Development of Green Catalytic Routes for the Synthesis of Commercially Important Chemicals

Thesis submitted in partial fulfillment of the requirements

For the degree of

Doctor of Philosophy

in

Chemical Engineering

by

Sumeet Kumar Sharma
(Rg. No. D05CH402)

Under the guidance of

Dr. Raksh V. Jasra
Former Deputy Director and Head
Discipline of Inorganic Materials and Catalysis, Central Salt & Marine Chemicals Research Institute, Bhavnagar, Gujarat

Prof. Parimal A. Parikh
Chemical Engineering Department
S.V. National Institute of Technology
Surat, Gujarat

Chemical Engineering Department
S.V. National Institute of Technology
Surat - 395 007 (Gujarat) INDIA

August 2008

Dedicated to,

My Grand Mother (Amma)

Thesis Approval for Doctor of Philosophy (Ph. D.)

Thesis entitled **"Development of Green Catalytic Routes for the Synthesis of Commercially Important Chemicals"** by Mr. Sumeet Kumar Sharma is approved for the degree of Doctor of Philosophy.

Examiners:

Supervisor(s):

Dr. Raksh V. Jasra
Former Deputy Director and Head
Discipline of Inorganic Materials and Catalysis, Central Salt & Marine Chemicals Research Institute, Bhavnagar (Gujarat)

Prof. Parimal A. Parikh
Chemical Engineering Department
S.V. National Institute of Technology, Surat (Gujarat)

Chairman:

Date:

Place: Surat

Certificate by the Ph.D. Supervisors

This is to certify that the contents of this thesis entitled "**Development of Green Catalytic Routes for the Synthesis of Commercially Important Chemicals**" are the original research work of **Mr. Sumeet Kumar Sharma** carried out under our supervision.

We further certify that the work has not been submitted either partially or fully to any other university/institution for the award of any diploma/degree.

Supervisor(s):

Dr. Raksh V. Jasra
Former Deputy Director and Head
Discipline of Inorganic Materials and Catalysis, Central Salt & Marine Chemicals Research Institute, Bhavnagar (Gujarat)

Prof. Parimal A. Parikh
Chemical Engineering Department
S.V. National Institute of Technology
Surat (Gujarat)

SARDAR VALLABHBHAI NATIONAL INSTITUTE OF TECHNOLOGY
SURAT - 395 007, GUJARAT, INDIA.

SEMESTER GRADE REPORT

DATE : 21-07-06 NO. 11

STUDENT'S NAME	EXAM NO.	SEM	YEAR
SUMEET KUMAR SHARMA	D05CH402	1	2005-2006

PROGRAMME : ~~M.Tech~~ Ph.D. DISCIPLINE : CHEMICAL

SPECIALIZATION : CHEMICAL ENGINEERING

COURSE NO.	COURSE NAME	GRADE	COURSE CREDIT
PHD 101	SEMINAR-I	AB	4
PHD 104/1	ASSIGNMENT-I	AB	1
PCHE 1003 T	ADVANCED PROCESS CONTROL	AB	4
PCHE 1004 T	SAFETY HEALTH & ENVIRONMENT	BB	3

REMARKS :

CURRENT SEMESTER PERFORMANCE			CUMULATIVE PERFORMANCE		
CREDITS	EARNED GRADE POINTS	SGPA	EARNED CREDIT	EARNED GRADE POINTS	CGPA
12	105	8.75	12	105	8.75

Patel N.N
CHECKED BY

DEPUTY REGISTRAR
ACADEMIC

Acknowledgements

It gives an immense pleasure to express my deep sense of gratitude and respect to Dr. Raksh V Jasra, former Deputy Director and Head, Discipline of Inorganic Materials and Catalysis, Central Salt and Marine Chemicals Research Institute (CSMCRI) and Prof. Parimal A. Parikh, Professor, Chemical Engineering Department, S.V. National Institute of Technology (SVNIT), Surat for their invaluable supervision with persistence, motivation, allowing me to think and work independently, seed innovations to my work and constant encouragement during the course of my work. Dr. Jasra's supportive critics and motivation for the inter–students collaborative work made me feel worthy and joyful throughout the period of my research. His eternal enthusiasm inspired me to accomplish my goal. Special thanks go to my Research Progress Committee members for their thoughtful constructive suggestions to enhance the quality of my research work.

I am also sincerely indebted to Dr. Ram S. Shukla and Dr. Sharad D. Bhatt for making healthy completive and friendly atmosphere in the High Pressure Laboratory. They have provided me constant encouragement, valuable suggestions and fruitful discussions related to not only my research work but also personal matters sometime. The invariable curiosity and fertile discussions from their profound knowledge made me reach at the present position.

I cannot fail to acknowledge my prodigious gratitude to Dr. Hari C. Bajaj for his kind support, encouragement and timely help during my research work, especially after resignation of Dr. Jasra from CSMCRI.

I am thankful to Dr. P.K. Ghosh (Director, CSMCRI), Prof. P.D. Pore (Director, SVNIT) and Prof. Z.V.P. Murthy for allowing me to carry out theoretical and experimental research work and extending me all the possible infrastructural facilities in CSMCRI–Bhavnagar and SVNIT–Surat.

Mr. A.H. Lakhanai, Technician, working in the High Pressure Laboratory, deserves for my exceptional thanks for his constant help in the work related to administration and purchase, maintenance of the instruments in high pressure lab and procurement of locally available stuffs related to my research work.

I extend my thankfulness to all my wonderful colleagues in High Pressure Laboratory for their assistance and friendship. I deeply appreciate the help obtained from my senior Dr. V.K. Srivastava and colleagues, Munir D. Khokhar, Jinka K. Mohan, Bharat K. Modhera, Asif A. Dabbawala, Mallikarjun V. Patil, Sudheesh N., C. Murugan, Hasmukh Patel and Kalpesh B. Siddhpuria, at various stages of my research work, discussions (sometimes hot) related to the nature of observed results in a typical experimental set–up and completion of inter–students collaborative work. Especial thanks to Mallikarjun V. Patil and Jinka K. Mohan for discussions related to the mechanistic aspects of the reactions.

I am extremely grateful to my friends and hostel–mates, Dr. R.K. Nagarale, Binsu R. Nagarale, Yogesh, Kunal N. Shah, Manoj Agrawal, Harish, Rajendra Patil, Gridhar Joshi with whom I enjoyed a lot during my stay in Bhavnagar as well as for their moral support in various matters.

I would like to place my respect and deep sense of gratitude to Dr. S.H.R. Abdi, Dr. R.I. Kureshy, Dr. R.S. Somani, Dr. S. Kannan, Dr. N.H. Khan, Dr. H.M. Modi, Dr. (Mrs.) Beena Tyagi, Dr. Jugnu Bhatt, Dr. A.B. Panda, Dr. A.B. Boricha, Dr. R.J. Tayade, Dr. A.S. Mehta, Dr. D.B. Shukla and Mr. Mehul Bhatt for their cooperation, in various ways, whenever I approached them.

I extend my thankfulness to the members from SVNIT, Dr. M. Chakraborty (Asist. Prof., Chemical Engineering Department), Mr. Kamal M. Desai (Academic section) and my colleges Alka Boricha, Paresh Patel and J.U. Kannedy for their time to time invaluable help related to the departmental documentations (especially Alka Boricha and Paresh Patel) as well as their moral support.

I am thankful to Mr. P.G.M. Pillai, Mr. J.M. Parmar, Mr. B.B. Parmar and. V.C. Zala who were also contributed in various ways to ensure the successful completion of my doctoral work.

I am also thankful to personnel from Workshop, Mr. J.H. Devmurari, Mr. S.N. Patel, Mr. J.N. Bhardia and Mr. L.M. Kachhadia. They were always available for maintenance and rectification of the minute and major problems of the autoclave reactor without which it was difficult to carry out Ph.D. work in hydroformylation reactions in appropriate time period.

I would also like to acknowledge the important technical assistance of Dr. (Mrs.) P. Bhatt, for P–XRD analysis, Mr. Vinod Agrawal for FT–IR analysis, Mr. Vinod P. Boricha for FT–NMR analysis, Prasanth K.P. and Ranjith S. for surface are measurements, Mr. C.K. Chandrakanth for SEM Analysis, Dr. Jagan Mohan and Harish for TGA Analysis. Without the support of these people, it is impossible to spread the shining of my research work in the world.

I would like to extend my special thanks to Mr. K. Rajagopalan (AO), R. Kashyap and Y. Trivadi for their kind support and cooperation during my crucial period in the CSMCRI. I convey my word of appreciation to R.P. Pillai for his keen interest and cooperation in the matters related to the CSMCRI research scholar's hostel, where I had stayed during my research work.

I take this opportunity to express my sincere gratitude to Mr. Pramod Makwana and his team members, IT Cell for their assistance in various problems related to computer hardwares and softwares.

I wish to express my sincere thanks to Mr. D.H. Khokhar and Mr. I.Y. Iyar for their helps in various ways for the procurements of chemicals and instruments related to my research work.

I would like to acknowledge Dr. Dharmesh U. Parmar, Dr. Chintan D. Chudasama, Dr. Yogi M. Badhika, Dr. Manish K. Mishra, Dr. Jince Sebastian, Dr. Surendra Singh, Dr. Irshad Ahmed, Dr. J. Krishnamurty, Sunil A.P., Praveen K. Surolia, Vishal J. Mayani, Seikh Basha, Kannan K., Achyut Bhatt, Kunal, Churchil, Jinesh, Kohol Raj, Gyanapraksham, Laxmi, Adarsh for the valuable discussions, moral support and friendship.

I render my thanks to all the students of Discipline of Inorganic Materials and Catalysis of CSMCRI for their prompt help and support.

I am grateful to Mr. M.J. Bariyaa for providing me the photo copies of research articles from the journals and helped me to search the location of journals and books in the institute library. I am also thankful to Mr. Vinu Solanki and all canteen members for providing me food in the institute premises.

It will be gaffe if I overlook them who had shaped me in early age to reach at the present position. Among them, at the outset, I am earnestly gratified to my grand mother (Amma) and her brother (Late Shri V.P. Sharma) who exposed me the world of knowledge in my early age. The highest gratitude goes to my grand mother, whose constant enthusiasm, hopeful disposition, timely encouragement, confidence, moral support and deep faith in God has motivated me to persevere and properly prioritize my life. My deep feelings of gratitude are also goes to my parents and my lovely brothers and sisters for their unwavering moral support and encouragement in successfully completion of my research work. My family members only installed in me the values of perseverance, a hard work ethic, value of common sense and responsibility, which were essential when working under pressure. Word “thank you” only scratch the surface of my gratitude for my family.

I must be doing injustice if I don’t mention a very special person, my wife *Sweta*, who has been my friend, scientific colleague and always beside me in my sunny and rainy days. Her help, cooperativeness, immensely friendly attitude and compromising nature have made me to learn so many things from her. I could not have completed my thesis without your love, respect, patience, appreciation, scientific discussions and faith with your charming presence, which kept my spirits alive.

My special heart felt thanks to my extraordinary graduation teachers, Prof Sanjay H. Amaley and Vijay Ganorkar from whom I learnt the aroma and taste of chemical reaction engineering fundamentals and the mantras of success. They have always inspired me and stood by me whenever I needed them.

I express my sincere thanks to Council of Scientific and Industrial Research (CSIR), India for providing me financial supports in terms of research scholarship and senior research fellowship.

Last but not least, I would also like to express my sincere thanks to all staff members of CSMCRI and Chemical Engineering Department, SVNIT–Surat for their cooperation and assistance directly or indirectly through out the tenure of my research work.

(Sumeet Kumar Sharma)

SRF–CSIR

Abstract

The research work in the present Thesis emphasizes the development of green catalytic routes for the synthesis of fine and commercially important chemicals using eco–friendly heterogeneous catalysts via hydroformylation, condensation and isomerization reactions. Chapters from second to fourth of this thesis are related to the development of multi-functional catalyst to reduce the multi–steps processes into a single pot for the synthesis of higher carbon chain length aldehydes/alcohols starting from low carbon number alkene as a reactant. For example, 2–ethylhexanal and 2–ethylhexanol, which are the commercially important intermediates for the synthesis of dioctylphthalate (DOP), are synthesized industrially from propylene in three steps process. The existing commercial processes for the manufacturing of C_8 aldol derivatives have drawbacks like, i) being a multi–step process, ii) use of hazardous liquid base KOH or NaOH in stoichiometric amount for aldol condensation reaction, iii) involving post synthesis work–up in the separation of spent KOH or NaOH from product mixture, iv) lower selectivity of product, corrosion of reactors and storage vessels. Therefore, the main focus was on the replacement of liquid bases, which are being used in stoichiometric amount, by the eco–friendly heterogeneous catalyst to carry out all three steps into a single pot by altering the reaction conditions.

The multi-functional [HF/HT] catalyst system was synthesized by the impregnation (Chapter 2) and intercalation (Chapter 3 and 4) of rhodium complex [HF] onto/into the interlayer space of hydrotalcite [HT] and its multi–functional potential was evaluated for the single pot selective synthesis of C_8 aldol derivatives (aldehydes/alcohols) from propylene. The Mg/Al ratio of [HT], amount of [HF] complex and [HT], and reaction temperature showed pronounced effect on the selectivity of C_8 aldol derivatives. Aldol condensation temperature T_2 played a significant role in the formation of 2–ethylhexanol in a single pot. As Mg/Al molar ratio and amount of [HT] increased, the selectivity of 2–ethylhexanal also increased due to the enhancement in the basicity of the catalyst. From kinetic experiments, it was observed that the rate of formation of 2–ethylhexanal is dependent on the rate of aldol condensation which is catalyzed by hydrotalcite present in the [HF/HT] catalyst.

Other commercial examples are the synthesis of perfumery chemicals such as, jasminaldehyde by the condensation of heptanal with benzaldehyde; *trans*–anethole and *trans*–isoeugenol by double bond isomerization of methyl chavicol and eugenol, respectively, using liquid KOH or NaOH in stoichiometric amounts. With increased environmental awareness, replacement of stoichiometric technologies by atom efficient greener catalytic routes with low E factor (kg of byproducts generated per kg of desired product) and substitution of toxic and/or

hazardous solvents/reagents with cleaner alternatives is today's demand. Therefore, it is desirable to find solid base catalysts which could substitute liquid bases.

The hydrotalcite samples of varied Mg/Al molar ratio were used as catalysts for synthesis of 2-methypentenal by aldol condensation of propanal (Chapter 5) and jasminaldehyde in solvent free condensation of 1–heptanal with benzaldehyde (Chapter 6). 97% conversion of propanal with 99% selectivity of 2–methylpentenal was achieved using activated hydrotalcite of Mg/Al molar ratio 3.5. From the kinetic data for aldol condensation of propanal using activated hydrotalcite (Mg/Al molar ratio 3.5), the initial rate of reaction was observed to increase on increasing the amount of catalyst. The activation energy for propanal condensation was calculated by Arrhenius plot and found to be 58 kJ/mol. The catalyst was recycled upto six cycles without loss in its activity. The selectivity of jasminaldehyde was observed to increase on increasing the M(II)/Al molar ratio of as–synthesized as well as activated hydrotalcite. The maximum selectivity of jasminaldehyde (86%) with 98% conversion of 1–heptanal was observed using as–synthesized Mg–Al hydrotalcite of Mg/Al molar ratio of 3.5 as a catalyst. The effect of activation of as–synthesized Mg–Al hydrotalcite samples of varied Mg/Al molar ratio on catalytic activity was studied and correlated with their basicity as determined from the model test reaction. The rate of reaction was calculated as 11.6 x 10^{-4} mol/(g_{cat} min) at optimum reaction conditions and catalyst was reused several times for the synthesis of jasminaldehyde..

The regioselective synthesis of *trans*–anethole from methyl chavicol via double bond isomerization of methyl chavicol using $RuCl_2(PPh_3)_3$ and $RuCl_3(AsPh_3)_2.CH_3OH$ complexes with detailed kinetics has been studied in Chapter 7. The incorporation of ruthenium in the hydrotalcite matrix was also carried out for double bond isomerization of perfumery related chemicals such as, methyl chavicol, eugenol, safrole, allylbenzene, dimethoxy allylbenzene, 3–carene. 98% conversion of methyl chavicol with 88% selectivity of *trans*–anethole was observed in 1 h reaction time. The effect of reaction temperature showed 41% conversion of methyl chavicol and 74% selectivity of *trans*–anethole at 100 °C which increased to 98% with 88% selectivity of *trans*–anethole on increasing temperature to 210 °C using Ru–Mg–Al as a catalyst. The activity of Ru–Mg–Al was compared with the various ruthenium impregnated catalysts such as, Ru–HT, Ru–MgO, Ru–CaO, Ru–SiO_2 and Ru–alumina. The Ru–Mg–Al catalyst was recycled upto fourth cycle without loss of its activity.

Keywords- Hydroformylation; Multi–functional catalyst; Condensation; Isomerization; Carbon monoxide; Solid base catalyst; Jasminaldehyde.

Contents

List of Figures

List of Tables

List of Schemes

Chapter 1

Introduction

"*It may appear that a field or even the whole of catalytic technology is relatively mature. This is, however, a misconception because history teaches us that fields which appear mature are suddenly revitalized by a major discovery.*"

– H. Heinemann

1.1. Introduction

Development of green catalytic routes for the synthesis of commercially important chemicals is a rewarding endeavor from environment and economic point of view. Green chemistry comprises designing, development and implementation of chemical products and processes to reduce or eliminate the use and generation of substances hazardous to the human health and environment. It is an innovative, non–regulatory, economically driven approach toward sustainability. Green technology is receiving significant attention as the awareness about environmental issues has increased. The term 'Green Chemistry' was suggested by Anastas, a member of the US Environmental Protection Agency (EPA) [1]. The concept for the design of environmentally benign products and processes is embodied in the 12 *Principles of Green Chemistry* as follow [1–2].

1. Waste prevention instead of remediation
2. Atom efficiency
3. Use of less hazardous/toxic chemicals
4. Design safer chemicals and products
5. Use innocuous solvents and reaction conditions
6. Design energy efficient processes
7. Preferably renewable raw materials
8. Shorter synthesis route and avoid derivatization
9. Use catalyst instead of stoichiometric reagents
10. Design products for degradation after use
11. Real time analytical methodologies for pollution prevention
12. Inherently safer processes to minimize the potentials for accidents

Catalysis plays a vital role in production of wide variety of products, which are having applications in drugs, plastics, agrochemicals, perfumery, detergents, food, clothing, fuels etc. [3]. In addition to these, it plays an important role in the balance of ecology and environment by providing cleaner alternative routes to stoichiometric technologies [4]. Green catalytic process efficiently utilize all the atoms of raw materials, eliminates waste and avoids the use of toxic and/or hazardous reagents and solvents in the manufacture and application of chemical products. The E Factor, i.e. kg of waste generated per kg of desired product, is a well accepted concept in the

modern green process to assess the impact of stoichiometric technologies on environment (Table 1.1). A higher E factor means more waste and, consequently, greater negative environmental impact. The ideal E factor is zero. Fine chemicals and pharmaceutical industries use processes having higher E factor, means more waste is generated per kg of desired product.

Table 1.1. E factor of some industrial sectors [5]

Industry sector	**Product range, tons/annum** [a]	**kg Byproducts/kg of products**
Oil Refining/Petrochemicals	$10^6 – 10^8$	~ 0.1
Bulk Chemicals	$10^4 – 10^6$	< 1–5
Fine Chemicals	$10^2 – 10^4$	5–50
Pharmaceuticals	$10 – 10^3$	25–100

[a] Annual production of product worldwide or at a single site

The enormous amounts of waste from the fine chemicals and pharmaceuticals industries, comprising of mainly inorganic salts, such as sodium chloride, sodium sulfate and ammonium sulfate, are formed in the reaction or in subsequent neutralization steps. The E factor increases dramatically on going downstream from bulk to fine chemicals and pharmaceuticals, partly because production of the latter involves multi–step syntheses but also owing to the use of stoichiometric reagents rather than catalysts. For example, an industry is reported an E factor 35 for particular process means that the 35 kg of waste generated for the production of 1 kg product.

Another concept in the green chemistry is the atom efficiency or atom economy introduced by Trost [6–7]. This is an extremely useful tool for rapid evaluation of the amounts of waste that will be generated by alternative processes. It is calculated by dividing the molecular weight of the desired product by the total sum of the molecular weights of all substances formed in the stoichiometric equation for the reaction involved.

The solid base catalysts provide an opportunity for eco–friendly synthesis of the commercially important chemicals that involve large amount of KOH or NaOH as a catalyst or sometimes as a reagent. The homogeneous processes have drawbacks like, corrosion of the reactor and vessels, use of hazardous liquid base KOH or NaOH in stoichiometric amounts, involving post synthesis work–up in the separation of spent KOH or NaOH from product mixture, disposal of spent catalyst, utilizing large amount of water and solvents for the treatment processes, lower selectivity of product, longer reaction time. High capital expenses are also connected with the

handling of strong liquid bases, KOH or NaOH. With increased environmental awareness, replacement of stoichiometric technologies by atom efficient greener catalytic routes with low E factor and substitution of toxic and/or hazardous solvents/reagents with cleaner alternatives is today's demand. Therefore, our main concern is the replacement of liquid bases, which are being used in stoichiometric amount with eco–friendly heterogeneous catalyst systems. The present thesis deals with the developments of heterogeneous eco–friendly catalysts for hydroformylation, condensation and isomerization reactions related to the fine and commercially important chemicals.

1.2. Hydroformylation of Alkenes (Oxo Reaction)

The reaction between double bond of an alkene with a mixture of hydrogen and carbon monoxide (syn–gas) in the presence of the catalyst, produces aldehydes (linear and branched) as primary products with an additional carbon atom as compared to the alkene is known as hydroformylation reaction (Scheme 1.1).

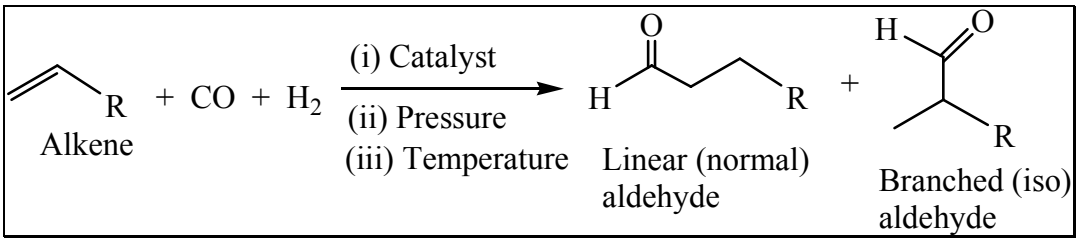

Scheme 1.1. Hydroformylation reaction.

The term hydroformylation (oxo reaction) for this reaction is introduced by Adkins, since an attack of hydrogen and formyl group (CHO) at the unsaturated center of the carbon chain of a alkene molecule [8]. The primary products of hydroformylation reaction are aldehydes only, however, the obtained aldehydes could be converted into various commercially important chemicals via subsequent reactions [9].

The hydroformylation reaction was discovered by Otto Roelen in 1938 while investigating the reaction mechanism of the Fischer–Tropsch (F–T) synthesis by addition of syn–gas to the ethylene [10–11]. The small amount of propanal (and diethyl ketone) was formed when a mixture of ethylene and synthesis gas was passed over a fixed bed of the catalyst containing cobalt at 150 °C and 100 atm. The selectivity of propanal increased significantly when the reaction was carried out at 51 atm and 150 °C. First real catalyst for the hydroformylation reaction was the conventional F–T catalyst. Later it was recognized that cobalt afforded higher conversion and selectivity of propanal when used as a catalyst in homogeneous conditions. Besides carbonylation of methanol to acetic acid and oxidation of *p*–xylene to DMT, hydroformylation of alkenes is next most important

industrial homogenously catalyzed reaction. Consequently, hydroformylation of alkenes is the most used and well–understood homogeneous catalytic reactions and is also a subject of exhaustive review [12–27].

1.2.1. Commercial Importance of Hydroformylation Products

World production and consumption of hydroformylation (oxo) chemicals is more than 8.8 million metric tons per year finding use in the manufacture of solvents, soaps, detergents, plasticizers and various intermediates for fine and perfumery chemical industry. *n*–Propanol and *n*–propyl acetate produced from ethylene hydroformylation are used in flexographic and gravure inks, which require volatile solvents to prevent spreading and ink accumulation on printing processes [22–23]. *n*–Propanol is also used as a solvent, pesticide intermediate, precursor for glycol ether, surface coating applications, grain and food preservatives, herbicides, etc.

Over 90% of world consumption of *n*–butanal, which is produced by hydroformylation of propylene, is for the production of 2–ethylhexanol (2–EH) and *n*–butanol. The main application of butanal is an intermediate for the production of plasticizers, rubber accelerators, synthetic resins, solvents and high molecular weight polymers. The reason for high production and demand of C_4 aldehydes is due to its use in the production of 2–ethylhexanol (2–EH). About 60% of the total C_4 aldehydes production capacity (or about 70% of the *n*–butanal production capacity) is consumed for the synthesis of 2–ethylhexanol. 2–Ethylhexanol is used for the production of dioctyl phthalate and other plasticizers, coatings, adhesives, stabilizers, low volatility solvent, perfumery and specialty chemicals (Figure 1.1). 2–Ethylhexanol derivatives are used as an additive for diesel fuel to reduce emissions and for lube and mining oils to improve their performance.

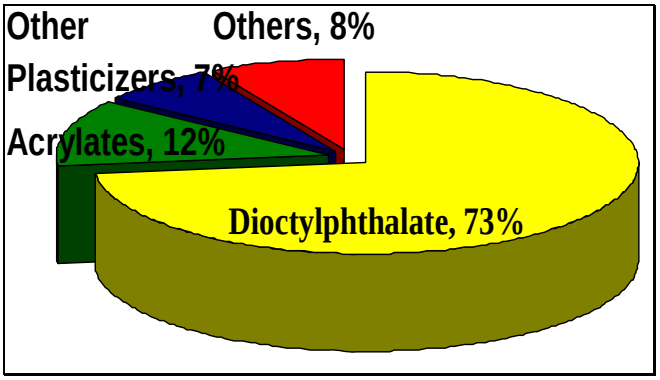

Figure 1.1. Global consumption of 2–ethylhexanol for various applications (wt %).

n–Butanol is a versatile intermediate for chemical industry. It reacts with acids to yield esters and with oxides to yield glycol ethers. *n*–Butanol is an intermediate chemical for the synthesis of esters like butyl acetate, butyl acrylate, butyl methacrylate, etc. and these esters are used as

solvents for coating. Other applications of *n*–butanol are solvent, cleaning fluids, herbicides, dyes, printing inks, personal care products, pharmaceuticals, plasticizers, textiles and lube additives. The global consumption of the butanol is shown in Figure 1.2.

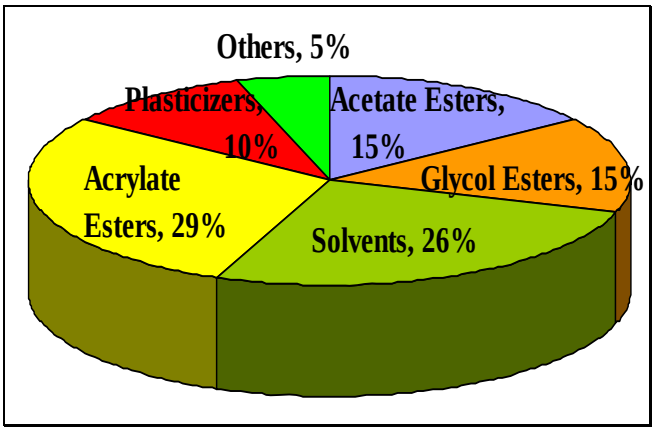

Figure 1.2. Global consumption of *n*–butanol and *iso*–butanol (wt %).

C_5 valeraldehyde derivatives are used predominantly to make lube oil additives, automotive anti–wear applications, aeromotive synthetic lube formulation and refrigerant lubricants. *n*–Valeric acid, which is prepared from the hydroformylation of butene followed by oxidation, is used for the synthesis of lubricants, biodegradable solvents, plasticizers, perfumery and pharmaceutical chemicals. $C_{6–15}$ oxo alcohols are used in the fine chemicals and perfumery industry, for the synthesis of neopolyol esters plasticizers and detergent applications [22].

1.2.2. Economic Aspects of Hydroformylation Reaction

The faster growing market for the oxo products is due to continuous growth of the hydroformylation processes. Figure 1.3 shows the growth in the production of oxo products around the world [22–23].

As seen from Figure 1.3 and 1.4, Asia, North America and Western Europe are contributing 32%, 23% and 30%, respectively to the world production capacity of oxo products and are major oxo producers today. USA and Germany with 23% and 21% of world's production are also leading producers. Within Asia, Japan, South Korea and China are the major manufacturers with as many as five other countries engaged in the production of oxo products (Figure 1.5). India is a minor producer contributing 0.66% to the world's production capacity and 2% to the Asia's production of oxo products. Between 1998 and 2002, approximately 1.8 million metric tons of oxo chemical capacity was added, mainly in Southeast Asia.

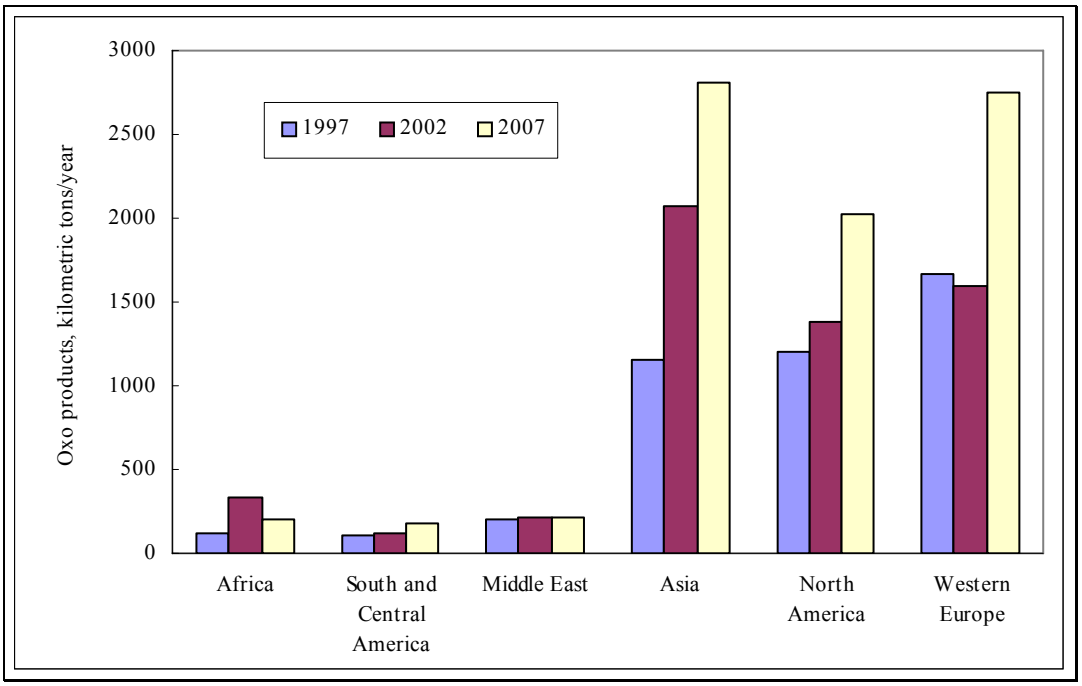

Figure 1.3. Worldwide growth in the production of oxo products.

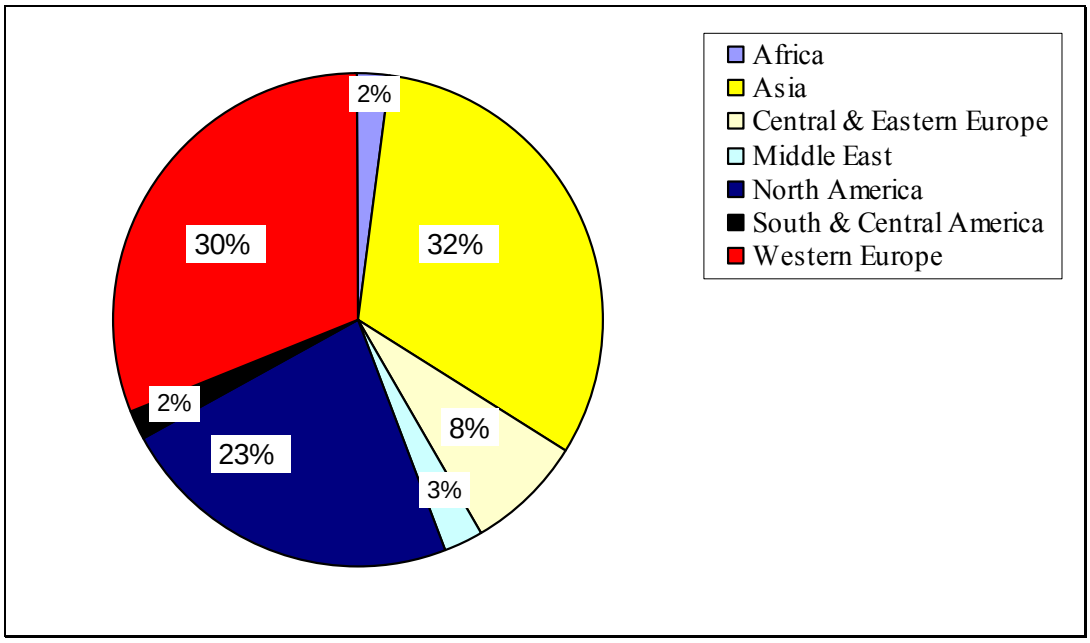

Figure 1.4. Region wise production statistics for oxo products (2003).

These data show that Asia has been the main growth center for these chemicals during last five year with North America and Western Europe showing stagnancy. It is estimated that in the coming five years too, Asia will witness the growth in oxo products with only a small increase in production capacities in other countries. The worldwide oxo product derivatives distribution is shown in Figure 1.6. The production rate of 2–ethylhexanol is high among all oxo derivatives, which is mostly consumed by the plastic industry, followed by production of butanol.

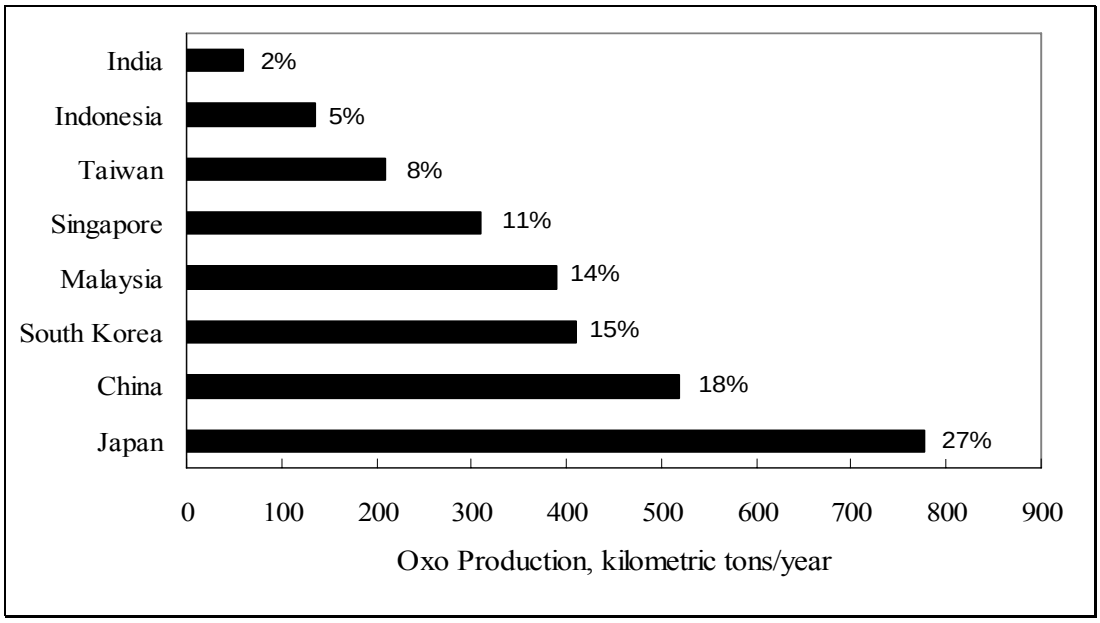

Figure 1.5. Statistics of oxo products for Asia region (2003).

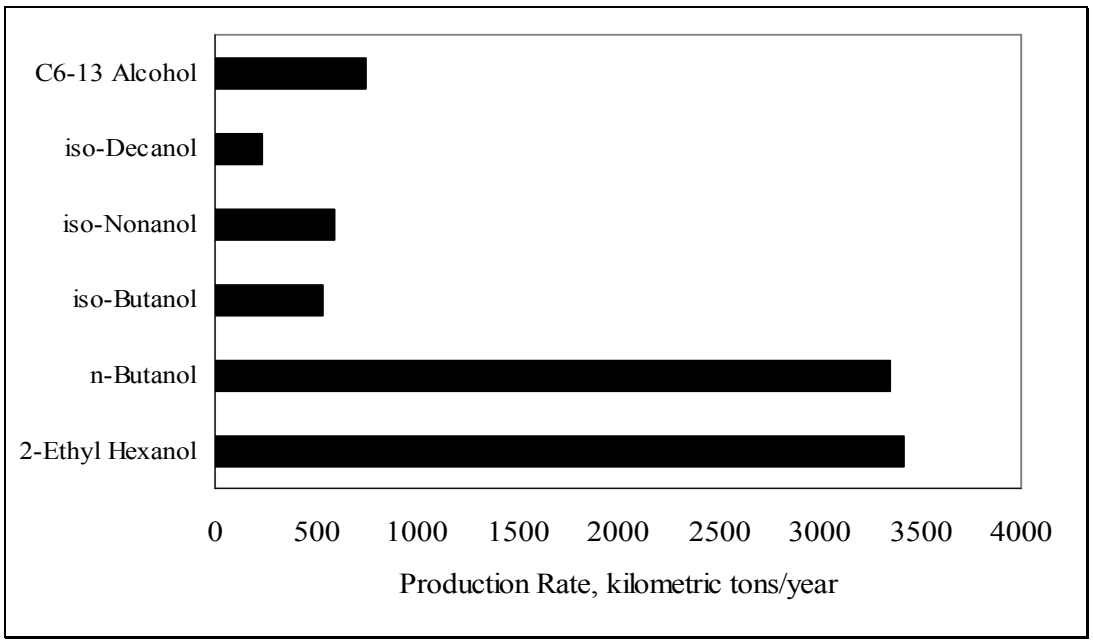

Figure 1.6. Worldwide oxo product derivatives distribution.

The detergent grade alcohols also have significant contribution in the world market, which are produced by oxo reaction. Figure 1.7 gives the estimated production capacities for the oxo products via hydroformylation reaction by worldwide known industries. It is observed from these data that around 57% of the oxo products are produced by seven companies namely BASF, Exxon, EON, Celanese, Dow, Eastman and Kyowo Hakko [22–23].

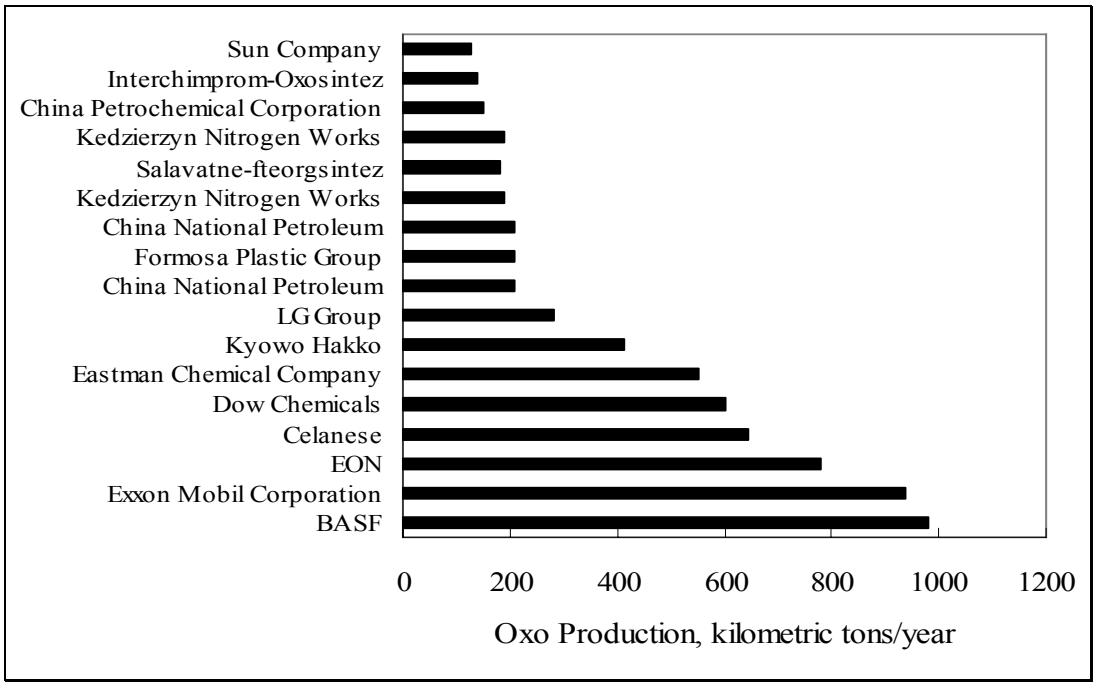

Figure 1.7. Production capacities for oxo products by worldwide known industries.

1.2.3. Hydroformylation Products: An Indian Scenario

The production of oxo products is limited mainly to 2–ethylhexanol and *n*–butanol in the India. During last few years, imports of 2–ethylhexanol and *n*–butanol have averaged about 10,000 to 14,000 tons per year. In India there are nine major producers (Figure 1.8) of oxo products, the reason behind tardy production in India is due to sluggish growth of market for plasticizers and other uses of oxo products.

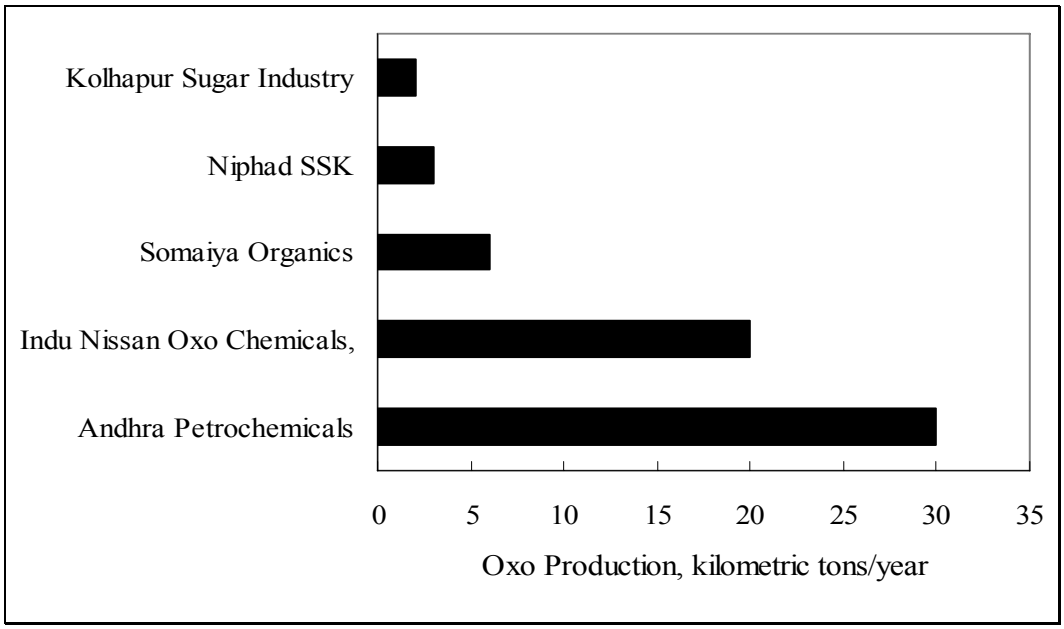

Figure 1.8. Production of oxo products in India.

At present, Andhra petrochemicals is a major producer of oxo products in India. Its production capacity is 30 kilometric tons/, which is consistent since 1999. Out of 30 kilometric tons/year, 25 kilometric tons/year 2–ethylhexanol is produced by propylene hydroformylation and rest is *n*–butanol, which is produced by the hydrogenation of butanal [22].

1.2.4. Catalysts for Hydroformylation Reaction

The hydroformylation catalysts, typically, consist of a transition metal atom (M), especially from the platinum group metals. These transition metal complexes interact with CO and hydrogen to form metal carbonyl hydride species, which is an active hydroformylation catalyst. Typically, complexes containing carbonyl ligands are known as unmodified catalysts. On the other hand, introduction of tailor–made ligand to the transition metals are known as the modified catalysts.

Three developmental stages for hydroformylation catalysts are reported in the literature. The first stage of hydroformylation was exclusively based on cobalt (Co) containing catalyst. The catalytic active species for hydroformylation reaction was the cobalt carbonyl hydrides in the pressure range of 240–300 bar at 150–200 °C temperature. Separation of products from the reaction mixture, severe reaction conditions and low activities of catalysts were the main limitations of this stage's processes. The research efforts led phosphine replacing carbonyl complexes as an electron donating ligand and this emerged as a fundamental step in metal carbonyl catalyzed reaction, which imparted ability to the scientists to tailor–make catalyst by modifying the electronic and steric properties of the ligand.

The second stage of hydroformylation reaction was the combined development in ligand modification and replacement of cobalt rhodium (Rh) metal. It took almost a decade of research before first rhodium catalyst based commercial process was launched in 1974 and the process was termed as Low Pressure Oxo (LPO) process. Compared to cobalt based processes, many advances were made in the second developmental stage of hydroformylation, especially with respect to material and energy utilization. Thus, second stage of hydroformylation was concluded with development of more effective Rh–phosphine catalyst. However, the industrial problems of first stage such as, separation of products from reaction mixture, catalyst recovery, loss of costly metals, use of corrosive solvents, etc. continued in the second stage too.

In the third stage, the attention was largely focused to design such a process wherein the separation of products from reaction mixture is facile and easy. The fundamental idea consisted in applying water–soluble catalysts by ligand modification and thus transferring the hydroformylation into aqueous phase. With the help of such catalysts, separations of desired products have become

an easy task. The idea of applying water–soluble Rh–complex as a catalyst for the hydroformylation of propylene and 1–butene was taken up and commercialized by Ruhrchemie AG [28–30]. The first plant was commissioned in 1984, only two years after the development on laboratory scale, followed by rapid further increases in capacity to more than 3 x 10^6 tons/year. An additional unit for the production of n–pentanal (*n*–valeraldehyde) from 1–butene [29–30] has been brought on stream in 1995. The developments of hydroformylation processes in different stages are shown in Table 1.2 and the catalysts used are presented in Scheme 1.2.

Table 1.2. Developments in hydroformylation processes

Catalyst metal	Cobalt	Cobalt	Rhodium	Rhodium	Rhodium
Ligand	none	phosphines	none	phosphines	phosphines
Process	1	2	3	4	5
Active catalyst species	$HCo(CO)_4$	$HCo(CO)_3PPh_3$	$HRh(CO)_4$	$HRh(CO)(PPh_3)_3$	$HRh(CO)(TPPTS)_3$
T (°C)	150–180	160–200	100–140	60–120	110–130
P (bar)	200–300	50–150	200–300	10–50	40–60
Catalyst/alkene molar ratio	0.1–1	0.6	10^{-4}–0.01	0.01–0.1	0.001–1
LHSV, h^{-1}	0.5–2	0.1–0.2	0.3–0.6	0.1–0.2	>0.2
Products	aldehydes	alcohols	aldehydes	aldehydes	aldehydes
By–products	high	high	low	low	low
n/iso of aldehydes	80:20	88:12	50:50	92:8	>95:5

1 = BASF, Ruhrchemie process; 2 = Shell process; 3 = Ruhrchemie process; 4 = Union Carbide process (LPO); 5 = Ruhrchemie–Rhone–Poulene process; LHSV = Liquid hourly space velocity

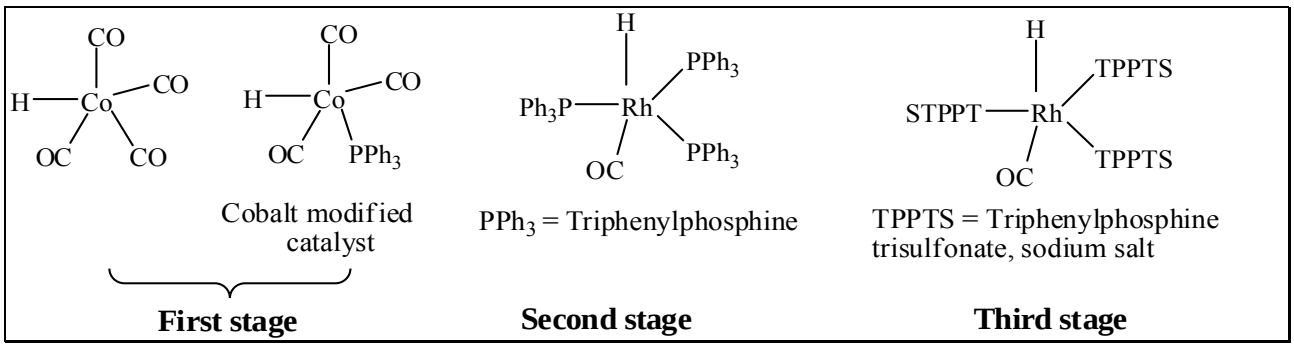

Scheme 1.2. Three stages of the catalyst development for the hydroformylation reaction.

Presently, most of the industrial plants are running successfully with rhodium and cobalt

based catalysts. Attempts had been made to compare the catalytic activity of group VIII and IX metals for hydroformylation of alkenes to understand the role of metal atom in hydroformylation reaction [31–36]. Ruthenium is attracting the attention of the researchers after rhodium and cobalt; nevertheless, it is yet to move from laboratory to pilot plant scale. The ligand plays a significant role in the hydroformylation reaction from the catalytic activity, selectivity and regio–selectivity point of view. Phosphines and phosphite based monodentate and bidentate ligands are most commonly used and accepted ligands for the hydroformylation reaction [37–44]. Nitrogen containing ligands showed lower reaction rates than phosphines due to their stronger coordination to the metal centers. A comparative study of Ph_3R (where R= elements of main group V) were made for the hydroformylation of 1–dodecane [45] and showed following order; $Ph_3P > Ph_3N > Ph_3As > Ph_3Sb > Ph_3Bi$. In another study, the activity of the triphenylphosphine, triphenylarsine and triphenylantimony ligands were compared for hydroformylation of ethylene and 1–hexene using transition metal catalysts [46]. Today, most of work in the homogeneous catalysis for hydroformylation is focused on the developments of the bulky phosphorous/phosphite ligands which include both monodentate and more bulky bidentate ligands.

1.2.5. Recent Trends in the Heterogeneous Hydroformylation Reaction

Commercial processes are using triphenylphosphine modified Rh–complex $[HRhCO(PPh_3)_3]$ as a catalyst for the hydroformylation of lower carbon chain length alkenes ($C_2 - C_5$) under milder reaction conditions. This catalyst is limited upto the hydroformylation of lower carbon chain alkenes such as, ethylene and propylene due to separation problems of Rh–complex from the product mixture after completion of the reaction. Conventionally, homogeneous catalyst is separated from the product mixture by stripping the products in vacuum (vacuum distillation). The thermal stress caused by the vacuum distillation process decomposes the expensive metal complex which is used as a catalyst for hydroformylation reaction. Most homogenous hydroformylation catalysts are thermally sensitive and decompose below 150 °C. This is the main reason, which limits the applicability of Rh–complex for hydroformylation of lower carbon chain length alkenes because in case of higher carbon chain length alkenes, decomposition of rhodium complex occurred during the separation of catalyst from higher boiling point product mixture. As far as hydroformylation reaction is concerned, Rh–complexes as catalysts typically work under mild conditions (80–100 °C, 20–40 atm), giving good activity & selectivity (95–99%) to the desired linear (*n*–) aldehyde. For the hydroformylation of higher alkenes, cobalt catalysts are widely used, which require drastic reaction conditions (200 °C, 200–250 atm) and yield poor selectivity for linear aldehyde. The cobalt catalyst is recycled after vacuum distillation of the product mixture by the "decobalting" procedure. In the decobalting process, regeneration of cobalt

catalyst after reaction is carried out by changing the oxidation state of cobalt either by hydrothermal treatment or by oxygen treatment in acidic medium. Typically, cobalt is recovered in the form of cobalt formate or acetate by addition of the oxygen and formic or acetic acid [21]. Although, cobalt catalyst is recycled for hydroformylation of alkenes, but still has drawbacks of higher temperature, pressure, longer reaction time and lower selectivity of the desired aldehyde as compared to rhodium based catalysts. Solving the product separation problem for the rhodium catalyzed hydroformylation in an effective and economically acceptable way, would present a major step forward in homogeneous catalysis. Therefore, development of a heterogeneous catalyst for hydroformylation in today's research scenario can be broadly classified into two categories. In the first category, catalyst is anchored or supported on the surface of solid inorganic material, which is used as heterogeneous catalyst either in continuous reactor (fixed bed) or in the high pressure batch reactor (autoclave). This type of process is often referred to as heterogenizaton of homogeneous catalysts. Second category is the designing of a water–soluble ligand, which is insoluble in the product mixture, is often referred to as biphasic systems. The reaction in biphasic system involves aqueous and organic phases (Figure 1.9).

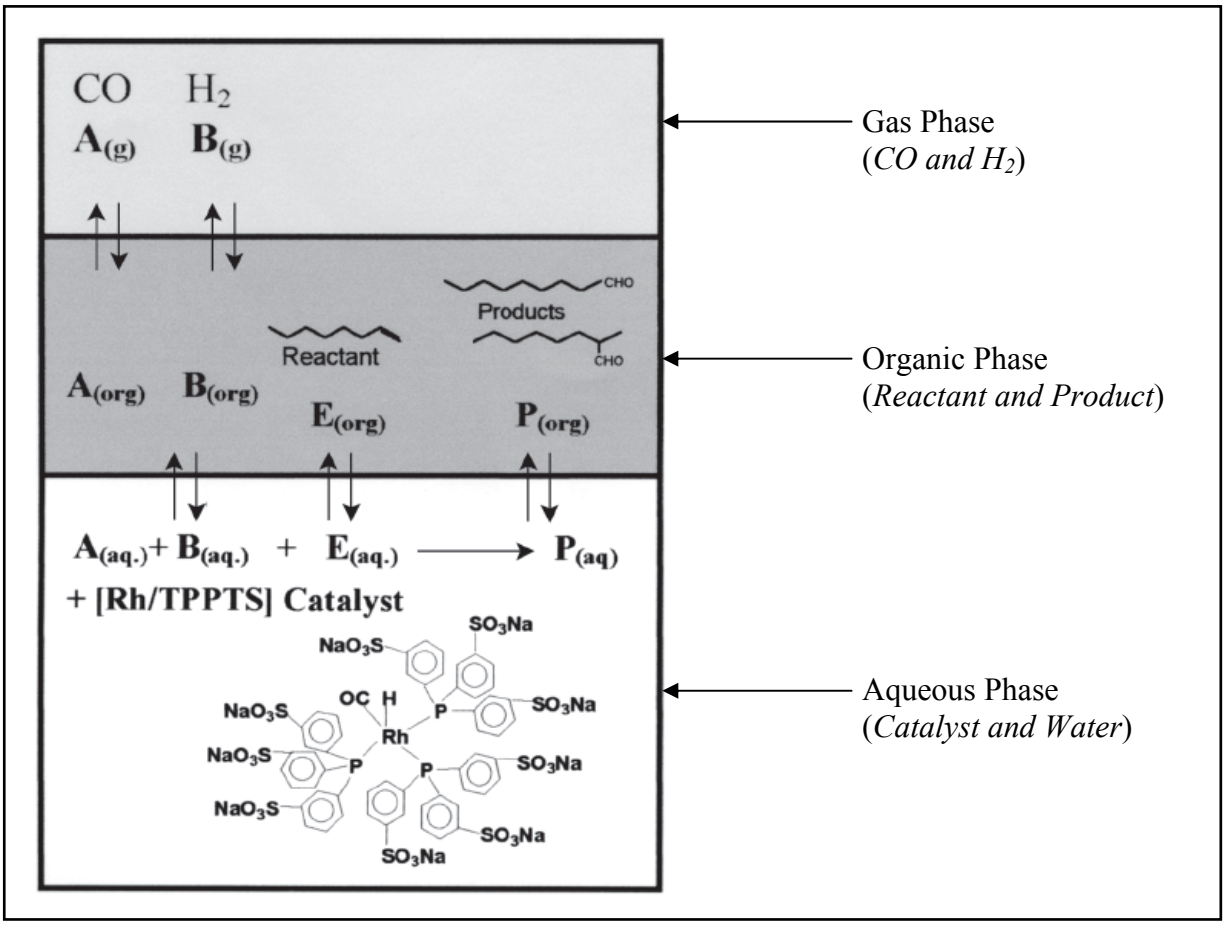

Figure 1.9. Hydroformylation reaction in biphasic medium.

Reaction takes place at the interphase. Catalyst is separated from the reaction mixture using phase separator [47–51]. There are some reports presented in the literature on the development of

cobalt and ruthenium biphasic systems for hydroformylation of alkenes [52–55]. Application of biphasic catalyst is limited to hydroformylation of propylene and butene due to lower solubility of higher carbon chain length alkenes in aqueous medium (water). Though, homogeneous catalysts give higher conversion and selectivity for desired product in short reaction time as compared to heterogeneous catalyst system, this have disadvantage in the separation of catalyst from the product mixture. Thus, efforts are directed towards the heterogenization of rhodium complex on the inorganic solid supports for hydroformylation of alkenes. In this concern, more attention in the present thesis has been paid on literature review related to the recent developments in the heterogenizaton of homogeneous catalysts on the inorganic solid supports for hydroformylation of alkenes.

Impregnation is the common method for heterogenizaton of homogeneous catalyst. In this method, inorganic solid support is mixed with the solution of homogeneous complex prepared by dissolving the complex in suitable solvent. Then, the suspension is stirred for long time either at room temperature or at a particular desired temperature. Ligands can also be anchored or impregnated onto solid inorganic materials, generally silica, zeolites or polymers. The ligand or complex anchored covalently to the solid support of high surface area ensures the reusability of the catalyst. Main problem in the heterogenizaton of homogeneous complex is the breaking of bonds between metal and ligand during the course of catalytic reaction and this is the cause of leaching of the active metal species responsible for the reaction. This "leaching" process leads to the loss of catalytic activity in the reusability experiments. The leaching problems can be solved upto certain extent by anchoring the homogeneous complex using some tethering agent or encapsulation inside the pores of the solid support used.

1.2.6. Heterogeneous Catalysts for Vapor Phase Hydroformylation of Alkenes

Most of the developments for rhodium based catalysts supported on various inorganic materials were studied for vapor phase hydroformylation of ethylene and propylene in a continuous flow (fixed bed) reactor. Since, the lower carbon number alkenes (ethylene and propylene) exist in gaseous form, it seems appropriate to produce aldehydes under continuous flow conditions over batch mode. In the 1980s, heterogenization of rhodium complex was performed by taking zeolites as solid supports. The series of highly active catalysts were synthesized by rhodium entrapping in the framework of zeolite X and Y and used as catalysts for vapor phase hydroformylation of propylene and ethylene (Scheme 1.3) [56–58].

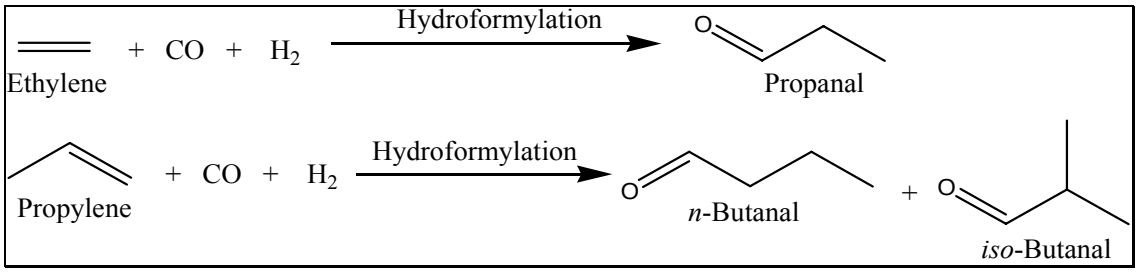

Scheme 1.3. Hydroformylation of ethylene and propylene.

Detailed comparative study for hydroformylation of ethylene and propylene were made by Davis et al. using Rh–Y and Rh–X as catalysts in the continuous flow reactor at an atmospheric pressure [57–58]. Activity of catalysts for the formation of propanal and butanal did nofall for a period of one month's continuous experimental run. The results concluded that the active sites were formed either at the entrance of pore or external surface can effectively catalyze the hydroformylation of ethylene and propylene. In another study, hydroformylation of propylene was investigated using palladium (Pd) trimethylphosphine carbonyl clusters entrapped in the cage of zeolite Na–Y [59]. The rate of reaction was reported to depend on calcination and reduction temperatures as well as concentration of trimethylphosphine. Excess concentration of trimethylphosphine results into the drop of catalytic activity of the catalyst [59].

Due to large surface area of silica as compared to zeolites, the Rh–complex was also heterogenized on the surface of silica for hydroformylation. Naito et al. found the rhodium supported silica to be the most selective catalyst for the formation of butanal via hydroformylation of propylene in fixed bed reactor [60]. There are some reports in which *In–situ* reduction of rhodium impregnated catalyst was claimed to convert it into nanocrystalline or amorphous metallic phase, which was very active for hydroformylation reaction. Lenarda et al. reduced the impregnated Rh on silica in a solution of tetrahydrofuran (THF) and 1 M lithium aluminum hydride at low temperature and obtained rhodium nanocrystals was used as a catalyst for propylene hydroformylation [61]. Apparent activation energy for the propylene hydroformylation was found to be 26 kJ/mol. Catalytic activity and selectivity of aldehyde could be improved by the addition of promoters or use of the bimetallic catalysts. The bimetallic nanocrystalline Rh–Co based catalysts with varied Rh/Co ratio were synthesized by the reduction of metal salts impregnated on silica with $NaBH_4$ in the nitrogen atmosphere [62]. The obtained catalyst showed high regio– and chemo–selectivity for aldehyde and catalytic activity was observed to increase with increase in the Rh/Co ratio. Effect of triphenylphosphine (PPh_3) on the rhodium impregnated silica (Rh/SiO_2) was also studied for hydroformylation of propylene using fixed bed reactor [63] and batch slurry reactor for hydroformylation of ethylene, 1–hexene and 1–octene [64]. The obtained results were compared with the $HRhCO(PPh_3)_3/SiO_2$ and $PPh_3–Rh/SiO_2$ systems. The coordination of PPh_3 was retained

in Rh/SiO_2 catalyst that was confirmed by solid state ^{31}P–nuclear magnetic resonance (NMR) and *in–situ* Fourier transform infrared (FT–IR) spectroscopic analysis. Excellent conversion of propylene with higher *n/iso* ratio of aldehydes was obtained using PPh_3–Rh/SiO_2 as a catalyst and deactivation of catalyst was not observed over a period of 1000 h reaction time on stream. The correlation of homogeneous and heterogeneous catalyst (Rh/SiO_2) for hydroformylation of ethylene was made based on the results obtained from the FT–IR spectroscopic study [65]. Later on infrared spectroscopic studies were continued for the hydroformylation of ethylene and propylene and developed the reaction mechanism and kinetic models. The coordination and formation of the intermediate species during hydroformylation of ethylene was studied by Chuang et al. using immobilized rhodium catalysts, mainly Rh/SiO_2 and manganese modified Mn–Rh/SiO_2. Progress of ethylene and propylene hydroformylation, formation of intermediate active species, mechanistic aspects and reaction kinetics were studied from the analysis of transient response of the formed product obtained by isotopic methods combined with *in–situ* infrared spectroscopy [66–74].

Advantage of supercritical carbon dioxide in the heterogeneous catalysis was reported by Abrahan et al. to study the effect of different supports on hydroformylation of propylene [75]. Recently, hydroformylation of propylene in continuous flow reactor was reported using rhodium catalyst synthesized in ordered mesoporous silica FSM–16 using Rh/Al heteropoly acid anions and/or $[Rh(COD)_2]^+$ complex. The activity of *in–situ* prepared catalyst was also compared with the impregnated Rh on FSM–16. The addition of molybdenum as a promoter results into increased selectivity of butanal and butanol (Figure 1.10) [76].

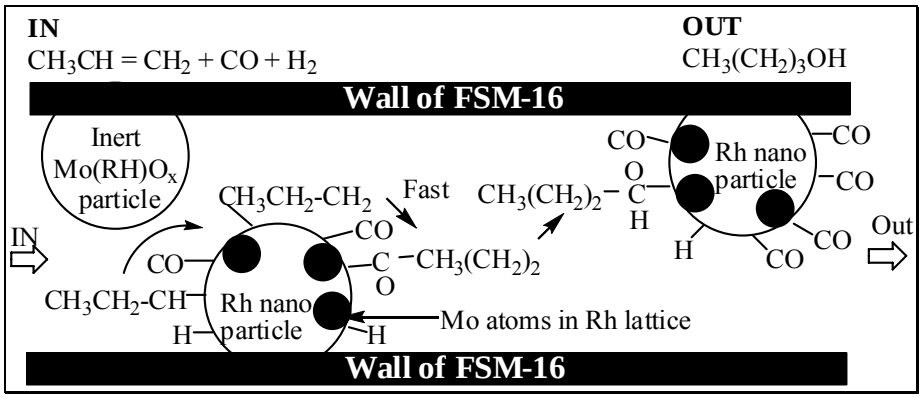

Figure 1.10. Proposed mechanism of selective *n*–butanol synthesis over $[RhMo_6O_{18}(OH)_6]^{3-}$ /FSM–16 catalyst.

Applicability of the supported ionic liquid phase (SILP) catalysts, prepared by impregnation of the partly dehydroxylated silica support with an anhydrous methanolic solution of ionic liquid [bmim][n–$C_8H_{17}OSO_3$] containing catalyst precursor [Rh(acac)$(CO)_2$] and bisphosphine ligand (Figure 1.11), was used as a effective catalyst for hydroformylation of propylene in a fixed bed

reactor [77]. Review articles for the applicability of supported ionic liquid as catalysts for hydroformylation of alkenes have recently appeared in the literature [78–84].

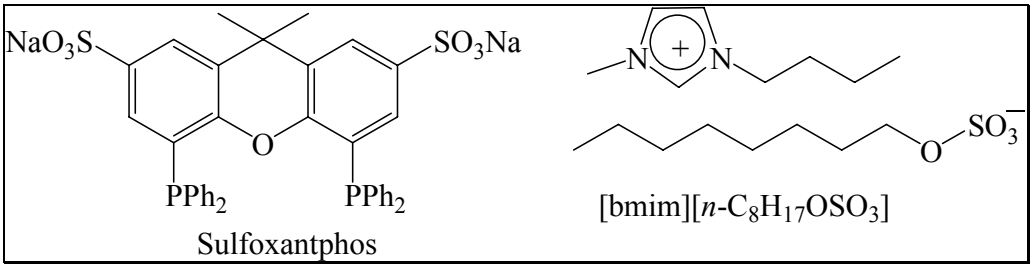

Figure 1.11. Ligand and ionic liquids used for hydroformylation reaction.

Applicability of the polymers for immobilization of rhodium complex for hydroformylation, hydrogenation and isomerization of lower alkenes was explored by Arai in 1978 [85]. Rhodium complex immobilized on polystyrene coated silica gel was used as a catalyst for hydroformylation of ethylene, propylene and 1–butene in the fixed bed reactor. Reactivity of the alkenes was reported in order: ethylene > propylene > 1–butene under identical reaction conditions and the obtained results using polymer immobilized catalyst were compared with the homogeneous Rh–complex [85]. Scholten et al. reported the gas phase hydroformylation of propylene at 90 °C and 10 atm total pressure using Rh–complex [$HRhCO(PPh_3)_3$] anchored on porous resin (polystyrene–divinylbenzene) [86]. In another study, cationic rhodium carbonyl complex bound to the copolymers of 2–vinylpyridine and methyl acrylate cross linked with 5% (mol) ethane diacrylate were used as catalysts for hydroformylation of propylene [87]. The catalyst deactivated very rapidly due to the formation of benzene during the reaction.

Except the applicability of Rh metal for hydroformylation of alkenes, the researchers also performed the experiments on the activity of ruthenium (Ru) exchanged pillared clay as a catalyst for hydroformylation of ethylene and propylene in a fixed bed reactor at atmospheric pressure in the temperature range of 100 – 220 °C. The Ru–catalyst showed constant rate of reaction even at the end of 1 week experimental run [88].

Effect of Promoters for Vapor Phase Hydroformylation of Ethylene and Propylene

Catalytic activity and selectivity of aldehyde in the vapor phase hydroformylation of alkenes over supported metal catalysts can be markedly influenced by other variables including supports and promoters. A catalyst promoter is defined as an element or compound without catalytic activity by itself, but when added to an active catalyst it accelerates the activity, selectivity, and stability of the catalyst. The use of an additive such as, iron (Fe), zinc (Zn), molybdenum (Mo), magnesium (Mg), manganese (Mn) and vanadium (V) showed pronounced

effect on the hydroformylation of ethylene and propylene. The $RhVO_4$ mixed oxide was synthesized by the simple impregnation method, in which respective salt solution was used as the metal source, and taken as a catalyst for the hydroformylation of ethylene [89]. Higher selectively of propanol was observed via hydroformylation of propanal even though the conversion of ethylene in the range of 0.07 to 1.88% at 10 atm total pressure and 300 °C reaction temperature. Hydroformylation activity of Rh–catalyst prepared by thermal decomposition of $Rh_6(CO)_{16}$ shows the order of support: ZnO>MgO>TiO_2, ZrO_2, La_2O_3>>>SiO_2, Al_2O_3 [90]. Modification of $Rh/SiO_2/ZrO_2$ catalyst by adsorbed sulfur [91] or selenium [92] showed a remarkable enhancement in the selectivity of aldehydes (up to four times that of un–promoted Rh/SiO_2) for the hydroformylation of propylene. Atoms of sulfur and selenium blocked the sites for hydrogen dissociation on the rhodium metal surface and suppress the alkene hydrogenation. Addition of Zn^{2+} or Fe^{3+} to Rh/SiO_2 also enhanced the selectivity of aldehydes [93]. Due to their Lewis acidity, these promoters can behave as electron acceptors activating Rh–bonded carbonyl ligand for nucleophilic attack of alkyls and stabilizing the acyl species. The presence of other Lewis acids such as TiO_x, MnO_x, ZrO_x and NbO_x [94], alkali earth metal oxides [95] or (Na^+) [96], increased the rate constant value for CO insertion step in the hydroformylation reaction catalyzed by Rh, Co, or Pd complex, although, change in the selectivity was not so significant since these promoters stimulate the hydrogenation abilities of Group VIII metals. In another study, Bando et al. studied the catalytic activity of supported rhodium dimers on the different supports such as, SiO_2, Al_2O_3, TiO_2, and MgO for ethylene hydroformylation [97]. The SiO_2–attached rhodium dimers showed highly active and selective catalyst for hydroformylation of ethylene. The structural changes and behavior of the rhodium sites during CO insertion process during in the hydroformylation reaction was also studied by *in–situ* FT–IR and EXAFS spectroscopy. The most of rhodium dimers supported on alumina (Al_2O_3) were degraded to monomers which exhibited no activity for hydroformylation reaction. In case of MgO support, the rhodium dimers on MgO were aggregated to metal clusters. The structural behavior of rhodium sites was explained in terms of the interaction between rhodium dimers and the supports [97].

Synthesis of higher oxygenates from hydroformylation of ethylene was also reported by Trevino et al. using Rh supported on zeolite as a catalyst and MnO as a promoter [98]. The effect of alkali cations (M = Li, Na, K, Rb, Cs) as promoters impregnated on silica–supported rhodium catalysts was studied for hydroformylation of propylene at 140 °C and 1 atm in fixed bed continuous flow glass reactor [99]. The catalysts were prepared by aqueous co–impregnation of $RhCl_3 \cdot 3H_2O$ and alkali–metal chloride on silica support. The hydroformylation activity for the aldehydes was reported in the order of; Li > Na > K > Rb >> Cs. This behavior shows that the more polarizing power of the cation results into more acidic properties of promoter and the greater

enhancement in the selectivity of aldehydes [99]. The above reports indicate that the promoter is playing an important role to provide a contact at the atomic level between alkene species and active sites of the catalyst to carry out hydroformylation reaction.

1.2.7. Heterogeneous Catalysts for Hydroformylation of Alkenes in Liquid Phase

Rhodium Metal Complex Encapsulated/Impregnated on the Zeolites and Zeotype Materials for Hydroformylation of Alkenes

The encapsulation of metal complexes has particular significance for the heterogenization of homogeneous complexes to prevent the leaching of active metal species. Zeolites and zeotype (molecular sieves) materials are of the interest due to their varied acidic and basic properties as well as uniform channel sizes, high surface areas, shape selectivity, thermal and chemical stability. These materials are largely used as a catalyst in oil refining, petrochemical, and fine chemical industries from the last four decades [100–103]. The main advantage of immobilization of metal complex in the pores of zeolites is the possibility of enhanced selectivity due to well defined pore structure and believed that the reaction could be performed selectively inside the pores of zeolite. The material from M41S family came into the picture due to lower pore sizes (less than 13 Å) of these types of zeolites and zeotype materials [104–107]. The M41S family has been generally classified as, MCM–41 (hexagonal), MCM–48 (cubic), and MCM–50 (lamellar). The properties of these mesoporous materials such as larger surface areas (>700 m^2/g), well–defined pore sizes (20–100 Å), and varied pore sizes distribution made them the most sought materials for catalytic applications. In the immobilization approach, metal complex is encapsulated or anchored inside the pores of the inorganic inert matrix (e.g., zeolites, M41S materials, clay, etc.) in such a way that the complex is tightly bound inside the pores and do not leach out from the pores during liquid phase catalytic reactions. The another benefits in case of immobilization of Rh–complex on large pore silica or MCM–41 by surface tethered phosphane ligands are, i) the bridging bidentate coordination of the ortho–metalated phosphane ligands promises strong coordination of catalyst with support, which prevent the catalyst leaching from the surface of support and ii) mesoporous structure of support should avoid the mass transfer problems [108]. Inorganic materials, such as silica, alumina have also been studied as inert supports to heterogenized Rh–complex for hydroformylation.

Davis et al. prepared a heterogeneous catalyst by ion exchange and mixing of rhodium metal during the synthesis of zeolite A and Na–X [109–111]. The Rh–zeolite A was used as a catalyst for hydroformylation of 1–hexene in liquid and vapor phase. Rh–zeolite A sample prepared by ion exchange process showed leaching of rhodium metal and reported that the reaction

takes place in the solution catalyzed by leached out Rh metal [109]. Chaudhari et al. reported a heterogeneous catalyst synthesized by tethering of $HRh(CO)(PPh_3)_3$ complex through phosphotungstic acid to zeolite Y support [112]. This catalyst showed excellent selectivity of aldehyde, stability, and improved activity for hydroformylation of various linear and branched alkenes. The heterogenized catalyst was reused several times without loss of its activity [112]. In another study, cationic rhodium complexes, [Rh(diphosphinite)(cod)] were formed by the reaction of $[RhCl(cod)]_2$ with ligands derived from (2*S*,4*R*), (2*S*,4*S*)–1–benzyl–4–hydroxy–4–phenyl–2–(1,1–diphenylmethyl)–pyrrolidinylmethanol and (2*S*,4*R*), (2*S*,4*S*)–1–(3–triethoxysilyl)propylamino carbonyl–4–hydroxy–4–phenyl–2–(1,1–diphenylmethyl)–pyrrolidinylmethanol [113]. These cationic rhodium complexes were coordinated covalently with triethoxysilyl groups of zeolite–Y and the obtained materials were used as heterogeneous catalysts for asymmetric hydroformylation of styrene. These catalysts showed enhanced activity and stability over prolonged time with the benefits of reusability of catalyst by filtration [113].

Mesoporous molecular sieves have highly uniform pore structure and the surface area, can give advantage to immobilize a large amount of metal complex uniformly. The larger shape selective pore size distribution can give the advantage to take larger size reactant molecules. Therefore, most of the recent research is focused on heterogenization of Rh–complex on MCM41 or –48 by different donor ligands via various methods. Huang et al., synthesized the heterogeneous catalysts by coordination of various rhodium complexes to silicates of aminated (–NH_2–) MCM–41 in the presence of triphenylphosphine analogues ligands and used as a catalyst for hydroformylation of 1–hexene, 1–octene and styrene [114–115]. Catalytic activity of various aminated MCM–41 tethered rhodium complexes were compared with the untethered complexes for hydroformylation of 1–hexene at 80 °C and found higher catalytic activity for aminated MCM–41 tethered Rh–complexes modified by the triphenylphosphine ligand.

To prevent leaching of transition metal complexes during hydroformylation reaction in liquid phase, Chaudhari et al. further approached for functionalization/encapsulation of $HRhCO(PPh_3)_3$ inside the pore of zeolites (Na–Y), MCM–41 and MCM–48 materials [116]. The functionalization of complex was carried out in the internal pores of MCM–41 (Figure 1.12) by coordination of silanols present outside the MCM–41 channels with $HRhCO(PPh_3)_3$, so that only surface ligands could be functionalized within the pores and transition metal complexes bound tightly inside the pores. These catalysts were claimed as highly active, stable and reusable catalysts for hydroformylation of alkenes.

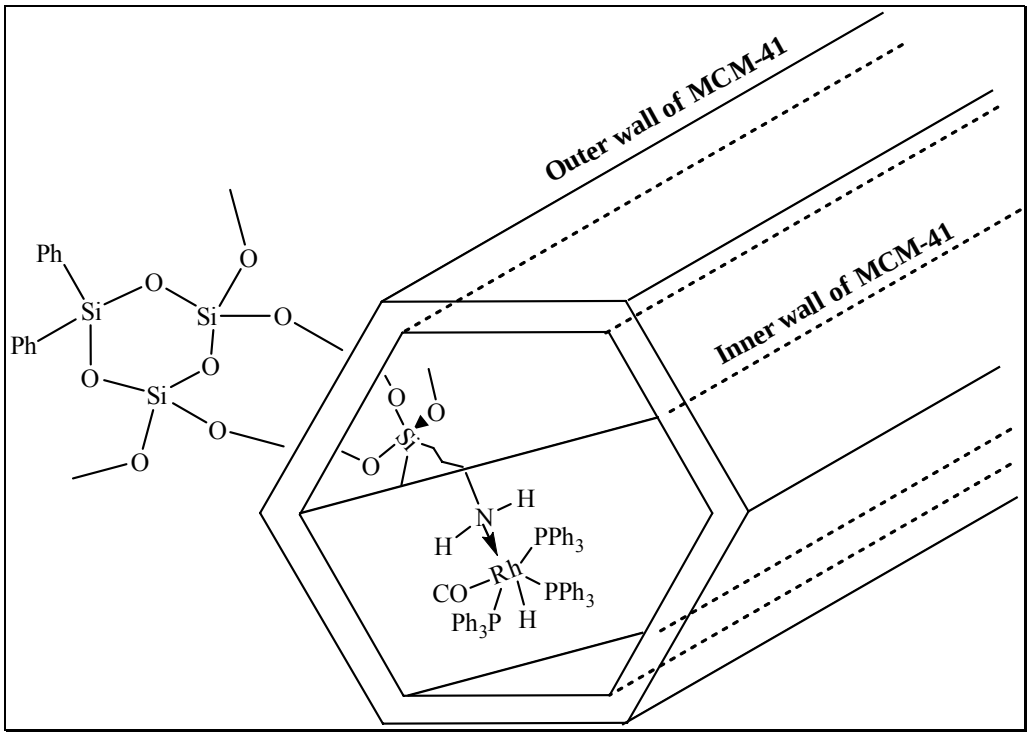

Figure 1.12. Encapsulation of the $HRhCO(PPh_3)_3$ inside the pore of MCM–41.

Huang et al. studied the hydroformylation of cyclohexene using $Rh_4(CO)_{12}$ complex immobilized on MCM–41 as a catalyst and surface properties of the immobilized catalyst was studied by FT–IR, X–Ray diffraction (PXRD) and N_2 adsorption–desorption measurements [117]. MCM–41 tethered catalyst showed good activity, selectivity and reusability for hydroformylation of cyclohexene. The effect of supported donor ligands on the activity and stability of tethered catalysts was also studied for hydroformylation reaction [117]. Ali et al. reported rhodium immobilized catalyst prepared by the impregnation of rhodium(I) and rhodium(III) complexes on MCM–41 with and without heteropoly acids for the hydroformylation of styrene and its derivatives [118]. The effect of pore size of MCM–41, presence of heteropoly acids and amount of water added showed promoting effect on the activity of catalysts. The catalysts were recycled several times without significant loss in their activities. In continuation of the previous studied for immobilization of Rh–complex, the Yuan et al immobilized rhodium–phosphine complexes for hydroformylation of 1–hexane by coordination of Rh–complex to the amino functionalities available on the surface of aminated MCM–41 and MCM–48 [119]. The interaction between surface amino groups with active rhodium species during immobilization process results into highly dispersed active rhodium moieties on the support. Activity of the immobilized catalyst for hydroformylation of 1–hexene was reported similar to its homogeneous counterpart, but easy catalyst separation from the product mixture is additional advantage of Rh–complex immobilization [119].

Synthesis of acetals in one pot by combination of hydroformylation and acetalization processes was reported using Rh(I) and Rh(III) impregnated on mesoporous supports such as MCM–41 as catalyst for hydroformylation of 1–hexene [120]. The formed aldehydes reacted with the alcohols in the hydroformylation conditions. Rh(I) supported on MCM–41 combined with the heteropoly acid $H_3PW_{12}O_{40}$ showed excellent catalytic activity towards the formation of acetals. However, Rh(III) supported catalysts showed higher catalytic activity in the absence of any additives. The effects of addition of different types of phosphine and phosphite ligands were also studied for hydroformylation of 1–hexene [120]. In an interesting approach by merging the concept of heterogeneous catalyst and ionic liquids, the $HRhCO(TPPTS)_3$ (Rh–TPPTS) complex was mixed in the various ionic liquids and immobilized on MCM–41. The resulting supported ionic liquid catalysts were used for hydroformylation of 1–hexene and found active and stable heterogeneous catalysts [121].

Rhodium Metal Complex Anchored/Impregnated on High Surface area Silica for Hydroformylation of Alkenes

Ding and coworkers modified the immobilized rhodium catalyst on SiO_2 by impregnation of triphenylphosphine $(PPh_3)_3$ and named as PPh_3–Rh/SiO_2 [122]. The interaction between Rh/SiO_2 and PPh_3 was confirmed by the ^{31}P NMR spectra and used as a catalyst for hydroformylation of 1–hexene and ethylene. Trzeciak et al. heterogenized the phosphorous containing Rh–complex by coordination of acidic sites of silica and surface hydroxyl groups for hydroformylation of 1–hexene [123]. In case of triphenylphosphine as a ligand, 98% conversion of 1–hexene with 94% selectivity of aldehydes (*n*/*iso* = 3.6) was reported for hydroformylation of 1–hexene. Hydroformylation of 1–hexene over heterogeneous rhodium catalysts in supercritical carbon dioxide demonstrates the opportunities that can be afforded through this unique reaction environment. The mechanism for hydroformylation of 1–hexene was derived from the well accepted mechanism in homogeneous conditions and compared with the observed kinetic results at the studied reaction conditions [124–125]. This study was continued by investigating the effect of various organic solvents on the progress of hydroformylation reaction in supercritical carbon dioxide expanded media using heterogeneous rhodium catalyst supported on silica [126]. Effect of the addition of a basic alkali metal salts such as Na_2CO_3, K_2CO_3 and NaH_2PO_4 on conversion and selectivity of the aldehydes was studied in detail using Rh–$TPPTS/SiO_2$ catalyst in aqueous phase [126]. In another study, the catalytic activity of rhodium impregnated on silica gel was evaluated for hydroformylation of perfumery related compounds. In general, the impregnated catalyst showed good conversion and reusability upto fourth cycles without any loss in the catalytic activity [127]. Zhao et al. reported the heterogenization of rhodium complex by the copolymerization of functionalized 3–

aminopropyltriethoxysilane with tetraethoxysilane via sol gel method [128]. The effect of reaction parameter on the conversion and selectivity of aldehydes was studied in order to optimize the reaction parameters. The catalyst showed 98.8% conversion of 1–hexene with 99.6% selectivity of the aldehydes (*n/iso* = 0.86) at optimum reaction conditions. The catalyst was recycled upto seven times without significant loss in activity [128]. In continuation of the immobilization of rhodium complex on silica support, Hang and Kawi reported the tethering of $RhCl(PPh_3)_3$ on silica via phosphine, amine and thiols ligands to make a stable heterogeneous catalyst for hydroformylation of cyclohexene [129]. The SiO_2 tethered rhodium complex with amine ligand showed highest conversion (87.9%) comparable to its homogeneous analogues and catalyst was reused several times for hydroformylation of cyclohexene [129].

In order to search suitable support of larger pore diameter to immobilized rhodium complex for hydroformylation reaction, Alper and Ajjou reported a catalyst prepared by the covalently coordination of rhodium trichloride to hexagonal mesoporous silica for hydroformylation of vinyl acetate and other related substrates [130]. The catalyst exhibited excellent activity with higher selectivity for aldehydes at the studied reaction conditions.

Allum et al. reported *n/iso* ratio of aldehyde 2.2:1 using rhodium complex immobilized on phosphinated silica as a catalyst for hydroformylation of 1–hexene at 43 atm (CO/H_2 = 1:1) and 100–120 °C [131]. A rhodium phosphine complex anchored on zirconium phosphate support was used as a catalyst to yield a regioselectivity of aldehydes near 3 with TOF of 110 (mol of aldehyde per mole of Rh per hour) for liquid–phase hydroformylation of 1–hexene [132]. To minimize rhodium loss via leaching, bidentate ligands such as a xanthene–based diphosphines were prepared by sol–gel techniques and were found to be active (TOF = 18.3 h^{-1}) and highly regioselective [*n/iso* ratio = 65] at 80 °C and 50 atm pressure of CO/H_2 (1:1) [133].

The use of supported aqueous–phase (SAP) catalysts for the hydroformylation using rhodium–based catalyst has become most popular due to higher catalytic activity as compared to those observed in homogeneous and biphasic conditions under similar reaction conditions. Yuan and co–researchers supported water soluble Rh–TPPTS complex on non–porous fumed silica nanoparticles, which acts as a supported aqueous phase catalyst for the hydroformylation of 1–hexene [134]. In an another report on the supported aqueous phase catalyst for hydroformylation reaction, catalytic activity of the rhodium supported on SiO_2 in aqueous–phase (SAP/Rh–SiO_2) and rhodium supported on SiO_2 modified by water–soluble TPPTS ligands (TPPTS–Rh/SiO_2) were compared for the hydroformylation of 1–hexene (Figure 1.13) [135–136]. But these SAP catalysts were not reused selectively for hydroformylation reaction due to leaching of the rhodium complex

in the aqueous medium.

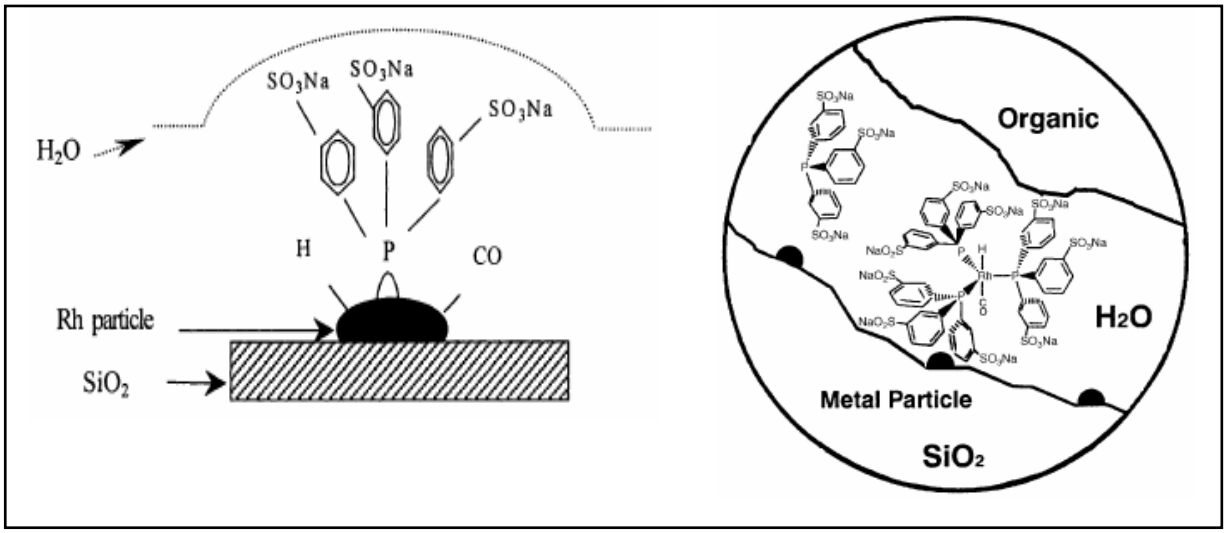

Figure 1.13. Schematic representation of supported aqueous phase catalyst.

Rhodium Metal Complex Immobilized on Resins/Polymeric Supports for Hydroformylation of Alkenes

The research for heterogenization of homogeneous complex on the resins and other polymeric supports, in which metal complex immobilized on resin/polymer surface through their surface functional groups, is of the current interest for hydroformylation reaction. Hydroformylation of 1–hexene in supercritical CO_2 ($scCO_2$) and other organic solvents was reported using polymer supported rhodium catalyst, which was prepared from polystyrene bound PPh_3 and dicarbonylacetylacetonatorhodium. The supported catalyst was reusable several times by means of simple filtration [137]. The method for synthesis of immobilized homogeneous catalyst by addition of a bi–functional ligand followed by a metal complex (rhodium, cobalt and platinum/tin) onto ion exchange resin (sulfonated styrene–divinylbenzene) for hydroformylation of 1–hexene was reported [138]. Uozumi et al., reported the synthesis and applicability of rhodium phosphine complexes supported on amphiphilic resin beads [polystyrene–poly(ethylene glycol) graft co–polymer (1% DVB cross–linked)] for the hydroformylation of alkenes in water. The supported catalyst showed excellent yields (upto 99%) of aldehydes for hydroformylation of various alkenes using water as a solvent [139]. Chaudhari et al. studied the kinetics of hydroformylation of 1–hexene using rhodium–TPPTS bounded on the surface of ion exchange resin, amberlite IRA–93 as a catalyst [140].

Recently, metal doped thermosetting epoxy resins, such as triglycidyl derivative of 4–aminophenol was synthesized by polymerization reaction using molybdenum, palladium, or rhodium complexes as initiators. These metal doped epoxy resins were observed as highly efficient

catalysts for hydroformylation reaction. These catalysts can be recovered by simply filtration and re–used without loss in its activity indicates reusability and stability of the catalyst [141].

Rhodium Metal Complex Impregnated on Activated Carbon for Hydroformylation of Alkenes

Activity of cobalt and rhodium metals supported on activated carbon was studied for low pressure hydroformylation of 1–hexene [142–145]. The effect of promoters such as platinum (Pt), palladium (Pd) and ruthenium (Ru) added to the catalyst showed higher catalytic activity for the hydroformylation reaction [142]. In continuation of rhodium supported on carbon, Fujimoto et al., impregnated Rh and Co metals on the surface of activated carbon and compared the catalytic activity for hydroformylation of 1–hexene. Co/activated carbon catalyst showed excellent catalytic performance in the alcoholic solvents only, while Rh/activated carbon catalyst exhibited good activity in the nonpolar solvents.

Rhodium Nanoparticles for Hydroformylation of Alkenes

Hydroformylation of 1–alkenes was reported in solvent free conditions using ligand–modified or unmodified Rh(0) nanoparticles prepared in imidazolium ionic liquids as catalyst precursors [146]. In another study, the synthesis of rhodium nanoparticles was carried out by reduction of aqueous rhodium chloride dispersed in toluene with amphiphilic tetraoctylammonium bromide and chiral (*R*)–BINAP [(R)–(+)–2,2'–bis(diphenylphosphino)–1,1'–binaphthyl] ligand [147]. The chirally stabilized rhodium nanoparticles (1.5–2.0 nm) were heterogenized by the impregnation of rhodium complex on the silica [Figure 1.14] and confirmed by spectroscopic techniques. The catalytic activity was evaluated for asymmetric hydroformylation of styrene and vinyl acetate showed high regioselectivity and chiral inductivities (92:8 *iso*/*n* ratio of aldehydes and 26% ee for styrene; 99:1 *iso*/*n* and 59% ee for vinylacetate) under mild reaction conditions [147–148]. The modification of chiral (*R*)–BINAP ligand impregnated on Rh/SiO_2 with the (S,S)–DIOP [(S,S)–(+)–2,3–O–isopropylidene–2,3–dihydroxy–1,4–bis(diphenylphosphino)butane] resulted into the enhanced catalytic activity for vinyl acetate hydroformylation [148].

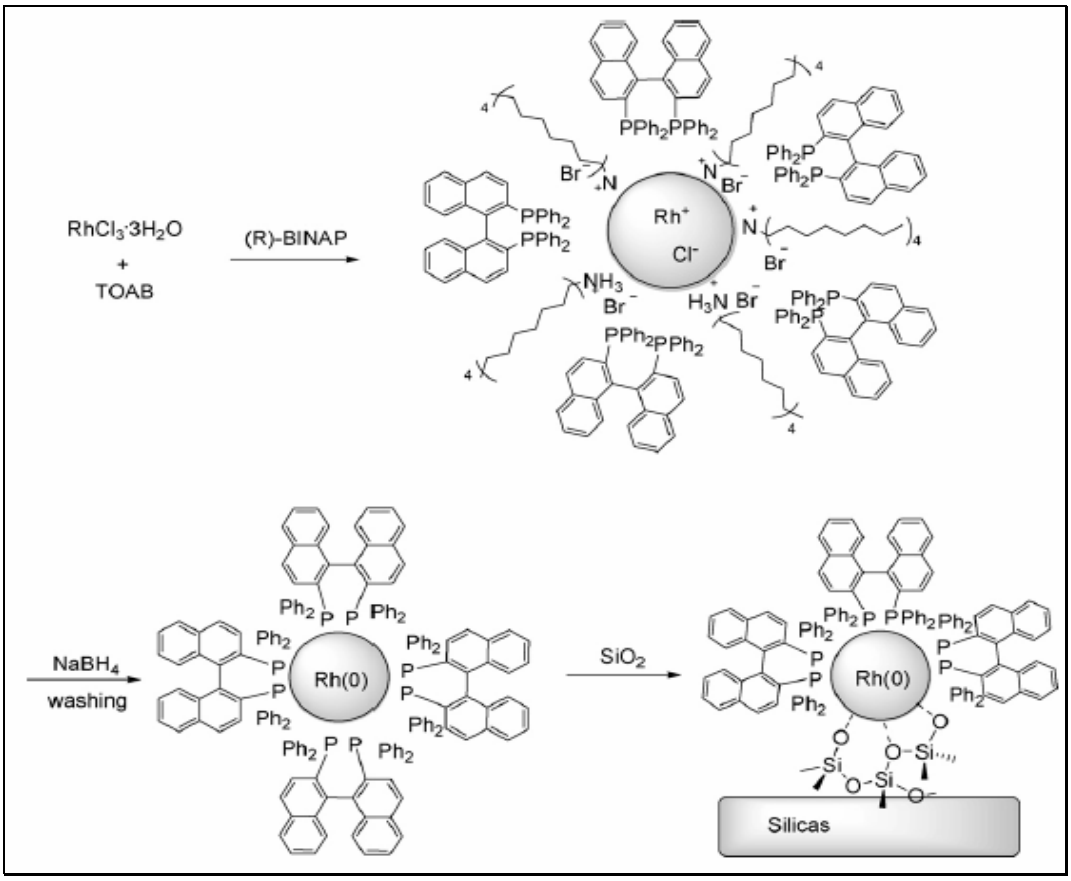

Figure 1.14. Synthesis of chirally stabilized rhodium nanoparticles [147].

Rhodium supported catalyst containing the dimeric complex of rhodium $[Rh_2Cl_2(CO)_4]$ grafted to multi–walled carbon nanotubes (Figure 1.15) was synthesized and used as a catalyst for hydroformylation of 1–hexene in liquid phase [149].

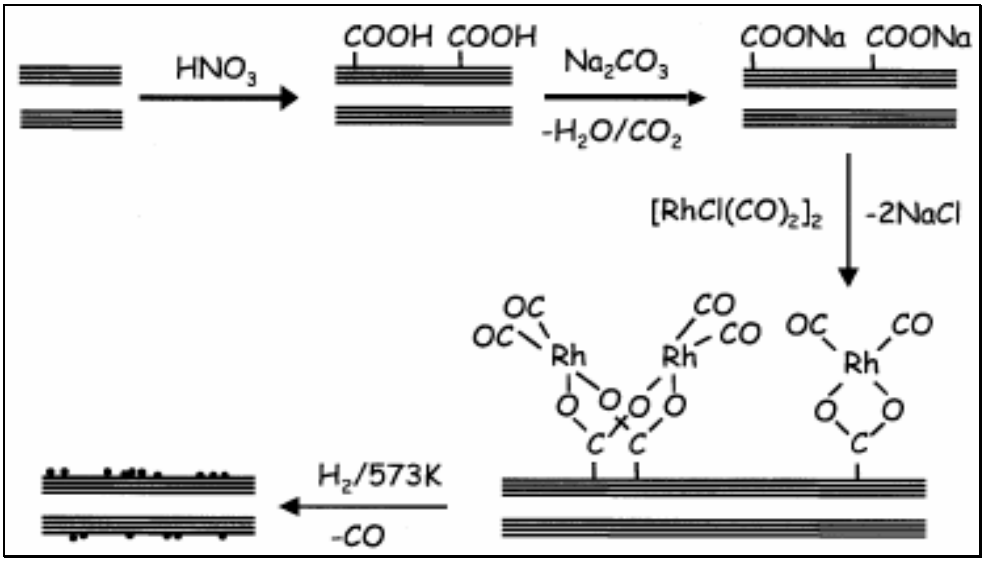

Figure 1.15. Surface mediated organometallic reaction between $[Rh_2(\mu–Cl)_2(CO)_4]$ and carbon nanotubes.

Rhodium Metal Complex and Bidentate Ligands Immobilization on Various Inorganic Supports for Hydroformylation of Alkenes

A truly heterogeneous catalyst system was reported by immobilization of xantphos (bidentate) ligands on silica surface by sol–gel method for the selective hydroformylation of alkenes [150–151]. The supported rhodium catalyst on silica showed high activity and selectivity for hydroformylation of alkenes under varied reaction conditions over a period of more than a year. The catalyst retains its activity and selectivity, providing a very rare example of a heterogeneous catalyst where leaching has been reduced to an acceptable level [152–153]. The immobilization of phenoxanthphosphino–modified xantphos–type ligand covalently anchored to polysiloxane support was reported as a heterogenized ligand for rhodium catalyzed hydroformylation of 1–octene. Catalytic activity of modified xantphos ligand was compared with the pristine xantphos ligand for hydroformylation of 1–octene. The immobilized catalyst systems were reused several times without leaching of the rhodium metal [154]. In another review article on the immobilization of xantphos ligand, the catalytic activity of xantphos immobilized catalyst was compared with the various other immobilized catalysts, such as SAP catalysts, sol–gel based catalysts and anchored catalysts on silica in an organic phase as well as in supercritical carbon dioxide ($scCO_2$). In all instances, high selectivity of the aldehydes was retained with more than 20 *n to iso* ratio of aldehydes. The isomerization of studied alkenes was rather low and comparable with the homogeneous counter part. The rates expressed in terms of turnover frequencies drop considerably except for the experiments in $scCO_2$, which were only half of those in homogeneous phase. Leaching of rhodium during the reaction was below to the detection limit of ICP–AES (1 ppm). Even the immobilization of homogenous rhodium catalyst on the surface of monolith was also reported for hydroformylation reaction. The rhodium complex immobilized monolith was fixed inside the agitator's blade and used as a catalyst for hydroformylation reaction (Figure 1.16). The encouraging results were reported using the immobilized rhodium complex on monolith as a catalyst for the hydroformylation of 1–octene. This heterogeneous catalyst system was found extremely stable in the studied reaction conditions.

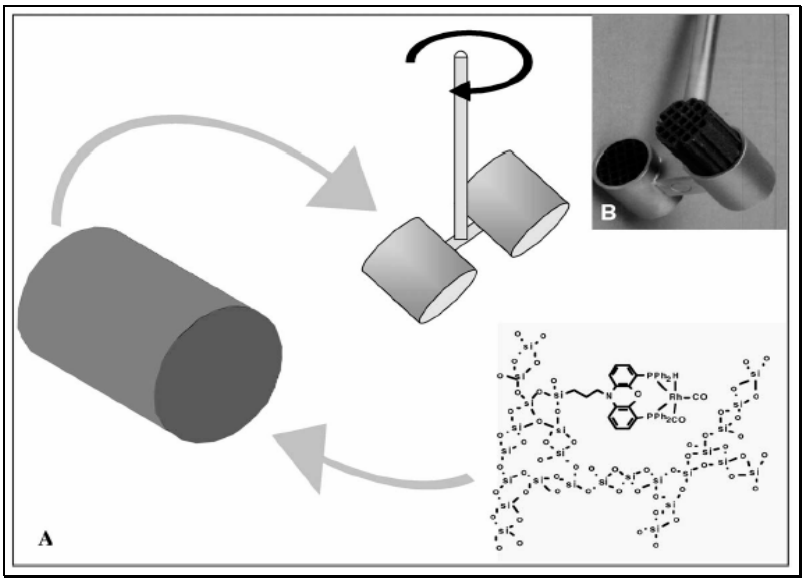

Figure. 1.16. A) Immobilization of homogeneous complex on monoliths, and the implementation of these monoliths in the blades of agitator of the reactor. B) Silicon–carbide monoliths in the stirrer [155].

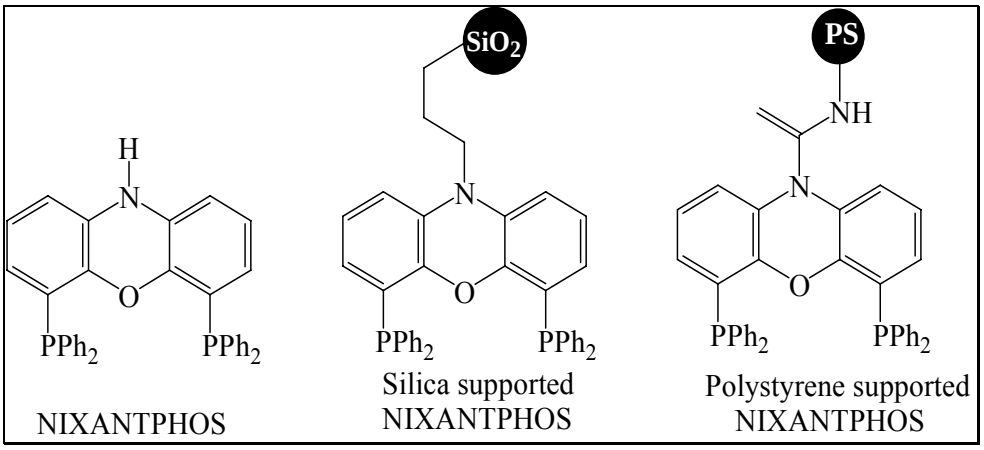

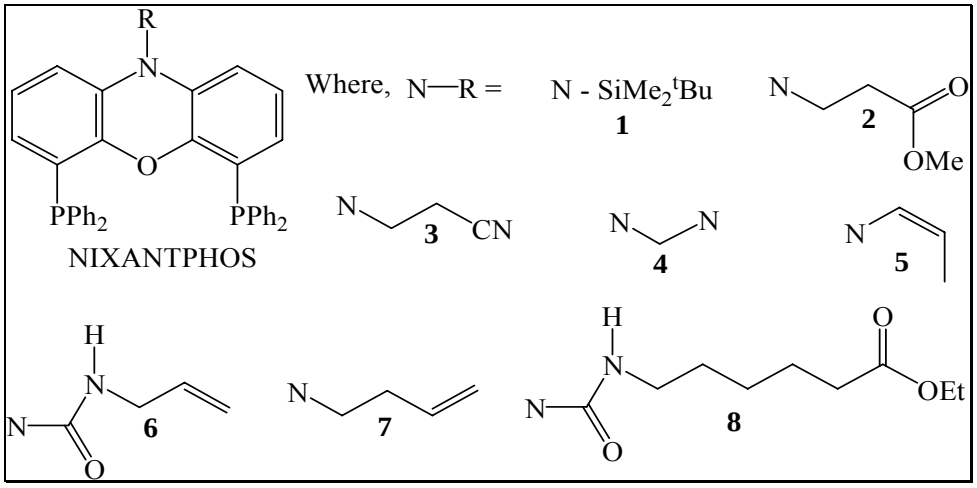

Figure 1.17a. NIXANTPHOS and its derivatives.

NIXANTPHOS as an effective ligand from the xantphos based diphosphine ligands family was modified at the nitrogen function and anchored on the silica and solid polymer support, such as dendrimers, polyglycerol, polyurethanes, [156] and polystyrene (Figure 1.17) [157]. The functionalized ligand was reused several times for the regioselective hydroformylation of 1–octene and *N*–allyl–phthalimide. The micro–dendrimeric NIXANTPHOS trimer and other ligands also showed the higher catalytic activity for hydroformylation reaction [156].

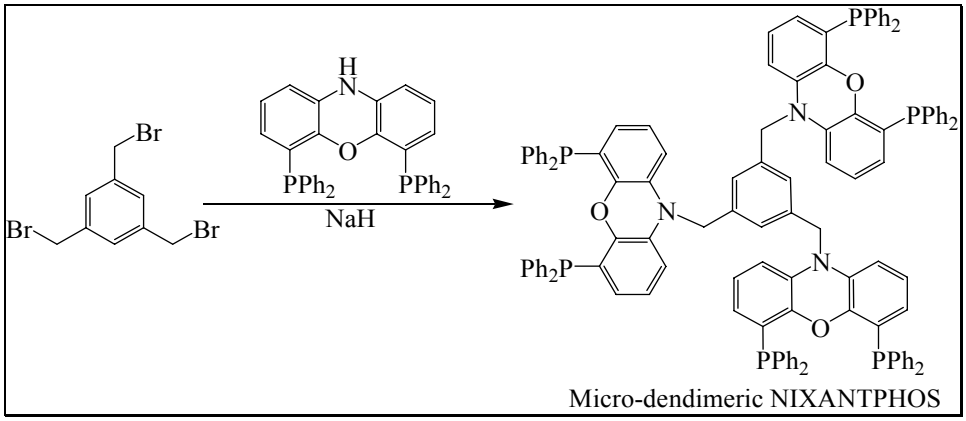

Figure 1.17b. Micro–dendrimeric NIXANTPHOS trimer

Rhodium Metal Complex with Supported Dendrimers as Ligands for Hydroformylation of Alkenes

There is a lot of scope to develop such a system that show high reactivity like homogeneous catalysis and are easy to separate from the reaction mixture. Dendrimers are relatively well defined macromolecules with emerging applications in the area of material and biological sciences [158–161]. In recent years, dendrimers have been synthesized as novel materials and applied to catalysis since its highly branched and bulky structures can provide multiple sites for coordination with transition metal complexes. The dendrimers are soluble in organic solvents, but can be separated by nanofiltration from the reaction mixture in liquid phase due to their large size. The coordination of dendrimers with transition metal complexes may bring forth enhanced catalytic performance due to positive dendritic effect [162–163]. Dendrimers are large (2 to 4 nm) tree–like molecules with a persistent globular shape, which makes them more suitable for ultrafiltration than soluble polymers, which may pass through filtration membranes more easily. The identical groups on periphery of dendrimers can also form complexes. The metal–binding groups are usually on the exteriors of dendrimers but can also be covered within shape–selective pockets. Advantageously, dendrimers may exhibit bidentate binding (through two donor atoms on the same dendrimer arm) to the metal. The chelate (ring–forming) effect will then ensure the minimum leaching of metal complex. Furthermore, if the metal separated from its dendrimer–bound ligand, it may be

sequestered again rapidly by one of the many identical binding sites nearby. Despite these advantages, the loss of activity upon recycling of the catalyst was observed on the used of ultrafiltration [164]. This may not be because of genuine leaching, but because the membranes are not designed for use with organic solvents, high temperatures and/or high pressures. One rather unexpected advantage of some dendrimers has emerged, however, they can show much higher selectivity to desired products than small–molecule analogs. For example, a dendrimers bearing 16 PPh_2 groups on its periphery (Figure 1.18), gives *n/iso* ratio of aldehyde 13.9:1 for hydroformylation of 1–octane as compared to 3.8:1 for small molecule analog [165].

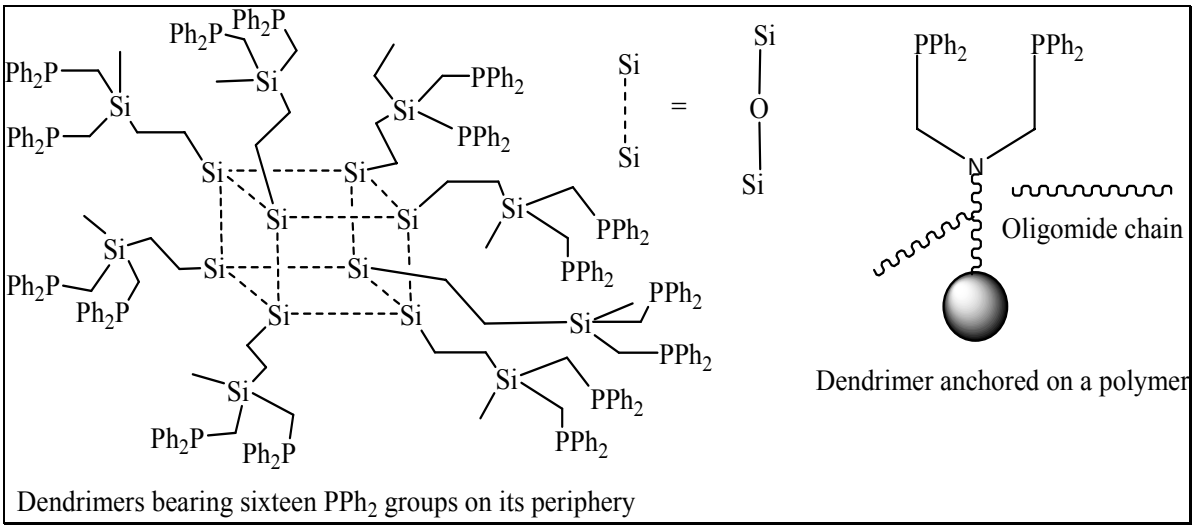

Figure 1.18. Supported dendrimers as ligands for hydroformylation reaction.

Dendrimer wedges (molecules that have dendrimer like properties but only form part of a sphere) were anchored to the beads of silica [166] or a polymer (Figure 1.19), using approaches developed for solid phase organic synthesis. They were used for hydroformylation reaction and can easily be removed by conventional filtration. This procedure combines the advantages of controlled environment of dendrimer–bound catalyst with the ease of separation of the supported catalyst. In this application, the metal–binding phosphine groups may be placed to the end of or along the arms of the dendrimer. Both types of binding allow high catalytic activities for hydroformylation of styrene and related substrates, but dendrimers in which, the rhodium is more deeply buried show better recyclability [167].

Polyaminoamido (PAMAM) diphosphonated dendrimers anchored onto silica gel were used as supported ligand for hydroformylation reactions [168]. The hydroformylation of styrene, substituted styrene and vinyl acetate were carried out by rhodium complexes with dendritic, phosphine ligands anchored the polymer beads. The catalysts were recycled several times and showed 99% conversion with excellent selectivity of branched aldehyde [169].

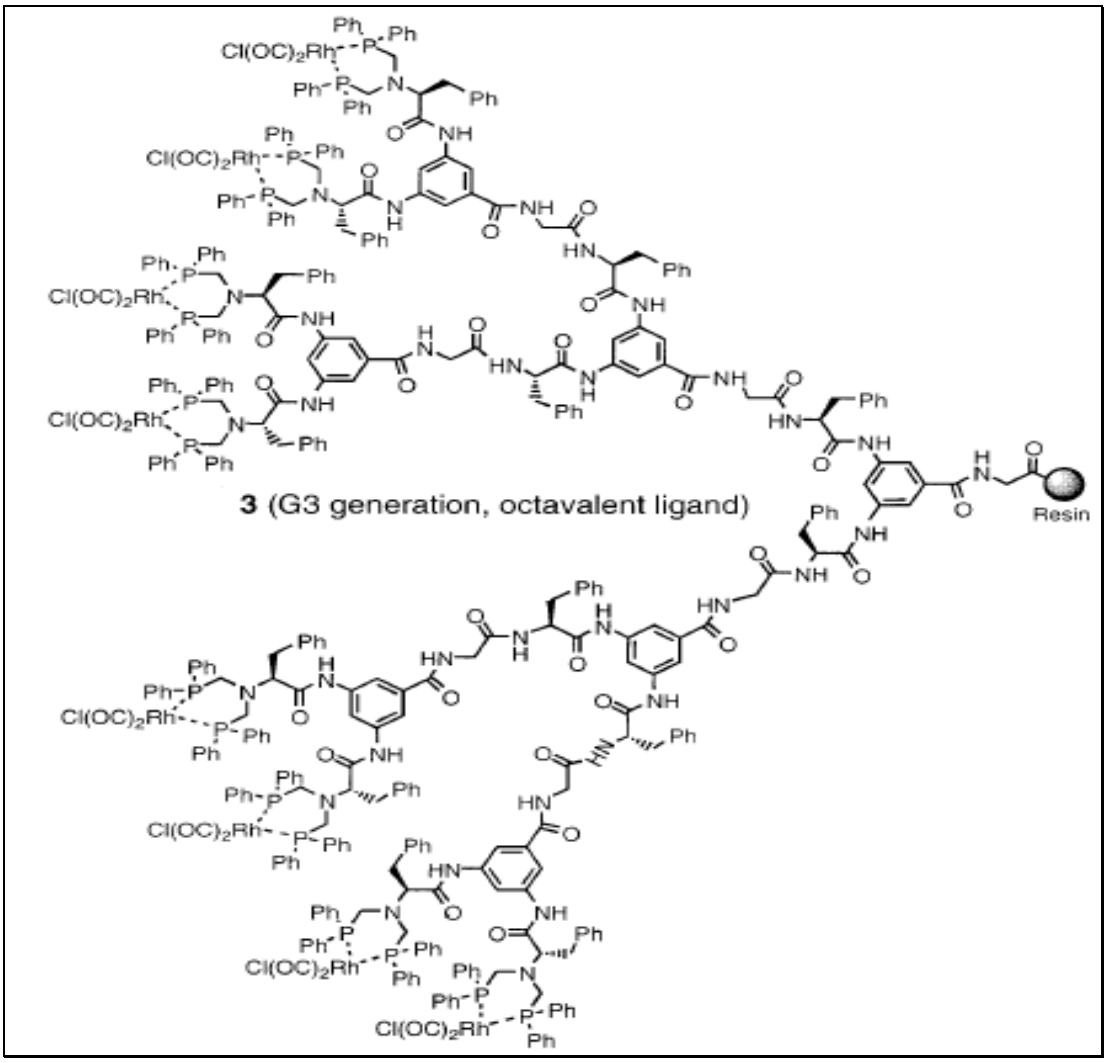

Figure 1.19. G_3 Generation, octavalent dendritic ligands on resin.

Alper et al. reported a method based on growing PAMAM dendrons on silica–coated magnetic nanoparticles [170]. After the dendronizing process, the stability of silica–coated magnetic nanoparticles increased significantly. The dendronized particles are phosphonated, complexed with $[Rh(COD)Cl]_2$, and applied for hydroformylation reactions. These new catalysts are reported to be highly selective for aldehydes. In continuation, Alper et al. developed another catalyst having Rh–complexed dendrimers supported on a resin (Figure 1.20) as an active catalyst for hydroformylation of aryl alkenes and vinyl esters [171]. This catalyst showed excellent yields of aldehydes even at room temperature. The dendritic catalysts were recycled by simple filtration upto tenth cycles without significant loss of activity and selectivity. These results represent a dramatic improvement over those previously described for rhodium–catalyzed (dendrimer and nondendrimer based) hydroformylation.

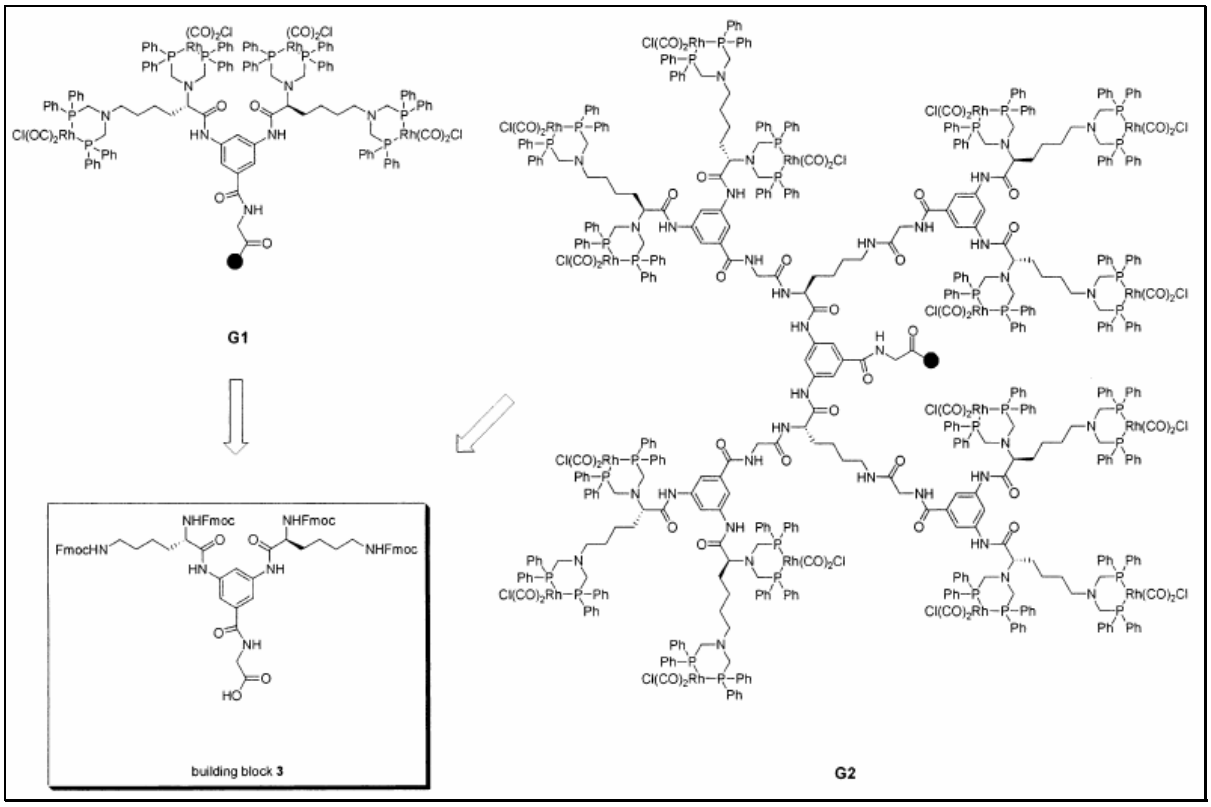

Figure 1.20. Synthesis of rhodium–complexed dendrimers on a resin [171].

In another study, PAMAM dendrimers were grown on the mesoporous SBA–15 support in order to immobilize rhodium complex [$RhCl(PPh_3)_3$] for hydroformylation of styrene [172–174]. Li et al. synthesized dendritic SBA–15 supported $HRh(CO)(PPh_3)_3$ complex for liquid phase hydroformylation of styrene [175]. The coordination of $HRh(CO)(PPh_3)_3$ complex was confirmed inside the channels of SBA–15 and PAMAM (polyamidoamine) dendrimers up to second generation were grown inside the SBA–15 channels. The performance of catalyst for hydroformylation of styrene was affected by the pore size and dendrimer generation, and the second–generation PAMAM was found to be optimal for these passivated dendritic SBA–15–supported rhodium catalysts [175].

MCM–41 and large pore Davisil silica have also been employed as a highly ordered mesoporous supports to grow dendrimers [176–177]. The combination of highly ordered mesoporous materials with the nano–sized highly branched dendrimers create a distinct architecture which is helpful for the dispersion of rhodium species due to high surface area of support and multiple binding sites of dendrimer for enhancement of regioselectivity due to the dendrimer and pore size effect [178]. However, the first generation G(1) and second generation G(2) catalysts did not have high loading of rhodium species although higher generation dendrimers are supposed to have more loading due to more binding dendritic sites. Results suggested that the shrinking pore volume and surface area impaired the binding sites during the growth of dendrimers

in mesoporous material. The result also suggests that some portion of dendrimers have been grown outside the external surface of the MCM–41 pores due to the greater accessibility of external surface [179].

Aldehydes produced via hydroformylation usually are not the final products. Due to the versatile chemistry of aldehyde group, they are further converted via reduction, oxidation, or other reactions to give alcohols, amines, carboxylic acid derivatives, aldol condensation products, and many others [180–181]. Following a general trend in organic chemistry, hydroformylation can also be integrated in tandem or domino reaction sequences. Thus, reduction, nucleophilic addition, or aldol condensation can be achieved directly under the reaction conditions of hydroformylation. This, however, is not possible in all cases, since additional reagents, products, or variations of reaction conditions optimized for hydroformylation may suppress or hinder the initial hydroformylation step. Thus, alcohols formation via reduction of aldehydes occurs under forcing reaction conditions and may lead to the formation of acetals with nonreduced aldehydes present. Similarly, many other reactions of metal acyl intermediates or final aldehydes may occur under hydroformylation reaction conditions. In the present thesis we have attempted to develop a multi–functional catalyst system to carry out hydroformylation, aldol condensation and hydrogenation reactions in a single pot.

1.3. Development of Solid Base Catalysts for Condensation and Isomerization Reactions

Solid acid and base catalysts are fast growing research area due to the environmental awareness. The main advantages of solid acid and base catalysts over conventionally used liquid catalysts in stoichiometric amounts are environmental friendly, reusable, non–corrosive catalysts and easily separable from product mixture. Furthermore, solid base catalysts can be designed to give higher activity, selectivity, and longer catalyst life. Upto now more than three hundreds solid acid and base catalysts are reported in the literature, among them, most of the area is covered by solid acid catalysts. The reason for rapid growth in the area of solid acid catalysts is due to faster developments and great progress of refining and petrochemical industries in the last 50 years. In refining processes also, special attentions were made to develop suitable heterogeneous catalyst for cracking as well as isomerization reactions. Very little studies were carried out for the developments of solid base catalysts as compared to the solid acid catalysts till date. A detailed classification as well as the commercially implemented processes showed 103, 10 and 14 processes based on solid acid, solid base, and solid acid–base bi–functional catalysts, respectively were commercialized upto 2004 (Figure 1.21) [182–183]. Of course, the total number of commercial

processes related to solid base and bi–functional catalysts is much less than that of solid acid catalysts. From percentage point of view, 81% of total processes are catalyzed by solid acid catalysts and rest processes 8 and 11% catalyzed by bi–functional and base catalysts, respectively. So far, heterogeneous catalysis has found few applications to the synthesis of fine chemicals and pharmaceuticals relative to its wide use in the petroleum and commodity chemicals sectors. Nevertheless, the application of heterogeneous catalysts to the synthesis of fine and specialty chemicals is receiving increased attention as it is a route to the design of safer, cleaner, and more sustainable environment friendly industrial processes.

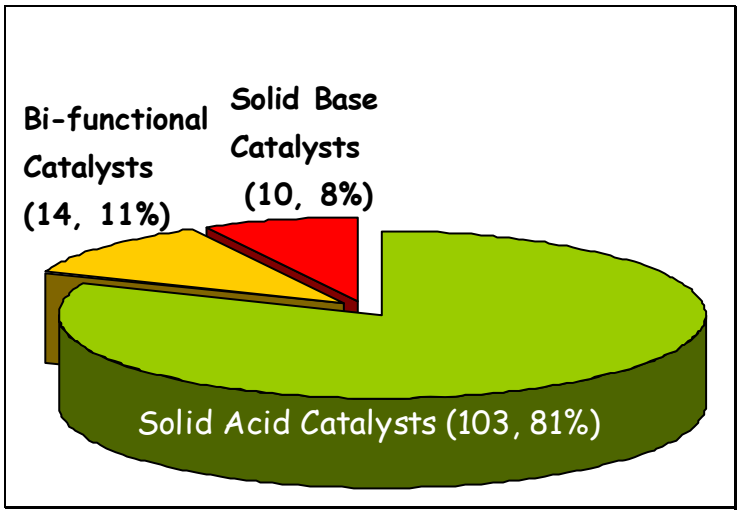

Figure 1.21. Industrial processes based on the solid acid, solid acid–base, solid base catalysts [182].

1.3.1. Types of Solid Base Catalysts

First heterogeneous basic catalysts was used in 1950s for double bond isomerization of alkenes using sodium metal dispersed on alumina as a catalyst by Pines et al. [184]. The study on the developments of solid base catalyst was extended to the single metal mixed oxide in 1970s. The breakthrough in the development of solid base catalyst came after 1970s, before that the catalysts were pretreated at lower temperature at which the basic sites covered by carbon dioxide, water and oxygen were not exposed properly to catalyzed the reaction. Removal of carbon dioxide, water and oxygen at higher pretreatment temperature from the surface of catalyst showed high catalytic activities for base catalyzed reactions. Presently, many solid base catalysts were developed starting from single metal oxide to mixed oxides, cation exchanged zeolites, functionalized mesoporous basic silica, oxynitrides, KF/Al_2O_3 and solid super–base catalysts for the various base catalyzed organic transformations [Table 1.3].

Table 1.3. Types of solid base catalysts [182, 185]

Typical catalyst	Details of the catalyst
Single metal oxide	MgO; CaO; SrO; BaO; Al_2O_3; La_2O_3;YbO_2; ZrO_2
Mixed oxides	MgO–Al_2O_3; Al_2O_3–B_2O_3; ZrO_2–MgO; ZrO_2–NaOH; ZrO_2–KOH; SiO_2–Al_2O_3; Al_2O_3–NaOH–Na; Al_2O_3–KOH–K; MgO–TiO_2
Alkali cation exchanged zeolites	K, Rb and Cs – exchanged zeolite X, Y; nitriles impregnated on zeolites
Mesoporous materials	MgO/SBA–15; MCM–41 functionalized with amino groups
Basic supported catalyst	KF/Al_2O_3; Na/NaOH/Al_2O_3; Na/MgO; Na/K_2CO_3
Clay and modified clay	As–synthesized, activated and rehydrated hydrotalcite of varied divalent and divalent to trivalent cations molar ratio; Magnesium silicate; talc modified by amino functionalities; chrysotile; sepiolite
Oxynitride	SiON; AlPON; ZrPON
Other	Modified natural phosphate (NP); Calcined $NaNO_3$/NP; Chitosin

Solid base catalysts listed in Table 1.3 may acts as acid catalysts also in some case. These materials may be called as solid base catalysts if it is acting as a base towards reaction by abstraction of a proton (Brønsted base) or by donation of an electron pair (Lewis base) to form anionic intermediate of the reactant in a particular catalytic cycle. The commercial processes those used sold base catalysts are shown in Table 1.4. The various review articles appeared in the literature in last decade showed the research work carried out in the direction of solid base catalysts for the synthesis of commercially important products [183, 185–193].

Alkaline Earth Oxides and Alkali Metal Supported on Metal Oxides

Alkaline earth oxides such as, magnesium oxide (MgO), calcium oxide (CaO), strontium oxide (SrO) and barium oxide (BaO) are active catalyst for base catalyzed reaction such as aldol condensation, Knoevenagel condensation, Michael addition, isomerization of alkenes, etc. Presently, synthesis of flavanones and chalcones was also carried out by the use of MgO as a catalyst [194–199]. Catalytic activity of the alkaline earth oxides is dependent upon the pretreatment temperature to remove adsorbed carbon dioxide and water molecules. For example,

after desorption of carbon dioxide and water molecules form the MgO surface, the oxygen anions become available to activate the reactant molecules.

Table 1.4. Commercial processes using solid base catalyst [183]

Process	**Catalyst**	**Year**
Alkylation of phenol with methanol	MgO	1970
iso–Butyraldehyde to *iso*–butylisobutyrate	ZrO_2	1974
Dehydration of 1–hexylethanol	ZrO_2	1986
Alkylation of cumene with ethylene	$Na/KOH/Al_2O_3$	1988
Isomerization of safrole to *iso*–safrole	$Na/KOH/Al_2O_3$	1988
Isomerization of 2,3–dimethyl–1–butene	$Na/KOH/Al_2O_3$	1988
Isomerization of 3,5–vinylbicyclo[2.2.1]heptene	$Na/KOH/Al_2O_3$	1988
Reduction of carboxylic acid to aldehyde	ZrO_2–Cr_2O_3	1988
Thiols from alcohols with hydrogen sulfide	$Alkali/Al_2O_3$	1988
Dehydration of propylamine–2–ol	ZrO_2–KOH	1992
Esterification of ethylene oxide with alcohol	Hydrotalcite	1994
Cyclization of imine with sulfur dioxide	Cs–zeolite	1995
Alkylation of *o*–xylene with butadiene	Na/K_2CO_3	1995
Isomerization of 1,2–propadiene to propyne	K_2O/Al_2O_3	1996
Dehydrotrimerization of *iso*–butyraldehyde	BaO–CaO	1998

Alkali metal deposited on the metal oxide supported by vapor deposition method has great importance to activate reactant molecules under mild reaction conditions. For example, the isomerization of 1–butene and 1–pentene was reported at room temperature using sodium metal deposited on alumina (Na/Al_2O_3) [200]. The sodium metal was also deposited on MgO showed high catalytic activity at 20 °C for isomerization of alkenes. [201]. The generation of strong basic sites was also reported by the reaction of alkali metal with holes trapped on oxygen anions near to the cationic vacancy [201]. Normally, catalysts which possess base sites stronger than pKa = 26 are called superbase and all the metal deposited catalysts comes under the superbase category. The side chain alkylation of aromatics and double bond isomerization of alkenes are the commercial examples for the applicability of solid superbase catalysts [202]. The generally applied solid superbase catalyst is shown in Table 1.5.

Table 1.5. Examples of solid superbase catalysts [187, 203]

Catalyst	Preparation method	Pretreatment temperature (K)	Basic strength (pKa)
CaO	$CaCO_3$	1173	26.5
SrO	$Sr(OH)_2$	1123	26.5
NaOH/MgO	(NaOH impregnated)	823	26.5
KNO_3/Al_2O_3, KNO_3/ZrO_2	(dry ground)	873	26.5
Na/MgO	(Na vaporized)	923	35
Na/Al_2O_3	(Na vaporized)	823	35
$Na/NaOH/Al_2O_3$	(NaOH, Na impregnated)	773	37
KNH_2/Al_2O_3	(KNH_2 impregnated)	573	>37
$K(NH_3)/Al_2O_3$	(ammoniacal K impregnated)	523–573	>37
K/MgO	(Na vaporized)	820	35

KF/Al_2O_3

Potassium fluoride supported on alumina (KF/Al_2O_3), introduced by Clark, is most widely studied as a solid base catalyst for condensation and isomerization reactions [204]. The KF/Al_2O_3 has wide application in organic chemistry due to its easy workup after completion of reaction. The idea of its catalytic active species is still controversial and mechanism of appearance of the basicity of KF/Al_2O_3 is not clarified. Moreover, conflicting conclusions have been reported on its basic strength, most authors considered as weak to moderate basicity, but few authors have claimed high or even super base catalyst [185, 205].

Main problem of above discussed supported catalysts such as, $Na/NaOH/Al_2O_3$, KF/Al_2O_3, metal or metal oxide supported on zeolites is the leaching of the active metal species in the reaction medium when the reaction carried out in liquid phase.

Basic Zeolites

Generally, zeolites are aluminosilicates, constructed from TO_4 tetrahedra (T = tetrahedral atom, e.g., Si, Al) with each apical oxygen atom shared with an adjacent tetrahedron (Figure 1.22). Zeolites are usually used as solid acid catalysts [101] but cation exchanged zeolites are known as weak base and can be activate toluene at higher reaction temperature. At the beginning of 1990s, zeolites were used as base catalysts in their ion–exchanged and impregnated forms [192].

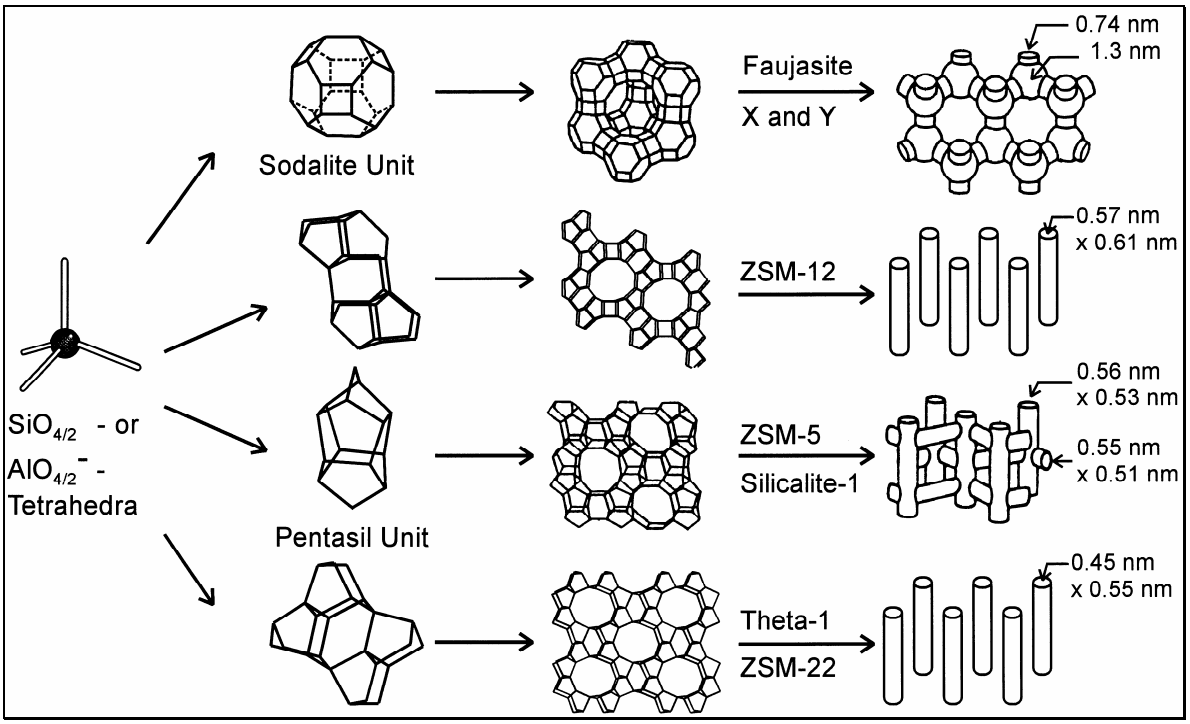

Figure 1.22. Structure of various zeolites [206].

There are two main kinds of basic zeolites– cation exchanged zeolites and supported zeolites. In general, the basic sites in cation exchanged zeolites are the framework oxygen ions and related to negative charge density on oxygen atoms, which depend on the zeolite structure and chemical composition. The basic strength and charge density of basic sites in alkali cation exchanged zeolites decrease with an increase in framework Si/Al ratio, while basic strength increases with an increase in electropositivity of the counteraction in zeolites [207–208]. Thus, relatively high aluminum content of zeolite X (Si/Al = 1–1.5) results into a substantial framework negative charge, which makes zeolite X one of the most basic zeolites when in the alkali cation exchanged form. Normally, the basic strength of cation exchanged zeolites depends on the exchangeable cations and decreases in the following order: $Cs^+ > Rb^+ > K^+ > Na^+ > Li^+$ [207–210]. Basic strength of the cation exchanged zeolite–X is higher than the corresponding zeolite–Y.

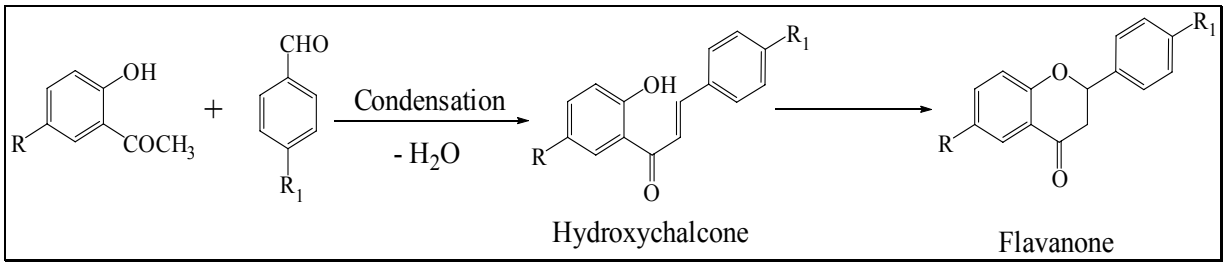

Scheme 1.4. Synthesis of chalcones and flavanones by the condensation reactions.

By generating framework and/or extra–framework basic sites mentioned above, it is possible to prepare basic zeolites with a very large spectrum of basicities. Then, depending on the

reaction to be catalyzed, it should be possible to select the most suitable basic zeolite from the very mild alkaline–exchanged zeolites up to very strong alkali– or alkaline–oxide–cluster containing zeolites. Therefore, until now, basic zeolites have been used as catalysts in a number of base–catalyzed reactions, such as toluene alkylation with methanol or ethylene, dehydrogenation of alcohols, double bond isomerization, condensation reactions (Scheme 1.4) and cycloaddition of CO_2 to epoxides. Recently, alkali earth oxides, such as MgO and BaO were also introduced into the zeolite cavity to produce strong basic sites [211–229]. Recently excellent review articles have been appeared in the literature for cation distributions in X and Y fujasite zeolites [205, 230–231].

Mesoporous Basic Materials

Although basic zeolites have been used in a broad variety of organic transformation reactions, but in some cases they have limitation, particularly, for the synthesis of fine chemicals, due to their small pore openings prevent the contact of bulky reactant molecules with active sites situated in zeolite cages. New families of mesoporous silica, such as MCM–41 and SBA–15 open the new opportunities due to tunable larger pore sizes and high surface area. Basic mesoporous materials may be prepared by following routes: a) cation exchange with alkali (e.g. Na^+ , K^+, Cs^+) metal cations; b) impregnation with alkali salts solution and calcination; c) functionalization with organic groups. The preparations of former two kinds of mesoporous materials are similar to those of basic zeolites.

Functionalized mesoporous basic materials can also be prepared by the immobilization of an organic base, such as amino groups, cinchonine, *β*–aminoalcohols or quaternary organic ammonium hydroxides, on the surface of mesoporous silica. Recently, aminopropylated mesoporous silica prepared by template free route was reported as an active catalyst for the synthesis of flavanones [232]. The aminopropylated mesoporous silica was synthesized by sol–gel method with orthosilicates and aminopropyltriethoxysilane under strong acidic conditions. The material was used as a catalyst for Claisen–Schmidt condensation between substituted benzaldehyde and substituted 2–hydroxyacetophenone and subsequent isomerization in the liquid phase reaction. Shin et al. impregnated magnesium oxide on MCM–41 and used as a solid base catalyst for the synthesis of jasminaldehyde [233–234]. The other examples of the modified mesoporous silica have been reported in the literature for the various solid base catalyzed reactions [235–239].

Organic–inorganic hybrid materials are less strongly basic than the corresponding free organic molecules and possess a wide distribution of the base sites with different strengths, which has been explained by an H–bonding interaction of amine functional groups with residual silanol

groups. Thus, these organic–inorganic hybrid materials have been reported as solid base catalyst for variety of reactions, including the Knoevenagel condensations, aldol condensations, Michael additions, syntheses of monoglycerides from fatty acids [240–245]. The magnesium oxide impregnated on Al–MCM–41 and amine groups grafted MCM–41 samples were used as active catalysts for synthesis of jasminaldehyde by condensation of benzaldehyde with 1–heptanal in mild reaction conditions (Scheme 1.5). These catalysts showed good yield of jasminaldehyde and reused several times without significant loss in the conversion and selectivity [233, 243].

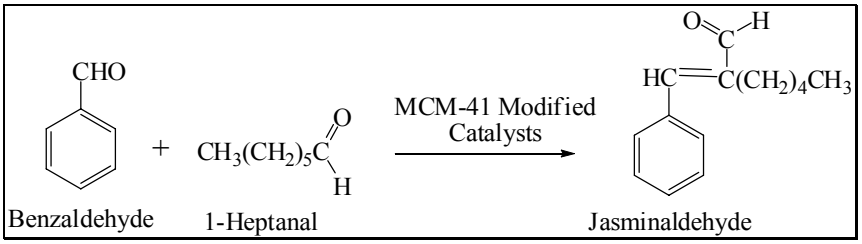

Scheme 1.5. Synthesis of jasminaldehyde using MCM–41 modified catalysts.

Oxynitrides

Lednor and Rulter synthesized silicon oxynitride, Si_2N_2O for first time, by a gas–solid reaction of amorphous silica with ammonia at 1100 °C [246] and used as a solid base catalyst for Knoevenagel condensation reactions [247–248]. Later on the aluminophosphate oxynitrides (AlPON) was prepared by the treatment of NH_3 at around 800 °C with amorphous aluminophosphate having high surface area. Amount of nitrogen incorporated increases with the time of exposure to NH_3 and reported as stronger base catalyst than the cation exchanged zeolites and weaker base catalyst as compared to MgO. The ALPON was used as a solid base catalyst for the synthesis of methyl isobutyl ketone, jasminaldehyde and Knoevenagel condensation reactions [249–253]. Incorporation of nitrogen in the aluminophosphate anionic framework seems to be an effective way to modify the surface acid–base properties of precursors and particularly to decrease the number of acid sites and to increase the number of basic sites. Recently, zirconophosphate oxynitride (ZrPON), galloaluminophosphate oxynitride (AlGaPON) and aluminovanadate oxynitride (VAlON) were also prepared in a similar method reported above and also used as solid base catalysts [249–260]. For oxynitrides, the identification of basic sites is more difficult than that of mixed oxide because several species present at the surface can act as basic sites. Among them the nitride nitrogen (N^{3-}), –(NH)–, and $–NH_2$ groups could be responsible for strong basicity, but presence of oxygen and hydroxyl groups whose charge would be modified by vicinity of the less electronegative framework nitrogen cannot be ignored.

Hydrotalcite or Layered double hydroxides (LDHs)

Hydrotalcite represent a class of anionic clay with general formula –

$$[M^{2+}_{1-x}M^{3+}_{x}(OH)_2]^{x+}(A_{A/m})^{m-}.nH_2O],$$

Where M^{2+} (divalent cations) = Mg, Zn, Ni, Cu, Ca, Mn, Fe, Co, etc.) and M^{3+} (trivalent cations = Al, Cr, Mn, Fe, Co, etc.) A is the exchangeable anions such as, OH^-, Cl^-, NO_3^-, CO_3^{2-}, SO_4^{2-}. The hydrotalcite has a structure similar to that of brucite sheet [$Mg(OH)_2$], where each Mg ion is octahedrally surrounded by six OH^- ions and different octahedral share edges to form infinite sheets. The sheets are mounted one on top of the other sheet and are held together by week interactions through hydrogen bonds. On replacing the Mg cation by another trivalent (M^{3+}) cation with similar radius to form hydrotalcite structure, the brucite like layers become positively charged and this charge is balanced by the compensation anions along with water molecules situated in the interlayer space (Figure 1.23). The value of x is varied from 0.17 to 0.33 [where, $x = M^{2+}/(M^{2+}+M^{3+})$] to synthesized pure hydrotalcite [271]. If the value of x is higher than the 0.33, this increase in the number of neighboring Al coordinating octahedra leads to the formation of $Al(OH)_3$, on the other hand lower x value leads to the segregation of $Mg(OH)_2$ due to the high density of Mg containing octahedral in the brucite like sheets.

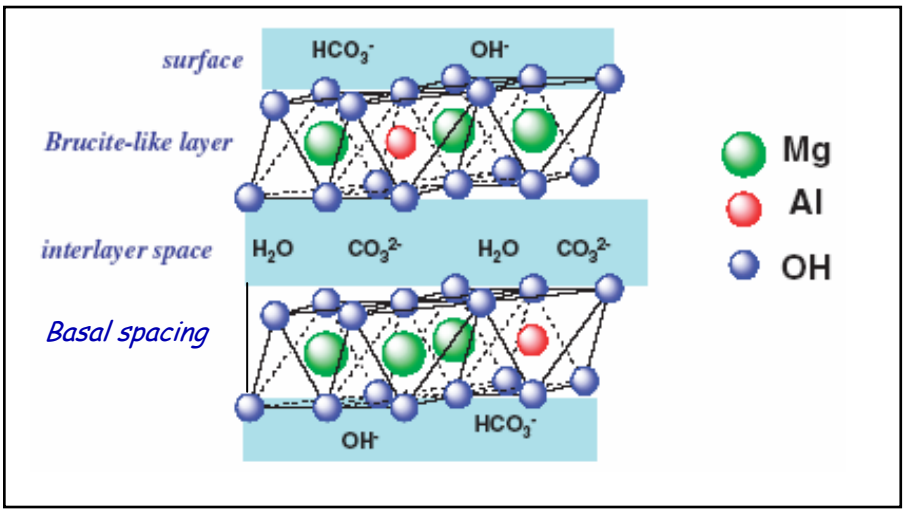

Figure 1.23. General structure of hydrotalcite.

Hydrotalcite has attracted much more attention due to their high anion exchange capacity along with high flexibility in the composition of brucite like layers, are often consider to be crucial parameters in tailoring of specific catalytic systems. Intercalation of metals containing anions in the interlayer space of hydrotalcite provides several advantages for an improved use in catalysis; its permits incorporation of a third metal component in the mixed oxide phase obtained upon thermal decomposition. In the materials, interlayer space provides unique space for the introduction of any

compound of our interest. The hydrotalcite has found many practical applications. The as–synthesized and calcined (activated) hydrotalcite have been used as a catalyst due to the following properties–

(a) Basic properties: –

Hydrotalcite offers an opportunity to play with the basicity in wider range to catalyze a variety of organic transformation reactions. As–synthesized hydrotalcite are considered as a mild base catalyst, whereas on activation of hydrotalcite at 450 °C, the basicity of hydrotalcite increases tremendously. The activation of hydrotalcite resulted into the formation of homogeneous mixture of thermally stable mixed oxides phase with very small crystal size having higher surface area as compared to the precursor. The P–XRD patterns of activated hydrotalcite showed diffuse MgO type structure with no segregate crystalline phase. Basicity of hydrotalcite can also be tuned by proper adjustment of Mg/Al molar ratio required to activate the reactant molecules. The basic properties of activated hydrotalcite (Mg–Al–O) is attributed to O^{2-} surface basic sites (strong basic sites), O^{-} located near the hydroxyl groups (medium strong sites), and OH^{-} groups (weak basic sites). The basic strength was measured by carbon dioxide temperature programmed desorption (CO_2–TPD) and titration method with different indicators in order to determine the number of active basic sites and maximum basic strength.

(b) Memory effect: –

When calcined hydrotalcite were rehydrated in water or in nitrogen flow saturated with water, hydrotalcite structure was recovered back to its original form, called reconstruction of hydrotalcite structure. This is due to the "memory effect" of calcined hydrotalcite. Reconstructed hydrotalcite contains mainly OH^{-} anions in the interlayer space. It is also possible to introduce OH^{-} anions by direct ion exchange method. Basic strength of reconstructed hydrotalcite containing OH^{-} anions is stronger than the original hydrotalcite containing CO_3^{2-} as compensation anions in the interlayer space. The OH^{-} ions are believed to be active sites for base catalyzed reactions using reconstructed hydrotalcite as a catalyst.

1.3.2. Hydrotalcite or Layered Double Hydroxides (LDHs) as a Solid Base Catalyst for the Condensation Reactions

Applicability of hydrotalcite as a catalyst is a potential substitute for commercially used alkaline base solution such as, NaOH or KOH in stoichiometric amounts, ammonia, ammonium salts or amines in the homogeneous conditions. Since, hydrotalcite is inexpensive, non–toxic, easily available, reusable by simple filtration and basic properties can be tailored to the process

requirement, the research is widely focused to develop environmental friendly processes using hydrotalcite as a solid base catalyst. The as–synthesized, activated and reconstruction hydrotalcite samples of varied Mg/Al molar ratio were reported as solid base catalysts in place of conventionally used NaOH or KOH for various reactions such as, aldol condensation, Knoevenagel condensation, Claisen–Schmidt condensation, Michael addition and double bound isomerization reactions.

In 1980s, aldol condensation of acetone by hydrotalcite of varied divalents and divalent to trivalent cations ratio was reported by Reichle [262]. He has also reported that the activated hydrotalcite samples are poor catalyst for isomerization and aromatization of 1,4–cyclohexadiene and limonene. Effect of anions present in the interlayer space of hydrotalcite on catalytic activity for aldol condensation of acetone was studied by the several researchers. Kustrowski et al. reported the aldol condensation of acetone using activated hydrotalcite of varied Mg/Al molar ratio from 2.1 to 3.6 containing nitrates and carbonates anions in the interlayer space [263–264]. The main products of the reaction are diacetone alcohol and mesityl oxide only (Scheme 1.6).

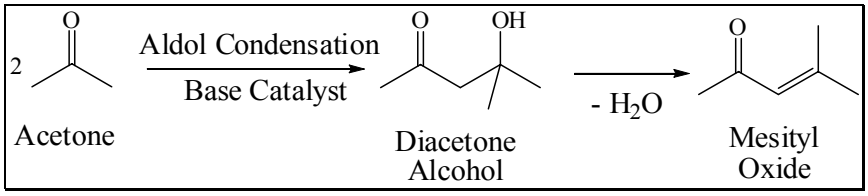

Scheme 1.6. Aldol condensation of acetone.

In another study, Tichit et al. reported aldol condensation of acetone in liquid phase using hydrotalcite as a catalyst having chlorides and carbonates as compensating anions in the interlayer space [265]. The activated hydrotalcite gave 20% conversion of acetone, which increased on increasing the Al content of hydrotalcite due to faster dehydration of diacetone alcohol on acid sites of the catalyst. The nature and amount of compensating anion in the hydrotalcite greatly influence the catalytic activity. Addition of the water in controlled amounts into reaction mixture enhanced the conversion of acetone and selectivity of diacetone alcohol. Experiments were also carried out using reconstructed hydrotalcite as a catalyst and reported that the conversion of acetone into diacetone alcohol reached the thermodynamic equilibrium (23%) in less than 1 h reaction time [265]. The hydrotalcite synthesized by hydrothermal treatment was activated, reconstructed and used for aldol condensation of acetone [266]. The activity of the reconstructed hydrotalcite was reported to increase linearly on increasing the amount of accessible Brønsted basic sites, which were determined by CO_2 adsorption. The number of accessible sites based on CO_2 adsorption was less than 5% and considered that the basic sites located near edges of

hydrotalcite platelets are participating for condensation reaction. Results also showed that the OH^- groups close to disordered edges gave higher activity as compared to the OH^- in a regular hydrotalcite structure [266]. In another study, effect of varied Mg/Al molar ratio of activated hydrotalcite samples from 0.5 to 9.0 was also studied for aldol condensation of acetone [267].

Activity of activated and reconstructed hydrotalcite samples was evaluated for C–C bond formation reactions such as, cross aldol condensation of citral and acetone [268–269]. The reconstructed hydrotalcite showed higher yield of desired product, pseudoionone as compared to commercially used NaOH in homogeneous conditions. Data for the citral–acetone condensation reaction was upscaled upto bench level. Hydrotalcite was not reused due to the deactivation of basic sites [268]. Reconstructed hydrotalcite synthesized by aging under sonication was found more active and gave 96% conversion of acetone with 99% selectivity for pseudoionone [269]. The other researchers also reported activity of the as–synthesized, activated and reconstructed hydrotalcite of varied Mg/Al molar ratio for condensation of citral and acetone (Scheme 1.7) [271–272].

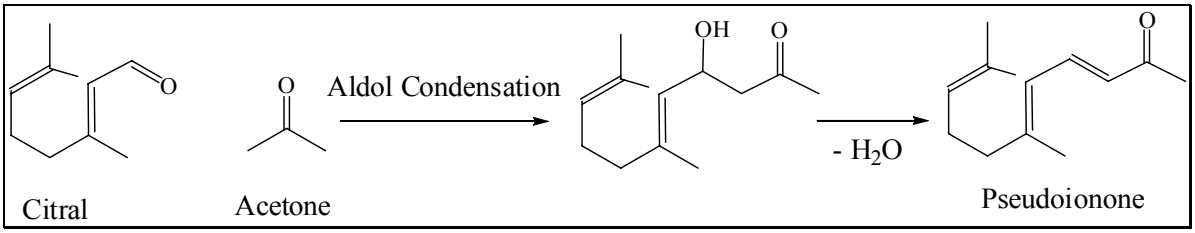

Scheme 1.7. Condensation of citral and acetone.

Abello et al. studied the influence of alkaline–doping agents (Na, Li, K) on the selectivity of pseudoionone obtained from condensation of citral and acetone using reconstructed hydrotalcite [273]. The amount of doped alkalines was varied from 0.5 to 4.9 % (by weight). The catalytic activity of reconstructed hydrotalcite was reported to increase on increasing the amount of alkaline metal. Increased behavior of the catalyst was correlated with their basic strength and number of basic sites. Leaching of the doped alkaline metal from hydrotalcite was observed during the reusability experiments [273]. The condensation of benzaldehyde and acetone to form 4–hydroxy,4–phenylbutan–2–one was studied to understand the role of activation procedure of hydrotalcite for the condensation reaction [274]. The higher catalytic activity of the activated samples was observed after the 450 °C activation temperature. The maximum yield (85%) of 4–hydroxy,4–phenylbutan–2–one was reported at optimum activation temperature. Catalytic activity of the activated samples increased significantly on the reconstruction of activated hydrotalcite by means of water vapors [274]. In order to observe the rate profile for condensation reaction using hydrotalcite as a catalyst, the kinetics of Claisen–Schmidt condensation of benzaldehyde with

acetone was performed in batch reactor. The maximum rate of reaction was observed as a function of calcination temperature of hydrotalcite and water content in the reaction mixture suggesting that the hydroxyl groups are playing an important role for the condensation reaction [275].

In another study, activated hydrotalcite was used as a catalyst for the condensation of campholenic aldehyde and methyl ethyl ketone (MEK), which find applications in the pharmaceutical and fragrance industries [276]. The presence of basic hydroxyl groups in the interlayer space leads to very active materials for aldol condensation reaction. This was achieved by the reconstruction of activated hydrotalcite by different procedure and used as a catalyst for condensation of campholenic aldehyde and MEK, and obtained results were compared with the catalytic activity of activated hydrotalcite samples. The reaction parameters were optimized by studying the effect of reaction temperature, molar ratio of the reactants and degree of reconstruction of the hydrotalcite [276]. The synthesis of cinamic acid, coumarin–3–carboxilic acid and their ethyl esters via Knoevenagel condensation was also reported under solvent free conditions using Mg–Al and modified Mg–Al hydrotalcite as a solid base catalyst [277]. The observed results were correlated with the basicity of hydrotalcite samples. In continuation of this, the activity of hydrotalcite synthesized by different procedures such as, conventional precipitation under hydrothermal aging, aging under microwave irradiation and sonication method were studied for Knoevenagel and aldol condensation reactions. Effect of the substitution of Mg cations by Ni on the catalytic activity of Ni–Al hydrotalcite for solvent free Knoevenagel condensation of different aldehydes with malononitrile and ethylcyanoacetate was studied in detail by Costantino et al [278]. The condensation of aliphatic and aromatic aldehydes gave excellent yield of Knoevenagel adducts in shorter reaction time (Scheme 1.8).

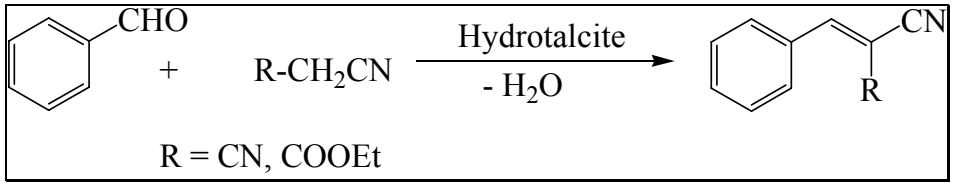

Scheme 1.8. Knoevenagel condensation catalyzed using hydrotalcite as a catalyst.

The catalyst was recycled several times, without loss of catalytic activity, and its performance was compared with the other solid base catalysts such as, zeolite A, potassium exchanged zirconium phosphate and amberlite [278]. Ebitani et al. reported reconstructed hydrotalcite as a highly active solid base catalyst for the Knoevenagel and Michael reactions of nitriles with carbonyl compounds [279]. Tichit et al. reported the condensation of acetaldehyde and heptanal using activated hydrotalcite of varied Mg/Al molar ratio and obtained data were compared with the MgO as a catalyst [280]. The strong solid base such as MgO favors the side reaction i.e., self condensation of

heptanal in the studied reaction conditions.

Claisen–Schmidt condensation between benzaldehyde and acetophenone was carried out in the presence of calcined and reconstructed hydrotalcite as solid base catalysts [281]. The results showed that the activated hydrotalcite of Al/(Al+Mg) molar ratio of 0.25 with 35% water content was the optimum catalyst which gave excellent activity for this reaction. The catalyst showed excellent selectivity for the synthesis of several chalcones with anti–inflammatory, antineoplasic, and diuretic pharmacological activities. The activity of reconstructed hydrotalcite was compared with commercially used KOH in homogeneous conditions, which showed that the reconstructed hydrotalcite can compete with the conventional KOH at higher reaction temperatures [281]. The pK value of activated hydrotalcite was reported to be in the range of 13.3 to 16.5 [282]. The hydrotalcite samples of varied divalent cations such as, calcium, magnesium, and zinc were also used as catalysts for synthesis of citronitril by the condensation of ethyl cyanoacetate and benzylacetone [283]. The effect of water content, reaction temperature and polarity of the solvents on conversion and selectivity was studied in detail [283]. The hydrotalcite was also used as a catalyst for the synthesis of flavanone [Scheme 1.9]

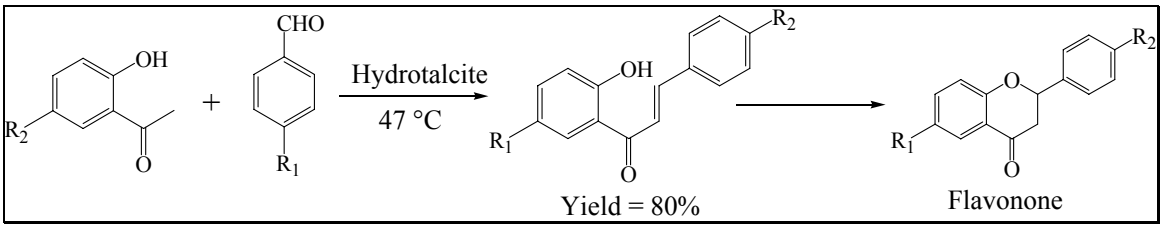

Scheme 1.9. Synthesis of flavanones.

Synthesis of vesidryl, an important diuretic drug was reported by the condensation of 2,4–dimethoxyacetophenone with *p*–anisaldehyde using hydrotalcite as a catalyst (Scheme 1.10) [227, 281, 284].

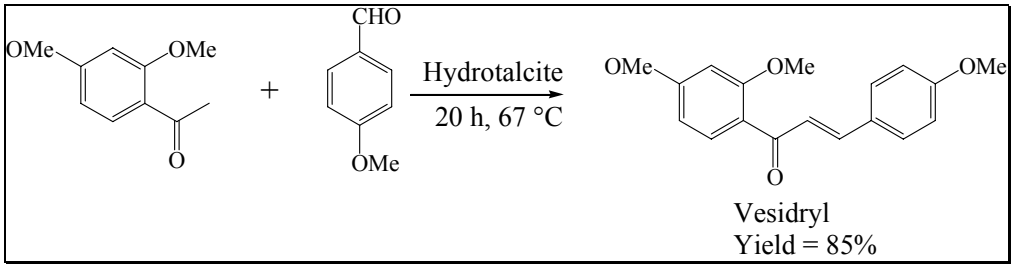

Scheme 1.10. Synthesis of vesidryl.

Michael addition of CH–acid compounds to methyl vinyl ketone gave high product yields with 100% selectivity using activated hydrotalcite of varied Mg/Al molar ratio from 0.6 to 3.0.

Acid–base properties of the activated hydrotalcite samples were investigated by (i) FT–IR spectroscopy after pyridine and CO_2 adsorption and (ii) microcalorimetry with CO_2 and benzoic acid suggests the presence of both acid sites (Lewis) and base sites (Lewis and Brønsted) on the surface of calcined hydrotalcite [285].

1.3.3. Bi–Functional Catalysts for the Synthesis of Commercially Important Chemicals in a Single Step

Replacement of multi–step, salt–generating chemical synthesis with efficiently catalyzed reactions that strive for atom economy is having a significant impact on the synthesis of fine chemicals and pharmaceutical intermediates. The development of multi–step synthesis processes into one–pot without separation of intermediate steps using multi–functional catalysts is an important strategy to carry out sustainable organic synthesis with a high atom and energy efficient way (Figure 1.24). The role multi–functional catalyst in one pot cascade reactions is the involvement of the different catalytic sites for different reactions simultaneously in a single reaction vessel. Multi–functional catalysts contain two or more catalytic functions (acid, base, metal, etc.) acting synergistically to carry out a multi–steps process in a single step. The use of multi–functional catalyst includes synthetic strategies that involve the sequential use of catalytic reactions with minimum workup, or without change in the reactors results into environmentally and economy more sustainable processes (higher atom economy and lower E factors), lower operating costs and lower waste generation. The synthesis of multi–steps reactions in a single pot constitutes a significant challenge for synthetic chemists and process development engineer presents a number of opportunities to improve chemical transformations. Multiple catalysts operating simultaneously could circumvent the time and yield losses associated with the isolation and purification of intermediates in multi–step sequences. Generating harmful chemicals *in–situ*, followed by incorporation into safer, more stable and larger molecular structures, would eliminate the inherent dangers associated with transportation of chemicals over long distances. Efficient multi–functional catalysts may allow the coupling of equilibrium–limited reactions with subsequent exothermic ones (Figure 1.24). This results into reduction in the number of equipments which leads to reduced investment costs and significant energy recovery or savings. Furthermore, improved product selectivity leads to a reduction in raw material consumption and hence, operating costs. Globally, process intensification through the use of multifunctional reactors permits significant reductions in both investment and plant operating costs. Cost reductions up to 30% could be obtained by optimizing the process. In an era of limited profit margins, it allows chemical producers more leverage in regard to competition in the global marketplace and good review articles are available on the cascade reaction in homogeneous conditions. [286–298]. Synthesis of the higher carbon

chain length aldehydes and ketones in one pot is highly appreciable and scare at commercial scale to save energy and the capital cost using multi–functional catalysts.

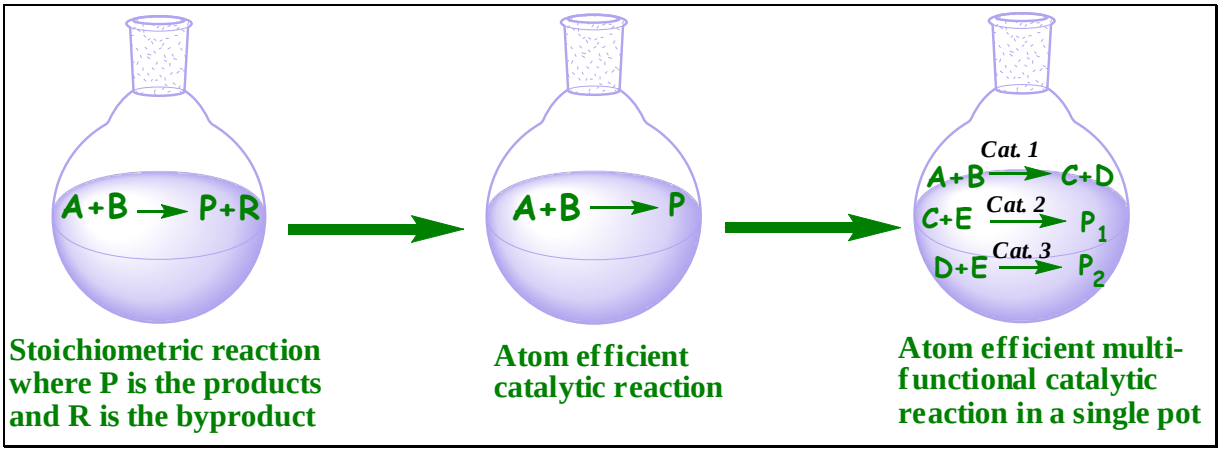

Figure 1.24. Representation of the function of multi–functional catalyst system.

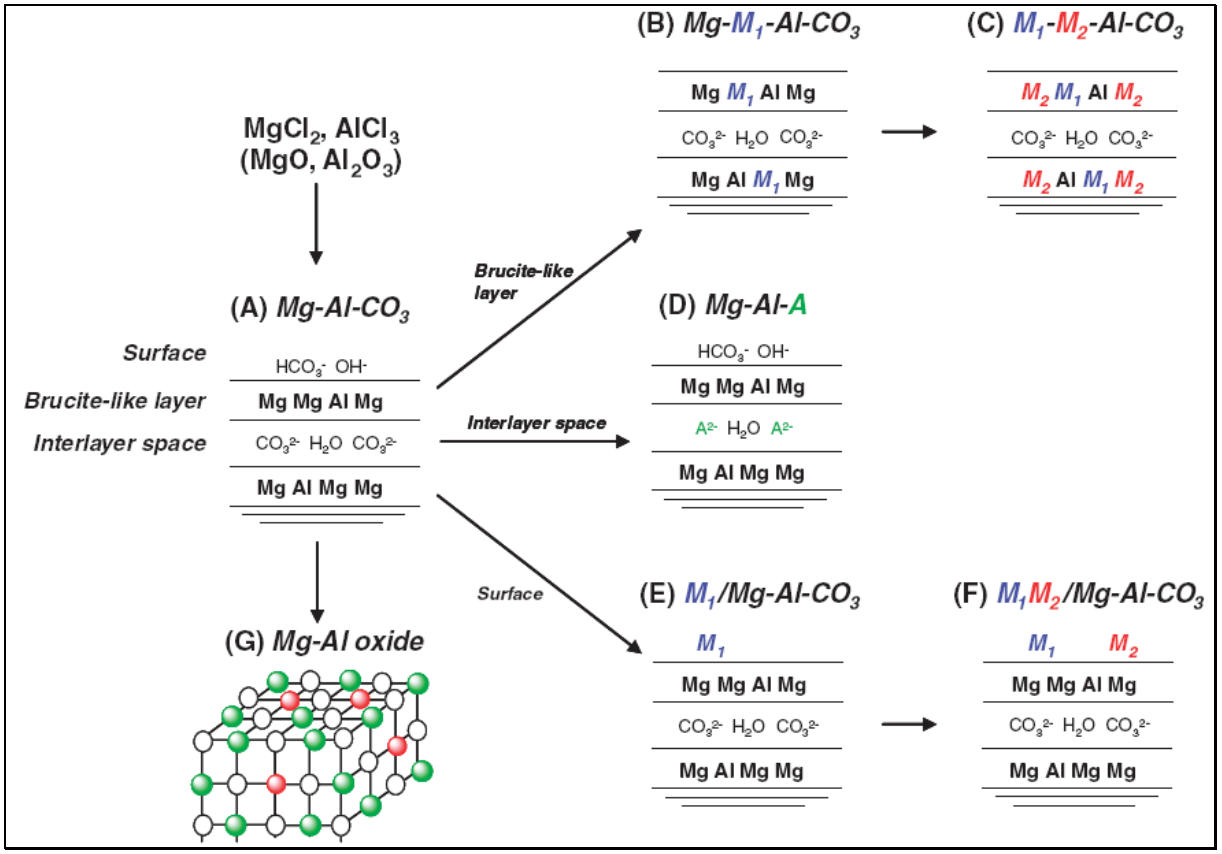

Figure 1.25. Synthesis of multi–functional catalyst [302].

Numerous transition metals can be introduced into the brucite–like layer, interlayer space, or on the hydrotalcite surface by using following characteristics: (i) cation–exchange ability of brucite layer, (ii) the anion–exchange ability of the interlayer, (iii) surface tunable basicity, and (iv) adsorption capacity [299–301]. The immobilized metal species can take the advantage of base sites available on the surface of hydrotalcite to synthesized multi–functional catalyst capable to catalyze

the sequential reactions in a single pot. Introduction of various metals in the hydrotalcite structure to synthesized heterogeneous multi–functional catalyst is shown in Figure 1.25.

A widely studied example of bi–functional catalysis is the synthesis of methyl isobutyl ketone (MIBK) from acetone (Scheme 1.11). The MIBK is used as a solvent for inks and lacquers and commercially prepared by a two step catalytic process involved base catalyzed aldol condensation of acetone to mesityl oxide (MO), then hydrogenation of MO using palladium or nickel metal. The step in which aldol condensation acetone takes place is also reported using acid catalysts such as zeolites [303], but in this section, literature related to solid base catalyst is included.

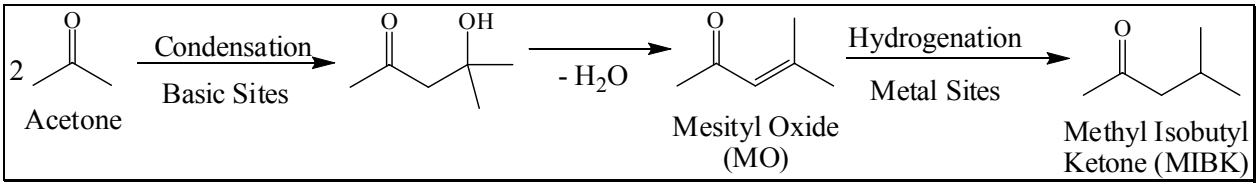

Scheme 1.11. Synthesis of methyl isobutyl ketone (MIBK) from acetone in a single pot.

Major reports describe the synthesis of bi–functional catalyst system by the impregnation of palladium on activated hydrotalcite and the catalytic performance was determined for single pot liquid phase synthesis of methyl isobutyl ketone by aldol condensation of acetone and subsequent hydrogenation of the condensed product [304–305]. Activity of palladium impregnated on activated hydrotalcite was compared with palladium supported on carbon nanofibers. The palladium impregnated on activated hydrotalcite showed higher activity since the dehydration reaction of diacetone alcohol to mesityl oxide over activated hydrotalcite is the rate–determining step in this process. A correlation between the number of active base sites, as determined by volumetric CO_2 adsorption measurements at low pressures, and activity of the catalyst was derived from the experimental data. Increasing amount of palladium loading on activated hydrotalcite gave the maximum selectivity for single pot synthesis of methyl isobutyl ketone, whereas no such effect was found when palladium supported on carbon nanofibers used as a catalyst [304]. In continuation of this, the activity of palladium impregnated on activated hydrotalcite of varied Mg/Al molar ratio was compared with the nickel impregnated on activated hydrotalcite as a catalyst for synthesis of methyl isobutyl ketone. These catalysts showed high conversion of acetone in the range of 35–40% with high selectivity to methyl isobutyl ketone (60–70%). A higher reduction temperature (>500 °C) was required to activate the nickel impregnated on activated hydrotalcite [306]. Impregnation of the copper and palladium on activated hydrotalcite was also claimed as a highly active catalyst for selective synthesis of methyl isobutyl ketone (90%) as compared to the palladium impregnated

on activated hydrotalcite. Impregnation of the platinum and palladium (0.1–1.5 wt%) on the activated Mg–Al hydrotalcite results into a highly active bi–functional catalyst for the synthesis of methyl isobutyl ketone from self condensation of acetone and hydrogenation of MO in a liquid phase batch micro–reactor at 99–153 °C and 400 psi pressure of hydrogen. Among the Pd– and Pt–based catalysts, 0.1 wt% Pd/HT sample gave maximum methyl isobutyl yield of about 32% as compared to the other studied catalysts [307]. Potential of ruthenium impregnated hydrotalcite was evaluated for the hydrogenation of α–alkylation of various nitriles with carbonyl compounds. The alkylated nitriles were synthesized by first aldol condensation on the basic sites available on the surface of hydrotalcite followed by hydrogenation catalyzed by ruthenium or palladium metal impregnated on the surface of hydrotalcite (Scheme 1.12) [308–309].

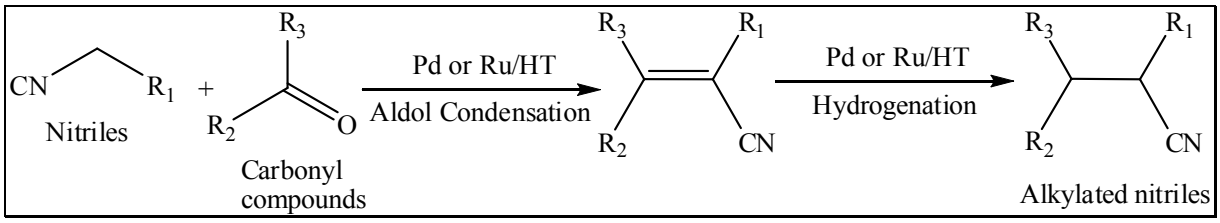

Scheme 1.12. Synthesis of alkylated nitriles in one step.

Synthesis of the 2–methyl–3–phenyl–propanal (Scheme 1.13), which is an important fragrance chemical, was reported by the condensation of benzaldehyde with propanal and subsequent hydrogenation of condensed product using palladium supported on activated hydrotalcite as a bi–functional catalyst system [310–312].

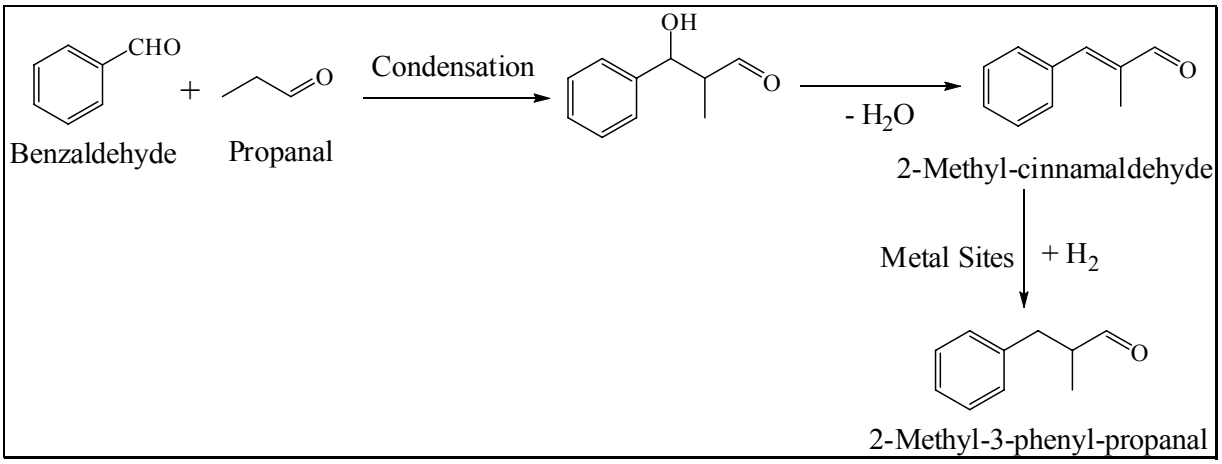

Scheme 1.13. Synthesis of 2–methyl–3–phenyl–propanal using palladium containing hydrotalcite as a catalyst.

The impregnation of copper and palladium on activated hydrotalcite was claimed as a highly active catalyst for selective synthesis of 2–methyl–3–phenyl–propanal (90%) as compared

to palladium impregnated on activated hydrotalcite as a catalyst [313]. The conversion of propanal increased to 96% with 97% selectivity of 2–methyl–3–phenyl–propanal using Pd–Mg–Al–O as a catalyst at propanal to benzaldehyde molar ratio 4. Addition of water into the reaction mixture enhanced the catalytic activity due to improvement in the Brønsted basicity of the catalyst [313].

Aim of the multi–steps synthesis can also be achieve in a single pot using different reaction conditions for different steps. For example, synthesis of a saturated cyanoester was reported over a rhodium grafted amino–containing mesoporous silica in two successive steps under different conditions (Scheme 1.14); (1) Knoevenagel condensation was carried out in the initial 1 h reaction time in inert atmosphere to avoid the undesired reaction, i.e., reduction of benzaldehyde; (2) then the hydrogenation of unsaturated intermediates was allowed for 12 h at 7 bar pressure of hydrogen [314]. In this synthesis strategies, amino–containing mesoporous silica offered the basic sites to carry out Knoevenagel condensation and rhodium was used for hydrogenation.

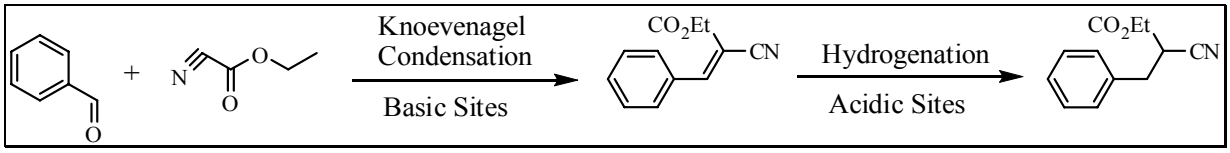

Scheme 1.14. Synthesis of a saturated cyanoester in a single pot.

Synthesis of 2–ethylhexanol, which is an important precursor for the synthesis of PVC and a useful plasticizer, from butanal is the best example of bi–functional catalyst in which aldol condensation of *n*–butanal takes place in liquid phase and hydrogenation of condensed product (2–ethylhexenal) gave 2–ethylhexanol (Scheme 1.15). Bi–functional catalyst was synthesized by the impregnation of nickel or palladium on the surface of Mg–Al hydrotalcite [315].

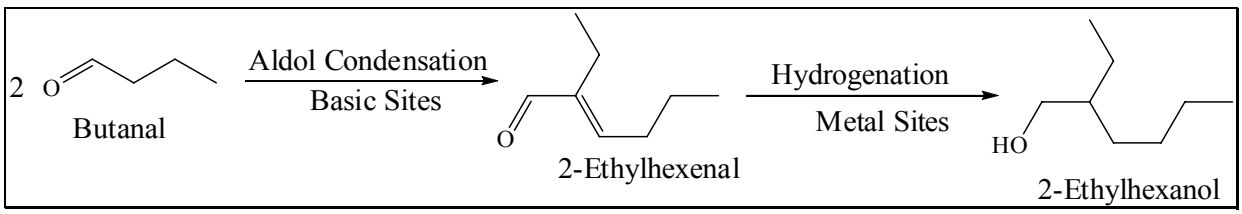

Scheme 1.15. Synthesis of 2–ethylhexanol from butanal in a single pot.

Aldol condensation of *n*–butanal and hydrogenation of 2–ethylhexenal to 2–ethylhexanal in a single pot using palladium impregnated on Na/SiO_2 catalyst system was studied in a fixed bed reactor by Kelly et al. [316–318]. Recently, Seki el al. also synthesized 2–ethylhexanal from crotonaldehyde in a single pot by the aldol condensation of crotonaldehyde to 2–ethylhexenal and finally hydrogenation to 2–ethylhexanal in supercritical CO_2 on fixed bed reactor using a bi–

functional catalyst containing palladium supported on acidic resin [319]. The maximum conversion of crotonaldehyde (98%) with 67% selectivity of 2–ethylhexanal was reported using palladium impregnated on amberlite–15 resin as a catalyst.

Quinoline is an important intermediate for the designing of various pharmacologically active compounds. The ruthenium impregnated hydrotalcite was reported as an active catalyst for the synthesis of quinolines from 2–aminobenzyl alcohols and various carbonyl compounds by oxidation followed by aldol condensation reactions in a single pot [320]. Similarly, citronitrile, a perfumery chemical with a citrus–like odor, was synthesized by the condensation of benzylacetone with ethylcyanoacetate, followed by hydrolysis and decarboxylation catalyzed by hydrotalcite in a single pot (Scheme 1.16) [283].

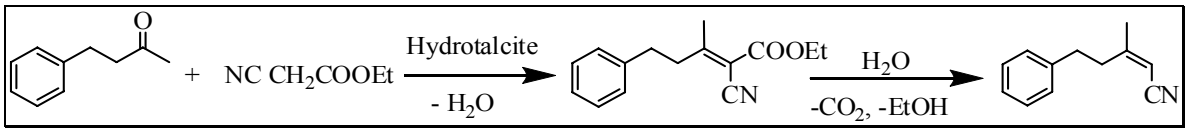

Scheme 1.16. Synthesis of citronitrile.

1.3.4. Isomerization of Perfumery Related Compounds

Double bond isomerization of perfumery chemicals is of great commercial importance for the production of number of key compounds where liquid bases such as KOH or NaOH are being used in stoichiometric amounts as catalysts (Scheme 1.17).

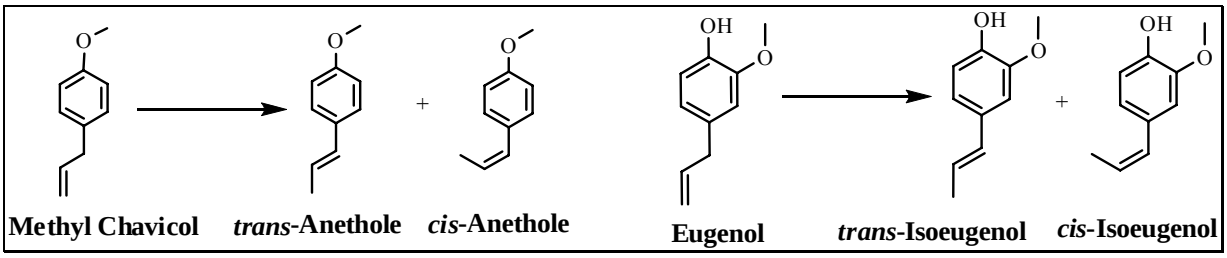

Scheme 1.17. Isomerization of methyl chavicol and eugenol.

The existing commercial processes for the double bond isomerization reaction possess demerits like use of strong liquid base in large amount, longer reaction time, lower conversion of reactant, lower selectivity of *trans*–isomer, higher reaction temperature, post synthesis work–up in separation of spent KOH from reactants/products mixture, disposal of effluent containing hazardous NaOH/KOH and separation of *cis* isomer from the products mixture. High capital expenses are also connected with the handling and storage of strong liquid bases, KOH/NaOH. Therefore, our main concern was on the replacement of liquid bases, which are being used in

stoichiometric amount, by the eco–friendly heterogeneous catalyst systems.

Bibb and Fla synthesized anethole via isomerization of methyl chavicol in the presence of liquid caustic alkali [321]. This process relates to the isomerization of pine oil which contains 4–25% methyl chavicol into anethole in the presence of 50% caustic soda solution at 200 °C for 2 h. The main drawback of this process is the use of hazardous, non–reusable caustic alkali compounds (50% caustic soda solution) at high temperature, which tends to split the ether linkage on methyl chavicol and form sodium compound of the resulting phenol. This process is not an eco–friendly route. The isomerization of safrole, eugenol, methyl chavicol was reported by the use of alkali metals (lithium, sodium, potassium, rubidium and other metals group I of the periodic table), alkali metal hydroxide (hydroxides of lithium, sodium, potassium, rubidium and other metals group I of the periodic table) and alumina in equimolar or less amount, which were heated at a temperature higher than the melting point of the respective alkali metal (preferably 200 to 500 °C for catalyst preparation) [322]. The substrate to catalyst ratio was kept at 5:1 in all experimental runs. Main drawback of this process is the use of hazardous non–recyclable alkali metals and metals hydroxides and the lower substrate to catalyst ratio.

Transition metals and their complexes have been known for double bond isomerization due to their strong affinity towards π–electrons of double bond [323]. The application of rhodium–containing compounds such as rhodium chloride, rhodium bromide, rhodium iodide, rhodium nitrate, rhodium sulfate, rhodium acetate for double bond isomerization of *cis/trans* mixture (*cis:trans* = 30:70) of anethole in an alcoholic medium at reflux temperature was reported by Martan and Reichenbacher [324]. In a typical experiment, 40 mg of rhodium trichloride per 100 grams of anethole (*cis/trans* mixture 30:70) was mixed with propanol and heated at 95 °C for 2 hours. After 2 hours the conversion of *cis/trans*–anethole was 5: 95. The main drawback of this route for the preparation of *trans*–anethole is the less availability of *cis* anethole as compared to methyl chavicol as a reactant. In another report, double bond isomerization of eugenol, safrole, allylbenzene, allyl phenols was reported by various ruthenium complexes [325].

In order to develop suitable solid base catalysts for double bond isomerization of perfumery related compounds, the base catalyzed isomerization of allylic compounds such as, eugenol, safrole was reported using various potassium salts impregnated on alumina and calcium oxide as solid base catalysts in solvent free conditions [326]. These catalysts showed moderate to good yield of *iso*–safrole and *iso*–eugenol in the studied reaction conditions.

Sodium–doped mesoporous alumina ($Na/mesoAl_2O_3$) was synthesized by doping of sodium azide and used as a catalyst for double bond migration of 2,3–dimethyl–1–butene at a low reaction

temperature (Scheme 1.18) [327]. The 81% yield of 2,3–dimethyl–2–butene was reported in 4 h reaction time to confirm the higher basicity of the synthesized catalyst. Na/mesoAl_2O_3 catalyst was also used for the isomerization of α–pinene to β–pinene, showed excellent selectivity of β–pinene in the range of 93–96% [327].

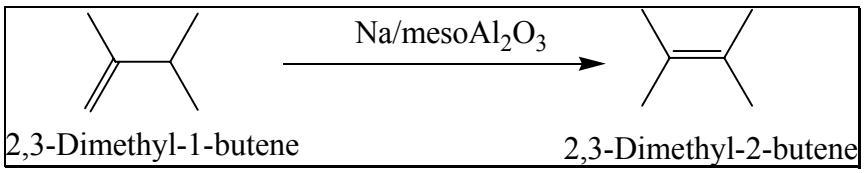

Scheme 1.18. Isomerization of 2,3–dimethyl–1–butane.

Potential of as–synthesized, activated hydrotalcite and ion exchanged zeolites as solid base catalysts was evaluated for isomerization of methyl chavicol to *trans*–anethole in the solvent free conditions in 10 h reaction time [328]. The lower activity of activated hydrotalcite samples was observed as compared to the as–synthesized hydrotalcite samples under identical reaction conditions. In another studies, Kannan et al., reported isomerization of eugenol, estragole (Scheme 1.17), safrole (Scheme 1.19), using as–synthesized hydrotalcite of varied divalent and trivalent metals cations as well as their ratios as catalysts in various polar and non polar organic solvents [329–332]. The hydrotalcite samples of different composition and varied divalent to trivalent cations ratio were used as catalysts for the isomerization of methyl chavicol in the presence of dimethyl formamide (DMF) as a solvent [332]. DMF was again used as a solvent to achieve 75% conversion of eugenol with 85% selectivity of *trans*–isoeugenol in 6 h at substrate to catalyst ratio 2:1 [329]. The conversion of eugenol was observed to 71% with 75% selectivity of *trans*–isoeugenol using ruthenium (2.5% by wt) impregnated hydrotalcite as a catalyst. Main drawbacks of this study are the use of DMF and other organic solvents, very low substrate to catalyst ratio, reusability of catalyst and lower selectivity of *trans* isomer using impregnated catalyst. The hydrotalcite as a catalyst was also showed excellent yields for isomerization of allylbenzene in liquid phase [333].

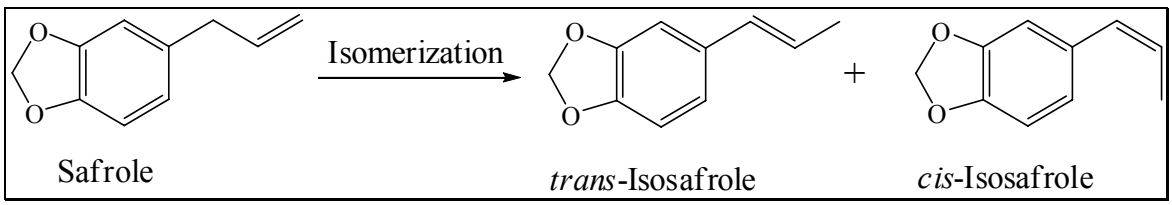

Scheme 1.19. Isomerization of safrole.

Figueras et al. demonstrated the applicability of hydrotalcite samples of varied Mg/Al molar ratio as a catalyst for double bond isomerization of β–isophorone to α–isophorone (Scheme

1.20). The catalytic activity of the hydrotalcite was also correlated with basicity of samples based on the results observed for isophorone isomerization and set as a model test reaction for the basicity measurements [334].

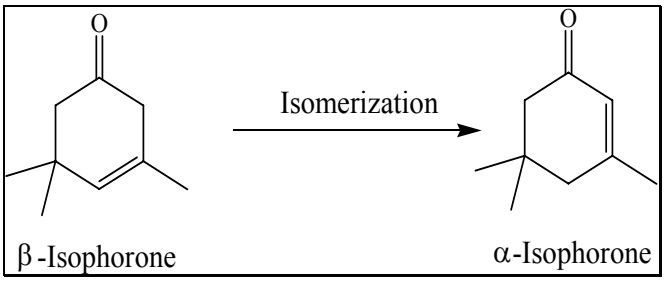

Scheme 1.20. Isomerization of β–isophorone.

2–Carene, which is synthesized by the isomerization of 3–carene (Scheme 1.21) finds application in fragrance and perfume industry and it is an intermediate for the synthesis of menthol. Tanabe et al. reported isomerization of 3–carene to 2–carene over metal oxides such as MgO, CaO, SrO, and ZrO as solid base catalysts. For MgO, 900 °C pretreatment temperature gave 46% conversion of 3–carene with 96% selectivity of 2–carene [335].

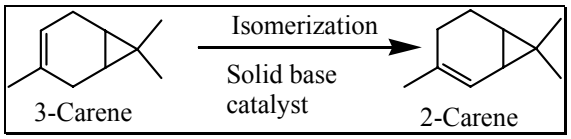

Scheme 1.21. Isomerization of 3–carene.

Meyer and Hoelderich performed vapor phase isomerization of 3–carene to 2–carene using basic zeolites prepared by ion exchange or impregnation of alkali metals and alkali metal acetates [336]. The maximum selectivity of 2–carene (78.4%) with 37% conversion of 3–carene was reported for Na/Na–X as a catalyst at 250 °C reaction temperature.

The work reported in the present Thesis aims to contribute towards the development of eco–friendly heterogeneous catalysts for synthesis of commercially importance products via hydroformylation, condensation and isomerization reactions. Thesis describes the synthesis of different heterogeneous catalysts, such as by impregnation and intercalation of rhodium complex into the hydrotalcite for hydroformylation, condensation and hydrogenation reactions in one pot and hydrotalcite of varied M(II) and M(II)/Al molar ratio [M(II) = Mg, Ni, Zn] for aldol condensation and isomerization reactions. Intercalation of ruthenium in the hydrotalcite matrix (replacement of aluminum by ruthenium cations) was also carried out and used as catalyst for isomerization of perfumery chemicals. The structural and textural properties of the synthesized

catalysts were studied by instrumental techniques such as, ^{31}P–Fourier Transform–Nuclear Magnetic Resonance (FT–NMR), Powder–X–Ray Diffraction (P–XRD), Fourier Transform–Infrared (FT–IR), Thermogravimetric Analysis (TGA), CHN analysis, Scanning Electron Microscopy (SEM) and Surface Area Measurements. Catalytic activities of these eco–friendly catalysts were studied for the synthesis of commercially important chemicals via hydroformylation, condensation and isomerization reactions.

1.4. References

[1] P. Anastas, J. C. Warner (Eds.), Green Chemistry: Theory and Practice, Oxford University Press, Oxford (1998).

[2] P.T. Anastas, M.M. Kirchhoff, Acc. Chem. Res. 35 (2002) 686–693.

[3] G.W. Parshall, Homogeneous Catalysis, John Wiley: New York, (1980).

[4] R.A. Sheldon, Chem. Ind. (1992) 903–906.

[5] R.A. Sheldon, Green Chem. 9 (2007) 1273–1283.

[6] B.M. Trost, Science 254 (1991) 1471–1477.

[7] B.M. Trost, Angew. Chem. Int. Ed. 34 (1995) 259–281

[8] H. Adkins, G. Krsek, J. Am. Chem. Soc. 70 (1948) 383–386.

[9] C.L. Aldridge, H.B. Jonassen, J. Am. Chem. Soc. 85 (1963) 886–891.

[10] Chemische Verwertungsgesellschaft Oberhausen (O. Roelen), DE Patent, 849548 (1938/1952) and US Patent, 2327006 (1943).

[11] O. Roelen, Chem. Exp. Didakt. 3 (1977) 119.

[12] A.J. Chalk, J.F. Harrod, Adv. Organomet. Chem. 11 (1968) 119.

[13] B. Cornils, W.A. Herrmann, Applied Homogeneous Catalysis with Organometallic Complexes, VCH, Weinheim, Germany, (1996).

[14] B. Cornils, W.A. Herrmann, M. Rasch, Angew. Chem. Int. Ed. Engl. 33 (1994) 2144–2163.

[15] B. Cornils, J. Mol. Catal. A. Gen. 143 (1999) 1–10.

[16] H.W. Bohnen, B. Cornils, Adv. Catal. 47 (2002) 1–64.

[17] B. Cornils, W.A. Herrmann, J. Catal. 216 (2003) 23–31

[18] L. Marko in Aspects of Homogeneous Catalysis (Ed. R. Ugo), D. Riedel, Dardrecht, Chapter 1 (1974).

[19] P. Pino, F. Piacenti, M. Bianchi in Organic Synthesis via Metal Carbonyls (Ed. I. Wender, P. Piano), Wiley, New York Chapter 2 (1977).

[20] R.L. Pruett, Adv. Organomet. Chem. 17 (1979) 1.

[21] S.K. Sharma, V.K. Srivastava, R.V. Jasra, in Catalysis in hydrocarbon processing and fertilizer industry (Ed. M.A. Siddiqui, R.P. Verma), Lovraj Kumar Memorial Trust, New Delhi.

[22] V.K. Srivastava, D.U. Parmar, R.V. Jasra, Chemical Weekly Part 1: Commercial Aspects, July 8 (2003) 173–178; Part 2: Technology, July 15 (2003) 181–190.

[23] Chemical Economic Handbook, Oxo Chemicals Report, SRI International, January (2003).

[24] S. Liu, J. Xiaom, J. Mol. Catal. A: Chem. 270 (2007) 1–43.

[25] F. Ungvary. Coord. Chem. Rev. 251 (2007) 2087–2102.

[26] F. Ungvary. Coord. Chem. Rev. 251 (2007) 2072–2086.

[27] A.M. Trzeciak, J.J. Ziolkowski, Coord. Chem. Rev. 190–192 (1999) 883–900.

[28] B. Cornils, E. Kuntz, J. Organomet. Chem. 502 (1995) 177–186.

[29] R. Anon., Chemical Marketing Reporter September 18, 1995.

[30] W.A. Herrmann, B. Cornils, Angew. Chem. Int. Ed. Engl. 36 (1997) 1048.

[31] V.K. Srivastava, S.D. Bhatt, R.S. Shukla, H.C. Bajaj, R.V. Jasra, React. Kinet. Catal. Lett. 85 (2005) 3–9.

[32] E.R. Tucci, Ind. Eng. Chem. Prod. Res. Dev. 25 (1986) 27–30.

[33] T.E. Nalesnik, J.H. Freudenberger, M. Orchin, J. Organomet. Chem. 236 (1986) 95–100.

[34] A. Fussi, E. Cesarotti, R. Ugo, J. Mol. Catal. 10 (1981) 213–221.

[35] V.K. Srivastava, R.S. Shukla, H.C. Bajaj, R.V. Jasra, J. Mol. Catal. A: Chem. 202 (2003) 65–72.

[36] L. Alvila, T.A. Pakkanen, T.T. Pakkanen O. Krause J. Mol. Catal. 73 (1992) 325–334.

[37] V.K. Srivastava, S.D. Bhatt, R.S. Shukla, R.V. Jasra, React. Kinet. Catal. Lett. 81 (2004) 99–105.

[38] G.S. Fink, G.F. Schmidt, J. Mol. Catal. 42 (1987) 361–366.

[39] V.K. Srivastava, S.K. Sharma, R.S. Shukla, N. Subramanyam, R.V. Jasra, Ind. Eng. Chem. Res. 44 (2005) 1764–1771.

[40] B. Cornils, New Synthesis with Carbon monoxide (Ed. J. Falbe), Springer, Berlin, (1980).

[41] D.U. Parmar, S.D. Bhatt, H.C. Bajaj, R.V. Jasra, J. Mol. Catal. A: Chem. 202 (2003) 9–15.

[42] C. Botteghi, G.D. Ponte, M. Marchetti, S. Paganelli, J. Mol. Catal. 93 (1994) 1–21.

[43] A. Polo, J, Real, C. Claver, S. Castillon, J.C. Bayon, J. Chem. Soc. Chem. Commun. (1990) 600–602.

[44] P.W.N.M. van Leeuwen, C.F. Roobek, J. Organomet. Chem. 258 (1983) 343–350.

[45] J.T. Carlock, Tetrahedron 40 (1984) 185–188.

[46] V.K. Srivastava, R.S. Shukla, H.C. Bajaj, R.V. Jasra, Appl. Catal. A: Gen. 282 (2005) 31–38.

[47] T.G. Southern, Polyhedron 8 (1989) 407–413.

[48] M. R. Barton, Y. Zhang, J. D. Atwood, J. Coord. Chem. 55 (2002) 969–983.

[49] P. Kalck, F. Monteil, Adv. Organomet. Chem. 34 (1992) 219.

[50] W.A. Herrmann, C.W. Kohlpaintner, Angew. Chem. Int. Ed. Engl. 32 (1993) 1524–1544.

[51] B. Cornils, E. Wiebus, Chemtech 25(1995) 33–38; E.G. Kuntz, Chemtech 17 (1987) 570–575.

[52] D.U. Parmar, H.C. Bajaj, R.V. Jasra, B.M. Moroz, V.A. Likholobov, J. Mol. Catal. A: Chem. 211 (2004) 83–87.

[53] D.U. Parmar, H.C Bajaj, S.D Bhatt, R.V Jasra, Bull. Catal. Soc. Ind. 2 (2003) 34–39.

[54] D. Evans, J.A. Osborn, G. Wilkinson, J. Chem. Soc. (A) (1968) 3133–3142.

[55] A.A. Dabbawala, D.U. Parmar, H.C. Bajaj, R.V. Jasra, J Mol. Catal. A: Chem. 282 (2008) 99–106.

[56] H. Arai, H. Tominaga, J. Catal. 75 (1982) 188–189.

[57] M.E. Davis, E. Rode, D. Taylor, B.E. Hanson, J. Catal. 86 (1984) 67–74.

[58] N. Takahashi, M. Kobayashi, J. Catal. 85 (1984) 89–97.

[59] Z. Karpinski, Z. Zhang, W.M.H. Sachtler, J. Mol. Catal. 77 (1992) 181–192.

[60] S. Naito, M. Tanimoto, J. Chem. Soc. Chem. Commun. (1989) 1403–1404.

[61] M. Lenarda, R. Ganzerla, S. Enzo, L. Storaro, R. Zanoni, J. Mol. Catal. 80 (1993) 105–116.

[62] L. Storaro, R. Ganzerla, M. Lenarda, R. Zanoni, G. Righini, J. Mol. Catal. 112 (1996) 43–54.

[63] L. Yan, Y.J. Ding, H.J. Zhu, J.M. Xiong, T. Wang, Z.D. Pan, L.W. Lin, J. Mol. Catal. A:

Chem. 234 (2005) 1–7.

[64] H.J. Zhu, Y.J. Ding, L. Yan, J.M. Xiong, Y. Lu, L.W. Lin, Catal. Today 93–94 (2004) 389–393.

[65] S.S.C. Chuang, S. Pien, J. Mol. Catal. 55 (1989) 12–22.

[66] M.W. Balakos, S.S.C. Chuang, J. Catal. 151 (1995) 253–265

[67] S.S.C. Chuang, M.A. Brundage, M.W. Balakos, Appl. Catal. A: Gen. 151 (1997) 333–354.

[68] M. A. Brundage, M.W. Balakos, S.S.C. Chuang, J. Catal. 173 (1998) 122–133.

[69] M. A. Brundage, S.S.C. Chuang, J. Catal. 164 (1996) 94–108.

[70] M.A. Brundage, S.S.C. Chuang, J. Catal. 174 (1998) 164–176.

[71] M.A. Brundage, S.S.C. Chuang, J. Catal. 174 (1998) 64–176.

[72] M.A. Brundage, S.S.C. Chuang, J. Catal. 151 (1995) 266–278.

[73] M.A. Brundage, S.S.C. Chuang, S.A. Hedrick, Catal. Today 44 (1998) 151–163.

[74] S.A. Hedrick, S.S.C. Chuang, A. Pant, A.G. Dastidar, Catal. Today 55 (2000) 247–257.

[75] G. Snyder, A. Tadd, M.A. Abraham, Ind. Eng. Chem. Res. 40 (2001) 5317–5325.

[76] Y. Izumi, K. Konishi, M. Tsukahara, D.M. Obaid, K. Aika, J. Phys. Chem. C 111 (2007) 10073–10081.

[77] A. Riisager, R. Fehrmann, S. Flicker, R. Hal, M. Haumann, P. Wasserscheid, Angew. Chem. Int. Ed. 44 (2005) 815–819.

[78] M. Haumann, A. Riisager, Chem. Rev. 108 (2008) 1474–1497.

[79] V.I. Parvulescu, C. Har, Chem. Rev. 107 (2007) 2615–2665

[80] J.D. Holbrey, K.R. Seddon, Clean Products Processes 1 (1999) 223–236.

[81] P. Wasserscheid, W. Keim, Angew. Chem. Int. Ed. 39 (2000) 3772–3789.

[82] C.P. Mehnert, R.A. Cook, N.C. Dispenziere, M. Afeworki, J. Am. Chem. Soc. 124 (2002) 12932–12933.

[83] C.P. Mehnert, Chem. Eur. J. 11 (2005) 50–56.

[84] A.Riisager, R. Fehrmann, M. Haumann, P. Wasserscheid, Eur. J. Inorg. Chem. (2006) 695–706.

[85] H. Arai, J. Catal. 51 (1978) 135–142.

[86] N.A. Demunck, M.W. Verbruggen, J.J.F. Scholten, J. Mol. Catal. 10 (1981) 313–330.

[87] B. Heinrich, Y. Chen, J. Hjortkjaer, J. Mol. Catal. 80 (1993) 365–375.

[88] M. Lenarda, R. Ganzerla, L. Storaro, A. Trovarelli, R. Zanoni, J. Kaspar, J. Mol. Catal. 72 (1992) 75–84.

[89] T. Yamagishi, S. Ito, K. Tomishige, K. Kunimori, Catal. Commun. 6 (2005) 421–425.

[90] M. Ichikawa, in Tailored Metal Catalysts, Y. Iwasawa (Ed.), D. Riedel, Dordrecht, Chapter 4 (1986).

[91] Y. Konishi, M. Ichikawa, W.M.H. Sachtler, J. Phys. Chem. 91 (1987) 6286–6291.

[92] Y. Izumi, K. Asakura, Y. Iwasawa, J. Catal. 132 (1991) 566–570.

[93] W.M.H. Sachtler, M. Ichikawa, J. Phys. Chem. 90 (1986) 4752–4758.

[94] A. Maeda, F. Yamakawa, K. Kunimori, T. Uchijima, Catal. Lett. 4 (1990) 107–110.

[95] K. Takeuchi, T. Hanaoka, T. Mastuzaki, Appl. Catal. 73 (1991) 281–287.

[96] S. Naito, M. Tanimoto, J. Catal. 130 (1991) 106–115.

[97] K.K. Bando, K. Asakura, H. Arakawa, K. Isobe, Y. Iwasawa, J. Phys. Chem. 100 (1996) 13636–13645.

[98] H. Trevino, T. Hyeon, W.M.H. Sachtler, J. Catal. 170 (1997) 236–243.

[99] L. Sordelli, M. Guidotti, D. Andreatta, G. Vlaic, R. Psaro, J. Mol. Catal. A: Chem. 204–205 (2003) 509–518.

[100] D.W. Breck, Zeolite Molicular Sieves: Chemistry and Uses, Wiley–New York, (1974).

[101] A. Corma, Chem. Rev. 95 (1995) 559–614.

[102] A. Corma, Chem. Rev. 97 (1997) 2373–2420.

[103] T.E. Bitterwolf, J.D. Newell, C.T. Carver, R.S. Addleman, J.C. Linehan, G. Fryxell, Inorg. Chim. Acta 357 (2004) 3001–3006.

[104] A. Taguchi, F. Schuth, Micropor. Mesopor. Mater. 77 (2005) 1–45.

[105] U. Ciesla, F. Schuth, Micropor. Mesopor. Mater. 27 (1999) 131–149.

[106] D.T. On, D.D. Giscard1, C. Danumah, S. Kaliaguine, Appl. Catal. A: Gen. 253 (2003) 545–602.

[107] G. Oye, J. Sjoblom, M. Stocker, Adv. Colloid Inter. Sci. 89–90 (2001) 439–466.

[108] M. Nowotny, T. Maschmeyer, B.F.G. Johnson, P. Lahuerta, J.M. Thomas, J.E. Davies,

Angew. Chem. Int. Ed. 40 (2001) 955–958.

[109] R.J. Davis, J.A. Rossin, M.E. Davis, J. Catal. 98 (1986) 477–486

[110] M.E. Davis, J. Schnitzer, J.A. Rossin, D. Taylor, B.E. Hanson, J. Mol. Catal. 39 (1987) 243–259.

[111] B.E. Hanson, M.E. Davis, D. Taylor, E. Rode, Inorg. Chem. 23 (1984) 52–56.

[112] K. Mukhopadhyay, R. V. Chaudhari, J. Catal. 213 (2003) 73–77.

[113] A. Fuerte, M. Iglesias, F. Sanchez, J. Organomet. Chem. 588 (1999) 186–194.

[114] L. Huang, Y. He, S. Kawi, J. Mol. Catal. A: Chem. 213 (2004) 241–249.

[115] L. Huang, Y. He, S. Kawi, Applied Catal. A: Gen. 265 (2004) 247–257.

[116] K. Mukhopadhyay, A.B. Mandale, R.V. Chaudhari, Chem. Mater. 15 (2003) 1766–1777.

[117] L. Huang, J.C. Wu, S. Kawi, J. Mol. Catal. A: Chem. 206 (2003) 371–387.

[118] B.E. Ali, J. Tijani, M. Fettouhi, M.E. Faer, A.A. Arfaj, Appl. Catal. A: Gen. 283 (2005) 185–196.

[119] Q. Peng, Y. Yang, Y. Yuan, J. Mol. Catal. A: Chem. 219 (2004) 175–181.

[120] B.E. Ali, J. Tijani, M. Fettouhi, Appl. Catal. A: Gen. 303 (2006) 213–220.

[121] Y. Yang, C. Deng, Y. Yuan, J. Catal. 232 (2005) 108–116.

[122] H. Zhu, Y. Ding, L. Yan, Y. Lu, C. Li, X. Bao, L. Lin, Chem. Lett. 33 (2004) 630–631.

[123] C.M.S. Hauser, T. Lummerstorfer, R. Schmid, H. Hoffmann, K. Kirchner, M. Puchberger, A.M. Trzeciak, E. Mieczynska, W. Tylus, J.J. Ziołkowski, J. Mol. Catal. A: Chem.210 (2004) 179–187.

[124] A.R. Tadd, A. Martell, M.R. Mason, J.A. Davis, M.A. Abraham, Ind. Eng. Chem. Res. 41 (2002) 4514–4522.

[125] S. Bektesevic, T. Tack, M.R. Mason, M.A. Abraham, Ind. Eng. Chem. Res. 44 (2005) 4973–4981.

[126] O. Hamminger, A. Marteel, M.R. Mason, J.A. Davies, A.R. Tadd, M.A. Abraham, Green Chem. 4 (2002) 507–512.

[127] M. Marchetti, S. Paganelli, E. Viel, J. Mol. Catal. A: Chem. 222 (2004) 143–151.

[128] J. Zhao, Y. Zhang, J. Han, Y. Jiao, J. Mol. Catal. A: Chem. 241 (2005) 238–243.

[129] L. Huang, S. Kawi, Catal. Lett. 92 (2004) 57–62.

[130] A.N. Ajjou, H. Alper, Molecules Online 2 (1998) 53–57.

[131] K.G. Allum, R.D. Hancock, I.V. Howell, R.C. Pitkethly, P.J. Robinson, J. Catal. 43 (1976) 322–330.

[132] M. Karlsson, C. Andersson, J. Hjortkjaer, J. Mol. Catal. A: Chem. 166 (2001) 337–343.

[133] A. Sandee, J.N.H. Reek, P.C.J. Kamer, P.W.N.M. van Leeuwen, J. Am. Chem. Soc. 123 (2001) 8468–8476.

[134] Z. Li, Q. Peng, Y. Yuan, Appl. Catal. A: Gen. 239 (2003) 79–86.

[135] H. Zhua, Y. Ding, H. Yin, L. Yana, J. Xiong, Y. Lua, H. Luoa, L. Lin, Appl. Catal. A: Gen. 245 (2003) 111–117.

[136] G. Fremy, E. Monflier, J.F. Carpentier, Y. Castanet, A. Mortreux, J. Catal. 162 (1996) 339–348.

[137] S.I. Fujita, S. Akihara, S. Fujisawa, M. Arai, J. Mol. Catal. A: Chem. 268 (2007) 244–250.

[138] S.C. Tang, T.E. Paxson, L. Kim, J. Mol. Catal. 9 (1980) 313–321.

[139] Y. Uozumi, M. Nakazono, Adv. Synth. Catal. 344 (2002) 274–277.

[140] M.M. Diwakar, R.M. Deshpande, R.V. Chaudhari, J. Mol. Catal. A: Chem. 232 (2005) 179–186.

[141] J. Artner, H. Bautz, F. Fan, W. Habicht, O. Walter, M. Doring, U. Arnold, J. Catal. 255 (2008) 180–189.

[142] M. Shinoda, Y. Zhang, Y. Shiki, Y. Yoneyama, K. Hasegawa, N. Tsubaki, Catal. Commun. 4 (2003) 423–427.

[143] Y. Zhang, K. Nagasaka, X. Qiu, N. Tsubaki, Catal. Today 104 (2005) 48–54.

[144] Y. Zhang, K. Nagasaka, X. Qiu, N. Tsubaki, Appl. Catal. A: Gen. 276 (2004) 103–111.

[145] B. Li, X. Li, K. Asami, K. Fujimoto, Energy Fuels 17 (2003) 810–816.

[146] A.J. Bruss, M.A. Gelesky, G.Machado, J. Dupont, J. Mol. Catal. A: Chem. 252 (2006) 212–218.

[147] D. Han, X. Li, H. Zhang, Z. Liu, G. Hu, C. Li, J. Mol. Catal. A: Chem. 283 (2008) 15–22.

[148] D. Han, X. Li, H. Zhang, Z. Liu, J. Li, C. Li, J. Catal. 243 (2006) 318–328.

[149] R. Giordano, P. Serp, P. Kalck, Y. Kihn, J. Schreiber, C. Marhic, J.L. Duvail, Eur. J. Inorg. Chem. (2003) 610–617.

[150] A.J. Sandee, L.A. van der Veen, J.N.H. Reek, P.C.J. Kamer, M. Lutz, A.L. Spek, P.W.N.M.

van Leeuwen, Angew. Chem. Int. Ed. 38 (1999) 3231–3235.

[151] A.C. Paez, S. Castillon, C. Claver, P.W.N.M. van Leeuwen, W.G.J. de Lange, Organomet. 17 (1998) 2543–2552.

[152] A.J. Sandee, R. S. Ubale, M. Makkee, J.N.H. Reek, P.C.J. Kamer, J.A. Moulijn, P.W.N.M. van Leeuwen, Adv. Synth. Catal. 343 (2001) 201–206.

[153] A.J. Sandee, J.N.H. Reek, P.C.J. Kamer, P.W.N.M. van Leeuwen, J. Am. Chem. Soc. 123 (2001) 8468–8476.

[154] R.P.J. Bronger, J.P. Bermon, J.N.H. Reek, P.C.J. Kamer, P.W.N.M. van Leeuwen, D.N. Carter, P. Licence, M. Poliakoff, J. Mol. Catal. A: Chem. 224 (2004) 145–152.

[155] P.W.N.M. van Leeuwen, A.J. Sandee, J.N.H. Reek, P.C.J. Kamer, J. Mol. Catal. A: Chem. 182–183 (2002) 107–123.

[156] S. Ricken, P.W. Osinski, P. Eilbracht, R. Haag, J. Mol. Catal. A: Chem. 257 (2006) 78–88.

[157] S. Deprele, J.L. Montchamp, Org. Lett. 6 (2004) 3805–3808.

[158] H.T. Chang, J.M.J. Frechet, J. Am. Chem. Soc. 121 (1999) 2313–2314.

[159] J.M.J. Frechet, Science 263 (1994) 1710–1714 and references therein.

[160] D.A. Tomalia, Aldrichimica Acta 26 (1993) 91–101 and references therein.

[161] J.R. McElhanon, D.V. McGarth, J. Am. Chem. Soc. 120 (1998) 1647–1656.

[162] M.T. Reetz, G. Lohmer, R. Schwickardi, Angew. Chem. Int. Ed. Engl. 36 (1997) 1526–1529.

[163] R. Breinbauer, E.N. Jacobsen, Angew. Chem. Int. Ed. Engl. 39 (2000) 3604–3607.

[164] D. de Groot, J.C. de Wilde, R.J. van Haaren, J.N.H. Reek, P.C.J. Kamer, P.W.N.M. van Leeuwen, E.B. Eggeling, D. Vogt, H. Kooijman, A.L. Spek, A.W. van der Made, Chem. Commun. (1999) 1623–1624.

[165] L. Ropartz, K.J. Haxton, D.F. Foster, R.E. Morris, A.M.Z. Slawin, D.J.C. Hamilton, J. Chem. Soc. Dalton Trans. (2002) 4323–4334.

[166] S. C. Bourque, H. Alper, L. E. Manzer, P. Arya, J. Am. Chem. Soc. 122 (2000) 956–957.

[167] P. Arya, G. Panda, N.V. Rao, H. Alper, S.C. Bourque, L.E. Manzer, J. Am. Chem. Soc. 123 (2001) 2889–2890.

[168] S.C. Bourque, F. Maltais, W.J. Xiao, O. Tardif, H. Alper, P. Arya, L.E. Manzer, J. Am. Chem. Soc. 121 (1999) 3035–3038.

[169] P. Arya, N.V. Rao, J. Singkhonrat, J. Org. Chem. 65 (2000) 1881–1885.

[170] R.A. Reziq, H. Alper, D. Wang, M.L. Post, J. Am. Chem. Soc. 128 (2006) 5279–5282.

[171] S.M. Lu, H. Alper, J. Am. Chem. Soc. 125 (2003) 13126–13131.

[172] D.Y. Zhao, Q. Huo, J.L. Feng, B.F. Chmelka, G.D. Stucky, J. Am. Chem. Soc. 120 (1998) 6024–6036.

[173] P. Li, S. Kawi, Catal. Today 131 (2008) 61–69.

[174] J.P.K. Reynhardt, Y. Yang, A. Sayari, H. Alper, Adv. Synth. Catal. 347 (2005) 1379–1388.

[175] P. Li, S. Kawi, J. Catal. 257 (2008) 23–31.

[176] J.P.K. Reynhardt, Y. Yang, A. Sayari, H. Alper, Chem. Mater. 16 (2004) 4095–4102.

[177] J.P.K. Reynhardt, Y. Yang, A. Sayari, H. Alper, Adv. Funct. Mater. 15 (2005) 1641–1646.

[178] C.T. Kresge, M.E. Leonowicz, W.J. Roth, J.C. Vartuli, J.S. Beck, Nature 359 (1992) 710–712.

[179] D.S. Shephard, W.Z. Zhou, T. Maschmeyer, J.M. Matters, C.L. Roper, S. Parsons, B.F.G. Johnson, M.J. Duer, Angew. Chem. Int. Ed. Engl. 37 (1998) 2719–2723.

[180] T.L. Ho, Tandem Organic Reactions, Wiley: New York, 1992; L.F. Tietze, U. Beifuss, Angew. Chem. Int. Ed. Engl. 32 (1993) 131–163.

[181] R.A. Bunce, Tetrahedron 51 (1995) 13103–13159; L.F. Tietze, Chem. Rev. 96 (1996) 115–136.

[182] K. Tanabe, W.F. Holderich, Appl. Catal. A: Gen. 181 (1999) 399–434.

[183] H. Hattori, J. Jpn. Petrol. Inst. 47 (2004) 67–81.

[184] H. Pines, J.A. Veseley, V.N. Ipatieff, J. Am. Chem. Soc. 77 (1955) 6314–6321.

[185] Y. Ono, J. Catal. 216 (2003) 406–415.

[186] T. Yamaguchi, Y. Wang, M. Komatsu, M. Ookawa, Catal. Sur. Jpn. 5 (2002) 81–89.

[187] Y. Ono, T. Baba, Catalysis, vol. 15, Royal Society of Chemistry, London, (2000) p. 8.

[188] F. Figueras, Top. Catal. 29 (2004) 189–196.

[189] W.F. Hoelderich, Catal. Today 62 (2000) 115–130.

[190] H. Hattori, Appl. Catal. A: Gen. 222 (2001) 247–259

[191] R.A. Sheldon, R.S. Downing, Appl. Catal. A: Gen. 189 (1999) 163–183

[192] J. Weitkamp, M. Hunger, U. Rymsa, Micropor. Msropor. Mater. 48 (2001) 255–270.

[193] M.J. Climent, A. Corma, S. Iborra, A. Velty, J. Catal. 182–183 (2002) 327–342.

[194] G. Zhang, H. Hattori, K. Tanabe, Bull. Chem. Soc. Jpn. 62 (1989) 2070–2072.

[195] T. Seki, H. Kabashima, K. Akutsu, H. Tachikaewa, H. Hattori, J. Catal. 204 (2001) 393–401.

[196] M.T. Drexler, M.D. Amiridis, Catal. Lett. 79 (2002) 175–181.

[197] M.T. Drexler, M.D. Amiridis, J. Catal. 214 (2003) 136–145.

[198] T. Seki, H. Hattori, Catal. Sur. Asia 7 (2003) 145–156.

[199] M.A. Aramendia, V.Borau, C. Jimenez, A. Marinas, J.M. Marinas, J.R. Ruiz, F.J. Urbano, J. Mol. Catal. A: Chem. 218 (2004) 81–90.

[200] J. Kijenski, S. Malinowski, React. Kinet. Catal. Lett. 3 (1975) 343–347.

[201] J. Kijenski, S. Malinowski, Bull. Acad. Pol. Sci. Ser. Chim. 25 (1977) 501.

[202] A. Mitsutani, Catal. Today 73 (2002) 57–63.

[203] T. Yamaguchi, Y. Wang, M. Komatsu, M. Ookawa, Catal. Sur. Jpn. 5 (2002) 81–89.

[204] J.H. Clark, Chem. Rev. 80 (1980) 429–452.

[205] Y. Ono, T. Baba, Catal. Today 38 (1997) 321–337.

[206] J. Weitkamp, Solid State Ion. 131 (2000) 175–188.

[207] D. Barthomeuf, Catal. Rev. Sci. Eng. 38 (1996) 521–612.

[208] R.J. Davis, J. Catal. 216 (2003) 396–405.

[209] D. Barthomeuf, J. Phys. Chem. 88 (1984) 42–45.

[210] H. Tsuji, F. Yagi, H. Hattori, Chem. Lett. (1991) 1881–1884.

[211] Y. Wang, J.H. Zhu, J.M. Cao, Y. Chun, Q.H. Xu, Micropor. Mesopor. Mater. 26 (1998) 175–184.

[212] K. Arishtirova, P. Kovacheva, A. Predoeva, Appl. Catal. A: Gen. 243 (2003) 191–196.

[213] J. Engelhardt, J. Szanyi, J. Valyon, J. Catal. 107 (1987) 296–306.

[214] W.S. Wieland, R.J. Davis, J.M. Garces, J. Catal. 173 (1998) 490–500.

[215] A. Corma, R.M.M. Aranda, F. Sanchez, J. Catal. 126 (1990) 192–198.

[216] A. Corma, V. Fornes, R.M.M. Aranda, H. Garcia, J. Primo, Appl. Catal. 59 (1990) 237–

248.

[217] A. Corma, R.M.M. Aranda, F. Sanchez, Stud. Surf. Sci. Catal. 59 (1991) 503–511.

[218] R. Ballini, F. Bigi, E. Gogni, R. Maggi, G. Sartori, J. Catal. 191 (2000) 348–353.

[219] P.T. Wierzchowski, L.W. Zatorski, Catal. Lett. 9 (1991) 411–414.

[220] M. Tu, R.J. Davis, J. Catal. 199 (2001) 85–91.

[221] M. Huang, S. Kaliaguine, M. Muscas, A. Auroux, J. Catal. 157 (1995) 266–269.

[222] P.E. Hathaway, M.E. Davis, J. Catal. 116 (1989) 263–278.

[223] F. Yagi, H. Tshji, H. Hattori, Micropor. Mater. 9 (1997) 237–245.

[224] J.C. Kim, H.X. Li, C.Y. Chen, M.E. Davis, Micropor. Mater. 2 (1994) 413–423.

[225] D.E.D. Vos, M. Dams, B.F. Sels, P.A. Jacobs, Chem. Rev. 102 (2002) 3615–3640.

[226] S.V. Bordawekar, R.J. Davis, J. Catal. 189 (2000) 79–90.

[227] M.J. Climent, A. Corma, S. Iborra, J. Primo, J. Catal. 151 (1995) 60–66.

[228] A. Simon, J. Kohler, P. Keller, J. Weitkamp, A. Buchholz, M. Hunger, Micropor. Mesopor. Mater. 68 (2004) 143–150.

[229] J. Li, J. Tai, R.J. Davis, Catal. Today 116 (2006) 226–233.

[230] T. Frising, P. Leflaive, Micropor. Mesopor. Mater. 114 (2008) 27–63.

[231] J. Weitkamp, Solid State Ion. 131 (2000) 175–188.

[232] X. Wang, Y.H. Tseng, J.C.C. Chan, S. Cheng, J. Catal. 233 (2005) 266–275.

[233] J.I. Yu, S.Y. Shiau, A.N. Ko, Catal. Lett. 77 (2001) 165–169.

[234] D. Brunel, A.C. Blanc, A. Galarneau, F. Fajula, Cat. Today 73 (2002) 139–152.

[235] D.J. Macquarrie, Green Chem. (1999) 195–198.

[236] D.J. Macquarrie, D.B. Jackson, S. Tailland, K.A. Utting, J. Mater. Chem. 11 (2001) 1843–1849.

[237] J.H. Clark, D.J. Macquarrie, S.J. Tavener, Dalton Trans. (2006) 4297–4309.

[238] X. Wang, K.S.K. Lin, J.C.C. Chan, S. Cheng, Chem. Commun. (2004) 2762–2763.

[239] D.D. Das, P.J.E. Harlick, A. Sayari, Catal. Commun. 8 (2007) 829–833.

[240] V.S. Rao, D.E. De Vos, P.A. Jacobs, Angew. Chem. Int. Ed. 36 (1997) 2661–2663.

[241] I. Rodriguez, S. Iborra, A. Corma, F. Rey, J.L. Jorda, Chem. Commun. (1999) 593–594.

[242] B.M. Choudary, M.L. Kantam, P. Sreekanth, T. Bandopadhyay, F. Figueras, A. Tuel, J. Mol. Catal. A: Chem. 142 (1999) 361–365.

[243] S. Jaenicke, G.K. Chuah, X.H. Lin, X.C. Hu, Micropor. Mesopor. Mater. 35–36 (2000) 143–153.

[244] X. Lin, G.K. Chuah, S. Jaenicke, J. Mol. Catal. A: Chem. 150 (1999) 287–294.

[245] A. Cauval, G. Renard, D. Brunel, J. Org. Chem. 62 (1997) 749–751.

[246] P.W. Lednor, R. de Ruiter, J. Chem. Soc. Chem. Commun. (1989) 320–321.

[247] P.W. Lednor, R. de Ruiter, J. Chem. Soc. Chem. Commun. (1991) 1625–1626.

[248] P.W. Lednor, Catal. Today 15 (1992) 243–261.

[249] Gandia, R. Malm, R. Marchand, R. Conanec, Y. Laurent, M. Montes, Appl. Catal. A: Gen. 114 (1994) L1–L7.

[250] P. Grange, P. Bastians, R. Conanec, R. Marchand, Y. Laurent, Appl. Catal. A: Gen. 114 (1994) L191–L196.

[251] J.J. Benitez, J.A. Odriozola, R. Marchand, Y. Laurant, P. Grange, J. Chem. Soc. Faraday Trans. 91 (1995) 4477–4479.

[252] A. Massinon, J.A. Odriozola, Ph. Bastians, R. Conanec, R. Marchand, Y. Laurant, P. Grange, Appl. Catal. A: Gen. 137 (1996) 9–23.

[253] M.J. Climent, A. Corma, V. Fornes, A. Frau, R.G. Lopez, S. Iborra, J. Primo, J. Catal. 163 (1996) 392–398.

[254] M. N. Fripiat, P. Grange, Chem. Commun. (1996) 1409–1410.

[255] N. Fripiat, R. Conanec, A. Auroux, R. Marchand, Y. Laurent, P. Grange, J. Catal. 167 (1997) 543–549.

[256] N. Fripiat, V. Parvulescu, V.I. Parvulescu, P. Grange, Appl. Catal. A: Gen. 181 (1999) 331–346.

[257] M.A. Centeno, S. Delsarte, P. Grange, J. Phys. Chem. B 103 (1999) 7214–7221.

[258] D. Delsarte, A. Auroux, P. Grange, Phys. Chem. Chem. Phys. 2 (2000) 2821–2827.

[259] H. Wiame, C. Cellier, P. Grange, J. Catal. 190 (2000) 406–418.

[260] H. Wiame, C. Cellier, P. Grange, J. Phys. Chem. B 104 (2000) 591–596.

[261] F. Cavani, F. Trifiro, A. Vaccari, Catal. Today 11 (1991) 173].

[262] W.T. Reichle, J. Catal. 94 (1985) 547–557.

[263] P. Kustrowski, D. Sulkowska, L. Chmielarz, A.R. Lasocha, B. Dudek, R. Dziembaj, Micropor. Mesopor. Mater. 78 (2005) 11–22.

[264] H.C. Greenwell, P.J. Holliman, W. Jones, B.V. Velasco, Catal. Today 114 (2006) 397–402.

[265] D. Tichit, M.N. Bennani, F. Figueras, R. Tessier, J. Kervennal, Appl. Clay Sci. 13 (1998) 401–415.

[266] J.C.A.A. Roelofs, D.J. Lensveld, A.J. van Dillen, K.P. de Jong, J. Catal. 203 (2001) 184–191.

[267] J.I.D. Cosimo, V.K. Diez, C.R. Apesteguia, Appl. Clay Sci. 13 (1998) 433–449.

[268] S. Abello, D.V. Shankar, J.P. Ramirez, Appl. Catal. A: Gen. 342 (2008) 119–125.

[269] M.J. Climent, A. Corma, S. Iborra, K. Epping, A. Velty, J. Catal. 225 (2004) 316–326.

[270] S. Abello, D.V. Shankar, J.P. Ramirez, Appl. Catal. A: Gen. 342 (2008) 119–125.

[271] J.C.A.A Roelofs, A.J. van Dillen, K.P. de Jong, Catal. Today 60 (2000) 297–303.

[272] C.N. Perez, C.A. Perez, C.A. Henriques, J.L.F. Monteiro, Appl. Catal. A: Gen. 272 (2004) 229–240.

[273] S. Abello, F. Medina, D. Tichit, J.P. Ramirez, X. Rodriguez, J.E. Sueiras, P. Salagre, Y. Cesteros, Appl. Catal. A: Gen. 281 (2005) 191–198.

[274] K.K. Rao, M. Gravelle, J.S. Valente, F. Figueras, J. Catal. 173 (1998) 115–121.

[275] A. Guida, M.H. Lhouty, D. Tichit, F. Figueras, P. Geneste, Appl. Catal. A: Gen. 164 (1997) 251–264.

[276] S. Abello, F. Medina, D. Tichit, J.P. Ramirez, J.E. Sueiras, P. Salagre, Y. Cesteros, Appl. Catal. B: Env. 70 (2007) 577–584.

[277] E. Angelescu, O.D. Pavel, R. Birjega, R. Zavoianu, G. Costentin, M. Che, Appl. Catal. A: Gen. 308 (2006) 13–18.

[278] U. Costantino, M. Curini, F. Montanari, M. Nocchetti, O. Rosati, J. Mol. Catal. A: Chem. 195 (2003) 245–252.

[279] K. Ebitani, K. Motokura, K. Mori, T. Mizugaki, K. Kaneda, J. Org. Chem. 71 (2006) 5440–5447.

[280] D. Tichit, D. Lutic, B. Coq, R. Durand, R. Teissier, J. Catal. 219 (2003) 167–175.

[281] M.J. Climent, A. Corma, S. Iborra, A. Velty, J. Catal. 221 (2004) 474–482.

[282] A. Corma, V. Fornés, R.M.M. Aranda, F. Rey, J. Catal. 134 (1992) 58–65.

[283] A. Corma, S. Iborra, J. Primo, F. Rey, Appl. Catal. A: Gen. 114 (1994) 215–225.

[284] M.J. Climent, A. Corma, S. Iborra, J. Primo, J. Catal. 151 (1995) 60–66.

[285] H.A. Prescott, Z.J. Li, E. Kemnitz, A. Trunschke, J. Deutsch, H. Lieske, A. Auroux, J. Catal. 234 (2005) 119–130.

[286] P. Eilbracht, L. Barfacker, C. Buss, C. Hollmann, B.E.K. Rzychon, C.L. Kranemann, T. Rische, R. Roggenbuck, A. Schmidt, Chem. Rev. 99 (1999) 3329–3366.

[287] D.E. Fogg, E.N. dos Santos, Coord. Chem. Rev. 248 (2004) 2365–2379.

[288] S. Chercheja, P. Eilbracht, Adv. Synth. Catal. 349 (2007) 1897–1905.

[289] J.C. Wasilke, S.J. Obrey, R.T. Baker, G.C. Bazan, Chem. Rev. 105 (2005) 1001–1020.

[290] A. Bruggink, R. Schoevaart, T. Kieboom, Org. Proc. Res. Dev. 7 (2003) 622–640.

[291] H. Lebel, C. Ladjel, J. Organom. Chem. 690 (2005) 5198–5205.

[292] S. Chercheja, P. Eilbracht, Adv. Synth. Catal. 349 (2007) 1897–1905.

[293] L. Garcia, C. Claver, M. Dieguez, A.M.M. Bulto, Chem. Commun. (2006) 191–193.

[294] F. Goettmann, P.L. Floch, C. Sanchez, Chem. Commun. (2006) 180–182.

[295] B. Fell, P. Herrmanns, H. Bahrmann, J. Prakt. Chem. 340 (1998) 459–460.

[296] A.J. Chalk in Catalysis of Organic Reactions, P.N. Rylander, H. Greenfield, R.L. Augustine, (Editors). Marcel Dekker, New York, (1988) p. 43.

[297] J. Goa, J. Evans, Chem. Abstr. 110 (1989) 191995a.

[298] J.F. Knifton, J.J. Lin, J. Mol. Catal. 81 (1993) 1–15.

[299] J. He, M. Wei, B. Li, Y. Kang, D.G. Evans, X. Duan, Struct. Bond 119 (2006) 89–119.

[300] K. Takehiraa, T. Shishido, Catal. Sur. Asia 11 (2007) 1–30.

[301] D. Tichit, B. Coq, Cattech 7 (2003) 206–217.

[302] K. Kaneda, K. Ebitani, T. Mizugaki, K. Mori, Bull. Chem. Soc. Jpn. 79 (2006) 981–1016.

[303] L. Melo, E. Rombi, J.M. Dominguez, P. Magnoux, M. Guisnet, Stud. Surf. Sci. Catal. 78 (1993) 701–706.

[304] F. Winter, M. Wolters, A.J. van Dillen, K.P. de Jong, Appl. Catal. A: Gen. 307 (2006) 231–238.

[305] N.N. Das, S.C. Srivastava, Bull. Mater. Sci. 25 (2002) 283–289.

[306] Y.Z. Chen, C.M. Hwang, C.W. Liaw, Appl. Catal. A: Gen. 169 (1998) 207–214.

[307] A.A. Nikolopoulos, B.W.L. Jang, J.J. Spivey, Appl. Catal. A: Gen. 296 (2005) 128–136.

[308] K. Motokura, N. Fujita, K. Mori, T. Mizugaki, K. Ebitani, K. Kaneda, Tetrahedron Lett. 46 (2005) 5507–5510.

[309] K. Motokura, D. Nishimura, K. Mori, T. Mizugaki, K. Ebitani, K. Kaneda, J. Am. Chem. Soc. 126 (2004) 5662–5663.

[310] D. Tichit, C. Gerardin, R. Durand, B. Coq, Top. Catal. 39 (2006) 89–96.

[311] D. Tichit, M. de J.M. Ortiz, D. Francova, C. Gerardin, B. Coq, R. Durand, F. Prinetto, G. Ghiotti, Appl. Catal. A: Gen. 318 (2007) 170–177.

[312] D. Tichit, B. Coq, S. Cerneaux, R. Durand, Catal. Today 75 (2002) 197–202.

[313] M. de J.M. Ortiz, D. Tichit, P. Gonzalez, B. Coq, J. Mol. Catal. A: Chem. 201 (2003) 199–210.

[314] F. Goettmann, D. Grosso, F. Mercier, F. Mathey, C. Sanchez, Chem. Commun. (2004) 1240–1241.

[315] B.F. Sels, D.E.D. Vos, P.A. Jacobs, Catal. Rev. Sci. Eng. 43 (2001) 443–488.

[316] G.J. Kelly, F. King, M. Kett, Green Chem. 4 (2002) 392–399.

[317] F. King, G.J. Kelly, Catal. Today 73 (2002) 75–81.

[318] C.A. Hamilton, S.D. Jackson, G.J. Kelly, Appl. Catal. A: Gen. 263 (2004) 63–70.

[319] T. Seki, J.D. Grunwaldt, A. Baiker, Chem. Commun. (2007) 3562–3564.

[320] K. Motokura, T. Mizugaki, K. Ebitani, K. Kaneda, Tetrahedron Lett. 45 (2004) 6029–6032.

[321] C.H. Bibb, P. Fla, US Patent, 2052744 (1936) to Newport Industries, Inc.

[322] T. Nagase, G. Suzukamo, M. Fukao, US Patent, 3852305 (1974) to Sumitomo Chemical Company.

[323] P.N. Rylander, Organic Synthesis with Nobel Metal Catalysts; Academic Press: New York, (1973) p. 145.

[324] M. Martan, P.H. Reichenbacher, US Patent, 4038325 (1977) to UOP.

[325] P. Gandilhon, B.R. Charly, US Patent, 4138411 (1979) to Rhone–Poulene.

[326] L.N. Thach, D.L. Hanh, N.B. Hiep, A.S. Radhakrishna, B.B. Singh, A. Loupy, Syn.

Commun. 23 (1993) 1379–1384.

[327] T. Seki, S. Ikeda, M. Onaka, Micropor. Mesopor. Mater. 96 (2006) 121–126.

[328] V.K. Srivastava, H.C. Bajaj, R.V. Jasra, Catal. Commun. 4 (2003) 543–548.

[329] D. Kishore, S. Kannan, Appl. Catal. A: Gen. 270 (2004) 227–235.

[330] D. Kishore, S. Kannan, J. Mol. Catal. A: Chem. 223 (2004) 225–230.

[331] D. Kishore, S. Kannan, Green Chem. 4 (2002) 607–610.

[332] D. Kishore, S. Kannan, J. Mol. Catal. A: Chem. 244 (2006) 83–92.

[333] M.A. Aramendia, V. Borau, C.Jimenez, A. Marinas, J.M. Marinas, F.J. Urbano, J. Catal. 211 (2002) 556–559.

[334] F. Figueras, J. Lopez, J.S. Valente, T.T.H. Vu, J.M. Clacens, J. Palomeque, J. Catal. 211 (2002) 144–149.

[335] K. Shimazu, H. Hattori, K. Tanabe, J. Catal. 48 (1977) 302–311.

[336] U. Meyer, W.F. Hoelderich, J. Mol. Catal. A: Chem. 142 (1999) 213–222.

Chapter 2

Part–1

Synthesis of C_8 Aldehydes and Alcohol from Propylene in a Single Pot using Heterogeneous Multi–Functional Catalyst

2.1.1. Introduction

Industrially, oxo products such as aldehydes and alcohols are synthesized by hydroformylation of alkenes with synthesis gas in the presence of cobalt or rhodium based catalysts. Nearly 86% of the total hydroformylation production capacity (9 million tons/year) is based on propylene hydroformylation to give butanals (*n*– and *iso*–) and butanols (*n*– and *iso*–) as major products [1]. *n*–Butanal is largely used for the production of C_8–aldol derivatives like 2–ethylhexanal and 2–ethylhexanol, which are valuable intermediates for the production of dioctyl phthalate (DOP) and other plasticizers, coatings, adhesives, lubricants, alkyd resins and fine chemicals. *n*–Butanol is an intermediate chemical for the synthesis of esters like butyl acetate, butyl acrylate, butyl methacrylate and also used as a solvent, cleaning fluids, herbicides, dyes, printing inks, personal care products, pharmaceuticals, plasticizers, textiles and lube additives.

Presently, the synthesis of C_8 aldehydes and alcohol from propylene is a three–steps process. In the first step, hydroformylation of alkene is carried out to produce aldehyde using rhodium (Rh) or cobalt (Co) based catalysts [2]. In the second step, obtained *n*–aldehyde undergoes aldol condensation in the presence of stoichiometric amount of a strong base, namely KOH or NaOH, to produce unsaturated aldol derivatives [3, 4]. Hydrogenation of unsaturated aldol derivatives is carried out in a fixed bed catalytic reactor using nickel (Ni) or copper (Cu) catalysts in the third step [5–8]. Thus, existing commercial strategies for the production of C_8 aldol derivatives involve multi–steps process using stoichiometric amounts of hazardous base solutions and require post synthesis work–up for the separation of spent KOH or NaOH from the products' mixtures. It is estimated that approximately, 1.0–1.5 tons of spent base solutions are generated for every 10 tons of product formed in homogeneous aldol condensation. In fact, 30% of the cost of C_8 aldol derivatives is estimated to be contributed by product purification, recovery and waste treatment [9].

Research efforts to develop catalytic processes alternative to existing environmentally and economically inefficient stoichiometric chemical processes are in progress. For example, single pot synthesis of methyl isobutyl ketone (MIBK) from acetone has been reported in the literature using Pd/Mg(Al)O catalyst [10]. The aldol condensation process during production of 2–ethylhexanol has also been modified by Mitsubishi Chemicals by converting *n*–butanal into 2–ethylhexenal in the second step using basic ion–exchanger as a catalyst in the temperature range of 80–100 °C [11]. The third hydrogenation step is carried out in vapor phase over either Ni or Cu catalysts. After a three–steps distillation process, pure products are obtained. Shell and Exxon both have developed a single pot process, known as 'Aldox' process, to produce

ethylhexanol directly from propylene by adding co–catalysts such as compounds of Ti, Sn, Zn, Al, or Cu or KOH, to the cobalt based hydroformylation catalyst [12]. However, these processes still have disadvantages like the use of strong base solutions for aldol condensation of *n*–butanal, low selectivity for C_8 aldol derivatives and relatively low liquid space velocity in the hydroformylation.

The present study reports a novel approach for single pot synthesis of C_8 aldol derivatives (aldehydes and alcohol) from propylene (Scheme 2.1.1) employing a multi–functional heterogeneous catalytst [HF/HT] prepared by impregnation of a rhodium complex, $HRh(CO)(PPh_3)_3$ [HF], on the surface of a solid base, hydrotalcite [HT] having general formula $Mg_{1-x}Al_x(OH_2)^{x+}(CO_3^{2-})_{x/n}\cdot mH_2O$ [13].

2.1.2. Experimental

2.1.2.1. Materials

Propylene (99.6%), carbon monoxide (CO, 99.8%) and hydrogen (H_2, 99.98%) were procured from Alchemie Gases and Chemicals Private Limited, India. The rhodium metal precursors $RhCl_3.3H_2O$, triphenylphosphine (PPh_3), sodium borohydride ($NaBH_4$, 99.98%) and formaldehyde (HCHO, 34%) were purchased from Sigma–Aldrich, USA for the synthesis of $HRh(CO)(PPh_3)_3$ [HF] complex. Magnesium nitrate ($Mg(NO_3)_2.6H_2O$, 98.9%), aluminum nitrate ($Al(NO_3)_3.9H_2O$, 99.1%), sodium carbonate (Na_2CO_3, 99.9%) and sodium hydroxide (NaOH, 99.9%) were purchased from s. d. Fine Chemicals, India for synthesizing $(Mg_{1-x}Al_x(OH_2))^{x+}(CO_3^{2-})_{x/n}\cdot mH_2O$) [HT]. Organic solvents required for the synthesis of [HF] complex were purchased from Rankem, India and were purified by the reported methods [14]. The double distilled milli–pore deionized water was used throughout the present study.

2.1.2.2. Catalyst Synthesis

Synthesis of $HRh(CO)(PPh_3)_3$ [HF] Complex

The [HF] complex was synthesized as per reported method [15]. A solution of $RhCl_3.3H_2O$ (7.6 mmol) in ethanol (70 mL) was added into a refluxing solution of triphenylphosphine (46.0 mmol) in ethanol (300 mL). After 2 min, aqueous formaldehyde solution (10 mL) was added drop wise and the resulted solution was observed to turn yellow with the formation of *trans*–$RhCl(CO)(PPh_3)_2$. Addition of the ethanolic solution of sodium borohydride (2.0 g) into this hot mixture yielded the yellow crystals of $HRh(CO)(PPh_3)_3$. The yellow crystals were washed with

ethanol to remove unreacted rhodium metal and dried in vacuum.

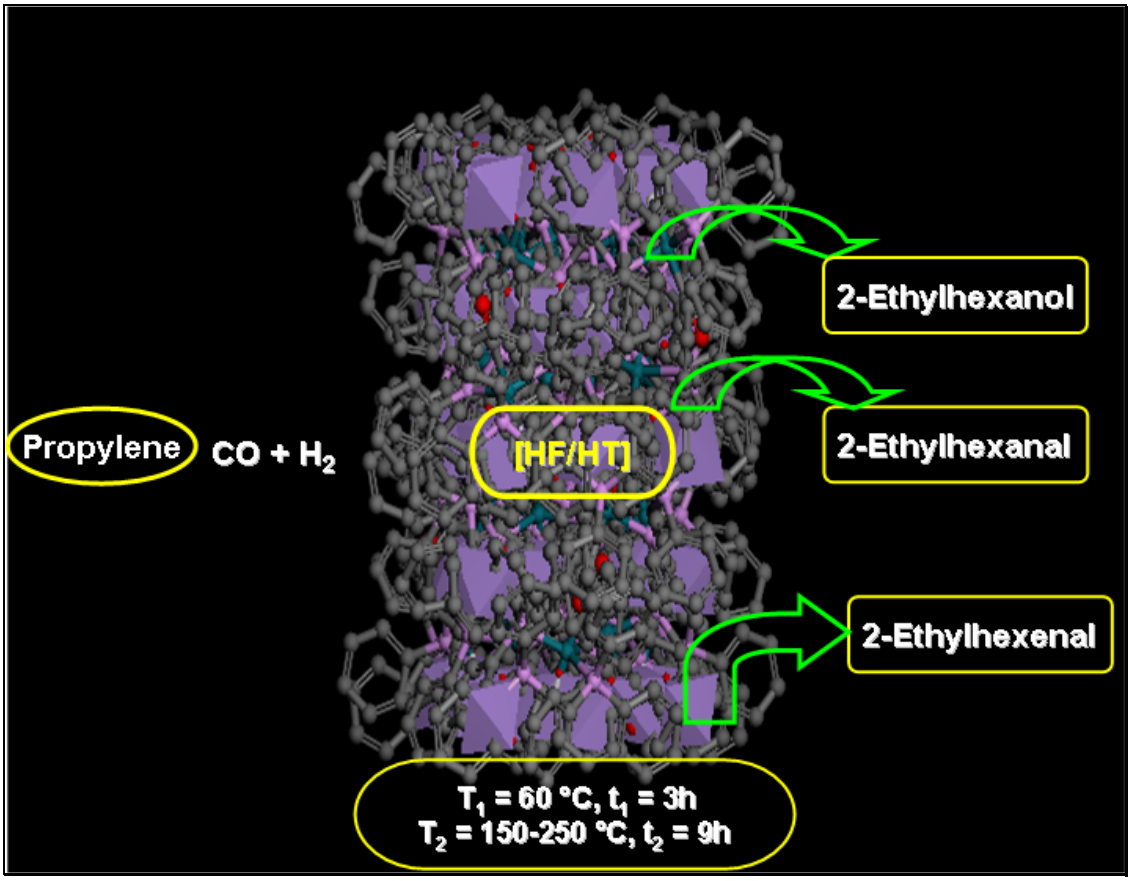

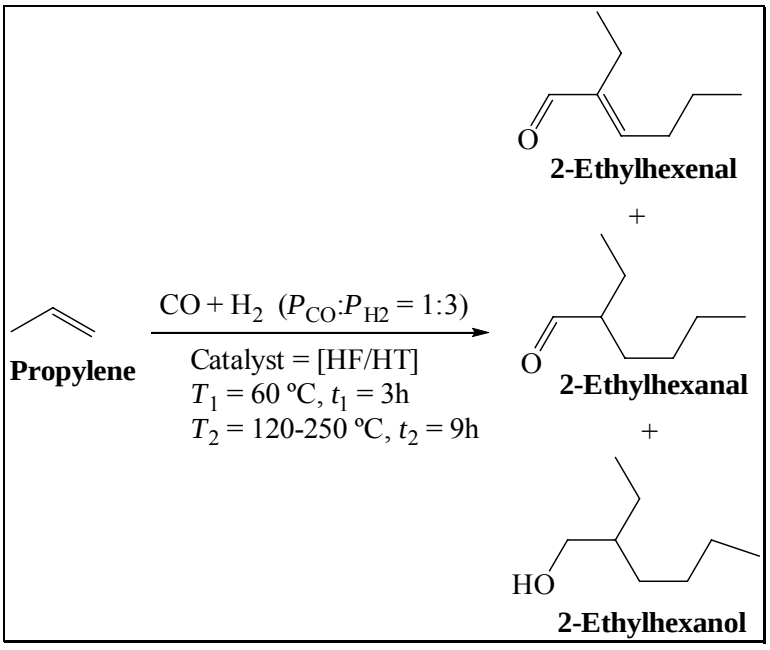

Scheme 2.1.1. Multi–functional heterogeneous catalyst [HF/HT] for single pot synthesis of C_8 aldehydes and alcohol from propylene.

Synthesis of Hydrotalcite [HT]

Co–precipitation method at constant pH was employed to synthesize the hydrotalcite [HT] samples with Mg/Al molar ratios varying from 1.5 to 3.5 [16]. Typically, an aqueous solution of $Mg(NO_3)_2.6H_2O$ (0.22 mol) and $Al(NO_3)_3.9H_2O$ (0.088 mol) in 200 mL double distilled deionized water was prepared. A second solution (200 mL) containing NaOH (0.72 mol) and Na_2CO_3 (0.21 mol) was prepared and then slowly added to the first solution in a 1 L round bottom flask over around 2 h under vigorous stirring at room temperature. The content was aged at 65 °C for 16 h. The precipitate formed was filtered and washed with hot distilled water until pH of the filtrate was neutral. The filter cake was dried in an oven at 80 °C for 12 h to give a hydrotalcite sample with Mg/Al molar ratio = 2.5. Similar procedure was followed for the synthesis of hydrotalcite samples of Mg/Al molar ratio from 1.5, 2.0, 3.0 and 3.5 by adding appropriate moles of $Mg(NO_3)_2.6H_2O$ and $Al(NO_3)_3.9H_2O$. Schematic representations for the synthesis of hydrotalcite samples of varied Mg/Al ratio are shown in Figure 2.1.1.

Synthesis of Multi–Functional Catalyst [HF/HT(X)]

Typically, a 10 mL toluene solution of [HF] complex $HRh(CO)(PPh_3)_3$ (500 mg) and triphenylphosphine (1050 mg) was added to a flask containing 3.5 g [HT(X)] (where X = Mg/Al ratio). The slurry was stirred for 32 h at room temperature under inert atmosphere (N_2). After 32 h, toluene was removed under vacuum. The final product obtained was a free flowing light yellow powder and was stored under inert atmosphere at room temperature.

2.1.2.3. Characterization of the Catalyst

Fourier transform nuclear magnetic resonance (NMR) characterization of [HF] complex was carried out on Bruker–Avance DPX 500 MHz FT–NMR system.

The C, H and N elemental analysis of [HF] complex was done by Perkin–Elmer CHNS/O 2400 analyzer.

Fourier transform infrared (FT–IR) spectra of [HF] complex, [HT(X)] and [HF/HT(X)] of different Mg/Al ratio (X) were recorded with a Perkin–Elmer spectrum GX Fourier transform infrared (FT–IR) spectrometer in the region of 400 to 4000 cm^{-1} using KBr pellets.

Powder X–ray diffraction (P–XRD) patterns of [HF] complex, [HT(X)] and [HF/HT(X)] were recorded with Phillips X'Pert MPD system equipped with XRK 900 reaction chamber, using Cu–Kα radiation (λ =1.5405 Å).

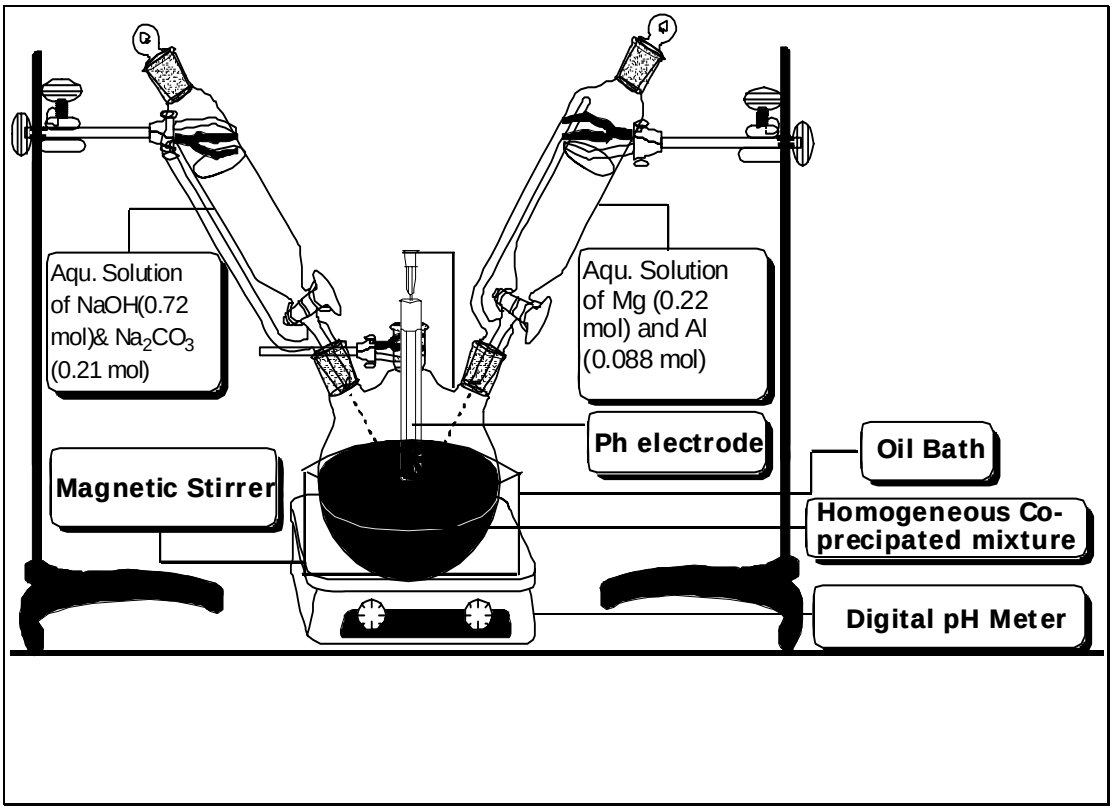

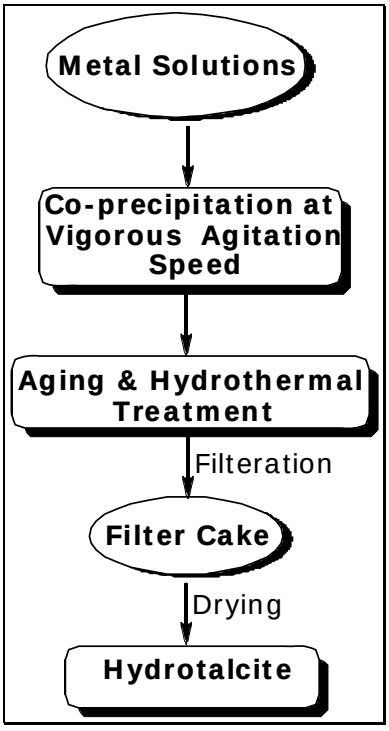

Figure 2.1.1. Synthesis of hydrotalcite.

Scanning electron microscopy (SEM) images of [HT(X)] and [HF/HT(X)] were measured on a microscope (Leo Series VP1430, Germany) having silicon detector equipped with EDX facility (Oxford instruments). The samples were coated with gold using sputter coating to avoid charging. Analysis was carried out at an accelerating voltage of 18 kV & probe current of 102 pA.

Thermogravimetric analysis (TGA) of [HF] complex, [HT(X)] and [HF/HT(X)] was carried out using a Mettler–Toledo TGA/SDTA 851e equipment in flowing N_2 (flow rate = 50 mL/min), at a heating rate of 10 °C/min and data were processed using Star^e software.

Surface area measurements of [HT(3.5)] and [HF/HT(3.5)] were carried out using ASAP 2010 Micromeritics, USA. The samples were activated at 80 °C for 4 h under vacuum (5 x 10^{-2} mmHg) prior to N_2 adsorption measurements. The specific surface area of the samples was calculated from N_2 adsorption isotherms measured at 77.4 K using Brunauer, Emmett, Teller (BET) method.

2.1.2.4. Single Pot Synthesis of C_8 Aldehydes and Alcohol

The Autoclave Reactor

All hydroformylation experiments were carried out in 100 mL stainless steel autoclave reactor (Autoclave Engineers, U.S.A.) equipped with a controlling unit. The reactor was kept in a fume cupboard having proper ventilation facilities with a strong exhaust fan. The autoclave reactor is made up for working up to 350 bar pressure and 400 °C temperature with a safety pressure rapture disc. The autoclave was designed with two gas inlet lines, one line for gas outlet and a sampling valve. The autoclave was provided with propeller type stirrer. A pressure transducer monitor system with high precision (±1%) was also connected to the reactor for online measurement of pressure drop in the autoclave reaction during the course of reaction. The temperature (±0.5 °C) and speed of stirrer (± 20 rpm) can be controlled by controlling unit, which is attached with the autoclave reactor. The controlling unit displays digitally rpm value of stirrer, pressure inside the reactor (psi) and temperatures (°C) inside and outside the autoclave reactor. The propellers in the reactor were fixed at a position in which an improved gas distribution was observed leading to intensive gas–liquid contacts with gas bubbles uniformly reacting in the liquid. The spraying of gases supplied inside the reactor occurred in such a way that sprayed gases cover all parts of the reactor. One cooling coil also provided in the reactor to control the inside reaction temperature effectively during the reaction by flowing the cooling liquid.

The safety aspects were always taken into consideration while dealing with carbon monoxide related high pressure reactions. All the high–pressure reactions were done in a high pressure laboratory, specially customized for conducting experiments at high pressure and temperature. A carbon monoxide gas detector system equipped with alarm, sensing for human tolerance limit (50 part per million) of CO, is kept in laboratory to avoid CO inhalation, in case of any leakage during handling of CO and its reaction. In addition to that, there is always medical

grade oxygen kept in laboratory to inhale in case of any emergency. The schematic representation of the autoclave reactor used for hydroformylation is shown in Figure 2.1.2.

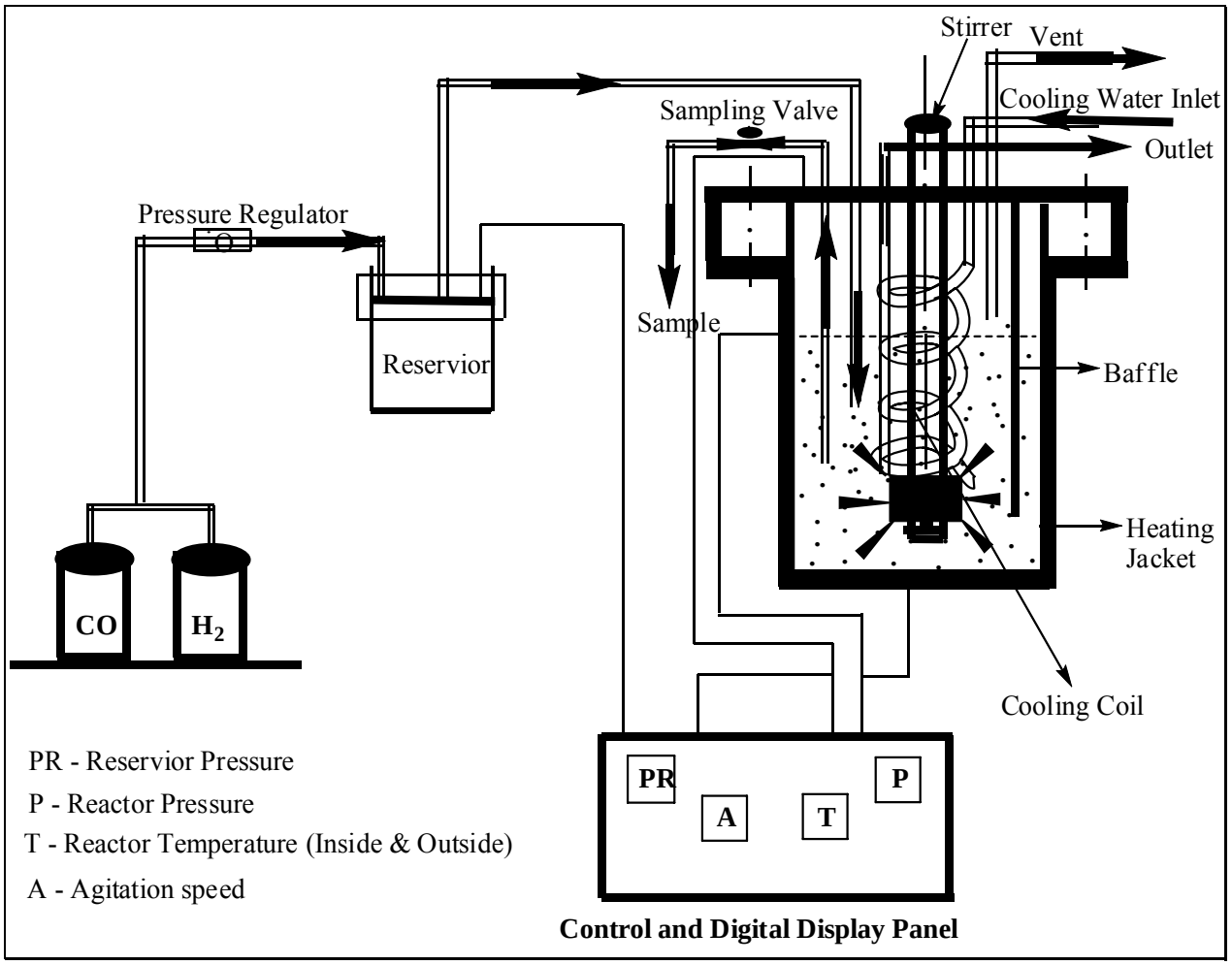

Figure 2.1.2. The autoclave reactor.

Reactions for the single pot synthesis of C_8 aldehydes and alcohol were carried out in 100 mL EZE–Seal stirred reactor supplied by Autoclave Engineers, USA, equipped with a controlling unit [17, 18]. The requisite amount of [HF/HT(X)] was added into the autoclave reactor having 50 mL toluene as a solvent. The autoclave was flushed twice with N_2 gas prior to introducing desired amount of propylene (10 atm). The reactor was then brought to 60 °C temperature (T_1) for hydroformylation reaction. Carbon monoxide and hydrogen (ratio = 1:3) gases were introduced in the reactor. The reaction was then initiated by starting the magnetic stirrer at 1000 rpm. The reaction was kept at 60 °C temperature for 3 h (t_1) following which, the reaction temperature was raised to T_2 °C to initiate aldol condensation reaction. The reaction was kept for 9 h (t_2) at T_2 °C. Reaction was continued at constant pressure by supplying CO & H_2 from the reservoir vessel. After 12 h total reaction time (t), the reactor was cooled to room temperature under flowing water in the coil provided inside the reactor. The product mixture was then analyzed using gas chromatography

(GC) and GC mass spectroscopy. For kinetic studies liquid samples were withdrawn for GC analysis by a sampling valve at different time intervals during the course of experiment [17].

2.1.2.5. Analysis of Product Mixture

Analysis of the product mixture was carried out by GC–MS (Shimadzu, GCMS–QP2010) and GC (Shimadzu 17A, Japan) equipped with 5% diphenyl and 95% dimethyl siloxane universal capillary column (60 m length and 0.25 mm diameter) and a flame ionization detector (FID). The GC oven temperature was programmed from 40 to 200 °C at the rate of 10 °C/min. N_2 was used as the carrier gas. The temperature of injection port and FID was kept constant at 250 °C. The retention time of different compounds were determined by injecting pure compound under identical GC conditions. The conversion of propylene was calculated by reported method [19, 20], using formula: $C_p = C_{po}(1–X_p)$; where X_p = conversion of propylene, C_{po} = initial concentration of propylene and calculated as $C_{po} = p_p/RT$; where p_p is the partial pressure of propylene initially. The conversion of propylene was found in the range of 95–99%. The percentage selectivity for each product was calculated by the earlier reported method [20]. To ensure reproducibility of the reaction, experiments were repeated under identical reaction conditions. The conversion and selectivity data were reproducible in the range of ± 5% variation.

In the catalyst thermal stability experiments, desired amount of [HF/HT(3.5)] catalyst was added in toluene (50 mL) as a solvent and charged into the reactor. The reactor was flushed with N_2 before introducing CO and H_2 at desired pressure. The CO and H_2 (1:3) were fed into the reactor at 20 atm. The reactor was then brought to set temperature. After 12 h reaction time, the reaction mixture was cooled to room temperature and the catalyst was filtered. The obtained solid material was dried under vacuum at room temperature. The dry solid material was characterized by the P–XRD and FT–IR analysis.

2.1.3. Results and Discussion

2.1.3.1. Characterization of the Catalyst

The appearance of doublet at 56.34 and 58.31 ppm [*J(Rh–P)* = 160 Hz] in ^{31}P–NMR spectrum of [HF] complex showed that the all three phosphorous atoms possess similar environment and are in the equatorial position. The hydride (H^-) and CO axial positions showed trigonal bipyramidal structure in the complex. The %C and %H for [HF] complex are: calculated (found): %C = 71.9 (71.6); %H = 5.0 (5.1). The %Rh in [HF] complex was calculated as 11.1%.

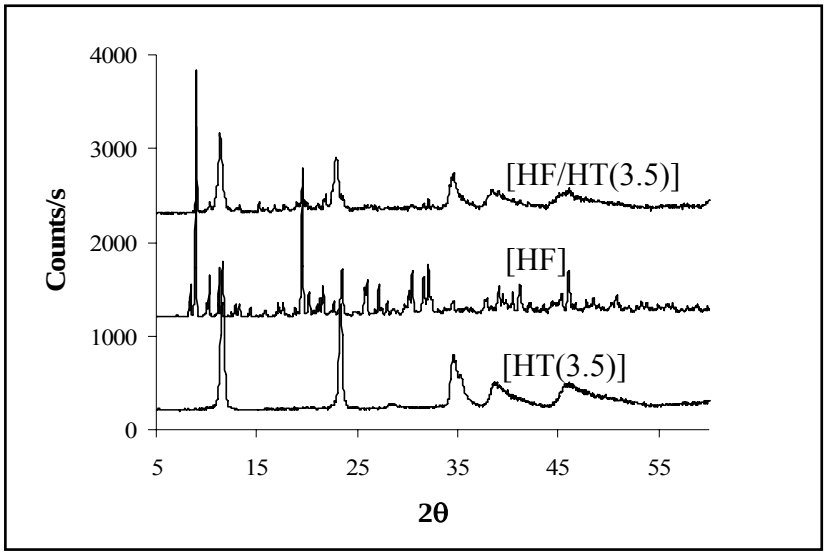

Figure 2.1.3a. P–XRD patterns of [HF] complex, [HT(3.5)] and [HF/HT(3.5)] samples.

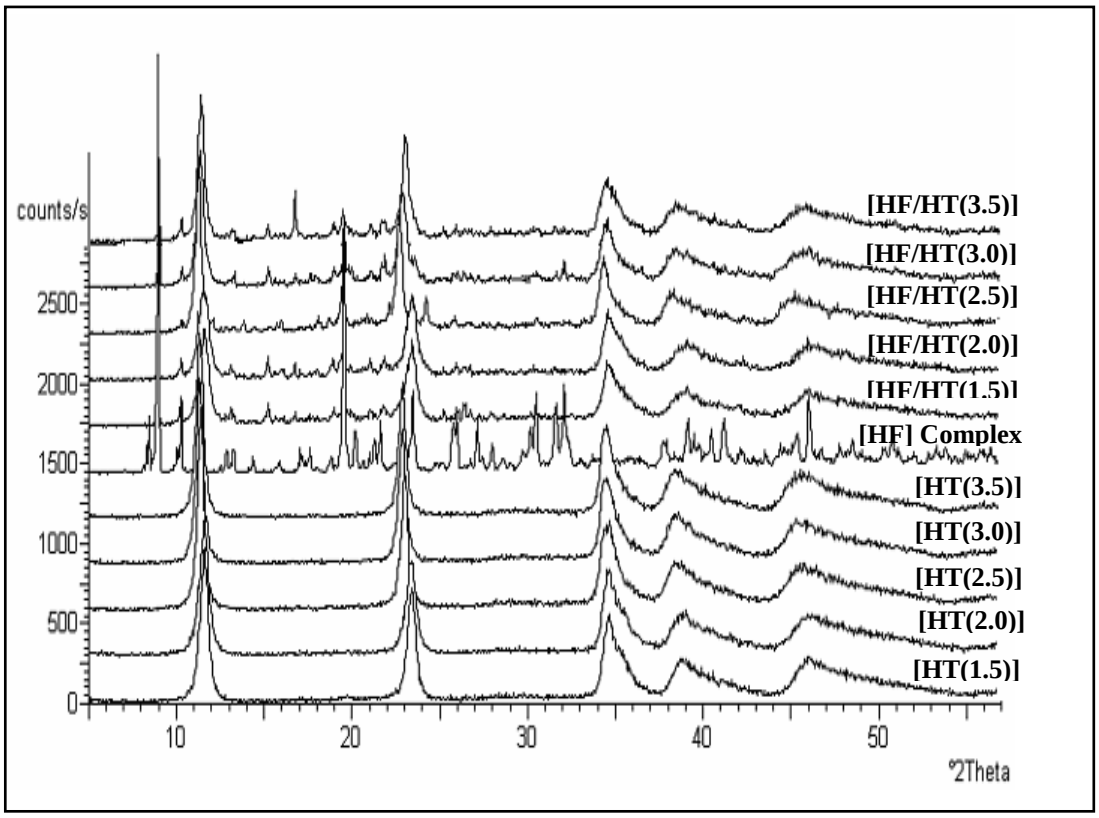

Figure 2.1.3b. P–XRD patterns of [HT] and [HF/HT] samples of varied Mg/Al molar ratio.

P–XRD patterns of [HT(X)], [HF] complex and [HF/HT(X)] are shown in Figures 2.1.3a & b. The P–XRD patterns of [HT(X)] showed sharp, intense and symmetric peaks at lower diffraction angles (2θ = 10–25) and broad asymmetric reflections at higher diffraction angles (2θ = 30–50), which are characteristics of hydrotalcite [21]. The sharp peaks at 2θ = 8.5 and 20 were observed in the P–XRD pattern of the [HF] complex and were also present in the P–XRD patterns of [HF/HT(X)] catalyst (Figure 2.1.3a). The P–XRD pattern of [HF/HT] catalyst showed that the characteristic planes of [HT] are retained after impregnation of [HF] complex. Intensity of the (00*l*)

planes of [HF/HT] catalyst, which is related to the crystallinity of [HT], decreased on the impregnation of [HF] complex. With increase in Mg/Al molar ratio of [HT] from 1.5 to 3.5, a slight shift towards lower 2θ values for the peaks corresponding to (003) and (006) planes was observed due to concurrent decrease of the positive charge of the layers of [HT] (Figure 2.1.3b). These small shifts in the peaks of the (003) and (006) planes were also observed in the P–XRD patterns of [HF/HT(X)] catalyst system. However, lack of broadening of the (00*l*) planes peaks of [HF/HT] compared to P–XRD patterns of starting [HT] sample, showed the absence of intercalation of [HF] complex into the interlayer space of [HT].

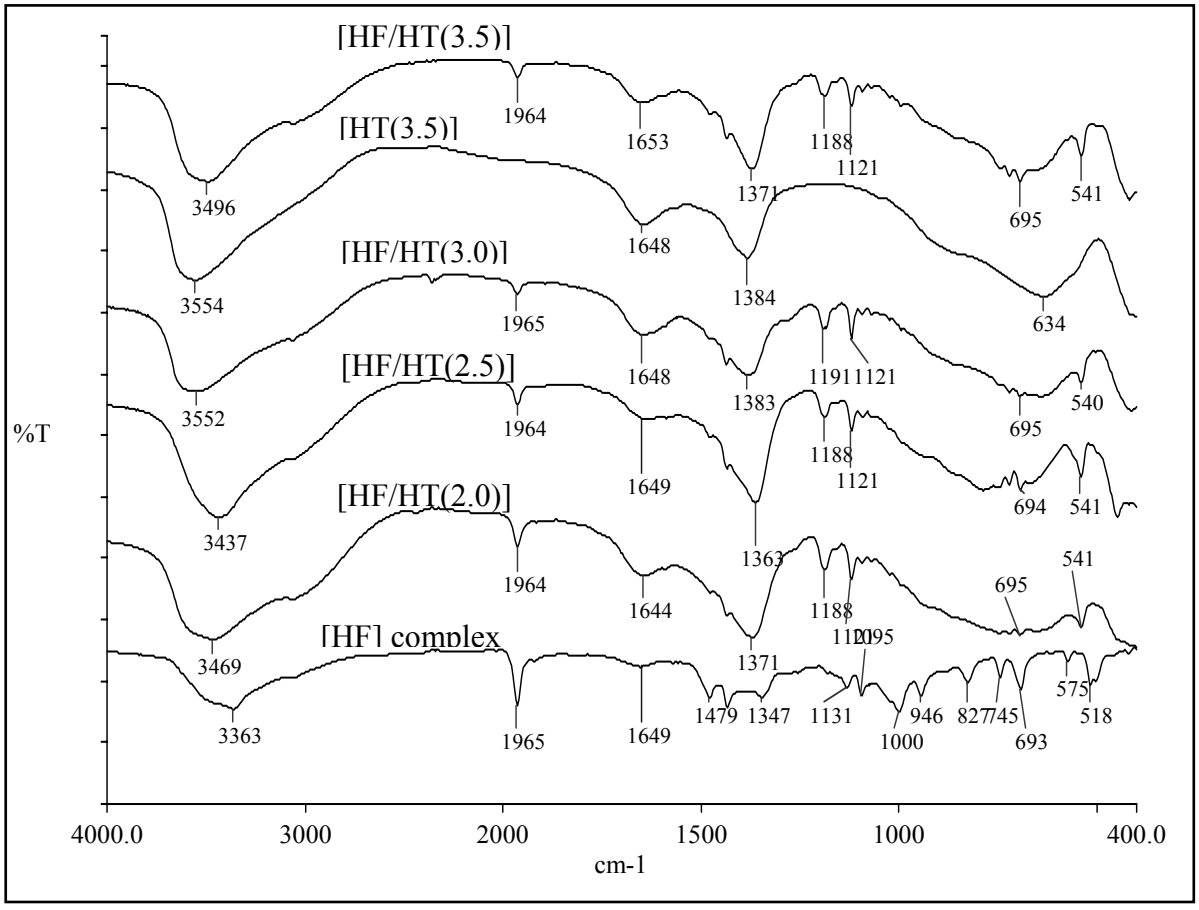

Figure 2.1.4. FT–IR spectra of [HF] complex, [HT(3.5)] and [HF/HT(X)] samples.

Appearance of band at 2036 cm^{-1} for $\nu_{(Rh-H)}$ and at 1965 cm^{-1} for $\nu_{(C=O)}$ in the FT–IR spectrum of the [HF] complex (Figure 2.1.4), confirmed the formation of [HF] complex. The FT–IR spectra of [HF/HT(X)] prepared at different Mg/Al molar ratio of HT(X) were quite similar, though, some difference was observed in the intensity and broadness of the bands. The absorption at 3500–3600 cm^{-1}, present in [HT(X)] is attributed to the H–bonding stretching vibrations of OH group in the brucite–like layer. The maximum of this band is shifted depending upon the Mg/Al molar ratio of [HT] [21]. The hydrogen stretching and bending frequencies in [HT] were increased with increase in the Mg/Al ratio from 2.0 to 3.5. In the FT–IR spectra of [HT(X)], appearance of the shoulders at 1647 cm^{-1} and 1435 cm^{-1} are the characteristic bands of H_2O and CO_3^{2-},

confirmed the formation of Mg–Al hydrotalcite samples having carbonate anions. The shoulder present at 3000 cm^{-1} is attributed to the hydrogen bonding between water molecules and the interlayer CO_3^{2-} anions. The vibration of carbonates (asymmetric stretching, ν_3) appeared at 1350–1380 cm^{-1} and could be assigned to interlayer carbonates (chelating or bridging bidentate). The lower wave number region showed a band at about 541 cm^{-1}, corresponding to the translation modes of hydroxyl groups, influenced by Al^{3+} cations. The peak appeared at 664 cm^{-1} (ν_4) is assigned to the in–plane carbonate bending [22].

SEM images were recorded to observe the effect of impregnation of [HF] complex on the morphology of the [HT]. The micrographs of the [HT(3.5)] and [HF/HT(3.5)] catalyst showed a well developed layered structure and possessed platelet structures. However, due to overlapping of such platelets spongy type structure was observed.

TGA of [HT(3.5)] showed two stages of weight loss accompanied by an endothermic transformation (Figure 2.1.5). The first weight loss (15%) was observed between 200–220 °C due to the loss of interlayer water molecules, without collapsing structure and this step is reversible [21]. The second weight loss (29%) was observed between 250–450 °C and is attributed to the removal of condensed water molecules (hydroxyl group) and carbon dioxide from the carbonate anion present in the interlayer space. The second weight loss usually appeared broad because of the simultaneous loss of water and carbon dioxide [21]. The weight loss in the TGA for [HF] complex at 150 °C is observed to be less than 4%. The 62% weight loss of [HF] complex is observed between 170–450 °C due to thermal decomposition of the complex. The weight loss observed for [HF/HT(3.5)] occurred in three steps. In the first step, only 5% weight loss was observed in temperature range 160–200 °C that increased upto 33% on increasing the temperature from 220 to 400 °C in the second step. However, on further increase in the temperature from 400 to 650 °C, the weight loss of 5% was observed. The weight losses for [HF/HT(3.5)] in the second and third steps are attributed to the removal of hydroxyl groups and carbon dioxide from the carbonate anions present in the brucite layer of [HT] and the thermal decomposition of [HF] complex.

The surface area of [HT(3.5)] was calculated as 86 m^2/g that decreased to 71 m^2/g after impregnation of [HF] complex on the surface of [HT(3.5)]. Decrease in the surface area of [HF/HT(3.5)] is due to the coverage of the pores and external surface of [HT(3.5)] by the lower surface area [HF] complex on impregnation.

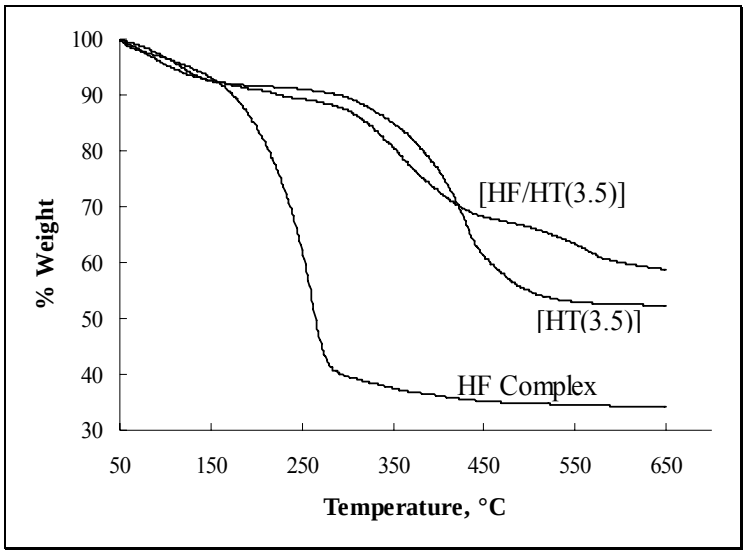

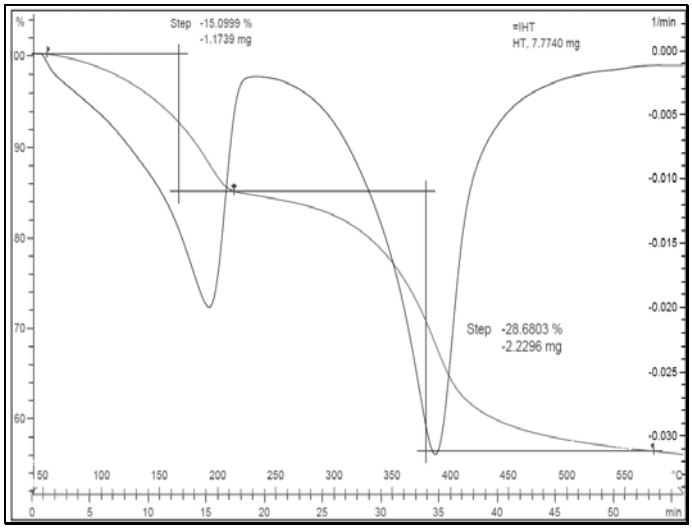

[HT(3.5)]

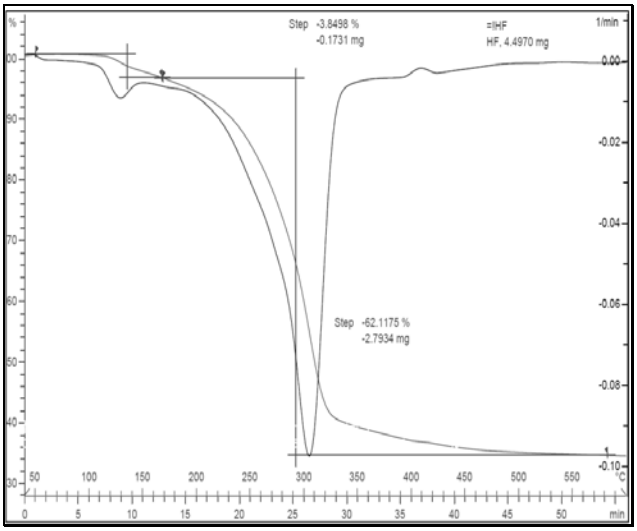

[HF Complex]

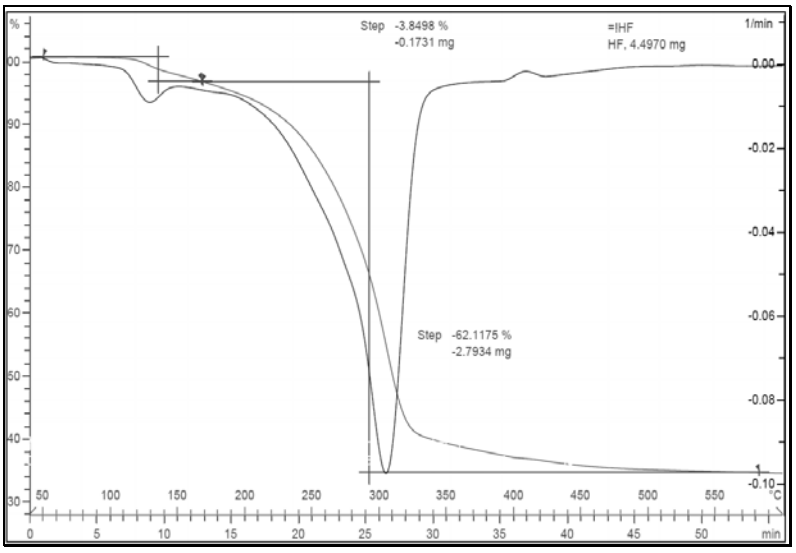

[HF/HT]

Figure 2.1.5. TGA of [HT(3.5)], [HF] complex and [HF/HT(3.5)] samples.

2.1.3.2. Single Pot Synthesis of C_8 Aldehydes and Alcohol

To understand the function of each component of multi–functional catalyst [HF/HT] during the synthesis of C_8 aldol derivatives from propylene, the proposed reaction pathways are shown in Scheme 2.1.2. The reaction gets initiated by formation of *n*–butanal via hydroformylation of propylene (Step **1**) by [HF] complex of the catalyst. This is followed by condensation step wherein two molecules of *n*–butanal undergo condensation reaction in the presence of a solid base [HT] to give 2–ethyl–3–hydroxyhexanal (β–hydroxy–aldehyde) and subsequently 2–ethylhexenal after removal of one molecule of water. The condensation of *n*–butanal is a base catalyzed reaction and dehydration of β–hydroxy–aldehyde is catalyzed by the Lewis acidic sites of the catalyst or thermal treatment [22, 23]. The [HT] constituent of the [HF/HT] catalyst facilitates the Steps **2** and **3**. The Step **4** is a hydrogenation step, which includes hydrogenation of 2–ethylhexenal to 2–ethylhexanal. As per stoichiometry, this step requires second hydrogen molecule. The [HF] complex under employed reaction conditions assists this hydrogenation step. The final Step **5** is again hydrogenation step, that involves reduction of 2–ethylhexanal to 2–ethylhexanol catalyzed by the [HF] complex. Stoichiometrically, the third hydrogen molecule is utilized in the Step **5**. Thus, the [HF] complex of the [HF/HT] catalyst plays role in three reactions, once in hydroformylation and twice in hydrogenation reactions during the single pot preparation of 2–ethylhexanol from propylene. However, possibilities of side reactions involved in one pot synthesis of 2–ethylhexanol from propylene under the hydroformylation conditions cannot be ignored. The most probable possibility is the reduction of butanals (*n*– and *iso*–) to their corresponding butanols (Step **6** and **7**) under the studied reaction conditions.

The [HF] complex can catalyze the reduction of butanals in the presence of hydrogen and this was confirmed by carrying out hydrogenation of *n*–butanal in a separate experiment by taking 2 g *n*–butanal, 20 mg [HF] complex in 50 mL solvent (toluene) at 30 atm (hydrogen) and 150 °C. Therefore, to avoid this competitive reaction, the amount of solid base [HT] in [HF/HT] catalyst and the reaction conditions, i.e., aldol reaction temperature (T_2), are to be optimized to divert the reaction towards Step **2** rather than Steps **6** and **7**. Another side reaction, cross aldol condensation of *n*– and *iso*–butanal was not observed in the present study.

The [HF/HT] catalyst was investigated in detail for the single pot synthesis of C_8 aldol derivatives from propylene under varied reaction parameters namely changing the amount of [HT] and [HF] complex, Mg/Al molar ratio (X) of [HT], aldol condensation temperature (T_2) and partial pressure of CO and H_2 at a fixed hydroformylation temperature (T_1).

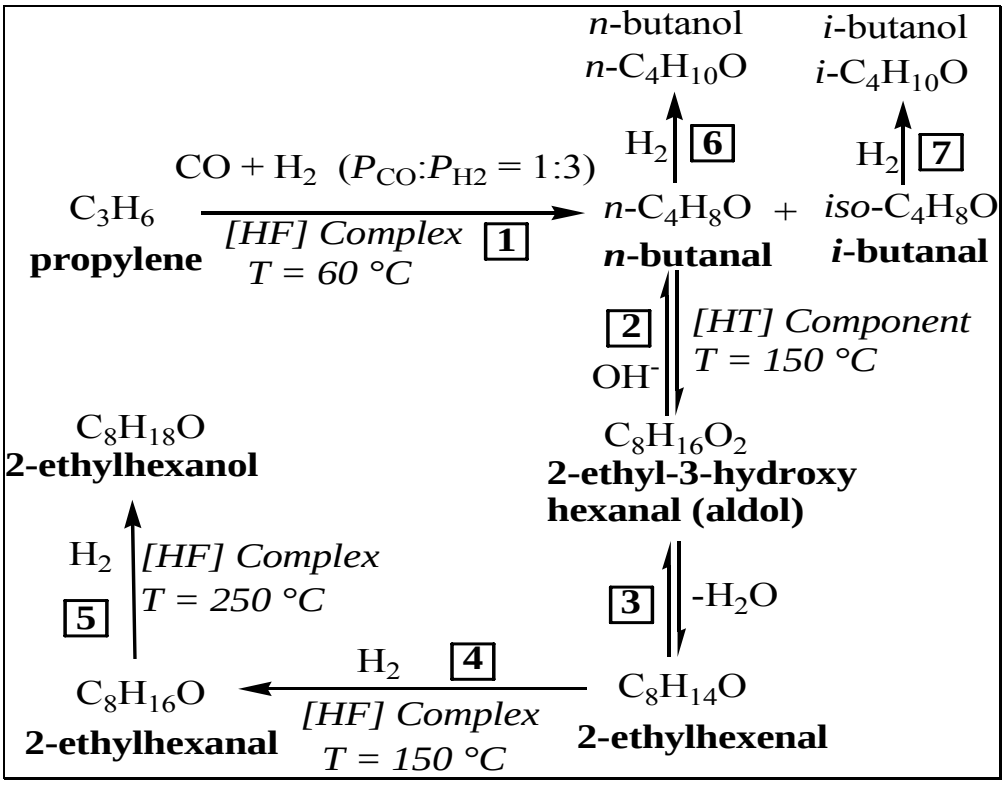

Scheme 2.1.2. Reaction pathways for the formation of 2–ethylhexanol from propylene in single step.

Preliminary experiments were carried out by taking [HF] complex and [HT] of varied Mg/Al molar ratio individually to confirm the catalytic activity of both of the components of multi-functional catalyst in our approach for the single pot synthesis of C_8 aldehydes and alcohols from propylene in a single pot. The effect of the Mg/Al molar ratio (X) of the [HT] in the [HF+HT(X)] on the selectivity of C_8 aldehydes was studied by varying the ratio from 1.5 to 3.5 and the corresponding results are given in Table 2.1.1. The selectivity of 2-ethylhexanal increased on increasing the Mg/Al molar ratio of [HT] in the [HF+HT(X)] system. The 46% selectivity of 2-ethylhexanal obtained at the ratio of 1.5 was found to be effectively increased upto 54% on increasing the ratio at 3.5. The concentration of butanals decreased in accordance to the increase of the concentration of C_8 aldol derivatives. Formation of butanols via hydrogenation of the butanals was also observed under studied experimental conditions. The results depicted in Table 2.1.1 confirmed that the both catalyst are working satisfactorily for the single pot synthesis of C_8 aldol derivatives from propylene. The further detail study was carried out by taking [HF] complex impregnated on [HT] as a multi-functional catalyst [HF/HT].

Table 2.1.1. Effect of Mg/Al Molar Ratio (X) of HT on the Selectivity of C_8 Aldehydes using [HF+HT(X)]

entry	Mg/Al molar ratio (X)	% selectivity			
		2-ethylhexanal	2-ethylhexenal	butanals	butanols
1	1.5	46	17	34	3
2	2.0	47	20	31	2
3	2.5	50	17	30	3
4	3.5	54	13	29	4

Reaction conditions: partial pressure of propylene = 10 bar, partial pressure of CO = 5 bar, partial pressure of H_2 = 15 bar, [HF+HT(X)] = 700 mg, T_1 = 60 °C, t_1 = 3h, T_2 = 150 °C, t_2 = 9 h, total time (t) = 12 h.

2.1.3.3. Effect of Mg/Al Molar Ratio (X) of [HT] in the [HF/HT(X)]

The effect of Mg/Al molar ratio (X) from 1.5 to 3.5 of [HT] in the [HF/HT(X)] catalyst was studied at 150 °C and 250 °C (Figures 2.1.6 and 2.1.7) aldol condensation temperatures (T_2) while keeping the hydroformylation temperature (T_1) constant at 60 °C. Mass fragmentation data of the product mixture is shown in Figure 2.1.8. The selectivity for 2–ethylhexanal was observed to increase linearly upto 45% on increase in the Mg/Al molar ratio of hydrotalcite from 1.5 to 3.5 at 150 °C aldol condensation temperature. The selectivity of butanal was found to decrease on increase in the Mg/Al molar ratio of hydrotalcite samples.

Significant amount of 2–ethylhexanol was formed by conducting the experiments at higher T_2 (250 °C) within 12 h reaction time by hydrogenation of 2–ethylhexanal. The selectivity for 2–ethylhexanol was observed to increase from 11 to 21% on increasing the Mg/Al molar ratio of [HT] from 1.5 to 3.5. On increasing the total reaction time to 24 h, the selectivity for 2–ethylhexanol was observed to increase upto 27% at the Mg/Al molar ratio of [HT] 1.5. Higher selectivity for C_4 and C_8 aldehydes was observed at 150 °C as compared to 250 °C. Lower selectivity for C_4 and C_8 aldehydes at 250 °C was observed due to continuous hydrogenation of aldehydes to the respective alcohols at employed reaction conditions, thereby, butanols and 2–ethylhexanol were formed as major products at higher T_2.

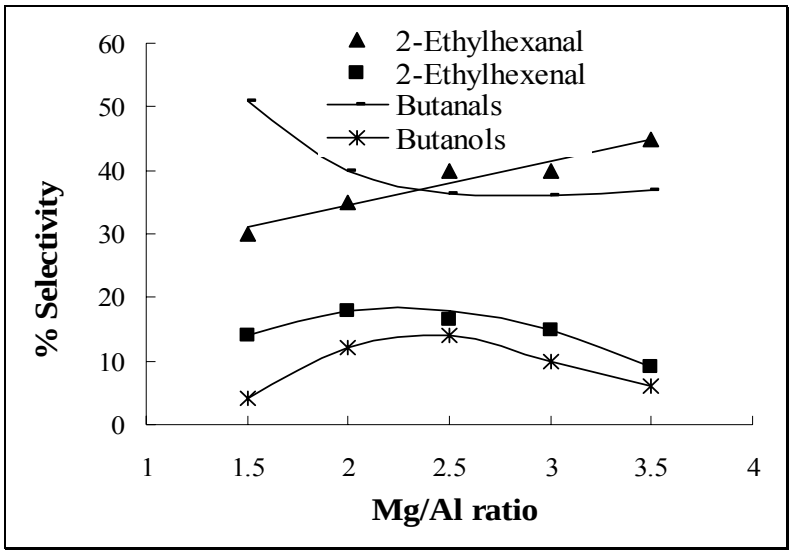

Figure 2.1.6. Effect of Mg/Al molar ratio of [HT] in [HF/HT] at 150 °C aldol temperature (T_2), partial pressure of propylene = 10 atm, CO = 5 atm, H_2 = 15 atm, [HF/HT] = 700 mg, HT/HF ratio =7, T_1 = 60 °C, t_1 = 3 h, T_2 = 150 °C, t_2 = 9 h, total time (t) = 12 h.

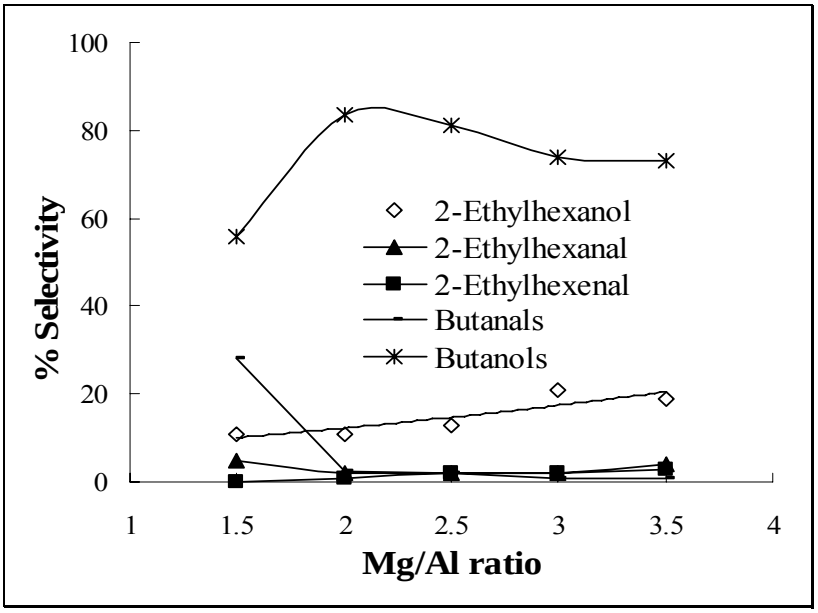

Figure 2.1.7. Effect of Mg/Al molar ratio of [HT] in [HF/HT] at 250 °C aldol temperature (T_2), partial pressure of propylene = 10 atm, CO = 5 atm, H_2 = 15 atm, [HF/HT] = 700 mg, HT/HF ratio =7, T_1 = 60 °C, t_1 = 3 h, T_2 = 250 °C, t_2 = 9 h, total time (t) = 12 h.

Increase in the selectivity for C_8 aldol derivatives with increasing magnesium content in [HT] is explained in terms of enhanced basicity of [HT] which aids condensation reaction. It is known that the basicity of a hydrotalcite increases with increasing the Mg/Al molar ratio of [HT][24–27]. Two types of basic sites are identified for hydrotalcite, one weaker Brønsted OH^- and second, stronger Lewis O^{2-} sites, but in the present study basicity of the hydrotalcite is mainly resulting from surface hydroxyl groups [23]. The Brønsted OH^- sites are responsible for the aldol

condensation of *n*–butanal to β–hydroxy–aldehyde and weak acidic sites are responsible for dehydration of β–hydroxy–aldehyde [22, 23]. 2–Ethylhexenal is produced by the dehydration of aldol condensation dimer by weaker acidic sites present on the hydrotalcite surface of [HF/HT] catalyst**.**

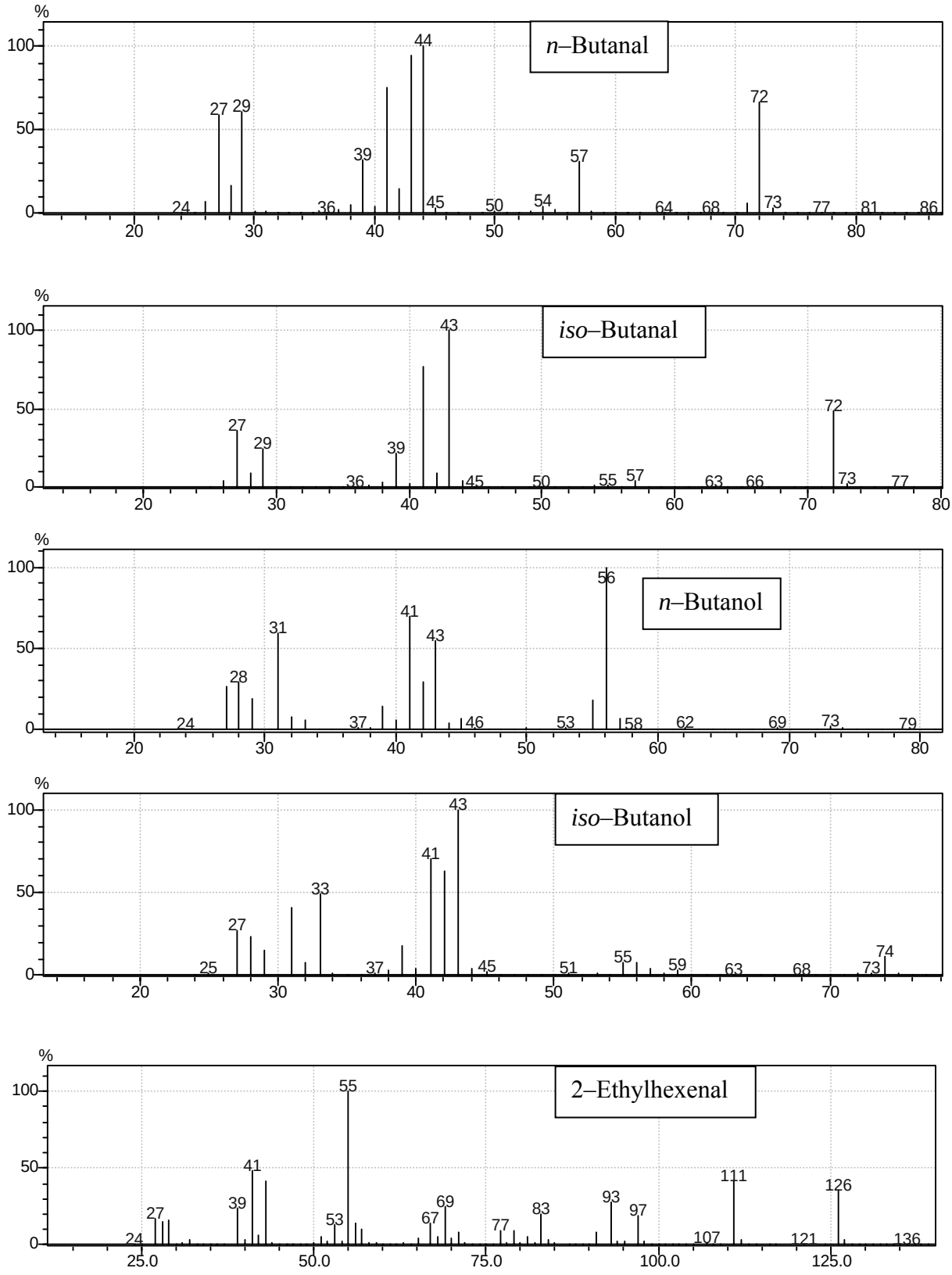

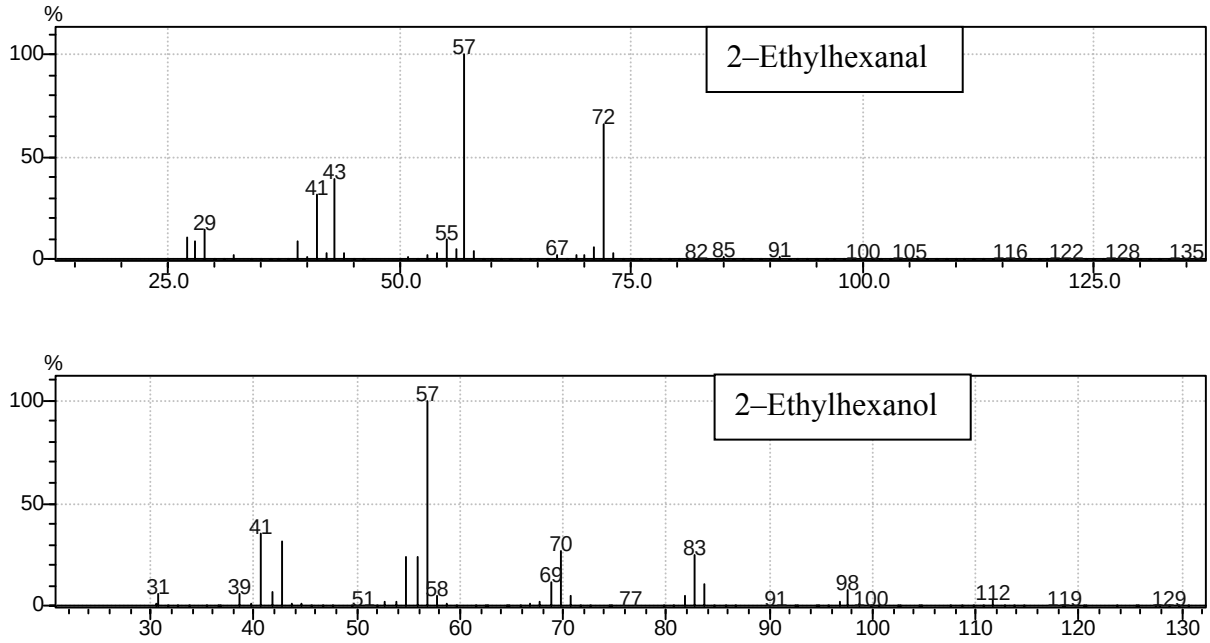

Figure 2.1.8. Mass fragmentation data of the product mixture for single pot synthesis of C_8 aldol derivatives from propylene.

2.1.3.4. Effect of [HT(3.5)] to [HF] Complex Ratio

Effect of the variation of [HT(3.5)] amount in the [HF/HT(3.5)] catalyst on the selectivity of C_8 aldol derivatives was studied by varying the amount of [HT(3.5)] from 100 to 1000 mg. The selectivity for 2–ethylhexanal was observed to increase from 7 to 48% (Table 2.1.2) on increase in the amount of [HT(3.5)] from 100 to 1000 mg. The selectivity of 2–ethylhexenal was observed to increase on increasing the amount of the [HT(3.5)]. Decrease in selectivity for butanals and butanols showed that the condensation reaction become predominant with increase in the amount of [HT] in [HF/HT(3.5)] catalyst.

The effect of amount of [HF] complex on the selectivity of products was studied by varying the amount of [HF] complex from 15 to 160 mg in the [HF/HT(3.5)] catalyst at constant amount of the [HT(3.5)] (Table 2.1.3). On increase in the amount of [HF] complex from 15 to 100 mg, the selectivity for 2–ethylhexanal increased significantly and was found to be maximum 45% at 100 mg [HF] complex amount. On further increasing the amount of [HF] complex, the selectivity for 2–ethylhexanal was observed to decrease at the expense of increase in the selectivity for butanols.

Table 2.1.2. Effect of [HT(3.5)] in [HF/HT(3.5)] on the selectivity for C_8 aldol derivatives

Run	[HT(3.5)] (mg)	% Selectivity [a]			
		2–Ethylhexanal	2–Ethylhexenal	Butanals	Butanols
1	100	7	0	43	50
2	300	24	8	50	18
3	500	43	6	45	6
4	700	45	9	40	6
5	1000	48	13	39	0

[a] **Reaction conditions:** propylene = 10 atm, CO = 5 atm, H_2 = 15 atm, [HF] complex = 100 mg, T_1 = 60 °C, t_1 = 3 h, T_2 = 150 °C, t_2 = 9 h, total time (t) = 12 h.

Table 2.1.3. Effect of [HF] complex in [HF/HT(3.5)] on the selectivity for C_8 aldol derivatives

Run	[HF] complex (mg)	% Selectivity [a]			
		2–Ethylhexanal	2–Ethylhexenal	Butanals	Butanols
1	15	24	10	51	15
2	30	29	12	41	18
3	50	37	20	31	12
4	100	45	9	40	6
5	125	43	22	14	21
6	160	27	16	17	40

[a] **Reaction conditions:** propylene = 10 atm, CO = 5 atm, H_2 = 15 atm, [HT(3.5)] = 700 mg, T_1 = 60 °C, t_1 = 3h, T_2 = 150 °C, t_2 = 9 h, total time (t) = 12 h.

Higher selectivity for butanols observed at lower amount of [HT(3.5)] could be due to the presence of insufficient amount of solid base in the [HF/HT(3.5)] catalyst to carry out aldol condensation reaction. The active catalyst for aldol condensation of *n*–butanal possesses basic sites (hydroxyl groups) on their surface which are responsible for the condensation reaction [28]. At the lower HT/HF ratio, amount of hydroformylation complex is more on the surface of [HT]. The impregnated [HF] complex on the surface could be blocking the basic sites of [HT], and thereby, suppressing the condensation reaction. Therefore, at higher amount of [HF] complex, the hydrogenation of aldehydes is observed to be more pronounced than the aldol condensation of *n*–

butanal. Maximum selectivity for C_8 aldol derivatives were observed at higher amount of [HT] due to the availability of more basic sites for the condensation reaction on the surface of the multi–functional catalyst.

2.1.3.5. Effect of Aldol Temperature (T_2)

The results given in Figures 2.1.6 and 2.1.7 show that the reaction is significantly influenced by the aldol condensation temperature (T_2). The effect of T_2 on the selectivity of C_8 aldol derivatives was studied at different T_2 (120 to 250 °C) using [HF/HT(3.5)] catalyst (Table 2.1.4). The selectivity for 2–ethylhexanal was found to increase from 14% to 61% on increasing the aldol condensation temperature (T_2) from 120 to 200 °C. The formation of 2–ethylhexanol was not observed in the T_2 range of 120 to 200 °C. On further increasing the temperature T_2 from 200 to 250 °C, the selectivity for 2–ethylhexanal was decreased from 61% to 4% due to the higher selectivity of the hydrogenation products of aldehydes. The selectivity for 2–ethylhexanol, which is formed by the hydrogenation of 2–ethylhexanal catalyzed by [HF] component of [HF/HT(3.5)] catalyst, was observed to 18%. At 250 °C, selectivity for the butanols sharply increased from 27% (at 200 °C) to 75%. The selectivity for butanals was found to decrease from 73% to 1% on increasing the T_2 from 120 °C to 250 °C. The rapid decrease in selectivity for butanals on increasing T_2 shows the consumption of butanals either for the aldol condensation or reduction to butanols.

Table 2.1.4. Effect of aldol reaction temperature (T_2) on the selectivity for C_8 aldol derivatives using [HF/HT(3.5)]

Run	T_2 °C	% Selectivity [a]				
		2–Ethylhexanol	2–Ethylhexanal	2–Ethylhexenal	Butanals	Butanols
1	120	–	14	2	73	11
2	150	–	45	9	40	6
3	200	–	61	3	9	27
4	250	18	4	2	1	75
5[b]	150	–	54	8	21	17
6[c]	250	27	4	5	1	63

[a] **Reaction conditions:** propylene = 10 atm, CO = 5 atm, H_2 = 15 atm, [HF/HT(3.5)] = 700 mg, HT/HF = 7, T_1 = 60 °C, t_1 = 3 h, t_2 = 9 h, total time (t) = 12 h.

[b] Single reaction temperature (T) = 150 °C for 12 h.

[c] Total time (t) = 24 h, Mg/Al molar ratio of [HT] = 1.5.

It was observed from the results (Table 2.1.4), that the higher temperature favored butanals reduction, that is catalyzed by the [HF] complex present in the [HF/HT(3.5)] catalyst. It is clear from the TGA data that the [HF] complex present in [HF/HT(3.5)] catalyst was stable upto 150 °C, and after that decomposition was observed. The decomposition of the [HF] complex may results into a rhodium species which could be more active for hydrogenation of aldehydes. To confirm this assumption, one separate experiment was carried out by taking *n*–butanal (2 g) as reactant in 50 mL of toluene as solvent at 250 °C and at 30 atm pressure of H_2 with 700 mg [HF/HT(3.5)] catalyst for 12 h reaction time. After 12 h, 72% selectivity for butanols was observed which are in accordance with the results observed in case of single pot synthesis using propylene as a reactant (Run 4, Table 2.1.4).

An important observation that was made regarding the selectivity for 2–ethylhexanal, increased from 45% to 54% on carrying out the experiment at a single temperature (T = 150 °C) rather than in two stages at temperatures at 60 °C and 150 °C (Run 2 and 5, Table 2.1.4). One of the possible reasons for higher selectivity on carrying the reaction at a single temperature (150 °C) could be the increased activity of solid base component [HT(3.5)] of multi–functional catalyst system for condensation reaction at the beginning of the reaction.

2.1.3.6. Effect of the Partial Pressures of CO and H_2

The effect of varied partial pressures of CO and H_2 (1: 3) from 13 to 80 atm on selectivity of C_8 aldol derivatives was studied using [HF/HT(3.5)] catalyst (Table 2.1.5). Partial pressures of CO and H_2 were varied at constant CO to H_2 ratio (1: 3).

Table 2.1.5. Effect of the partial pressures of CO and H_2 on the selectivity for C_8 aldol derivatives using [HF/HT(3.5)]

Run	Pressures, atm		% Selectivity [a]			
	CO	H_2	2–Ethylhexanal	2–Ethylhexenal	Butanals	Butanols
1	3	10	38	12	42	8
2	5	15	45	9	40	6
3	10	30	47	7	38	8
4	15	45	40	7	39	14
5	20	60	47	9	31	13

[a] **Reaction conditions:** propylene = 10 atm, [HF/HT(3.5)] = 700 mg, HT/HF = 7, T_1 = 60 °C, t_1 = 3 h, T_2 = 150 °C, t_2 = 9 h, total time (t) = 12 h.

For example, selectivity of 2–ethylhexanal was observed to increase from 38 to 47% on increasing the partial pressures of CO and H_2 from 13 to 40 atm. After that, the selectivity decreased from 47 to 40% on increasing the partial pressures of CO and H_2 from 40 to 60 atm. However, the selectivity of 2–ethylhexanal was found to increase from 40 to 47% on increasing the partial pressures of CO and H_2 from 60 to 80 atm. The formation of butanols was observed via hydrogenation of butanals with higher selectivity at higher partial pressure of CO and H_2.

2.1.3.7. Kinetic Profiles for Single Pot Synthesis of C_8 Aldol Derivatives

In order to calculate the rate of reaction for hydroformylation of propylene, aldol condensation of *n*–butanal and hydrogenation of 2–ethylhexenal, separate experiments were conducted by taking propylene, *n*–butanal and 2–ethylhexenal as a reactant under the reaction conditions identical to those used for single pot synthesis of C_8 aldol derivatives from propylene. Initially, kinetic experiments were carried out by varying the agitation speed from 100 to 1200 rpm. The rate of reaction was observed to be independent on agitation speed after 600 rpm, which indicate negligible diffusional (mass transfer) resistance. To ensure the reaction is in purely kinetic region, all the kinetic experiments were performed at 1000 rpm agitation speed. The rate of reaction for hydroformylation of propylene, aldol condensation of *n*–butanal and hydrogenation of 2–ethylhexenal were found to be 20 x 10^{-2} M/h, 2.8 x 10^{-2} M/h and 8 x 10^{-2} M/h, respectively. These rate of reaction values showed that the hydroformylation of propylene for synthesis of butanals is the fastest reaction. Condensation of *n*–butanal for the production of 2–ethylhexenal is the slowest reaction among all the three subsequent reactions. These rates of reactions were followed the order of $k_1 > k_3 > k_2$. The rate of 2–ethylhexenal formation is dependent on the rate of aldol condensation of *n*–butanal, which is catalyzed by [HT] of [HF/HT] catalyst. The rate of hydrogenation of 2–ethylhexenal is also slower than the hydroformylation of propylene. After the hydroformylation of propylene, butanals can either undergo aldol condensation or hydrogenation depending on the reaction conditions. Kinetic profile shown in Figure 2.1.9 for the single pot synthesis of C_8 aldol derivatives using [HF/HT] catalyst gave important information for the formation of various products at different stages with time to arrive at the actual reaction pathways. The formation of butanals via propylene hydroformylation at 60 °C catalyzed by the [HF] complex of [HF/HT(3.5)] catalyst was observed upto 3 h. The rate (k_1) of butanals formation by propylene hydroformylation (Equation 1) was calculated as 20 x 10^{-2} M/h.

$$k_1 = d\,[\text{butanals}]/\,dt \qquad (1)$$

As the T_1 increased to T_2, the formation of 2–ethylhexenal was seen after 3.25 h via aldol condensation of *n*–butanal. The rate (k_{-1}) of consumption of butanals (Equation 2) in terms of the

decrease in concentration of butanals was found to be 2.6 x 10^{-2} M/h .

$k_{-1} = -$ d [butanals]/ dt (2)

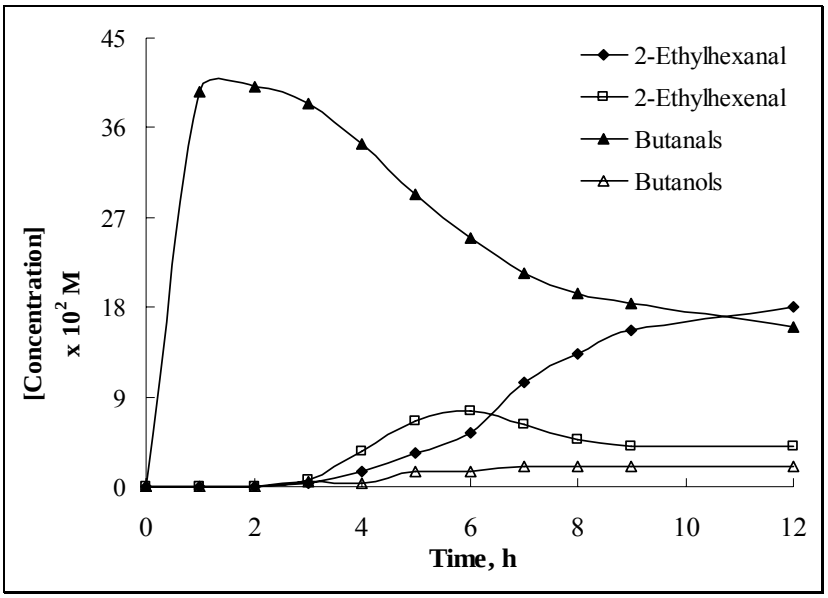

Figure 2.1.9. Kinetic profiles for synthesis of C_8 aldol derivatives from propylene in single step using [HF/HT(3.5)] catalyst at partial pressure of propylene = 10 atm, CO = 5 atm, H_2 = 15 atm, [HF/HT(3.5)] = 700 mg, HT/HF ratio =7, T_1 = 60 °C, t_1 = 3 h, T_2 = 150 °C, t_2 = 9 h, t = 12 h.

The concentration of 2–ethylhexenal was linearly increased up to 6 h with appreciable rate (k_2, Equation 3), 2.28 x 10^{-2} M/h and after that its concentration decreased with rate (k_{-2}, Equation 4), 0.9 x 10^{-2} M/h.

k_2 = d [2–ethylhexenal]/ dt (3)

$k_{-2} = -$ d [2–ethylhexenal]/ dt (4)

The decrease in the concentration of 2–ethylhexenal indicates its consumption for the formation of 2–ethylhexanal in the presence of hydrogen. Similar to the formation of 2–ethylhexenal, the formation of its hydrogenated product 2–ethylhexanal was observed after 3.25 h reaction time. As the reaction time increased, the formation of 2–ethylhexanal was found to be increased up to 9 h, with decrease in the concentration of 2–ethylhexenal, due to the simultaneous consumption of 2–ethylhexenal into the formation of 2–ethylhexanal. Concentration of 2–ethylhexanal was observed to increase with its formation rate (k_3, Equation 5), 2.13 x 10^{-2} M/h.

k_3 = d [2–ethylhexanal]/ dt (5)

After 9 h reaction time, no significant changes in the concentration of 2–ethylhexanal and

2–ethylhexenal were observed. Formation of butanols was also observed with very slow rate (k_4, Equation 6), 0.20 x 10^{-2} M/h started almost at the same time when formations of C_8 aldol derivatives were observed.

$$k_4 = d\,[\text{butanols}]/\,dt \qquad (6)$$

Most of the butanals concentration was found to contribute for the formation of 2–ethylhexenal with a little formation of butanols since a nice balance in the rate of formation of products and consumption of butanals ($k_{-1} = \sim(k_2 + k_4)$) was observed under the employed reaction conditions. Summation of the rates k_2 and k_4 ($k_2 + k_4$ = 2.48 x 10^{-2} M/h) was found to be almost identical with the rate k_{-1}(2.60 x 10^{-2} M/h).

The detailed kinetics including the rates of formation of butanals, butanols, 2–ethylhexenal, and 2–ethylhexanal was investigated as a function of Mg/Al molar ratio of [HT] in the [HF/HT(3.5)] catalyst, aldol condensation temperature (T_2) at a fixed hydroformylation temperature (T_1), amount of [HT] and [HF] complex using [HF/HT(3.5)] catalyst for the synthesis of C_8 aldol derivatives from propylene in a single pot.

Effect of Mg/Al molar ratio of [HT] on the rates of products formation at 150 and 250 °C aldol temperature (T_2)

Effect of Mg/Al molar ratio of [HT] on the rates of formation of products was studied at 150 and 250 °C aldol temperature (T_2) by varying the Mg/Al molar ratio of [HT] from 1.5 to 3.5 in the [HF/HT] catalyst (Table 2.1.6). At 150 °C, the rate of formation of 2–ethylhexanal was observed to increase on increasing the Mg/Al molar ratio of [HT]. At Mg/Al molar ratio of 1.5, the rate of formation of 2–ethylhexanal determined to be 1.41 x 10^{-2} M/h was increased to 2.13 x 10^{-2} M/h on increasing the Mg/Al molar ratio of [HT] upto 3.5. Similar to the rate of formation of 2–ethylhexanal, the rate of formation of 2–ethylhexenal was also observed to increase on increasing the Mg/Al molar ratio of [HT]. At all the studied Mg/Al molar ratios, the rate of formation of 2–ethylhexenal was observed to be slightly higher than the rate of formation of 2–ethylhexanal. The rate of formation of butanals was decreased regularly from 27.5 x 10^{-2} M/h at Mg/Al molar ratio 1.5 to 20 x 10^{-2} M/h at Mg/Al molar ratio of [HT] 3.5. Rates of the formation of butanols were extremely slow. At 150 °C aldol temperature, the formation of the 2–ethylhexanol was not observed in the entire studied reaction conditions for the single pot synthesis of C_8 aldol derivatives from propylene.

Table 2.1.6. Effect of the Mg/Al molar ratio of [HT] on the rates of products formation at 150 °C aldol temperature (T_2) [a]

Run	Mg/Al Molar ratio	$k_3 \times 10^2$ M/h	$k_2 \times 10^2$ M/h	$k_1 \times 10^2$ M/h	$k_4 \times 10^2$ M/h
1	1.5	1.41	1.52	27.5	0.12
2	2.0	1.62	1.67	24.2	0.36
3	2.5	1.83	1.90	23.1	0.44
4	3.0	1.90	1.97	22.4	0.32
5	3.5	2.13	2.28	20.0	0.19

[a] **Reaction conditions:** propylene = 10 atm, CO = 5 atm, H_2 = 15 atm, [HF/HT] = 700 mg, HT/HF ratio = 7, T_1 = 60 °C, T_2 = 150 °C, t_1 = 3 h, t_2 = 9 h, total time (t) = 12 h at 1000 rpm.
k_1 = rate of formation of butanals
k_2 = rate of formation of 2–ethylhexenal
k_3 = rate of formation of 2–ethylhexanal
k_4 = rate of formation of butanols.

Table 2.1.7. Effect of the Mg/Al molar ratio of [HT] on the rates of products formation at 250 °C aldol temperature (T_2) [a]

Run	Mg/Al Molar ratio	$k_5 \times 10^2$ M/h	$k_3 \times 10^2$ M/h	$k_2 \times 10^2$ M/h	$k_1 \times 10^2$ M/h	$k_4 \times 10^2$ M/h
1	1.5	0.59	0.23	–	14	1.76
2	2.0	0.61	0.1	–	0.5	2.68
3	2.5	0.65	0.11	0.26	0.5	2.62
4	3.0	1.13	0.14	0.26	0.5	2.30
5	3.5	1.21	0.19	0.26	0.5	2.37

[a] **Reaction conditions:** propylene = 10 atm, CO = 5 atm, H_2 = 15 atm, [HF/HT] = 700 mg, HT/HF ratio = 7, T_1 = 60 °C, T_2 = 250 °C, t_1 = 3 h, t_2 = 9 h, total time (t) = 12 h at 1000 rpm. *total time = 24 h, k_5 = rate of formation of 2–ethylhexanol.

On conducting the experiments at 250 °C aldol condensation temperature (T_2), the formation of 2–ethylhexanol was observed by further hydrogenation of 2–ethylhexanal (Table 2.1.7).

$k_5 =$ d [2–ethylhexanol]/ dt (7)

Similar to the results observed at 150 °C aldol temperature, the rate of formation of 2–ethylhexanol was observed to increase on increasing the Mg/Al molar ratio of [HT]. At the Mg/Al molar ratio of [HT] 1.5, rate of formation of 2–ethylhexanol was calculated as 0.59 x 10^{-2} M/h and increased to 1.21 x 10^{-2} M/h on increasing the ratio to 3.5.

Effect of the amount of [HT(3.5)] and [HF] complex in [HF/HT(3.5)] system on the rates of products formation

Rates of the formation of C_8 aldehydes, butanals and butanols were determined by varying the amount of [HT] in the range of 100–1000 mg at constant amount of [HF] complex to understand the effect of [HT] amount on the kinetics of the reaction (Table 2.1.8). The rate (k_3) of formation of 2–ethylhexanal was observed to increase on increasing the amount of [HT]. On varying the amount of [HT] from 100 mg to 1000 mg, the rate k_3 was continuously increased from 0.33 x 10^{-2} to 2.28 x 10^{-2} M/h. A similar trend of increasing the rate of formation of 2–ethylhexenal (k_2) was also observed on increasing the amount of [HT]. The rate k_2 was regularly increased from 0.13 x 10^{-2} to 2.4 x 10^{-2} M/h on varying [HT] in the range of 100–1000 mg. The rates of formation of butanals and butanols both were observed to decrease on increasing the amount of [HT]. In the studied range of the amount of [HT], the rate k_1 was decreased from 32.5 x 10^{-2} to 19.5 x 10^{-2} M/h. The rate of formation of butanols was decreased from 1.56 x 10^{-2} to 0 .19 x 10^{-2} M/h and no butanols formation was observed at 1000 mg [HT].

Table 2.1.8. Effect of [HT(3.5)] amount in [HF/HT(3.5)] on the rates of products formation [a]

Run	[HT(3.5)] (mg)	k_3 x 10^2 M/h	k_2 x 10^2 M/h	k_1 x 10^2 M/h	k_4 x 10^2 M/h
1	100	0.33	0.13	32.5	1.56
2	300	1.14	1.04	28.2	0.56
3	500	2.04	1.78	25.1	0.19
4	700	2.13	2.28	20.0	0.19
5	1000	2.28	2.4	19.5	0

[a] **Reaction conditions:** propylene = 10 atm, CO = 5 atm, H_2 = 15 atm, [HF] complex = 100 mg, T_1 = 60 °C, t_1 = 3 h, T_2 = 150 °C, t_2 = 9 h, total time (t) = 12 h.

Table 2.1.9 shows the effect of variation of the amount of [HF] complex on the rates of formation of 2–ethylhexanal, 2–ethylhexenal, butanals and butanols for the synthesis of C_8

aldehydes from propylene in a single pot. The rates of formation of 2–ethylhexenal and 2–ethylhexanal were observed to give a mixed trend on increasing the amount of [HF] complex. The rates were increased upto certain amount of [HF] complex and afterwards on further increasing the amount, rates were decreased significantly. The rate k_3 was found to be increase from 1.14 x 10^{-2} M/h (at 15 mg) to 2.13 x 10^{-2} M/h (at 100 mg). On further increase in the amount of the [HF] complex to 160 mg, the rate of formation of 2–ethylhexanal was decreased to 1.28 x 10^{-2} M/h. The rate of formation of 2–ethylhexenal was also observed to increase upto 100 mg of [HF] complex (2.58 x 10^{-2} M/h) and decreased to 1.67 x 10^{-2} M/h at 160 mg. An increasing trend on the rates of formation of butanals and butanols were observed on increasing the amount of [HF] complex. Hence, on increasing the amount of [HF] complex, all the rates corresponding to k_1, k_2, k_3 and k_4 were increased. However after 100 mg of [HF], the rates k_2 and k_3 were decreased, indicated that the amount of [HF] complex plays an significant role. There was not much significant difference in the rate of formation of 2–ethylhexanal at 15 mg and 160 mg of [HF] complex. This may be due to the less accessibility of [HT(3.5) component of [HF/HT(3.5)] catalyst. The lower amount of [HF] complex causes lower rate for the hydrogenation of 2–ethylhexenal to 2–ethylhexanal and hydroformylation reaction. On the other hand, higher amount of [HF] complex favors the faster hydroformylation of propylene and hydrogenation of butanals.

Table 2.1.9. Effect of [HF] complex amount in [HF/HT(3.5)] on the rates of products formation [a]

Run	[HF] complex (mg)	k_3 x 10^2 M/h	k_2 x 10^2 M/h	k_1 x 10^2 M/h	k_4 x 10^2 M/h
1	15	1.14	1.3	12.5	0.47
2	30	1.38	1.56	15.5	0.50
3	50	1.76	2.06	18.2	0.55
4	100	2.13	2.58	20.0	0.59
5	125	1.98	2.08	27.7	0.66
6	160	1.28	1.67	29.8	1.26

[a] **Reaction conditions:** propylene = 10 atm, CO = 5 atm, H_2 = 15 atm, [HT(3.5)] = 700 mg, T_1 = 60 °C, t_1 = 3h, T_2 = 150 °C, t_2 = 9 h, total time (t) = 12 h.

Effect of the aldol temperature (T_2) using [HF/HT(3.5)]

The effect of aldol condensation temperature (T_2) on the rates of formation of products is shown in Table 2.1.10. Formation of 2–ethylhexanol was observed at 250 °C. Upto 200 °C, 2–ethylhexanal and 2–ethylhexenal was formed as C_8 aldol derivatives. The rate of formation of

2–ethylhexanal was observed to increase on increasing the reaction temperature upto 200 °C, after that the rate decreased significantly due to consumption of 2–ethylhexanal in the formation of the 2–ethylhexanol via hydrogenation reaction. The rate of formation of 2–ethylhexanal determined to be 0.66 x 10^{-2} M/h at 120 °C was increased upto 2.87 x 10^{-2} M/h at 200 °C. The rate of formation of 2–ethylhexenal was decreased from 2.25 x 10^{-2} to 0.25 x 10^{-2} M/h on increasing the temperature from 120 to 200 °C. The rate of formation of butanals decreased drastically from 36.5 x 10^{-2} M/h (at 120 °C) to 0.5 x 10^{-2} M/h (at 250 °C). This may be due to the faster consumption of butanals for further consecutive reactions such as aldol condensation and hydrogenation at higher temperature. The rate of formation of butanols via hydrogenation of butanals increased significantly on increasing the aldol temperature. At lower aldol temperature (120 °C), lower rate of formation (0.34 x 10^{-2} M/h) of butanol was obtained, which increased to 2.37 x 10^{-2} M/h at 250 °C.

Table 2.1.10. Effect of aldol reaction temperature (T_2) on the rates of products formation [a]

Run	T_2 °C	k_5 x 10^2 M/h	k_3 x 10^2 M/h	k_2 x 10^2 M/h	k_1 x 10^2 M/h	k_4 x 10^2 M/h
1	120	–	0.66	2.25	36.5	0.34
2	150	–	2.13	2.28	20	0.19
3	200	–	2.87	1.39	4.5	0.85
4	250	1.20	0.20	0.25	0.5	2.37

[a] **Reaction conditions:** propylene = 10 atm, CO = 5 atm, H_2 = 15 atm, [HF/HT(3.5)] = 700 mg, HT/HF = 7, T_1 = 60 °C, t_1 = 3 h, t_2 = 9 h, total time (t) = 12 h.

Effect of the partial pressures of CO and H_2 using [HF/HT(3.5)]

The effect of partial pressure of CO and H_2 at constant CO to H_2 ratio (1:3) on the rates of formation of products is depicted in Table 2.1.11. At lower partial pressures of CO and H_2, lower rate of formation of 2–ethylhexanal was observed, enhanced on increasing the partial pressures. The rates of formation of 2–ethylhexenal and butanals were found to decrease on increasing the partial pressure of CO and H_2. These observations indicated that the consumption of 2–ethylhexenal and butanals for the formation of 2–ethylhexanal and butanols, respectively become predominant at higher partial pressures of CO and H_2. The rates of formation of butanols were also increased on increasing the partial pressures of CO and H_2. Hence, increase in partial pressures of CO and H_2 increases the consumption of 2–ethylhexenal and butanals, which in turn enhance the rates of their hydrogenated products, 2–ethylhexanal and butanols, respectively.

Table 2.1.11. Effect of partial pressures of CO and H_2 on the rates of products formation [a]

Run	CO	H_2	$k_3 \times 10^2$	$k_2 \times 10^2$	$k_1 \times 10^2$	$k_4 \times 10^2$
	atm	atm	M/h	M/h	M/h	M/h
1	2.5	10	1.01	2.56	24	0.11
2	5	15	2.13	2.28	20	0.19
3	10	30	2.43	0.91	19	0.25
4	15	45	2.61	0.81	17.5	0.44
5	20	60	2.68	0.78	15	0.41

[a] **Reaction conditions:** propylene = 10 atm, [HF/HT(3.5)] = 700 mg, HT/HF = 7, T_1 = 60 °C, t_1 = 3 h, T_2 = 150 °C, t_2 = 9 h, total time (t) = 12 h.

2.1.3.8. Thermal Stability of Multi–Functional [HF/HT] Catalyst

The experiments were conducted at different temperatures to study the thermal stability of [HF/HT(3.5)] catalyst at partial pressures of CO and H_2 at 20 atm; 700 mg of [HF/HT(3.5)]; 50 mL toluene and 12 h reaction time. The thermal treatment temperature was varied from 30–250 °C by keeping the other reaction parameters constant. The P–XRD patterns of original [HF/HT(3.5)] catalyst and thermally treated catalyst are shown in Figure 2.1.10.

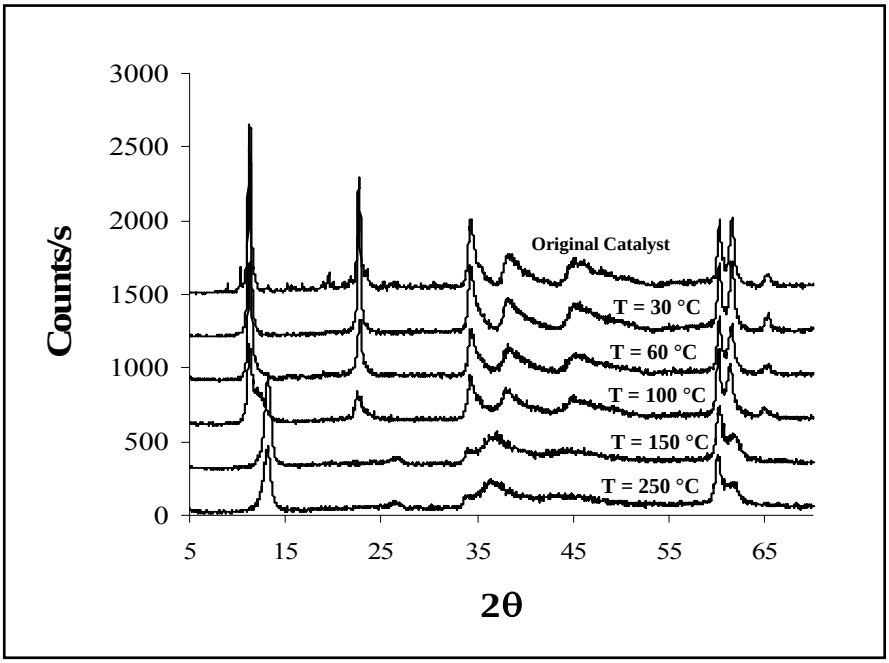

Figure 2.1.10. P–XRD Patterns for the study of thermal stability of [HF/HT(3.5)].

P–XRD patterns of the thermally treated [HF/HT(3.5]] catalyst are divided into two categories. In the first category (T = 30–100 °C), sharp and intense peaks at low diffraction angles

(2θ = 10–27°) and broad reflections at high angles (2θ = 30–67°) were observed, the patterns being identical to the original [HF/HT(3.5)] catalyst. In the second category, (T = 150 to 250 °C), significant changes in the P–XRD patterns were observed. For example, the peaks corresponding to the (003) and (006) planes were shifted to higher angles, 13.2° and 26.6°, respectively, when compared to the original catalyst (11.3° and 22.7°, respectively). Furthermore, as the treatment temperature was raised up to 250 °C, the intensity of all peaks decreased. The maximum decrease in peak intensity was observed in the 2θ range 20–50°. In contrast, the region around 2θ = 60° was less affected by the rise in temperature. The temperature at which these changes appear (transition temperature) in the P–XRD patterns was found to depend on the Mg/Al molar ratio of [HT]. The transition temperature was decreased with increasing the Mg/Al molar ratio of [HT]. The observed changes are due to the reaction between interlayer carbonates and interlayer water molecules, producing hydroxyl anions in the interlayer gallery of this phase. The TGA of [HF] complex confirmed the stability of complex up to 150 °C, where decomposition of [HF] resulting in the observed shifting of the peaks of the (003) and (006) planes of [HF/HT]. The layered structure of [HF/HT(3.5)] was still maintained above this temperature, but it contained hydroxyl anions in the interlayer, which are less bulky than the carbonate anions found in the interlayers of the original catalyst. The observed P–XRD patterns of [HF/HT] are more comparable to that of [HT] than to that of [HF]. Similar observations have been reported in the literature for hydrotalcite at different temperatures characterized by high temperature *in–situ* powder XRD (HTXRD) [29, 30]. All the peaks of original [HF/HT(3.5)] catalyst were found in the FT–IR spectra of the thermally treated [HF/HT(3.5)] catalysts (Figure 2.1.11).

High temperature treatment in the presence of hydrogen may form the clusters [HF] complex into Rh(0) supported aggregates, which is an efficient catalyst for hydrogenation, but less active for the hydroformylation of propylene. Keeping this point in view, we have checked the catalytic activity of [HF/HT(3.5)] after four successive runs, using the same catalyst under identical reaction conditions. The results are shown in Table 2.1.12. As seen from the data presented in the Table 2.1.12, no changes in the activity of [HF] complex were observed for hydroformylation and hydrogenation reactions after high temperature treatment in the presence of excess hydrogen atmosphere. Therefore, it can be safely said that under the conditions employed in our reaction, the formation of Rh(0) is less likely. However, the activity of [HT] for the aldol condensation of aldehyde was influenced significantly with a loss of selectivity for C_8 aldehydes/alcohols. This can be attributed to the structural changes of hydrotalcite as evidenced by X–ray diffraction (Figure 2.1.10). This clearly shows that the [HF/HT] catalyst is thermally stable up to 150 °C and slow decomposition follows up to 200 °C. This is consistent with our experimental data, which showed that excellent selectivity with respect to C_8 aldol derivatives was

observed in the temperature range 150–200 °C.

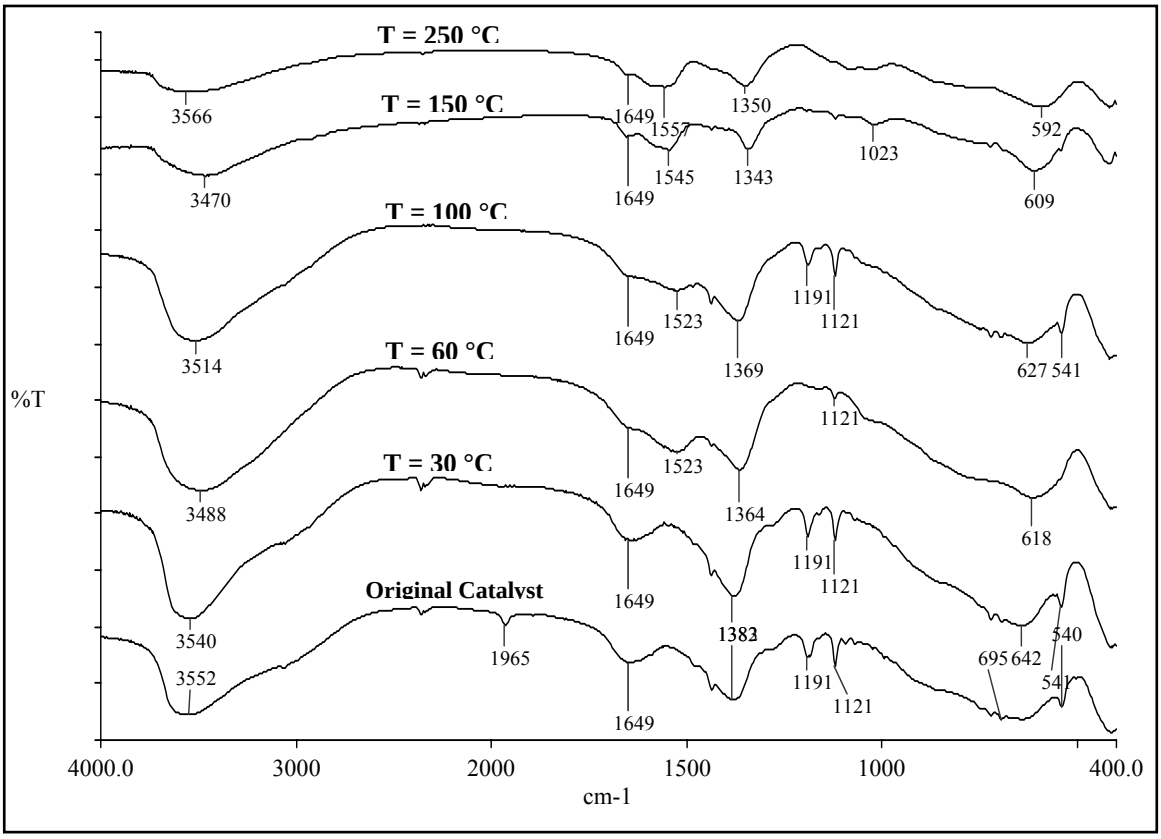

Figure 2.1.11. FT–IR spectra for the study of thermal stability of [HF/HT(3.5)].

Table 2.1.12. Effect of the high temperature treatment on the activity of catalyst

	% Selectivity [a]		
	C_4 Aldehydes	C_4 Alcohols	C_8 Aldehydes/alcohols
Fresh catalyst	40	6	54
Second run	28	71	<1
Third run	23	76	<1
Fourth run	22	77	<1

[a] **Reaction conditions:** propylene = 10 atm, CO = 5 atm, H_2 = 15 atm, [HF/HT (3.5)] = 700mg, HT/HF = 7, T_1 = 60 °C, t_1 = 3 h, T_2 = 150 °C, t_2 = 9 h, total time (t) = 12 h.

2.1.4. Conclusions

Rhodium complex, $HRh(CO)(PPh_3)_3$ [HF] and hydrotalcite, $(Mg_{1-x}Al_x(OH_2))^{x+}(CO_3^{2-})_{x/n}{\cdot}mH_2O)$ [HT] based catalyst [HF/HT] was developed and its multi–functional potential was evaluated for

the single pot selective synthesis of C_8 aldol derivatives (aldehydes/alcohol) from propylene. The [HF/HT] catalyst has shown catalytic activity for hydroformylation, aldol condensation and hydrogenation reactions in a single pot. The Mg/Al ratio of [HT], amount of [HF] complex and [HT], and reaction temperature showed pronounced effect on the selectivity of C_8 aldol derivatives. Aldol condensation temperature T_2 played a significant role in the formation of 2–ethylhexanol in a single pot. As the Mg/Al molar ratio and amount of [HT] increased, selectivity of 2–ethylhexanal also increased due to enhancement in the basicity of the catalyst. The amount of [HF] complex in the catalyst significantly influenced the selectivity of 2–ethylhexanal. From the kinetic experiments, it was observed that the rate of formation of 2–ethylhexanal is dependent on the rate of aldol condensation which is catalyzed by hydrotalcite component of [HF/HT] catalyst. The reaction pathways and role of each component of multi–functional catalyst [HF/HT] for the synthesis of 2–ethylhexanol is discussed with the help of kinetic profiles of the reaction with time.

2.1.5. References

[1] V.K. Srivastava, D.U. Parmar, R.V. Jasra, Chem. Weekly July 8 (2003) 173–178 and July 15 (2003) 181–190; Chemical Economic Handbook, Oxo Chemical Report, SRI International, January (2003).

[2] D. Frohning, C.W. Kohlpaintner, in Applied Homogeneous Catalysis with Organometallic Compounds, ed. B. Cornils, W. A. Hermann, Wiley–VCH, Weinheim, (2000) vol. 1, ch. 2, p. 29.

[3] A.D. Godwin, R.H. Schlosberg, F. Hershkowitz, M.G Matturro, G. Kiss, K.C. Nadler, P.L Buess, R.C Miller, P.W. Allen, H.W. Deckman, R. Caers, E.J. Mozeleski, J. Edmund, R.P. Reynolds, US Patent 6307093 (2001).

[4] F.J. Doering, G.F. Schaefer, J. Mol. Catal. 41 (1987) 313–328; B.J. Arena, J.S. Holmgren, US Patent, 5144089 (1992).

[5] G. Horn, C.D. Frohning, H. Liebern, W. Zgorzelski, US Patent, 5475161 (1995).

[6] W. Bueschken, J. Hummel, US Patent, 5756856 (1998).

[7] H.G. Lueken, U. Tanger, W. Droste, G. Ludwig, D. Gubisch, US Patent, 4968849 (1990).

[8] T. Mori, K. Fujita, H. Hinoishi, US Patent, 5550302 (1996).

[9] J.J. Spivey, M.R. Gogate, Pollution Prevention in Industrial Condensation Reactions, Research Triangle Institute, USEPA Grant, (1996); G.J. Kelly, F. King, M. Kett, Green Chem. 4 (2002) 392–399.

[10] D. Tichit, B. Coq, Cattech 7 (2003) 206–217.

[11] M. Tomoyuki, O. Yasukazu, F. Koichi, E. Hiroki and T. Akio, JP Patent, 11269118 (1999).

[12] C.R. Greene, US Patent, 3278612 (1966).

[13] R.V. Jasra, V.K. Srivastava, R.S. Shukla, H.C. Bajaj, S.D. Bhatt, US Patent, 7294745 B2 (2007).

[14] D.D. Perrin, W.L.F. Armarego, D.D. Perrin, Purification of Laboratory Chemicals, 2nd ed., (1980) Pegamon Press, Oxford.

[15] D. Evans, G. Yagupsky, G. Wilkinson, J. Chem. Soc. (A) (1968) 2660–2665.

[16] M. J. Climent, A. Corma, S. Iborra, K. Epping, A. Velty, J. Catal. 225 (2004) 316–326.

[17] V.K. Srivastava, S.K. Sharma, R.S. Shukla, N. Subrahmanyam, R.V. Jasra, Ind. Eng. Chem. Res. 44 (2005) 1764–1771.

[18] V.K. Srivastava, R.S. Shukla, H.C. Bajaj, R.V. Jasra, Appl. Catal. A: Gen. 282 (2005) 31–38.

[19] O. Levenspiel, Chemical Reaction Engineering, 3rd ed., (1998) Wiley.

[20] V.K. Srivastava, S.K. Sharma, R.S. Shukla, R.V. Jasra, Catal. Commun. 7 (2006) 881–886.

[21] F. Cavani, F. Trifiro, A. Vaccari, Catal. Today 11 (1991) 173–301.

[22] S. Abello, F. Medina, D. Tichit, J.P. Ramirez, J.C. Groen, J.E. Sueiras, P. Salagre, Y. Cesteros, Eur. Chem. J. 11 (2005) 728–739.

[23] H. Liu, E. Min, Green Chem. 8 (2006) 657–662.

[24] F. Basile, G. Fornasari, V. Rosetti, F. Trifirò, A. Vaccari, Catal. Today 91–92 (2004) 293–297.

[25] J.M. Herman, P.J. Van Den Berg and J.J.F. Scholten, Chem. Eng. J. 35 (1987) 25–35.

[26] S. Ueno, K. Ebitani, A. Ookubo, K. Kaneda, Appl. Sur. Sci. 121–122 (1997) 366–371.

[27] K. Kaneda, K. Yamaguchi, K. Mori, T. Mizugaki, K. Ebitani, Catal. Sur. Jap. 4 (2000) 31–38.

[28] H. Tsugi, F. Yagi, H. Hattori, H. Kita, J. Catal. 148 (1994) 759–770.

[29] E. Kanezaki, Inorg. Chem. 37 (1998) 2588–2590.

[30] E. Kanezaki, Solid State Ion. 106 (1998) 279–284.

Chapter 2

Part–2

Synthesis of 2–Methylpentanol and 2–Methylpentenal (C_6 Alcohol and Aldehydes) from Ethylene in a Single Pot using Heterogeneous Multi–Functional Catalyst

2.2.1. Introduction

2–Methylpentenal and 2–methylpentanol are commercially important chemicals that find application in fragrances, flavors, cosmetics and as an intermediate for the synthesis of various pharmacologically active compounds [1–3]. Commercially, 2–methylpentenal and 2–methylpentanol are synthesized by a process which involves hydroformylation, aldol condensation and hydrogenation reactions being carried out separately. In the first step, propanal is produced by the hydroformylation of ethylene using rhodium based catalyst [4–5]. The propanal produced undergoes aldol condensation in the presence of liquid base like KOH or NaOH used in stoichiometric amount in the second step [1–3]. Under optimum reaction conditions, 95% conversion of propanal is achieved with 86% selectivity of 2–methylpentenal using a liquid base [1]. Third step involves the hydrogenation of 2–methylpentenal (obtained by the condensation of propanal) to 2–methylpentanol in a fixed bed reactor using nickel or copper based catalyst [6–7]. The existing commercial process for the synthesis of 2–methylpentenal/2–methylpentanol from propanal is a multi–step process. Besides, this process has other drawbacks like use of KOH or NaOH in large stoichiometric amount, lower selectivity, separation of spent KOH/NaOH from product mixture, post synthesis reaction mixture, and disposal of spent liquid base. The alkali metal hydroxides require large amount of water for the neutralization and washing after completion of the reaction. Replacement of currently used homogeneous alkaline liquid by solid bases can result in the reusability of catalyst and minimization of waste stream [8]. It is desirable to find solid base catalysts which could substitute liquid base and possess all the advantages of heterogeneous catalysis, i.e., ease of separation of the products, decreased corrosion of the reactor, and possible regeneration of the catalyst. Therefore, research efforts are directed to develop a catalytic process, which can produce 2–methylpentenal or 2–methylpentanol from ethylene in single pot with high selectivity employing eco–friendly reusable catalyst (Scheme 2.2.1).

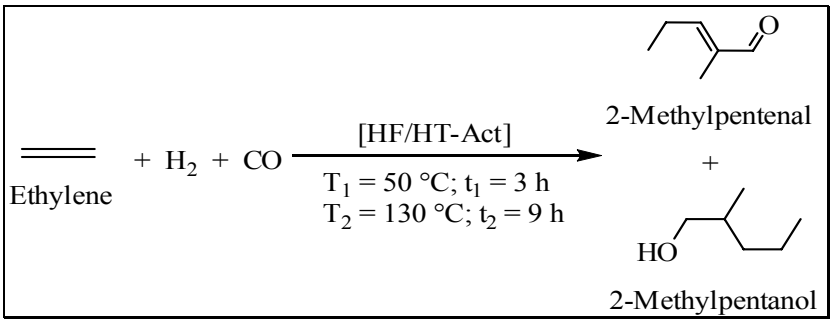

Scheme 2.2.1. Single pot synthesis of 2–methylpentanol and 2–methylpentenal from ethylene using [HF/HT–Act] as a multi–functional catalyst.

In our earlier study, a novel idea was conceptualized to integrate the hydroformylation with

aldol condensation and hydrogenation using an eco–friendly multi–functional catalyst prepared by impregnation and mechanical mixing of $HRh(CO)(PPh_3)_3$ on the surface of a solid base catalyst, as–synthesized hydrotalcite for single pot synthesis of C_8 aldehydes and alcohols from propylene [9–11]. This catalyst showed excellent conversion of propylene and selectivity of C_8 aldehydes/ alcohol. Kinetic study for the single pot synthesis of C_8 aldehydes and alcohols from propylene suggested that the overall rate of reaction depends on the aldol condensation step. If the rate of aldol condensation is higher, then hydrogenation of hydroformylation products could be suppressed. Therefore, in order to select highly active solid base catalyst for aldol condensation step various alkali ion–exchanged zeolites, modified synthetic talc, alumina, alkali impregnated alumina, as–synthesized and activated hydrotalcite of varied Mg/Al molar ratio were used as catalysts in a separate study by selecting propanal as a model reactant [12–13]. The activated hydrotalcite samples were observed to be more active catalyst among all the studied catalysts. Higher conversion of propanal and selectivity of 2–methylpentenal was found using activated hydrotalcite of Mg/Al molar ratio of 3.5 as a catalyst due to higher basicity of hydrotalcite on its activation at 450 °C. Therefore, in the present study we have chosen activated hydrotalcite of varied Mg/Al molar ratio as a base component of the multi–functional catalyst. Multi–functional catalyst [HF/HT–Act] was synthesized by impregnation of a rhodium complex, $HRh(CO)(PPh_3)_3$ [HF] complex, on the surface of activated hydrotalcite [HT–Act] and used as a catalyst for single pot synthesis of 2–methylpentenal/2–methylpentanol from ethylene.

2.2.2. Experimental

2.2.2.1. Materials

Ethylene (99.6%), hydrogen (99.999%) and carbon monoxide (99.99%) were procured from Alchemie Gases and Chemicals Private Limited, India. Triphenylphosphine (PPh_3; 99%), rhodium metal precursor $RhCl_3.3H_2O$ (99.99%), formaldehyde (HCHO) and sodium borohydride ($NaBH_4$; 99%) were purchased from Sigma–Aldrich, USA. Magnesium nitrate ($Mg(NO_3)_2.6H_2O$; 98.9%), aluminum nitrate ($Al(NO_3)_3.9H_2O$; 99.1%), sodium carbonate (Na_2CO_3; 99.9%), sodium hydroxide (NaOH; 99.9%), toluene (99.9%) were purchased from s. d. Fine Chemicals Ltd., Mumbai, India. The double distilled milli–pore de–ionized water was used for the synthesis of catalyst.

2.2.2.2. Catalyst Synthesis

Synthesis of [HF] Complex and [HT]

The synthesis of [HF] complex, $HRh(CO)(PPh_3)_3$ and hydrotalcite [HT] samples of varied Mg/Al molar ratio from 1.5 to 3.5 were carried out by the procedure mentioned in the *Chapter 2.1, Section 2.1.2.2.*

Activation of [HT]

The activation (calcination) of [HT] samples of varied Mg/Al molar ratio were carried out at 450 °C for 4 h in a muffle furnace and thus activated samples are represented as [HT–Act]. The freshly activated samples were used for the synthesis of multi–functional [HF/HT–Act] catalyst.

Synthesis of [HF/HT–Act] Catalyst

The [HF/HT–Act] catalyst was synthesized by dissolving 500 mg of [HF] complex and 1050 mg of triphenylphosphine into a round bottom flask having 10 mL toluene as a solvent. Appropriate amount of [HT–Act] (4 g) was added into the above solution at vigorous stirring under inert atmosphere. Slurry was stirred for 32 h at room temperature under nitrogen atmosphere. After 32 h, toluene was removed under vacuum and was a free–flowing light yellow powder obtained. This powder was stored under vacuum and used as a catalyst for synthesis of 2–methylpentanol from ethylene.

2.2.2.3. Characterization of Catalyst

^{31}P–NMR spectra of [HF] complex and [HF/HT–Act] catalyst were measured using Bruker–Avance II–500 (FT–NMR–500 MHz) spectrometer.

FT–IR spectra of [HF] complex, [HT], [HT–Act] and [HF/HT–Act] catalyst were recorded with a Perkin–Elmer spectrum GX–Fourier transform infrared spectrometer (FT–IR) system in the region of 400 to 4000 cm^{-1} using KBr pellets.

P–XRD patterns of [HF] complex, [HT], [HT–Act] and [HF/HT–Act] were recorded on a Philips X'Pert MPD system equipped with XRK 900 reaction chamber, using Ni–filtered Cu–K_α radiation (λ = 1.54056Å) over a 2θ range of 2–70°. The data were processed with Philips X'Pert (version 1.2) software.

TGA of [HF] complex, [HT], [HT–Act] and [HF/HT–Act] was carried out using Mettler–Toledo TGA/SDTA 851e equipment in 50 mL/min nitrogen flow at a heating rate of 10 °C/min.

Surface area measurements of [HT–Act] and [HF/HT–Act] were carried out using ASAP 2010 Micromeritics, USA. The samples were activated at 80 °C for 4 h under vacuum

(5 x 10^{-2} mmHg) prior to N_2 adsorption measurements. The specific surface area of the samples was calculated from N_2 adsorption isotherms measured at 77.4 K using Brunauer, Emmett, Teller (BET) method.

2.2.2.4. Catalytic Reaction

The synthesis of 2–methylpentenal and 2–methylpentanol from ethylene was carried out in 100 mL EZE–Seal stirred reactor supplied by Autoclave Engineers, USA. The desired amount of [HF/HT–Act] (HT–Act to [HF] complex ratio = 8) was added into the autoclave reactor having 50 mL toluene as a solvent. The autoclave was flushed with nitrogen prior to introducing ethylene at 10 atm. Carbon monoxide (CO) and hydrogen (H_2) were introduced in the reactor upto 40 atm pressure. The reactor was brought to 50 °C (T_1) for hydroformylation of ethylene. The reaction was then initiated by starting the stirrer at 1000 rpm and kept at 50 °C for 3 h (t_1) following which, the reaction temperature was raised to T_2 °C for 9 h (t_2) to initiate aldol condensation of propanal and hydrogenation of condensed product. The reaction was continued at constant pressure by supplying CO and H_2 from the reservoir cylinders. After 12 h total reaction time (t), the reactor was cooled to ambient temperature by circulation of cold water in the coil provided inside the reactor. For kinetic studies liquid samples were withdrawn through a sampling valve at desired time intervals during the course of experiments and analyzed using gas chromatography.

2.2.2.5. Reaction Product Analysis

The analysis of product mixture was carried out by GC–MS (Shimadzu, GCMS–QP2010) and gas chromatography (GC) (Shimadzu 17A, Japan) equipped with 5% diphenyl and 95% dimethyl siloxane universal capillary column (60 m length and 0.25 mm diameter) and a flame ionization detector (FID). The GC oven temperature was programmed from 40 to 200 °C at the rate of 10 °C/min. Nitrogen gas was used as a carrier gas. The temperatures of injection port and FID were kept constant at 200 °C. The retention time of each compound was determined by injecting pure compound under identical GC conditions. The conversion of ethylene and selectivity of formed products were calculated by the reported methods [10–11]. Overall conversion of ethylene was found to be in the range of 97–100% except the studies for the effect of partial pressure of ethylene on selectivity of 2–methylpentanol. To ensure the reproducibility of reaction, repeated experiments were carried out under identical reaction conditions. The obtained results including conversion and selectivity data were found to be reproducible in the range of ± 5% variation.

2.2.3. Results and Discussion

2.2.3.1. Characterization of Catalyst

The ^{31}P–NMR spectra of [HF] complex and [HF/HT–Act] are shown in Figure 2.2.1. Appearance of the doublet at 43.41 ppm [*J(Rh–P)* = 154 Hz] in ^{31}P–NMR spectrum of [HF] complex shows that all the three phosphorous atoms are present in the equivalent environment and are in the equatorial position. The hydride (H) and CO find axial positions showing trigonal bipyramidal structure in the complex. The %C and %H for the [HF] complex are; calculated (found): %C = 71.9 (71.6); %H = 5.0 (5.1). The ^{31}P solid state NMR spectrum of [HF/HT–Act] catalyst also showed doublet at 41.42 and 52.79 ppm, confirming the impregnation of the [HF] complex on the surface of [HT–Act] without decomposition.

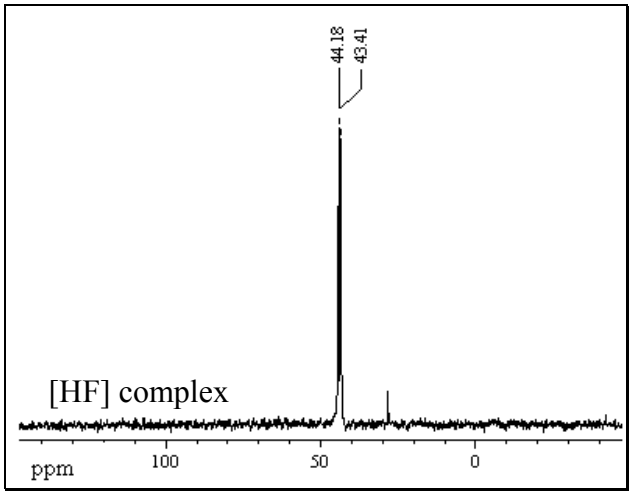

Figure 2.2.1. (a) ^{31}P–NMR of [HF] complex in C_6D_6.

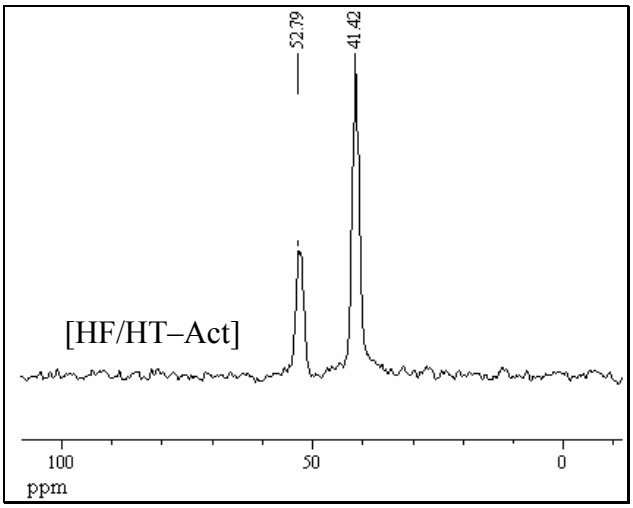

Figure 2.2.1. (b) Solid state ^{31}P–NMR of [HF/HT–Act].

Formation of [HF] complex was also confirmed by the appearance of bands at 2037 cm^{-1} for $\nu_{(Rh–H)}$ and 1964 cm^{-1} for $\nu_{(C=O)}$ in the FT–IR spectrum of [HF] complex (Figure 2.2.2). FT–IR

spectra of [HT] and [HT–Act] matched well with reported spectra in the literature which confirmed the formation of hydrotalcite [14]. The absorption band at 3440 cm^{-1} in FT–IR spectrum of [HF/HT–Act] catalyst is attributed to the H–bonding stretching vibrations of OH group in the brucite–like layer. The bands at 2037 cm^{-1} for $\nu_{(Rh–H)}$ and 1964 cm^{-1} for $\nu_{(C=O)}$ appearing in the FT–IR spectrum of [HF/HT–Act] catalyst, again showed that the [HF] complex impregnated on the surface of [HT–Act] without decomposition. Appearance of shoulders at 1645 cm^{-1} and 1435 cm^{-1} are the characteristic bands of H_2O and CO_3^{2-}. The low frequency region showed a band at about 541 cm^{-1}, corresponding to the translation modes of hydroxyl groups, influenced by Al^{3+} cations. The peak at the 664 cm^{-1} (ν_4) is assigned to in–plane carbonate bending [15].

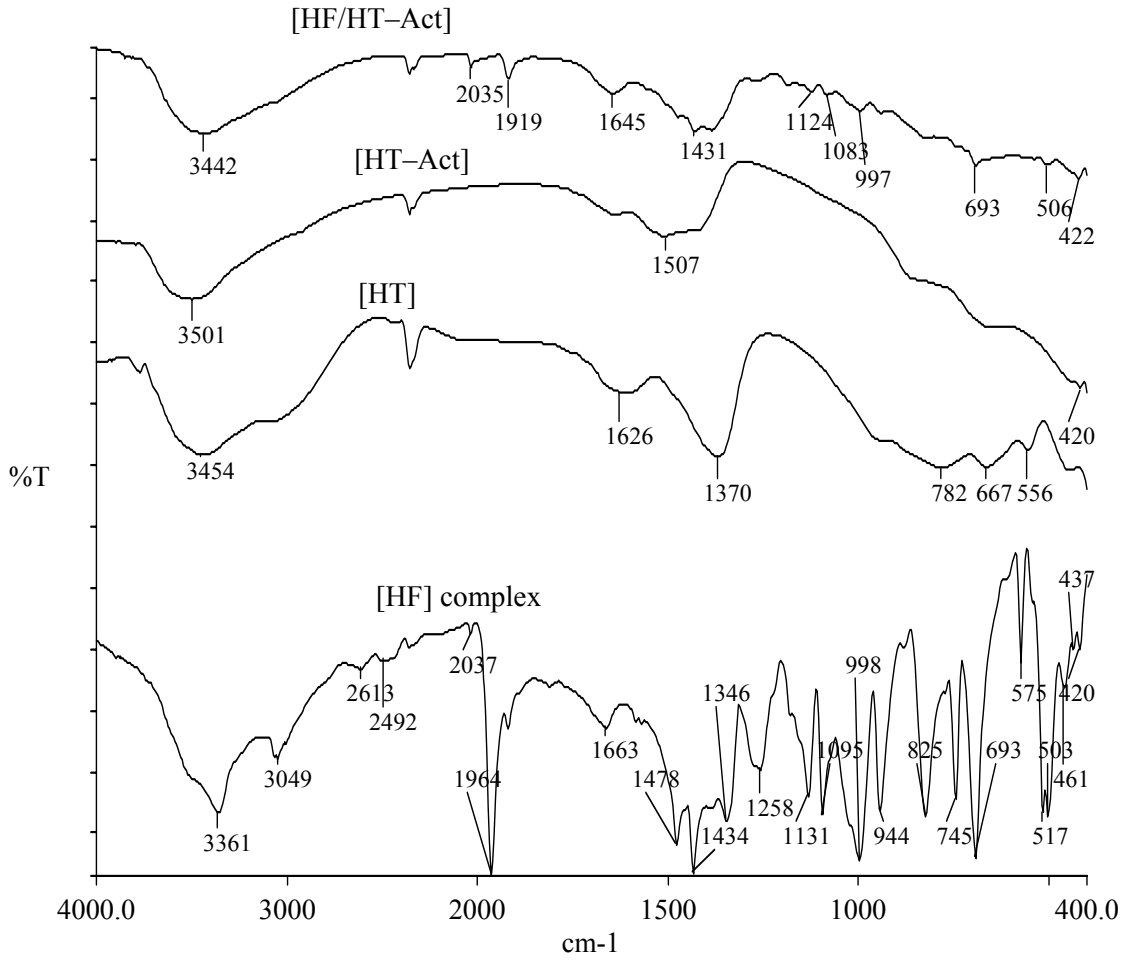

Figure 2.2.2. FT–IR of [HF] complex, [HT], [HT–Act] and [HF/HT–Act] samples.

The P–XRD patterns of [HF] complex, [HT], [HT–Act] and [HF/HT–Act] samples are given in Figure 2.2.3. The P–XRD patterns of [HT] showed sharp, intense and symmetric peaks at lower diffraction angles (2θ = 10–25) and broad asymmetric reflections at higher diffraction angles (2θ = 30–50), which are characteristics of hydrotalcite [14]. The P–XRD patterns of [HT–Act] consist of broadened peaks that can be assigned to a mixed oxide phase $Mg(Al)O_x$, with diffraction lines at values very similar to that of MgO. The sharp peaks at 2θ = 8.5 and 20 were observed in

the P–XRD pattern of the [HF] complex and were present in the P–XRD pattern of [HF/HT–Act] catalyst. The P–XRD patterns of [HF/HT–Act] catalyst showed that the characteristic original planes of [HT–Act] are retained after impregnation of [HF] complex.

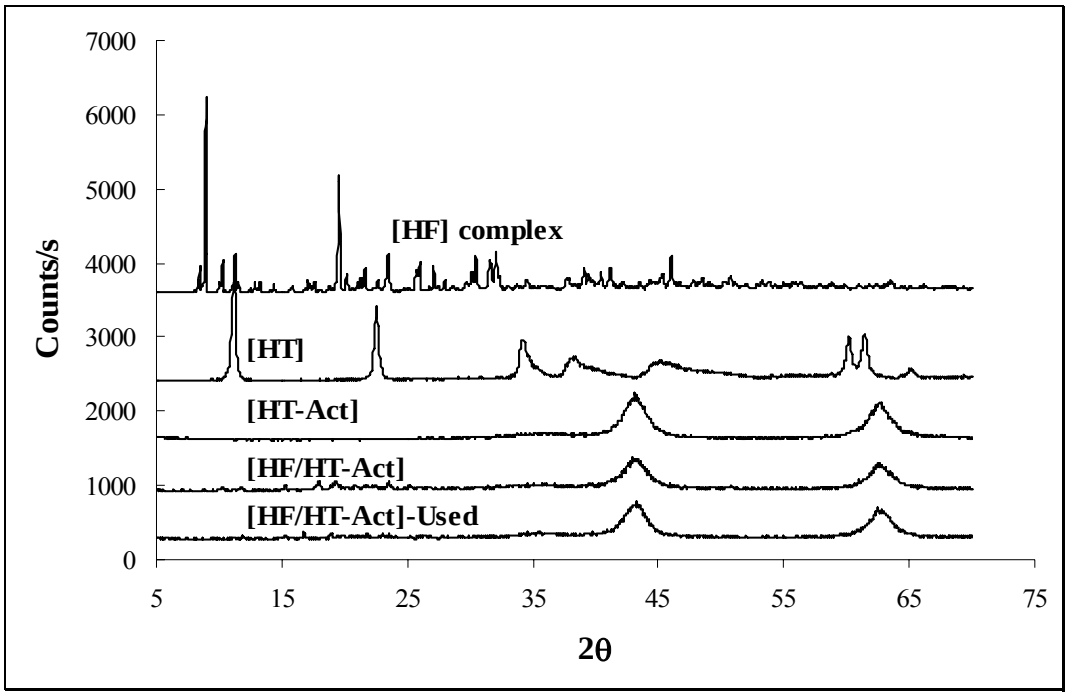

Figure 2.2.3. P–XRD of [HF] complex, [HT], [HT–Act], [HF/HT–Act] and used [HF/HT–Act] samples.

The TGA data of [HF] complex, [HT], [HT–Act] and [HF/HT–Act] samples are shown in Figure 2.2.4. Two stages of weight loss accompanied by an endothermal transformation were observed in the TGA of [HT]. 16% weight loss was observed in the first stage between 160–220 °C due to loss of physically adsorbed water molecules, without collapse of the structure. The second weight loss (28%) was observed in the temperature range of 300–450 °C and is attributed to the removal of condensed water molecules (hydroxyl group) and carbon dioxide from carbonate anion present in the interlayer space of [HT]. The activated hydrotalcite [HT–Act] showed only 5% weight loss in the entire temperature range. The major weight loss (63%) of [HF] complex was observed in the temperature range of 200–360 °C due to thermal decomposition of the [HF] complex. Only 5% weight loss of the [HF/HT–Act] catalyst was observed in temperature range 200–220 °C and increased upto 32% on increasing the temperature from 250 to 570 °C. The major weight loss in the second stage is due to the thermal decomposition of the [HF] complex from [HF/HT–Act] catalyst. The TGA data shows that the [HF/HT–Act] can be used as a catalyst upto 200 °C reaction temperature without thermal decomposition.

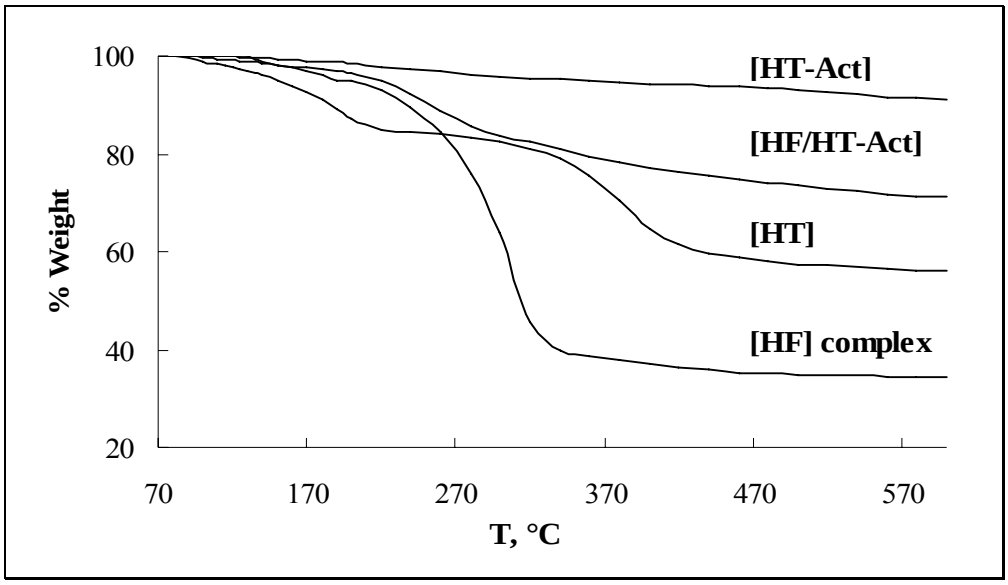

Figure 2.2.4. TGA of [HF] complex, [HT], [HT–Act] and [HF/HT–Act] samples.

The surface area of [HT(3.5)–Act] was calculated as 197 m^2/g that decreased upto 144 m^2/g after impregnation of [HF] complex on the surface of [HT(3.5)–Act]. The decrease in the surface area of [HF/HT–Act] is due to the coverage of the pores and external surface of hydrotalcite by the lower surface area [HF] complex on impregnation.

2.2.3.2. Reaction Pathways for the Synthesis of 2–Methylpentanol from Ethylene in a Single Pot

Before discussion of the obtained results, it is worthwhile to understand the function of each constituent of [HF/HT–Act] catalyst involved in the production of 2–methylpentanol from ethylene (Scheme 2.2.2). The reaction is initiated by the hydroformylation of ethylene to form propanal (**I**) catalyzed by [HF] complex of [HF/HT–Act] catalyst at 50 °C. Then two molecules of (**I**) undergo condensation step to give 3–hydroxy–2–methylpentanal (**II**) catalyzed by [HT–Act] component of catalyst and subsequently after removal of water molecule gave 2–methylpentenal (**III**). Reaction temperature for condensation step should be more than 100 °C to obtain excellent selectivity of 2–methylpentenal [12]. The [HF] complex of the catalyst also plays important role for hydrogenation of (**III**) to 2–methylpentanal (**IV**) and of (**IV**) to 2–methylpentanol (**V**). This hydrogenation step requires two hydrogen molecules and the reaction temperature similar to the condensation step. Thus, the [HF] complex of [HF/HT–Act] system catalyzes three reactions namely, hydroformylation, double bond (C=C) hydrogenation and (C=O) carbonyl hydrogenation during the single step preparation of 2–methylpentanol from ethylene. However, possibility of side reactions involved in the present studied conditions cannot be ignored. The most probable side reaction is the reduction of propanal to propanol (**VI**) under the reaction conditions similar to the

condensation step. The [HF] complex is efficient for the reduction of propanal in the presence of hydrogen. Potential of [HF] complex for hydrogenation of propanal was again confirmed by performing a separate experiment. Hence, in order to avoid this competitive side reaction, the amount and basicity of [HT–Act] component of [HF/HT–Act] catalyst must be sufficient enough to divert the reaction pathway in the direction of aldol condensation of propanal rather than the hydrogenation of propanal. The condensation temperature (T_2) and reaction conditions also played an important role for the diversion of reaction pathway from hydrogenation of propanal to condensation of propanal.

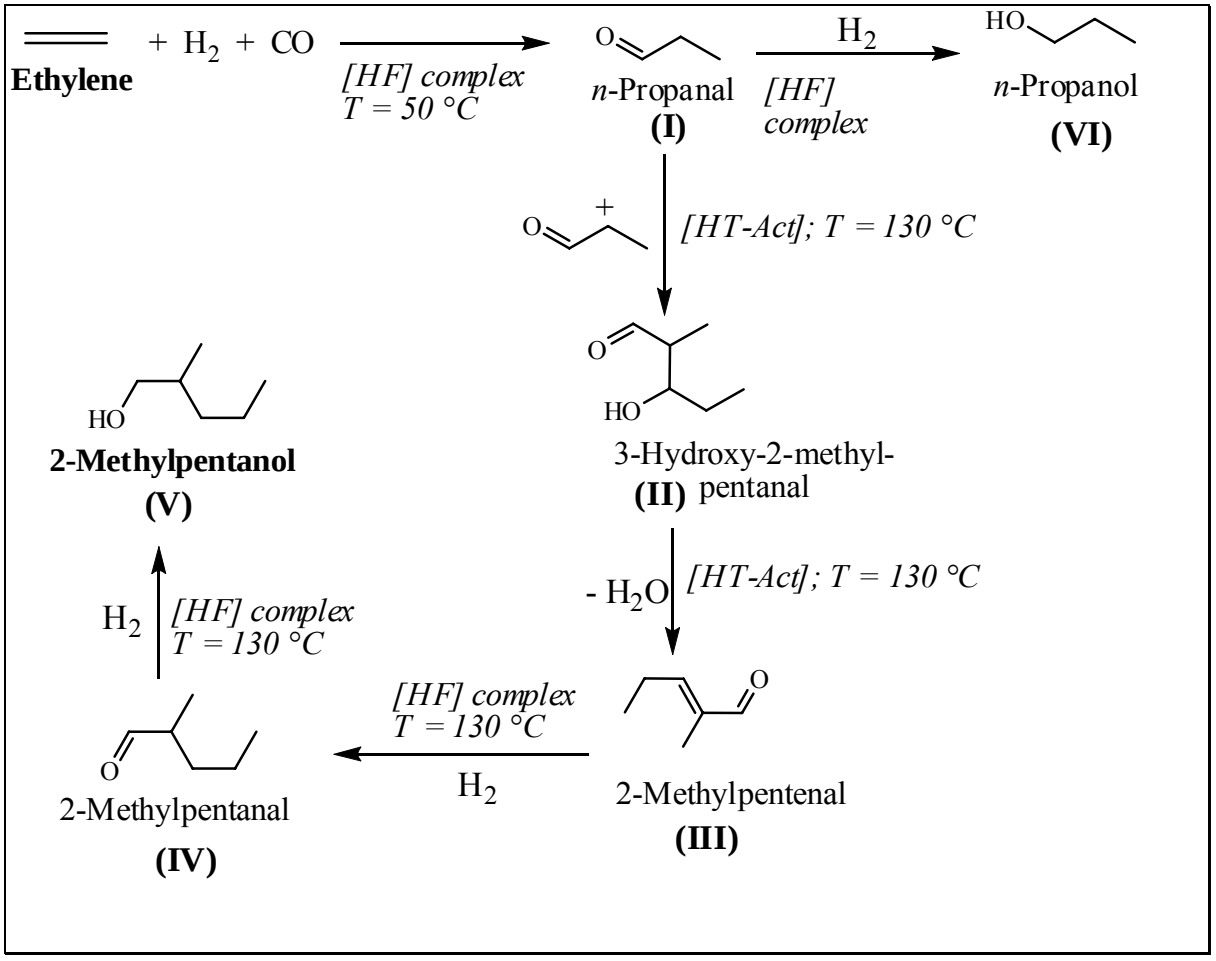

Scheme 2.2.2. Reaction pathways for the synthesis of 2–methylpentanol from ethylene in a single pot.

In order to optimize the reaction parameters for single step synthesis of 2–methylpentanol from ethylene using [HF/HT–Act] catalyst, the experiments were carried out by varying the aldol condensation temperature (T_2) at a fixed hydroformylation temperature (T_1). The effect of Mg/Al molar ratio of [HT–Act] at constant [HT–Act]/[HF] complex ratio (8), partial pressure of ethylene,

CO to H_2 ratio and nature of solvents on the selectivity of 2–methylpentanol was studied in detail by varying one variable at a time.

2.2.3.3. Effect of Aldol Condensation Temperature (T_2)

The condensation of propanal, which takes place after hydroformylation reaction (Scheme 2.2.2), is influenced by the temperature (T_2). Experiments were conducted by varying T_2 from 60 to 180 °C at constant Mg/Al molar ratio of [HT–Act] 3.5 (Table 2.2.1). The mass fragmentation data of the product mixture is shown in Figure 2.2.5. Significant effect on the conversion of ethylene was not observed, therefore, results are explained in terms of selectivity of products formed. The lower selectivity of 2–methylpentanol was observed at lower T_2, which increased on increasing the T_2. The selectivity of 2–methylpentanol was observed to increase from 0 to 79% on increasing the T_2 from 60 to 130 °C. However, on further increasing the T_2 to 180 °C, the selectivity of 2–methylpentanol was observed to decrease to 55%. The lower selectivity of 2–methylpentanol in the T_2 range of 60–100 °C indicates that this temperature range is not suitable for hydrogenation of 2–methylpentenal to 2–methylpentanol. However, higher selectivity of 2–methylpentenal in the lower T_2 range suggested that the lower reaction temperature is also suitable for condensation of propanal. The observed lower selectivity of 2–methylpentanol at higher T_2 is due to the higher selectivity of propanol via hydrogenation of propanal. At higher T_2, hydrogenation reaction is predominant as compared to the condensation of propanal. As the T_2 increased from 60–180 °C, selectivity of propanal was also observed to decrease constantly which is attributed to the consumption of propanal for condensation and hydrogenation reactions. Similar trends in the selectivity of products formation were observed in our earlier reports for the single step synthesis of C_8 aldehydes and alcohols from propylene [10–11]. As the effect of T_1 on the ethylene hydroformylation reaction is well documented in the literature, therefore, we have not studied this effect in the present work. The 130 °C aldol temperature was selected as T_2 for further study on optimization of reaction parameters for the synthesis of 2–methylpentanol from ethylene in one pot.

2.2.3.4. Effect of Mg/Al Molar Ratio of [HT–Act]

The effect of Mg/Al molar ratio of [HT–Act] on the selectivity of 2–methylpentanol was studied by varying the ratio from 1.5 to 3.5 and the corresponding results are depicted in Table 2.2.2. Selectivity of 2–methylpentanol increased on increasing Mg/Al molar ratio of [HT–Act].

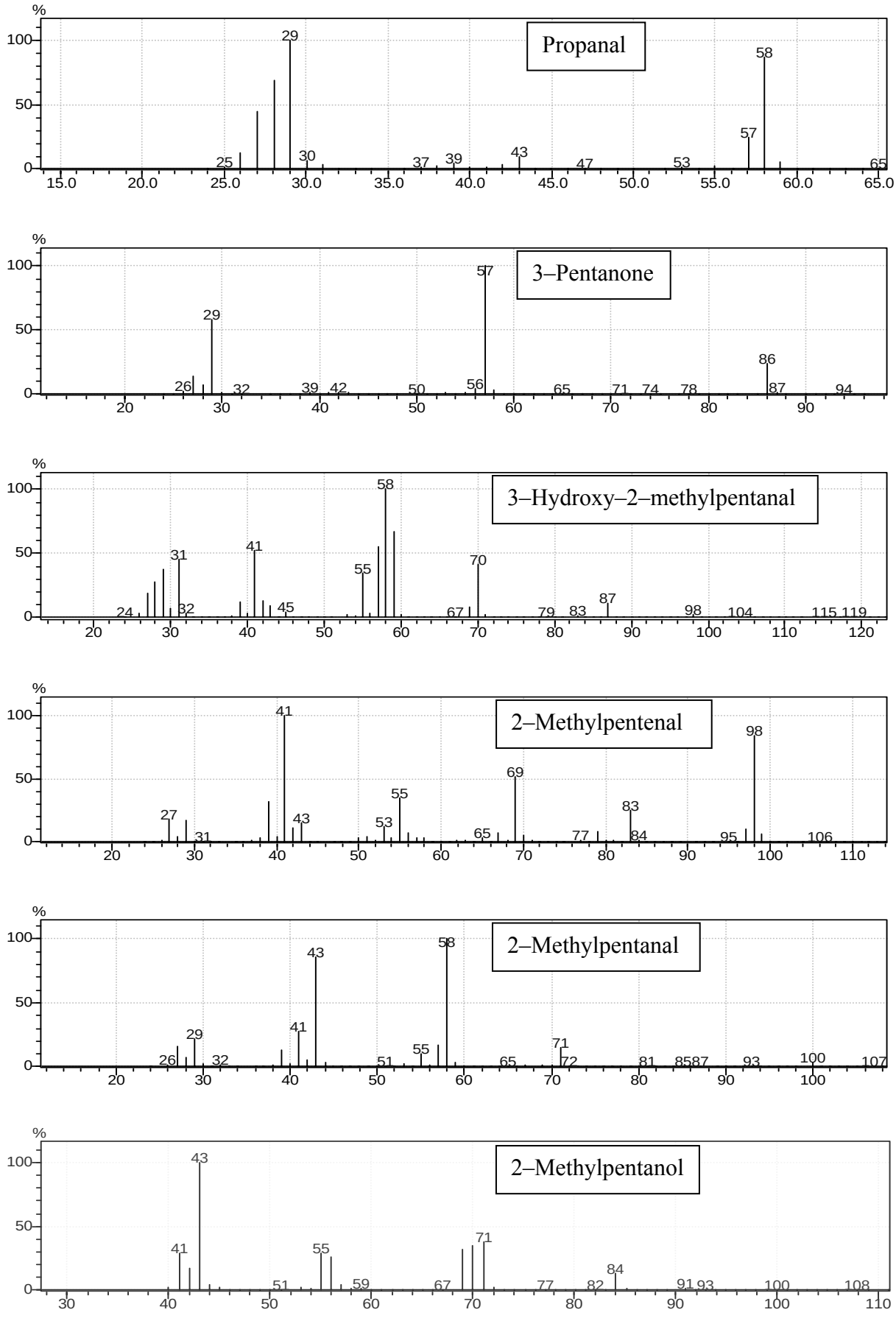

Figure 2.2.5. Mass fragmentation data of the product mixture

The 56% selectivity of 2–methylpentanol obtained at the ratio of 1.5 was found to increase significantly upto 79% on increasing the molar ratio at 3.5. At lower Mg/Al molar ratio, higher selectivity of propanol was observed. The selectivity of propanol was found to be 27% at Mg/Al = 1.5, which decreased to 7% on increasing the molar ratio to 3.5. The significant effect on the selectivity of propanal and 3–pentanone was not observed in the studied Mg/Al molar ratio.

Table 2.2.1. Effect of T_2 (aldol temperature) on the selectivity of 2–methylpentanol and 2–methylpentenal

Run	T_2, °C	% Selectivity [a]				
		2–Methylpentanol	2–Methylpentenal	Propanal	Propanol	3–Pentanone
1	60	0	46	49	0	5
2	80	2	52	40	0	6
3	100	8	54	25	5	8
4	130	79	0	4	7	10
5	150	64	0	0	23	13
6	180	55	0	0	28	17

[a] **Reaction conditions:** ethylene = 10 atm, CO = 5 atm, H_2 = 15 atm, [HF/HT–Act] = 700 mg, T_1 = 50 °C, t_1 = 3 h, t_2 = 9 h.

Table 2.2.2. Effect of Mg/Al molar ratio of [HT–Act] on the selectivity of 2–methylpentanol

Run	Mg/Al molar ratio	% Selectivity [a]			
		2–Methylpentanol	Propanal	Propanol	3–Pentanone
1	1.5	56	6	27	11
2	2.0	65	5	20	10
3	2.5	68	6	16	10
4	3.0	72	6	11	11
5	3.5	79	4	7	10
6*	3.5	62	14	12	12

[a] **Reaction conditions:** ethylene = 10 atm, CO = 5 atm, H_2 = 15, [HF/HT–Act] = 700 mg, T_1 = 50 °C, t_1 = 3 h, T_2 = 130 °C, t_2 = 9 h.

* [HF/HT] catalyst presented in the Ref. 10 and 11.

The increase in the selectivity of 2–methylpentanol with increasing Mg/Al molar ratio of hydrotalcite is explained in terms of the increased basicity of [HT–Act] which enhanced the aldol condensation reaction. The basicity of hydrotalcite can be tuned either by increasing the Mg/Al molar ratio or activation at appropriate temperature. The basicity of the [HT–Act] is mainly due to their O^{2-} (Lewis basicity) and hydroxyl groups (Brønsted basicity; small amount) present in it. The increment of Mg–content in [HT] increases the basic character of hydrotalcite, which results into the increase of 2–methylpentanol selectivity. Higher selectivity of aldol derivatives was observed in the present study using [HF/HT–Act] catalyst as compared to the study reported in the Chapter 2.1 on the use of [HF/HT] as a multi–functional catalyst for single pot synthesis of C_8 aldol derivatives from propylene. The higher selectivity of corresponding alcohol in the present report might be due to enhanced basicity of the activated hydrotalcite as compared to the as–synthesized hydrotalcite in studied in Chapter 2.1 along with the size of the reactant and products molecules. For the confirmation of enhanced basicity, we have carried out a reaction for the synthesis of 2–methylpentanol from ethylene in a single pot using the multi–functional catalyst [HF/HT] reported in Chapter 2.1. The selectivity of 2–methylpentanol was observed to 62% with 12% selectivity of propanol. The 14% propanal was still un–reacted using [HF/HT] catalyst system. Another reason for higher activity of catalyst in the present study could be the higher surface area of [HF/HT–Act] catalyst (144 m^2/g) as compared to the 71 m^2/g observed in the earlier report [11]. Due to higher surface area of the catalyst, more numbers of active sites are exposed at the surface of catalyst to activate reactant for the product formation. These results clearly show that the [HF/HT–Act] catalyst is more active as compared to the [HF/HT] catalyst for single pot synthesis reactions. Keeping in view of the higher selectivity of 2–methylpentanol observed at Mg/Al molar ratio of [HT–Act] 3.5, the effect of other reaction parameters were studied by taking [HT–Act] of Mg/Al molar ratio 3.5 as a solid base constituent of multi–functional catalyst.

2.2.3.5. Effect of Partial Pressure of Ethylene

The effect of partial pressure of ethylene on the selectivity of 2–methylpentanol was studied by varying the pressure from 3 to 20 atm (Table 2.2.3). As the partial pressure of ethylene increased, the conversion of ethylene was observed to decrease. The conversion of ethylene was calculated as 100% at 3 atm which decreased to 80% at 20 atm pressure of ethylene. The selectivity of 2–methylpentanol were observed to increase upto 79% at 10 atm that decreased to 64% at 20 atm. The 38% selectivity of propanol was found when partial pressure of ethylene was 3 atm.

Table 2.2.3. Effect of partial pressure of ethylene on the selectivity of 2–methylpentanol

Run	P_{ethy} (atm)	% Conv	% Selectivity [a]			
			2–Methylpentanol	Propanal	Propanol	3–Pentanone
1	3	100	45	10	38	7
2	5	100	55	20	20	5
3	7	100	61	14	18	7
4	10	99	79	4	7	10
5	14	95	71	5	13	11
6	17	89	67	6	15	12
7	20	80	64	5	20	11

[a] **Reaction conditions:** CO = 5 atm, H_2 = 15 atm, [HF/HT–Act] = 700 mg, T_1 = 50 °C, t_1 = 3 h, T_2 = 130 °C, t_2 = 9 h.

P_{ethy} = Partial pressure of ethylene; Conv = conversion

2.2.3.6. Effect of CO to H_2 ratio

The effect of CO to H_2 ratio (partial pressures) on the selectivity of aldol derivatives was studied by varying the ratio from 1:1 to 1:5 at constant pressure of p_{CO+H2} = 30 atm using [HF/HT–Act] catalyst (Table 2.2.4). The lower selectivity of 2–methylpentanol was observed at lower CO to H_2 ratio. For example, on increasing the CO to H_2 ratio from 1:1 to 1:3, the selectivity of 2–methylpentanol increased from 24 to 79%. However, at 1:1 and 1:2 CO to H_2 ratio, formation of 2–methylpentanal and 2–methylpentenal was observed due to insufficient hydrogen for hydrogenation of 2–methylpentenal to 2–methylpentanol in the studied reaction conditions. On further increase in the CO to H_2 ratio from 1:3 to 1:5, the selectivity of 2–methylpentanol decreased from 79 to 50%. The decrease in the selectivity of 2–methylpentanol at higher CO to H_2 ratio (above 1:3) is due to presence of excess hydrogen which assist the another side reaction i.e., hydrogenation of propanal to propanol. On increasing the CO to H_2 ratio, the selectivity of 3–pentanone and propanol was observed to increase significantly. From these experiments, 1:3 is the optimum CO to H_2 ratio to obtained maximum selectivity of 2–methylpentanol.

2.2.3.7. Effect of Solvent

The effect of the nature of solvents used for single pot synthesis of 2–methylpentanol from ethylene is presented in Table 2.2.5. Polar solvents like, methanol and *n*–butanol showed slightly

higher selectivity for 2–methylpentanol as compared to non polar, non cordinating solvent toluene. The selectivity of 2–methylpentanol was observed to 86% for methanol as a solvent which decreased to 79% for toluene as a solvent. For *n*–hexane as a solvent, selectivity of 2–methylpentanol was found to be 60%. Higher selectivity in case of polar solvents is attributed to the higher solubility of CO, H_2 and ethylene.

Table 2.2.4. Effect of CO: H_2 ratio on the selectivity of 2–methylpentanol and 2–methylpentenal

Run	$P_{CO:H2}$	% Selectivity [a]				
		2–Methylpentanol	2–Methylpentenal/ 2–Methylpentanal	Propanal	Propanol	3–Pentanone
1	1:1	24	51	12	6	7
2	1:2	40	35	10	8	7
3	1:3	79	–	4	7	10
4	1:4	62	–	4	18	16
5	1:5	50	–	3	30	17

[a] **Reaction conditions:** ethylene = 10 atm, p_{CO+H2} = 30 atm, [HF/HT–Act] = 700 mg, T_1 = 50 °C, t_1 = 3 h, T_2 = 130 °C, t_2 = 9 h.

Table 2.2.5. Effect of solvent on the selectivity of 2–methylpentanol

Solvent	% Selectivity [a]			
	2–Methylpentanol	Propanal	Propanol	3–Pentanone
Methanol	86	2	2	10
n–Butanol	83	3	4	10
Toluene	79	4	7	10
Benzene	74	6	8	12
n–Hexane	60	16	10	14

[a] **Reaction conditions:** ethylene = 10 atm, CO = 5 atm, H_2 = 15 atm, [HF/HT–Act] = 700 mg, T_1 = 50 °C, t_1 = 3 h, T_2 = 130 °C, t_2 = 9 h.

2.2.3.8. Reusability of [HF/HT–Act] Catalyst

The spent [HF/HT–Act] catalyst after completion of reaction was filtered and washed with 100 mL toluene and dried in vacuum for 12 h. Then the material was used as catalyst for the single pot synthesis of 2–methylpentanol from ethylene in single pot and the results are shown in Table

2.2.6. The significant drop in the conversion of ethylene was not observed upto third cycle and decreased to 87% in the fourth cycle. The selectivity of aldol derivatives gradually decreased in each cycle of reusability. The selectivity of 2–methylpentanol decreased from 79 to 34% at the end of fourth cycle. This indicates the deactivation of basic component [HT–Act] of [HF/HT–Act] catalyst, which is used for condensation of propanal. Therefore, the reaction is forwarding towards hydrogenation of propanal rather than the condensation step. This is also confirmed by the observed higher selectivity of propanal and propanol at the end of each cycle. This shows that the [HF/HT–Act] catalyst is still active for hydroformylation and hydrogenation reactions at the end of fourth cycle, but not active for the aldol condensation of propanal.

Table 2.2.6. Reusability of [HF/HT–Act] catalyst

Cycles	% Conversion	% Selectivity [a]			
		2–Methylpentanol	Propanal	Propanol	3–Pentanone
First	99	79	4	7	10
Second	98	66	13	7	14
Third	94	57	20	15	8
Fourth	87	34	24	33	9

[a] **Reaction conditions:** ethylene = 10 atm, CO = 5 atm, H_2 = 15 atm, T_1 = 50 °C, t_1 = 3 h, T_2 = 130 °C, t_2 = 9 h.

2.2.3.9. Reaction Kinetic Profile

In order to have an insight into the kinetic profile and rates of the products formation during the synthesis of 2–methylpentanol, which could provide significant information for the stages of formation of various products with time and to understand the reaction pathways, time dependent experiments were conducted using [HF/HT–Act] catalyst system at 130 °C, the temperature at which maximum selectivity for 2–methylpentanol was obtained. The kinetic profiles for products formation during the synthesis of 2–methylpentanol in single pot gives significant information with respect to time to understand the actual reaction pathway for the formation of various products at different stages. The results for the selectivity of products formed with respect to time are shown in Figure 2.2.6 to understand the activity of the [HF/HT–Act] catalyst.

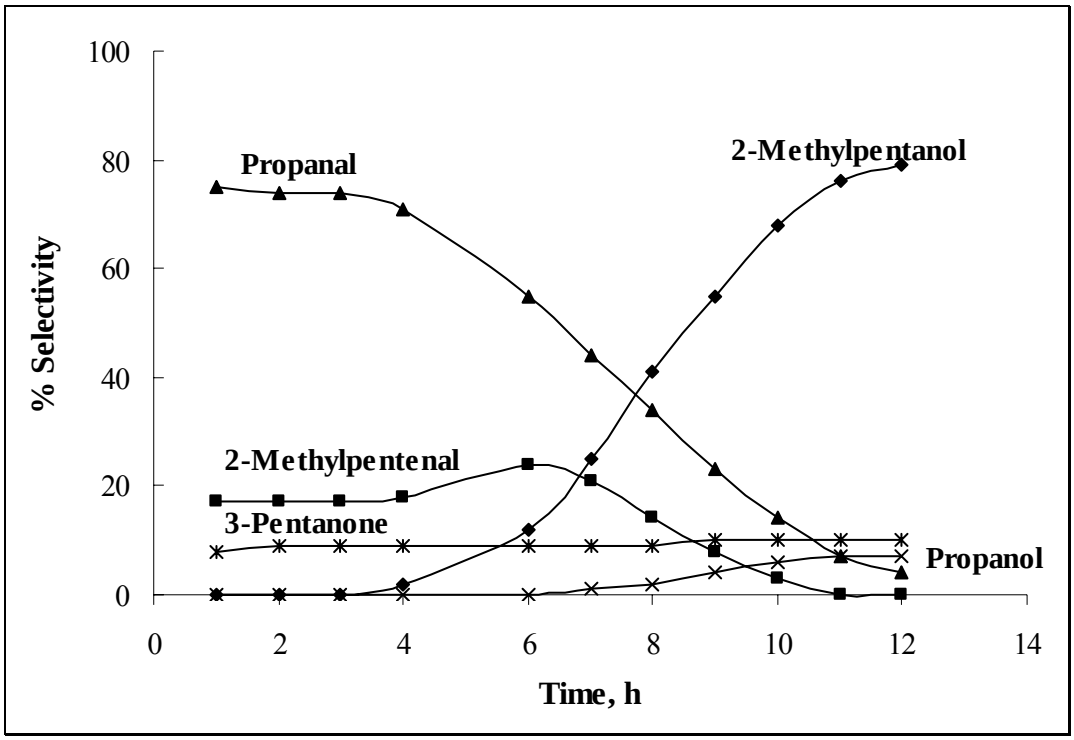

Figure 2.2.6. Effect of reaction time on the formation of products during single pot synthesis of 2–methylpentanol from ethylene using [HF/HT–Act] as a catalyst.

The hydroformylation of ethylene catalyzed by [HF] complex of [HF/HT–Act] catalyst was completed in 3 h where maximum formation of propanal takes place upto 2 h. Simultaneously, formation of 2–methylpentenal was also observed by the aldol condensation of propanal at 50 °C catalyzed by [HT–Act] component of multi–functional catalyst. After 3 h reaction time, reaction temperature was increased from 50 to 130 °C. Formation of 2–methylpentanol was started after 4 h and increased gradually. Linear increase in the selectivity of 2–methylpentanol after 6 h was observed which indicates that the condensation and hydrogenation of condensed product is faster during this reaction time period. The selectivity of 2–methylpentenal was also increased on increasing the reaction temperature, which indicates faster aldol condensation reaction at higher temperature. Linear decrease in the selectivity of propanal was observed due to its continuous consumption for condensation reaction. As the reaction time increased, the selectivity of 2–methylpentanol increased continuously upto 12 h, with decrease in the selectivity of the 2–methylpentenal, due to the simultaneous consumption of the 2–methylpentenal into 2–methylpentanol. Almost complete consumption of 2–methylpentenal for 2–methylpentanol was observed within 12 h via hydrogenation reaction catalyzed by [HF] complex of multi–functional catalyst. Significant changes in the selectivity of 3–pentanone was not observed throughout the reaction. The formation of propanol was also observed after 7 h via hydrogenation of propanal.

Table 2.2.7. Rate of reaction calculated from separate reaction performed by taking individual reactants and single pot synthesis of 2–methylpentanol from ethylene using [HF/HT–Act] as a catalyst

Run	Catalyst	Reaction*	Rate x 10^2 M/h
1	[HF/HT–Act] [a]	Hydroformylation	16.4
2	[HF/HT–Act] [b]	Hydrogenation [f]	9.8
3	[HF/HT–Act] [c]	Aldol condensation	5.2
4	[HF/HT–Act] [d]	Hydroformylation	14.3
		Aldol condensation	4.8
		Hydrogenation [f]	5.1
		Hydrogenation [g]	0.7

Reaction conditions:

[a] [HF/HT–Act] catalyst = 700 mg, T_1 = 50 °C for 3 h.

[b] [HF/HT–Act] catalyst = 700 mg, 2–methylpentenal = 0.4 M, T_2 = 130 °C for 9 h.

[c] [HF/HT–Act] = 700 mg, propanal = 0.4 M T_2 = 130 °C for 9 h.

[d] ethylene = 10 atm, CO = 5 atm, H_2 = 15 atm, [HF/HT–Act] = 700 mg, T_1 = 50 °C for 3 h; T_2 = 130 °C for 9 h.

[f] formation of 2–methylpentanol, [g] rate for formation of propanol.

From the comparison point of view, the rate of reaction was calculated for hydroformylation of ethylene, aldol condensation of propanal and hydrogenation of 2–methylpentenal by conducting experiments separately taking ethylene, propanal and 2–methylpentenal as a reactant under the reaction conditions identical to those used for single pot synthesis of 2–methylpentanol from ethylene (Table 2.2.7**)**. The rate of reaction for the hydroformylation of the ethylene, aldol condensation of the propanal and hydrogenation of 2–methylpentenal were found to be 16.4 x 10^{-2}, 9.8 x 10^{-2} and 5.2 x 10^{-2} M/h, respectively, when the all three reactions were performed separately in the reaction conditions similar to those of single pot synthesis of 2–methylpentanol. The rate of reaction for ethylene hydroformylation was found to be 14.3 x 10^{-2} M/h and 5.1 x 10^{-2} M/h for the formation of 2–methylpentanol in the single pot synthesis of 2–methylpentanol from ethylene using [HF/HT–Act] as a catalyst. The rate of condensation reaction was calculated as 4.8 x 10^{-2} M/h due to the basic solid component (activated hydrotalcite) of the multifunctional catalyst. The higher rate of reaction for hydrogenation as compared to aldol condensation step showed the faster hydrogenation of 2–methylpentenal to 2–methylpentanol. Generally, lower reaction rates were observed in case of single pot synthesis of

2–methylpentanol from ethylene using [HF/HT–Act] catalyst as compared to the separate reaction performed by taking individual reactants shows the complexity of the reaction for various subsequent reactions and side reactions in the single pot. However, significant difference in the rate of reaction was not observed for hydrogenation of 2–methylpentenal step in single pot reaction as compared to the separate reaction performed by taking individual reactants using [HF/HT–Act] catalyst.

2.2.4. Conclusions

Multi–functional catalyst [HF/HT–Act] was synthesized by impregnation of [HF] complex on the surface of [HT–Act] of varied Mg/Al molar ratio and its multi–functional potential was evaluated for selective synthesis of 2–methylpentanol from ethylene via hydroformylation, aldol condensation and hydrogenation reactions in single pot. ^{31}P–NMR and FT–IR spectra of [HF/HT–Act] catalyst showed that the [HF] complex was impregnated on the surface of [HT–Act] without decomposition. The Mg/Al ratio of [HT], aldol condensation temperature (T_2), CO to H_2 ratio and partial pressure of ethylene showed pronounced effect on the selectivity of 2–methylpentanol. As the Mg/Al molar ratio of [HT–Act] increased from 1.5 to 3.5, the selectivity for 2–methylpentanol also increased from 56 to 79% due to the enhancement in the basicity of catalyst. The selectivity of 2–methylpentanol was observed to increase from 0 to 79% on increasing the aldol temperature (T_2) from 60 to 130 °C. On further increase in the T_2 upto 180 °C, the selectivity of 2–methylpentanol decreased to 55% due to the hydrogenation of propanal to propanol. As the partial pressure of ethylene was increased upto 10 atm, the selectivity of 2–methylpentanol was observed to increase. The polar solvents showed higher selectivity of 2–methylpentanol as compared to non polar solvents. The [HF/HT–Act] catalyst is reusable for hydroformylation and hydrogenation reactions even at the end of fourth cycle, but not active for the aldol condensation of propanal. The reaction pathways and role of each component of multi–functional catalyst [HF/HT–Act] for the synthesis of 2–methylpentanol was discussed with the help of the kinetic profile of the reaction with time.

2.2.5. References

[1] A.D. Godwin, R.H. Schlosberg, F. Hershkowitz, M.G. Matturro, G. Kiss, K.C. Nadler, P.L. Buess, R.C. Miller, P.W. Allen, H.W. Deckman, R. Caers, E.J. Mozeleski, R.P. Reynolds, US Patent, 6307093 B1 (2001).

[2] W. Schoenlebe, H. Hoffmann, W. Lengsfeld, DE Patent, 2727330 (1979).

[3] P.Y. Blanc, A.Perret, F. Teppa, Helv. Chim. Acta 47 (1964) 567–575.

[4] D. Frohning, C.W. Kohlpaintner, in Applied Homogeneous Catalysis with Organometallic Compounds, ed. B. Cornils, W. A. Hermann, Wiley–VCH, Weinheim, (2000) vol. 1, ch. 2, pp. 29–104.

[5] V.K. Srivastava, D.U. Parmar, R.V. Jasra, Chem. Weekly July 8 (2003) 173–178 and July 15 (2003) 181–190; Chemical Economic Handbook, Oxo Chemical Report, SRI International, January (2003).

[6] H.G. Lueken, U. Tanger, W. Droste, G. Ludwig, D. Gubisch, US Patent, 4968849 (1990).

[7] T. Mori, K. Fujita, H. Hinoishi, US Patent, 5550302 (1996).

[8] J.J. Spivey, M.R. Gogate, Pollution Prevention in Industrial Condensation Reactions, Research Triangle Institute, USEPA Grant, (1996); G.J. Kelly, F. King, M. Kett, Green Chem. 4 (2002) 392–399.

[9] R.V. Jasra, V.K. Srivastava, R.S. Shukla, H.C. Bajaj, S.D. Bhatt, US Patent, 7294745B2 (2007); V.K. Srivastava, S.K. Sharma, R.S. Shukla, R.V. Jasra, Ind. Eng. Chem. Res. 47 (2008) 3795–3803.

[10] V.K. Srivastava, S.K. Sharma, R.S. Shukla, R.V. Jasra, Catal. Commun. 7 (2006) 879–884.

[11] S.K. Sharma, V.K. Srivastava, R.S. Shukla, P.A. Parikh, R.V. Jasra, New J. Chem. 31 (2007) 277–286.

[12] S.K. Sharma, P.A. Parikh, R.V. Jasra, J. Mol. Catal. A: Chem. 278 (2007) 135–144.

[13] H.A. Patel, S.K. Sharma, R.V. Jasra, J. Mol. Catal. A: Chem. 286 (2008) 31–40.

[14] F. Cavani, F. Trifiro, A. Vaccari, Catal. Today 11 (1991) 173–301.

[15] S. Abello, F. Medina, D. Tichit, J.P. Ramirez, J.C. Groen, J.E. Sueiras, P. Salagre Y. Cesteros, Chem. Eur. J. 11 (2005) 728–739.

Chapter 3

Eco–Friendly Hydroformylation of Alkenes using Multi–Functional Catalyst having $HRh(CO)(TPPTS)_3$ Complex Intercalated into the Interlayer Space of Hydrotalcite

3.1. Introduction

Hydroformylation or oxo reaction employed for the synthesis of aldehyde and alcohol starting from alkene is an important reaction from industrial and academic perspective. Approximately, 9 million metric tons per year of aldehydes and alcohols are produced by hydroformylation reaction. These products find applications in the manufacturing of soaps, fragrances, detergents, adhesives**,** plasticizers and solvents [1–3]. Commercially, triphenylphosphine modified rhodium based complex is used as a catalyst for hydroformylation of lower carbon chain length alkenes ($C_2 – C_5$) under mild reaction conditions. However, this is not used for higher carbon chain length alkenes due to the decomposition of rhodium complex during separation of the catalyst from product mixture. Hydroformylation of higher alkenes is carried out using cobalt based catalysts under homogeneous conditions. These catalysts require higher temperature, pressure and longer reaction time as compared to rhodium based catalysts. Though, homogeneous catalysts give higher conversion and selectivity for desired product in short reaction time as compared to heterogeneous catalyst system, yet they have disadvantage in the separation of catalyst from product mixture. Thus, research efforts are directed towards the heterogenization of rhodium complex for hydroformylation of alkenes. The problem of catalyst separation from reaction mixture is solved by using a water soluble $[HRh(CO)(TPPTS)_3]$ catalyst in biphasic system for the hydroformylation of alkenes [4]. The application of biphasic catalyst system is limited to hydroformylation of propylene and butene due to lower solubility of higher carbon chain length alkenes in aqueous medium. Numerous supported rhodium complexes have been reported in the literature for hydroformylation of alkenes. The support materials studied include MCM–41, silica, alumina, zeolites, active carbons, polymeric organic, inorganic and hybrid supports and supported aqueous phase catalysis (SAPC) [5–14]. The main disadvantages of these supported catalysts are include leaching of rhodium complex during the reaction, complicated synthesis procedure, lower catalyst activity and lower thermal stability of the catalyst.

Hydrotalcite or layered double hydroxides (LDHs) is synthetic anionic clay having positively charged brucite–like sheets with general formula $[M(II)_{1-x}M(III)x(OH)_2]^{x+}A^{n-}{}_{x/n}$ $(1-3x/2)H_2O$, $(0.20 < x \leq 0.33)$. Where M(II) and M(III) are divalent and trivalent cations in the octahedral sites within the hydroxyl layers, x is the molar ratio of M(III)/[M(II)+M(III)] and A is the exchangeable interlayer anions [15]. Due to excellent anions exchange property of hydrotalcite, variety of organic and inorganic anions can be intercalated into the interlayer space of hydrotalcite and composite material can be used for specific purposes [16–27]. Intercalation of transition metal complexes such as $PtCl_6$, palladium, cobalt(II)–phthalocyanine, ruthenium–, chromium–, iron(III)–hexacyano, copper(II)– and nickel(II)– nitrilotriacetate in LDHs has been reported in the literature

[28–37]. Intercalation of *trans*–RhCl(CO)$(TPPTS)_2$ into Zn–Al LDHs was reported by Duan et al., however, they have not reported its catalytic activity [38]. In another study, $RhCl(TPPTS)_3$ complex was heterogenized onto Zn–Al LDHs via ion exchange method and used as a heterogeneous catalyst for hydrogenation of bicyclo[2.2.2]octenes [39]. In the present study, intercalation of $HRh(CO)(TPPTS)_3$ complex in the interlayer space of Mg–Al hydrotalcite of Mg/Al molar ratio of 3.5 was carried out (Scheme 3.1) and applicability of intercalated complex as a heterogeneous catalyst for hydroformylation of alkenes was studied.

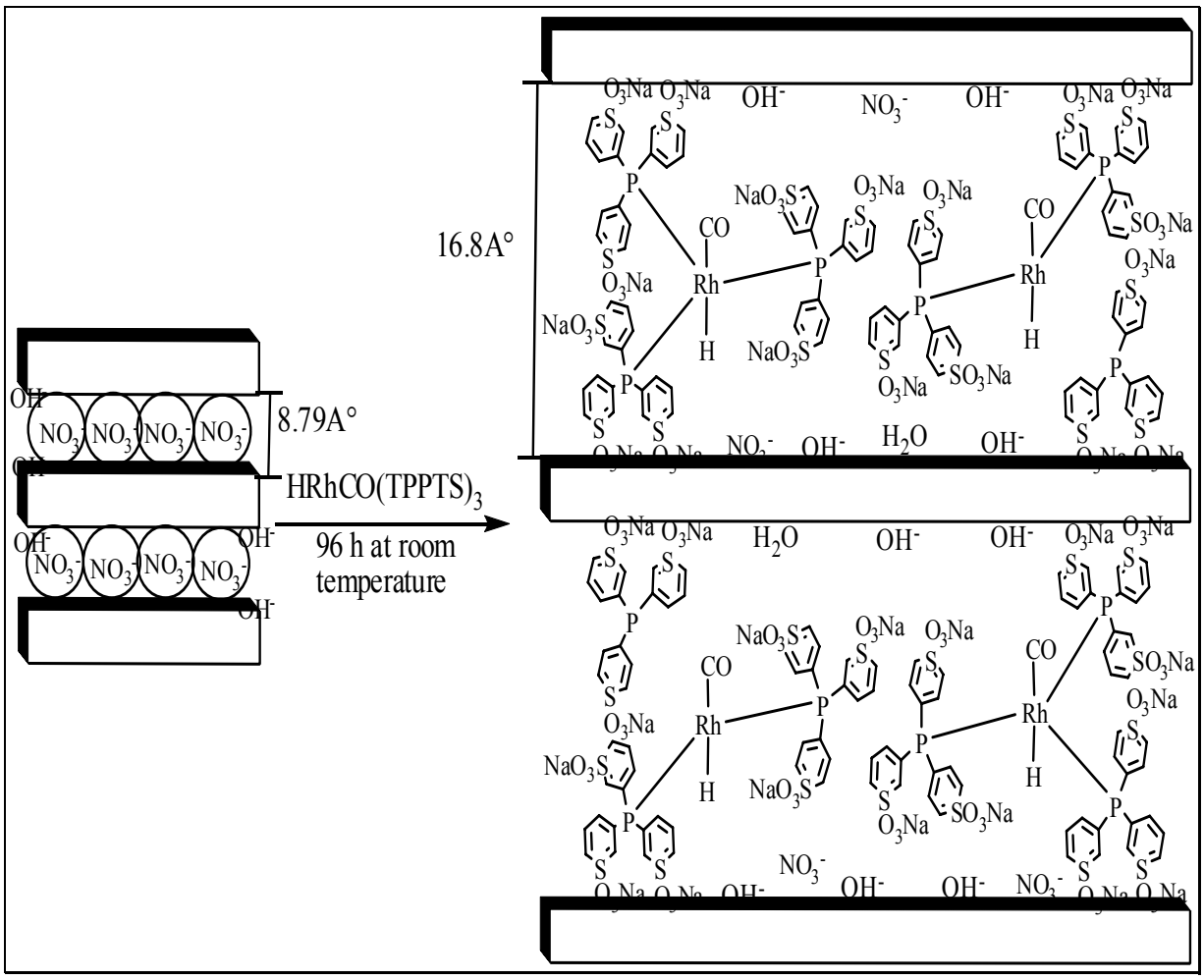

Scheme 3.1. Intercalation of $HRh(CO)(TPPTS)_3$ complex into the interlayer space of hydrotalcite.

3.2. Experimental

3.2.1. Materials

The (acetylacetonato)dicarbonylrhodium ($Rh(CO)_2(acac)$; 98%), tris(3–sodium sulfonatophenyl) phosphine (TPPTS; P(*m*–$C_6H_4SO_3Na)_3$), and alkenes were purchased from Sigma–Aldrich, USA. Magnesium nitrate ($Mg(NO_3)_2.6H_2O$, 98.9%), aluminum nitrate ($Al(NO_3)_3.9H_2O$, 99.1%), sodium nitrate ($NaNO_3$, 99.9%), ammonia solution (40%) and toluene

(99.9%) were purchased from s.d. Fine Chemicals, India. CO (99.9%) and H_2 (99.99%) gases were purchased from Alchemie Gases and Chemicals Pvt. Ltd., India. Alkenes used in the present study, were purchased from Sigma–Aldrich, USA. Double distilled milli–pore deionized water was used during the synthesis of $HRh(CO)(TPPTS)_3$ complex and hydrotalcite.

3.2.2. Synthesis of $HRh(CO)(TPPTS)_3$ Complex

Synthesis of $HRh(CO)(TPPTS)_3$ complex was carried out by the reported procedure [40]. In a typical procedure, 400 mg of TPPTS (0.704 mmol) was dissolved in 1 mL water followed by addition of 50 mg of $Rh(CO)_2(acac)$ under inert atmosphere. Mixture was warmed gently till the complete dissolution of $Rh(CO)_2(acac)$. Syn–gas ($CO + H_2 = 1:1$) was charged into solution from top of the flask. Color of the solution changed from maroon to yellow on passing syn–gas. After 6 h, solution was filtered to remove unreacted rhodium metal under inert atmosphere. Yellow precipitate was obtained by adding saturated ethanol (8 mL) with syn–gas into the filtrate. The precipitated material was again filtered, washed with ethanol and dried under vacuum.

3.2.3. Synthesis of Hydrotalcite [HT(3.5)–N] containing Nitrates in the Interlayer Space

The hydrotalcite of Mg/Al molar ratio 3.5 [HT(3.5)–N] was synthesized by co–precipitation of metals salt solutions at constant pH [15]. Typically, for synthesis of hydrotalcite of Mg/Al molar ratio 3.5, an aqueous solution (A) of $Mg(NO_3)_2.6H_2O$ (0.105 mol) and $Al(NO_3)_3.9H_2O$ (0.03 mol) in 80 mL double distilled deionized water was prepared. The solution A was added drop wise into a second solution (B) containing $NaNO_3$ (0.10 mol) in 80 mL double distilled deionized water, for about 1 h under vigorous stirring at room temperature. The pH of the content was maintained at 9.5 by adding the ammonia solution. The content was aged at 70 °C for 14 h under autogenous pressure. The formed precipitate was filtered and washed with hot distilled water until pH of filtrate was reached to 7. The washed precipitate was dried in vacuum at room temperature.

3.2.4. Intercalation of $HRh(CO)(TPPTS)_3$ Complex into the Interlayer Space of Hydrotalcite [HT(3.5)–INT]

Intercalation of $HRh(CO)(TPPTS)_3$ complex into interlayer space of [HT(3.5)–N] was carried out by the addition of 3.24 g hydrotalcite in a solution of 1.04 g $HRh(CO)(TPPTS)_3$ complex in 25 mL deionized double distilled water. Suspension was stirred at room temperature for 96 h under inert atmosphere of nitrogen gas. After 96 h, the yellow colored suspension was filtered and dried in vacuum and the catalyst thus obtained is termed as [HT(3.5)–INT].

3.2.5. Characterization of Catalyst

Powder X–ray diffraction (P–XRD) patterns of $HRh(CO)(TPPTS)_3$ complex, [HT(3.5)–N] and [HT(3.5)–INT] were recorded using Phillips X'Pert MPD system equipped with XRK 900 reaction chamber, using Ni–filtered Cu–Kα radiation (λ =1.5405 Å) over a 2θ range of 2–70°. The percentage crystallinity of [HT(3.5)–N] and [HT(3.5)–INT] were calculated by the summation of integral intensities of (003) and (006) planes. The crystallinity of [HT(3.5)–INT] catalyst was calculated by assuming 100% crystallinity of pristine hydrotalcite [HT(3.5)–N]. The values of unit cell parameters (*a* and *c*) of [HT(3.5)–N] and [HT(3.5)–INT] were calculated by the formula; a = $2(d_{110})$ and c = $3(d_{003})$; where d_{110} and d_{003} are the basal spacing values of (110) and (003) planes, respectively [41].

Fourier transform infrared (FT–IR) spectra of $HRh(CO)(TPPTS)_3$ complex, [HT(3.5)–N] and [HT(3.5)–INT] were recorded using Perkin–Elmer spectrum GX FT–IR spectrometer in the region of 400 to 4000 cm^{-1} using KBr pellets.

^{31}P solid state Fourier transform nuclear magnetic resonance (FT–NMR) spectra of TPPTS, $HRh(CO)(TPPTS)_3$ complex and [HT(3.5)–INT] were recorded on Bruker–Avance II–500 (FT–NMR 500 MHz) spectrometer.

Thermogravimetric analysis (TGA) of $HRh(CO)(TPPTS)_3$ complex, [HT(3.5)–N] and [HT(3.5)–INT] was carried out using Mettler–Toledo TGA/SDTA 851e equipment in nitrogen flow (flow rate = 50 mL/min) at a heating rate of 10 °C/min.

Surface morphology of [HT(3.5)–N] and [HT(3.5)–INT] was determined using scanning electron microscope (SEM; Leo Series VP1430, Germany) having silicon detector. The samples were coated with gold using sputter coating prior to measurement. Analysis of samples was carried out at an accelerating voltage of 15 kV.

Surface area measurements of [HT(3.5)–N] and [HT(3.5)–INT] were carried out using ASAP 2010 Micromeritics, USA. The samples were activated at 80 °C for 4 h under vacuum (5×10^{-2} mmHg) prior to N_2 adsorption measurements. Specific surface area of the samples was calculated from N_2 adsorption isotherms measured at 77.4 K using Brunauer, Emmett, Teller (BET) method. The pore size distribution was determined from desorption branch using the Barrett, Joyner and Halenda method [42].

3.2.6. Hydroformylation Reaction

Hydroformylation reaction was carried out in 100 mL EZE–Seal stirred reactor supplied by Autoclave Engineers, USA, equipped with a controlling unit [43–44]. In a typical reaction procedure, 0.025 mol of 1–hexene and 0.1 g tridecane (as an internal standard) dissolved in 50 mL of toluene as a solvent with 100 mg of [HT(3.5)–INT] catalyst were fed into the reactor. The reactor was flushed twice with nitrogen after that the synthesis gas (CO/H_2 = 1:1) was introduced into the reactor upto 40 atm. The reactor temperature was brought upto 80 °C by heating and stirrer of the reactor was started at 1000 rpm. Constant pressure was maintained during the reaction by supplying the syn–gas from reservoir. After completion of reaction, the reactor was cooled to room temperature by circulation of cold water in the coil provided inside the reactor. Product mixture was then analyzed by gas chromatography (GC) and GC–mass spectroscopy (GC–MS).

For finding out the reusability of [HT(3.5)–INT], the catalyst after completion of the reaction was filtered from the reaction mixture, washed with 100 mL toluene and dried in vacuum. The catalyst obtained after drying was used again for hydroformylation of 1–hexene under reaction conditions similar to that of the fresh catalyst.

3.2.7. Reaction Product Analysis

Analysis of product mixture was carried out by GC–MS (Shimadzu, GCMS–QP2010) and GC (Shimadzu 17A, Japan) equipped with 5% diphenyl and 95% dimethyl siloxane universal capillary column (60 m length and 0.25 mm diameter) and a flame ionization detector (FID). The GC oven temperature was programmed from 40 to 200 °C at the rate of 6 °C/min. Nitrogen gas was used as a carrier gas. Temperature of injection port and FID were kept constant at 250 °C. Retention time of different compounds was determined by injecting pure compounds under identical GC conditions. To ensure reproducibility of the reaction, repeated experiments were carried out under identical reaction conditions. Conversion and selectivity data were found to be reproducible in the range of ± 4% variation. The % conversion of alkenes, % selectivity of aldehydes and TOF values were calculated by the following formula–

$$\% \text{ Conversion} = \frac{\text{Moles of alkene reacted}}{\text{Moles of alkene fed}} \times 100$$

$$\% \text{ Selectivity of aldehydes} = \frac{\text{Moles of aldehydes formed}}{\text{Moles of (aldehydes + isomerized alkene + alkane + ketone)}} \times 100$$

$$TOF = \frac{\text{Moles of aldehydes formed}}{\text{(Moles of Rh present in the catalyst x time)}}$$

3.3. Results and Discussion

3.3.1. Characterization of Catalyst

P–XRD patterns of $HRh(CO)(TPPTS)_3$, [HT(3.5)–N] and [HT(3.5)–INT] samples are shown in Figure 3.1. P–XRD pattern of [HT(3.5)–N] shows sharp and symmetric peaks at lower diffraction angles (2θ = 10–25) and broad asymmetric reflections at higher 2θ angles (2θ = 30–50), which are typical characteristics of pure hydrotalcite. The presence of NO_3^- anions in interlayer space of [HT(3.5)–N] was confirmed by the *d*–spacing of (003) and (006) planes, 8.79 Å and 4.48 Å, respectively. P–XRD pattern of intercalated hydrotalcite [HT(3.5)–INT] shows all characteristics peaks of pristine hydrotalcite without any additional peak of $HRh(CO)(TPPTS)_3$ complex. This indicates intercalation of $HRh(CO)(TPPTS)_3$ complex into the interlayer space of [HT(3.5)–N]. However, in our earlier work reported in Chapter 2 for the synthesis of multi–functional catalyst system by impregnation of $HRh(CO)(PPh_3)_3$ complex on the surface of hydrotalcite, we have observed the peaks of $HRh(CO)(PPh_3)_3$ complex in the P–XRD patterns of multi–functional catalyst [45–46]. The main diffraction peaks at 2θ values 5.62 (003), 11.32 (006) and 61.1 (110) were observed in P–XRD pattern of [HT(3.5)–INT] sample. The observed shift in P–XRD pattern of intercalated [HT(3.5)–INT] sample towards lower 2θ values of (003) and (006) planes with respect to pristine hydrotalcite confirmed the intercalation of $HRh(CO)(TPPTS)_3$ complex. The intercalation of $HRh(CO)(TPPTS)_3$ complex was further confirmed by the broadening in *d*–spacing value of (003) plane of [HT(3.5)–INT] from 8.79 to 16.8 Å. The crystallinity of [HT(3.5)–INT] was observed to decrease upto 43% on intercalation of $HRh(CO)(TPPTS)_3$. The values of unit cell parameters *a* was calculated as 3.0 Å for both, [HT(3.5)–N] and [HT(3.5)–INT] samples. The value of *c* was observed to change significantly for the intercalated sample [HT(3.5)–INT]. The value of *c* was calculated as 26.4 Å for [HT(3.5)–N], which increased to 59.4 Å for [HT(3.5)–INT] sample. Increase in the *c* value for [HT(3.5)–INT] sample is due to the intercalation of $HRh(CO)(TPPTS)_3$ complex in the interlayer space of [HT(3.5)–N].

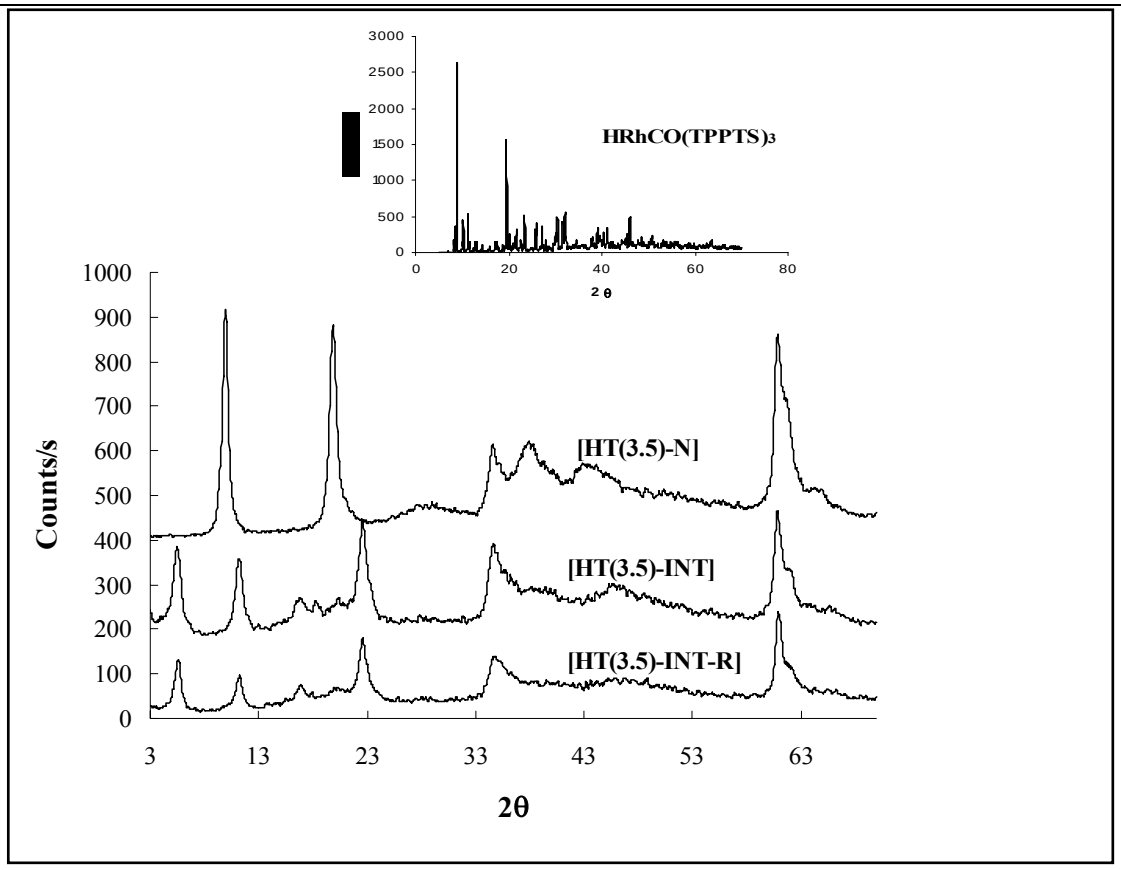

Figure 3.1. P–XRD patterns of $HRh(CO)(TPPTS)_3$ complex, [HT(3.5)–N], [HT(3.5)–INT] and [HT(3.5)–INT–R] samples.

The FT–IR spectra of $HRh(CO)(TPPTS)_3$, [HT(3.5)–N] and [HT(3.5)–INT] samples are shown in Figure 3.2. The formation of $HRh(CO)(TPPTS)_3$ complex was confirmed by the appearance of bands at 2006 cm^{-1} for ν_{Rh-H}, 1926 cm^{-1} for $\nu_{C=O}$, 3868 and 1632 cm^{-1} for ν_{O-H}, 1465 and 1399 cm^{-1} for ν_{ph}, 1195 cm^{-1} for ν_{SO3}^{-}, 1096 cm^{-1} for ν_{SO} and 623 cm^{-1} for ν'_{SO} [38]. The band appeared at 1380 cm^{-1} in FT–IR spectrum of [HT(3.5)–N] confirmed the presence of nitrate anions in the interlayer space of hydrotalcite [15]. Bands that appeared at 1195 cm^{-1} (ν_{SO3}^{-1}), 1096 cm^{-1} (ν_{SO}) and 623 cm^{-1} (ν'_{SO}) in the spectrum of $HRh(CO)(TPPTS)_3$ complex was observed to shift towards low frequency region in the FT–IR spectrum of [HT(3.5)–INT] catalyst. The shifting of these bands in the direction of low frequency region is due to coordination between oxygen atom of sulfonate group of $HRh(CO)(TPPTS)_3$ complex with layers of hydroxides present in the hydrotalcite network. The intensity of band at 1380 cm^{-1} was observed to decrease significantly in the FT–IR of [HT(3.5)–INT] catalyst, which confirmed that the nitrate anions present in the interlayer space of hydrotalcite were replaced by $HRh(CO)(TPPTS)_3$ complex. The other vibrations of the FT–IR spectra of $HRh(CO)(TPPTS)_3$ complex and [HT(3.5)–N] were found to be present in FT–IR spectrum of [HT(3.5)–INT] catalyst. Above data show that the $HRh(CO)(TPPTS)_3$ complex was intercalated into interlayer space of [HT(3.5)–N].

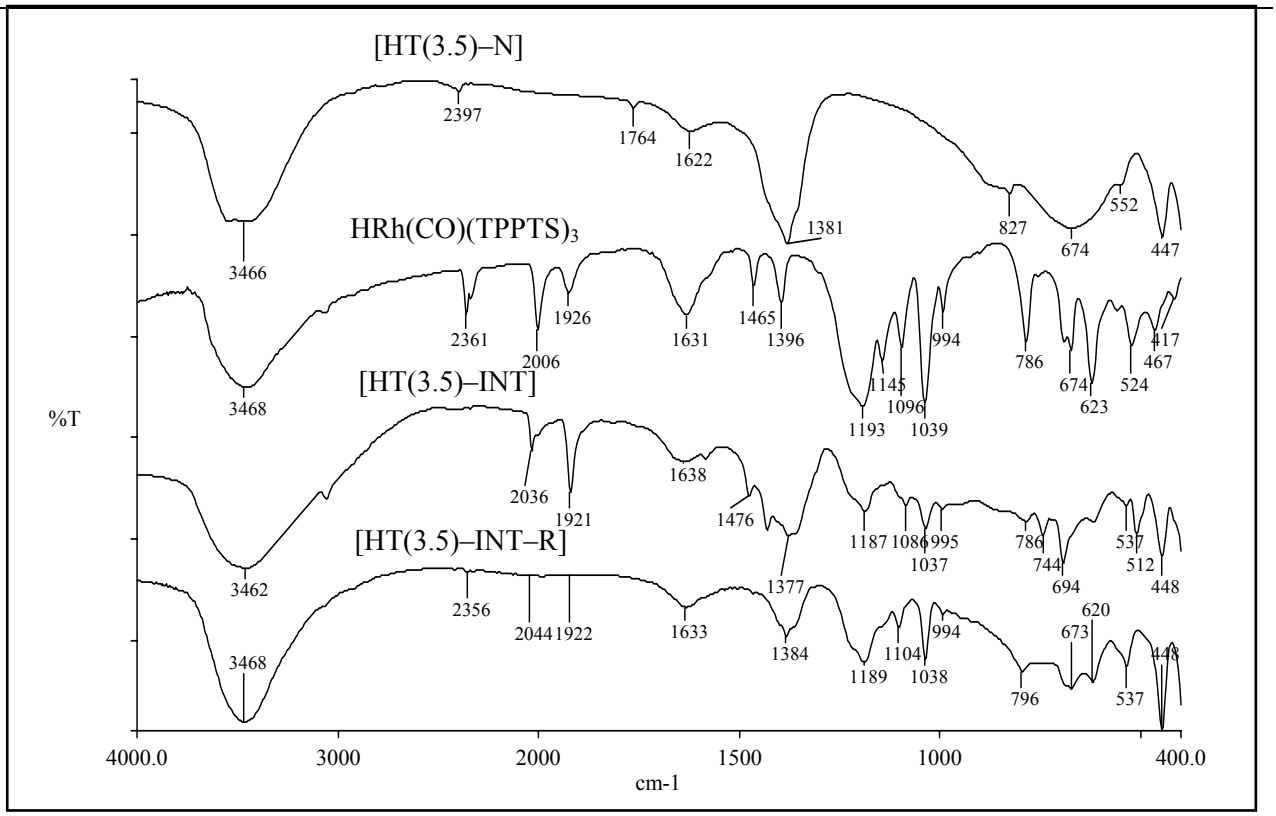

Figure 3.2. FT–IR spectra of [HT(3.5)–N], $HRh(CO)(TPPTS)_3$ complex, [HT(3.5)–INT] and [HT(3.5)–INT–R] samples.

^{31}P MAS NMR spectra of TPPTS, $HRh(CO)(TPPTS)_3$ complex and [HT(3.5)–INT] samples are shown in Figure 3.3. The ^{31}P–NMR spectrum of TPPTS shows peaks at –5.4 and 34.65 ppm attributed to the uncoordinated TPPTS and oxides of TPPTS, respectively (Figure 3.3a).

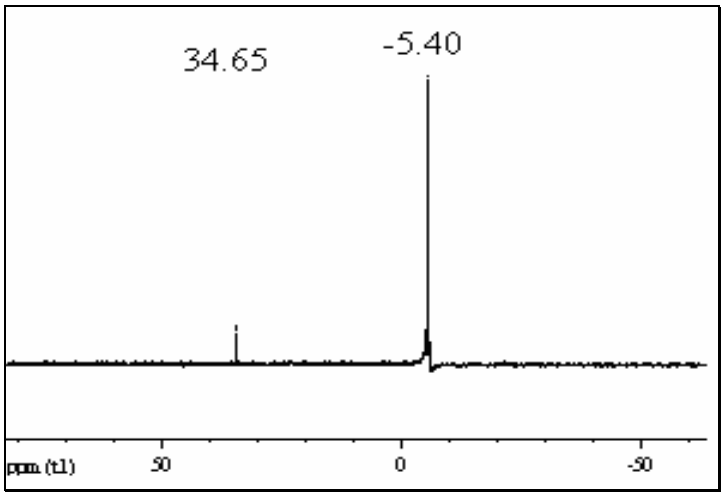

Figure 3.3a. ^{31}P NMR spectrum of TPPTS in D_2O.

The appearance of doublet at 44.32 [J(Rh–P) = 152 Hz] in ^{31}P–NMR spectrum of $HRh(CO)(TPPTS)_3$ complex (Figure 3.3b) shows the trigonal bipyramidal structure with three phosphorous atoms present in the same environment and are in equatorial plane. The hydride (H)

and CO are in axial positions [40]. Doublet at 42.34 ppm was observed in solid state ^{31}P–NMR spectrum of [HT(3.5)–INT] catalyst (Figure 3.3c) confirming that the $HRh(CO)(TPPTS)_3$ complex was intercalated into the interlayer space of hydrotalcite. The peaks observed at 37.59 ppm and –31.48 ppm in solid state ^{31}P–NMR spectrum of [HT(3.5)–INT] catalyst are attributed to the intercalated $HRh(CO)(TPPTS)_2$ and TPPTS, respectively, in the interlayer space of hydrotalcite. During the intercalation process, dissociation of TPPTS molecule from $HRh(CO)(TPPTS)_3$ complex is also reported in the literature [47–48].

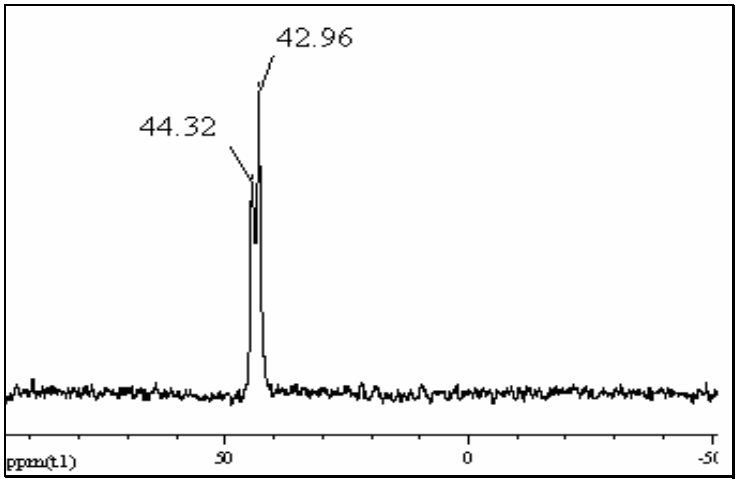

Figure 3.3b. ^{31}P NMR spectrum of $HRh(CO)(TPPTS)_3$ in D_2O.

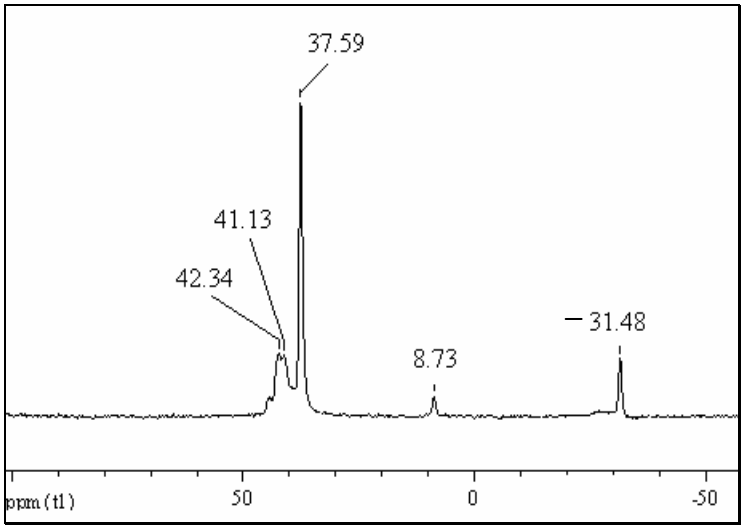

Figure 3.3c. ^{31}P solid state NMR spectrum of [HT(3.5)–INT] catalyst.

Thermal stability of $HRh(CO)(TPPTS)_3$, [HT(3.5)–N] and [HT(3.5)–INT] samples were evaluated by TGA and results are shown in Figure 3.4. TGA of $HRh(CO)(TPPTS)_3$ showed 63% weight loss in the temperature range of 180 to 300 °C due to thermal decomposition of complex. However, only 3% weight loss of $HRh(CO)(TPPTS)_3$ was observed upto 140 °C due to removal of water molecules. TGA of [HT(3.5)–N] showed weight loss in two stages, which is a typical

characteristic of pure hydrotalcite sample [15]. The weight loss in first stage (9%) was observed in the temperature range of 200–220 °C due to loss of physically adsorbed water molecules on the surface without collapse of the structure. The weight loss in second stage (30%) was attributed to the removal of hydroxyl groups and nitrate anions in the temperature range of 300–550 °C. TGA curve of [HT((3.5)–INT] catalyst was observed similar to $HRh(CO)(TPPTS)_3$ complex. TGA of intercalated catalyst [HT((3.5)–INT] showed 10% weight loss in the temperature range of 180–240 °C due to removal of water molecules. The major weight loss (42%) was observed in second stage due to removal of anions from interlayer space of hydrotalcite in the temperature range of 300–550 °C. Higher weight loss in [HT((3.5)–INT] as compared to pristine [HT((3.5)–N] is due to decomposition of bulkier anions (TPPTS) present in the interlayer space of [HT((3.5)–N]. The observed higher thermal stability of [HT((3.5)–INT] catalyst as compared to $HRh(CO)(TPPTS)_3$ complex is due to the strong interaction of $HRh(CO)(TPPTS)_3$ complex and interlayer network of hydrotalcite structure. Due to the higher thermal stability of [HT((3.5)–INT], it has potential applications in catalysis as a heterogeneous catalyst for hydroformylation and hydrogenation reaction.

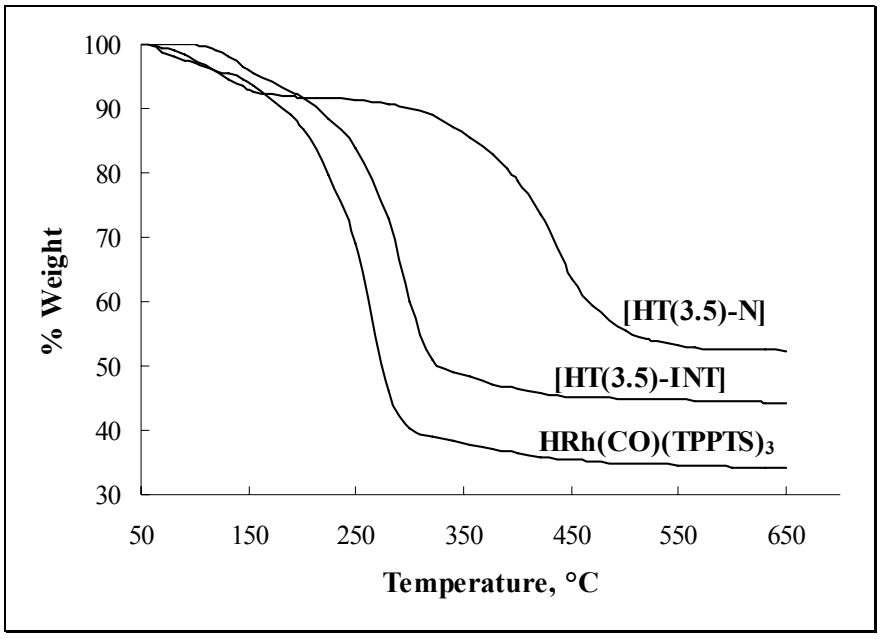

Figure 3.4. TGA of $HRh(CO)(TPPTS)_3$ complex, [HT(3.5)–N] and [HT(3.5)–INT] samples.

The SEM images of [HT(3.5)–N] and [HT(3.5)–INT] are given in Figure 3.5. The micrographs of [HT(3.5)–N] and [HT(3.5)–INT] show a well developed layered structure and possess platelet structures. However, due to overlapping of such platelets spongy type structure is exhibited.

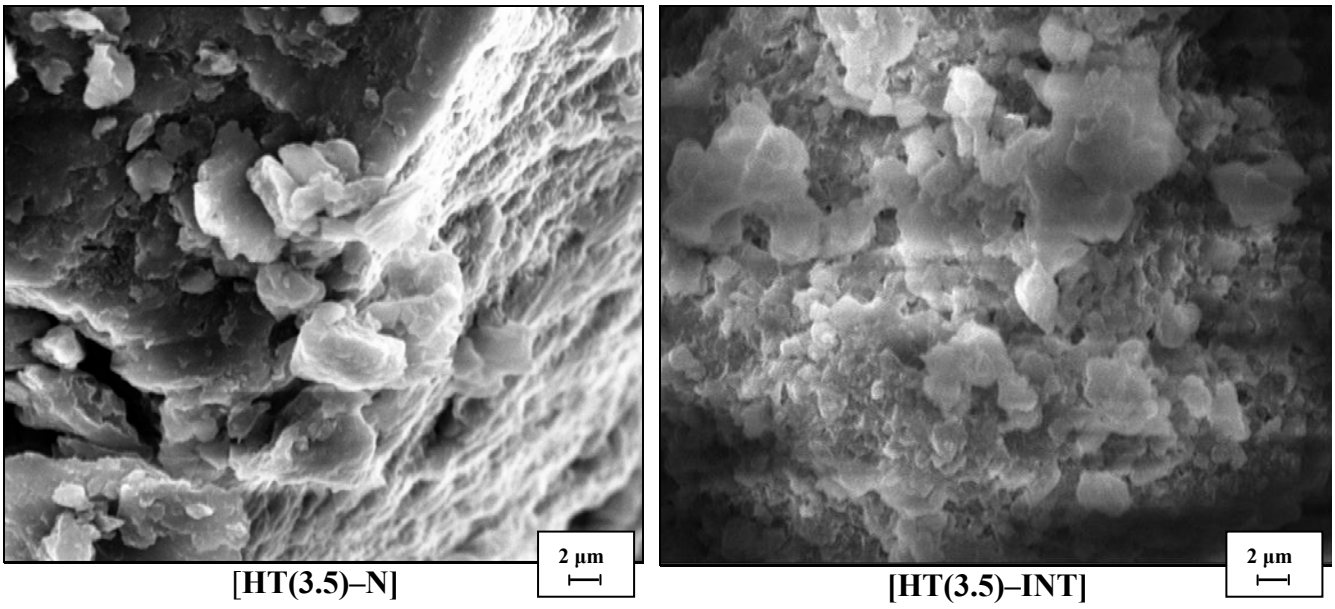

Figure 3.5. SEM images of [HT(3.5)–N] and [HT(3.5)–INT] catalyst.

Nitrogen adsorption–desorption isotherms of [HT(3.5)–N] and [HT(3.5)–INT] measured at liquid nitrogen temperature are shown in Figure 3.6. The surface area, pore size distribution and pore volume of [HT(3.5)–N] and [HT(3.5)–INT] are given in Table 3.1. The surface area of [HT(3.5)–N] was calculated as 76 m^2/g that decreased upto 33 m^2/g after intercalation of $HRh(CO)(TPPTS)_3$ in the interlayer space of [HT(3.5)–N]. The pore volume of [HT(3.5)–N] was also observed to decrease from 0.4 to 0.1 cm^3/g for intercalated [HT(3.5)–INT] catalyst. The surface area measurements data also support the results observed in P–XRD analysis of [HT(3.5)–INT] catalyst.

Table 3.1. Characterization of [HT(3.5)–N] and [HT(3.5)–INT] samples

Sample	[HT(3.5)–N]	[HT(3.5)–INT]
Crystallinity, %	100	42
Surface area, m^2/g	76	33
Pore volume, cm^3/g	0.4	0.1
Unit cell parameter (*a*), Å	3.0	3.0
Unit cell parameter (*c*), Å	26.4	59.4

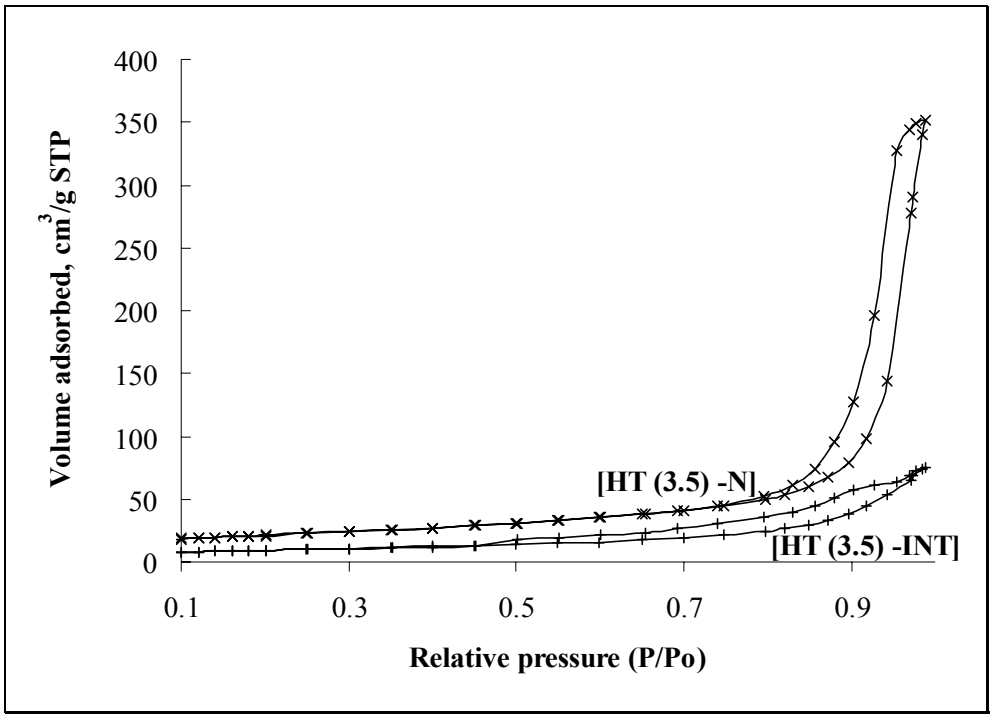

Figure 3.6. Surface area measurements of [HT(3.5)–N] and [HT(3.5)–INT] samples.

3.3.2. Catalytic Activity for Hydroformylation of Alkenes

The catalytic activity of intercalated [HT(3.5)–INT] catalyst was evaluated for hydroformylation of linear alkenes with varied carbon chain length from C_5 to C_{13} and some cyclic alkenes (Table 3.2). The mass fragmentation data for the hydroformylation products of studied alkenes are given in Figure 3.7. As the carbon chain length of linear alkenes increases, the selectivity for aldehydes was observed to decrease. For example, 100% conversion with 98% selectivity of aldehydes was achieved for hydroformylation of 1–pentene in 10 h reaction time at 80 °C, which decreased to 99% conversion of 1–decene with 83% selectivity of aldehydes. However, for hydroformylation of 1–tridecene, conversion further decreased to 88% with 56% selectivity of aldehydes. This decrease in the selectivity of aldehydes on increasing the carbon chain length of alkenes is due to isomerization of alkene and formation of ketone under the studied experimental conditions. The reactivity of the catalyst for hydroformylation of linear alkenes under identical reaction conditions was found to be in the order of; 1–pentene > 1–hexene > 1–heptene > 1–octene> 1–nonene > 1–decene > 1–undecene > 1–dodecene > 1–tridecene. The *n/iso* ratio of aldehydes for linear alkenes was observed in the range of 0.6 – 1.3.

Table 3.2. Effect of carbon chain length of alkenes on catalytic activity of [HT(3.5)–INT]

Run	Alkene	% Conv.	% Selectivity [a]				
			Aldehydes	*n/iso* Ratio of aldehydes	Isomerization of alkene	Hydrogenation of alkene	Ketone
1	 1–Pentene	100	98	1.3	2	–	–
2	 1–Hexene	100	97	0.8	3	–	–
3	 1–Heptene	100	95	0.8	5	–	–
4	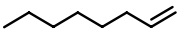 1–Octene	100	95	0.7	5	–	–
5[b]	 1–Nonene	100	88	0.7	7	–	5
6[c]	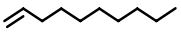 1–Decene	99	83	0.7	11	–	6
7[d]	 1–Undecene	97	72	0.6	18	–	10
8[e]	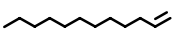 1–Dodecene	95	67	0.6	21	–	12
9[f]	 1–Tridecene	88	56	0.6	29	–	15
10	 Cyclohexene	98	100	–	–	–	–
11[g]	 Cycloheptene	90	–	–	–	2	–
12	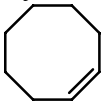 *cis*– Cyclooctene	42	95	–	–	5	–
13	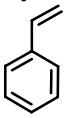 Styrene	95	92	0.5	–	8	–
14	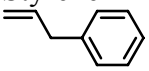 allylbenzene	64	89	1.1	6	5	–

[a] **Reaction conditions:** alkene = 0.2 mmol, catalyst = 100 mg, syn–gas = 40 atm (CO/H_2 = 1/1), temperature = 80 °C, time = 10 h.

[b] 3–Decanone (m/z = 156); [c] undecanone; [d] 3–Dodecanone (m/z = 184); [e] Tridecanone (m/z = 198); [f] 2–Tetradecanone (m/z = 212); [g] 98% selectivity for cycloheptanemethanol (m/z = 128).

The main reason for lower *n/iso* ratio of aldehydes observed in present study could be due to the strong coordination of ligand to the hydrotalcite matrix in [HT(3.5)–INT] catalyst. Therefore, movement of ligand molecules is restricted in the intercalated catalyst as compared to that in its biphasic analogues [$HRh(CO)(TPPTS)_3$] catalyzed hydroformylation in biphasic medium], as a result, the steric effect of ligand is less operative to increase the n/iso ratio of aldehydes in the present study. Another reason for lower *n/iso* ratio of aldehydes is the absence of excess ligand (TPPTS) in this study. It is well known in hydroformylation reaction that the higher *n/iso* ratio of aldehydes can be achieved by adding excess amount of ligand to suppress the isomerization of alkenes, this creates a sterically demanding environment around the rhodium metal centre which results into the higher *n/iso* ratio of aldehydes. Lower *n/iso* ratio of aldehydes in the range of 0.5 to 0.64 was also reported by the Chaudhary et al. for hydroformylation of alkenes using $HRh(CO)(TPPTS)_3$ supported on carbon surface [49]. In case of hydroformylation of cyclic alkenes, 98% conversion of cyclohexene with 100% selectivity for cyclohexanal (m/z = 112) was observed. The conversion decreased to 42% for hydroformylation of *cis*–cyclooctene with 95% selectivity for cyclooctanal (m/z = 140). However, for the hydroformylation of 1–cycloheptene, 98% selectivity for cycloheptanemethanol (m/z = 128) was observed, which was formed via subsequent hydrogenation of hydroformylation product (aldehyde). Order of the catalytic activity for hydroformylation of cyclic alkenes was observed as; cyclohexene > cycloheptene > cyclooctene under identical reaction conditions. For hydroformylation of styrene, 95% conversion with 92% selectivity of aldehydes (3–phenylpropanal, α–phenylpropionaldehyde; m/z = 134) was observed, while the conversion decreased to 64% with 89% selectivity of aldehydes (benzenebutanal, α–ethyl–benzeneacetaldehyde; m/z = 148) for the hydroformylation of allylbenzene. 1–Hexene was selected as a model reactant to study the effect of reaction parameters such as, alkene concentration, amount of catalyst, partial pressure of CO and H_2 and reaction temperature on the catalytic activity of intercalated catalyst. Experiments to study the reusability of catalyst was also carried out by performing repeated experiments under reaction conditions similar to those used for the fresh catalyst.

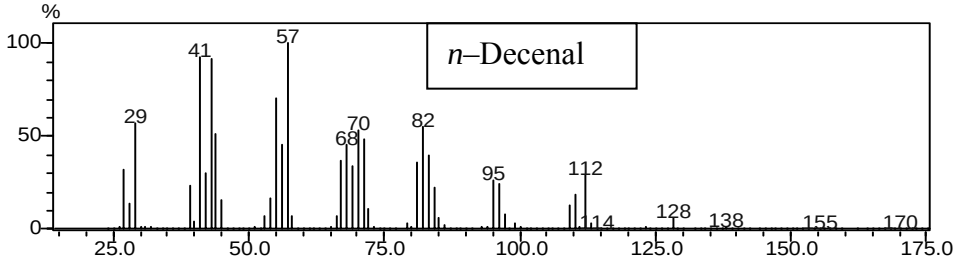

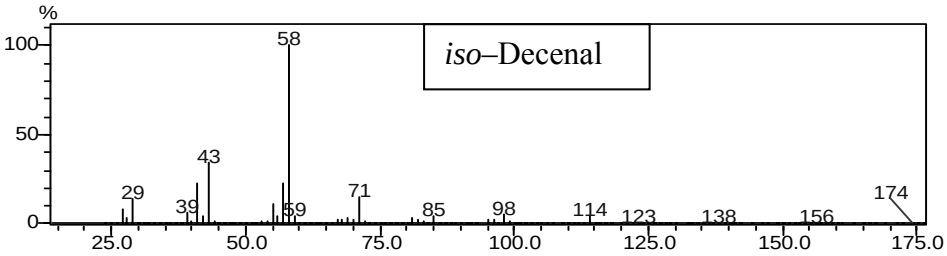
%
100
50
0
iso–Decenal
58
43
29
39
59
71
85
98
114
123
138
156
174
25.0
50.0
75.0
100.0
125.0
150.0
175.0

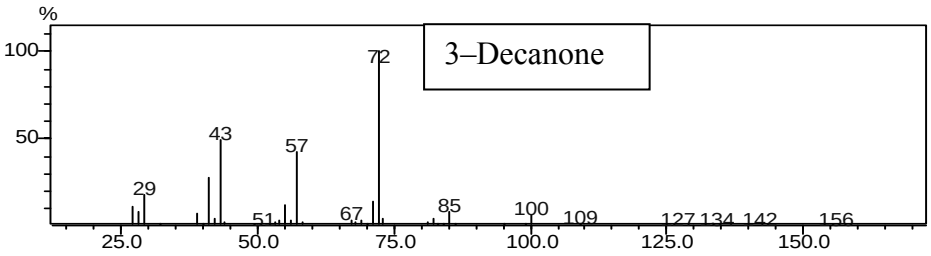
%
100
50
3–Decanone
72
43
57
29
51
67
85
100
109
127
134
142
156
25.0
50.0
75.0
100.0
125.0
150.0

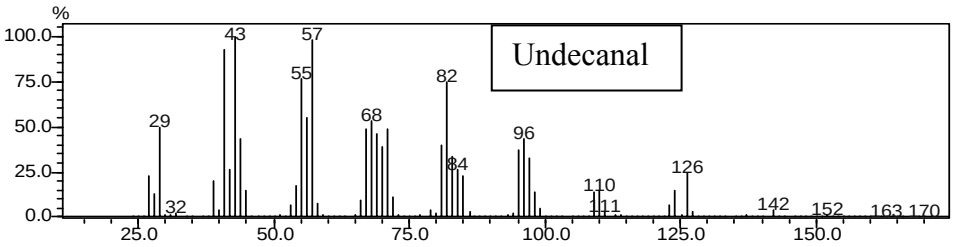
%
100.0
75.0
50.0
25.0
0.0
Undecanal
43
57
55
82
29
68
96
84
126
110
111
32
142
152
163
170
25.0
50.0
75.0
100.0
125.0
150.0

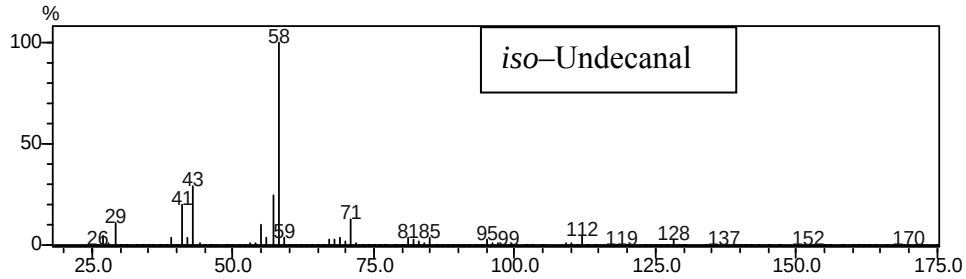
%
100
50
0
iso–Undecanal
58
43
41
29
26
59
71
81
85
95
99
112
119
128
137
152
170
25.0
50.0
75.0
100.0
125.0
150.0
175.0

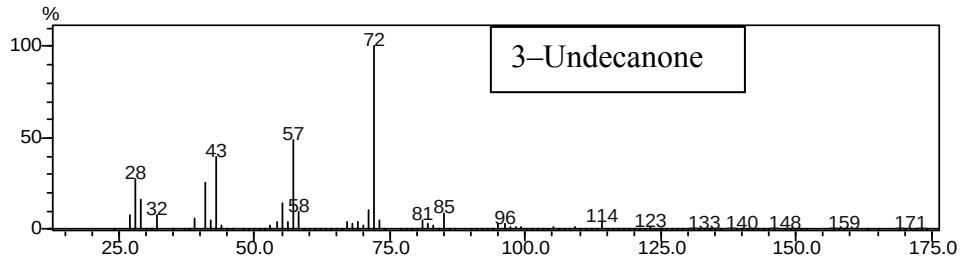
%
100
50
0
3–Undecanone
72
57
43
28
32
58
81
85
96
114
123
133
140
148
159
171
25.0
50.0
75.0
100.0
125.0
150.0
175.0

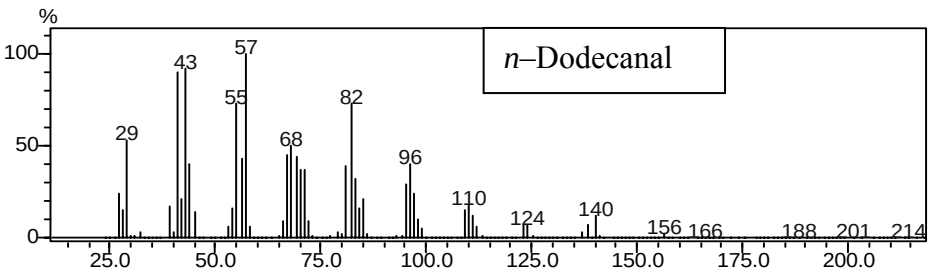
%
100
50
0
n–Dodecanal
57
43
55
82
29
68
96
110
124
140
156
166
188
201
214
25.0
50.0
75.0
100.0
125.0
150.0
175.0
200.0

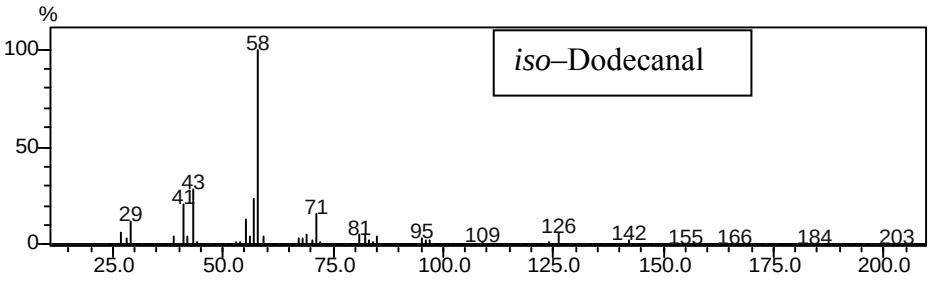
%
100
50
0
58
43
41
29
71
81
95
109
126
142
155
166
184
203
25.0
50.0
75.0
100.0
125.0
150.0
175.0
200.0
iso–Dodecanal

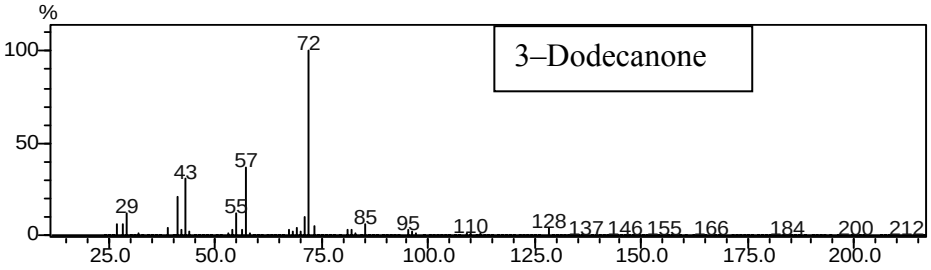
%
100
50
0
72
57
43
29
55
85
95
110
128
137
146
155
166
184
200
212
25.0
50.0
75.0
100.0
125.0
150.0
175.0
200.0
3–Dodecanone

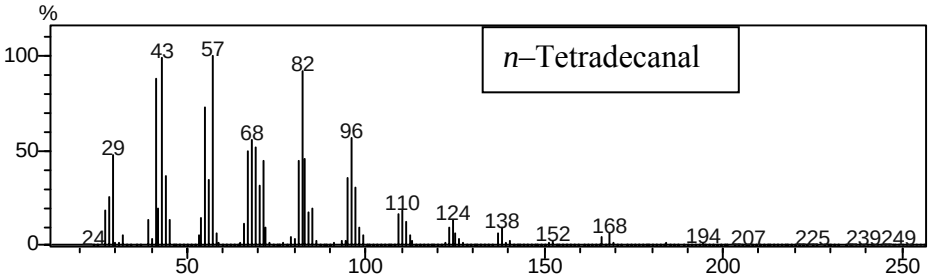
%
100
50
0
43
57
82
29
68
96
110
124
138
152
168
194
207
225
239
249
24
50
100
150
200
250
n–Tetradecanal

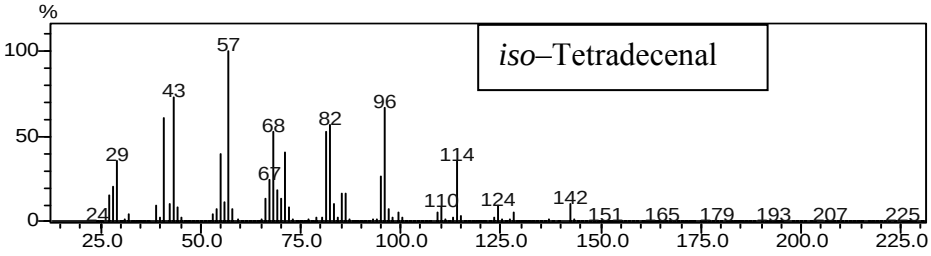
%
100
50
0
57
43
96
68
82
29
114
67
110
124
142
151
165
179
193
207
225
24
25.0
50.0
75.0
100.0
125.0
150.0
175.0
200.0
225.0
iso–Tetradecenal

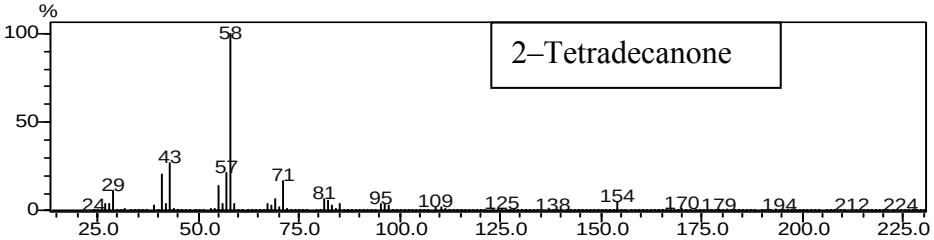
%
100
50
0
58
43
57
29
71
81
95
109
125
138
154
170
179
194
212
224
24
25.0
50.0
75.0
100.0
125.0
150.0
175.0
200.0
225.0
2–Tetradecanone

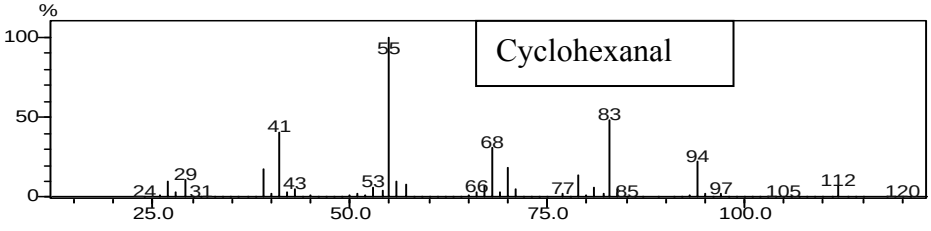
%
100
50
0
55
41
83
68
29
94
24
31
43
53
66
77
85
97
105
112
120
25.0
50.0
75.0
100.0
Cyclohexanal

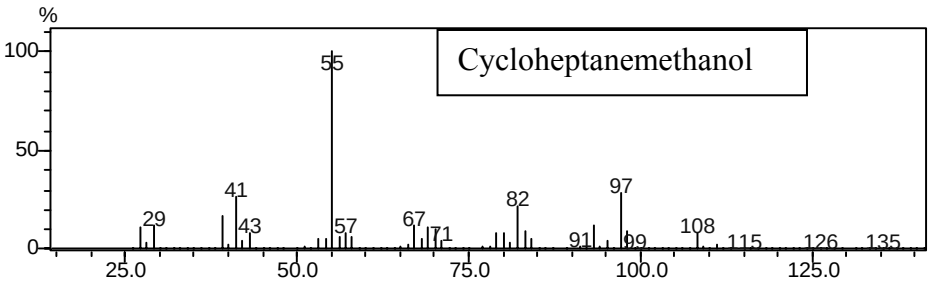
Cycloheptanemethanol
%
100
50
0
55
41
29
43
57
67
71
82
97
91
99
108
115
126
135
25.0
50.0
75.0
100.0
125.0

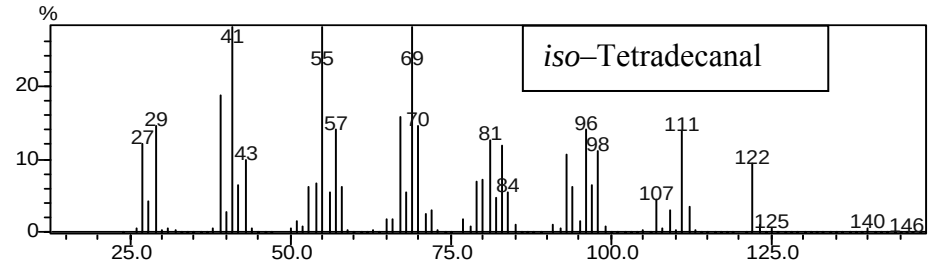
iso–Tetradecanal
%
20
10
0
41
55
69
29
27
57
70
43
81
96
98
111
122
84
107
125
140
146
25.0
50.0
75.0
100.0
125.0

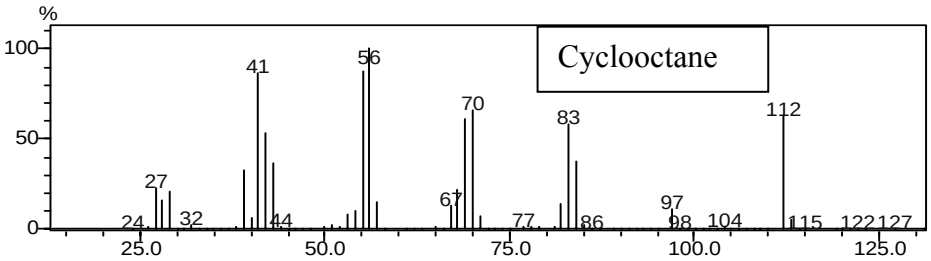
Cyclooctane
%
100
50
0
41
56
70
83
112
27
24
32
44
67
77
86
97
98
104
115
122
127
25.0
50.0
75.0
100.0
125.0

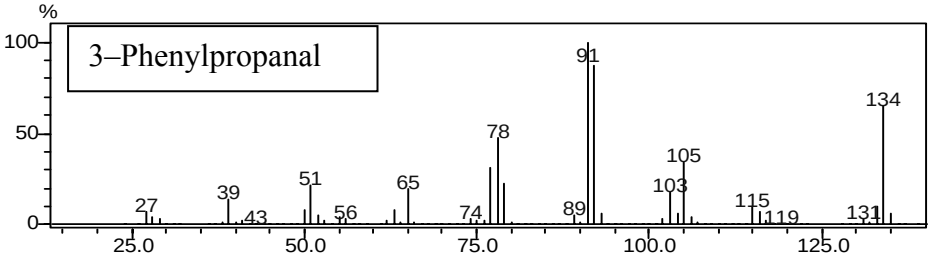
3–Phenylpropanal
%
100
50
0
91
134
78
105
103
39
51
65
27
43
56
74
89
115
119
131
25.0
50.0
75.0
100.0
125.0

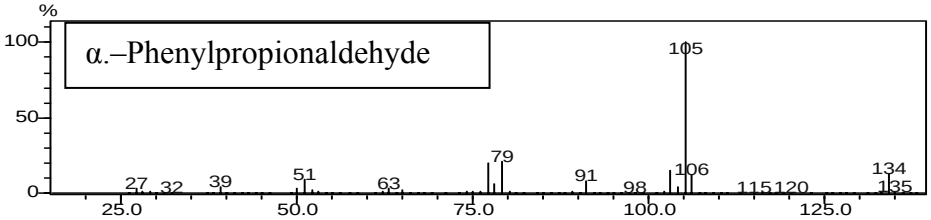
α.–Phenylpropionaldehyde
%
100
50
0
105
79
27
32
39
51
63
91
106
98
115
120
134
135
25.0
50.0
75.0
100.0
125.0

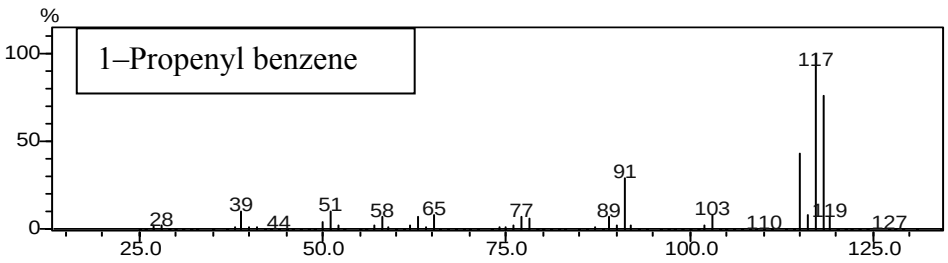
1–Propenyl benzene
%
100
50
0
117
91
28
39
44
51
58
65
77
89
103
110
119
127
25.0
50.0
75.0
100.0
125.0

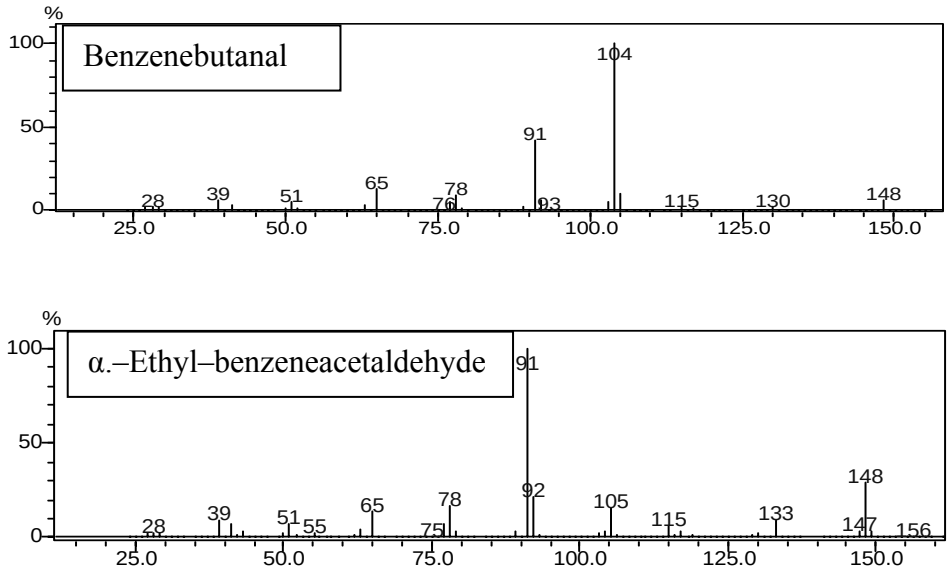

Figure 3.7. Mass fragmentation data for the products of hydroformylation of studied alkenes in Table 3.2.

3.3.3. Effect of 1–Hexene Concentration and Amount of Catalyst

Data on the conversion and selectivity for 1–hexene hydroformylation depicting the effect of varied concentration of 1–hexene and amount of catalyst are given in Table 3.3. The concentration of 1–hexene was varied from 6 to 120 mmol by keeping amount of catalyst constant at 100 mg. The complete conversion of 1–hexene was observed upto 70 mmol concentration of 1–hexene which decreased to 90% on further increasing the concentration of 1–hexene to 120 mmol. The selectivity of aldehydes was observed to increase upto 25 mmol concentration of 1–hexene. On further increasing the concentration of 1–hexene, selectivity of aldehydes was found to decrease significantly. *n/iso* Ratio of aldehydes was observed to increase upto 30 mmol of 1–hexene concentration, on further increasing the concentration to 120 mmol, *n/iso* ratio was observed to decrease from 0.8 to 0.6 . The higher catalytic activity for isomerization of 1–hexene to 2/3–hexene at higher substrate concentration results into the lower *n/iso* ratio of aldehydes (Scheme 3.2). Hydrogenation of 1–hexene and aldehydes was not observed in the present study. The calculated TOF values were found to increase from 52 to 696 on increasing the 1–hexene concentration from 6 to 120 mmol. The maximum conversion of 1–hexene and selectivity for aldehydes (*n* to *iso* ratio = 0.8) were observed at 25 mmol of 1–hexene concentration. Therefore, 25 mmol concentration of 1–hexene was taken to study the effect of other parameters on the conversion and selectivity for 1–hexene hydroformylation.

Table 3.3. Effect of 1–hexene concentration and amount of catalyst on the selectivity of aldehydes

Run	1–Hexene, mmol	Catalyst, mg	% Conversion	% Selectivity [a]			TOF, h^{-1}
				Aldehydes	*n/iso* Ratio of aldehydes	2/3–Hexene	
1	6	100	100	74	0.6	26	52
2	12	100	100	89	0.7	11	125
3	18	100	100	94	0.7	6	198
4	25	100	100	95	0.8	5	281
5	30	100	100	92	0.8	8	323
6	40	100	100	89	0.7	11	375
7	50	100	100	83	0.7	17	466
8	70	100	100	77	0.7	23	648
9	90	100	97	68	0.6	32	649
10	120	100	90	55	0.6	45	696
11	25	10	91	35	0.9	65	1014
12	25	20	93	54	0.8	46	798
13	25	50	100	79	0.9	21	383
14	25	100	100	95	0.8	5	281
15	25	200	100	96	0.8	4	142
16	25	300	100	92	0.8	8	91
17	25	500	100	78	0.8	22	47

[a] **Reaction conditions:** syn–gas = 40 atm (CO/H_2 = 1/1), temperature = 80 °C, time = 8 h.

Effect of the amount of catalyst on conversion and selectivity for 1–hexene hydroformylation was studied by varying the amount of catalyst from 10 to 500 mg at constant 1–hexene concentration (25 mmol). Selectivity of aldehydes was observed to increase upto 200 mg catalyst. On further increase in the amount of catalyst, selectivity of aldehydes was observed to decrease significantly due to the higher selectivity of 1–hexene isomerization products. The TOF values were expectedly observed to decrease on increasing the amount of catalyst. TOF value was calculated as 1014 at 10 mg catalyst amount, which decreased to 47 at 500 mg of catalyst amount.

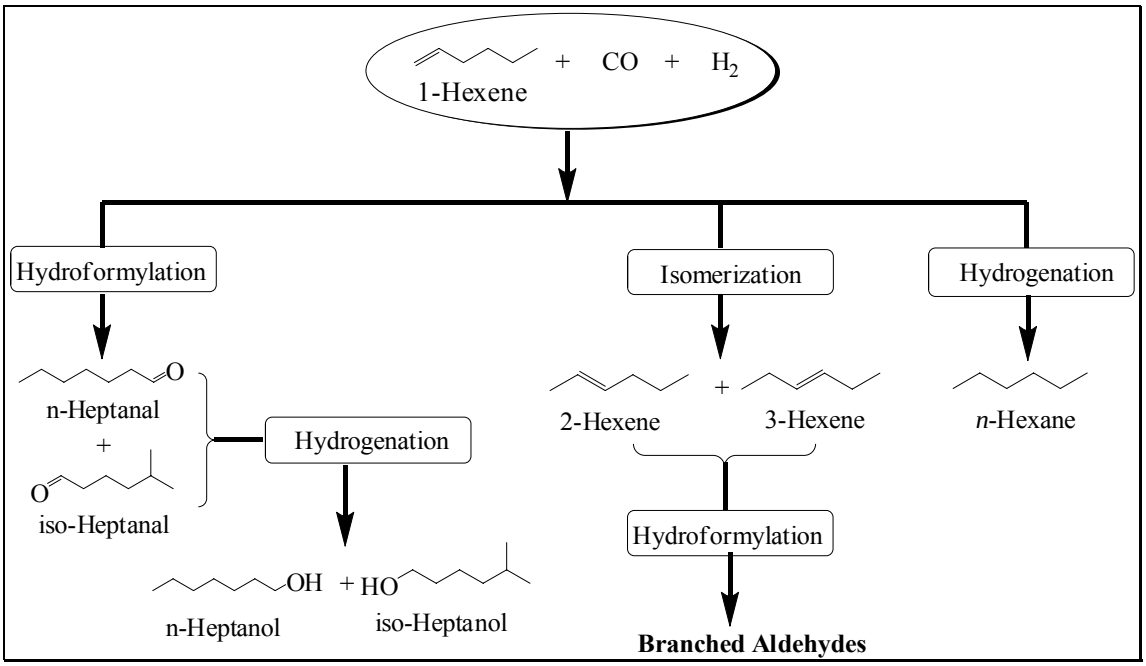

Scheme 3.2. Products of 1–hexane hydroformylation.

3.3.4. Effect of Partial Pressures of H_2 and CO

Partial pressures of H_2 and CO have significant effect on the selectivity of aldehydes (Table 3.4). Effect of partial pressure of H_2 was studied by varying the pressure of hydrogen from 2 to 30 atm at constant pressure of CO (20 atm). The conversion of 1–hexene was found to increase from 96 to 100% by increasing the partial pressure of H_2 from 2 to 10 atm. At lower partial pressure of H_2, lower selectivity of aldehydes was observed due to slow hydroformylation of 1–hexene as compared to its isomerization. Selectivity of aldehydes was observed to increase significantly upto 20 atm, however, on further increase in partial pressure of H_2, no significant effect was observed. Selectivity of aldehydes was found to increase from 26 to 95% by increasing the pressure of H_2 from 2 to 20 atm. Selectivity of isomerization products (2/3–hexene) was observed to decrease from 74 to 4% on increasing the partial pressure of H_2 from 2 to 30 atm. The TOF was calculated as 75 at 2 atm and it increased to 287 at 30 atm partial pressure of hydrogen. Hydrogenation products of 1–hexene and aldehydes were not obtained under the studied reaction conditions.

The effect of partial pressure of CO on conversion and selectivity was also studied at constant H_2 pressure (20 atm). The selectivity of aldehydes was observed to increase from 20% at 2 atm to 98% at 30 atm of CO pressure. The selectivity of 2/3–hexene decreased significantly from 80 to 8% on increasing the partial pressure of CO from 2 to 20 atm and selectivity of 2/3–hexene again decreased to 2% on further increasing the partial pressure of CO to 30 atm. The TOF values were observed to increase from 58 to 290 on increasing the partial pressure of CO from 2 to 30 atm. The reason for lower selectivity of aldehydes at low partial pressure of CO is the insufficient

concentration of CO to carry out hydroformylation reaction. Most of the 1–hexene consumed for 2/3–hexene via isomerization reaction. As partial pressure of CO increased, the selectivity of aldehydes was observed to increase due to the enhancement in the CO concentration.

Table 3.4. Effect of partial pressures of H_2 and CO on the selectivity of aldehydes

Run	Partial pressure of		% Conversion	% Selectivity [a]			TOF, h^{-1}
	H_2, atm	CO, atm		Aldehydes	*n/iso* Ratio of aldehydes	2/3–Hexene	
1	2	20	96	26	0.7	74	75
2	5	20	98	34	0.7	66	99
3	10	20	100	50	0.7	50	148
4	15	20	100	89	0.7	11	263
5	20	20	100	95	0.8	5	281
6	25	20	100	95	0.8	5	281
7	30	20	100	96	0.8	4	287
8	20	2	97	20	0.6	80	58
9	20	5	97	47	0.7	53	135
10	20	10	100	78	0.7	22	231
11	20	15	100	92	0.7	8	272
12	20	20	100	95	0.8	5	281
13	20	25	100	97	0.8	3	287
14	20	30	100	98	0.8	2	290

[a] **Reaction conditions:** 1–hexene = 25 mmol, catalyst = 100 mg, temperature = 80 °C time = 8 h.

3.3.5. Effect of Reaction Temperature

The reaction temperature was varied from 50 to 100 °C at 40 atm pressure of syn–gas ($CO/H_2 = 1$), 100 mg catalyst and 25 mmol of 1–hexene concentration (Table 3.5). The selectivity of aldehydes was observed to increase from 78% to 95% on increasing the reaction temperature from 50 °C to 80 °C. On further increase in the reaction temperature to 100 °C, the selectivity of aldehydes decreased to 53%. The observed decrease in the aldehydes selectivity is due to the increased isomerization of 1–hexene to 2/3–hexene at higher reaction temperature. At 80 °C, 5% isomerization of 1–hexene was obtained and it increased to 47% at 100 °C. *n/iso* Ratio of aldehydes was also found to decrease from 1.1 to 0.8 on increasing the temperature from 50 to 100 °C. At higher temperatures, it is expected that the thermal motion of intermediate catalytic species

increases due to significant decrease in steric factors of the catalyst which results into increased in polarity of M–H bond favoring Markovnikov addition that results into higher selectivity of *iso*–aldehyde. Calculated TOF values were observed to increase upto 80 °C and decreased on further increase in the reaction temperature.

Table 3.5. Effect of temperature on the selectivity of aldehydes

Run	Temperature °C	% Conversion	% Selectivity [a]			TOF, h^{-1}
			Aldehydes	*n/iso* Ratio of aldehydes	2/3–Hexene	
1.	50	100	78	1.1	22	230
2.	60	100	89	0.9	11	263
3.	70	100	93	0.9	7	275
4.	80	100	95	0.8	5	281
5.	90	100	82	0.8	8	242
6.	100	100	53	0.8	47	157

[a] **Reaction conditions:** 1–hexene = 25 mmol, catalyst = 100 mg, syn–gas = 40 atm (CO/H_2 = 1/1) time = 8 h.

3.3.6. Kinetics Measurements and Reusability of the Catalyst

The reaction profile with respect to time for hydroformylation of 1–hexene using heterogeneous [HT(3.5)–INT] catalyst at 80 °C and 40 atm syn–gas pressure is shown in Figure 3.8. Rapid consumption of 1–hexene was observed for hydroformylation and isomerization reactions. Initially, most of 1–hexene isomerized to 2/3–hexene in the studied experimental conditions. About 95% conversion of 1–hexene into 2/3–hexene was observed within 60 min reaction time. After complete consumption of 1–hexene, 2/3–hexene was converted into aldehydes (mostly for 2–methylhexanal and 2–ethylpentanal) via hydroformylation reaction which results into lower *n/iso* ratio of aldehydes. Higher rate of reaction was obtained for isomerization of 1–hexene to 2/3–hexene as compared to hydroformylation reaction. The higher rate of isomerization reaction is due to the well known property of Rh–complex and hydrotalcite for double bond isomerization reaction [50–51]. Hydrogenation products were not observed during the course of kinetics experiment.

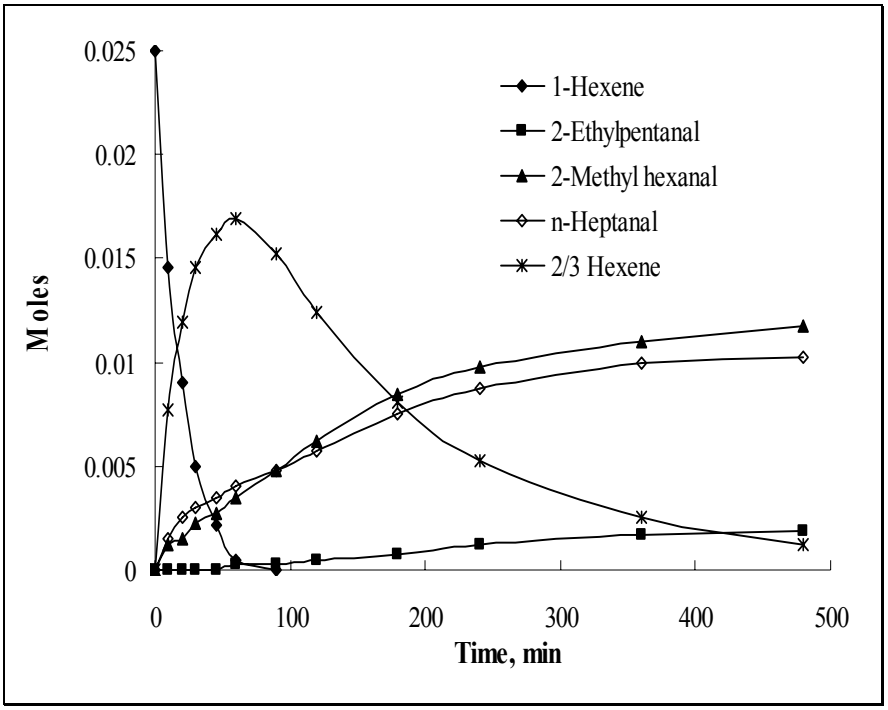

Figure 3.8. Kinetic profile for hydroformylation of 1–hexene using [HT(3.5)–INT] as a catalyst.

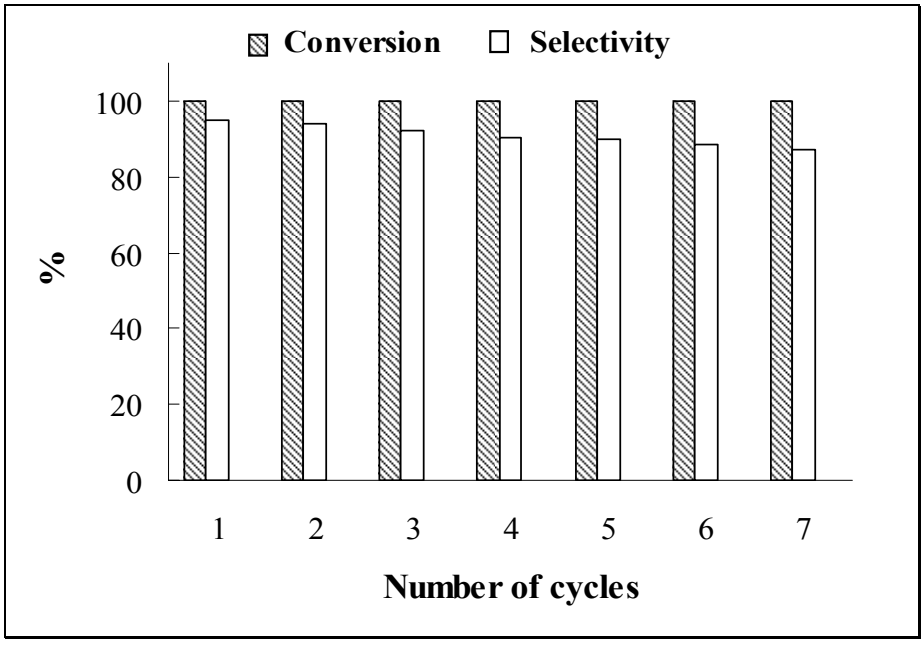

Figure 3.9. Reusability of [HT(3.5)–INT] catalyst for hydroformylation of 1–hexane.

The catalyst was recycled upto seven times for hydroformylation of 1–hexene (Figure 3.9). Complete conversion of 1–hexene (100%) was observed in seventh cycle, however, selectivity of the aldehydes (*n* and *iso*) was observed to decrease after fifth cycle. 93% selectivity of aldehydes was obtained at fifth cycle that decreases to 87% at seventh cycle. The decrease in selectivity of aldehydes could be due to handling losses of the catalyst during reusability experiments. The P–

XRD and FT–IR spectrum of used [HT(3.5)–INT] catalyst shown in Figures 3.1 & 3.2 also supported that the structure of [HT(3.5)–INT] catalyst was not disturbed after repeated experiments for reusability experiments. All peaks of fresh catalyst were observed in the P–XRD and FT–IR spectrum of used [HT(3.5)–INT] catalyst.

3.4. Conclusions

Intercalation of $HRh(CO)(TPPTS)_3$ complex into interlayer space of hydrotalcite was confirmed by ^{31}P–NMR, P–XRD and FT–IR spectra of intercalated [HT(3.5)–INT] catalyst. The intercalated material was used as a heterogeneous catalyst for hydroformylation of linear alkenes with varied carbon chain length (C_5 to C_{13}) and cyclic alkenes. As carbon chain length of linear alkenes increases, the selectivity of aldehydes was observed to decrease. The activity of catalyst for hydroformylation of linear alkenes under identical reaction conditions was found to be in the order of; 1–pentene > 1–hexene > 1–heptene > 1–octene> 1–nonene > 1–decene > 1–undecene > 1–dodecene > 1–tridecene. For hydroformylation of cyclic alkenes, the order of catalytic activity of [HT(3.5)–INT] catalyst was observed as; cyclohexene > cycloheptene > cyclooctene under identical reaction conditions. The catalyst was recycled upto five cycles without significant loss in conversion and selectivity for hydroformylation of 1–hexene. The P–XRD and FT–IR spectrum of used [HT(3.5)–INT] catalyst showed that the structure of [HT(3.5)–INT] catalyst was not disturbed even after several repeated experiments to ensure reusability of the catalyst. The rate of reaction was calculated from the kinetic plot for hydroformylation of 1–hexene at optimum reaction conditions. Higher rate of reaction was obtained for isomerization of 1–hexene to 2/3–hexene as compared to the hydroformylation of 1–hexene for the production of aldehydes.

3.5. References

[1] D. Frohning, C.W. Kohlpaintner, in Applied Homogeneous Catalysis with Organometallic Compounds, ed. B. Cornils, W. A. Hermann, Wiley–VCH, Weinheim, (2000), vol. 1, ch. 2, p. 29.

[2] V.K. Srivastava, D.U. Parmar, R.V. Jasra, Chem. Weekly July 8 (2003) 173–178 and July 15 (2003) 181–190.

[3] Chemical Economic Handbook, Oxo Chemical Report, SRI International, January (2003).

[4] E.G. Kunzu, FR Patent, 2 733 516 (1976) to Rhone–Poulenc.

[5] K. Mukhopadhyay, R.V. Chaudhari, J. Catal. 213 (2003) 73–77.

[6] L. Huang, Y. He, S. Kawi, J. Mol. Catal. A: Chem. 213 (2004) 241–249.

[7] L. Huang, S. Kawi, Catal. Lett. 92 (2004) 57–62.

[8] R.J. Davis, J.A. Rossin, M.E. Davis, J. Catal. 98 (1986) 477–486.

[9] M.W. Balakos, S.S.C. Chuang, J. Catal. 151 (1995) 266–278.

[10] A. Riisager, P. Wasserscheid, R. Hal, R. Fehrmann, J. Catal. 219 (2003) 452–455.

[11] H. Arai, J. Catal. 51 (1978) 135–142.

[12] K. Mukhopadhyay, A.B. Mandale, R.V. Chaudhari, Chem. Mater. 15 (2003) 1766–1777.

[13] M. Ichikawa, J. Catal. 59 (1979) 67–78.

[14] Y. Zhang, K. Nagasaka, X. Qiu, N. Tsubaki, Appl. Catal. A: Gen. 276 (2004) 103–111.

[15] F. Cavani, F. Trifiro, A. Vaccari, Catal. Today 11 (1991) 173–301.

[16] D.G. Evans, X. Duan, Chem. Commun. (2006) 485–496.

[17] A.I. Khan, D. O'Hare, J. Mater. Chem. 12 (2002) 3191–3198.

[18] E.L. Crepaldi, P.C. Pavan, J.B. Valim, Chem. Commun. (1999) 155–156.

[19] R. Schollhorn, B. Otto, J.Chem. Soc., Chem. Commun. (1986) 1222–1223.

[20] K. Chibwe, W. Jones, J. Chem. Soc. Chem. Commun. (1989) 926–927.

[21] A.I. Khan, L. Lei, A.J. Norquist, D. O'Hare, Chem. Commun. (2001)2342–2343.

[22] G.R. Williams, T.G. Dunbar, A.J. Beer, A.M. Fogg, D. O'Hare, J. Mater. Chem. 13 (2006) 1231–1237.

[23] K.M. Parida, S. Parija, J. Das, P.S. Mukherjee, Catal. Commun. 7 (2006) 913–919.

[24] J. Das, K.M. Parida, J. Mol. Catal. A: Chem. 264 (2007) 248–254.

[25] E. Kanezaki, K. Kinugawa, Y. Ishikawa, Chem. Phy. Lett. 226 (1994) 325–330.

[26] F. Malherbe, J.P. Besse, J. Solid State Chem. 155 (2000) 332–341.

[27] E.L. Crepaldi, P.C. Pavan, J. Tronto, J.B. Valim, J. Col. Inter. Sci. 248 (2002) 429–442.

[28] V.I. Iliev, A.I. Ileva, L.D. Dimitrov, Appl. Catal. A: Gen. 126 (1995) 333–340.

[29] B.M. Choudary, M.L. Kantam, N.M. Reddy, N.M. Gupta, Catal. Lett. 82 (2002) 79–83.

[30] M. Chibwe, T.J. Pinnavaia, J. Chem. Soc., Chem. Commun. (1993) 278–280.

[31] S. Hamada, K, Ikeue, M. Machida, Chem. Mater. 17 (2005) 4873–4879.

[32] J. Inacio, C.T.Gueho, S.M. Therias, M.E. Roy, J.P. Besse, J. Mater. Chem. 11 (2001) 640–643.

[33] E.P. Giannelis, D.G. Nocera, T.J. Pinnavaia, Inorg. Chem. 26 (1987) 203–205.

[34] I. Crespo, C. Barriga, V. Rives, M.A. Ulibarri, Solid State Ion. 101–103 (1997) 729–735.

[35] M. Arco, S. Gutierrez, C. Martin, V. Rives, Inorg. Chem. 42 (2003) 4232–4240.

[36] I. Carpani, M. Berrettoni, M. Giorgetti, D. Tonelli, J. Phys. Chem. B 110 (2006) 7265–7269.

[37] N.H. Gutmann, L. Spiccia, T.W. Turney, J. Mater. Chem. 10 (2000) 1219–1224.

[38] X. Zhang, M. Wei, M. Pu, X. Li, H. Chen, D.G. Evans, X. Duan, J. Solid State Chem. 178 (2005) 2701–2708.

[39] F. Iosif, V.I. Parvulescu, M.E.P. Bernal, R.J.R. Casero, V. Rives, K. Kranjc, S. Polanc, M. Kocevar, E. Genin, J.P Genet, V. Michelet, J. Mol. Catal. A: Chem. 276 (2007) 34–70.

[40] J.P. Arhancet, M.E. Davis, J.S. Merola, B.E. Hanson, J. Catal. 121 (1990) 327.

[41] Y. Zhao, F. Li, R. Zhang, D.G. Evans, X. Duan, Chem. Matter. 14 (2002) 4286–4291.

[42] E.P. Barrett, L.G. Joyner, P.P. Halenda, J. Am. Chem. Soc. 73 (1951) 373–380.

[43] V.K. Srivastava, S.K. Sharma, R.S. Shukla, N. Subrahmanyam, R.V. Jasra, Ind. Eng. Chem. Res. 44 (2005) 1764–1771.

[44] V.K. Srivastava, R.S. Shukla, H.C. Bajaj, R.V. Jasra, Appl. Catal. A: Gen. 282 (2005) 31–38.

[45] S.K. Sharma, V.K. Srivastava, R.S. Shukla, P.A. Parikh, R.V. Jasra, New J. Chem. 31 (2007) 277–286.

[46] V.K. Srivastava, S.K. Sharma, R.S. Shukla, R.V. Jasra, Catal. Commun. 7 (2006) 881–886.

[47] C. Bianchini, H.M. Lee, A. Meli, F. Vizza, Organometallics 19 (2000) 849–853.

[48] H. Zhu, Y. Ding, H. Yin, L. Yan, J. Xiong, Y. Lu, H. Luo, L. Lin, Appl. Catal. A: Gen. 245 (2003) 111–117 and reference cited therein.

[49] N.S. Pagar, R.M. Deshpande, R.V. Chaudhari, Catal. Lett. 110 (2006)129–133.

[50] V.K. Srivastava, H.C. Bajaj, R.V. Jasra, Catal. Commun. 4 (2003) 543–548.

[51] S.K. Sharma, V.K. Srivastava, P.H. Pandya, R.V. Jasra, Catal. Commun. 6 (2005) 205–209.

Chapter 4

Single Pot Synthesis of 2–Ethylhexanal from Propylene using Eco–Friendly Multi–Functional Catalyst Prepared by Intercalation of $HRh(CO)(TPPTS)_3$ Complex in the Interlayer Space of Hydrotalcite

4.1. Introduction

The field of intercalation chemistry has long been a point of interest to the researchers so as to alter the material's electrical, optical and magnetic properties with negligible structural changes in the host materials. The intercalation of organic and inorganic anions in the interlayers of hydrotalcite having general formula $[M(II)_{1-x}M(III)x(OH)_2]^{x+}A^{n-}{}_{x/n}(1-3x/2)H_2O$, $(0.20 < x \leq 0.33)$, where M(II) and M(III) are divalent and trivalent cations, x is molar ratio of M(III)/[M(II)+M(III)] and A is the exchangeable anions, is currently attaining greater interest among the researchers to develop new materials of wider applicability in the area of catalysis or composite materials [1–4]. Hydrotalcite is a positively charged layered structure formed by the octahedral units with shared edges where that charge is balanced by the exchangeable anions. Each octahedron consists of M(II) and M(III) cations surrounded by the six hydroxyl groups. The positive charge in the layers is generated due to the replacement of M(II) by M(III) cations, which is compensated by the exchangeable anions in the interlayer space of hydrotalcite. Therefore, due to excellent anions exchange property of hydrotalcite, variety of functionalized organic compounds, inorganic anions and transition metals complexes can be intercalated into the interlayer space of hydrotalcite [4–15]. Intercalation of anions in the interlayer space of hydrotalcite is carried out by three methods. i) The general co–precipitation method in which solution of desired anions is mixed during the crystallization of hydrotalcite. ii) Ion exchange method in which synthesized hydrotalcite is stirred with the concentrated solution of the desired anions. iii) The intercalation of anions by stirring the suspension of activated hydrotalcite with the solution of anions to be intercalated in the inert atmosphere. By the use of above methods, various transition metals complexes such as $PtCl_6$, palladium, cobalt(II)–phthalocyanine, ruthenium–, chromium–, iron(III)– hexacyano, copper(II)– and nickel(II)– nitrilotriacetate and other anions were intercalated in layered double hydroxide [16–28]. Intercalation of *trans*–$RhCl(CO)(TPPTS)_2$ into Zn–Al layered double hydroxides was reported by Duan et al., however, they have not evaluated its catalytic activity [26]. In another study, $RhCl(TPPTS)_3$ complex was heterogenized into Zn–Al layered double hydroxides via ion exchange method and used as a heterogeneous catalyst for hydrogenation of bicyclo[2.2.2]octenes [27].

2–Ethylhexanal and 2–ethylhexanol are commercially important intermediate chemicals for the synthesis of dioctylphthalate (DOP) and other plasticizers, coatings, adhesives, lubricants, alkyd resins and fine chemicals. Presently, 2–ethylhexanal and 2–ethylhexanol are synthesized from propylene in a three steps process. Hydroformylation of propylene is carried out to produce butanal in the first step using rhodium based catalysts [29]. In the second step, the obtained butanal undergoes aldol condensation in the presence of stoichiometric amount of a strong base, namely

KOH or NaOH, to produce 2–ethylhexenal [30, 31]. Hydrogenation of 2–ethylhexenal is carried out using Ni or Cu catalysts in the third step [32–35]. Thus, existing commercial strategies for the production of 2–ethylhexanol involved multi–steps process using stoichiometric amounts of hazardous liquid base solutions and require post synthesis work–up for the separation of spent KOH or NaOH from the product mixture. The above process requires three reactors for each step as well as many of the purification units, which add into capital cost of the plant. The strong liquid base catalyst KOH or NaOH, which is used in stoichiometric amounts, causes corrosion in the reactors and vessels. It is estimated that approximately, 1.0–1.5 tons of spent base solutions are generated for every 10 tons of product formed in homogeneous aldol condensation. In fact, 30% of the selling price of the product synthesized by the catalyst used in stoichiometric amounts is estimated to be contributed by product purification, recovery and waste treatment [36–37].

For the synthesis of 2–ethylhexanol from propylene, Shell has developed a single step process, known as 'Aldox' process. In this process, cobalt carbonyl was used as a catalyst for hydroformylation along with potasium hydroxide, sodium hydroxide or secondary/tertiary amines of higher carbon chain length as a catalyst for condensation of the butanal [38]. This process has disadvantages like, use of strong base catalyst in liquid phase for aldol condensation of *n*–butanal, use of cobalt carbonyl along with phosphine as a homogeneous catalyst for hydroformylation of propylene which requires higher reaction temperature and pressure, and relatively low liquid space velocity. In another study, multi–functional catalyst system was developed by impregenation of $HRh(CO)(PPh_3)_3$ complex on hydrotalcite of varied Mg/Al molar ratio for the synthesis of C_8 aldol derivatives from propylene in a single pot [39–40]. The drawbacks of this process are the leaching of $HRh(CO)(PPh_3)_3$ complex from hydrotalcite during the reaction and lower thermal stability of multi–functional catalyst. The catalyst was not reused for the further cycles. Therefore, in order to avoid leaching of the active hydroformylation complex from multi–functional catalyst, intercalation of hydroformylation catalyst [$HRh(CO)(TPPTS)_3$] was carried out in the interlayer space of hydrotalcite and used as a multi–functional catalyst for the synthesis of C_8 aldol derivatives from propylene in a single pot.

The present study describes a novel approach for the synthesis of 2–ethylhexanal and 2–ethylhexanol from propylene via hydroformylation, aldol condensation and hydrogenation reactions in a single pot using heterogeneous eco–friendly multi–functional catalyst [HF/HT–INT] synthesized by the intercalation of $HRh(CO)(TPPTS)_3$ [HF] complex in the interlayer space of Mg–Al hydrotalcite of Mg/Al molar ratio of 3.5 [HT(3.5)] (Scheme 4.1).

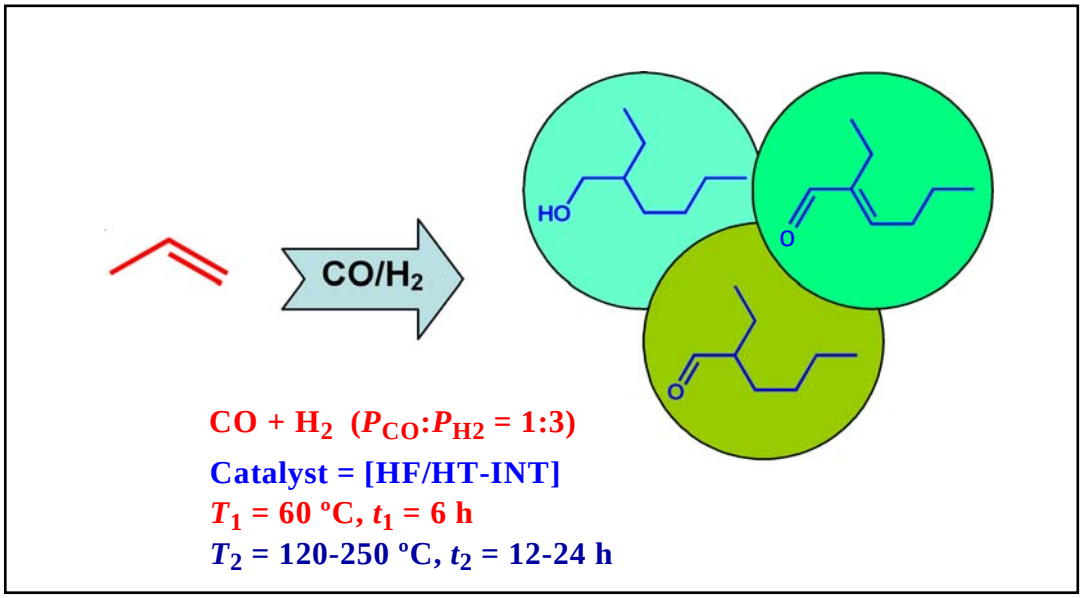

Scheme 4.1. Single pot synthesis of 2–ethylhexanal and 2–ethylhexanol from propylene using [HF/HT–INT] as a catalyst.

4.2. Experimental

4.2.1. Materials

The (acetylacetonato)dicarbonylrhodium ($Rh(CO)_2(acac)$; 98%) and tris(3–sodium sulfonatophenyl) phosphine (TPPTS; $P(m\text{–}C_6H_4SO_3Na)_3$) were purchased from Sigma–Aldrich, USA. Magnesium nitrate ($Mg(NO_3)_2.6H_2O$, 98.9%), aluminum nitrate ($Al(NO_3)_3.9H_2O$, 99.1%), sodium nitrate ($NaNO_3$, 99.9%), ammonia solution (40%) and toluene (99.9%) were purchased from s.d. Fine Chemicals, India. Propylene (99.6%), carbon monoxide (CO, 99.8%) and hydrogen (H_2, 99.98%) were procured from Alchemie Gases and Chemicals Private Limited, India. Double distilled milli–pore deionized water was used during the synthesis of $HRh(CO)(TPPTS)_3$ complex and hydrotalcite.

4.2.2. Synthesis of $HRh(CO)(TPPTS)_3$ [HF] Complex, Hydrotalcite [HT] and Intercalation of [HF] Complex into the Interlayers of [HT] [HF/HT–INT]

The experimental procedure for synthesis of $HRh(CO)(TPPTS)_3$ [HF] complex, hydrotalcite [HT] and [HF/HT–INT] by the intercalation of [HF] complex into interlayer space of [HT] was carried out by the reported procedure in Chapter 3, Sections 3.2.2 to 3.2.4 (Refer [HT(3.5)–INT] in Chapter 3).

4.2.3. Characterization of the Catalyst

Characterization of the [HF/HT–INT] catalyst was carried out by Fourier transform nuclear magnetic resonance (FT–NMR), powder X–ray diffraction (P–XRD) patterns, Fourier transform infrared (FT–IR) spectroscopy, thermogravimetric analysis (TGA), surface area analysis and scanning electron microscopy (SEM) images. The detailed characterization procedure of [HF/HT–INT] catalyst is reported in Chapter 3, Section 3.2.5.

4.2.4. Synthesis of 2–Ethylhexanal and 2–Ethylhexanol from Propylene in a Single Pot

Synthesis of 2–ethylhexanal and 2–ethylhexanol from propylene in a single pot was carried out in 100 ml EZE–Seal stirred reactor supplied by Autoclave Engineers, USA, equipped with a controlling unit [41]. The catalyst [HF/HT–INT] with 200 mg [HT] was added into the autoclave reactor having 50 ml toluene as a solvent. The reactor was flushed with nitrogen gas prior to introducing desired concentration of propylene. The CO and H_2 gases were introduced in the reactor in specified ratio. The reactor was then brought to 60 °C temperature (T_1) for hydroformylation reaction. Reaction was then initiated by starting the agitator at 1000 rpm. The reaction was carried out at 60 °C temperature for 6 h (t_1) following which, the reaction temperature was raised to T_2 °C for aldol condensation of formed aldehydes. The reaction temperature (T_2 °C) was kept for 12 and 24 h (t_2). Reaction was then continued at constant pressure by supplying CO and H_2 from the reservoir vessel. After completion of the reaction, reactor was cooled to room temperature by circulation of cold water in the coil provided inside the reactor. The catalyst was separated from products mixture by simple filtration and filtrate was analyzed by GC–MS (Shimadzu, GCMS–QP2010) and GC (Shimadzu 17A, Japan). The conversion was calculated from the propylene consumption data and was found in the range of 95–99%. The conversion of propylene was calculated by reported method [39], using formula: $C_p = C_{po}\ (1–X_p)$; where X_p = conversion of propylene, C_{po} = initial concentration of propylene and calculated as $C_{po} = p_p /RT$; where p_p is the partial pressure of propylene initially. To ensure the reproducibility of reaction, experiments were repeated under identical reaction conditions. The conversion and selectivity were reproduced in the range of ± 5% variation. The percentage selectivity for each product was calculated by following formula –

$$\%\,\text{n-Butanal} = \left(\frac{\text{moles of n-butanal}}{\text{moles of (n-butanal+ iso-butanal+ n-butanol+ iso-butanol+ 2-ethylhexenal+ 2-ethylhexanal+ 2-ethylhexanol)}}\right) X\ 100$$

$$\%\,\text{iso-Butanal} = \left(\frac{\text{moles of iso-butanal}}{\text{moles of (n-butanal+ iso-butanal+ n-butanol+ iso-butanol+ 2-ethylhexenal+ 2-ethylhexanal+ 2-ethylhexanol)}}\right) X\ 100$$

$$\%\,\text{n-Butanol} = \left(\frac{\text{moles of n-butanol}}{\text{moles of (n-butanal+ iso-butanal+ n-butanol+ iso-butanol+ 2-ethylhexenal+ 2-ethylhexanal+ 2-ethylhexanol)}}\right) X\ 100$$

$$\%\,\text{iso-Butanol} = \left(\frac{\text{moles of iso-butanol}}{\text{moles of (n-butanal+ iso-butanal+ n-butanol+ iso-butanol+ 2-ethylhexenal+ 2-ethylhexanal+ 2-ethylhexanol)}}\right) X\ 100$$

$$\%\,\text{2-Ethylhexenal} = \left(\frac{\text{moles of 2-ethylhexenal}}{\text{moles of (n-butanal+ iso-butanal+ n-butanol+ iso-butanol+ 2-ethylhexenal+ 2-ethylhexanal+ 2-ethylhexanol)}}\right) X\ 100$$

$$\%\,\text{2-Ethylhexanal} = \left(\frac{\text{moles of 2-ethylhexanal}}{\text{moles of (n-butanal+ iso-butanal+ n-butanol+ iso-butanol+ 2-ethylhexenal+ 2-ethylhexanal+ 2-ethylhexanol)}}\right) X\ 100$$

$$\%\,\text{2-Ethylhexanol} = \left(\frac{\text{moles of 2-ethylhexanol}}{\text{moles of (n-butanal+ iso-butanal+ n-butanol+ iso-butanol+ 2-ethylhexenal+ 2-ethylhexanal+ 2-ethylhexanol)}}\right) X\ 100$$

4.3. Results and Discussion

4.3.1. Characterization of Catalyst

Intercalation of [HF] complex in the interlayer space of [HT] was confirmed by P–XRD pattern and ^{31}P solid state NMR and FT–IR spectra of [HF/HT–INT] catalyst. The observed shift in P–XRD pattern of intercalated [HT(3.5)–INT] sample with respect to pristine hydrotalcite confirmed the intercalation of $HRh(CO)(TPPTS)_3$ complex. The intercalation of $HRh(CO)(TPPTS)_3$ complex was confirmed by the broadening in *d*–spacing value of (003) plane of [HF/HT–INT] catalyst from 8.79 to 16.8 Å and shifting of the values of (003) and (006) planes towards lower 2θ as compared to pristine [HT]. The doublet at 42.34 ppm was observed in solid state ^{31}P–NMR spectrum of [HF/HT–INT] catalyst confirming that the [HF] complex was intercalated without decomposition into the interlayer space of hydrotalcite. Intercalation of [HF] complex without decomposition was further confirmed by FT–IR spectrum of [HF/HT–INT] catalyst. TGA data of [HF/HT–INT] sample showed that the catalyst is thermally stable upto 200 °C. Complete discussion on the characterization of [HF/HT–INT] catalyst was presented in detail in the Chapter 3, Section 3.3.1 (Refer [HT(3.5)–INT] in Chapter 3).

4.3.2. Reaction Pathways for the Synthesis of 2–Ethylhexanol and 2–Ethylhexanal in a Single Pot

It looks important to understand the role played by the each component of [HF/HT–INT] catalyst system for each steps involved in the production of 2–ethylhexanol and 2–ethylhexanal from propylene before discussing the obtained results (Scheme 4.2).

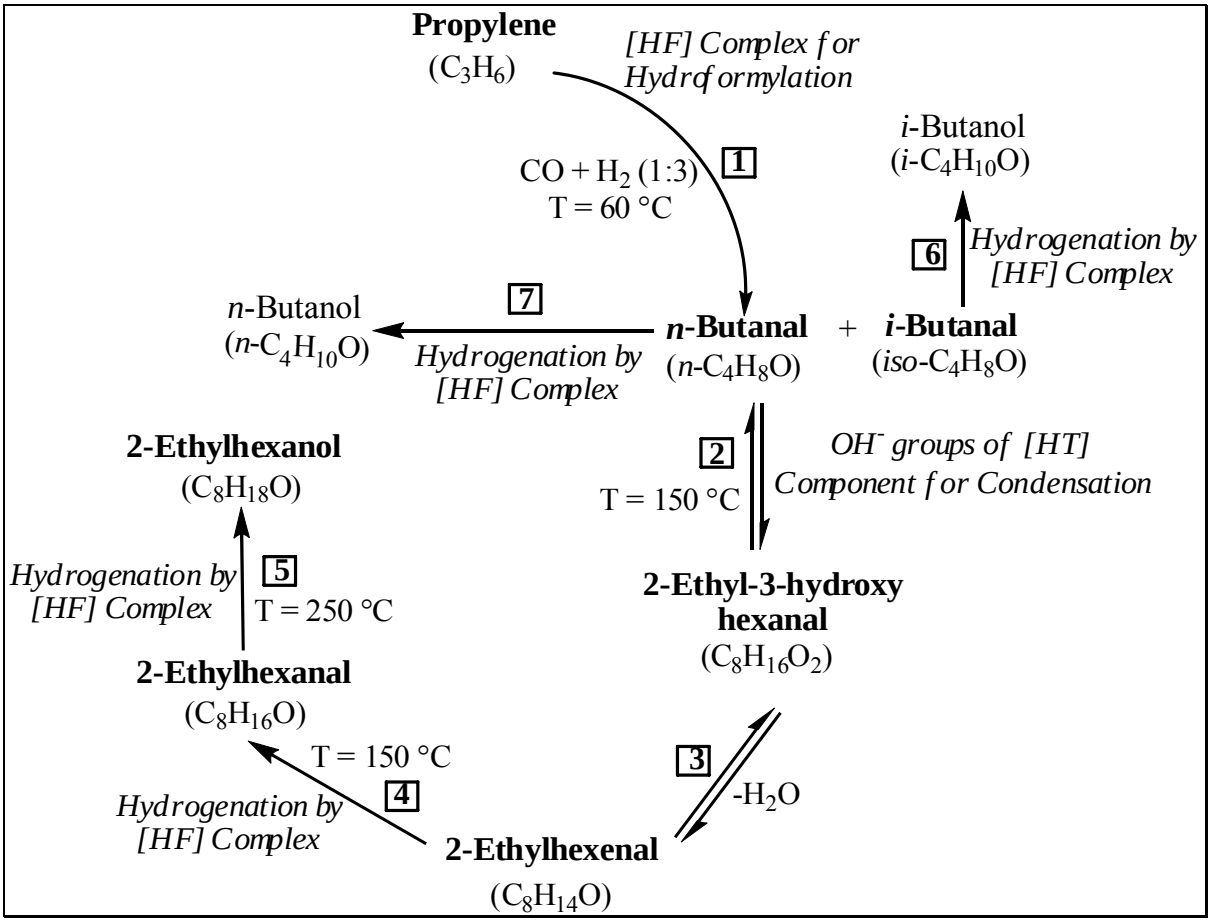

Scheme 4.2. Reaction pathways for the synthesis of 2–ethylhexanol from propylene in a single pot using [HF/HT–INT].

Reaction is initiated by the formation of butanal (*n* and *iso*) by hydroformylation of propylene catalyzed by intercalated [HF] component of the [HF/HT–INT] system (**1**) at 60 °C reaction temperature. The obtained *n*–butanal from hydroformylation step is subsequently consumed for aldol condensation (**2**) at 150 °C, wherein two molecules of *n*–butanal undergo condensation reaction catalyzed by HT component of [HF/HT–INT] to give 2–ethyl–3–hydroxyhexanal (aldol product) and subsequently 2–ethylhexenal after removal of one water molecule (**3**). The hydrogenation of 2–ethylhexenal to 2–ethylhexanal catalyzed by intercalated [HF] component of [HF/HT–INT] catalyst takes place in the step **4** at 150 °C temperature and above. The last step (**5**) is again hydrogenation of 2–ethylhexanal to 2–

ethylhexanol catalyzed by [HF] component of [HF/HT–INT] catalyst. This step required higher reaction temperature (250 °C in the present study) to carry out hydrogenation reaction. Two reactions in a single pot synthesis were catalyzed by intercalated [HF] component of [HF/HT–INT] catalyst, one is the hydroformylation of propylene and second is hydrogenation of 2–ethylhexenal. The possible side reaction, which affect the selectivity of 2–ethylhexanol significantly, is the reduction of butanals (*n*– and *iso*–) to their corresponding butanols (Step **6** and **7**), which also catalyzed by the intercalated [HF] component of [HF/HT–INT] catalyst in the studied experimental conditions. Therefore, in order to avoid this competitive reaction, amount of solid base, basicity of catalyst and reaction conditions should be optimized to divert the reaction in the direction of step **2**.

4.3.3. Catalytic Activity for Synthesis of 2–Ethylhexanal and 2–Ethylhexanol from Propylene in a Single Pot – Effect of Partial Pressure of Propylene

Catalytic performance of [HF/HT–INT] system for selective synthesis of 2–ethylhexanal and 2–ethylhexanol was investigated in detail as function of various reaction parameters by conducting a series of experiments at constant hydroformylation temperature (T_1). The effects of partial pressure of propylene, aldol reaction temperature (T_2), and amount of catalyst on the selectivity of 2–ethylhexanal and 2–ethylhexanol at a fixed hydroformylation temperature (T_1 = 60 °C) were studied by varying one variable at a time for the single pot synthesis of 2–ethylhexanal and 2–ethylhexanol. Extensive literature is available for the effect of temperature (T_1) on hydroformylation, therefore, the effect of T_1 on hydroformylation reaction was not studied and kept constant at 60 °C in the present study. The higher selectivity of 2–ethylhexanal and 2–ethylhexanol was observed for the hydrotalcite as a basic component of multi–functional catalyst with Mg/Al molar ratio 3.5 due to higher basicity of the catalyst (Chapter 2). Therefore, hydrotalcite of Mg/Al molar ratio of 3.5 was selected for the intercalation of $HRh(CO)TPPTS)_3$ [HF] complex which act as a basic component of the multi–functional [HF/HT–INT] catalyst for single pot synthesis of 2–ethylhexanol from propylene via hydroformylation aldol condensation and hydrogenation reactions.

The concentration of reactant has a vital role for the selectivity of desired product. Therefore, effect of partial pressure of propylene on the selectivity of 2–ethylhexanal and 2–ethylhexanol was studied by varying the partial pressure of propylene from 3 to 10 atm at constant amount of [HF/HT–INT] catalyst (700 mg) and aldol temperature (T_2 = 150 °C) (Table 4.1).

Table 4.1. Effect of partial pressure of propylene on the selectivity of C_8 aldehydes

Run	Propylene, atm	% Selectivity [a]						t, h
		2–Ethylhexanal	*2*–Ethylhexenal	*n*–Butanal	*i*–Butanal	*n*–Butanol	*i*–Butanol	
1	3	4	2	40	54	–	–	12
2	5	7	4	38	51	–	–	12
3	7	10	7	40	43	–	–	12
4	10	21	8	27	33	8	3	12
6	3	11	3	27	48	6	5	24
7	5	21	4	20	40	7	10	24
8	7	26	7	17	27	7	16	24
9	10	30	12	16	20	8	14	24

[a] **Reaction conditions:** partial pressure of CO = 5 atm, partial pressure of hydrogen = 15 atm, catalyst = 700 mg, T_1 = 60 °C, t_1 = 6 h, T_2 = 150 °C.

To observe the progress of reaction, the reaction mixture was withdrawn from the reactor through sampling valve at two different time intervals first at 12 h and finally at 24 h. Formation of 2–ethylhexanol was not observed in the entire studied range of partial pressure of propylene. At lower partial pressure of propylene (3 atm), 6% selectivity for C_8 aldehydes (2–ethylhexanal and 2–ethylhexenal) were observed that increased to 14% on increasing the reaction time to 24 h. The selectivity of *n*–butanal also decreased on increasing the reaction time from 12 to 24 h. The decrease in the selectivity of butanal at higher reaction time is due to its consumption either for condensation reaction or for the reduction to butanol. This is supported by the observed 11% selectivity of butanols at 24 h and 3 atm pressure of propylene. The selectivity of C_8 aldehydes increased from 6 to 11% in 12 h and 14 to 25% in 24 h on increasing the partial pressure of propylene from 3 to 5 atm. On further increase in the partial pressure of propylene to 7, the selectivity of C_8 aldehydes were found to be 17% in 12 h which further increased to 33% within 24 h. Maximum selectivity of C_8 aldehydes (29%) were obtained at 10 atm propylene in 12 h that increased to 42% on increasing the reaction time to 24 h. The selectivity of *n*– and *iso*–butanal was also observed to decrease on increasing the partial pressure of propylene. Selectivity of *n*–butanal was observed to decrease from 40% at 3 atm to 27% at 10 atm in 12 h. On increase in the reaction time to 24 h, 27% selectivity of *n*–butanal was achieved at 3 atm that decreased to 16% on increasing the partial pressure of propylene to 10 atm. Similar to *n*–butanal, selectivity of *iso*–butanal was also observed to decrease on increasing partial pressure of propylene. Hydrogenation of butanals was not observed in the lower partial pressure of propylene in 12 h

reaction time, however, formation of butanols was observed when the reaction continued for 24 h. These results show that the higher reaction time is favoring the higher selectivity of desired C_8 aldehydes products along with hydrogenation of butanals.

The lower selectivity of C_8 aldehydes were observed in the present study at 10 atm pressure of propylene as compared to our earlier reports (Chapter 2.1) on the use of impregnated [HF] complex onto hydrotalcite of Mg/Al molar ratio 3.5. In the present study, most of the [HF] complex is intercalated in the interlayer space of hydrotalcite that limits the movement of ligand to initiate the hydroformylation reaction and the [HF] complex connected to edges of the hydrotalcite is catalyzing the hydroformylation and hydrogenation reaction. However, in our earlier reports, the [HF] complex was impregnated on the surface of hydrotalcite and ligand could move freely to initiate the reaction which results into higher selectivity of C_8 aldehydes in shorter reaction time. In view of the maximum selectivity of 2–ethylhexanal and 2–ethylhexanol observed at 10 atm partial pressure of propylene in the present study, further optimization of reaction parameter such as, aldol condensation temperature (T_2), amount of the [HF/HT–INT] catalyst and reusability experiments were carried out by taking partial pressure of propylene to 10 atm.

4.3.4. Effect of Aldol Condensation Temperature (T_2)

The second step temperature (T_2) in a single pot synthesis of 2–ethylhexanal and 2–ethylhexanol from propylene named as aldol condensation temperature because at this temperature condensation of *n*–butanal and hydrogenation of condensed product (2–ethylhexenal) takes place for the selective synthesis of C_8 aldehydes. The effect of aldol condensation temperature (T_2) on the selectivity of C_8 aldehydes was studied by varying T_2 from 80 to 250 °C (Table 4.2).

At lower T_2, lower selectivity of C_8 aldehydes was observed. For example, at 80 °C, only *n*– and *iso*–butanals were formed even after 12 h. As T_2 increased to 100 °C, 9% selectivity of C_8 aldehydes were observed that increase to 21% at 125 °C temperature. On further increase in T_2 to 200 °C, the selectivity of C_8 aldehydes increased to 33% in 12 h. This shows that the higher temperature favors the formation of 2–ethylhexenal and 2–ethylhexanal even though 2–ethylhexanol was not observed. The hydrogenation of butanals to butanols catalyzed by [HF] complex was not observed in the temperature range of 80 to 125 °C. On further increase in the T_2, hydrogenation of butanals increased significantly. The selectivity of *n*–butanal decreased significantly on increasing T_2 from 80 to 200 °C. At 80 °C, 78% selectivity of *n*–butanal was observed which decreased to 14% on increasing the aldol temperature to 200 °C in 12 h. As the reaction time increased to 24 h, the selectivity of C_8 aldehydes were observed to increase

significantly as compared to results obtained in 12 h in the studied T_2 range. Formation of C_8 aldehydes were not observed at 80 °C even after 24 h, however, C_8 aldehydes formed significantly (25% selectivity) on increasing the temperature to 100 °C in similar reaction time.

Table 4.2. Effect of aldol temperature (T_2) on the selectivity of 2–ethylhexanal and 2–ethylhexanol

Run	T_2, °C	% Selectivity [a]						t, h
		2–Ethylhexanal	2–Ethylhexenal	*n*–Butanal	*i*–Butanal	*n*–Butanol	*i*–Butanol	
1	80	–	–	78	32	–	–	12
2	100	3	6	50	41	–	–	12
3	125	6	15	37	38	–	–	12
4	150	21	8	27	33	8	3	12
5	200	29	4	14	24	12	18	12
6	80	–	–	76	29	2	3	24
7	100	7	18	30	35	4	6	24
8	125	16	12	29	32	5	6	24
9	150	30	12	16	20	8	14	24
10	200	32	10	3	16	18	21	24
11*	250	5	1	0	1	45	36	24

[a] **Reaction conditions:** partial pressure of propylene = 10 atm, partial pressure of CO = 5 atm, partial pressure of hydrogen = 15 atm, catalyst = 700 mg, T_1 = 60 °C, t_1 = 6 h.

* = 12% selectivity of 2–ethylhexanol

The selectivity of C_8 aldehydes increased to 28% at 125 °C. On further increasing the T_2 to 200 °C, the selectivity of C_8 aldehydes increased significantly to 42%. As the aldol temperature again increased to 250 °C, surprisingly, 12% selectivity of 2–ethylhexanol was observed with 6% selectivity for C_8 aldehydes in 24 h reaction time. At higher temperatures the selectivity of butanol was also observed to increase significantly. From the results presented in Table 4.2, only 5% selectivity of butanols was obtained at 80 °C, which further increased to 11% at 125 °C and 22% at 150 °C in 24 h reaction time. As temperature T_2 rose to 200 °C, the selectivity of butanols increased significantly. At 200 °C, the selectivity of butanols was achieved to 39% which increased to 81% on increasing the T_2 from 200 to 250 °C. The higher selectivity at 250 °C aldol temperature shows that the [HF/HT–INT] catalyst became more selective for the synthesis of butanols instead of C_8 aldehydes. Selectivity of *n*– and *iso*–butanals was also decreased significantly on increasing the T_2 from 80 to 250 °C which again confirmed the selective hydrogenation of butanols at 250 °C. Selectivity of butanals reduced from 95% at 80 °C to 61% at 125 °C. On further increase in the T_2

to 200 °C, selectivity of butanals dropped to 19%. All most complete consumption of butanals was observed at 250 °C due to faster hydrogenation of butanals to butanols catalyzed by intercalated [HF] complex of the multi–functional catalyst in the studied reaction conditions. In the lower T_2 range (80–150 °C), most of *n*–butanal was consumed for the synthesis of C_8 aldehydes with little amount for the hydrogenation of *n*–butanal to *n*–butanol. Whereas, *iso*–butanal was consumed completely for the hydrogenation reaction to give *iso*–butanol.

One of the possible reasons for higher selectivity of C_8 aldehyde on increasing the reaction temperature upto 200 °C could be the increased catalytic activity due to activation of solid base component [HT] of [HF/HT–INT] for condensation of aldehydes. The kinetics data presented in the Chapter 2.1 suggested that the overall rate of reaction depends upon the condensation of *n*–butanal step. If aldol condensation reaction is faster then the formation of C_8 aldehydes will also be faster. Higher rate of condensation of aldehydes at higher temperature was also confirmed by performing the reactions for condensation of aldehydes separately in Chapter 5 and 6 using hydrotalcite as a catalyst. The observed reduction of butanals at higher temperature is due to the engagement of intercalated [HF] complex present in the [HF/HT–INT] catalyst for hydrogenation of butanals rather than the hydrogenation of condensed products. The another reason for increase in the selectivity of C_8 aldehydes upto 200 °C is due to the thermal stability of [HT/HT–INT] catalyst as seen from TGA curves. TGA data shows that the intercalated [HF] complex present in [HF/HT–INT] catalyst was stable upto 200 °C, and after that decomposition was observed. The decomposition of [HF] complex may result into a rhodium species which could be more active for the hydrogenation of aldehydes. To confirm this assumption, one separate experiment was carried out by taking *n*–butanal (0.4 M) as reactant in 50 ml of toluene as solvent at 250 °C at 30 atm of H_2 with 700 mg [HF/HT–INT] for 12 h reaction time. After 12 h, 78% selectivity for butanols was observed which is in accordance with the results observed in case of propylene as a reactant. The lower selectivity of C_8 aldehydes was also observed at lower T_2. The reason for lower activity of catalyst at lower temperature could be attributed to the strong adsorption of intermediate/products molecules on the surface of [HF/HT–INT]. Therefore, high temperature is required to avoid this undesirable adsorption which leads to decreased catalytic activity. Significant effect on the selectivity of C_8 aldehydes were not observed between the temperature of 150 and 200 °C, therefore, lower (150 °C) aldol condensation temperature was selected as T_2 to study the effect of amount of catalyst on the selectivity of 2–ethylhexanal and 2–ethylhexanol.

4.3.5. Effect of Amount of Catalyst

The amount of catalyst was varied from 100 to 1200 mg at constant T_2 (150 °C), 10 atm

pressure of propylene, CO and H_2 at 1:3 (Table 4.3). Formation of the 2–ethylhexanol was not observed in the studied variations in the amount of catalyst which again confirmed that the higher temperature (T_2) must be required to obtain 2–ethylhexanol in single pot using [HF/HT–INT] catalyst. The selectivity of C_8 aldehydes were observed to increase on increasing amount of catalyst. At 100 mg, 14% selectivity of C_8 aldehydes were obtained in 12 h which increased to 26% at 500 mg catalyst amount. On further increase in the catalyst amount to 1000 mg, excellent selectivity of C_8 aldehydes (44%) was achieved which further increased to 47% on increasing the amount to 1200 mg.

Table 4.3. Effect of amount of catalyst on the selectivity of C_8 aldehydes

Run	Catalyst, mg	% Selectivity [a]						t, h
		2–Ethylhexanal	2–Ethylhexenal	*n*–Butanal	*i*–Butanal	*n*–Butanol	*i*–Butanol	
1	100	9	5	42	30	8	6	12
2	250	14	3	40	31	7	6	12
3	500	23	3	23	25	8	7	12
4	700	21	8	27	33	8	3	12
5	1000	29	15	20	25	5	7	12
6	1200	31	16	19	25	4	5	12
7	100	15	6	34	26	14	20	24
8	250	18	7	20	24	13	18	24
9	500	26	15	12	23	15	19	24
10	700	30	12	16	20	8	14	24
11	1000	36	9	8	15	13	17	24
12	1200	39	12	6	12	16	15	24

[a] **Reaction conditions:** partial pressure of propylene = 10 atm, partial pressure of CO = 5 atm, partial pressure of hydrogen = 15 atm, T_1 = 60 °C, t_1 = 6 h, T_2 = 150 °C.

The selectivity of *n*–butanal was also observed to decrease on increase in the amount of catalyst, however, no significant decrease in the selectivity of *iso*–butanol was observed in the catalyst range of 100 to 700 mg. On increasing the reaction time from 12 h to 24 h, the selectivity of C_8 aldehydes increased significantly higher than the results obtained in 12 h. At 100 mg, the selectivity of C_8 aldehydes increased from 14% (12 h) to 21% in 24 h. 41% Selectivity of C_8 aldehydes were obtained for 500 mg, which increased to 45% at 1000 mg and finally 51% for 1200 mg catalyst amount in 24 h. The selectivity of *n*– and *iso*–butanal also decreased from 34 to 6%

and 26 to 12%, respectively, in 24 h reaction time.

Higher selectivity for C_8 aldehydes observed at increasing amount of [HF/HT–INT] catalyst could be due to the availability of sufficient amounts of solid base components in [HF/HT–INT] catalyst to affect aldol condensation reaction. The active catalyst for aldol condensation of *n*–butanal possesses basic sites on their surface to carry out the reaction. In the present multi–functional catalyst, the active sites for condensation of *n*–butanal are the hydroxyl groups located on the surface of the hydrotalcite which acts as Brønsted basic sites. The lower selectivity of C_8 aldehydes at lower catalyst amount is due to less availability of total number of active basic sites on the surface of hydrotalcite. As the amount of catalyst increases, total number of active basic sites responsible for the condensation reaction also increased significantly to enhance condensation of *n*–butanal. Therefore, at higher amounts of catalyst, maximum selectivity of C_8 aldehydes were observed in the present study.

4.3.6. Reusability of [HF/HT–INT] Catalyst

For the reusability experiments, spent [HF/HT–INT] catalyst was filtered from the product mixture after completion of the reaction and was washed several times with 100 ml toluene. During washing with toluene, all physically adsorbed products on the surface of catalyst were dissolved in the toluene without leaching of [HF] complex. The washed [HF/HT–INT] catalyst was dried for 8 h under vacuum at room temperature. Then the catalyst was reused for single pot synthesis of 2–ethylhexanal and 2–ethylhexanol from propylene by taking 1000 mg regenerated catalyst, CO and H_2 in 1:3 ratio at 10 atm partial pressure of propylene and 150 °C T_2 (Table 4.4). No significant decrease in the selectivity of C_8 aldehydes were observed upto second run. Afterwards, the selectivity of C_8 aldehydes decreased significantly on each reusability experiments. Increase in the selectivity of butanals was observed at the end of each reusability cycle which suggested that the [HF/HT–INT] catalyst is active for carrying out the hydroformylation reaction even at fourth cycle but the basic component [HT] of [HF/HT–INT] catalyst, which is responsible for the aldol condensation of the butanal obtained form the hydroformylation step, is deactivating slowly at the end of each cycle. Therefore, apart from handling loss of the catalyst, reaction for the single pot synthesis of C_8 aldehydes is slow down at the end of each reusability cycle due to deactivation of [HT].

Table 4.4. Reusability of [HF/HT–INT] catalyst

Cycle	% Selectivity [a]					
	2–Ethylhexanal	2–Ethylhexenal	*n*–Butanal	*i*–Butanal	*n*–Butanol	*i*–Butanol
Fresh	36	9	6	15	13	19
First	32	6	17	23	9	14
Second	30	6	20	30	4	10
Third	22	7	25	36	3	7
Fourth	16	5	35	44	–	–

[a] **Reaction conditions:** partial pressure of propylene = 10 atm, partial pressure of CO = 5 atm, partial pressure of hydrogen = 15 atm, catalyst = 1000 mg, T_1 = 60 °C, t_1 = 6 h, T_2 = 150 °C, t = 24 h.

4.3.7. Kinetic Profiles and Rate of Reaction for Synthesis of C_8 Aldehydes in a Single Pot

In order to have an insight into the kinetic profiles and rates of formation of the products for synthesis of C_8 aldehydes from propylene in a single pot, which could provide significant information to understand the reaction pathways involved in the formation of products at different stages with time, the experiments were conducted using [HF/HT–INT] catalyst at the conditions which gave optimum selectivity for formation of C_8 aldehydes, i.e., 150 °C aldol condensation temperature (T_2), 1200 mg catalyst amount and 10 atm partial pressure of propylene in 50 ml toluene as a solvent. The calculated rates of reaction for the single pot synthesis of C_8 aldehydes were compared with the rate of reaction determined individually, for hydroformylation of propylene, aldol condensation of *n*–butanal and hydrogenation of 2–ethylhexenal catalyzed by [HF/HT–INT] using propylene, *n*–butanal and 2–ethylhexenal, respectively as reactants under the reaction conditions identical to those used for the single pot synthesis of C_8 aldehydes from propylene in this study. Kinetic profiles for the formation of each product in single pot synthesis of C_8 aldehydes are shown in Figure 4.1 which give important information to understand the progress of reaction at different stages with time to arrive at the actual reaction pathway. The formation of butanals via propylene hydroformylation at 60 °C catalyzed by intercalated [HF] complex was seen upto 6 h. Except the *n*– and *iso*–butanal, the formation of other products were not observed upto 5 h. In the 6 h reaction time, small amount of butanols via hydrogenation of butanals and 2–ethylhexanal via condensation of *n*–butanal was observed.

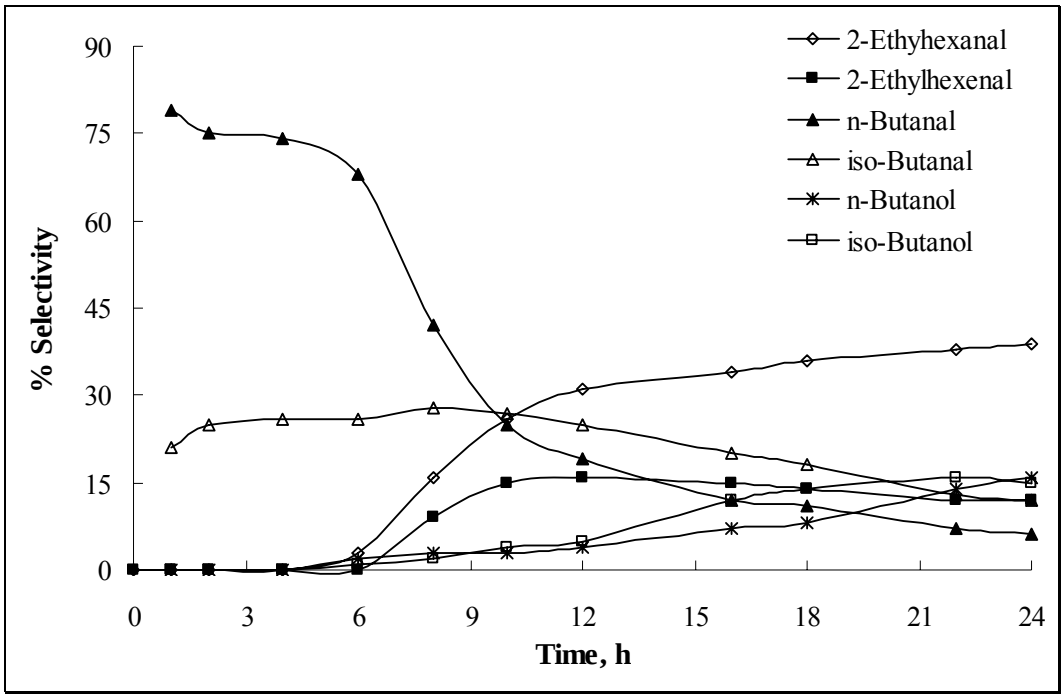

Figure 4.1. Effect of reaction time on the formation of products during single pot synthesis of C_8 aldehydes from propylene using [HF/HT–INT] as a catalyst.

As the hydroformylation temperature (T_1) increased to aldol condensation temperature (T_2), the formation of C_8 aldehydes via aldol condensation of *n*–butanal, which is subsequently consumed into 2–ethylhexanal in the presence of hydrogen and the reduction of butanals to butanols were observed after 7 h. As the reaction time increased from 7 to 12 h, selectivity of 2–ethylhexenal and 2–ethylhexanal were found to increase linearly. After 12 h, slow increase in the selectivity of 2–ethylhexanal was observed. However, decrease in the selectivity of 2–ethylhexenal confirmed its simultaneous consumption for the synthesis of 2–ethylhexanal. Significant increase in the selectivity of butanols was observed due to the hydrogenation of butanals after 12 h. The observed increase in the selectivity of *iso*–butanol suggests that most of *iso*–butanal undergoes for the hydrogenation reaction. The selectivity of *n*–butanal decreased sharply after 6 h indicating its regular consumption for the formation of C_8 aldehydes and butanols. It was interesting to see that the formation of butanols also started after 6 h, the time after which formation of C_8 aldehyde were observed. Formation of 2–ethylhexanol was not observed in the entire range of studied reaction conditions in present kinetic study even after 24 h reaction time.

Table 4.5. Rate of reaction calculated from separate reaction performed by taking propylene, *n*–butanal, 2–ethylhexenal as reactants and one pot synthesis of C_8 aldehydes from propylene using [HF/HT–INT] as a catalyst

Run	Catalyst	Reaction	Rate x 10^2, M/h
1	[HF/HT–INT] [b]	hydroformylation	21.7
2	[HF/HT–INT] [c]	hydrogenation	12.6
3	[HF/HT–INT] [d]	aldol condensation	4.6
4	[HF/HT–INT] [a]	hydroformylation	19.3
		aldol condensation	3.3
		hydrogenation [f]	2.6
		hydrogenation [g]	1.0

[a] **Reaction conditions:** partial pressure of propylene = 10 atm, partial pressure of CO = 5 atm, partial pressure of H_2 = 15 atm, [HF/HT–INT] = 1200 mg, T_1 = 60 °C, t_1 = 6 h, T_2 = 150 °C, t = 24 h.

[b] [HF/HT–INT] = 1200 mg, T_1 = 60 °C for 6 h.

[c] [HF/HT–INT] = 1200 mg, 2–ethylhexenal = 0.4 M, T_2 = 150 °C for 12 h.

[d] [HF/HT–INT] = 1200 mg, *n*–butanal = 0.4 M; T_2 = 150 °C for 12 h.

Formation of 2–ethylhexanal [f] and butanol [g]

The rates of formation of the products were determined separately, for hydroformylation of propylene, aldol condensation of *n*–butanal and hydrogenation of 2–ethylhexenal catalyzed by [HF/HT–INT] using propylene, *n*–butanal and 2–ethylhexenal as reactants under identical reaction conditions those used for the single pot synthesis of 2–ethylhexanal and 2–ethylhexanol from propylene and the corresponding results are listed in Table 4.5. The individual rates for hydroformylation of propylene, aldol condensation of *n*–butanal and hydrogenation of 2–ethylhexenal indicated that the hydroformylation is the fastest reaction and aldol condensation of *n*–butanal for the production of 2–ethylhexenal is the slowest reaction. The rate of hydrogenation of 2–ethylhexenal is also slower than the hydroformylation of propylene. With [HF/HT–INT] catalyst in the single pot, the rate of hydroformylation and aldol condensation was observed to be comparable with the calculated rate from individual reactions. The fastest rate of hydroformylation of propylene followed by rate of aldol condensation of *n*–butanal and rate for hydrogenation of 2–ethylhexenal was observed for single pot synthesis of C_8 aldehydes from propylene. The rate of aldol condensation (3.3 x 10^{-2} M/h) and hydrogenation of 2–ethylhexenal (2.6 x 10^{-2} M/h) indicate that the rate of hydrogenation of 2–ethylhexenal to 2–ethylhexanal is lower than the rate of aldol

condensation of *n*–butanal in the studied reaction conditions. This could be attributed to the lower rate of reaction for hydrogenation of 2–ethylhexenal to 2–ethylhexanal which is an intermediate for the production of 2–ethylhexanol. The rate of butanol formation was found to be lower (1.0×10^{-2} M/h) than that of 2–ethylhexanal (2.6×10^{-2} M/h). The rate of formation of the 2–ethylhexenal is dependent on the rate of aldol condensation which is catalyzed by [HT] component of [HF/HT–INT] catalyst. The rate of hydrogenation of 2–ethylhexenal is also lower as compared to hydroformylation of propylene. After the hydroformylation of propylene, butanal can either undergo aldol condensation or hydrogenation depending on the applied reaction conditions.

4.4. Conclusions

A novel eco–friendly multi–functional [HF/HT–INT] catalyst was synthesized by the intercalation of $HRhCO(TPPTS)_3$ in the interlayer space of hydrotalcite for single pot synthesis of C_8 aldehydes from propylene. The catalyst showed excellent activity for hydroformylation, aldol condensation and hydrogenation reaction in a single pot by changing the reaction conditions. The effect of various reaction parameters on the selectivity of 2–ethylhexanal and 2–ethylhexanol was studied in order to optimize the reaction conditions. Formation of 2–ethylhexanol (12%) was observed at higher aldol condensation temperature (T_2 = 250 °C). The selectivity of C_8 aldehydes was observed to increase on increasing the T_2 and maximum selectivity (42%) obtained in the range of 150 to 200 °C aldol temperature at 10 atm partial pressure of propylene in 24 h reaction time. The amount of [HF/HT–INT] catalyst was varied from 100 to 1200 mg in order to optimize the amount of catalyst for the maximum selectivity of C_8 aldehydes. The selectivity of C_8 aldehydes increased from 21% at 100 mg to 51% at 1200 mg. The catalyst was reused upto second cycle without significant loss in the conversion of propylene and selectivity of C_8 aldehydes. The reusability experiments suggested that the [HF/HT–INT] catalyst is active even at fourth cycle for carrying out hydroformylation reaction but the basic component [HT] of [HF/HT–INT] catalyst was deactivated which is responsible to catalyze the aldol condensation of *n*–butanal obtained from the hydroformylation step. Rate of formation of the various products was calculated from the kinetic profile and compared with the rates of formation of products which determined separately, for hydroformylation of propylene, aldol condensation of *n*–butanal and hydrogenation of 2–ethylhexenal catalyzed by [HF/HT–INT] using propylene, *n*–butanal and 2–ethylhexenal as reactants under identical reaction conditions those used for the single pot synthesis of C_8 aldehydes from propylene.

4.5. References

[1] D.G. Evans, X. Duan, Chem. Commun. (2006) 485–496.

[2] Q.Z. Yang, D.J. Sun, C.G. Zhang, X.J. Wang, W.A. Zhao, Langmuir 19 (2003) 5570–5574.

[3] G.G. Aloisi, U. Costantino, F. Elisei, L. Latterini, C. Natali, M. Nocchetti, J. Mater. Chem. 12 (2002) 3316–3323.

[4] A.I. Khan, D. O'Hare, J. Mater. Chem. 12 (2002) 3191–3198.

[5] V. Rives, Layered Double Hydroxides: Present and Future, Nova Science Publishers, Inc., New York, (2001).

[6] E.L. Crepaldi, P.C. Pavan, J.B. Valim, Chem. Commun. (1999) 155–156.

[7] R. Schollhorn, B. Otto, J.Chem. Soc., Chem. Commun. (1986) 1222–1223.

[8] K. Chibwe, W. Jones, J. Chem. Soc., Chem. Commun. (1989) 926–927.

[9] A.I. Khan, L. Lei, A.J. Norquist, D. O'Hare, Chem. Commun. (2001) 2342–2343.

[10] G.R. Williams, T.G. Dunbar, A.J. Beer, A.M. Fogg, D. O'Hare, J. Mater. Chem. 13 (2006) 1231–1237.

[11] K.M. Parida, S. Parija, J. Das, P.S. Mukherjee, Catal. Commun. 7 (2006) 913–919.

[12] J. Das, K.M. Parida, J. Mol. Catal. A: Chem. 264 (2007) 248–254.

[13] E. Kanezaki, K. Kinugawa, Y. Ishikawa Chem. Phy. Lett. 226 (1994) 325–330.

[14] F. Malherbe, J.P. Besse, J. Solid State Chem. 155 (2000) 332–341.

[15] E.L. Crepaldi, P.C. Pavan, J. Tronto, J.B. Valim, J. Col. Inter. Sci. 248 (2002) 429–442.

[16] V.I. Iliev, A.I. Ileva, L.D. Dimitrov, Appl. Catal. A: Gen. 126 (1995) 333–340.

[17] B.M. Choudary, M.L. Kantam, N.M. Reddy, N.M. Gupta, Catal. Lett. 82 (2002) 79–83.

[18] M. Chibwe, T.J. Pinnavaia, J. Chem. Soc., Chem. Commun. (1993) 278–280.

[19] S. Hamada, K. Ikeue, M. Machida, Chem. Mater. 17 (2005) 4873–4879.

[20] J. Inacio, C.T.Gueho, S.M. Therias, M.E. Roy, J.P. Besse, J. Mater. Chem. 11 (2001) 640–643.

[21] E.P. Giannelis, D.G. Nocera, T.J. Pinnavaia, Inorg. Chem. 26 (1987) 203–205.

[22] I. Crespo, C. Barriga, V. Rives, M.A. Ulibarri, Solid State Ion. 101–103 (1997) 729–735.

[23] M. Arco, S. Gutierrez, C. Martin, V. Rives, Inorg. Chem. 42 (2003) 4232–4240.

[24] I. Carpani, M. Berrettoni, M. Giorgetti, D. Tonelli, J. Phys. Chem. B 110 (2006) 7265–7269.

[25] N.H. Gutmann, L. Spiccia, T.W. Turney, J. Mater. Chem. 10 (2000) 1219–1224.

[26] X. Zhang, M. Wei, M. Pu, X. Li, H. Chen, D.G. Evans, X. Duan, J. Solid State Chem. 178 (2005) 2701–2708.

[27] F. Iosif, V.I. Parvulescu, M.E.P. Bernal, R.J.R. Casero, V. Rives, K. Kranjc, S. Polanc, M. Kocevar, E. Genin, J.P Genet, V. Michelet, J. Mol. Catal. A: Chem. 276 (2007) 34–70.

[28] Y. Zhao, F. Li, R. Zhang, D.G. Evans, X. Duan, Chem. Matter. 14 (2002) 4286–4291.

[29] D. Frohning, C.W. Kohlpaintner, in Applied Homogeneous Catalysis with Organometallic Compounds, ed. B. Cornils, W. A. Hermann, Wiley–VCH, Weinheim, (2000), vol. 1, ch. 2, p. 29.

[30] A.D. Godwin, R.H. Schlosberg, F. Hershkowitz, M.G Matturro, G. Kiss, K.C. Nadler, P.L Buess, R.C Miller, P.W. Allen, H.W. Deckman, R. Caers, E.J. Mozeleski, J. Edmund, R.P. Reynolds, US Patent, 6307093 (2001).

[31] F.J. Doering, G.F. Schaefer, J. Mol. Catal. 41 (1987) 313–328; B.J. Arena, J.S. Holmgren, US Patent, 5144089 (1992).

[32] G. Horn, C.D. Frohning, H. Liebern, W. Zgorzelski, US Patent, 5475161 (1995).

[33] W. Bueschken, J. Hummel, US Patent, 5756856 (1998).

[34] H.G. Lueken, U. Tanger, W. Droste, G. Ludwig, D. Gubisch, US Patent, 4968849 (1990).

[35] T. Mori, K. Fujita, H. Hinoishi, US Patent, 5550302 (1996).

[36] J.J. Spivey, M.R. Gogate, Pollution Prevention in Industrial Condensation Reactions, Research Triangle Institute, USEPA Grant, (1996).

[37] G.J. Kelly, F. King, M. Kett, Green Chem. 4 (2002) 392–399.

[38] C.R. Greene, US Patent, 3278612 (1966) to Shell oil company.

[39] S.K. Sharma, V.K. Srivastava, R.S. Shukla, P.A. Parikh, R.V. Jasra, New J. Chem. 31 (2007) 277–286.

[40] V.K. Srivastava, S.K. Sharma, R.S. Shukla, R.V. Jasra, Catal. Commun. 7 (2006) 881–886.

[41] V.K. Srivastava, S.K. Sharma, R.S. Shukla, N. Subrahmanyam, R.V. Jasra, Ind. Eng. Chem. Res. 44 (2005) 1764–1771.

Chapter 5

Solvent Free Aldol Condensation of Propanal to 2–Methylpentenal using Solid Base Catalysts

5.1. Introduction

2–Methylpentenal is a commercially important chemical that finds applications in fragrances, flavors, cosmetics and as an intermediate for the synthesis of various pharmacologically active compounds [1]. Industrially, 2–methylpentenal is synthesized by aldol condensation of propanal in the presence of liquid base like KOH or NaOH used in stoichiometric amounts [1–3]. Under optimum reaction conditions, 95% conversion of propanal is achieved with 86% selectivity of 2–methylpentenal using a liquid base [3]. Existing process for the synthesis of 2–methylpentenal from propanal is not eco–friendly and have other drawbacks like the use of KOH or NaOH in large stoichiometric amount, lower selectivity, separation of spent KOH or NaOH from post synthesis reaction mixture, effluent treatment and disposal of spent liquid base. The alkali metal hydroxides require large amount of water for neutralization and washing after the completion of reaction. Replacement of currently used homogeneous alkaline liquid by solid bases will not only allow the reusability of the catalyst but could also minimize waste stream. It is desirable to find alternative catalyst which could substitute liquid bases and have ease of separation from the products, decreased corrosion of the reactors, and possible regeneration of the catalyst. Therefore, research efforts are directed to develop a catalytic process, which can produce 2–methylpentenal from propanal with high selectivity employing eco–friendly re–usable solid base catalyst (Scheme 5.1).

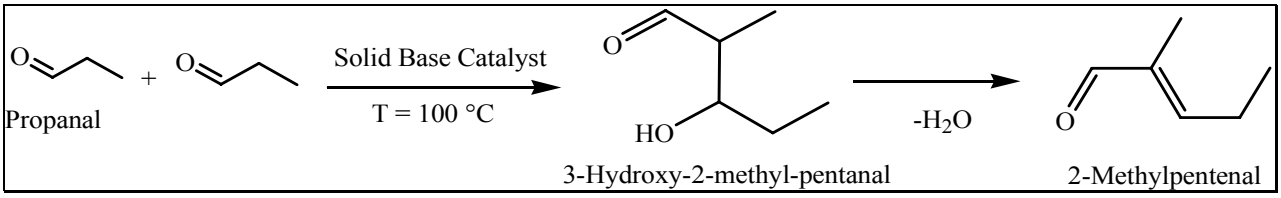

Scheme 5.1. Aldol condensation of propanal.

The synthesis of C_6 aldehydes from propanal via aldol condensation in ionic liquid media with NaOH as a catalyst was studied by Mehnert et al. The authors have reported 100% conversion of propanal with 83% selectivity for C_6 aldehydes at 80 °C in 3 h reaction time using [bdmin]PF_6 ionic liquid as a solvent with sodium hydroxide as a catalyst [4]. Matsui et al. studied the effect of CO_2 pressure on selectivity of condensation products in the presence of MgO with small amount of water. In the supercritical region, 94% selectivity of 2–methylpentenal was obtained near the critical pressure of 12 MPa [5]. The vapor phase aldol condensation of propanal was studied by Scheidt et al., and achieved more than 95% selectivity of 2–methylpentenal by passing the vapors of propanal over heated lithium phosphate [6]. In another study, Tang et al. reported the synthesis of 2–methylpentenal from self condensation of propanal using ion–exchanged resins [7]. 94% yield

of 2–methylpentenal was obtained in 2 h reaction time at 30 °C using benzene as a solvent.

Hydrotalcite (HT) and cation exchanged zeolites have received much attention in view of their potential applications as adsorbents, and most importantly, as solid base catalysts [8–10]. Thermal decomposition of hydrotalcite at about 450 °C results into highly active uniformly mixed oxides, which is a potential base catalyst for variety of organic transformations such as condensation, isomerization, anion exchangers and epoxidation reactions [11–15]. Numerous studies are reported on self condensation of butanal, acetone, and cross condensation using hydrotalcite samples or other solid base catalysts [16–18], but only limited literature is available on the self condensation of propanal using solid base catalysts.

The aim of present investigation is to develop a suitable solid base catalyst for aldol condensation of propanal in solvent free environment. The various alkali ion–exchanged zeolites, alumina, alkali impregnated alumina and hydrotalcite samples were synthesized, characterized and their catalytic activities were evaluated.

5.2. Experimental

5.2.1. Materials

Propanal and 2–methylpentenal were purchased from Sigma–Aldrich, USA and used without further purification. Zeolite powder (Si/Al = 1.25) procured from Zeolites and Allied products, Mumbai, India, was used without any further purification. The chloride salts of cesium, potassium and rubidium were purchased form Sigma–Aldrich, USA. Magnesium nitrate ($Mg(NO_3)_2.6H_2O$), aluminum nitrate ($Al(NO_3)_3.9H_2O$), sodium carbonate (Na_2CO_3) and sodium hydroxide (NaOH) were purchased from s.d. Fine Chemicals, India for the synthesis of hydrotalcite samples. The double distilled milli–pore deionized water was used for the synthesis of hydrotalcite samples.

5.2.2. Catalyst Synthesis

Synthesis of Alkali Exchanged Zeolites

The exchange of various alkali ions (cations) into the zeolites framework was carried out by reported procedure [12–19]. The alkali ion–exchanged zeolites Cs–X, Rb–X and K–X were prepared by four times ion–exchange of Na–X zeolite with 1 M aqueous solution of corresponding salts of cesium, rubidium and potassium at 80 °C for 4 h. The resulting Cs–X, Rb–X and K–X were washed with deionized distilled water. The alkali ion–exchanged zeolite samples were dried in

oven at 110 °C and activated for 4 h at 450 °C in a muffle furnace.

Impregnation KOH on Alumina

The impregnation of KOH on the surface of neutral alumina was carried out by stirring of neutral alumina with 10%, 20%, 30%, and 50% concentrated solution of KOH at room temperature for 12 h. After 12 h, the solids were separated by filtration, followed by overnight drying at 110 °C. The impregnated samples were calcined at 450 °C for 4 h in a muffle furnace.

Synthesis of Hydrotalcite of Varied Mg/Al Molar Ratio

The hydrotalcite samples with Mg/Al molar ratios in the range of 1.5 to 3.5 were synthesized by co–precipitation method at constant pH. Typically, for hydrotalcite sample with Mg/Al molar ratio = 2.5, an aqueous solution (A) of $Mg(NO_3)_2.6H_2O$ (0.22 mol) and $Al(NO_3)_3.9H_2O$ (0.088 mol) in 200 mL double distilled deionized water was prepared. The solution A was added dropwise into a second solution (B) containing NaOH (0.72 mol) and Na_2CO_3 (0.21 mol) in 200 mL double distilled deionized water, in around 2 h under vigorous stirring at 30 °C. The content was then transferred into teflon coated stainless steel autoclave and aged at 70 °C for 12 h under autogenous water vapor pressure. After 14 h, the precipitate formed was filtered and washed thoroughly with hot distilled water until pH of filtrate was 7. The washed precipitate was dried in an oven at 80 °C for 14 h. Hydrotalcite samples with varied Mg/Al molar ratio (1.5–3.5) were synthesized as per above procedure having appropriate amounts of $Mg(NO_3)_2.6H_2O$ and $Al(NO_3)_3.9H_2O$. The hydrotalcite samples of Mg/Al molar ratio from 1.5 to 3.5 were activated (calcination) at 450 °C for 4 h in a muffle furnace. The solid material was then cooled and used as a catalyst for aldol condensation of propanal. Freshly activated (calcined) catalyst was always used in the present study. Reconstruction of the activated hydrotalcite was carried out by stirring of 1 g of freshly activated hydrotalcite with 75 mL decarbonated water for 48 h. After 48 h, the suspension was filtered and dried in vacuum. The detail procedure on the reconstruction of hydrotalcite has been reported in Chapter 6.

5.2.3. Characterization of the Catalyst

Powder X–ray diffraction (P– XRD) patterns of alkali ion–exchanged zeolites, KOH treated alumina and hydrotalcite samples were recorded with Phillips X'Pert MPD system equipped with XRK 900 reaction chamber, using Ni–filtered Cu–Kα radiation (λ =1.54050 Å) over a 2θ range of 0–70°. Fourier transform infrared (FT–IR) spectra of hydrotalcite samples were recorded from 400 to 4000 cm^{-1} with a Perkin–Elmer spectrum GX FT–IR system using KBr pellets. Thermogravimetric analysis (TGA) of the hydrotalcite samples was carried out using Mettler–

Toledo TGA/SDTA 851e equipment in flowing nitrogen or argon (flow rate, 50 mL/min), at a heating rate of 10 °C/min and the data were processed using Star^e software. Scanning electron microscopy (SEM) images of the hydrotalcite samples were taken on a microscope (Leo Series VP1430, Germany) having silicon detector equipped with EDX facility (Oxford instruments). The samples were coated with gold using sputter coating to avoid charging. Analysis was carried out at an accelerating voltage of 15 kV.

5.2.4. Aldol Condensation Reaction

Typically, aldol condensation of propanal was carried out in a 25 mL oven dried double necked round bottom flask in which pre–calculated amount of propanal and solid base catalyst were taken with 0.01 g *n*–decane as an internal standard. One neck of flask was fitted with 2.25 feet long refluxing condenser having spiral tube inside and another neck of flask was blocked with silicon rubber septa. The top of the refluxing condenser was blocked by standard cork. The water at 15 °C was circulated in refluxing condenser during the course of reaction from water chiller at flow rate of 6 liter/min. The entire experimental setup was kept in an oil bath equipped with temperature and agitation speed controlling unit. The reaction is carried out at 100 °C for 10 h. The reaction mixture was cooled to room temperature after set reaction time and was subjected to filtration. The silicon grease was used in all joints to prevent vapor loss of propanal and conversion of propanal was calculated by internal standard method. However, the weight of initial reaction mixture and product mixture after the completion of reaction was compared to ensure no vapor loss of propanal. The kinetic studies were carried out by taking 5 g propanal and 0.5 g catalyst. The 0.01 mL sample each time was withdrawn during the kinetic experiment using 1 mL size glass syringe at different time intervals. The analysis of reaction mixture samples were carried out by gas chromatography (GC) (Shimadzu 17A, Japan) and GC–MS (mass spectrophotometer, Shimadzu–QP2010, Japan). The GC has a 5% diphenyl and 95% dimethyl siloxane universal capillary column (60 m length and 0.25 mm diameter) and a flame ionization detector (FID). The initial column temperature was increased from 40 to 200 °C at the rate of 10 °C/min. Nitrogen gas was used as a carrier gas. Temperatures of the injection port and FID were kept constant at 250 °C during the analysis of reaction mixture. The retention time of different compounds were determined by injecting pure compound under identical gas chromatography conditions.

5.2.5. Kinetic Analysis and Reproducibility

The parameters, which might have pronounced effect on the rate of aldol condensation of propanal include, concentration of reactant and solvent, amount of catalyst and reaction temperature. Therefore, the kinetic experiments were carried out by varying these parameters. In

each case, the change in concentration of reactant was determined by gas chromatography at fixed time intervals. The initial rate of reaction was calculated by the method reported in literature [20]. In the present experimental conditions, 2–methylpentenal and 3–hydroxy–2–methylpentanal were only the major products observed to form in the aldol condensation of propanal. However, formation of 3–pentanone in small amount cannot be ignored in some experimental conditions during the course of aldol condensation of propanal.

To ensure the reproducibility of condensation of propanal, repeated experiments were carried out under identical reaction conditions. The results obtained, including conversion and selectivity data were found to be reproducible within less than 7% variation, confirming the reproducibility of the results. A typical concentration profile of reactant consumption and product formation is shown in Figure 5.1. The conversion of propanal and selectivity of 2–methylpentenal was observed to increase linearly upto 3.5 h. After 3.5 h, the slow rate of increment in the conversion and selectivity was seen upto 6 h and it attains saturation on further increase in the reaction time.

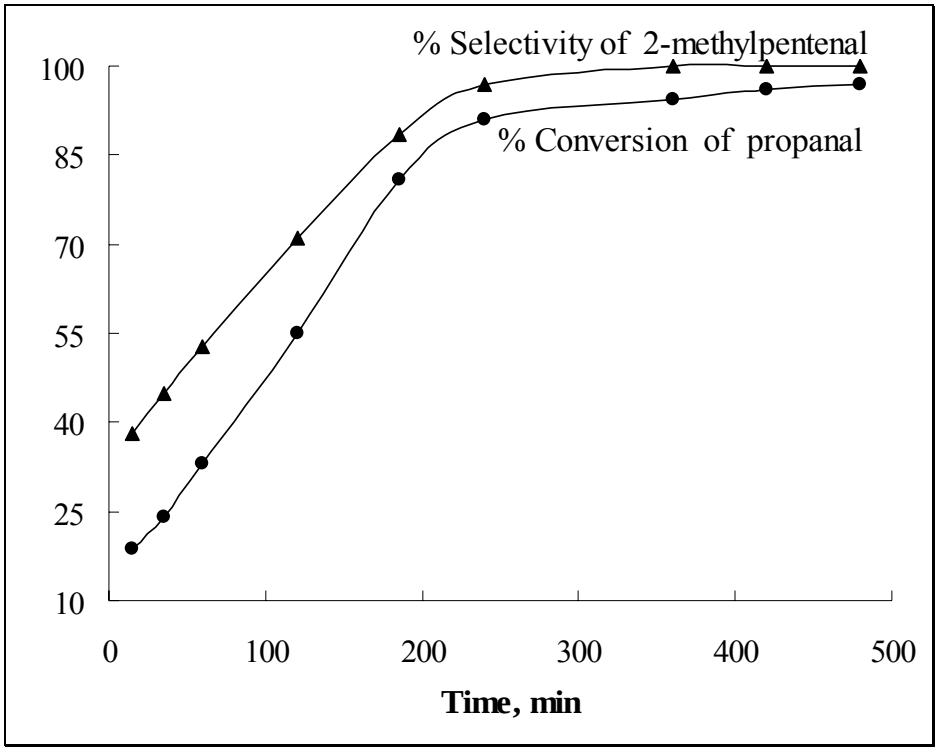

Figure 5.1. Concentration–time profile for aldol condensation of propanal.

5.3. Results and Discussion

5.3.1. Catalyst Characterization

P–XRD Patterns of Alkali Ion–Exchanged Zeolites and KOH Impregnated on Neutral Alumina and Hydrotalcite Samples

P–XRD patterns of the alkali ion–exchanged zeolites and KOH impregnated alumina are shown in Figures 5.2 and 5.3. P–XRD profiles of original and modified zeolite samples showed all characteristic peaks of zeolite structure closely matching with the reported reflections for highly crystalline zeolite Na–X at 2θ values 6.1°, 10.0°, 15.5°, 20.1°, 23.9°, 26.7°, 29.4°, 30.7°, 31.0°, 33.5°, 36.8° and 42.4° (Figure 5.2). Percentage crystallinity of the alkali ion–exchanged zeolites was observed to decrease on increasing the cations size as compared to the Na–X zeolite sample (Table 5.1). For example, crystallinity of Na–X was observed to decrease from 100 to 91% on the exchange of potassium cation in the cages of Na–X. For Rb–X zeolite, the crystallinity was found to be 88% which decreased to 62% for Cs–X.

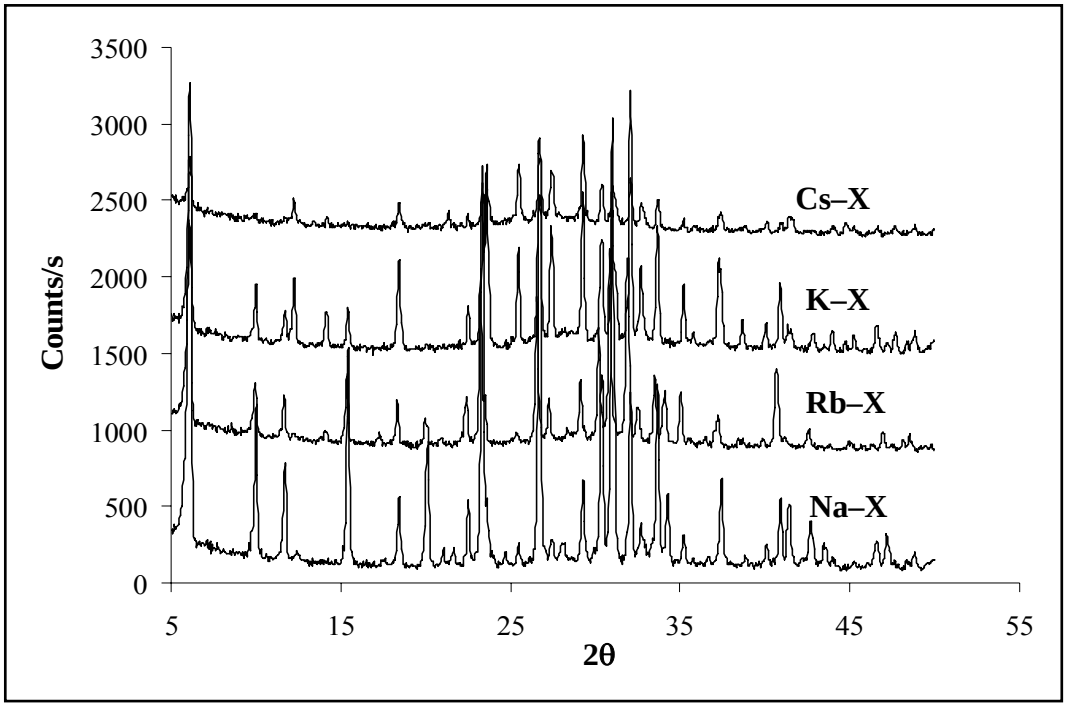

Figure 5.2. P–XRD patterns of alkali ion–exchanged zeolites.

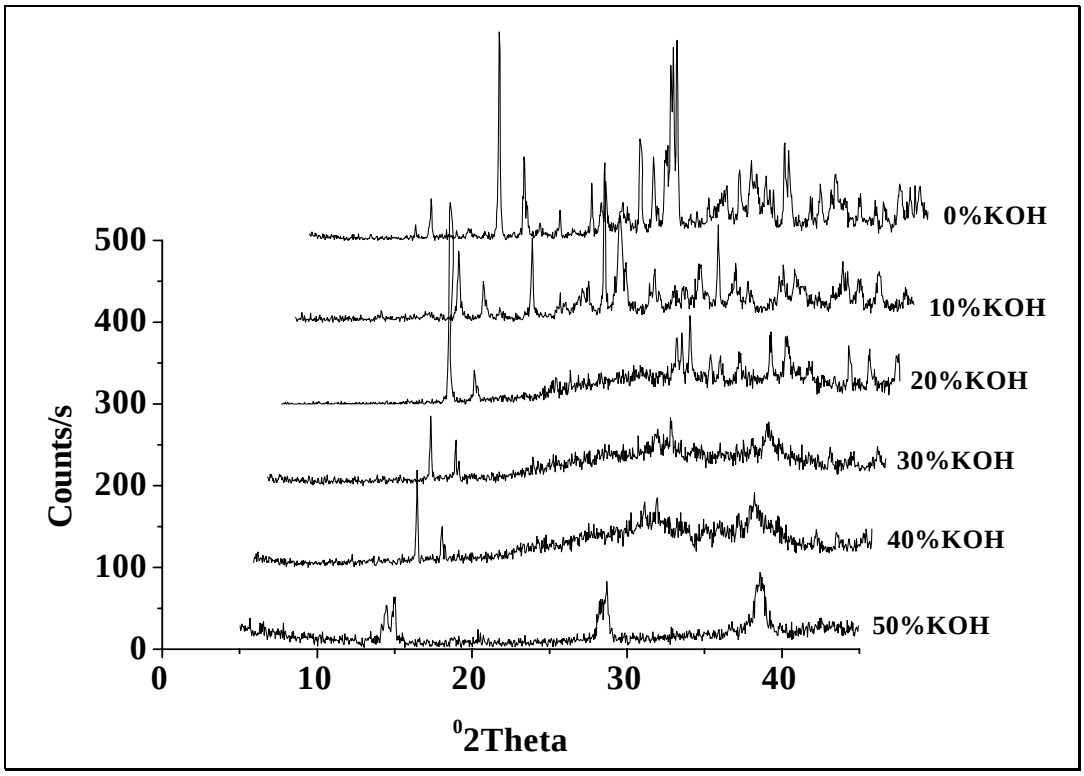

Figure 5.3. P–XRD patterns of KOH treated neutral alumina samples.

Table 5.1. Physico–chemical characterization of catalysts used

Catalyst Sample	Chemical Composition	% Crystallinity	Surface Area, m^2/g
Na–X	$Na_{88}Al_{88}Si_{104}O_{384}$	100	542
K–X	$K_{88}Al_{88}Si_{104}O_{384}$	91	496
Rb–X	$Rb_{84}Na_4Al_{88}Si_{104}O_{384}$	88	476
Cs–X	$Cs_{76}Na_{12}Al_{88}Si_{104}O_{384}$	62	245
HT(1.5)	$[Mg_{0.6}Al_{0.4}(OH)_2](CO_3)_{0.20}.0.84H_2O$	94	58
HT(2.0)	$[Mg_{0.67}Al_{0.33}(OH)_2](CO_3)_{0.165}.0.81H_2O$	100	62
HT(2.5)	$[Mg_{0.72}Al_{0.28}(OH)_2](CO_3)_{0.14}.0{\cdot}6H_2O$	88	67
HT(3.0)	$[Mg_{0.75}Al_{0.25}(OH)_2](CO_3)_{0.125}{\cdot}0.76H_2O$	77	69
HT(3.5)	$[Mg_{0.78}Al_{0.22}(OH)_2](CO_3)_{0.11}{\cdot}0.58H_2O$	72	75
Alumina	Al_2O_3	100	180
10 % KOH on Alumina	10 % KOH on Al_2O_3	88	132
20 % KOH on Alumina	20 % KOH on Al_2O_3	69	59
30 % KOH on Alumina	30 % KOH on Al_2O_3	47	32
50 % KOH on Alumina	50 % KOH on Al_2O_3	30	7

The P–XRD pattern of pure alumina shows the maximum crystallinity and is considered as 100% crystalline material for the comparison of crystallinity after impregnation of KOH (Figure 5.3). It was observed that the crystallinity of KOH impregnated alumina decreased significantly on increasing the amount of KOH. The alumina became almost amorphous after impregnation of 30% KOH on the surface of neutral alumina as shown in the P–XRD patterns.

P–XRD Patterns of As–Synthesized, Activated, Reconstructed and Activated Reconstructed Hydrotalcite Samples

The P–XRD patterns of as–synthesized [HT (3.5)], activated [HT (3.5)–A], reconstructed [HT (3.5)–R] and activated reconstructed hydrotalcite [HT (3.5)–AR] samples are shown in Figure 5.4. The P–XRD patterns of as–synthesized hydrotalcite showed sharp, intense and symmetric peaks at lower diffraction angles (2θ = 10–25°) and broad asymmetric reflections at higher diffraction angles (2θ = 30–50°), which are characteristics of highly crystalline layered structure.

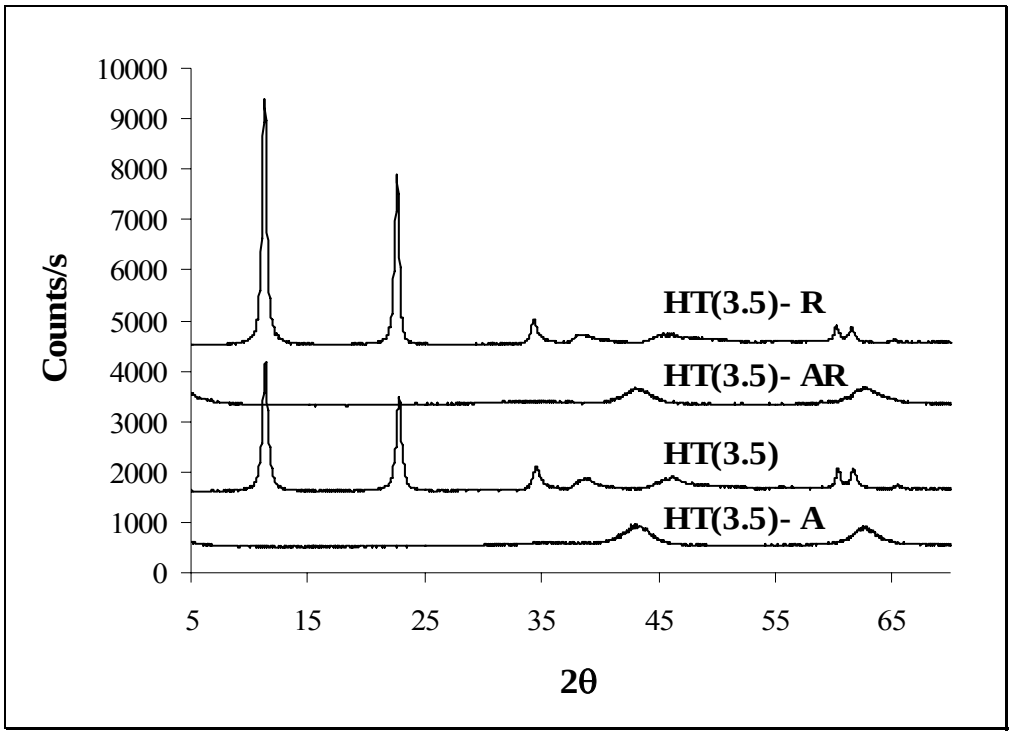

Figure 5.4. P–XRD patterns of as–synthesized [HT(3.5)], activated [HT(3.5)–A], reconstructed [HT(3.5)–R] and activated reconstructed [HT(3.5)–AR] hydrotalcite samples

The percentage crystallinity of hydrotalcite samples of Mg/Al molar ratio from 1.5 to 3.5 were calculated by comparing the summation of integral intensities of 003 (2θ = 10.5°) and 006 (2θ = 23.3°) planes and the sample having maximum intensity of above plane [HT (2.5)] was considered as a 100% crystalline sample. The crystallinity of hydrotalcite samples decreased with

increase in Mg/Al molar ratio. Decrease in the crystallinity on increasing the Mg/Al molar ratio of hydrotalcite samples is due to increase in amount of divalent cation (Mg^{2+}) [21]. The P–XRD patterns of activated hydrotalcite consisted of broadened peaks that can be assigned to a mixed oxide phase $Mg(Al)O_x$, with diffraction lines very similar to that of MgO. The original hydrotalcite structure was recovered via reconstruction (rehydration) of activated hydrotalcite in liquid phase using de–carbonated water under inert atmosphere. The Mg and Al coordination modes were restored completely to the original octahedral hydrotalcite structure [22]**.** The peak intensities of (003) and (006) planes of reconstructed hydrotalcite were observed to increase as compared to original hydrotalcite indicating the higher crystallinity of reconstructed samples. This may be attributed to the mechanical stirring effect during the liquid phase rehydration process. The P–XRD pattern of activated reconstructed hydrotalcite was observed to be similar to the activated hydrotalcite.

FT–IR Spectra of As–Synthesized, Activated, Reconstructed and Activated Reconstructed Hydrotalcite Samples

The FT–IR spectra of [HT (3.5)], [HT (3.5)–A], [HT (3.5)–R] and [HT (3.5)–AR] are shown in Figure 5.5. The absorption at 3450–3550 cm^{-1}, present in all hydrotalcite samples is due to H–bonding stretching vibrations of OH group in the brucite–like layer. Shoulder present around 3000 cm^{-1} is attributed to hydrogen bonding between water molecules and interlayer CO_3^{2-} anions. Appearance of the shoulder at 1650 cm^{-1} is the characteristic band of H_2O. The asymmetric stretching, ν_3, appears at around 1380 cm^{-1} could be assigned to interlayer carbonates, and confirms the formation of Mg–Al hydrotalcite with intercalated carbonate anions. The low frequency region showed bands at about 550, 790, 940 cm^{-1}, corresponding to the Al–OH and the band at 635 cm^{-1} is assigned to Mg–OH [21]. FT–IR of the calcined sample showed the disappearance of bands at 1650 cm^{-1} (water bending vibrations), and around 3000 cm^{-1} (interaction of H_2O–CO_3^{2-} in the interlayer). Intensity of the band at 3450–3550 cm^{-1} also decreases significantly due to the dehydroxylation which confirmed the removal of water molecules and hydroxyl groups from the interlayer space of hydrotalcite. The disappearance of vibration assigned to interlayer carbonates at around 1380 cm^{-1} was observed in the calcined hydrotalcite samples. The appearance of strong bands around 3550, 3000 and 1650 cm^{-1} in rehydrated samples confirmed the presence of significantly large amount of hydroxyl groups and water molecules. The FT–IR spectrum of the activated reconstructed hydrotalcite was observed to be similar to that of activated hydrotalcite.

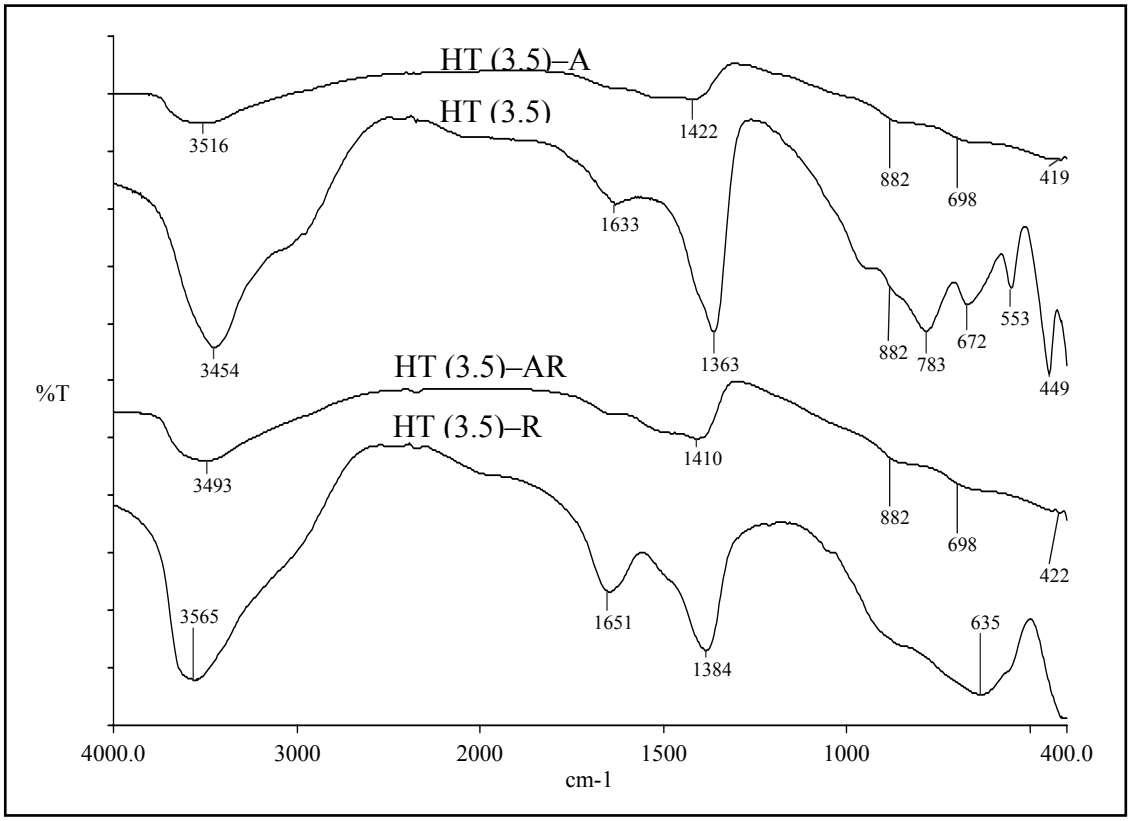

Figure 5.5. FT–IR spectra of as–synthesized [HT(3.5)], activated [HT(3.5)–A], reconstructed [HT(3.5)–R] and activated reconstructed [HT(3.5)–AR] hydrotalcite samples.

TGA of As–Synthesized, Activated, Reconstructed and Activated Reconstructed Hydrotalcite Samples

TGA curves of [HT (3.5)], [HT (3.5)–A], [HT (3.5)–R] and [HT (3.5)–AR] are shown in Figure 5.6. The TGA profiles are in good agreement with those available in the literature for hydrotalcite [8]. TGA of hydrotalcite showed two stages weight loss accompanied by an endothermal transformation. The first weight loss in as–synthesized hydrotalcite (12%) was observed between 200–220 °C due to the loss of interlayer water molecules, without collapse of the structure. This step is reversible [8]. The second weight loss (38%) was observed between 250–440 °C and is attributed to the removal of condensed water molecules (hydroxyl groups) and carbon dioxide from the carbonate anions present in the interlayers. The second weight loss usually appeared broad because of the simultaneous loss of condensed water molecules and carbon dioxide. Slightly higher weight loss observed in the reconstructed hydrotalcite as compared to as–synthesized hydrotalcite is due to increase of compensating OH^- anions and water molecules present in the interlayer space of reconstructed hydrotalcite. The [HT (3.5)–A] and [HT (3.5)–AR] also showed TGA patterns similar to that of [HT(3.5)]. Lower weight loss in the TGA of [HT (3.5)–A] and [HT (3.5)–AR] was observed as compared to the as–synthesized hydrotalcite.

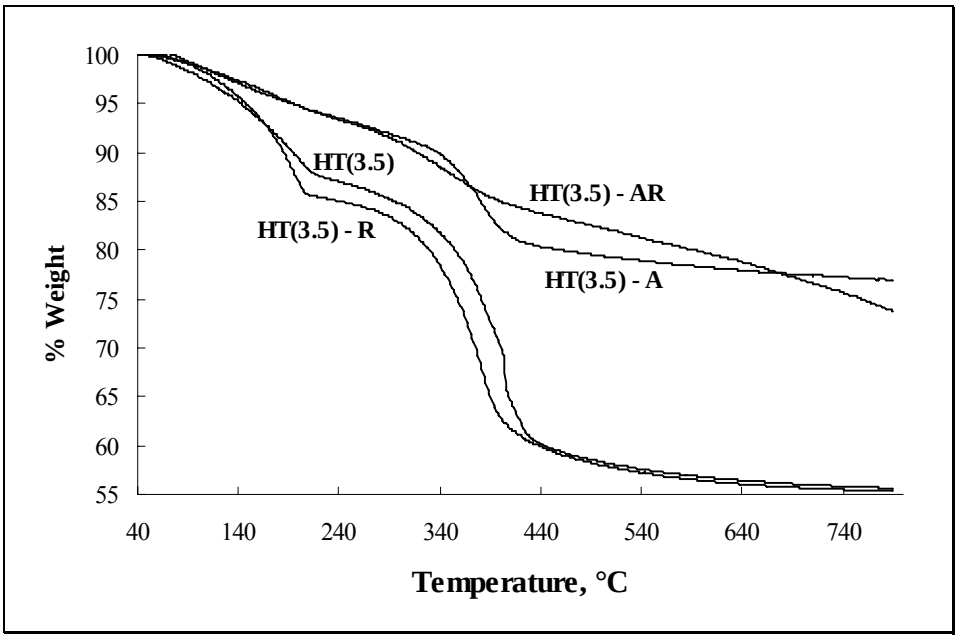

Figure 5.6. TGA of as–synthesized [HT(3.5)], activated [HT(3.5)–A], reconstructed [HT(3.5)–R] and activated reconstructed [HT(3.5)–AR] hydrotalcite samples.

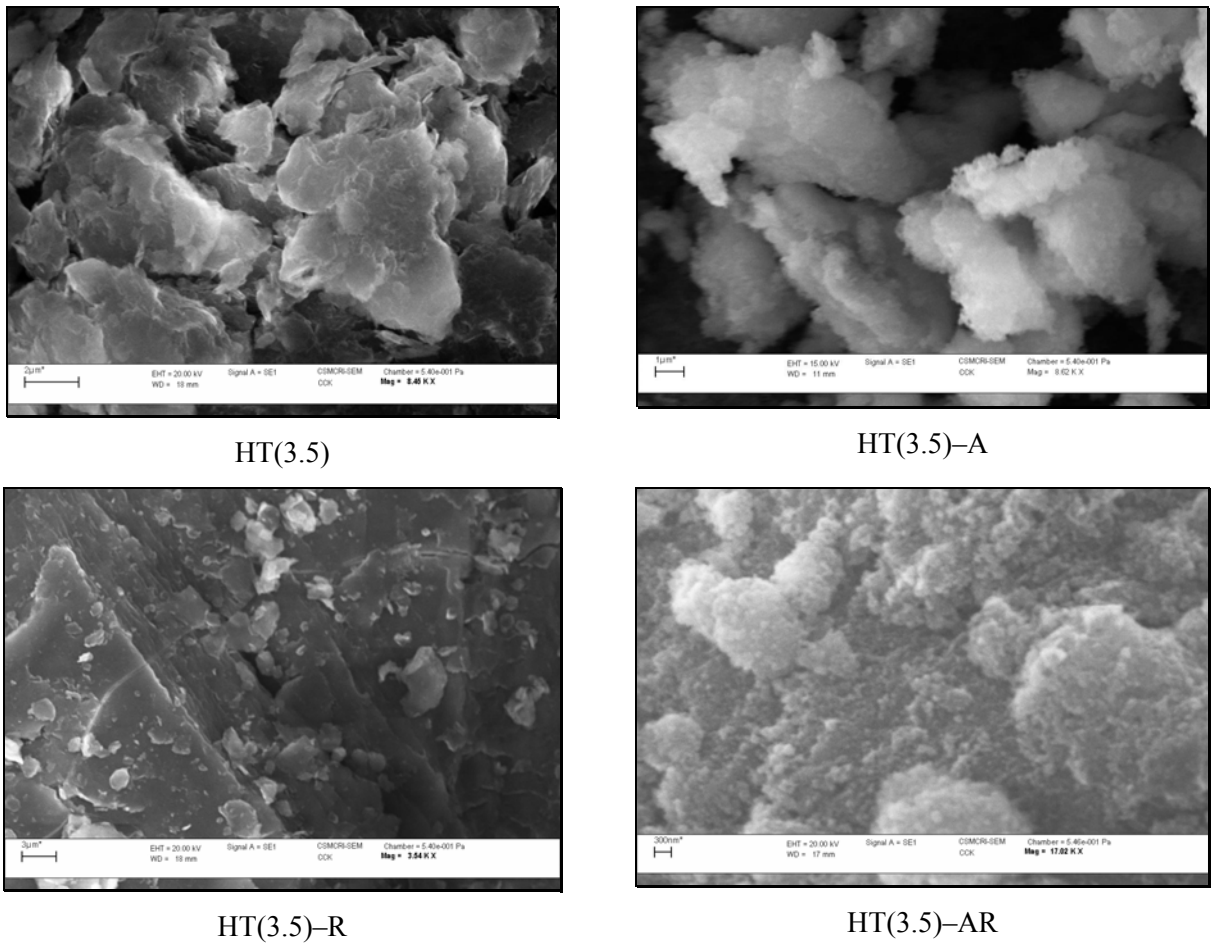

HT(3.5) HT(3.5)–A

HT(3.5)–R HT(3.5)–AR

Figure 5.7. SEM images of as–synthesized [HT(3.5)], activated [HT(3.5)–A], reconstructed [HT(3.5)–R] and activated reconstructed [HT(3.5)–AR] hydrotalcite samples.

SEM images of [HT(3.5)] and [HT(3.5)-A] are in shown in Figure 5.7. The micrographs of all hydrotalcites shows well developed layers with platelet structure. The morphology of Mg-Al mixed oxides obtained upon calcination seems to be similar to that of as-synthesized hydrotalcite.

5.3.2. Catalytic Activity for the Aldol Condensation of Propanal

Conversion of propanal varied from 22–42% with 92–94% selectivity of 2–methylpentenal using alkali ion–exchanged zeolites which are known to be weak bases without any thermal treatment or activation (Table 5.2, Entry 1–4). On activation of ion–exchanged zeolites at 450 °C for 4 h, the conversion of propanal decreased with increase in the selectivity of 2–methylpentenal (Table 5.2, Entry 5–8). Zeolite X has pore opening of 7.4 Å and pore cavity of 11.8 Å. The molecular dimensions of n–propanal and 2–methylpentenal are 4.6 and 6.7 Å, respectively, which are smaller than the pore opening diameter of zeolite. Therefore, the effect of microporosity was excluded in the present study. The results obtained using alkali ion–exchanged zeolites as catalysts indicate that the aldol condensation of propanal depend on the type of alkali metal ion trapped in the zeolite cage. Conversions obtained, follow the order Cs–X > Rb–X > K–X > Na–X which is in agreement with the order of basicity reported in the literature for these solids [24–25]. Overall basicity of the alkali ion–exchanged zeolites depends upon the nature of extra–framework cations and presence of polarizable cations. The cations such as cesium or rubidium resulted into more basic zeolites as compared to those formed by sodium or lithium exchange [26]**.** This is also supported by the calculation of average partial charge on oxygen atom using Sanderson electronegativity methods for the Cs–X, Rb–X, K–X, Na–X zeolite samples [27]. These were observed to be –0.45, –0.44, –0.43, –0.41, respectively, indicating the basicity order of zeolites as Cs–X > Rb–X > K–X > Na–X.

The aldol condensation of propanal was carried out using alumina based catalysts and the conversion of propanal was found to be 42% with 97% selectivity of 2–methylpentenal using neutral alumina without activation. The conversion increased upto 46% with neutral alumina activated at 450 °C for 4 h (Table 5.2, Entry 9–10). The conversion of propanal strongly depends on the amount of impregnated KOH on the neutral alumina (Table 5.2, Entry 11–14). It decreased significantly from 42 to 21% on impregnation of 10% KOH on the surface of neutral alumina. Conversion data for the alumina impregnated samples with different percentage of KOH showed that lower the KOH impregnation, higher is the conversion and selectivity for propanal condensation. The surface area of KOH impregnated alumina samples was observed to decrease significantly on increasing the amount of KOH (Table 5.1). This could be due to pore blocking of alumina on impregnation of KOH. The formation of potassium aluminate is also expected by the

reaction of alumina with KOH. The KOH molecules are expected to be well dispersed on alumina surface at lower impregnation. However, with increased KOH impregnation, the poor KOH dispersion and lower surface area was achieved [12], and hence, lower catalytic activity for aldol condensation of propanal was observed in the present study.

Table 5.2. Aldol condensation of propanal using various solid base catalysts

Run	Catalyst	Activation temp/time	% Conversion	% Selectivity [a]	
				2–Methyl pentenal	3–Hydroxy–2–methylpentanal
1	Cs–X	Without act.	42	94	6
2	Rb–X	Without act.	35	94	6
3	K–X	Without act.	27	95	5
4	Na–X	Without act.	22	92	8
5	Ce–X	450 °C/4 h	38	99	1
6	Rb–X	450 °C/4 h	30	98	2
7	K–X	450 °C/4 h	26	98	2
8	Na–X	450 °C/4 h	19	97	3
9	Alumina–Neutral	Without act.	42	97	3
10	Alumina–Neutral	450 °C/4 h	46	97	3
11	10 % KOH on Alumina	Without act.	21	98	2
12	20 % KOH on Alumina	Without act.	17	98	2
13	30 % KOH on Alumina	Without act.	15	97	3
14	50 % KOH on Alumina	Without act.	12	96	4

[a] **Reaction conditions:** propanal = 1.0 g, catalyst = 0.1 g, *n*–decane (internal standard) = 0.01 g, temperature = 100 °C, reaction time = 10 h.

The catalytic activity of the as–synthesized, activated, reconstructed and activated reconstructed hydrotalcite samples of Mg/Al molar ratio from 1.5 to 3.5 was evaluated for aldol condensation of propanal (Tables 5.3 and 5.4) at 100 °C reaction temperature for 10 h. The conversion of propanal was found to increase from 40 to 83% with increase in the Mg/Al ratio of as–synthesized hydrotalcite from 1.5 to 3.5 (Table 5.3, Entry 1–5). Selectivity of 2–methylpentenal was observed to increase from 48 to 86% on increasing Mg/Al ratio of as–synthesized hydrotalcite samples.

Table 5.3. Aldol condensation of propanal using as–synthesized and activated hydrotalcite samples of varied Mg/Al molar ratio from 1.5 to 3.5

Run	Catalyst	Activation Temp/Time	% Conversion	% Selectivity [a]		
				2–Methyl pentenal	3–Hydroxy–2–methylpentanal	3–Pentanone
1	HT (1.5)	Without act.	40	48	52	–
2	HT (2.0)	Without act.	45	52	48	–
3	HT (2.5)	Without act.	52	80	17	3
4	HT (3.0)	Without act.	58	83	15	2
5	HT (3.5)	Without act.	83	86	9	5
6*	Ni–Mg–Al	Without act.	66	98	–	2
7	HT (1.5)	450 °C/4 h	44	68	30	2
8	HT (2.0)	450 °C/4 h	47	83	17	–
9	HT (2.5)	450 °C/4 h	80	92	8	–
10	HT (3.0)	450 °C/4 h	86	96	4	–
11	HT (3.5)	450 °C/4 h	97	99	–	1
12*	Ni–Mg–Al	450 °C/4 h	90	97	2	1

[a] **Reaction conditions:** propanal = 1.0 g, catalyst = 0.1 g, *n*–decane (internal standard) = 0.01 g, temperature = 100 °C, reaction time = 10 h. *Mg/Al = 3.0.

The conversion and selectivity of aldehyde increased significantly on activation of as–synthesized hydrotalcite at 450 °C for 4 h under identical reaction conditions (Table 5.3, Entry 7–11). The maximum conversion of propanal was observed to be 83% with 86% selectivity of 2–methylpentenal in case of as–synthesized hydrotalcite of Mg/Al molar ratio 3.5, which increased up to 97% with 99% selectivity of 2–methylpentenal using activated hydrotalcite (Mg/Al = 3.5) as a catalyst. The Ni–Mg–Al was also observed to be more effective catalyst for aldol condensation of propanal as compared to the binary hydrotalcite of Mg/Al molar ratio 3.0. 66% conversion of propanal with 98% selectivity of 2–methylpentenal was observed in reaction catalyzed by as–synthesized Ni–Mg–Al hydrotalcite (Table 5.3, Entry 6). However, conversion of propanal increased upto 90% with 97% selectivity of 2–methylpentenal using Ni–Mg–Al hydrotalcite sample activated at 450 °C for 4 h (Table 5.3, Entry 12).

For any base catalyzed reaction, catalytic activity depends upon total base strength required to activate the particular reactant molecule. Increase in the conversion of propanal and selectivity of 2–methylpentenal on increasing Mg–content (Mg/Al molar ratio) in hydrotalcite is explained in terms of increased basicity of [HT] which aids aldol condensation reaction. The basicity of hydrotalcite is mainly due to their hydroxyl functions and it can be adjusted by either changing the Mg/Al molar ratio in the brucite like sheets or selection of suitable anion in the interlayer space. The most active basic sites for aldol condensation are available on the surface of hydrotalcite. In the present study, observed increase in conversion of propanal and selectivity of 2–methylpentenal on increasing the Mg/Al molar ratio of hydrotalcite samples is due to increment in basic character of hydrotalcite as discussed above. Two types of basic sites are identified in hydrotalcite, one weaker Brønsted OH^- and second, stronger Lewis O^{2-} sites [8]. At 450 °C, as–synthesized hydrotalcite converts into well dispersed mixture of magnesium and aluminium mixed oxides with high surface area, strong Lewis basic sites (O^{2-} anions) and weakly basic sites (OH^- groups) on the surface [28]. Activated hydrotalcite has more Lewis basic sites as compared to Brønsted basic sites. Activated hydrotalcite is more basic as compared to the as–synthesized and reconstructed hydrotalcite samples, both in terms of basic strength and number of basic sites [29]. Basic properties of calcined hydrotalcite also strongly depend upon the Mg/Al molar ratio, increasing Al content in activated hydrotalcite resulted into decrease in total number of basic sites [30]. Thus, higher Mg/Al molar ratio in the activated hydrotalcite gives the higher basicity and enhanced catalytic activity. The active sites for aldol condensation in activated hydrotalcite samples [Mg(Al)O] are – weakly basic sites (hydroxide groups), medium–strong sites connected to the oxygen of O^{2-}–Mg^{2+} acid–base pairs and strong basic sites (O^{2-} anions on surface) [31–32]. The O^{2-}–Mg^{2+} acid–base pairs and isolated O^{2-} anions sites are highly efficient for aldol condensation reactions [33–34]. The overall numbers of these basic sites are not influenced significantly by the Mg/Al molar ratio of hydrotalcite samples. However, fraction of strong and medium–strong sites increases with increasing Mg/Al molar ratio and calcination temperature [35]. In view of the higher conversion and selectivity for propanal condensation using activated hydrotalcite as a catalyst, the basicity of activated hydrotalcite samples of Mg/Al ratio 1.5, 2.5 and 3.5 was evaluated by isomerization of β–isophorone to α–isophorone as a model test reaction reported for basicity measurement (Scheme 5.2) [13]. The initial rate of reaction was observed to increase on increasing Mg/Al molar ratio of hydrotalcite (Figure 5.8). Initial rate of reaction was calculated as 37 x 10^{-4} mol/(g_{cat} sec) for activated hydrotalcite of Mg/Al molar ratio 1.5 and increased to 48 x 10^{-4} mol/(g_{cat} sec) for Mg/Al molar ratio 3.5. The initial rate of the reaction for isophorone isomerization is reproducible within ± 6% variation. The β–isophorone to α–isophorone is a zero order reaction; hence, the value of initial rate of reaction is equal to the rate constant. The value of

rate constant for isophorone isomerization is proportional to the number basic sites [13]. The increasing Al content in the activated hydrotalcite resulted into decrease in total number of basic sites. Thus, higher Mg/Al molar ratio in the activated hydrotalcite gives the higher basicity and maximum catalytic activity.

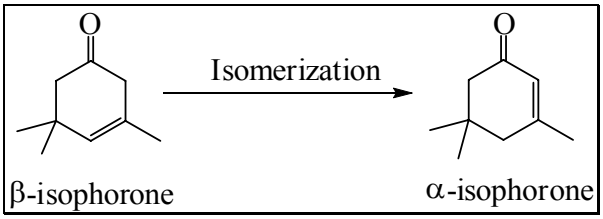

Scheme 5.2. Isomerization of β–isophorone to α–isophorone as a model test reaction for basicity measurement.

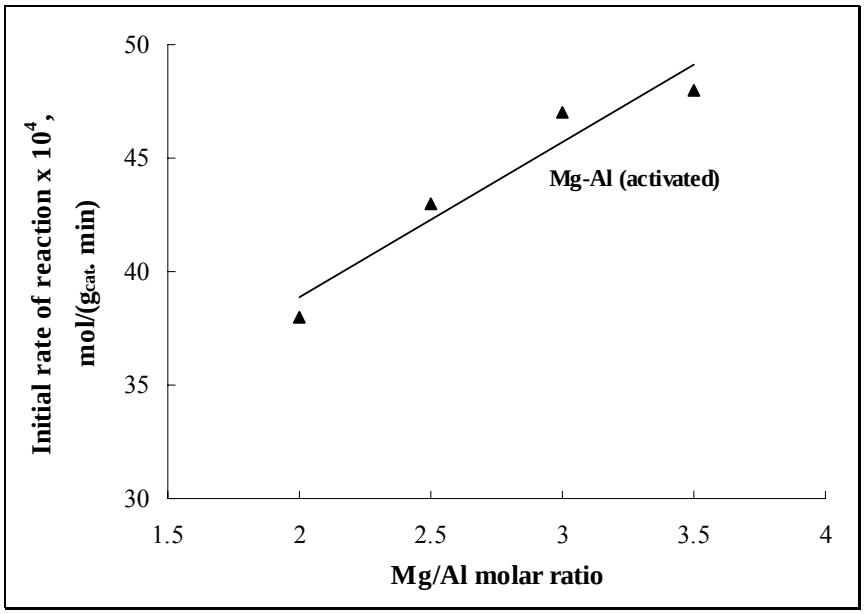

Figure 5.8. Initial rate of reaction for isomerization of β–isophorone to α–isophorone as a model test reaction for basicity measurements of hydrotalcite samples

Catalytic activity of the reconstructed and activated reconstructed hydrotalcite samples of Mg/Al molar ratio 1.5 to 3.5 was evaluated for aldol condensation of propanal under reaction conditions similar to those used for as–synthesized hydrotalcite samples. The conversion and selectivity data are presented in Table 5.4. Higher propanal conversion with greater selectivity for 2–methylpentenal was observed in case of reconstructed hydrotalcite catalyzed condensation as compared to as–synthesized hydrotalcite. However, significant changes in the conversion and selectivity were not observed in case of activated reconstructed hydrotalcite as compared to the activated hydrotalcite under identical reaction conditions. The conversion of propanal was observed to increase from 47 to 92% with 68 to 95% selectivity of 2–methylpentenal using

reconstructed hydrotalcite samples of Mg/Al molar ratio from 1.5 to 3.5 as catalyst (Table 5.4, Entry 1–5). The conversion was observed to increase upto 96% with 97% selectivity of 2–methylpentenal using activated reconstructed hydrotalcite of Mg/Al molar ratio of 3.5 (Table 5.4, Entry 6–10).

Table 5.4. Aldol condensation of propanal using reconstructed and activated reconstructed hydrotalcite samples of varied Mg/Al molar ratio from 1.5 to 3.5

Run	Catalyst	Activation Temp/Time	% Conversion	% Selectivity [a]		
				2–Methyl pentenal	3–Hydroxy–2–methylpentanal	3–Pentanone
1	HT (1.5)	Without act.	47	68	28	4
2	HT (2.0)	Without act.	55	83	14	3
3	HT (2.5)	Without act.	60	90	8	2
4	HT (3.0)	Without act.	73	93	4	3
5	HT (3.5)	Without act.	92	95	3	2
6	HT (1.5)	450 °C/4 h	51	72	26	2
7	HT (2.0)	450 °C/4 h	59	88	11	1
8	HT (2.5)	450 °C/4 h	77	94	5	1
9	HT (3.0)	450 °C/4 h	88	95	4	1
10	HT (3.5)	450 °C/4 h	96	97	3	–

[a] **Reaction conditions:** propanal = 1.0 g, catalyst = 0.1g, *n*–decane (internal standard) = 0.01 g, temperature = 100 °C, reaction time = 10 h.

When calcined hydrotalcite is stirred with decarbonated water under inert atmosphere, restoration of the original layered structure with mainly OH^- ions in the interlayer space takes place due to 'memory effect', yielding a highly active solid base catalyst for liquid phase aldol condensation reactions. Higher catalytic activity of the reconstructed hydrotalcite as compared to the as–synthesized hydrotalcite is due to the presence of higher numbers of Brønsted basic sites (OH^- groups), which are active towards aldol condensation of aldehydes in liquid phase. Stronger basicity of the reconstructed hydrotalcite is very well known as compared to the well ordered hydrotalcite structure obtained by ion–exchange process [36].

Among the studied alkali ion–exchanged zeolites, alumina and KOH impregnated alumina, as–synthesized, activated, reconstructed and activated reconstructed hydrotalcite samples, the best

conversion and selectivity were obtained using activated hydrotalcite for aldol condensation of propanal. Therefore, further studies for aldol condensation of propanal were carried out using activated hydrotalcite of Mg/Al molar ratio of 3.5 as a catalyst. The effect of reactant to catalyst ratio and temperature on the conversion of propanal, selectivity of 2–methylpentenal and rate of condensation reaction were studied in detail.

5.3.3. Effect of Amount of Catalyst on Conversion of Propanal, Selectivity of 2–Methylpentenal and Initial Rate of Reaction

The effect of amount of catalyst on conversion of propanal, selectivity of 2–methylpentenal and rate of reaction was studied by varying the amount of catalyst at constant amount of propanal at 100 °C reaction temperature. At lower amount of catalyst, the lower conversion of propanal was observed (Table 5.5). For example, at 0.02 g catalyst amount, 40% conversion of propanal was obtained, which increased upto 63% on increasing the amount of catalyst to 0.05 g. However, further increase in the catalyst amount to 0.1 g, the conversion of propanal increased upto 97%. Conversion of propanal was found to be independent on further increase in the amount of catalyst. The selectivity of the 2–methylpentenal also followed the similar trend. Highest selectivity (100%) of 2–methylpentenal was observed in the range of 0.1 to 0.2 g catalyst amount.

Table 5.5. Effect of reactant to catalyst ratio (by weight) on the conversion and selectivity for propanal condensation

Run	Catalyst, mg	% Conversion	% Selectivity [a]		
			2–Methylpentenal	3–Hydroxy–2–methylpentanal	3–Pentanone
1	0.02	40	73	27	–
2	0.04	51	82	18	–
3	0.05	63	85	15	–
4	0.07	85	88	10	2
5	0.08	96	96	2	2
6	0.10	97	99	–	1
7	0.13	97	100	–	–
8	0.20	97	100	–	–

[a] **Reaction conditions:** propanal = 1.0 g, *n*–decane (internal standard) = 0.01 g, temperature = 100 °C, time = 10 h.

Effect of reaction time on the conversion of propanal at different reactant to catalyst ratio is shown in Figure 5.9a. It was observed that the conversion of propanal decreased from 85% at ratio 5 within 60 min to 40% on increasing the reactant to catalyst ratio to 12. The 20% conversion of propanal was obtained within 60 min at reactant to catalyst ratio 15, similar propanal conversion was found within 10 min reaction time at reactant to catalyst ratio 5.

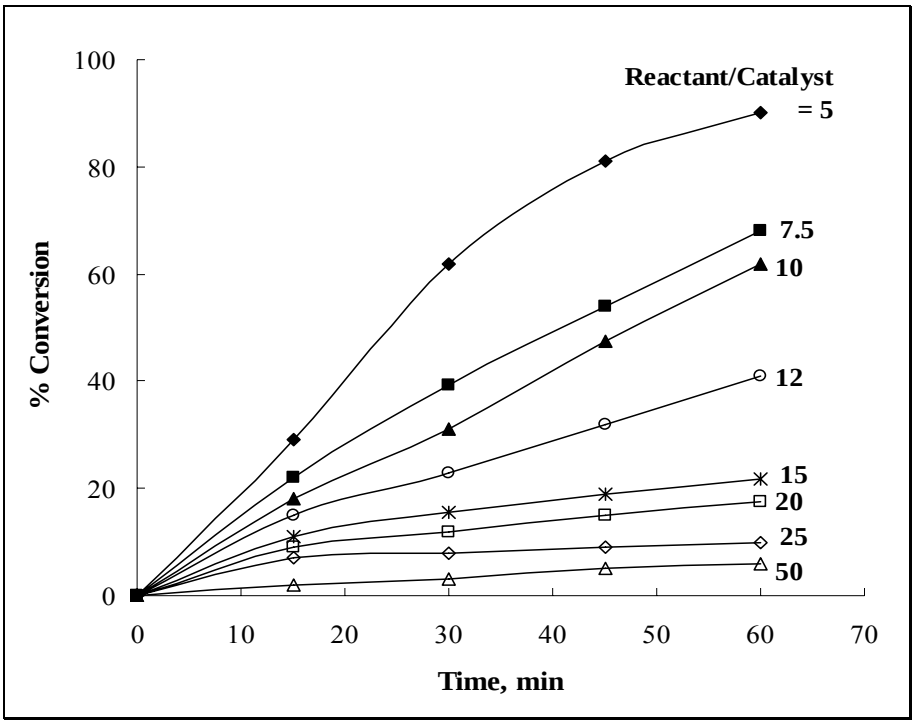

Figure 5.9a. Effect of reactant to catalyst ratio on conversion with respect to time.

Effect of catalyst amount on initial rate of reaction is shown in Figure 5.9b. The amount of catalyst was varied from 0.02 to 2 g to study its effect on initial rate of reaction. The initial rate of reaction was observed to increase on increasing the amount of catalyst. Initially, the rate of reaction was calculated as 17 x 10^{-4} mol/(g_{cat} sec) at 0.02 g catalyst. The rate of reaction increased linearly upto 0.1 g amount of catalyst. On further increase in the amount of catalyst upto 2 g, slight increase in the initial rate of reaction was observed. This indicates that the reaction is in kinetic region at 0.1 g of catalyst amount where mass transfer resistance can be neglected. Higher conversion and initial rate of reaction at higher amount of catalyst is due to the availability of sufficient amount of strong basic sites on the surface of activated hydrotalcite to catalyze the reaction. As the amount of catalyst decreases, the total number of active basic sites present for condensation reaction on the surface of catalyst also decrease and hence lower catalytic activity was observed at lower amount of catalyst. Another possible reason for lower activity of the catalyst is strong adsorption of reactant molecules on the surface of activated hydrotalcite at lower amount of catalyst, this could block the active basic sites present on the surface of catalyst for condensation reaction.

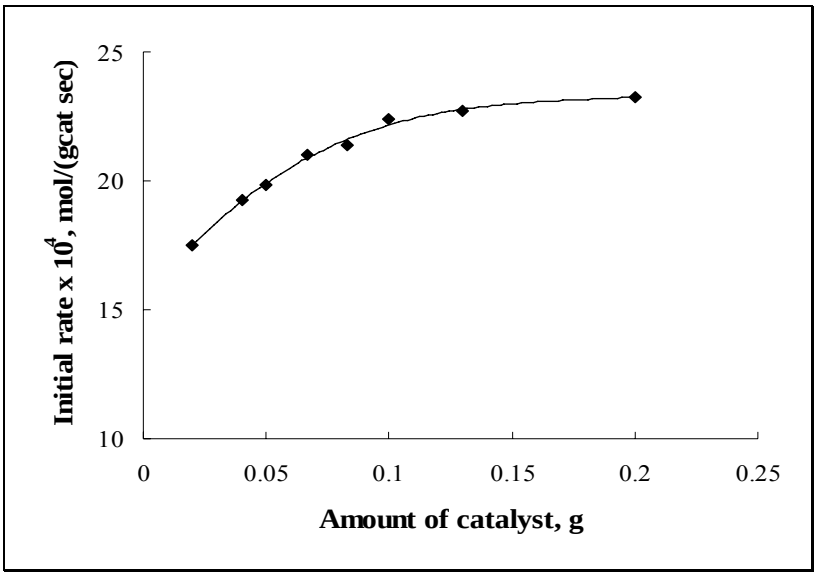

Figure 5.9b. Effect of amount of catalyst on initial rate of reaction.

5.3.4. Effect of Temperature on Conversion of Propanal, Selectivity of 2–Methylpentenal and Initial Rate of Reaction

The effect of temperature on aldol condensation of propanal was studied by varying the reaction temperature from 45 to 100 °C at constant amount of propanal (5 g) and 0.5 g activated hydrotalcite of Mg/Al molar ratio of 3.5 as a catalyst (Table 5.6). The higher conversion of propanal (97%) with 99% selectivity of 2–methylpentenal was observed at 100 °C.

Table 5.6. Effect of reaction temperature on the conversion and selectivity for aldol condensation of propanal

Run	T °C	% Conversion	% Selectivity [a]		
			2–Methylpentenal	3–Hydroxy–2–methylpentanal	3–Pentanone
1	45	43	69	31	–
2	50	56	78	22	–
3	60	60	84	14	2
4	70	77	85	13	2
5	80	81	88	9	3
6	90	95	93	4	3
7	100	97	99	–	1

[a]**Reaction conditions:** *n*–decane (internal standard) = 0.01 g, time = 10 h.

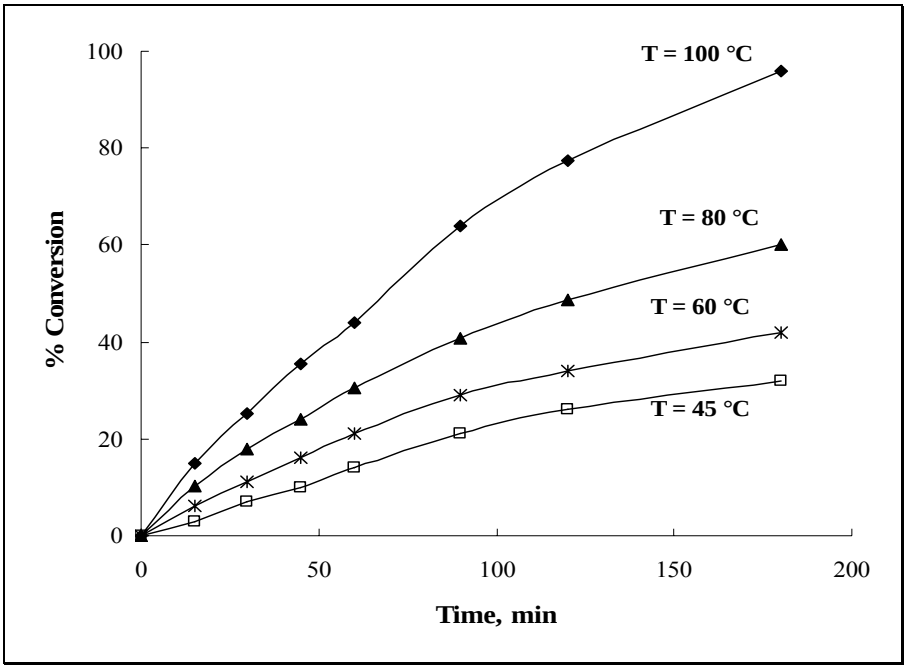

Figure 5.10a. Effect of reaction temperature on conversion with respect to time.

The reaction kinetic was also observed to be significantly influenced by the reaction temperature (Figure 5.10a). The effect of reaction temperature on initial rate of reaction is shown in the Figure 5.10b. The initial rate of reaction was found to increase linearly with increase in the reaction temperature. The initial rate of reaction was calculated as 3.7 x 10^{-4} mol/(g_{cat} sec) at 45 °C, which increased upto 16.4 x 10^{-4} mol/(g_{cat} sec) at 80 °C. On further increasing the temperature to 100 °C, the rate of reaction increased to 22.5 x 10^{-4} mol/(g_{cat} sec).

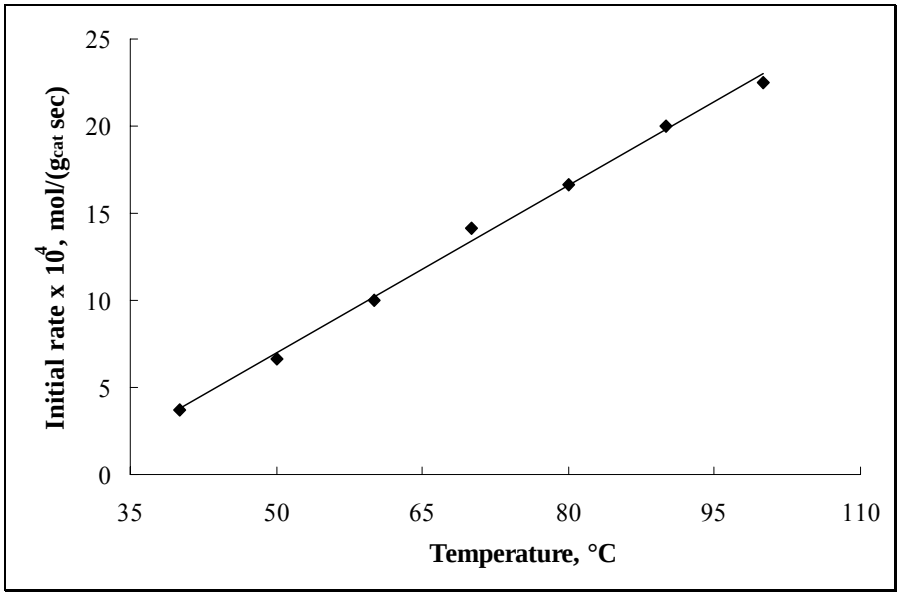

Figure 5.10b. Effect of reaction temperature on initial rate of reaction.

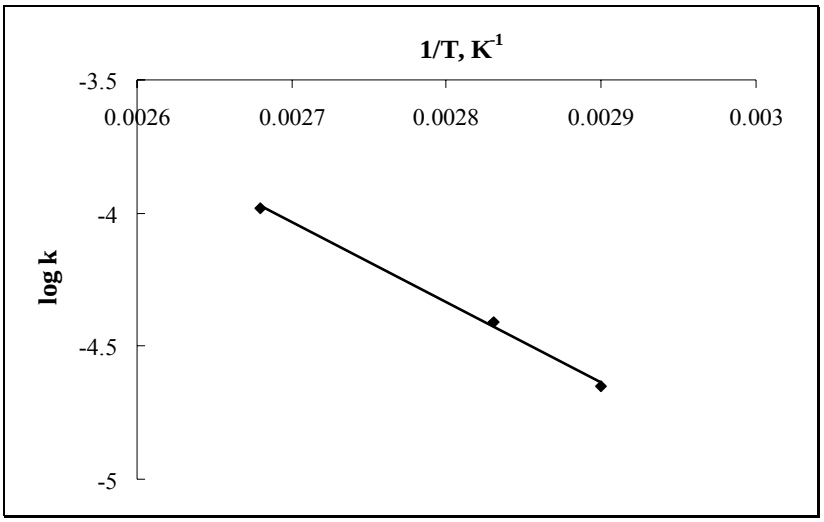

Figure 5.10c. Arrhenius plot.

The activation energy for propanal condensation was calculated by plotting ln k *vs* 1/T (Arrhenius plot, Figure 5.10c) and was found to be 58 kJ/mol. Calculated activation energy in the present study was not observed in the range of 8 to 25 kJ/mol, which again indicates that the reaction is far away from the diffusional (mass transfer) limitations. Low activity of the catalyst for aldol condensation of propanal at lower temperature is due to the strong adsorption of propanal molecules on the surface of catalyst [37]. Therefore, high temperature is required to avoid this undesirable adsorption which leads to decreased catalytic activity.

5.3.5. Reusability of Catalyst

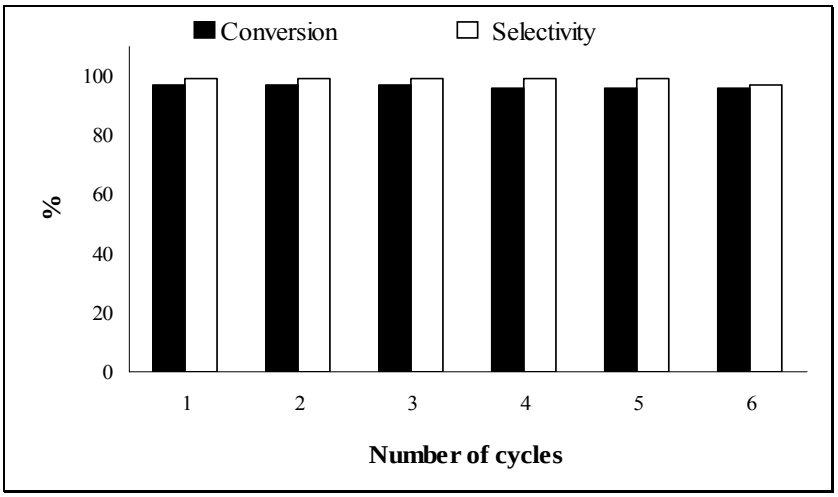

Figure 5.11. Reusability of the catalyst.

The spent catalyst was regenerated in air flow at 450 °C for 4 h. The regenerated catalyst was used for aldol condensation of propanal under reaction conditions similar to those used for activated hydrotalcite of Mg/Al molar ratio of 3.5. From the data on conversion of propanal and

selectivity of 2–methylpentenal given in Figure 5.11, it is observed that the catalyst was reusable upto six cycles without any significant loss in its activity for aldol condensation of propanal.

5.3.6. Tentative Reaction Mechanism

Tentative reaction mechanism for aldol condensation of propanal catalyzed by hydrotalcite is proposed as shown in Scheme 5.3. Aldol condensation of propanal is a three steps reaction. The OH^- species present on the surface of hydrotalcite abstracts an acidic proton from α–carbon of propanal (**I**) in the first step to form a stabilized enolate (**II**).

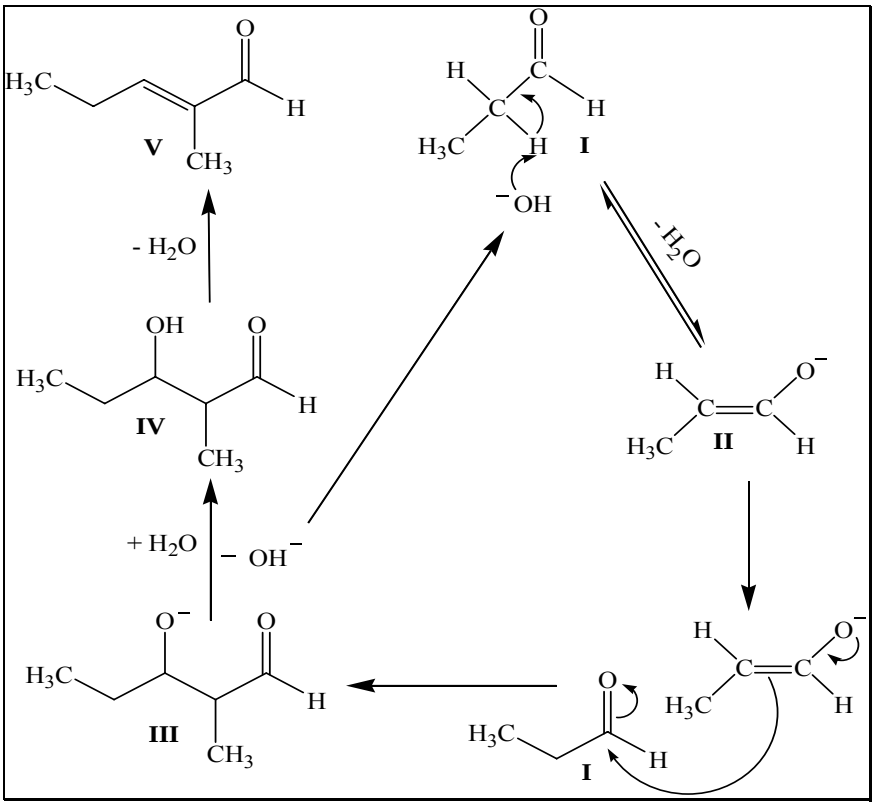

Scheme 5.3. Proposed reaction mechanism for aldol condensation of propanal using hydrotalcite as a solid base catalyst.

In the second step, formation of 2–methyl–1–oxo–pentan–3–ol anion (**III**) takes place by the nucleophilic addition of α–carbon of enolate anion to the carbonyl group of another propanal. The resulting 2–methyl–1–oxo–pentan–3–ol anion (**III**) reacts with water to form the product of aldol addition (**IV**; 3–hydroxy–2–methyl–pentanal) and release the OH^- species. Dehydration of 3–hydroxy–2–methyl–pentanal (**IV**) to 2–methylpentenal (**V**) i.e. α, β unsaturated aldehyde occurs in the third step. The species OH^- present on the hydrotalcite surface efficiently acts as Brønsted basic sites in the presence of water and provides a highly hydrophilic environment for aldol condensation of propanal [38].

5.4. Conclusions

The higher conversion of propanal was observed using hydrotalcite as a solid base catalyst among the various studied solid base catalysts namely, alkali ion–exchanged zeolites, alumina, alkali treated alumina and hydrotalcite of varied Mg/Al molar ratio. The conversion of propanal and selectivity of 2–methylpentenal increased with increasing Mg/Al molar ratio of hydrotalcite. 97% conversion of propanal with 99% selectivity of 2–methylpentenal was achieved using activated hydrotalcite of Mg/Al molar ratio 3.5. The basicity of activated hydrotalcite of Mg/Al ratio 1.5, 2.5 and 3.5 was evaluated by isomerization of β–isophorone to α–isophorone as a model test reaction reported for basicity measurements. From the kinetic data for aldol condensation of propanal using activated hydrotalcite (Mg/Al molar ratio 3.5), the initial rate of reaction was observed to increase on increasing the amount of catalyst. The reaction kinetics was also observed to be significantly influenced by the reaction temperature. The activation energy for propanal condensation was calculated by Arrhenius plot and found to be 58 kJ/mol. The catalyst was recycled upto six cycles without any significant loss in its activity for aldol condensation of propanal.

5.5. References

[1] A.D. Godwin, R.H. Schlosberg, F. Hershkowitz, M.G. Matturro, G. Kiss, K.C. Nadler, P.L. Buess, R.C. Miller, P.W. Allen, H.W. Deckman, R. Caers, E.J. Mozeleski, R.P. Reynolds, US Patent, 6307093 B1 (2001).

[2] W. Schoenlebe, H. Hoffmann, W. Lengsfeld, DE Patent, 2727330 (1979).

[3] P.Y. Blanc, A.Perret, F. Teppa, Helv. Chim. Acta 47 (1964) 567.

[4] C.P. Mehnert, N.C. Dispenziere, R.A. Cook, Chem. Commun. (2002) 1610–1611.

[5] K. Matsui, H. Kawanami, Y. Ikushima, H. Hayashi, Chem Commun. (2003) 2502–2503.

[6] F.M. Scheidt, J. Catal. 3 (1964) 372–378.

[7] S.P. Tang, H.Q. Li, D.L. Yin, Hunan Shifan Daxue Ziran Kexue Xuebao 24 (2001) 42.

[8] F. Cavani, F. Trifiro, A. Vaccari, Catal. Today 11 (1991) 173–301.

[9] G.J. Kelly, F. King, M. Kett, Green Chem. 4 (2002) 392–399.

[10] J. Weitkamp, M. Hunger, U. Rymsa, Micropor. Mesopor. Mater. 48 (2001) 255–270.

[11] J.C.A.A. Roelofs; D.J. Lensveld, A.J. van Dillen, K.P. de Jong, J. Catal. 203 (2001) 184–191.

[12] V.K. Srivastava, H.C. Bajaj, R.V. Jasra, Catal. Commun. 4 (2003) 543–548.

[13] F. Figueras, J. Lopez, J.S. Valente, T.T. H. Vu, J.M. Clacens, J. Palomeque, J. Catal. 211 (2002) 144–149; J.S. Valente, F. Figueras, M. Gravelle, J. Lopez, J.P. Besse, J. Catal. 189 (2000) 370–381.

[14] M. A. Ulibarri, I. Pavlovic, C. Barriga M.C. Hermosin, Appl. Clay Sci. 18 (2001) 17–27.

[15] D. Carriazo, C. Martin, V. Rives, A. Popescu, B. Cojocaru, I. Mandache, V.I. Parvulescu, Micropor. Mesopor. Mater. 95 (2006) 39–47.

[16] D. Tichit, B. Coq, S. Cerneaux, R. Durand, Catal. Today 75 (2002) 197–202; C.A. Hamilton, S.D. Jackson, G.J. Kelly, Appl. Catal. A: Gen. 263 (2004) 63–70.

[17] D. Tichit, M.J. M. Ortiz, D. Francová, C. Gérardin, B. Coq, R. Durand, F. Prinetto, G. Ghiotti, Appl. Catal. A: Gen. 318 (2007) 170–177; P. Kuśtrowski, D. Sułkowska, L. Chmielarz, R. Dziembaj, Appl. Catal. A: Gen. 302 (2006) 317–324.

[18] D. Tichit, D. Lutic, B. Coq, R. Durand, R. Teissier, J. Catal. 219 (2003) 167–175.

[19] J. Sebastian, K.M. Jinka, R.V. Jasra, J. Catal. 244 (2006) 208–218.

[20] S.K. Sharma, V.K. Srivastava, R.V. Jasra, J. Mol. Catal. A: Chem. 245 (2005) 200–209.

[21] P. Kustrowski, D. Sulkowska, L. Chmielarz, A.R. Lasocha, B. Dudek, R. Dziembaj, Micropor. Mesopor. Mater. 78 (2005) 11–22.

[22] J.A. van Bokhoven, J.C.A.A Roelofs, K.P. de Jong, D.C. Koningsberger, Chem. Eur. J. 7 (2001) 1258–1265.

[23] S. Abello, F. Medina, D. Tichit, J.P. Ramirez, J.C. Groen, J.E. Sueiras, P. Salagre Y. Cesteros, Chem. Eur. J. 11 (2005) 728–739.

[24] L. Yang, Y. Aizhen, X. Qinhua, Appl. Catal. 67 (1991) 169–177.

[25] M. Huang, S. Kaliaguine, A. Auroux, Stud. Surf. Sci. Catal. 97 (1995) 31.

[26] M.F. Ciraolo, J.C. Hanson, C.P. Grey, Micropor. Mesopor. Mater. 49 (2001) 111–124.

[27] R.T. Sanderson, Chemical Bonds and Bond Energy, Academic Press, New York, (1976) p. 218.

[28] J.I. Di Cosimo, V.K. Díez, M. Xu, E. Iglesia, C.R. Apesteguía, J. Catal. 178 (1998) 499–510.

[29] K. K. Rao, M. Gravelle, J.S. Valente, F. Figueras, J. Catal. 173 (1998) 115–121.

[30] T. Nakatsuka, H. Kawasaki, S. Yamashita, S. Kohijiya, Bull. Chem. Soc. Jpn. 52 (1979)

2449–2450.

[31] W.T. Reichle, S.Y. Kang, D.S. Everhardt, J. Catal. 101 (1986) 352–359.

[32] D. Tichit, C. Gerardin, R. Durand, B. Coq, Top. Catal. 39 (2006) 89–96.

[33] A. Corma, V. Forncs, R.M.M. Aranda, J. Catal. 134 (1992) 58–65.

[34] D. Tichit, M. Lhouty, A. Guida, B. Chiche, F. Figueras, A. Auroux, D. Bartalini, E. Garrone, J. Catal. 151 (1995) 50–59.

[35] M.J. Climent, A. Corma, S. Iborra, J. Primo, J. Catal. 151 (1995) 60–66.

[36] D. Tichit, B. Coq, Cattech 7 (2003) 206–217.

[37] M.J. Climent, A. Corma, S. Iborra, A. Velty, Green Chem. 4 (2002) 474–480.

[38] K. Ebitani, K. Motokura, K. Mori, T. Mizugaki, K. Kaneda, J. Org. Chem. 71 (2006) 5440–5447.

Chapter 6

Eco–Friendly Synthesis of Jasminaldehyde by Condensation of 1–Heptanal with Benzaldehyde using Hydrotalcite as a Solid Base Catalyst

6.1. Introduction

Jasminaldehyde or α–pentylcinnamaldehyde is a perfumery chemical of commercial interest and is synthesized by the condensation of 1–heptanal with benzaldehyde in the presence of liquid alkali like, NaOH or KOH taken in more than stoichiometric amounts as a homogeneous catalyst [1]. The main drawbacks of homogeneous process for synthesis of jasminaldehyde include lack of reusability of the catalyst, hazardous nature of liquid base like KOH or NaOH and post reaction work–up of spent liquid bases. Therefore, it is desirable to develop suitable solid base catalysts, which would overcome these disadvantages and provide a commercial process having easy handling of the catalyst, easy separation of products, decreased corrosion of the reactors and vessels, possible regeneration and re–use of the catalyst. The applicability of various solid acid and base catalysts has been reported for the synthesis of jasminaldehyde in the literature [1–8]. Corma et al. reported the applicability of large pore HY and beta zeolites, mesoporous MCM–41 aluminosilicates (Al–MCM–41) and amorphous aluminophosphate (ALPO) as solid acid catalysts for the synthesis of jasminaldehyde [2–4]. These processes involve two steps. The heptanal dimethyl acetal is formed in the first step by reaction of 1–heptanal with excess methanol. In the second step, methanol is distilled in vacuum and benzaldehyde is added to the formed heptanal dimethyl acetal followed by heating of the system at desired temperature for synthesis of jasminaldehyde. With ALPO as a catalyst, 96% conversion of 1–heptanal with 86% selectivity of jasminaldehyde was achieved by varying the benzaldehyde to 1–heptanal molar ratio from 1 to 10 [2–4]. In another study, Al–MCM–41 supported magnesium oxide was used as a solid base catalyst and 31% conversion of 1–heptanal with 40% selectivity of jasminaldehyde was found in 2 h reaction time at 150 °C and benzaldehyde to heptanal molar ratio 10 [5]. Jaenicke et al. reported 90% conversion of 1–heptanal and 50% selectivity of jasminaldehyde for MCM–41 based hybrid materials as catalysts in a batch reactor at 160 °C with benzaldehyde to 1–heptanal molar ratio 1.5 [6]. The selectivity of jasminaldehyde is very important in the condensation of 1–heptanal with benzaldehyde. 2–n–Pentyl–2–nonenal is a major by–product of this reaction, which is also a base catalyzed product formed by aldol condensation of 1–heptanal. The selectivity of jasminaldehyde can be enhanced by tailoring the acidic and basic properties of the catalyst. Therefore, the research efforts are directed to develop a catalytic process, which can produce jasminaldehyde with high selectivity from condensation of 1–heptanal with benzaldehyde using eco–friendly reusable solid base catalysts (Scheme 6.1).

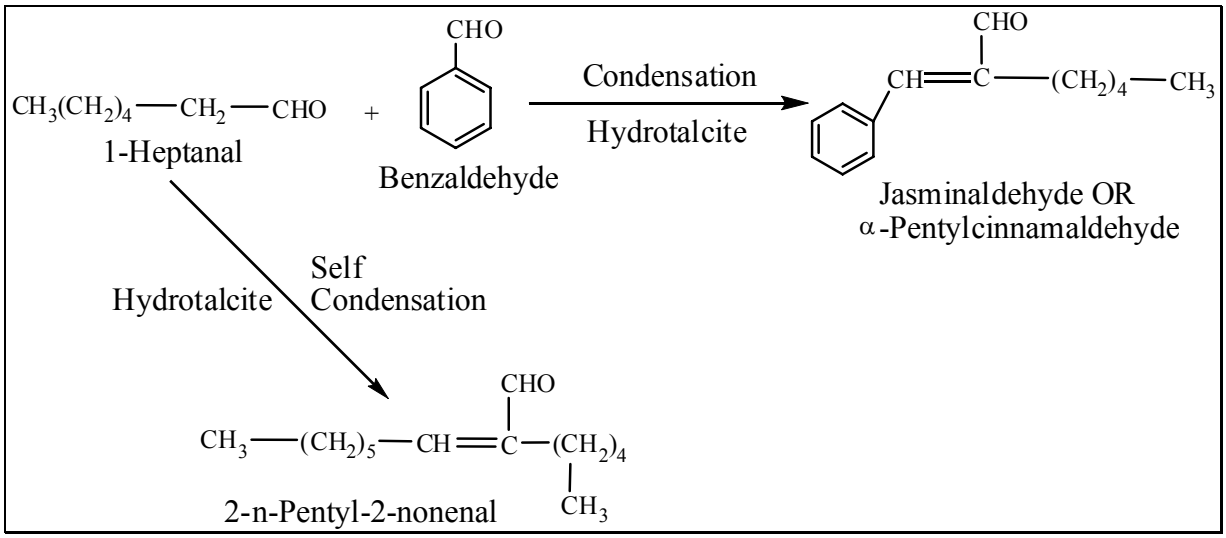

Scheme 6.1. Synthesis of jasminaldehyde.

Hydrotalcite (layered double hydroxides) has recently received much attention as solid base catalysts [9]. The basicity of the hydrotalcite could be modified either by changing the divalent to trivalent cations molar ratio [M(II)/M(III)] or intercalation of a suitable anion in the interlayer space. The as–synthesized hydrotalcite is converted into aluminum–magnesium mixed oxide on thermal decomposition at about 450 °C, which is reported to be a potential solid base catalyst for a variety of organic transformations such as condensation, isomerization, anion exchangers and epoxidation reactions [10–19]. Numerous studies are reported on self condensation of butanal, acetone, and cross condensation of aldehydes and ketones using hydrotalcite or other solid base catalysts. However, the detail study on applicability of as–synthesized hydrotalcite of varied divalent metal cations [M(II)] and divalent to trivalent cations molar ratio [M(II)/Al; M(II) = Mg, Ni, Zn] as solid base catalysts for the synthesis of jasminaldehyde is being reported for the first time in the present study.

The aim of present study is to evaluate catalytic activity of as–synthesized and activated hydrotalcite of varied divalent metal cations [M(II)] and divalent to trivalent cations molar ratio [M(II)/Al; M(II) = Mg, Ni, Zn] for synthesis of jasminaldehyde by solvent free condensation of 1–heptanal with benzaldehyde. The hydrotalcite of varied divalent metal cations and M(II)/Al molar ratio were synthesized, characterized and their catalytic activity was evaluated for condensation of 1–heptanal with benzaldehyde.

6.2. Experimental

6.2.1. Materials

Magnesium nitrate ($Mg(NO_3)_2.6H_2O$; 98.9%), aluminum nitrate ($Al(NO_3)_3.9H_2O$; 99.1%), nickel nitrate ($Ni(NO_3)_2.6H_2O$; 98%), zinc nitrate ($Zn(NO_3)_2.6H_2O$; 98%), sodium carbonate (Na_2CO_3; 99.9%) and sodium hydroxide (NaOH; 99.9%) were purchased from s.d. Fine Chemicals, India for the synthesis of hydrotalcite samples. The double distilled milli–pore deionized water was used during the synthesis. β–Isophorone, 1–heptanal and benzaldehyde were purchased from Sigma–Aldrich and used as received.

6.2.2. Catalyst Synthesis

The Mg–Al hydrotalcite samples with Mg/Al molar ratio in the range of 2.0 to 3.5 were synthesized by co–precipitation method at constant pH [9]. For example, during the synthesis of hydrotalcite of Mg/Al molar ratio 2.5, an aqueous solution (A) of $Mg(NO_3)_2.6H_2O$ (0.22 mol) and $Al(NO_3)_3.9H_2O$ (0.088 mol) was prepared in 200 mL double distilled deionized water. The solution A was added dropwise into a second solution (B) containing NaOH (0.72 mol) and Na_2CO_3 (0.21 mol) in 200 mL double distilled deionized water, in around 2 h under vigorous stirring at room temperature. The content was then transferred into the teflon coated stainless steel autoclave and aged at 70 °C for 14 h under autogenous pressure. After 14 h, the precipitate formed was filtered and washed thoroughly with hot distilled water until pH of the filtrate was reached to 7. The washed precipitate was dried in an oven at 80 °C for 14 h. The hydrotalcite samples of varied Mg/Al molar ratio from 2.0–3.5 were synthesized as per above procedure using appropriate amounts of $Mg(NO_3)_2.6H_2O$ and $Al(NO_3)_3.9H_2O$. Similar procedure was followed for the synthesis of Ni–Al and Zn–Al hydrotalcite samples. The activation of as–synthesized Mg–Al hydrotalcite samples was carried out at 450 °C in muffle furnace for 4 h in the presence of air.

6.2.3. Characterization of the Catalyst

Powder X–ray diffraction (P–XRD) patterns of hydrotalcite and reconstructed hydrotalcite samples were recorded with powder diffractometer (Philips, X'Pert MPD system) using PW3123/00 curved Cu–filtered Cu–Kα (λ=1.54056 Å) over a 2θ range of 2–70°. The data were processed with Philips X'Pert (version 1.2) software. The operating voltage and the current were 40 kV and 40 mA, respectively. Percentage crystallinity of hydrotalcite samples were calculated by comparing the summation of integral intensities of (003) (2θ = 11.5°) and (006) (2θ = 23.3°) planes with a commercially available hydrotalcite (Pural MG70, supplied by SASOL, Germany) of Mg/Al molar ratio 2.0. Fourier transform infrared (FT–IR) spectra of the hydrotalcite and reconstructed hydrotalcite samples were recorded with Perkin–Elmer spectrum GX–FTIR system using KBr pellet in the wavelength range of 400 to 4000 cm^{-1}. Thermogravimetric analysis (TGA) of hydrotalcite and reconstructed hydrotalcite samples was carried out using Mettler–Toledo

TGA/SDTA 851e equipment in flowing nitrogen (flow rate, 50 mL/min), at a heating rate of 10 °C/min.

6.2.4. Synthesis of Jasminaldehyde

The desired amounts of benzaldehyde, 1–heptanal (benzaldehyde to 1–heptanal molar ratio = 5) and catalyst were taken with 0.01 g of tetradecane as an internal standard in an oven dried double necked round bottom flask for condensation of 1–heptanal with benzaldehyde. One neck of flask was fitted with 0.7 m long refluxing condenser having spiral tube inside the condenser and silicon rubber septum was inserted in second neck of flask. Top of the refluxing condenser was closed by a cork of standard joint size. Water at 15 °C was circulated in spiral tube of refluxing condenser continuously during the course of reaction from water chiller at a flow rate of 6 L/min. Flask fitted with refluxing condenser was kept in an oil bath equipped with temperature and agitation speed controlling unit. Reaction was carried out at 125 °C for 8 h. After completion of the reaction, reaction mixture was cooled down to room temperature and was subsequently filtered. The weight of initial reaction mixture and product mixture after reaction was compared to ensure the absence of vapor loss of reaction mixture. This reaction was carried out in the nitrogen atmosphere to avoid oxidation of 1–heptanal and benzaldehyde. Progress of reaction was monitored in terms of consumption of 1–heptanal. Analysis of product mixture was carried out by gas chromatography (GC) (Shimadzu 17A, Japan) & GC–MS (Shimadzu–QP2010, Japan). GC has a 5% diphenyl and 95% dimethyl siloxane universal capillary column (60 m length and 0.25 mm diameter) and a flame ionization detector (FID). The retention time of different compounds was determined by injecting pure compounds into GC column under identical GC conditions. Conversion and selectivity data calculated in the present study are reproducible within ± 5% error. The conversion and selectivity were calculated by the following formula –

$$\% \text{ Conversion} = \frac{\text{Moles of 1-heptanal reacted}}{\text{Moles of 1-heptanal fed}} \times 100$$

$$\% \text{ Selectivity of jasminaldehyde} = \frac{\text{Moles of jasminaldehyde}}{\text{Moles of (jasminaldehyde + 2-n-pentyl-nonenal)}} \times 100$$

6.2.5. Isomerization of β–Isophorone

The isomerization of β–isophorone to α–isophorone was performed as a model test reaction for basicity measurement of as–synthesized and activated hydrotalcite samples (Scheme 6.2) [12, 14]. 10 mL of isophorone was mixed into 30 mL heptane as a solvent in a 50 mL oven dried double

necked round bottom flask. The nitrogen was purged to remove CO_2 present in the reaction atmosphere and agitation was started at 35 °C temperature and 1000 rpm. After 2 min, 0.1 g catalyst was added to this mixture from side neck of the round bottom flask and reaction was continued by stirring at 1000 rpm. The analysis of product mixture was carried out by GC–MS (Shimadzu–QP2010, Japan).

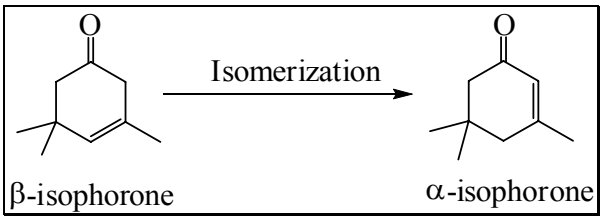

Scheme 6.2. Isomerization of β–isophorone to α–isophorone as a model test reaction for basicity measurement.

6.3. Results and Discussion

6.3.1. Characterization of Catalyst

P–XRD Patterns of As–Synthesized and Activated Hydrotalcite Samples of Varied Divalent Cations (Mg, Ni) to Aluminum Molar Ratio

P–XRD patterns of as–synthesized Mg–Al, Ni–Al and activated Mg–Al(A) hydrotalcite samples are shown in Figure 6.1. P–XRD patterns of as–synthesized hydrotalcite samples showed sharp, intense and symmetric peaks at lower diffraction angles (2θ = 10–25°) and broad asymmetric reflections at higher diffraction angles (2θ = 30–50°), which are characteristic of highly crystalline layered structure [9]. Presence of CO_3^{2-} anions in interlayer space of hydrotalcite was confirmed by the characteristic basal spacing $d_{(003)}$ = 7.65Å. P–XRD patterns of Ni–Al and Zn–Al hydrotalcite were observed to be similar to that of the Mg–Al hydrotalcite. On calcination of hydrotalcite at 450 °C, P–XRD patterns of Mg–Al(3.5A) revealed broad peaks that can be assigned to Mg–Al mixed oxide [Mg(Al)O] phase, with diffraction lines similar to that of MgO. The crystallinity of hydrotalcite samples decreased with increase in M(II)/Al molar ratio (Table 6.1). For Mg–Al hydrotalcite samples, 98% crystallinity of hydrotalcite of Mg/Al molar ratio 2.0 was observed, which decreased to 79% on increasing the Mg/Al molar ratio to 3.5. The decrease in the crystallinity on increasing Mg/Al molar ratio of hydrotalcite samples is due to increase in amount of divalent cations (Mg^{2+}) which have ionic radii 0.65 Å that favors the formation of brucite by replacing the smaller ionic radii trivalent cations (Al^{3+}) [20]. *d*–Spacing of (003) plane of hydrotalcite was found to increase on increasing the Mg/Al molar ratio of hydrotalcite samples.

Similar to the crystallinity of Mg–Al hydrotalcite, the crystallinity of Ni–Al and Zn–Al hydrotalcite samples were also observed to decrease on increasing the Ni/Al or Zn/Al molar ratio.

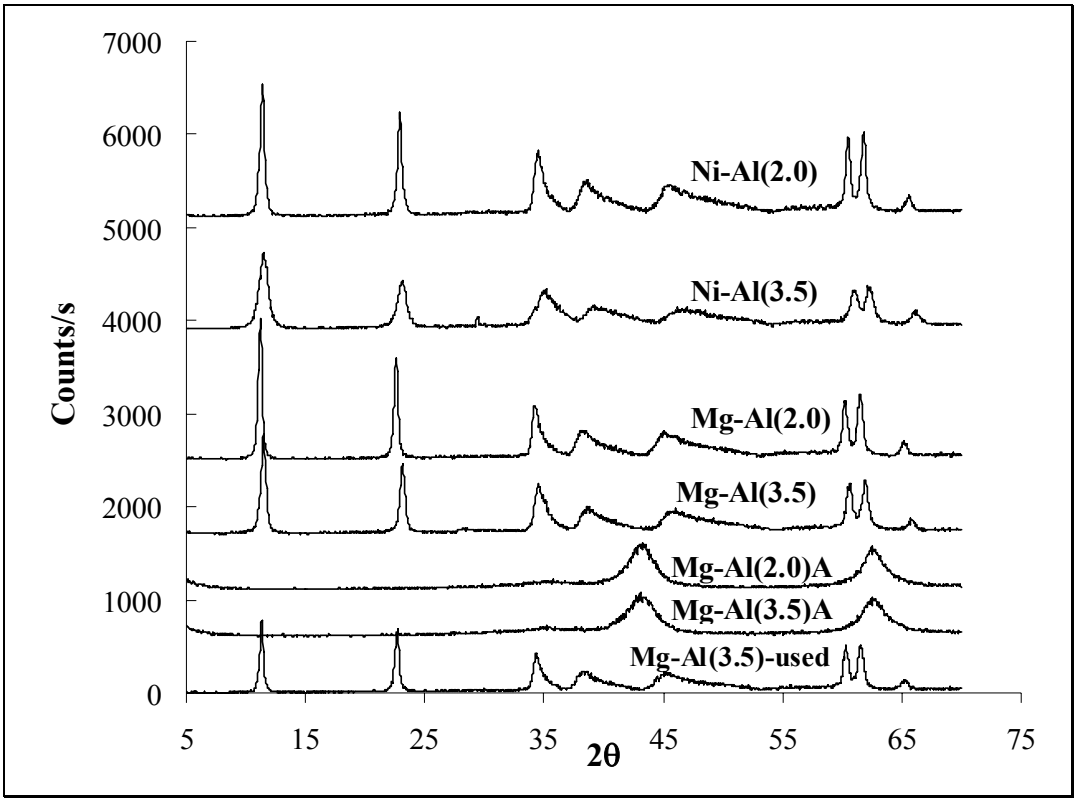

Figure 6.1. P–XRD patterns of Ni–Al, Mg–Al hydrotalcite samples and Mg–Al(3.5)–used catalyst.

Table 6.1. Chemical composition and crystallinity of the catalysts used

Catalyst Sample	Chemical Composition	% Crystallinity	*d*–Spacing (Å) (003) plane
Mg–Al(2.0)	$[Mg_{0.67}Al_{0.33}(OH)_2](CO_3)_{0.165}.mH_2O$	98	7.58
Mg–Al (2.5)	$[Mg_{0.72}Al_{0.28}(OH)_2](CO_3)_{0.14}.mH_2O$	91	7.63
Mg–Al (3.0)	$[Mg_{0.75}Al_{0.25}(OH)_2](CO_3)_{0.125}\cdot mH_2O$	86	7.65
Mg–Al (3.5)	$[Mg_{0.78}Al_{0.22}(OH)_2](CO_3)_{0.11}\cdot mH_2O$	79	7.74
Ni–Al(2.0)	$[Ni_{0.66}Al_{0.34}(OH)_2](CO_3)_{0.17}\cdot mH_2O$	95	7.63
Ni –Al (2.5)	$[Ni_{0.72}Al_{0.28}(OH)_2](CO_3)_{0.14}\cdot mH_2O$	88	7.65
Ni –Al (3.0)	$[Ni_{0.75}Al_{0.25}(OH)_2](CO_3)_{0.125}\cdot mH_2O$	82	7.67
Ni –Al (3.5)	$[Ni_{0.77}Al_{0.23}(OH)_2](CO_3)_{0.11}\cdot mH_2O$	76	7.71
Zn–Al(2.0)	$[Mg_{0.67}Al_{0.33}(OH)_2](CO_3)_{0.165}.mH_2O$	94	7.62
Zn–Al(3.5)	$[Zn_{0.78}Al_{0.22}(OH)_2](CO_3)_{0.11}\cdot mH_2O$	76	7.69

FT–IR Spectra of As–Synthesized and Activated Hydrotalcite Samples of Varied Divalent Cations (Mg, Ni) to Aluminum Molar Ratio

FT–IR spectra of Mg–Al(3.5) and Mg–Al(3.5A) hydrotalcite samples are shown in Figure 6.2. Peak in the range of 3450–3550 cm^{-1} present in all hydrotalcite samples, is due to OH stretching mode of hydroxyl groups, both from interlayer water molecules and hydroxyls in the brucite–like layer. Shoulder present at around 3000 cm^{-1} is attributed to hydrogen bonding between water molecules and interlayer CO_3^{2-} anions. Appearance of shoulder at 1650 cm^{-1} is the characteristic of H_2O. Asymmetric stretching, ν_3, appeared at around 1380 cm^{-1} could be assigned to interlayer carbonates. The bands observed at 950 and 1050 cm^{-1} are due to Al–OH deformation and at 760 and 550 cm^{-1} are attributed to Al–OH translation. The band at 860 cm^{-1} is due to out–of–plane CO_3^{2-} anions. The band at 554 cm^{-1} is assigned to translation modes of hydroxyl groups influenced by Al^{3+} cations (Mg/Al–OH translation) and band at 635 cm^{-1} is assigned to Mg–O [21]. Disappearance of bands at about 1650 cm^{-1} (water bending vibrations) and 3000 cm^{-1} (interaction of H_2O–CO_3^{2-} in interlayer) in the FT–IR spectra of activated hydrotalcite samples, confirmed that the water molecules were removed on calcination of as–synthesized hydrotalcite samples. Intensity of band at 3450–3550 cm^{-1} also decreases significantly due to dehydroxylation process. Absence of carbonates anions was confirmed by disappearance of peak at around 1380 cm^{-1} in the FT–IR spectra of activated hydrotalcite samples. Peak appeared at 600 cm^{-1} in the FT–IR spectra of Ni–Al hydrotalcite samples is attributed to Ni–OH translation mode.

TGA of As–Synthesized and Activated Hydrotalcite Samples

TGA curves of Mg–Al(3.5) and Mg–Al(3.5)A are shown in Figure 6.3. TGA curves showed two steps weight loss which is in good agreement with the results reported for hydrotalcite [9]. First weight loss (14%) of Mg–Al (3.5) hydrotalcite was observed in the temperature range of 140 to 220 °C due to removal of physically adsorbed water. Weight loss in second step increased to 42% due to removal of hydroxyl groups (dehydroxylation) and carbonate anions (decarboxylation) from the interlayer space of hydrotalcite in the temperature range of 350 to 460 °C. Only 12% weight loss was observed in TGA of Mg–Al(3.5)A hydrotalcite in the temperature range of 260 to 470 °C.

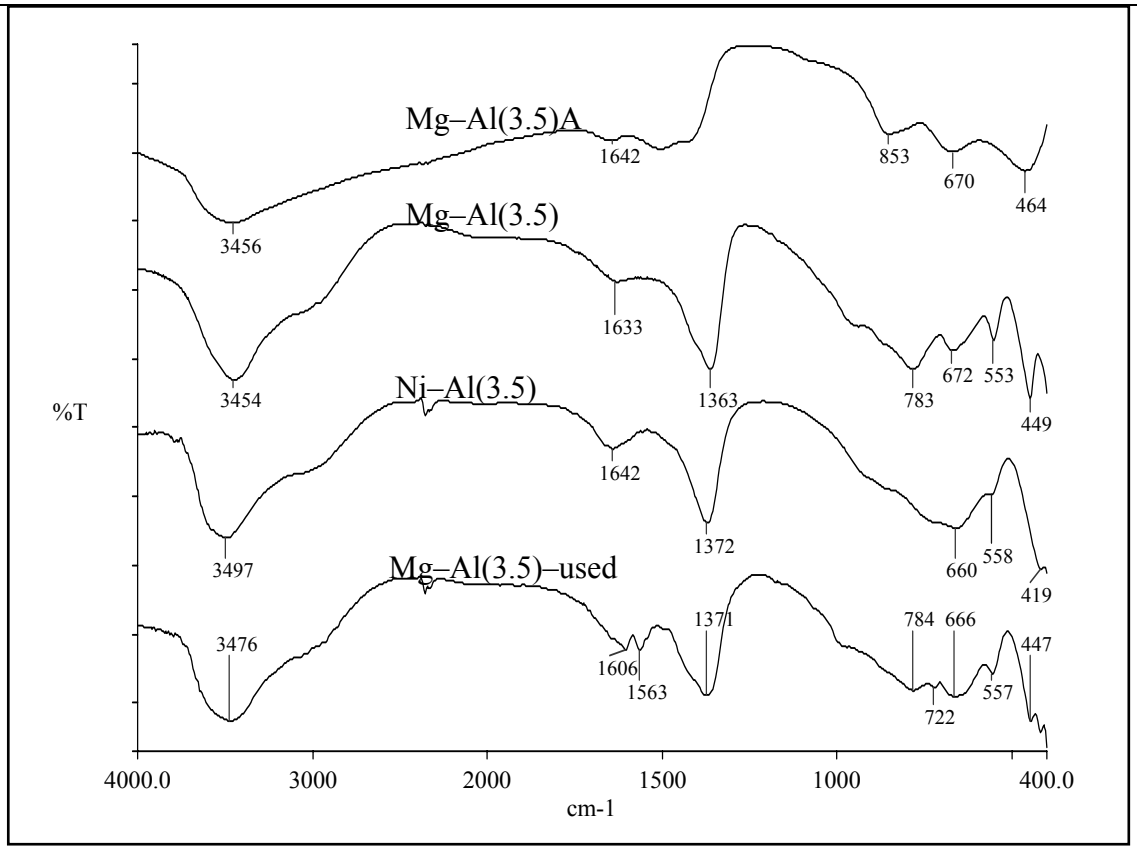

Figure 6.2. FT–IR spectra of Mg–Al(3.5)A, Mg–Al(3.5), Ni–Al hydrotalcite samples and Mg–Al(3.5)–used catalyst.

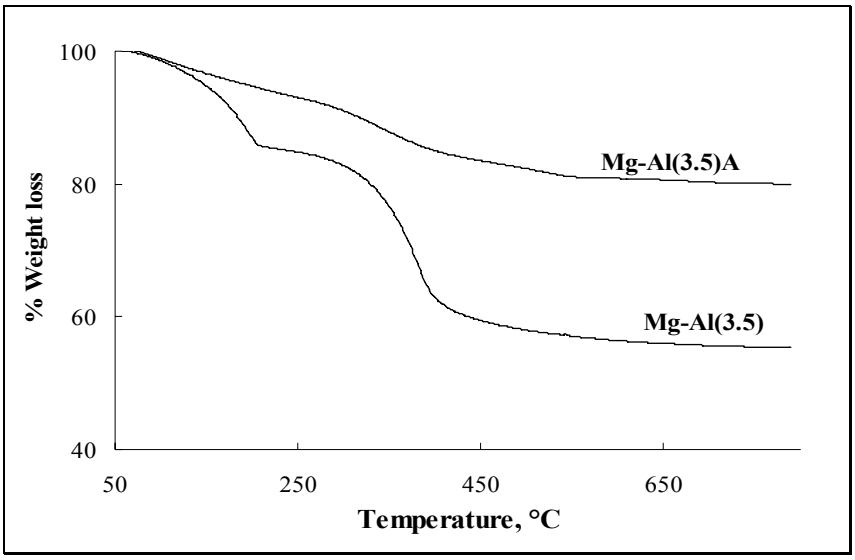

Figure 6.3. TGA of Mg–Al(3.5) and Mg–Al(3.5)A hydrotalcite samples.

6.3.2. Catalytic Activity

Catalytic activity of hydrotalcite samples of varied M(II)/Al molar ratio as catalysts was evaluated for the synthesis of jasminaldehyde by condensation of 1–heptanal with benzaldehyde are given in Table 6.2. 1–Heptanal conversion in the range of 96–99% was observed for the studied

catalysts. This shows that no significant change in the conversion of 1–heptanal was observed on varying Mg/Al molar ratio of as–synthesized and activated Mg–Al hydrotalcite samples. Selectivity of jasminaldehyde was observed to increase from 83% at Mg/Al molar ratio of hydrotalcite 2.0 to 86% at Mg/Al molar ratio 3.5. GC–MS fragmentation data of 1–heptanal, benzaldehyde, jasminaldehyde and 2–n–pentyl–2–nonenal are given in Figure 6.4. The mass data showed standard fragmentation pattern corresponding to 1–heptanal (m/z: 114, 70, 55, 44, 41, 29), benzaldehyde (m/z: 106, 77, 51), jasminaldehyde (m/z: 202, 145, 129, 117, 91) and 2–n–pentyl–2–nonenal (m/z: 210, 153, 125, 97, 81, 55, 41, 29). On activation of Mg–Al hydrotalcite samples, the selectivity of jasminaldehyde decreased significantly from 86% to 75% (Mg/Al = 3.5). The conversion of 1–heptanal was obtained as 98% with 78% selectivity of jasminaldehyde using MgO as a catalyst. Selectivity of jasminaldehyde decreased to 62% using activated MgO at 450 °C as a catalyst. In view of higher selectivity of jasminaldehyde observed in case of as–synthesized Mg–Al hydrotalcite used as a catalyst, the experiments were conducted using Ni–Al and Zn–Al hydrotalcite samples as catalysts without activation to observe the effect of divalent cations on their catalytic activity. As–synthesized Ni–Al hydrotalcite showed 97% conversion of 1–heptanal, which is similar to the conversion observed in case of as–synthesized Mg–Al hydrotalcite. The selectivity of jasminaldehyde was observed to increase from 73 to 78% by varying the Ni–Al molar ratio of hydrotalcite from 2.0 to 3.5. The selectivity of jasminaldehyde increased from 78% to 84% by introducing Mg in Ni–Al(3.5) hydrotalcite sample. The selectivity of jasminaldehyde was observed to decrease to 72% on activation of Ni–Mg–Al(3.5) catalyst. 1–Heptanal conversion of 96% with 70% selectivity of jasminaldehyde was observed using Zn–Al hydrotalcite of Zn/Al molar ratio 2.0 which showed small increase in conversion (97%) and selectivity of jasminaldehyde (76%) on increasing the Zn/Al molar ratio 3.5.

Catalytic activity of hydrotalcite depends upon its basicity which in case of as–synthesized hydrotalcite is mainly due to their hydroxyl groups which act as Brønsted basic sites for condensation of 1–heptanal with benzaldehyde. Higher selectivity of jasminaldehyde observed in case of as–synthesized hydrotalcite as a catalyst confirms that the material having weak basic sites (hydroxyl groups) is appropriate for this reaction. Decrease in the selectivity of jasminaldehyde on activation of as–synthesized hydrotalcite shows that the catalyst having strong basic sites is not suitable for selective synthesis of jasminaldehyde. This was also confirmed by the data obtained on performing a reaction using MgO as a catalyst, which is known to be a strong base catalyst. The basicity of as–synthesized and activated hydrotalcite samples of Mg/Al ratio 2.0, 2.5, 3.0 and 3.5 were evaluated by isomerization of β–isophorone to α–isophorone as a model test reaction reported for basicity measurement to support our observations in the present study [12, 14].

Table 6.2. Condensation of 1–heptanal with benzaldehyde using solid base catalysts

Run	Catalyst		% Conversion	% Selectivity [a]	
				Jasminaldehyde	2–n–Pentyl – 2–nonenal
1	Mg–Al(3.5)	Without activation	98	86	14
2	Mg–Al(3.0)	Without activation	98	84	16
3	Mg–Al(2.5)	Without activation	98	82	18
4	Mg–Al(2.0)	Without activation	97	83	17
5	Mg–Al(3.5A)	Activated at 450 °C/4h	98	75	25
6	Mg–Al(3.0A)	Activated at 450 °C/4h	99	75	25
7	Mg–Al(2.5A)	Activated at 450 °C/4h	99	74	26
8	Mg–Al(2.0A)	Activated at 450 °C/4h	99	72	28
9	MgO	Without activation	98	78	22
10	MgO(A)	Activated at 450 °C/4h	99	62	38
11	Ni–Al(3.5)	Without activation	97	78	22
12	Ni–Al(3.0)	Without activation	97	77	23
13	Ni–Al(2.5)	Without activation	97	74	26
14	Ni–Al(2.0)	Without activation	96	73	27
15	Ni–Mg–Al	Without activation	96	84	16
16	Ni–Mg–Al(A)	Activated at 450 °C/4h	98	72	28
17	Zn–Al(3.5)	Without activation	97	76	24
18	Zn–Al(2.0)	Without activation	96	70	30

[a] **Reaction conditions:** benzaldehyde = 39.6 mmol, heptanal = 7.9 mmol, catalyst = 75 mg, temperature = 125 °C, time = 8 h.

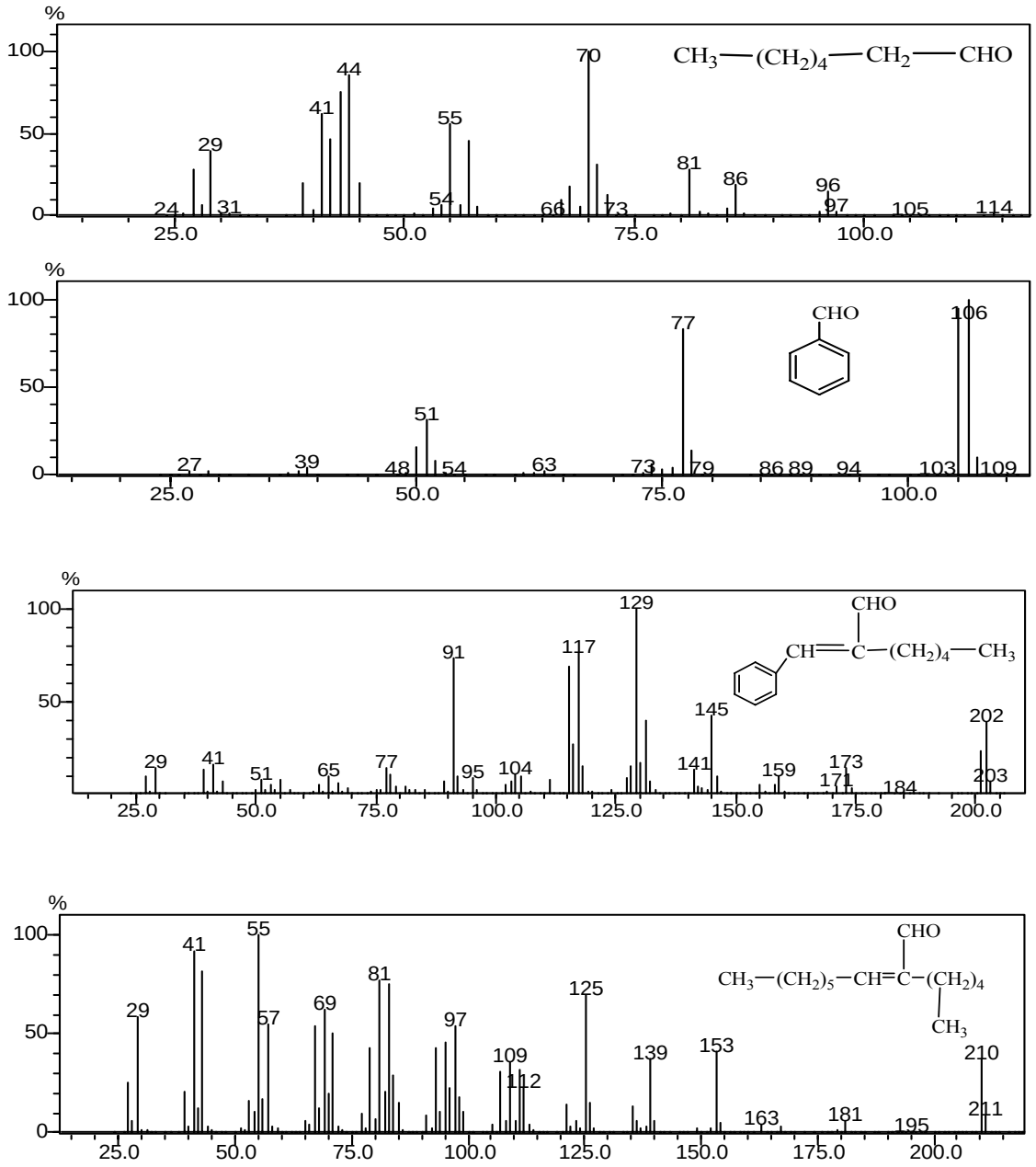

Figure 6.4. GC–MS fragmentation data of 1–heptanal, benzaldehyde, jasminaldehyde and 2–n–pentyl–2–nonenal.

Initial rate of reaction was observed to increase significantly on activation of as–synthesized hydrotalcite samples of different Mg/Al molar ratio (Figure 6.5). The initial rate of reaction for as–synthesized hydrotalcite of Mg/Al molar ratio 2.0 was calculated as 18 x 10^{-4} mol/(g_{cat} sec) which increased to 38 x 10^{-4} mol/(g_{cat} sec) for activated hydrotalcite of Mg/Al molar ratio 2.0. For as–synthesized hydrotalcite of Mg/Al molar ratio 3.5, the initial rate of reaction was found to be 26 x 10^{-4} mol/(g_{cat} sec) that increased to 48 x 10^{-4} mol/(g_{cat} sec) with activated hydrotalcite sample.

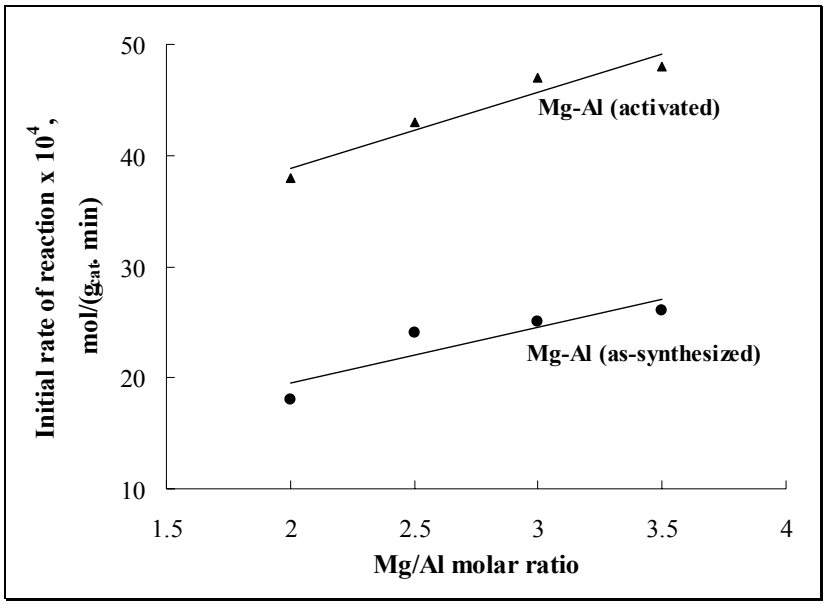

Figure 6.5. Initial rate of reaction for isomerization of β–isophorone to α–isophorone as a model reaction to test basicity of as–synthesized and activated Mg–Al hydrotalcite samples.

The isomerization of β–isophorone to α–isophorone is a zero order reaction; hence, the value of initial rate of reaction is equal to the value of rate constant. The value of rate constant for isophorone isomerization is reported to be directly proportional to the number of basic sites [12, 14]. The higher values of initial rate of reaction obtained on activation of hydrotalcite indicate that the basicity increased significantly on activation of catalyst. From these results, it is clear that the activated hydrotalcite samples are stronger base catalysts as compared to as–synthesized hydrotalcite samples. However, the initial rate of reaction was also observed to increase on increasing the Mg/Al molar ratio of as–synthesized and activated hydrotalcite. But the extent of increase in initial rate of reaction at varied Mg/Al molar ratio of as–synthesized hydrotalcite is significantly less as compared to the difference in the initial rate of reaction of activated hydrotalcite.

The trend observed in present study shows that the strong solid base catalysts such as MgO, activated hydrotalcite gave higher conversion of 1–heptanal but poor selectivity of jasminaldehyde. Similar observations are also reported in the literature [8]. The reason for lower selectivity of jasminaldehyde is the competitive side reaction, i.e., self condensation of 1–heptanal catalyzed by strong base catalyst such as activated hydrotalcite. Activation of as–synthesized hydrotalcite at 450 °C gives a well dispersed mixture of magnesium and aluminium mixed oxides having strong Lewis (isolated O^{2-} anions) and weaker Brønsted (OH^- anions) basic sites on the surface. [22]. The numbers of stronger Lewis O^{2-} sites are higher as compared to weaker Brønsted OH^- sites on the surface of activated hydrotalcite. Therefore, activated hydrotalcite is a strong basic catalyst compared to as–synthesized hydrotalcite, both in terms of basic strength and number of basic

sites [23]. Keeping in view of the higher conversion and selectivity of jasminaldehyde observed for Mg as a divalent cation of as–synthesized hydrotalcite, further experiments were carried out using as–synthesized Mg–Al hydrotalcite of Mg/Al molar ratio 3.5 [Mg–Al(3.5)] as a catalyst.

6.3.3. Effect of the Catalyst Amount

In order to optimize the amount of catalyst for synthesis of jasminaldehyde, experiments were carried out by increasing the amount of catalyst [Mg–Al(3.5)] from 25 to 500 mg at constant benzaldehyde to 1–heptanal molar ratio 5 at 125 °C (Table 6.3). The conversion of 1–heptanal was observed to increase with decrease in selectivity of jasminaldehyde on increasing the amount of catalyst. The maximum conversion (100%) was found at 100 mg of the catalyst amount with 85% selectivity of jasminaldehyde. Beyond 100 mg catalyst, the conversion of 1–heptanal was found to be independent of the catalyst amount. The selectivity of jasminaldehyde was observed to decrease to 78% on increasing the amount of catalyst to 250 mg. On further increase in the amount of catalyst to 500 mg, selectivity of jasminaldehyde further decreased to 70%. The decrease in selectivity of jasminaldehyde on increasing the amount of catalyst is due to simultaneous self condensation of 1–heptanal to 2–n–pentyl–2–nonenal on increased availability of basic sites on the surface of catalyst. The self condensation of 1–heptanal is also a base catalyzed reaction.

Table 6.3. Effect of the amount of catalyst [Mg–Al(3.5)] on the selectivity of jasminaldehyde

Run	[Mg–Al(3.5)], mg	% Conversion	% Selectivity [a]	
			Jasminaldehyde	2–n–Pentyl–2–nonenal
1	25	70	86	14
2	50	86	85	15
3	75	98	86	14
4	100	100	85	15
5	125	100	85	15
6	150	100	83	17
7	250	100	78	22
8	500	100	70	30

[a] **Reaction conditions:** benzaldehyde = 39.6 mmol, heptanal = 7.9 mmol, temperature = 125 °C, time = 8 h.

6.3.4. Effect of Benzaldehyde to 1–Heptanal Molar Ratio

The effect of benzaldehyde to 1–heptanal molar ratio was studied by varying their molar ratio from 1 to 10 at constant amount of catalyst [Mg–Al(3.5)] (Table 6.4). At benzaldehyde to 1–heptanal molar ratio 1, 94% conversion with 56% selectivity of jasminaldehyde was observed. Conversion of 1–heptanal was found to increase upto 96% with 74% selectivity of jasminaldehyde on increasing this ratio to 3. The jasminaldehyde selectivity was observed to increase upto 86 with 98% conversion of 1–heptanal at benzaldehyde to 1–heptanal molar ratio 5. No significant effect on conversion and selectivity data was observed on further increase in the ratio, which indicates that the optimum benzaldehyde to 1–heptanal molar ratio is 5 under the studied experimental conditions. Probability of faster adsorption of carbocations of 1–heptanal is higher as compared to that of benzaldehyde on active sites of catalysts at lower benzaldehyde to 1–heptanal molar ratio. This could result into the higher selectivity of 2–n–pentyl–2–nonenal, which is a base catalyzed self condensation product of 1–heptanal. However, at higher benzaldehyde to 1–heptanal molar ratio, the concentration of benzaldehyde will be higher which leads to increased interaction probability of benzaldehyde rather than 1–heptanal molecules with the active sites of catalyst. Similar observations were reported by Corma et al. for higher benzaldehyde to 1–heptanal molar ratio [3].

Table 6.4. Effect of benzaldehyde to 1–heptanal molar ratio on the selectivity of jasminaldehyde

Run	Benzaldehyde/ 1–heptanal molar ratio	% Conversion	% Selectivity [a]	
			Jasminaldehyde	2–n–Pentyl–2–nonenal
1	1	94	56	44
2	2	96	67	33
3	3	96	74	26
4	5	98	86	14
5	7	98	85	15
6	10	98	86	14

[a] **Reaction conditions:** Catalyst [Mg–Al(3.5)] = 75 mg, temperature = 125 °C, reaction time = 8 h.

6.3.5. Effect of the Reaction Temperature

The effect of reaction temperature on selectivity of jasminaldehyde was studied in the temperature range of 60 to 170 °C at constant benzaldehyde to 1–heptanal molar ratio 5 and 75 mg catalyst amount. Lower conversion on 1– heptanal was found at lower reaction

temperature (Table 6.5). The conversion of 1–heptanal was observed to increase from 38 to 98% by increasing the reaction temperature from 60 to 125 °C. On further increase in the temperature to 140 °C, conversion increased to 100%. Higher selectivity of jasminaldehyde was observed at lower reaction temperature. The selectivity of jasminaldehyde was observed to decrease from 88 to 81% on increasing the reaction temperature from 60 to 170 °C.

Table 6. 5. Effect of reaction temperature on the selectivity of jasminaldehyde

Run	Temperature, °C	% Conversion	% Selectivity [a]	
			Jasminaldehyde	2–n–Pentyl–2–nonenal
1	60	38	88	12
2	80	57	87	13
3	100	80	86	14
4	125	98	86	14
5	140	100	84	16
6	170	100	81	19

[a] **Reaction conditions:** benzaldehyde = 39.6 mmol, heptanal = 7.9 mmol, catalyst [Mg–Al(3.5)] = 75 mg, reaction time = 8 h.

6.3.6. Reaction Kinetics and Reusability of the Catalyst [Mg–Al(3.5)]

The effect of reaction time on conversion of 1–heptanal and selectivity of jasminaldehyde was studied at optimum reaction conditions, i.e., 75 mg catalyst, benzaldehyde/1–heptanal molar ratio = 5 and reaction temperature = 125 °C. 1–Heptanal conversion and selectivity of jasminaldehyde with respect to reaction time is shown in Figure 6.6. The conversion of 1–heptanal was observed to increase on increasing the reaction time. For example, 62% conversion of 1–heptanal was observed at 2 h reaction time and increased to 80% in 4 h. Finally the conversion of 1–heptanal reached to 98% at 8 h reaction time. The selectivity of jasminaldehyde was observed to increase from 60 to 66% within 2 h reaction time. On increasing the reaction time upto 8 h, the selectivity of jasminaldehyde also increased from 66 to 86%. The order of reaction was calculated from the kinetic data and found to be second order reaction with respect to reactants. The rate of reaction was calculated as 11.6 x 10^{-4} mol/(g_{cat} min) in the lower conversion range (< 20%).

The spent catalyst [Mg–Al(3.5)] obtained after completion of reaction was washed with 100 mL methanol and dried at 100 °C for 6 h in an oven. The dried material was used as a catalyst for reusability experiments under similar reaction conditions (Table 6.2; Run 1) as that of fresh catalyst. The catalyst was recycled upto three cycles without significant loss in the conversion of

1–heptanal and selectivity of jasminaldehyde (Table 6.6).

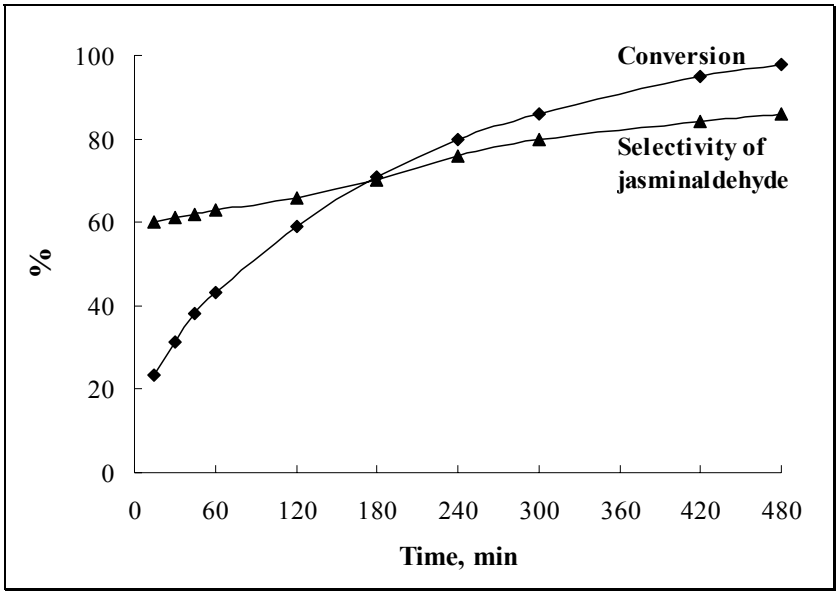

Figure 6.6. Kinetic profile with respect to time using Mg–Al(3.5) as a catalyst.

Table 6.6. Reusability of the catalyst

Cycles	% Conversion	% Selectivity [a]	
		Jasminaldehyde	2–n–Pentyl–2–nonenal
1	98	86	14
2	98	85	15
3	97	83	17
4	94	77	27
5	92	71	29
6	81	70	30

[a] **Reaction conditions:** benzaldehyde = 39.6 mmol, heptanal = 7.9 mmol, temperature = 125 °C, reaction time = 8 h.

After that the conversion and selectivity data was observed to decrease significantly. The decrease in conversion and selectivity of jasminaldehyde may be attributed to deactivation of active basic sites present on the surface of catalyst. Spent catalyst was analyzed by P–XRD and FT–IR spectroscopy to observe the structural changes of spent catalyst (Figure 6.1 & 6.2). P–XRD of spent catalyst showed all characteristic peaks of pure hydrotalcite. The crystallinity of spent catalyst was observed to decrease significantly. Any new peak was not observed in the FT–IR spectrum of spent catalyst after first cycle. FT–IR data of spent catalyst after sixth cycle showed the absorption of jasminaldehyde intermediates (skeletal vibrations of phenyl rings) on the catalyst

as evident from the peaks observed at 1606 and 1563 cm^{-1} (Figure 6.7). This could results into the decrease in relative concentration of jasminaldehyde in the reaction mixture as determined by GC analysis. Therefore, the observed selectivity values after third cycle of catalyst reusability are apparent selectivities.

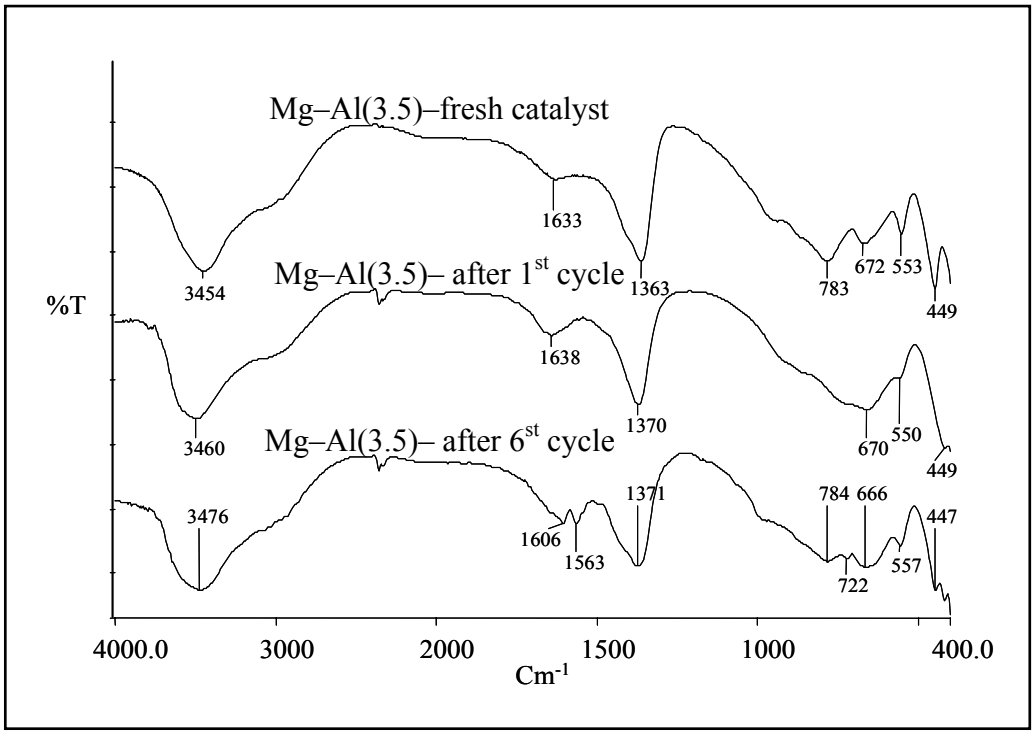

Figure 6.7. FT–IR spectra of Mg–Al(3.5)–fresh catalyst, Mg–Al(3.5)– after 1st cycle and Mg–Al(3.5)– after sixth cycle during reusability study.

6.3.7. Tentative Reaction Mechanism

Tentative reaction mechanism proposed for the synthesis of jasminaldehyde by condensation of 1–heptanal with benzaldehyde using solid base catalyst is presented in Scheme 6.3. The reaction is initiated by activation of 1–heptanal (**I**) molecule to form a stabilized carbanion (**II**) on the OH^- sites of catalyst by abstracting an acidic proton from α–carbon of (**I**). Nucleophilic addition of α–carbon of enolate anion (**II**) to carbonyl carbon of benzyaldehyde (**III**) takes place in the next step to form intermediate species (**IV**). The species (**IV**) abstracts a proton from the in–situ generated water molecules to form condensation product (**V**). In this step, the OH^- sites of catalyst are recycled for the further reaction. Jasminaldehyde (**VI**) is formed by dehydration of specie (**V**).

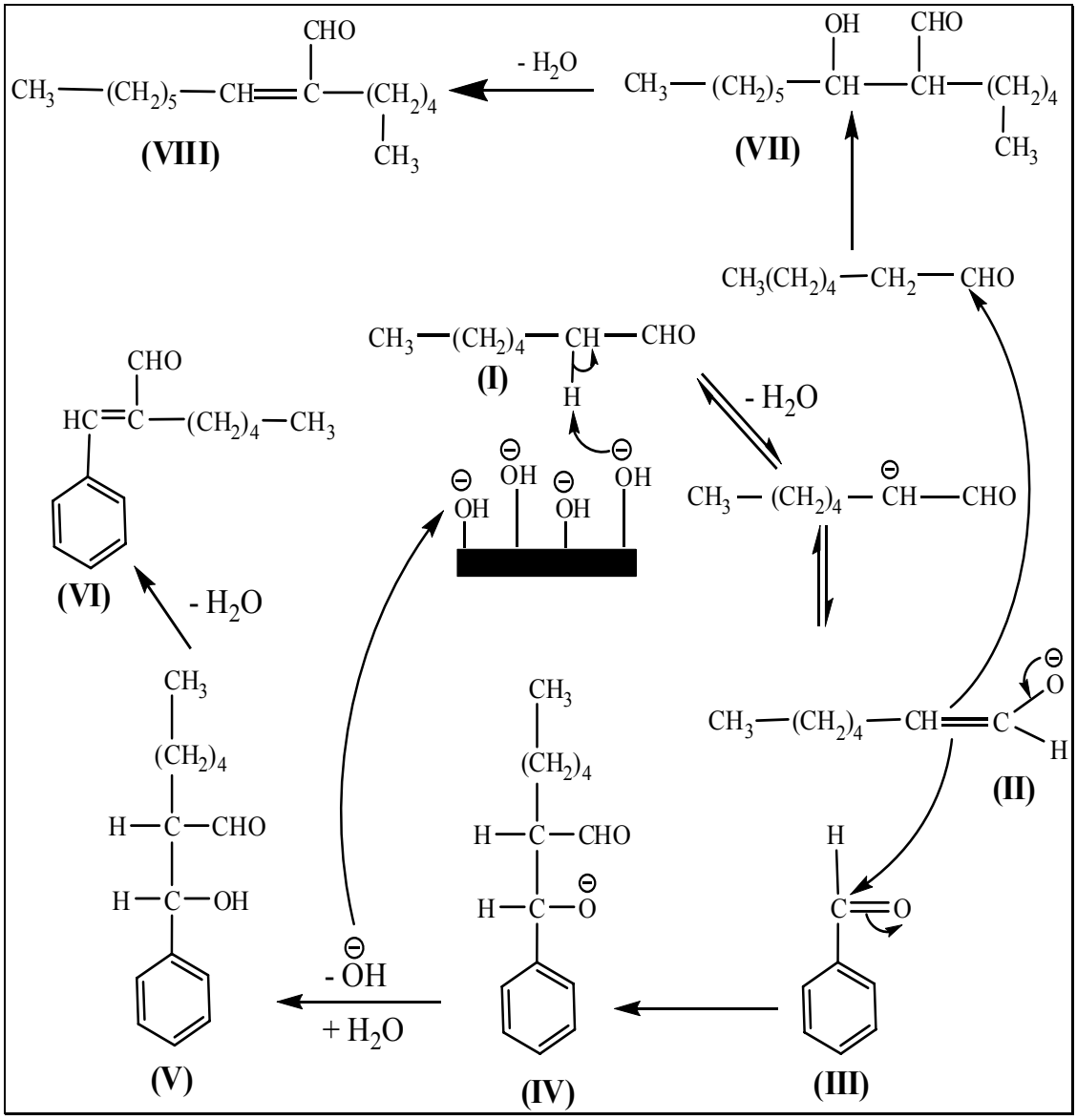

Scheme 6.3. Proposed reaction mechanism for the synthesis of jasminaldehyde using solid base catalyst.

The self condensation of (**I**) also follows the similar pathway. The formation of (**VII**) takes place by nucleophilic addition of α–carbon of enolate anion to the carbonyl group of another (**I**) molecule and the resulting anion reacts with water to form the product of aldol addition (**VII**). Dehydration of species (**VII**) gives the self condensation product of 1–heptanal, i.e., 2–n–pentyl–2–nonenal.

6.4. Reconstructed hydrotalcite of Mg/Al Molar ratio 3.5 as a Solid Base Catalyst for the Synthesis of Jasminaldehyde

The results discussed above clearly showed that the as–synthesized hydrotalcite of Mg/Al molar ratio 3.5 gives maximum selectivity of jasminaldehyde (86%) as compared to activated hydrotalcite (75%) of similar molar ratio, which is known as a strong base catalyst. However, significant difference in the conversion of 1–heptanal was not observed on activation of hydrotalcite. This indicates that the hydroxyl groups are playing an important role for the selective synthesis of jasminaldehyde and can be enhanced by proper tuning of the acidic and basic properties of the hydrotalcite. The catalyst having Brønsted basicity (hydroxyl groups) was observed to be more effective towards the selective synthesis of jasminaldehyde as compared to the catalyst having Lewis basicity (O^{2-} sites). The hydroxyl anions present in the hydrotalcite can be intercalated in control way by the reconstruction process at specific reconstruction time of hydrotalcite, gives the proper combination of acidic and basic properties required for the reaction. When the calcined hydrotalcite sample is stirred with water vapours or de–carbonated water under inert atmosphere, a highly active solid base catalyst is obtained by restoration of the original layered structure of hydrotalcite which contain mainly hydroxyl groups as compensating anions in the interlayer space, called reconstruction process (Figure 6.8). The reconstructed hydrotalcite samples have basic strength due to presence of hydroxyl groups in major amounts as charge balancing anions as compared to as–synthesized hydrotalcite sample in which hydroxyl groups alongwith carbonate anions are used as charge balancing anions. The reconstruction time and degree of reconstruction have pronounced effect on the structural and catalytic activity of hydrotalcite. The effect of reconstruction time on the structural properties of hydrotalcite is documented in the literature [21, 24–28]. However, literature is silent for the effect of reconstruction time on catalytic activity of the reconstructed hydrotalcite. Therefore, the present study describes the effect of reconstruction time on the catalytic activity of the reconstructed hydrotalcite for synthesis of jasminaldehyde by condensation of 1–heptanal with benzaldehyde.

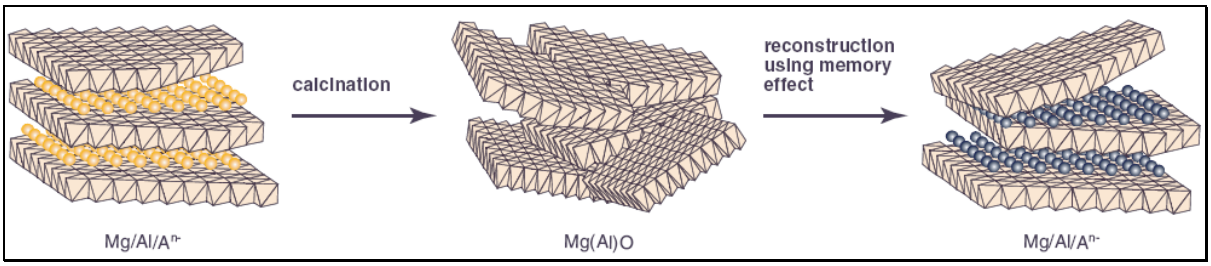

Figure 6.8. Reconstruction process of hydrotalcite [19].

The aim of present study is to study the effect of reconstruction time on catalytic activity of reconstructed hydrotalcite of Mg/Al molar ratio of 3.5 for synthesis of jasminaldehyde by condensation of 1–heptanal with benzaldehyde in the solvent free conditions. The reconstructed hydrotalcite of at different reconstruction time were synthesized, characterized to study the

structural changes during the reconstruction period and used as a catalyst for synthesis of jasminaldehyde.

6.4.1. Synthesis and Characterization of Reconstructed Hydrotalcite

Synthesis of Reconstructed Hydrotalcite Samples

The reconstructed hydrotalcite of Mg/Al molar ratio of 3.5 was synthesized by the stirring of activated hydrotalcite in decarbonated water at 30 °C. Initially, hydrotalcite sample of Mg/Al molar ratio of 3.5 was synthesized by co–precipitation method at constant pH [9] by taking an aqueous solution (A) of $Mg(NO_3)_2.6H_2O$ (0.0522 mol) and $Al(NO_3)_3.9H_2O$ (0.0149 mol) in 50 ml double distilled deionized water. The solution A was added drop wise into a second solution (B) containing Na_2CO_3 (0.079 mol) in 50 ml double distilled deionized water, in around 45 min under vigorous stirring at 25 °C. Constant pH of the mixture was maintained by adding 1 M NaOH solution. The content was then transferred into the teflon coated stainless steel autoclave and aged at 60 °C for 16 h under autogenous pressure. Then the precipitate formed was cool down to room temperature, filtered and washed thoroughly with hot deionized distilled water until pH of the filtrate was reached to 7. The washed precipitate was dried in an oven at 80 °C for 14 h. The activation of hydrotalcite was carried out at 450 °C in a muffle furnace for 4 h. Then the material was subjected for reconstruction procedure in liquid phase. For the synthesis of reconstructed hydrotalcite samples at varied reconstruction time, the freshly activated hydrotalcite (1.5 g) was mixed in 1 M NaOH solution prepared in 100 mL decarbonated deionized water under nitrogen atmosphere. The suspension was stirred at 800 rpm for desired reconstruction time in the nitrogen atmosphere at 30 °C. Then the suspension was filtered and washed thoroughly with hot distilled water until pH of the filtrate was reached to 7. The washed filter cake was dried in vacuum and crushed the sample to convert it into powder form. The reconstructed hydrotalcite powder was stored in the vacuum and used as a catalyst for synthesis of jasminaldehyde.

P–XRD Patterns of Reconstructed Hydrotalcite Samples at Varied Reconstruction Time

The reconstructed hydrotalcite samples were characterized by P–XRD, FT–IR and thermogravimetric analysis. The P–XRD patterns of as–synthesized, activated (calcined) and reconstructed hydrotalcite at varied reconstruction time are shown in Figure 6.9. The P–XRD pattern of as–synthesized hydrotalcite was well matched with the reported in the literature [9]. The sharp and intense peaks of (003) and (006) planes in the 2θ range from 10 to 25° and broad asymmetric reflections at higher diffraction angles (2θ = 30–70°) confirmed the formation of highly crystalline hydrotalcite structure. The Basel spacing of (003) plane *d*-spacing = 7.55 Å is

attributed to the presence of hydroxides anions in the interlayer space of hydrotalcite. P–XRD pattern of activated hydrotalcite consist of broadened peaks that can be assigned to a mixed oxide phase $Mg(Al)O_x$, with diffraction lines at values very similar to that of MgO. Pristine hydrotalcite structure was recovered via reconstruction of activated hydrotalcite in liquid phase using decarbonated water under inert atmosphere. All characteristic peaks of pristine hydrotalcite were observed in the reconstructed hydrotalcite sample within 1 h reconstruction time shows that the Mg and Al coordination modes were restored completely to the original octahedral hydrotalcite structure [24]**.** Reconstruction in the liquid phase took shorter time to completely recover the hydrotalcite structure. Rapid reconstruction of hydrotalcite is due to the efficient wetting of the surface of mixed oxides with the solution. As the reconstruction time of hydrotalcite increases, the peaks intensities of (003) and (006) planes, which are directly proportional to the crystallinity of hydrotalcite were also observed to increase.

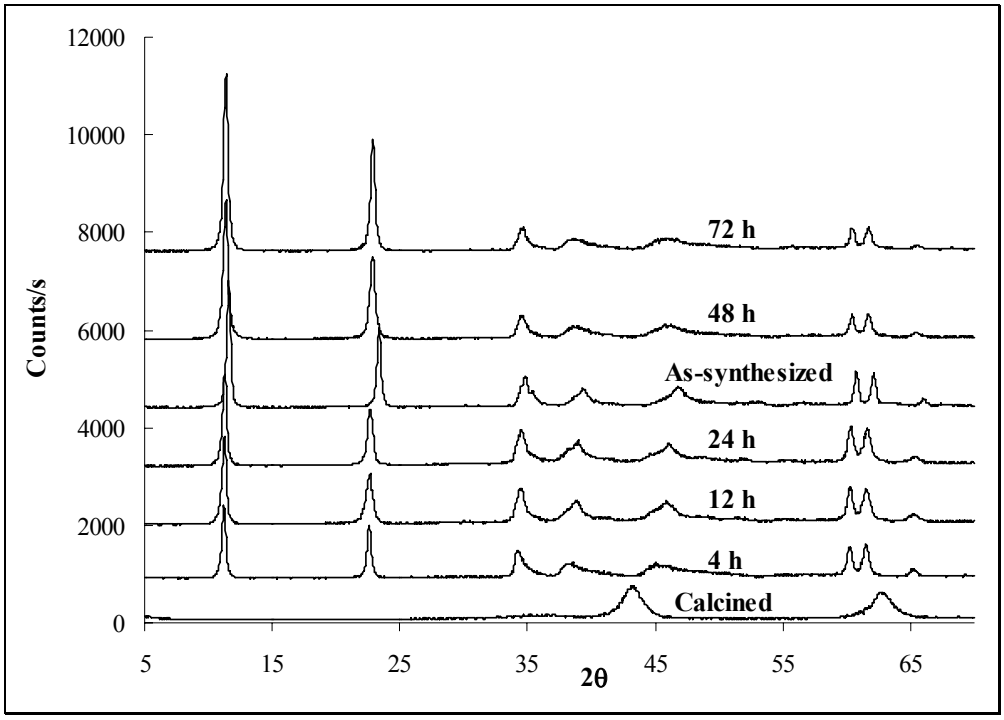

Figure 6.9. P–XRD patterns of as–synthesized, calcined and reconstructed hydrotalcite at different reconstruction time.

The degree of reconstruction (α) with respect to time was calculated by comparing the peak intensities of (003) and (006) planes of each sample with the peak intensities of (003) and (006) planes obtained at 72 h reconstruction time. The 72 h sample was assumed as a completely reconstructed hydrotalcite sample [25]. The degree of reconstruction was observed to increase linearly upto 12 h (Figure 6.10). As the time increased from 12 to 72 h, slow increase in the degree of reconstruction was observed.

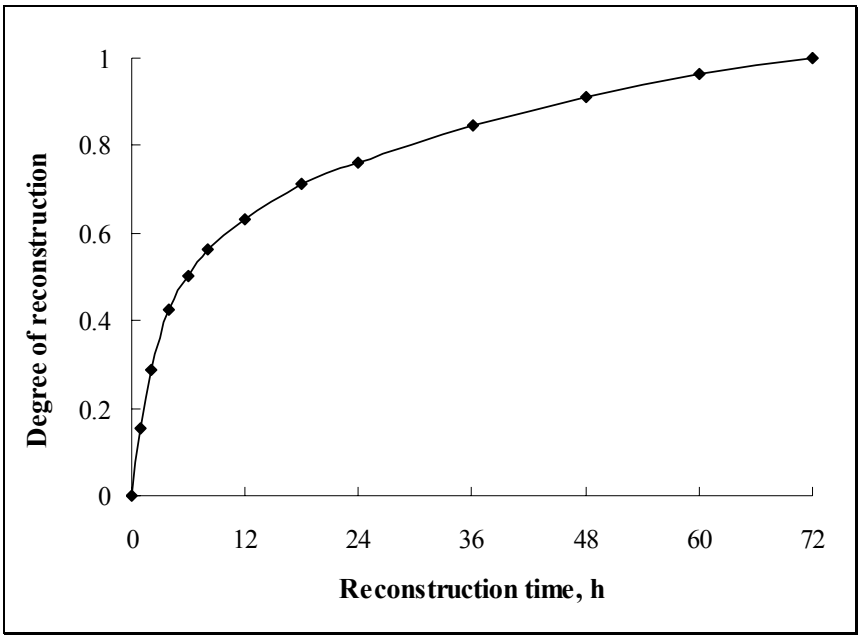

Figure 6.10. Degree of reconstruction of hydrotalcite with respect to time.

FT–IR Spectra of Reconstructed Hydrotalcite Samples at Varied Reconstruction Time

FT–IR spectra of as–synthesized, calcined and reconstructed hydrotalcite at different reconstruction time are shown in Figure 6.11. The absorption band at 3450–3550 cm^{-1}, present in all hydrotalcite samples is due to stretching vibrations of structural OH group in the brucite–like layer. The shoulder present at around 3000 cm^{-1} is attributed to hydrogen bonding between water molecules and interlayer CO_3^{2-} anions. Appearance of shoulder at 1650 cm^{-1} is the characteristic band of interlayer water molecules. The asymmetric stretching vibrations appeared at around 1380 cm^{-1} could be assigned to interlayer carbonates anions. Low frequency region showed bands at about 550, 790, 940 cm^{-1} corresponding to the translation mode of hydroxyl groups mainly influenced by aluminum cations and the band at 635 cm^{-1} is assigned to translation mode of hydroxyl groups mainly influenced by magnesium cations [29]. Calcination of hydrotalcite at 450 °C shows that the water molecules have been removed and this is confirmed by the disappearance of bands at 1650 cm^{-1} (water bending vibrations), and 3000 cm^{-1} (interaction of H_2O–CO_3^{2-} in the interlayer). The intensity of the band at 3450–3500 cm^{-1} also decreased significantly due to the dehydroxylation of hydroxyl groups. Appearance of vibrations at about 3500 and 1380 cm^{-1} showed that the 450 °C is not sufficient calcination temperature for completely removal of hydroxyl groups and carbonate anions present in the interlayers of hydrotalcite (dehydroxylation and decarboxylation). The band appeared at about 447 cm^{-1} is attributed to the vibrations of mixed oxides (MgO and Al_2O_3). Reconstruction of activated hydrotalcite in decarbonated water induced a recovery of original hydrotalcite structure.

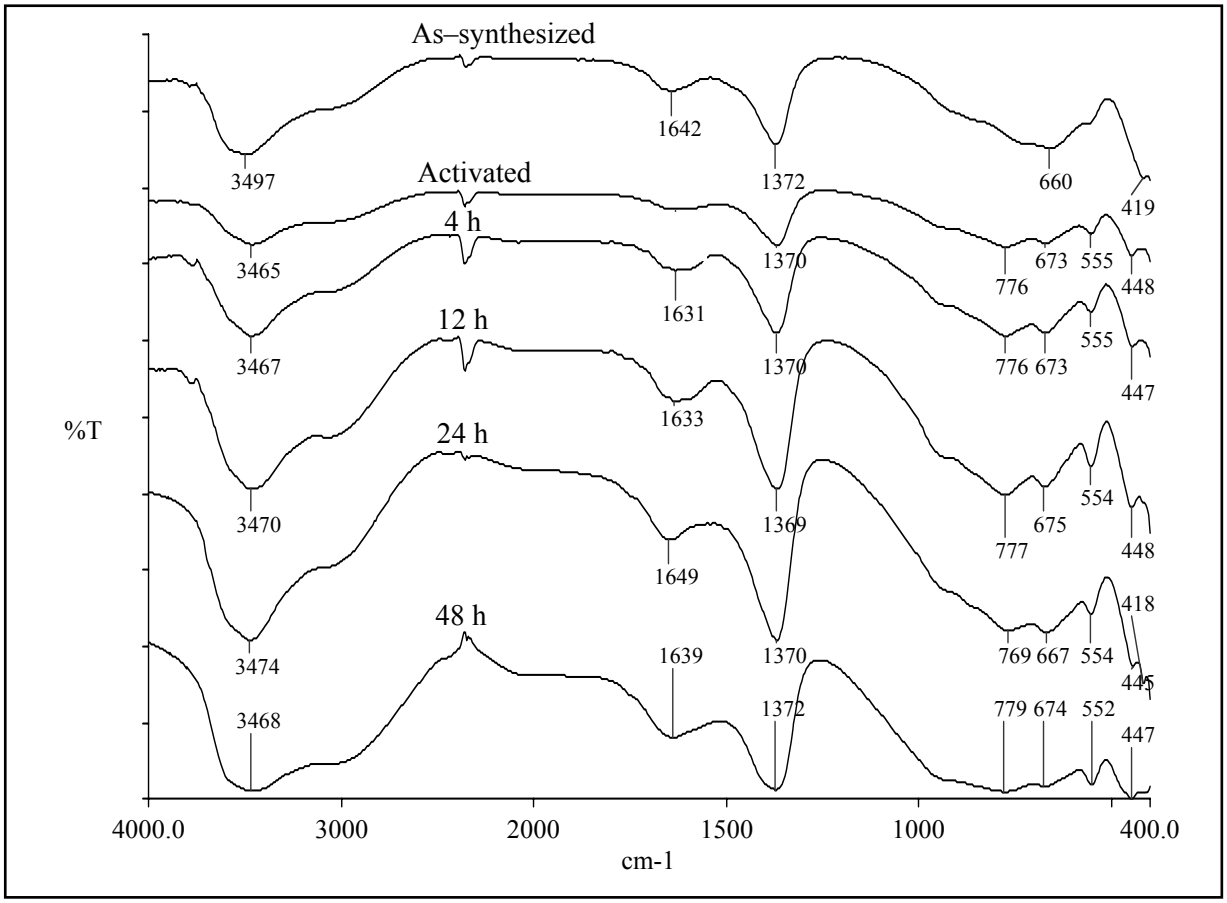

Figure 6.11. FT–IR spectra of as–synthesized, activated and reconstructed hydrotalcite at different reconstruction time.

The presence of band at 3470 cm^{-1} in all reconstructed hydrotalcite samples is due to the presence of structural hydroxyl groups which confirmed the recovery of hydrotalcite structure. The appearance of strong bands at around 3000 and 1650 cm^{-1} also confirmed the presence of water molecules in reconstructed hydrotalcite samples. As the reconstruction time increases, the intensity and broadening of bands at 3470 and 3000 cm^{-1} also increased, which show that the amount of water/hydroxyl groups increased on increasing reconstruction time. Translation modes of hydroxyl groups, influenced by Al^{3+} cations (Mg/Al–OH translation) were remain present in the FT–IR spectra of reconstructed hydrotalcite. The peak at 1380 cm^{-1} assigned to the carbonate anions indicates that the carbonates are still present in the reconstructed hydrotalcite samples.

TGA of Reconstructed Hydrotalcite Samples at Varied Reconstruction Time

Two steps weight loss at respective temperatures were calculated from thermogravimetric analysis (TGA) curves of hydrotalcite samples, shown in Table 6.7. The weight loss in first step is reversible and attributed to the loss of physically adsorbed water molecules with relatively smaller amounts of condensed water without collapse of hydrotalcite structure upto 120 °C. The weight loss in second step was observed due to removal of condensed water molecules (dehydroxylation

of hydroxyl groups) and carbon dioxide from the carbonate anions (decarboxylation) present in interlayer space of hydrotalcite in the temperature range of 420 °C.

Table 6.7. Weight loss of as–synthesized, activated and reconstructed hydrotalcite at different reconstruction time

Reconstruction time, h	T_1, °C	T_2, °C	W_1, %	W_2, %	Total weight loss, %
As–synthesized	125	400	10	26	36
Activated	100	420	2	6	8
0.5	110	410	6	12	18
1	115	410	7	18	25
2	115	400	9	20	29
4	120	390	10	22	32
8	125	405	12	22	34
12	125	410	12	26	38
24	120	400	14	29	43
48	125	400	13	33	46
72	125	410	16	35	51

W_1 =First weight loss at temperature T_1; W_2 =Second weight loss at temperature T_2

In this weight loss, interlayer carbonate anions were thermally oxidized by a nearby interlayer water molecule to produce volatile CO_2 and interlayer hydroxyl anions. The weight loss in the reconstructed hydrotalcite sample was observed to increase on increasing the reconstruction time. For example, 18% total weight loss in the reconstructed hydrotalcite sample was calculated for 0.5 h reconstruction time, which increased to 32% for 4 h and finally 51% for the 72 h reconstruction time. The increase in the weight loss indicates that the amount of hydroxyl groups/water molecules increased on increasing reconstruction time. This is also supported by the observed increase and broadening of peak intensity at about 3470 cm^{-1} in the FT–IR spectra of reconstructed hydrotalcite samples.

6.4.2. Catalytic Activity of Reconstructed Hydrotalcite of Varied Reconstruction Time

Effect of Reconstruction Time on the Catalytic Activity of Reconstructed Hydrotalcite for Synthesis of Jasminaldehyde

The effect of reconstruction time on the catalytic activity of reconstructed hydrotalcite was investigated for the synthesis of jasminaldehyde by condensation of 1–heptanal with benzaldehyde at 130 °C, 1–heptanal to catalyst ratio 10 (by wt) and benzaldehyde to 1–heptanal molar ratio 5 in 3 h reaction time (Figure 6.12). The hydrotalcite of Mg/Al molar ratio 3.5 was taken as precursor for the reconstruction experiments due to its higher basicity and the reconstruction time was varied from 0.5 to 72 h. The conversion of 1–heptanal and selectivity of jasminaldehyde was observed to increase on increasing reconstruction time from 0.5 to 8 h. At 0.5 h reconstruction time, 78% conversion of 1–heptanal was achieved with 70% selectivity of jasminaldehyde. The conversion of 1–heptanal increased to 90% with 80% selectivity of jasminaldehyde using reconstructed hydrotalcite of 6 h reconstruction time as a catalyst. After that small increase in the conversion and selectivity of jasminaldehyde was observed for the hydrotalcite sample of reconstruction time in the range of 8 to 12 h. The conversion of 1–heptanal decreased to 85% for hydrotalcite having 24 h reconstruction time. On further increase in the reconstruction time of hydrotalcite, no significant effect on the conversion of 1–heptanal was observed. The selectivity of jasminaldehyde was also not affected significantly by the reconstruction time of hydrotalcite after 12 h. In view of the higher catalytic activity of reconstructed hydrotalcite sample of 8 to 12 h reconstruction time, the further study for optimization of reaction parameters was carried out by taking reconstructed hydrotalcite of 8 h reconstruction time as a solid base catalyst for the synthesis of jasminaldehyde.

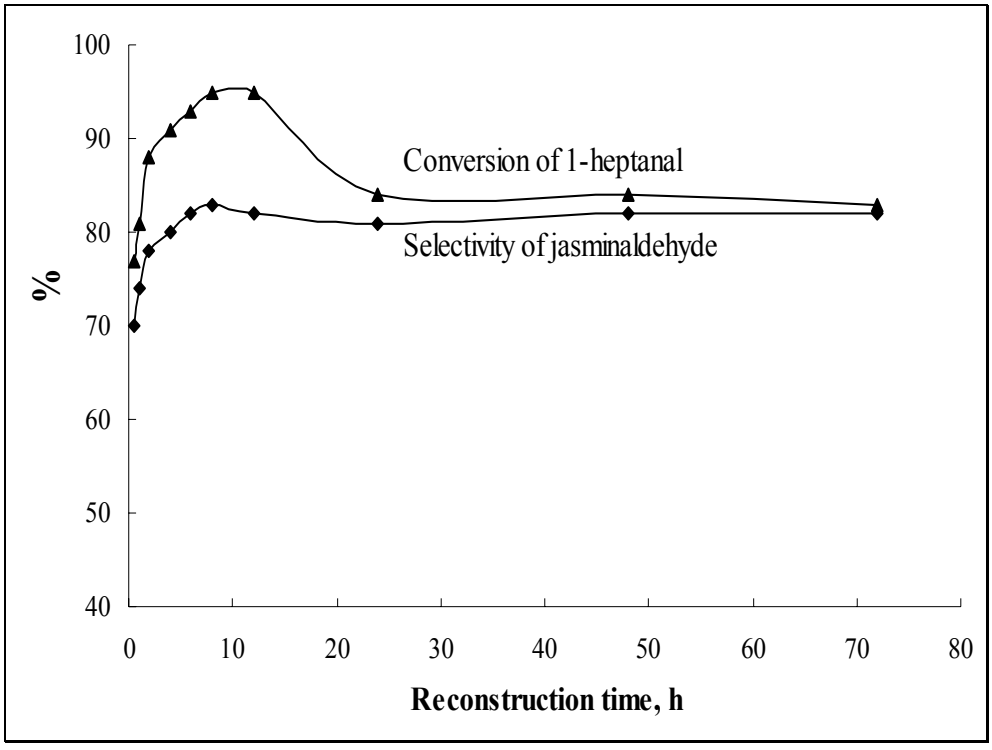

Figure 6.12. Effect of reconstruction time on conversion and selectivity for the synthesis of jasminaldehyde.

The catalytic activity of as–synthesized, calcined and reconstructed hydrotalcite samples was compared for synthesis of jasminaldehyde in order to understand the effect of reconstruction on the progress of reaction at 130 °C, 1–heptanal to catalyst ratio 10 (by wt) and benzaldehyde to 1–heptanal molar ratio 5. The higher conversion of 1–heptanal in shorter reaction time was observed for reconstructed hydrotalcite as a catalyst (Figure 6.13a). 87% conversion of 1–heptanal was achieved in 1 h using reconstructed hydrotalcite as a catalyst, while 43 and 30% conversion of 1–heptanal was achieved using as–synthesized and calcined hydrotalcite, respectively as a catalyst in the similar reaction time (Figure 6.13a). In case of reconstructed hydrotalcite, the conversion of 1–heptanal reached to the 98% within 2 h reaction time, however, 60 and 47% conversion was obtained using as–synthesized and calcined hydrotalcite, respectively, as a catalyst in 2 h reaction time. Higher selectivity of jasminaldehyde was achieved in case of reconstructed hydrotalcite as a catalyst as compared to as–synthesized hydrotalcite (Figure 6.13b). For example, 66% selectivity of jasminaldehyde was found in 2 h reaction time using as–synthesized hydrotalcite, which increased to 82% for reconstructed hydrotalcite as a catalyst. Lower selectivity of jasminaldehyde was achieved in case of the calcined hydrotalcite as a catalyst as compared to the as–synthesized hydrotalcite. Similar to the as–synthesized hydrotalcite, the selectivity of jasminaldehyde was observed to increase on increasing the reaction time.

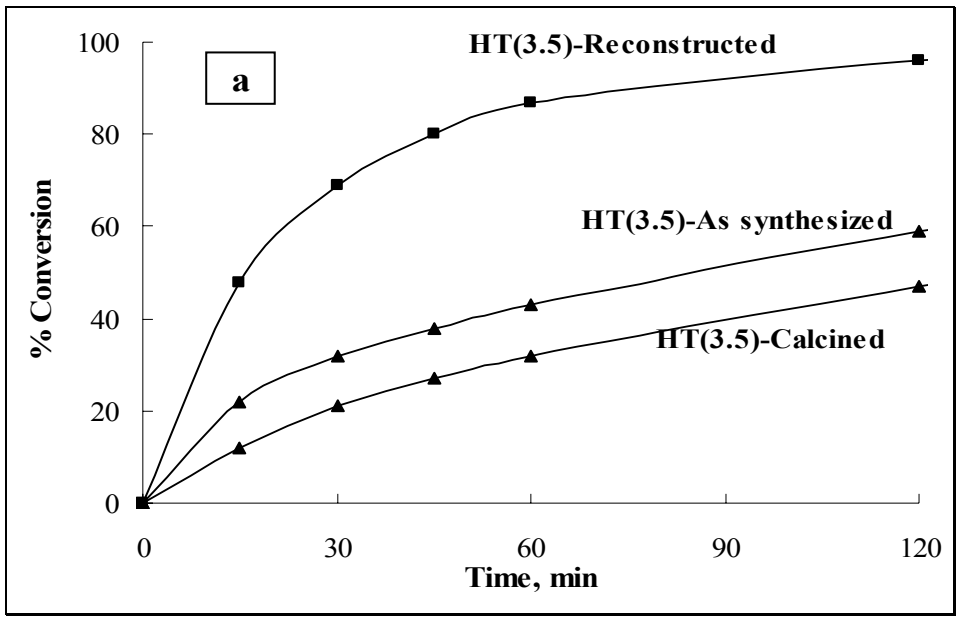

Figure 6.13. (a) Conversion of 1–heptanal using as–synthesized, activated and reconstructed hydrotalcite as catalysts for synthesis of jasminaldehyde.

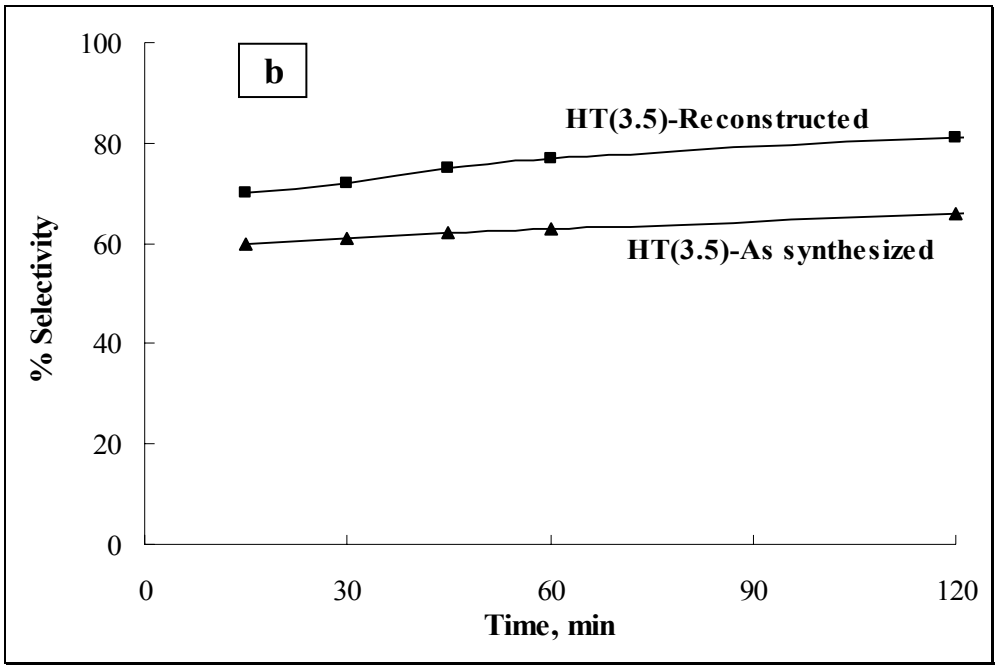

Figure 6.13. (b) selectivity of jasminaldehyde using as–synthesized and reconstructed hydrotalcite as catalysts for synthesis of jasminaldehyde.

When calcined hydrotalcite is stirred with water vapours or immersed in the decarbonated water under inert atmosphere, restoration of original layered structure which contain mainly hydroxyl groups in the interlayer space, takes place due to 'memory effect', yielding a highly active solid base catalyst for the condensation reactions. Higher catalytic activity of the reconstructed hydrotalcite as compared to as–synthesized hydrotalcite is attributed to the presence of higher number of Brønsted basic sites (OH^- groups), which are more active for aldol condensation of aldehydes. Although, lower basicity of the surface in terms of basic strength and number of sites are reported for reconstructed hydrotalcite as compared to activated hydrotalcite, but the main purpose of reconstruction of hydrotalcite is to increase the rate of reaction rather than conversion and selectivity. Only less than 5% of the OH^- compensating anions of the reconstructed hydrotalcite are active to catalyze the aldol condensation reaction [11]. This suggests that the active hydroxyl groups are located on the defective sites at the edge of layers of reconstructed hydrotalcite. These hydroxyl groups are likely to be bonded to low coordination sites which exhibit much stronger basicity than those present in the well ordered structure obtained by ion–exchange process or general co–precipitation method instead of reconstruction process [10]. The basic strength of reconstructed hydrotalcite can be controlled by modifying the number of defects in the framework. The basic strength of activated hydrotalcite is similar to super base, but can be decreased to medium level by absorption of water or used as a catalyst where water is generated during the reaction. The higher conversion of 1–heptanal and selectivity of jasminaldehyde in lower reaction time is due to the accessibility of large amount of Brønsted basic sites available on

the defective sites of reconstructed hydrotalcite samples. The another reason for higher activity of the reconstructed hydrotalcite could be attributed to the decrease in agglomerization during the nucleation and crystal growth process which results into smaller crystals size as compared to the as–synthesized hydrotalcite.

6.4.3. Kinetic Study for the Synthesis of Jasminaldehyde using Reconstructed Hydrotalcite as a Catalyst

Effect of other reaction parameters such as, stirring speed, amount of catalyst, reaction temperature and benzaldehyde to 1–heptanal molar ratio on the conversion of 1–heptanal and selectivity of jasminaldehyde was studied by taking reconstructed hydrotalcite of 8 h reconstruction time as a catalyst.

Effect of Stirring Speed on the Conversion of 1–Heptanal, Selectivity of Jasminaldehyde and Rate of Reaction

In order to ensure the pure kinetic regime and negligence of mass transfer resistance, the reaction was carried out first by varying the stirring speed and amount of catalyst. The stirring speed was varied from 0 to 1000 rpm at benzaldehyde to 1–heptanal molar ratio 5 and 1–heptanal to catalyst ratio (by wt) 10. In all the case 96 to 98% conversion of 1–heptanal was achieved within 2 h reaction time at 130 °C temperature (Figure 6.14a).

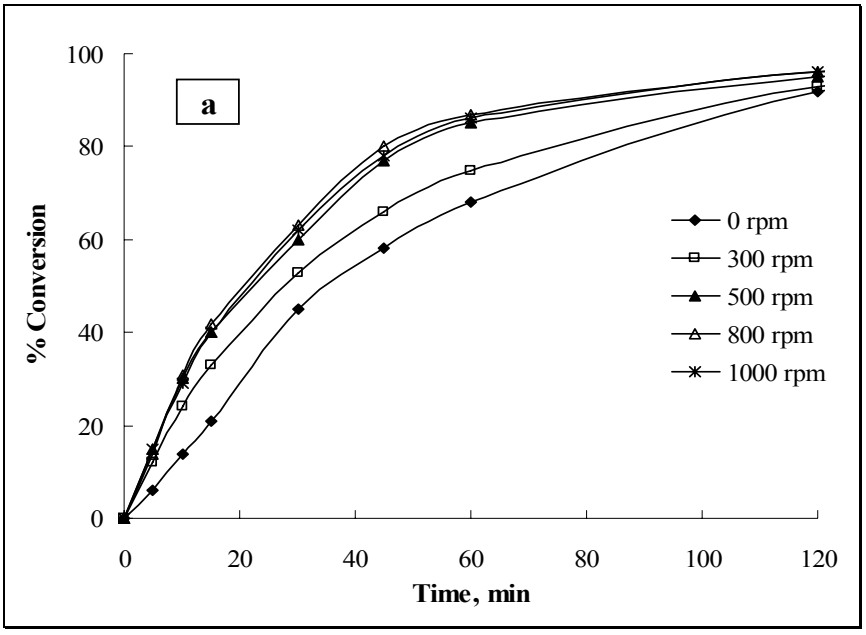

Figure 6.14a. Effect of stirring speed on conversion of 1–heptanal using reconstructed hydrotalcite as a catalyst for the synthesis of jasminaldehyde.

However, difference in the conversion could be seen clearly in lower reaction time region. Without stirring, 68% conversion of 1–heptanal was observed at 0 rpm which increased to 80% on increasing the stirring speed to 500 rpm. On further increase in the agitation speed of reaction from 500 to 800 and finally 1000 rpm, significant effect on conversion was not observed. Any direct linear correlation of stirring speed with the selectivity of jasminaldehyde was not observed, however, selectivity of jasminaldehyde increased significantly on increasing the reaction time (Figure 6.14b). The selectivity of jasminaldehyde was found to increase with the reaction time. For example, at lower stirring speed (300 rpm), the selectivity of jasminaldehyde was observed to increase form 66% in 5 min to 78% in 2 h reaction time. Similarly at 800 rpm, the selectivity of jasminaldehyde increased from 68% in 5 min to 86% in 2 h reaction time.

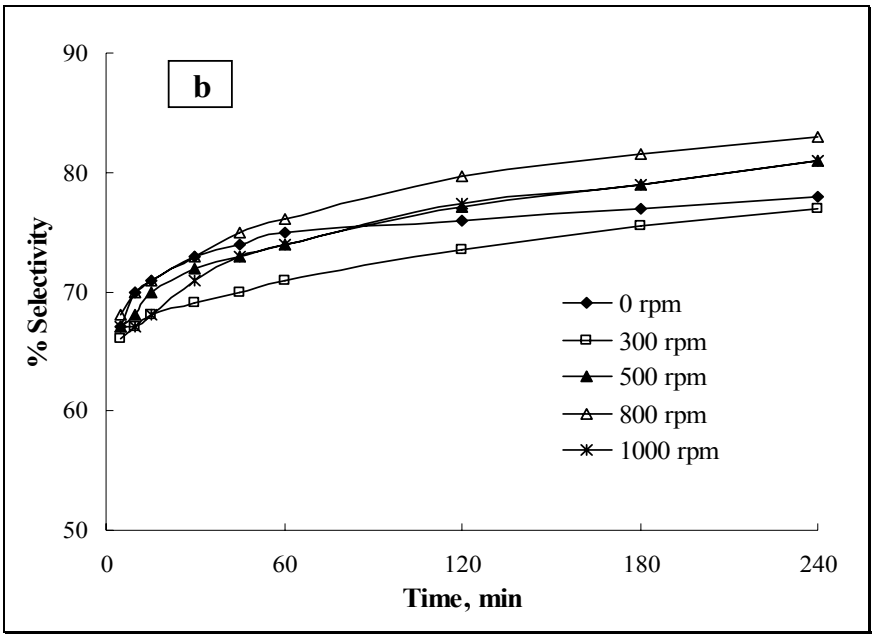

Figure 6.14b. Effect of stirring speed on selectivity of jasminaldehyde using reconstructed hydrotalcite as a catalyst for the synthesis of jasminaldehyde.

The initial rate of reaction calculated in the lower conversion of 1–heptanal (<10%) was found to increase from 0 to 500 rpm (Figure 6.14c). After 500 rpm, the rate of reaction was not affected significantly by the stirring speed. The increase in the rate of reaction upto 500 rpm is due to the combined effect of the mass transfer resistances or diffusional limitations and kinetic effect. However, after 500 rpm the effect of mass transfer resistance in not prominent and reaction moved into pure kinetic region. Therefore, the effect of all other reaction parameters on the selectivity of jasminaldehyde was studied at 800 rpm to ensure the reaction in purely kinetic region. The absence of mass transfer resistance was further confirmed by the effect of catalyst amount on initial rate of reaction.

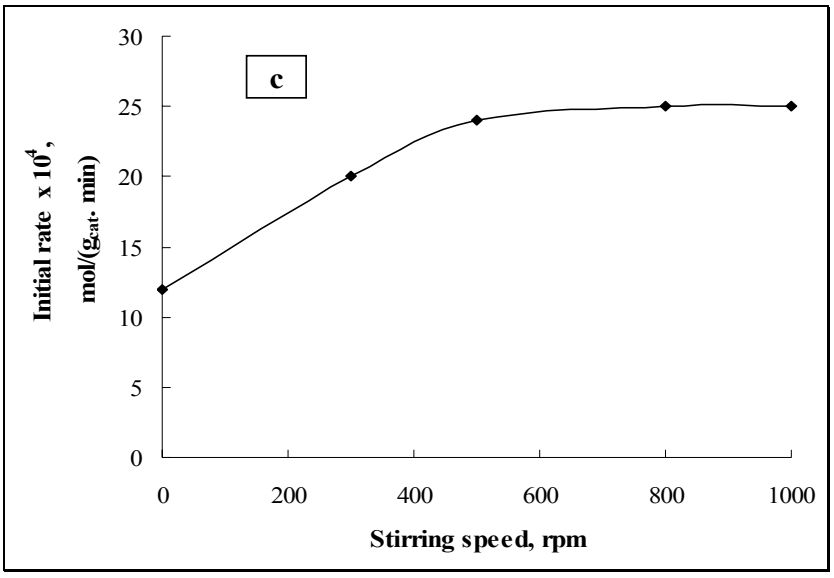

Figure 6.14c. Effect of stirring speed on initial rate of reaction using reconstructed hydrotalcite as a catalyst for the synthesis of jasminaldehyde.

Effect of Catalyst Amount on the Conversion of 1–Heptanal, Selectivity of Jasminaldehyde and Rate of Reaction

The effect of catalyst amount on conversion of 1–heptanal, selectivity of jasminaldehyde and rate of reaction was studied by varying the amount of catalyst from 12 to 250 mg at 130 °C temperature, benzaldehyde to 1–heptanal molar ratio 5 and 800 rpm. The conversion of 1–heptanal was affected significantly by changing the amount of catalyst (Figure 6.15a).

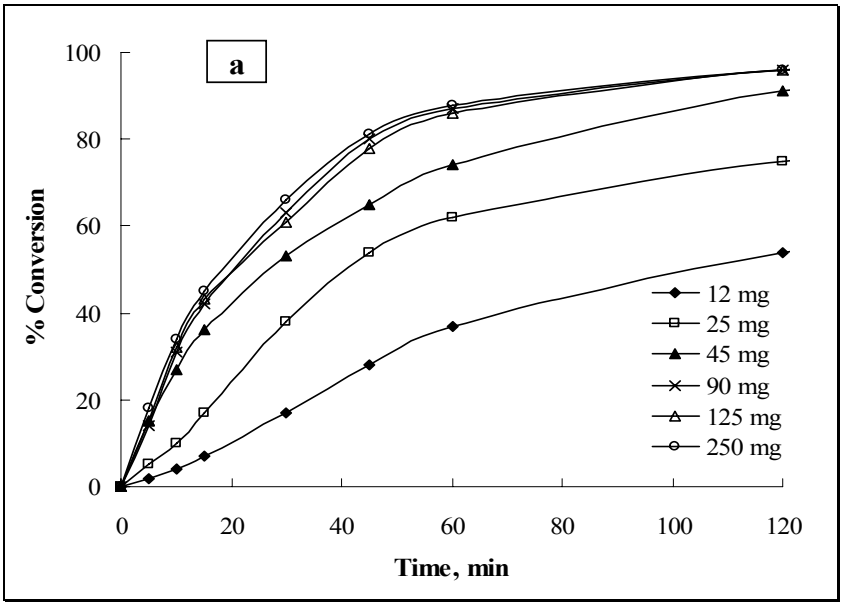

Figure 6.15a. Effect of catalyst amount on conversion of 1–heptanal using reconstructed hydrotalcite as a catalyst for the synthesis of jasminaldehyde.

Lower conversion of 1–heptanal with higher selectivity of jasminaldehyde was observed at lower amount of catalyst. At 12 mg catalyst amount, only 36% conversion of 1–heptanal was achieved with 81% selectivity of jasminaldehyde. The conversion of 1–heptanal increased to 64% at 25 mg and 75% at 45 mg catalyst amount in 60 min reaction time at the cost of slight decrease in the selectivity of jasminaldehyde. On further increase in the amount of catalyst from 90 to 250 mg, no significant effect on the conversion of 1–heptanal was observed. However, selectivity of jasminaldehyde was observed to decrease significantly on increasing the amount of catalyst (Figure 6.15b).

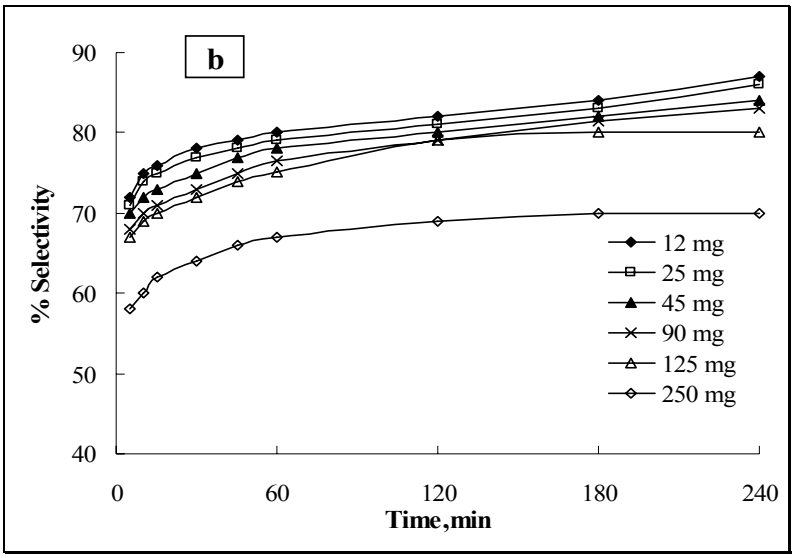

Figure 6.15b. Effect of catalyst amount on selectivity of jasminaldehyde using reconstructed hydrotalcite as a catalyst for the synthesis of jasminaldehyde.

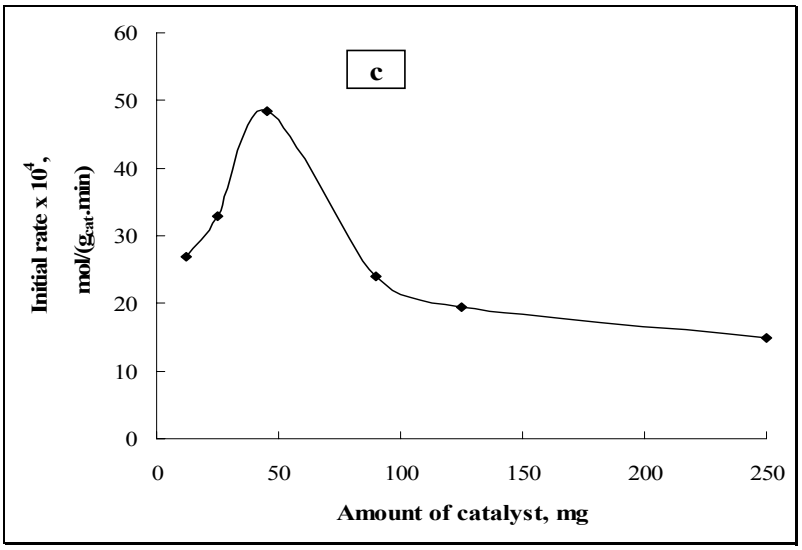

Figure 6.15c. Effect of catalyst amount on initial rate of reaction using reconstructed hydrotalcite as a catalyst for the synthesis of jasminaldehyde.

The initial rate of reaction was observed to increase linearly upto 50 mg catalyst amount (Figure 6.15c). The rate of reaction decreased significantly on increasing the amount of catalyst upto 90 mg. On further increase in the catalyst amount, no significant effect on the rate of reaction was observed which indicate that the reaction was not affected by the mass transfer resistances or diffusional limitations behind 90 mg catalyst amount.

Effect of Benzaldehyde to 1–Heptanal Molar Ratio on the Conversion of 1–Heptanal, Selectivity of Jasminaldehyde and Rate of Reaction

The effect of benzaldehyde to 1–heptanal molar ratio has significant effect not only on rate of reaction but also on the conversion of 1–heptanal and selectivity of jasminaldehyde. Higher conversion of 1–heptanal with lower selectivity of jasminaldehyde was observed at lower benzaldehyde to 1–heptanal ratio due to faster consumption of 1–heptanal either for the jasminaldehyde or 2–n–pentyl–2–nonenal. Almost 91% conversion of 1–heptanal was observed in case of benzaldehyde to 1–heptanal molar ratio in the range of 1–3 in 60 min reaction time (Figure 6.16a).

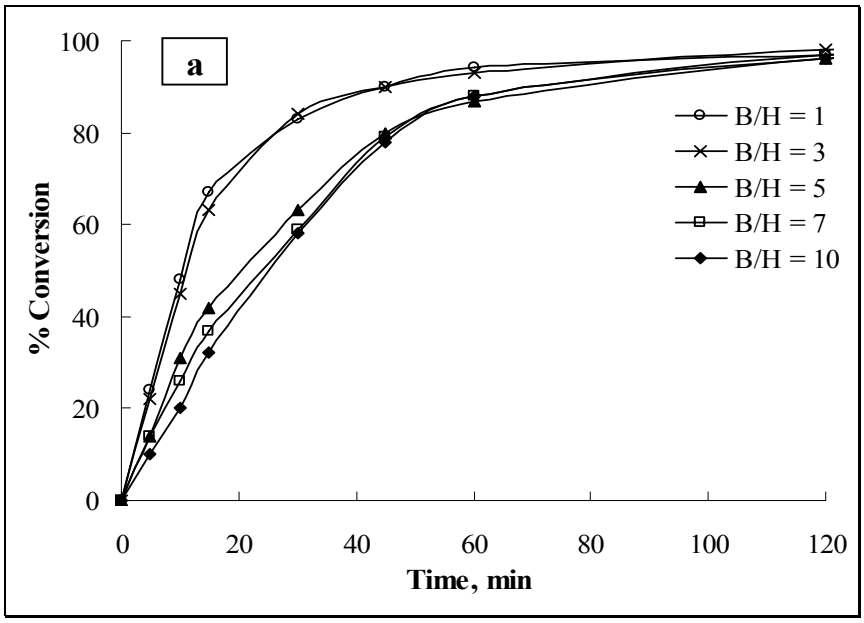

Figure 6.16a. Effect of benzaldehyde to 1–heptanal molar ratio on conversion of 1–heptanal using reconstructed hydrotalcite as a catalyst for the synthesis of jasminaldehyde.

Increasing this ratio to 5, the conversion of 1–heptanal decreased to 80% in similar reaction time. No significant effect on the conversion was observed in the range of benzaldehyde to 1–heptanal molar ratio 5–10 within 60 min reaction time, however, some differences could be seen in the lower reaction time (less than 25 min). For example, 42% conversion of 1–heptanal was observed for benzaldehyde to 1–heptanal molar ratio 5 which decreased to 34% for the ratio 10

within 15 min reaction time. Selectivity of jasminaldehyde was observed to increase on increasing the ratio (Figure 6.16b). At lower benzaldehyde to 1–heptanal molar ratio (1), 44% selectivity of jasminaldehyde was achieved which increased to 63% on increasing the ratio to 3 in 60 min reaction time. For benzaldehyde to 1–heptanal molar ratio 10, 83% selectivity of jasminaldehyde was obtained in 60 min reaction time that increased to 88% on increasing the reaction time to 240 min. The results showed that the conversion of 1–heptanal and selectivity of jasminaldehyde increases significantly on increasing the reaction time. The lower selectivity of jasminaldehyde at lower benzaldehyde to 1–heptanal ratio is due to the presence of 1–heptanal in higher concentration which favors the self condensation reaction rather than the condensation of 1–heptanal with benzaldehyde.

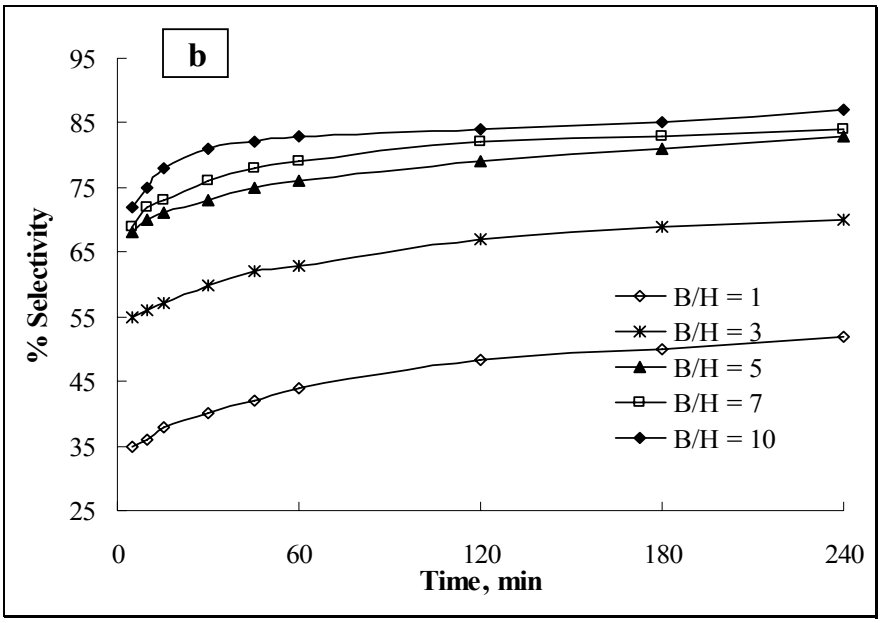

Figure 6.16b. Effect of benzaldehyde to 1–heptanal molar ratio on selectivity of jasminaldehyde using reconstructed hydrotalcite as a catalyst for the synthesis of jasminaldehyde.

Initial rate of reaction for the synthesis of jasminaldehyde was observed to decrease on increasing the benzaldehyde to 1–heptanal molar ratio (Figure 6.16c). At lower molar ratio, for example 1, higher rate of reaction [45 x 10^{-4} mol/(g_{cat} min)] was achieved. The rate of reaction decreased to 37 x 10^{-4} mol/(g_{cat} min) on increasing the molar ratio to 3. On further increase to benzaldehyde to 1–heptanal molar ratio to 5, the initial rate of reaction was found to decrease to 25 x 10^{-4} mol/(g_{cat} min). Significant effect on initial rate of reaction was not observed in the range of benzaldehyde to 1–heptanal molar ratio 5–10.

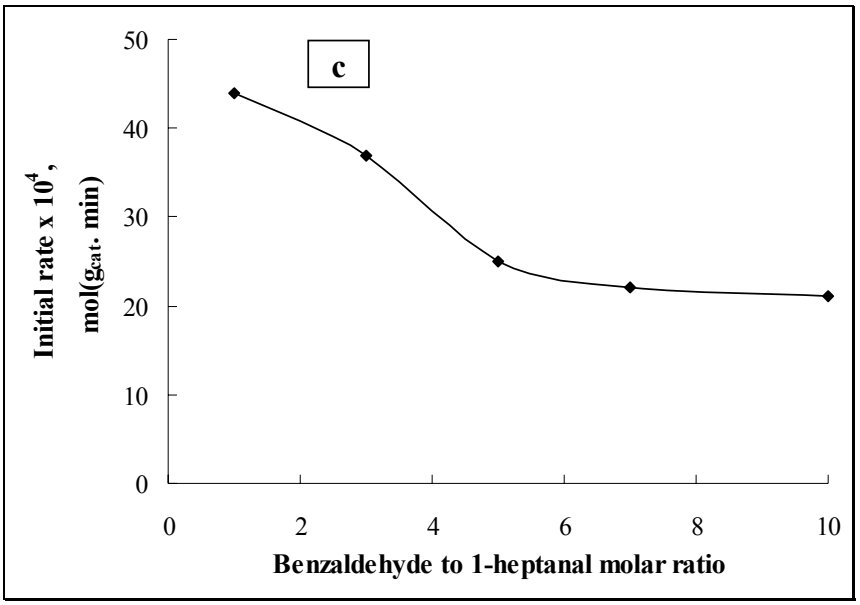

Figure 6.16c. Effect of benzaldehyde to 1–heptanal molar ratio on initial rate of reaction using reconstructed hydrotalcite as a catalyst for the synthesis of jasminaldehyde.

Effect of Reaction Temperature on the Conversion of 1–Heptanal, Selectivity of Jasminaldehyde and Rate of Reaction

The reaction temperature has significant effect on the conversion1–heptanal, selectivity of jasminaldehyde and initial rate of reaction studied in the temperature range of 70 to 170 °C at benzaldehyde to 1–heptanal molar ratio 5 and 1–heptanal to catalyst ratio (by wt) 10 at 800 rpm. Two regions could be visualized clearly from Figure 6.17a; one is the temperature bellow 100 °C and another region is the above 100 °C. The maximum conversion of 1–heptanal (32%) was observed at 70 °C that increased to 52% on increasing the reaction temperature to 100 °C in 120 min. On further increase in the temperature to 130 °C, the conversion reached to 85% within 60 min and 98% in 120 min reaction time. More than 90% conversion of 1–heptanal was achieved within 15 min reaction time by conducting the reaction at 170 °C. Conversion of 1–heptanal increased to 98% in 30 min reaction time at similar reaction temperature. Higher reaction temperature is favoring the faster consumption of 1–heptanal, either for jasminaldehyde or 2–n–pentyl–nonenal. The selectivity data clearly showed that the self condensation of 1–heptanal is faster then the condensation of 1–heptanal with benzaldehyde at higher temperatures (Figure 6.17b). Higher selectivity of jasminaldehyde (87%) was achieved in lower reaction time (45 min) at 70°C. On increasing the temperature 120 °C, similar selectivity of jasminaldehyde was obtained in 240 min. Significant decrease in the selectivity of jasminaldehyde was observed on further increase in the reaction temperature to 170 °C.

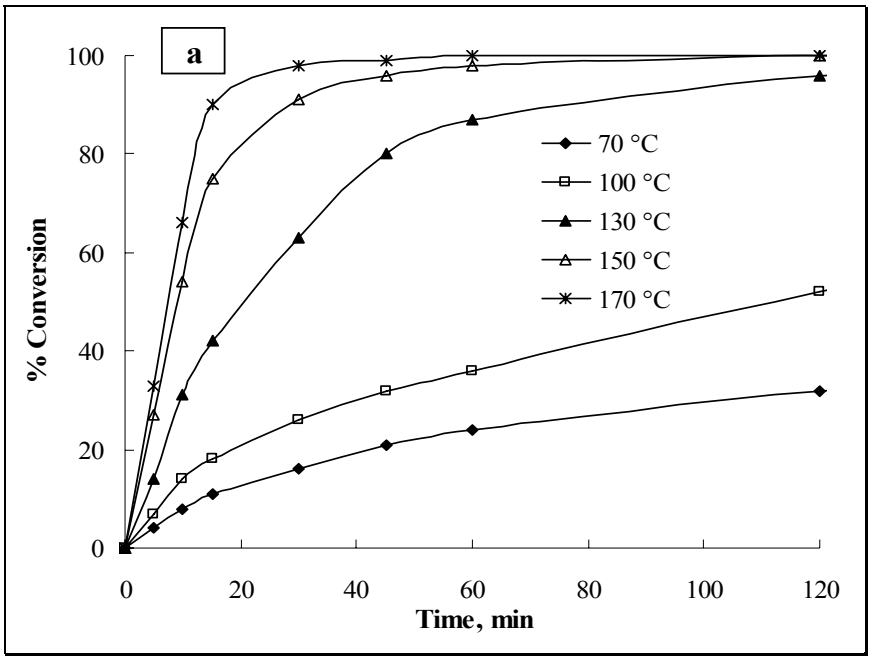

Figure 6.17a. Effect of reaction temperature on conversion of 1–heptanal using reconstructed hydrotalcite as a catalyst for the synthesis of jasminaldehyde.

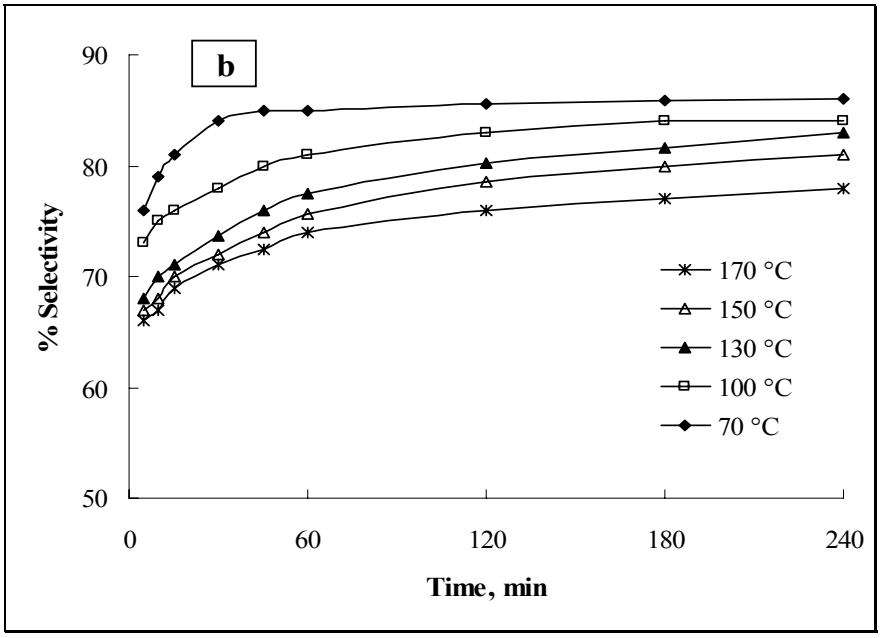

Figure 6.17b. Effect of reaction temperature on selectivity of jasminaldehyde using reconstructed hydrotalcite as a catalyst for the synthesis of jasminaldehyde.

Decrease in the selectivity of jasminaldehyde on increasing reaction temperature is due to the higher self condensation of 1–heptanal to 2–n–pentyl nonenal as compared to the condensation of 1–heptanal with benzaldehyde. The initial rate of reaction was observed to increase on increasing the reaction temperature. Activation energy was calculated by plotting ln k versus 1/T in the temperature range of 130–170 °C (Arrhenius plot; Figure 6.17c). The activation energy was

found to be 37.6 kJ/mol. The calculated activation energy in the present study was not observed in the range of 8–25 kJ/mol, which again indicates that the reaction is far away from the diffusional or mass transfer resistances.

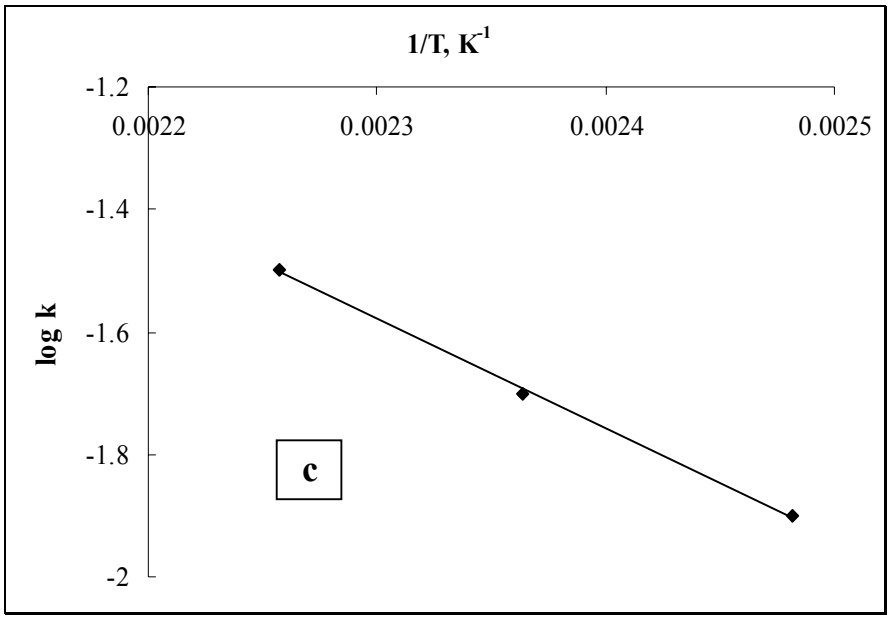

Figure 6.17c. Arrhenius plot.

6.5. Conclusions

The catalytic activity of hydrotalcite ($[M(II)_{1-x}M(III)_x(OH_2)]^{x+}(CO_3^{2-})_{x/n}\cdot mH_2O$; where M(II) = Mg, Ni, Zn and M(III) = Al) was evaluated for the synthesis of jasminaldehyde by solvent free condensation of 1–heptanal with benzaldehyde. The selectivity of jasminaldehyde was observed to increase on increasing the M(II)/Al molar ratio of as–synthesized as well as activated hydrotalcite samples. The maximum selectivity of jasminaldehyde (86%) with 98% conversion of 1–heptanal was observed using as–synthesized Mg–Al hydrotalcite of Mg/Al molar ratio of 3.5 as a catalyst. The effect of activation of as–synthesized Mg–Al hydrotalcite samples of varied Mg/Al molar ratio on catalytic activity was studied and correlated with their basicity as determined from the model test reaction. The activated hydrotalcite was found to be more active for self condensation of 1–heptanal as compared to the condensation of 1–heptanal with benzaldehyde. The effect of reaction parameters such as, amount of catalyst, benzaldehyde to 1–heptanal molar ratio and reaction temperature on conversion of 1–heptanal and selectivity of jasminaldehyde was studied in detail. The conversion of 1–heptanal was observed to increase from 70 to 100% with decrease in selectivity of jasminaldehyde from 86 to 70% on increasing the amount of Mg–Al(3.5) as a catalyst from 20 to 500 mg. Benzaldehyde to 1–heptanal molar ratio was observed to influence the selectivity of jasminaldehyde significantly. The rate of reaction was calculated as 11.6 x 10^{-4}

mol/(g_{cat} min) at optimum reaction conditions. No significant losses in the conversion of 1–heptanal and selectivity of jasminaldehyde were observed upto three cycles, which shows the reusability of the catalyst. On reconstruction of hydrotalcite in liquid phase, catalytic activity of the reconstructed hydrotalcite was observed to increase significantly as compared to as–synthesized and activated hydrotalcite samples as a catalyst for synthesis of jasminaldehyde. The reconstructed hydrotalcite samples of 8–12 h reconstruction time showed higher conversion of the 1–heptanal and higher selectivity of jasminaldehyde in the studied reaction conditions. Kinetics for the synthesis of jasminaldehyde was carried out which include to the effect of reconstruction time, stirring speed, amount of catalyst, benzaldehyde to 1–heptanal molar ratio and reaction temperature. The activation energy calculated from Arrhenius plot in the temperature range of 130–170 °C was found to be 37.6 kJ/mol.

6.6. References

[1] L.S. Payne, EP Patent, 0392579 A2 (1990) to Unilever.

[2] M.J. Climent, A. Corma, V. Fornes, R.G. Lopez, S. Ibora, Adv. Syn. Catal. 344 (2002) 1090–1096.

[3] M.J. Climent, A. Corma, H. Garcia, R.G. Lopez, S. Ibora, V. Fornes, J. Catal. 197 (2001) 385–393.

[4] M.J. Climent, A. Corma, R.G. Lopez, S. Ibora, J. Primo, J. Catal. 175 (1998) 70–79.

[5] J.I. Yu, Y. Shiau, A.N. Ko, Catal. Lett. 77 (2001) 165–169.

[6] S. Jaenicke, G.K. Chuah, X.H. Lin, X.C. Hu, Micropor. Mesopor. Mater. 35–36 (2000) 143–153.

[7] J.I. Yu, Y. Shiau, A.N. Ko, React. Kinet. Catal. Lett. 72 (2001) 365–372.

[8] M.J. Climent, A. Corma, S. Ibora, A. Velty, J. Mol Catal. A: Chem. 182–183 (2002) 327–342.

[9] F. Cavani, F. Trifiro, A. Vaccari, Catal. Today 11 (1991) 173–301.

[10] G.J. Kelly, F. King, M. Kett, Green Chem. 4 (2002) 392–399; D. Tichit, M.J.M. Ortiz, D. Francova, C. Gerardin, B. Coq**,** R. Durand, F. Prinetto, G. Ghiotti, Appl. Catal. A: Gen. 318 (2007) 170–177.

[11] J.C.A.A. Roelofs, D.J. Lensveld, A.J. van Dillen, K.P. de Jong, J. Catal. 203 (2001) 184–191.

[12] F. Figueras, J. Lopez, J. Sanchez–Valente, T.T. H. Vu, J.M. Clacens, J. Palomeque, J. Catal. 211 (2002) 144–149.

[13] D. Carriazo, C. Martin, V. Rives, A. Popescu, B. Cojocaru, I. Mandache, V.I. Parvulescu, Micropor. Mesopor. Mater. 95 (2006) 39–47.

[14] J.S. Valente, F. Figueras, M. Gravelle, J. Lopez, J.P Besse, J. Catal. 189 (2000) 370–381.

[15] V.K. Srivastava, H.C. Bajaj, R.V. Jasra, Catal. Commun. 4 (2003) 543–548.

[16] D.J. Macquarrie, D.B. Jackson, Chem. Commun. (1997) 1781–1782; D. Tichit, B. Coq**,** S. Cerneaux, R. Durand, Catal. Today 75 (2002) 197–202.

[17] M.J. Climent, A. Corma, S. Iborra, J. Primo, J. Catal. 151 (1995) 60–66.

[18] D. Tichit, M.N. Bennani, F. Figueras, R. Tessier, J. Kervenal, Appl. Clay Sci. 13 (1998) 401–415.

[19] D. Tichit, D. Lutic, B. Coq, R. Durand, R. Teissier, J. Catal. 219 (2003) 167–175; D. Tichit, B. Coq, Cattech. 7 (2003) 206–217.

[20] P. Kustrowski, D. Sulkowska, L. Chmielarz, A.R. Lasocha, B. Dudek, R. Dziembaj, Micropor. Mesopor. Mater. 78 (2005) 1–22.

[21] S. Abello, F. Medina, D. Tichit, J.P. Ramirez, J.C. Groen, J.E. Sueiras, P. Salagre, Y. Cesteros, Chem. Eur. J. 11 (2005) 728–739.

[22] J.I. Di Cosimo, V.K. Díez, M. Xu, E. Iglesia, C.R. Apesteguia, J. Catal. 178 (1998) 499–510.

[23] K.K. Rao, M. Gravelle, J.S. Valente, F. Figueras, J. Catal. 173 (1998) 115–121.

[24] J.A. van Bokhoven, J.C.A.A. Roelofs, K.P. de Jong, D.C. Koningsberger, Chem. Eur. J. 7 (2001) 1258–1265.

[25] J.P. Ramirez, S. Abello, N.M. van der Pers, Chem Eur. J. 13 (2007) 870–878.

[26] F. Millange, R.I. Walton, D. O'Hare, J. Mater. Chem. 10 (2000) 1713–1720.

[27] A.I. Khan, D. O'Hare, J. Mater. Chem. 12 (2002) 3191–3198 and reference cited therein.

[28] F. Delorme, A. Seron, M. Bizi, V.J. Prost, D. Martineau, J. Mater. Sci. 41 (2006) 4876–4882.

[29] F. Millange, R. I. Walton, D. O'Hare, J. Mater. Chem. 10 (2000) 1713–1720.

Chapter 7

Selective Double Bond Isomerization of Perfumery Related Chemicals Catalyzed by Transition Metals in Homogeneous and Heterogeneous Conditions

7.1. Introduction

The allyl phenyl ethers have unique importance in perfumery, fragrance and food industries and among the allyl phenyl ethers, *trans*–anethole and isoeugenol have high industrial demand as intermediates for the synthesis of various perfumery chemicals [1–3]. Besides, *trans*–anethole also finds application in alcoholic beverage industry, food industry and in the formulation of oral sanitation products. It is one of the precursors for synthesis of anisic aldehyde, synthetic intermediate for fragrance and flavor industries. The total annual global production of *trans*–anethole is approximately 0.75 million metric tons. *trans*–Isoeugenol which is also known as 2–methoxy–4–(1–propenyl) phenol, is widely used for the synthesis of perfumery chemical, stabilizers and antioxidants for plastic and rubber industries. It is also used in antiseptic and analgesic medicines, as well as for the production of vanillin.

Generally, most of the *trans*–anethole is extracted from the natural sources like anise oil (80–90%), star anise oil (>90%), anise seeds, and fennel oil (80%). The demand of *trans*–anethole in the world market has increased rapidly during last few years due to its growing applications in various products. To meet the growing demand without depending on natural crop, alternative routes for the synthetic preparation of *trans*–anethole have been developed from anisole [4] and methyl chavicol [5]. The existing synthesis of *trans*–anethole from anisole is a multiple step process. Presently, *trans*–anethole is commercially produced by double bond isomerization of methyl chavicol using liquid bases like KOH and/or NaOH in stoichiometric amounts at 200 °C reaction temperature. Under these conditions 56% conversion is achieved in 12 h reaction time with a *trans to cis* anethole ratio of 82:18 in the product mixture. Additionally, anethole obtained from certain natural sources and synthesized from methyl chavicol is always accompanied with the *trans* and *cis* isomers (mostly cis isomer >15%). Thermodynamically, *trans*–isomer is more stable as compared to *cis* and commercially *trans*–isomer is an important valuable product for various applications. According to food regulatory instructions, more than 1% cis isomer cannot be tolerated due to its toxicity and sharp, unpleasant taste. On the other hand, present commercial process using liquid base like KOH or NaOH produce *trans* to *cis* ratio of anethole is 82:18. Therefore, the single step preparation of anethole (mixture of *trans* and *cis* isomers) from methyl chavicol via double bond isomerization has drawn a special attention [5–11]. Furthermore, isomerization process in which lower formation of *cis* isomer is desired so that fractional distillation may be effective to separate *cis* isomers from the product mixture [7].

Interestingly, isoeugenol at the commercial level is also being produced by the prolonged heating of eugenol with the stoichiometric amount of liquid base like KOH in the presence of

alcohol, mostly higher alcohols, at higher reaction temperature [12–14].

Thus, the existing commercial processes for the synthesis of *trans*–anethole from methyl chavicol and *trans*–isoeugenol from eugenol via double bond isomerization reaction is beset with demerits like use of strong liquid base in large amount, longer reaction time, lower conversion of reactant, lower selectivity of *trans*–isomer, higher reaction temperature, post synthesis work–up in separation of spent KOH or NaOH from reactant/product mixture, hazardous post reaction effluent disposal problems and separation of *cis* isomer from the product mixture.

>C=C< double bond isomerization is commercially important reactions in many industrial process [15–17] and, therefore, selective double bond isomerization under mild conditions using eco–friendly reusable catalyst is highly desired research goal. Transition metals and their complexes have been known to isomerise the double bond due to their strong affinity towards π–electrons of double bond [17]. Although catalytic double bond isomerization of alkenes by transition metal complexes has been well documented and applied to commercial processes, the stereo–selectivity and activity control is still a concern in these processes [15-16, 18-19]. Additionally, studies on the effect of various ligands on the metal for double bond isomerization reactions are not reported in literature. Therefore, present chapter explore the applicability of transition metals with various ligands as catalysts for selective double bond isomerization of methyl chavicol to trans–anethole and eugenol to *trans*–isoeugenol in homogeneous conditions. The heterogenization of ruthenium, which observed to be more selective catalyst for double bond isomerization reaction in homogeneous conditions among all studied metals, was carried out on the different solid supports. The activity and reusability of the various ruthenium supported catalysts were studied for isomerization of methyl chavicol and other perfumery compounds.

7.2. Experimental

7.2.1. Materials

Magnesium nitrate [$Mg(NO_3)_2.6H_2O$; 98.9%], aluminum nitrate [$Al(NO_3)_3.9H_2O$; 99.1%], magnesium chloride [$MgCl_2.6H_2O$; 98%], aluminum chloride [$AlCl_3.9H_2O$; 98%], sodium carbonate [Na_2CO_3; 99.9%], sodium hydroxide [NaOH; 99.9%], silica [SiO_2], CaO, MgO and alumina [Al_2O_3] were purchased form s. d. Fine Chemicals Ltd., Mumbai, India and used as such received. Ruthenium trichloride [$RuCl_3.3H_2O$], triphenylphosphine [PPh_3], triphenylarsine [$AsPh_3$], triphenylantimony [$SbPh_3$], methyl chavicol (98%), eugenol (98%), safrole (98.5%), allylbenzene (99.3%), 3–carene (99%), dimethoxy allylbenzene (99.2%) and tetradecane (99.8%) were procured from Sigma Aldrich, USA and used without further purification. The double distilled deionized

milli–pore water was used for the synthesis of catalysts. The precursors of rhodium and palladium for the synthesis of the metal complexes were purchased from Sigma Aldrich, USA.

7.2.2. Synthesis of Rhodium (Rh), Ruthenium (Ru) and Palladium (Pd) Metal Complexes

The metal complexes $RhCl(PPh_3)_3$, $RhCl(AsPh_3)_3$, $RhCl(SbPh_3)_3$, $RuCl_2(SbPh_3)_3$, $PdCl_2(PPh_3)_2$, $PdCl_2(AsPh_3)_2$ and $PdCl_2(SbPh_3)_2$ were synthesized by the reported procedures [20–23].

Synthesis of tris(triphenylphosphine)chlororhodium(I), $RhCl(PPh_3)_3$

A solution of $RhCl_3.3H_2O$ (2.0 g) in hot ethanol (70 mL) was added to a solution of PPh_3 (12.0 g) in hot ethanol (350 mL) and the resulting solution was heated under reflux for 30 min in N_2 atmosphere. The hot solution was filtered and red crystal of the complex was washed with ethanol followed by diethyl ether (50 mL) and then dried in vacuum.

Synthesis of tris(triphenylarsine)chlororhodium(I), $RhCl(AsPh_3)_3$

The complex $RhCl(AsPh_3)_3$ cannot be obtained in adequate yield directly from the solutions of $RhCl_3.3H_2O$ in ethanol contrast to the phosphine case. The arsine and antimony complexes of rhodium were synthesized from bis(ethylene)chlororhodium(I), $RhCl(C_2H_4)_2$.

Synthesis of bis(ethylene)chlororhodium(I), $RhCl(C_2H_4)_2$

$RhCl_3.3H_2O$ (1.0 g) was dissolved in 5 mL of degassed 10% aqueous methanol in a thick–walled glass tube. Ethylene was condensed in, and the sealed tube was shaken vigorously for 2 h. The orange crystal (0.48 g), yield 65% (based on Rh) were collected, dried in nitrogen stream and was used immediately. The filtrate could be treated again with ethylene to produce an additional amount of complex.

Synthesis of tris(triphenylarsine)chlororhodium(I), $RhCl(AsPh_3)_3$

$RhCl(C_2H_4)_2$ (0.2 g) was added to a solution of $AsPh_3$ (5.0 g) in hot methanol (15 mL) and the resulted solution was refluxed for 20 min under N_2 atmosphere. Nitrogen saturated anhydrous diethyl ether (15 mL) was then added and the solution was refluxed until brown crystals of complex were formed. Crystals were collected and washed with diethyl ether and dried in vacuum.

Synthesis of tris(triphenylantimony)chlororhodium(I), $RhCl(SbPh_3)_3$

$RhCl(C_2H_4)_2$ (0.2 g) was added to a solution of $SbPh_3$ (5.0 g) in hot methanol (15 mL) and the resulted solution was refluxed for 20 min under N_2 atmosphere. Nitrogen saturated anhydrous diethyl ether (15 mL) was then added and solution was refluxed until bright purple powder of the complex was precipitated. The precipitated material was filtered and washed with diethyl ether and dried in vacuum.

Synthesis of dichlorotris(triphneylphosphine)ruthenium(II), $RuCl_2(PPh_3)_3$

$RuCl_3.3H_2O$ (0.2 g) was dissolved in methanol (50 mL) and six–fold excess (1.2 g) of PPh_3 was added. The solution was refluxed for 4 h under N_2 atmosphere. The resulting reddish brown crystals of the complex were washed with methanol followed by diethyl ether and dried in vacuum.

Synthesis of trichlorobis(triphneylarsine)(methanol)ruthenium(II), $RuCl_3(AsPh_3)_2.CH_3OH$

$RuCl_3.3H_2O$ (0.2 g) was dissolved in methanol (50 mL) and six–fold excess (1.2 g) of $AsPh_3$ was added. The solution was refluxed for 2 h under N_2 atmosphere. The resulting green crystals of the complex were washed with methanol followed by diethyl ether and dried in vacuum.

Synthesis of dichlorotris(triphneylantimony)ruthenium(II), $RuCl_2(SbPh_3)_3$

$RuCl_3.3H_2O$ (0.2 g) was dissolved in methanol (50 mL) and six–fold excess (1.2 g) of $SbPh_3$ was added. The solution was refluxed for 2 h under N_2 atmosphere. The resulting deep red micro–crystals of the complex were washed with methanol followed by diethyl ether and dried in vacuum.

Synthesis of dichlorobis(triphneylphosphine)palladium(II), $PdCl_2(PPh_3)_2$

1.0 mmol solution of $K_2[PdCl_4]$ dissolved in water (5 mL) was added to 2.0 mmol of PPh_3 dissolved in absolute alcohol (5 mL). The reaction mixture was allowed to stirring for 3 min under N_2 atmosphere. The resulting bright yellow solids were isolated by vacuum filtration, washed with slight amount of water, ethanol and finally with diethyl ether and dried in vacuum.

Synthesis of dichlorobis(triphneylarsine)palladium(II), $PdCl_2(AsPh_3)_2$

1.0 mmol solution of $K_2[PdCl_4]$ dissolved in water (5 mL) was added to 2.0 mmol of $AsPh_3$ dissolved in absolute alcohol (5 mL). The reaction mixture was allowed to stirring for 5 min under N_2 atmosphere. The resulting light yellow solids were isolated by vacuum filtration, washed with slight amount of water, ethanol and finally with diethyl ether and dried in vacuum.

Synthesis of dichlorobis(triphneylantimony)palladium(II), $PdCl_2(SbPh_3)_2$

1.0 mmol solution of $K_2[PdCl_4]$ dissolved in water (5 mL) was added to 2.0 mmol of $SbPh_3$ dissolved in absolute alcohol (5 mL). The reaction mixture was allowed to stirring for 5 min under N_2 atmosphere. The resulting yellowish green solids were isolated by vacuum filtration, washed with slight amount of water, ethanol and finally with diethyl ether and dried in vacuum.

7.2.3. Heterogenization of Ruthenium on Solid Base as Supports

Synthesis of Ruthenium Grafted Hydrotalcite [Ru–Mg–Al]

Ruthenium grafted hydrotalcite was prepared by the co–precipitation method at pH = 9±0.5 [24]. In a typical synthesis procedure, an aqueous solution (A) containing $MgCl_2{\cdot}6H_2O$ (0.0522 mol), $AlCl_3{\cdot}H_2O$ (0.0144 mol) and $RuCl_3.3H_2O$ (0.0005 mol) in 50 mL double distilled deionized water was prepared. The solution A was added drop wise into a second solution (B) containing Na_2CO_3 (0.079 mol) in 50 mL double distilled de–ionized water, in around 45 min under vigorous stirring at 30 °C. The constant pH of the mixture was maintained by adding 1 M NaOH solution. The content was then transferred into the teflon coated stainless steel autoclave and aged at 80 °C for 16 h under autogenous water vapor pressure. After 16 h, the precipitate formed was filtered and washed thoroughly with hot distilled water until the filtrate was free from Cl^- ions (silver nitrate test). The obtained filter cake was dried in an oven at 80 °C for 14 h. The solid material (yield = 6.1 g) named as Ru–Mg–Al, was ground and stored under vacuum. The activation of Ru–Mg–Al was carried out in a muffle furnace at 450 °C for 4 h.

Synthesis of Hydrotalcite [HT(3.5)]

The Mg–Al hydrotalcite sample with Mg/Al molar ratio of 3.5 was synthesized by co–precipitation method at constant pH (9±0.5) [25]. In the typical procedure, an aqueous solution (A) of $MgCl_2{\cdot}6H_2O$ (0.0522 mol) and $AlCl_3{\cdot}H_2O$ (0.0149 mol) in 50 mL double distilled deionized water was prepared. The solution A was added drop wise into a second solution (B) containing Na_2CO_3 (0.079 mol) in 50 mL double distilled deionized water, in around 45 min under vigorous stirring at 30 °C. The constant pH of the mixture was maintained by adding 1M NaOH solution. The content was then transferred into the teflon coated stainless steel autoclave and aged at 80 °C for 16 h under autogenous water vapor pressure. After 16 h, the precipitate formed was filtered and washed thoroughly with hot distilled water until pH of the filtrate was 7 and free from Cl^- ions. The washed filter cake was dried in an oven at 80 °C for 14 h. The solid material labeled as HT(3.5) was ground and used as a catalyst for the double bond isomerization of methyl chavicol.

The activation of HT(3.5) was carried out in a muffle furnace at 450 °C for 4 h.

Synthesis of Impregnated Ruthenium Catalyst

Impregnation of ruthenium on various solid base supports namely HT(3.5), MgO, CaO, alumina, SiO_2 was carried out to compare the catalytic activity of Ru–Mg–Al by the following procedure. An aqueous solution of $RuCl_3.3H_2O$ (0.0005 mol) in 40 mL deionized double distilled water was added dropwise to the suspension of 6.1 g respective solid support in 40 mL water at vigorous stirring under N_2 atmosphere. The mixture was stirred for 16 h at 30 °C. The slurry was filtered and washed with hot distilled water until the filtrate free from Cl^- ions (silver nitrate test). Then the solids were dried at 80 °C for 14 h.

7.2.4. Characterization of Catalyst

Fourier transform nuclear magnetic resonance (FT–NMR; ^1H and ^{31}P) for the characterization of transition metal complexes was performed using Bruker–Avance DPX 200 MHz FT–NMR spectroscopy. C, H and N elemental analysis was done using Perkin–Elmer CHNS/O 2400 analyzer.

Fourier transform infrared (FT–IR) spectra of metal complexes, HT(3.5) and Ru–Mg–Al samples were recorded with a Perkin–Elmer spectrum GX–Fourier transform infrared spectrometer (FT–IR) system in the region of 400 to 4000 cm^{-1} using KBr pellets.

Thermogravimetric analysis (TGA) of HT(3.5) and Ru–Mg–Al samples was carried out using a Mettler–Toledo TGA/SDTA 851e equipment in flowing nitrogen (flow rate = 50 mL/min) at a heating rate of 10 °C/min and the data were processed using star^e software.

Surface area measurements of HT(3.5) and Ru–Mg–Al samples were carried out using ASAP 2010 Micromeritics, USA. The samples were activated at 120 °C for 4 h under vacuum (5 x 10^{-2} mmHg) prior to N_2 adsorption measurements. The specific surface area of the samples was calculated from N_2 adsorption isotherms measured at 77.4 K according to the Brunauer, Emmett, Teller (BET) method.

Scanning electron microscopy (SEM) images of HT(3.5) and Ru–Mg–Al samples were obtained using Leo Series VP1430, Germany microscope having silicon detector equipped with EDX facility (Oxford instruments), where the samples were coated with gold using sputter coating to avoid charging. Analyses were carried out at an accelerating voltage of 18 kV and probe current of 102 pA.

7.2.5. Isomerization Reaction and Product Analysis

In a typical experimental reaction, double bond isomerization of methyl chavicol was carried out in a 25 mL oven dried double necked round bottom flask in which calculated amount of methyl chavicol and catalyst were taken with 0.01 g tetradecane as an internal standard. One neck of the flask was fitted with refluxing condenser and another neck of the flask was blocked with silicon rubber septa. The entire experimental setup was kept in an oil bath equipped with temperature and agitation speed controlling unit. The reaction was carried out at desired temperature under nitrogen atmosphere. Progress of the reaction was monitored by taking the samples at different time interval during the course of reaction and analyzed by gas chromatography. Reaction mixture was cooled to room temperature after set reaction time and was subjected for filtration. For kinetic studies, samples (0.01 mL) were taken out during the experiment using glass syringe at different time intervals. The analysis of product mixture was carried out by gas chromatography (GC; Shimadzu 17A, Japan), having 5% diphenyl and 95% dimethyl siloxane universal capillary column (60 m length and 0.25 mm diameter) and flame ionization detector (FID). The initial column temperature was increased from of 100 to 220 °C at the rate of 10 °C/min using nitrogen as a carrier gas. The temperature of injection port and FID were kept 250 and 300 °C, respectively, during the analysis of product mixture. The retention times for each compound were determined by injecting pure compounds under identical GC conditions. The % conversion and selectivity for each product were calculated as follows –

$$\% \text{ Conversion} = \left(\frac{\text{moles of methyl chavicol reacted}}{\text{moles of methyl chavicol fed}} \right) \times 100$$

$$\% \text{ Selectivity for } \textit{trans}\text{-anethole} = \left(\frac{\text{moles of } \textit{trans}\text{-anethole}}{\text{moles of } \textit{trans}\text{-anethole + moles of } \textit{cis}\text{-anethole}} \right) \text{ x } 100$$

$$\% \text{ Selectivity for } \textit{cis}\text{-anethole} = \left(\frac{\text{moles of } \textit{cis}\text{-anethole}}{\text{moles of } \textit{trans}\text{-anethole + moles of } \textit{cis}\text{-anethole}} \right) \text{ x } 100$$

7.3. Results and Discussion

7.3.1. Characterization of Transition Metal Complexes

The ^{31}P–NMR spectra of the complexes $PdCl_2(PPh_3)_2$ (in $CHCl_3$), $RuCl_2(PPh_3)_3$ (in

CH_2Cl_2), $HRh(CO)(PPh_3)_3$ and $RhCl(PPh_3)_3$ (in C_6H_6) gave doublets at 41.42 ppm, 43.04 ppm, 48.89 ppm and 47.32 ppm, respectively which verifies the formation of complexes. The appearance of $\nu_{(Pd-P)}$, $\nu_{(Pd-As)}$ and $\nu_{(Pd-Sb)}$ bands at 506 cm^{-1}, 468 cm^{-1} and 442 cm^{-1}, respectively confirms the formation of corresponding palladium complexes. The FT–IR spectra of rhodium and ruthenium complexes are shown in Figure 7.1. Metal Complexes; C, H calculated (found): $RhCl(PPh_3)_3$; C: 70.1 (70.0); H: 4.9 (5.0); $RhCl(AsPh_3)_3$; C: 61.3 (61.1); H 4.9 (4.8), $RhCl(SbPh_3)_3$; C: 54.1 (54.0); H 3.8 (3.6), $HRh(CO)(PPh_3)_3$; C: 71.9 (71.8), H: 5.0 (5.1)**,** $RuCl_2(PPh_3)_3$; C: 67.7 (67.5); H: 4.7 (4.5), $RuCl_3(AsPh_3)_2.CH_3OH$; C 52.2 (52.1); H 4.0 (4.1), $RuCl_2(SbPh_3)_3$; C:52.7 (52.5); H 3.7 (3.6), $PdCl_2(PPh_3)_2$; C: 61.6 (61.4); H: 4.3 (4.2), $PdCl_2(AsPh_3)_2$; C: 54.7 (54.3); H:3.8 (3.7) and $PdCl_2(SbPh_3)_2$; C: 48.9 (48.7); H: 3.4 (3.5).

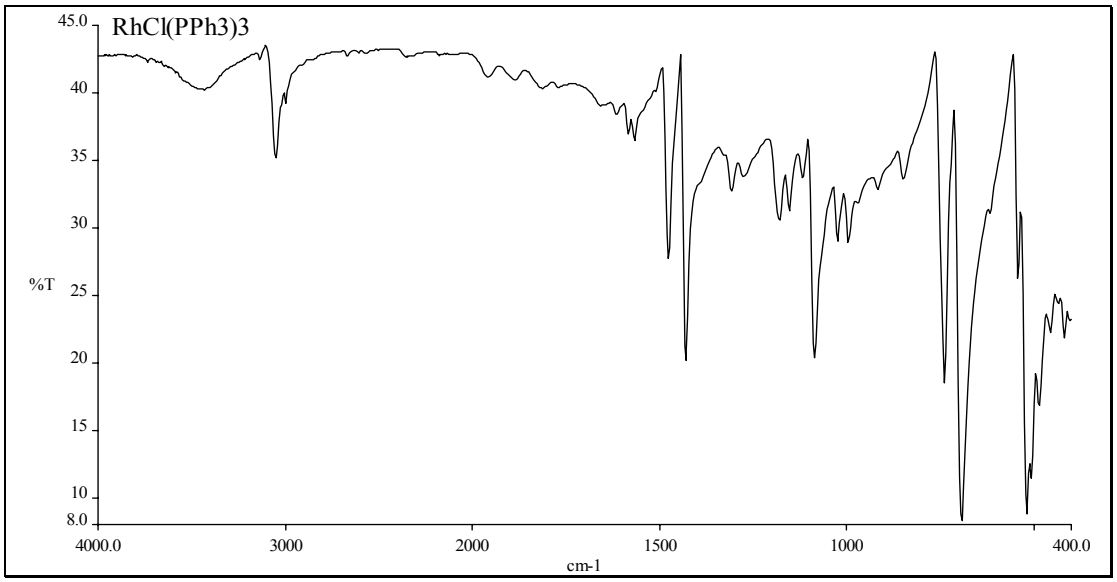

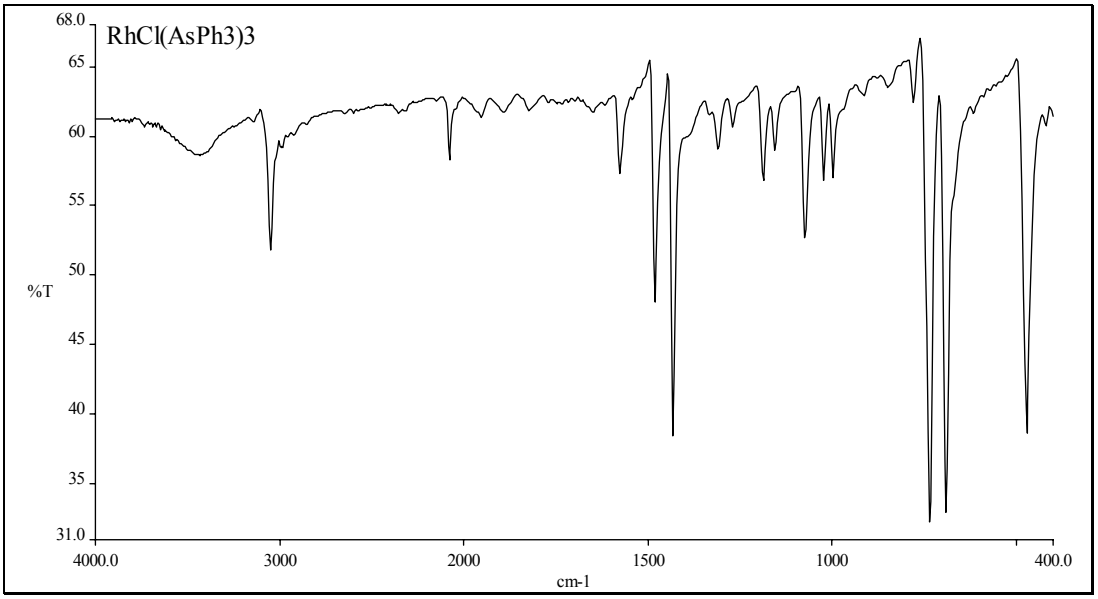

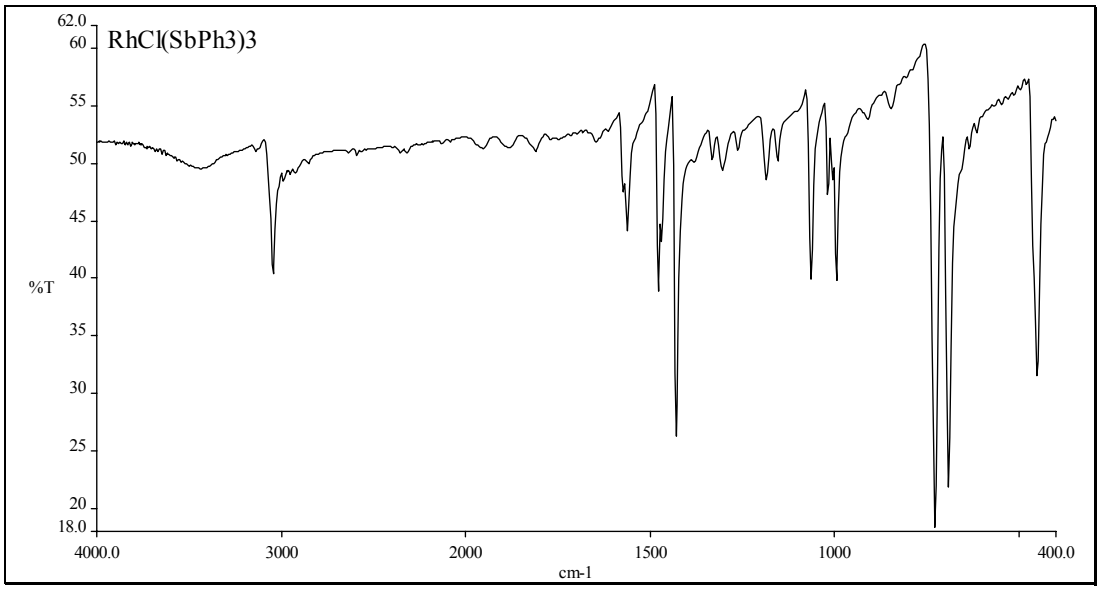
RhCl(SbPh3)3
%T
cm-1
4000.0
3000
2000
1500
1000
400.0

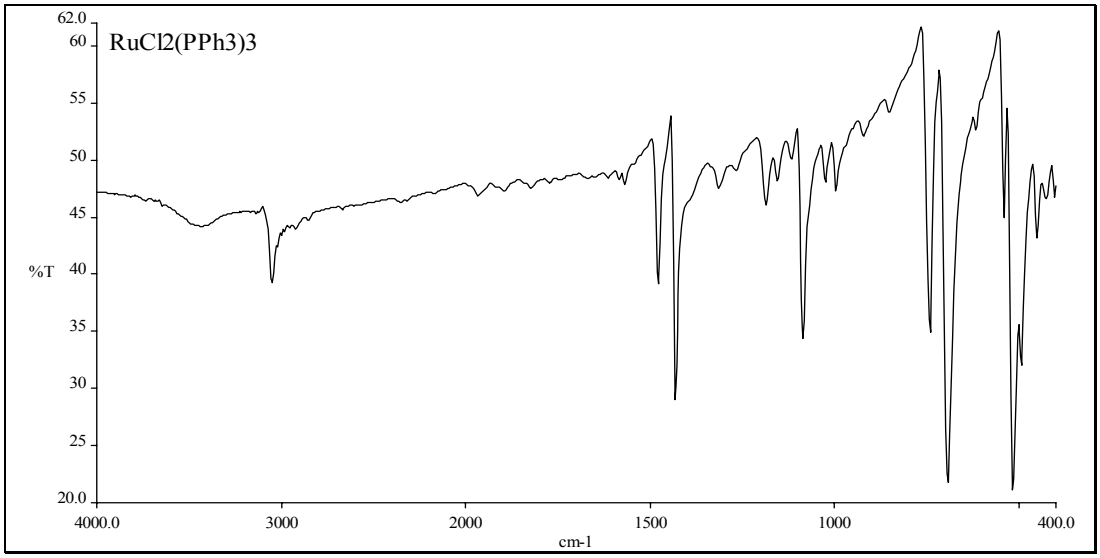
RuCl2(PPh3)3
%T
cm-1
4000.0
3000
2000
1500
1000
400.0

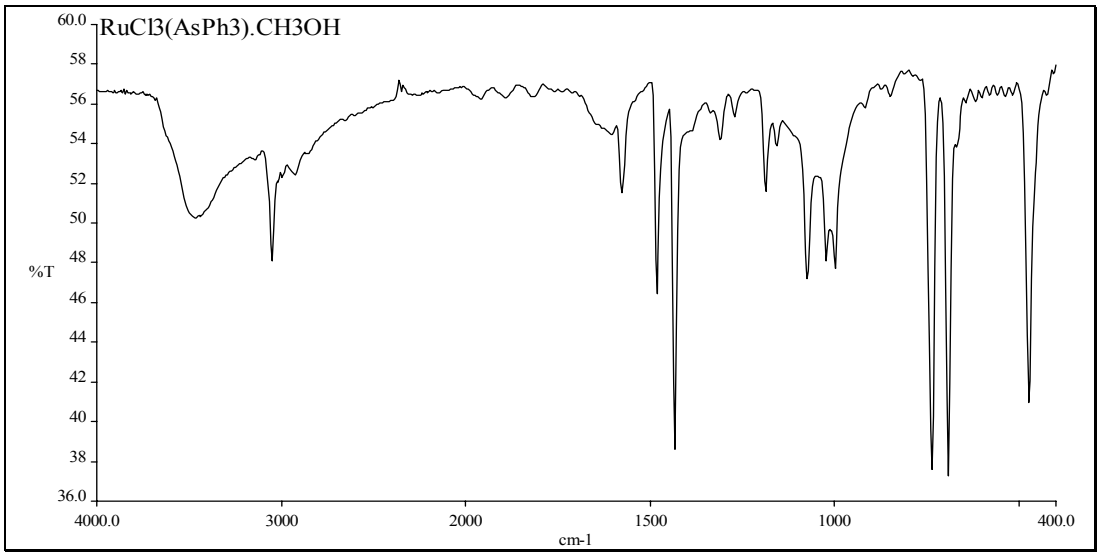
RuCl3(AsPh3).CH3OH
%T
cm-1
4000.0
3000
2000
1500
1000
400.0

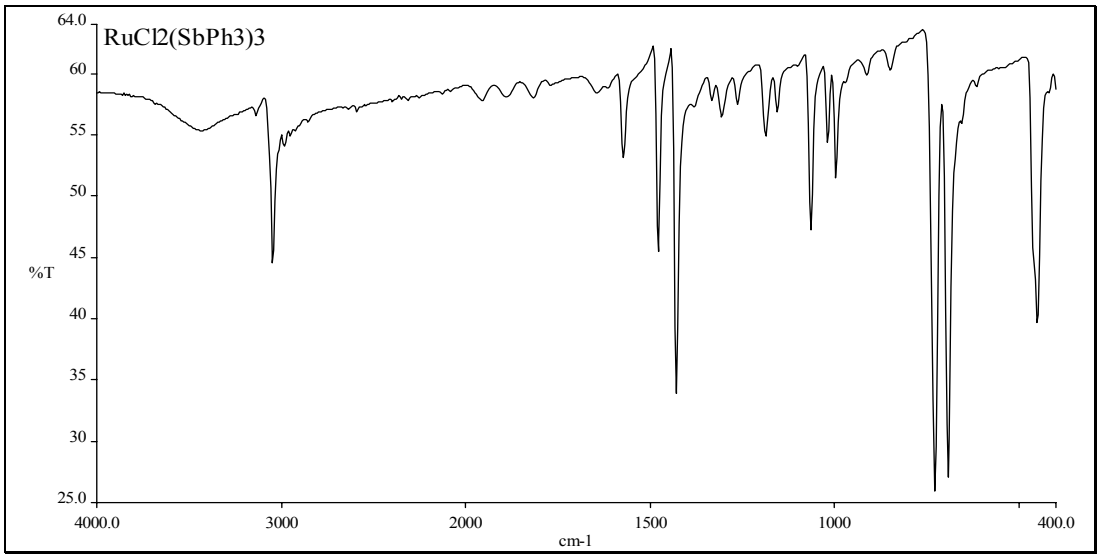

Figure 7.1. FT–IR spectra of rhodium and ruthenium metal complexes.

7.3.2. Screening of the Catalysts for Isomerization of Methyl Chavicol and Eugenol

The catalytic activity of rhodium, ruthenium and palladium complexes was evaluated for double bond isomerization of methyl chavicol and eugenol in the solvent free conditions. It was observed from conversion and selectivity data (Table 7.1) that the palladium and rhodium metal precursors showed higher conversion at the cost of lower selectivity of *trans*–anethole than their corresponding complexes. However, ruthenium complexes showed better conversion of methyl chavicol and selectivity of *trans*–anethole than the ruthenium metal precursor. Among the palladium metal complexes, $Pd/SbPh_3$ system showed highest conversion and selectivity toward *trans*–anethole followed by Pd/PPh_3 and $Pd/AsPh_3$ systems. Similar results were observed for rhodium metal complexes, $Rh/SbPh_3$ system gave higher conversion and selectivity for *trans*–anethole than corresponding Rh/PPh_3 and $Rh/AsPh_3$ systems. However, in case of ruthenium metal complexes, the conversion and selectivity for *trans*–anethole was higher for $Ru/AsPh_3$ as compared to Ru/PPh_3 and $Ru/SbPh_3$ systems.

The variation in the conversion and selectivity for *trans*–anethole with time was also studied (Figure 7.2) under identical experimental conditions of the results presented in Table 7.1 using $Ru/AsPh_3$ as a catalyst since this catalyst showed higher activity for the double bond isomerization of methyl chavicol to *trans*–anethole among the all studied catalyst systems.

Table 7.1. Conversion and selectivity data for solvent free isomerization of methyl chavicol to anethole using transition metal complexes as catalysts

Run	Catalyst	% Conversion	% Selectivity [a]	
			trans–Anethole	*cis*–Anethole
1	$PdCl_2.3H_2O$	60	65	35
2	$PdCl_2(PPh_3)_2$	27	71	29
3	$PdCl_2(AsPh_3)_2$	12	86	14
4	$PdCl_2(SbPh_3)_2$	31	88	12
5	$RhCl_3.3H_2O$	96	68	21
6	$RhCl(PPh_3)_3$	69	74	26
7	$RhCl(AsPh_3)_3$	63	76	24
8	$RhCl(SbPh_3)_3$	90	78	22
9	$HRhCO(PPh_3)_3$	81	73	27
10	$RuCl_3.3H_2O$	85	70	30
11	$RuCl_2(PPh_3)_3$	93	78	22
12	$RuCl_3(AsPh_3)_2.CH_3OH$	97	87	13
13	$RuCl_2(SbPh_3)_3$	90	80	20

[a] **Reaction conditions:** methyl chavicol = 1.0 g, catalyst = 0.01 g, temperature = 220 °C (refluxing), reaction time = 5 h.

From the concentration–time profile data, it was observed that the conversion of methyl chavicol was 95% in 30 min. A small increase in the conversion from 95 to 97% was observed on increasing the reaction time from 30 to 60 min, after which it achieved a steady state, i.e., conversion was independent of time. Similar trend was also observed for selectivity of *trans*–anethole. After attaining 82% selectivity in 30 min, the selectivity of *trans*–anethole increased from 82 to 87% in 60 min reaction time, after which the selectivity was independent of time.

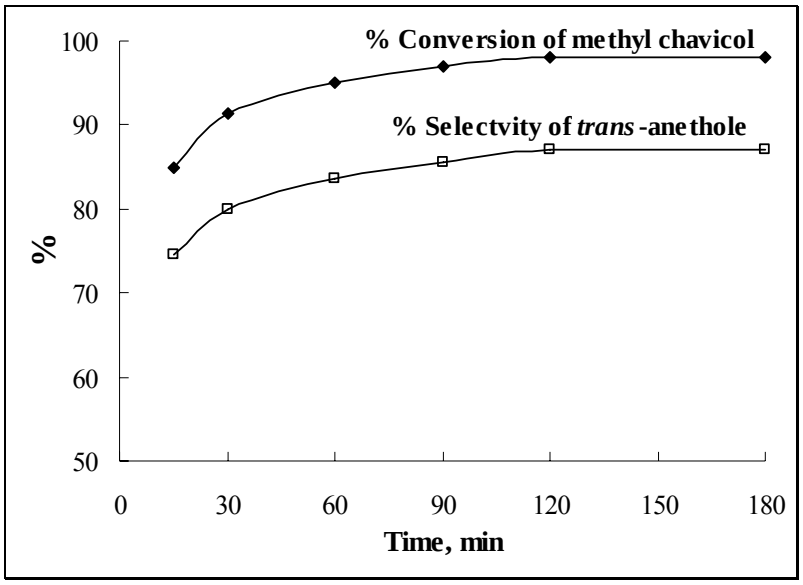

Figure 7.2. Conversion and selectivity with respect to time for solvent free isomerization of methyl chavicol to *trans*–anethole using $RuCl_3(AsPh_3)_2.CH_3OH$ as a catalyst.

Table 7.2. Conversion and selectivity data for solvent free isomerization of eugenol to isoeugenol using transition metal complexes as catalysts

Run	Catalyst	% Conversion	% Selectivity [a]	
			trans–Isoeugenol	*cis*– Isoeugenol
1	$PdCl_2.3H_2O$	33	6	0
2	$PdCl_2(SbPh_3)_2$	62	21	5
3	$RhCl_3.3H_2O$	25	8	7
4	$RhCl(SbPh_3)_3$	80	63	12
5	$RuCl_3.3H_2O$	46	59	14
6	$RuCl_2(PPh_3)_3$	9	49	0
7	$RuCl_3(AsPh_3)_2.CH_3OH$	86	79	17

[a] **Reaction conditions:** eugenol = 1.0 g, catalyst = 0.01 g, temperature = 240 °C (refluxing), reaction time = 5 h.

In order to observe the effect of transition metal complex catalysts for the isomerization of other allylphenyl compounds, the double bond isomerization of eugenol to *trans*–isoeugenol was also carried out (Table 7.2). It is interesting to note that again $Ru/AsPh_3$ system showed the highest conversion and selectivity than the other studied catalysts for double bond isomerization of eugenol to *trans*–isoeugenol. However, the trend of activity of the catalytic systems within the same metal for double bond isomerization of eugenol to *trans*–isoeugenol

(Table 7.2) was almost in contrast to the trend which was observed for double bond isomerization of methyl chavicol to *trans*–anethole. One of the possible reason of lower activity of studied transition metal complex as a catalyst for the double bond isomerization eugenol to *trans*–isoeugenol may be due to less acidity of benzylic carbon in eugenol since there are two electron–donating group (–OH and $–OCH_3$) attached to the ring which would reduce the acidity by increasing electron density on benzylic carbon.

An important step in isomerization reactions is the interconversion of π– and σ–bonded organometallic complexes [5]. Generally, the electron density is donated from the filled π–orbital of alkene into an empty metal orbital, while back–bonding occurs from filled orbital to the π*–orbital of the bound alkene. Hence, the double bond isomerization of methyl chavicol to *trans*–anethole would be highly influenced by the nature of metals and ligands used as a catalyst. The vacant orbitals present and the factors which affect the vacancy of orbitals in the metals are major governing aspect for isomerization of methyl chavicol to *trans*–anethole. Among the ligands, the σ–donor/π–acceptor ratio for EPh_3 (E = P, As, Sb) ligand show the following trend $SbPh_3$ > PPh_3 > $AsPh_3$ [26–27]. The π–electrons of the alkenes gets transferred to vacant orbitals of metals and the back–donation of electrons to the alkenes is affected by nature of metals and the ligand present with the metal. As it is clear from the trend of σ–donor/π–acceptor ratio for EPh_3 (E = P, As, Sb), $SbPh_3$ ligand has highest σ–donor ability of electrons, hence, the isomerization of methyl chavicol to *trans*–anethole will be favored when the metals have $SbPh_3$ ligand followed by PPh_3 and $AsPh_3$ ligand. The results obtained for isomerization of methyl chavicol to *trans*–anethole with palladium and rhodium metal complexes (Table 7.1) follow this order. However, as far as ruthenium metal complexes are concerned, the results obtained were exactly opposite than the results obtained with palladium and rhodium metal complexes. The most active catalytic system for isomerization of methyl chavicol to *trans*–anethole was $Ru/AsPh_3$ followed by Ru/PPh_3 and $Ru/SbPh_3$. One of the possible reasons for the higher conversion of methyl chavicol to *trans*–anethole with $Ru/AsPh_3$ system may be due to the higher oxidation state of ruthenium metal with $AsPh_3$ ligand (Ru^{III}) than Ru/PPh_3 and $Ru/SbPh_3$ systems (Ru^{II}). Higher the oxidation state of the metal, more number of vacant orbital with metals and hence the interaction of π–electrons of alkenes with metals will be more. Therefore, $Ru/AsPh_3$ system has high interaction with allylic electrons of methyl chavicol than Ru/PPh_3 and $Ru/SbPh_3$ system.

On comparing Pd, Rh, Ru metal precursors and their complexes of phosphine, arsine and antimony, the ruthenium metal complexes showed better activity than palladium and rhodium metals for double bond isomerization of methyl chavicol to *trans*–anethole and eugenol to isoeugenol. Among the phosphine, arsine and antimony complexes of Pd, Rh and Ru, the $M/SbPh_3$

(M = Pd, Rh) system gave higher conversion and selectivity towards *trans*–anethole except for ruthenium complexes. In the view of the higher catalytic activity of the ruthenium metal complexes, namely $RuCl_2(PPh_3)_3$ and $RuCl_3(AsPh_3)_2.CH_3OH$, the detailed kinetic study includes, nature of solvent used, effect of reaction parameters on the activity of the catalyst, rate of reaction and reusability of the catalyst was studied for double bond isomerization of methyl chavicol and eugenol.

7.3.3. Kinetic Analysis and Reproducibility for the Isomerization of Methyl Chavicol and Eugenol using $RuCl_2(PPh_3)_3$ (Ru/PPh_3) and $RuCl_3(AsPh_3)_2.CH_3OH$ (Ru/$AsPh_3$) Complexes as Catalysts

The parameters, which might have pronounced effect on the rate of isomerization reaction include, concentration of reactants, catalysts, solvents and the reaction temperature. Therefore, the kinetic experiments were carried out by varying these parameters. In each case, the changes in concentration of reactant were determined by gas chromatography at fixed time intervals. The initial rate of reaction was calculated by plotting the concentration of reactant in the range of initial period wherein the concentration of reactant did not change significantly (<10%) with time, giving a polynomial fit and the analysis was carried out by differential method. Under the kinetics experimental conditions, *trans* and *cis* isomers were only the major products formed during all the studied isomerization reactions.

To ensure reproducibility of isomerization of methyl chavicol and eugenol using Ru metal complex catalysts in the solvent, repeated experiments were carried out under identical reaction conditions. The results obtained, including conversion and selectivity was found to be within less than 2% variation, confirming the reproducibility of the results. In order to check the material balance of the reaction, the moles of products formed and moles of reactant consumed were compared. The concentration profile of reactant consumption and products formation are shown in Figure 7.3a (for isomerization of methyl chavicol) and Figure 7.3b (for eugenol isomerization).

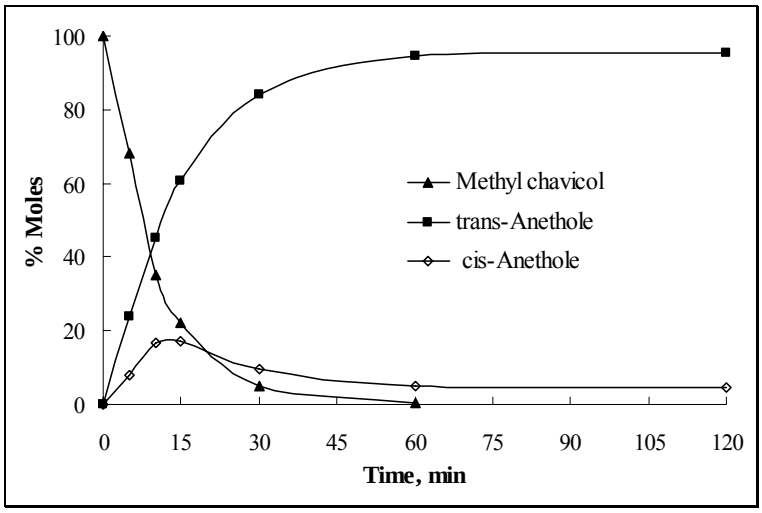

Figure 7.3a. Concentration profile for the isomerization of methyl chavicol with respect to time.

Reaction conditions: methyl chavicol = 6.75 mmol, $RuCl_2(PPh_3)_3$ = 5.2 x 10^{-3} mmol, solvent (ethanol) = 65.22 mmol, reaction time = 2 h, 85 °C

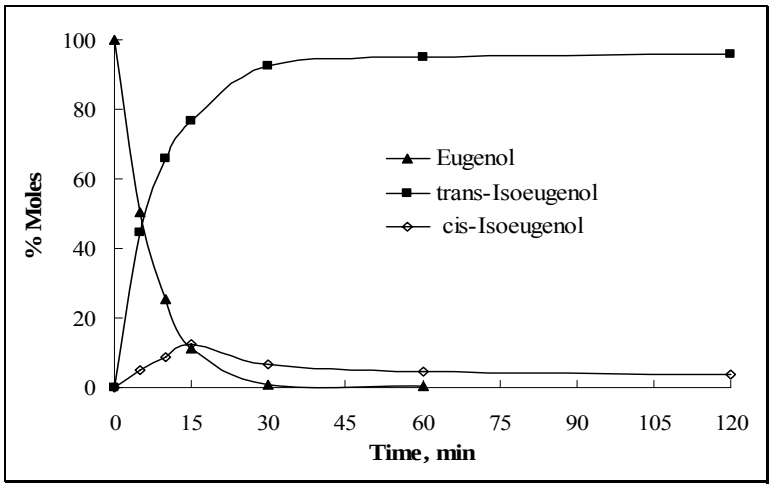

Figure 7.3b. Concentration profile for the isomerization of eugenol with respect to time.

Reaction conditions: eugenol = 6.75 mmol, $RuCl_2(PPh_3)_3$ = 5.2 x 10^{-3} mmol, solvent (ethanol) = 65.22 mmol, reaction time = 2 h, at 85 °C

7.3.4. Solvent Effect

Nature of the solvent used has a substantial influence on isomerization of methyl chavicol and eugenol, as seen from the conversion and selectivity data given in Tables 7.3 and 7.4. The isomerization of methyl chavicol and eugenol was carried out at the refluxing temperature. Conversion of methyl chavicol was observed to be 4.7% and 8.2% in highly polar aprotic solvents such as DMSO and acetonitrile, respectively, using $RuCl_2(PPh_3)_3$ catalyst. Whereas, in case of $RuCl_3(AsPh_3)_2.CH_3OH$ catalyst, conversion of methyl chavicol was obtained to 2% and 6% using

DMSO and acetonitrile, respectively (Table 7.3). Similar behavior with the highly polar aprotic solvents was observed during the double bond isomerization of eugenol to isoeugenol. The conversion of eugenol was found to be 5% using DMSO as a solvent and $RuCl_2(PPh_3)_3$ as a catalyst.

Table 7.3. Effect of nature of solvents on the isomerization of methyl chavicol

Run	Solvent [a]	$RuCl_2(PPh_3)_3$ catalyst		$RuCl_3(AsPh_3)_2.CH_3OH$ catalyst*		Refluxing temp., °C
		(%) Conversion of methyl chavicol	(%) Selectivity of *trans*–anethole	(%) Conversion of methyl chavicol	(%) Selectivity of *trans*–anethole	
1	DMSO	4.7	80.9	2.0	82.0	197
2	Chloroform	58.5	60.4	72.5	93.4	68
3	Benzene	63.0	82.4	58.2	92.3	87
4	Toluene	82.8	77.4	90.6	93.0	115
5	Cyclohexane	87.4	77.8	34.3	92.2	86
6	*n*–Butanol	98.8	94.2	92.6	96.2	112
7	*n*–Hexane	67.7	86.7	20.6	93.7	72
8	Ethanol	99.7	95.4	93.8	97.2	85
9	Methanol	86.7	94.0	94.2	98.6	85
10	*iso*–Propanol	99.6	94.3	92.1	96.5	85
11	*iso*–Butanol	99.2	94.0	93.0	95.8	112
12	Acetonitrile	8.2	84.6	6	90	85
13	Tetrahydofuran	69.5	88.7	66.4	95.4	70
14	Dichloromethane	61.7	86.2	52.7	93.4	48

[a] **Reaction conditions:** methyl chavicol = 6.75 mmol, solvent = 65.22 mmol, solvent* = 93.75 mmol, catalyst =5.2 x 10^{-3} mmol, [catalyst*] = 5.88 x 10^{-3} mmol, reaction time = 3 h.

The highest conversion (99.7%) of methyl chavicol with 95.4% selectivity for *trans*–anethole was observed in moderate polar protic solvents such as ethanol followed by *iso*–propanol (99.6% conversion, 94.3% selectivity), *n*–butanol (98.8%, 94.2%) and *iso*–butanol (99.2%, 94%) in $RuCl_2(PPh_3)_3$ catalyzed isomerization reaction (Table 7.3). While, in case of $RuCl_3(AsPh_3)_2.CH_3OH$ catalyzed reaction, the highest conversion of methyl chavicol (94.2%) with 98.6% selectivity for *trans*–anethole was observed in methanol followed by other polar protic

solvents. Similar behavior was observed in case of double bond isomerization of eugenol (Table 7.4) to isoeugenol catalyzed by $RuCl_2(PPh_3)_3$ complex. The highest conversion (99.8%) of eugenol with 95.6% selectivity for *trans*–isoeugenol was observed in moderate polar protic solvents such as ethanol followed by *iso*–propanol (99.8% conversion, 95.2% selectivity), *n*–propanol (99.7%, 94.0%), *iso*–butanol (99.7%, 94.6%) and *n*–butanol (99.5%, 92.2%) in $RuCl_2(PPh_3)_3$ catalyzed isomerization reaction. However, significantly lower conversion and selectivity of eugenol to isoeugenol were observed in $RuCl_3(AsPh_3)_2.CH_3OH$ catalyzed reaction.

Table 7.4. Effect of nature of solvents on the isomerization of eugenol

Run	Solvent [a]	$RuCl_2(PPh_3)_3$ catalyst		$RuCl_3(AsPh_3)_2.CH_3OH$ catalyst*		Refluxing temp., °C
		(%) Conversion of eugenol	(%) Selectivity of trans–isoeugenol	(%) Conversion of eugenol	(%) Selectivity of trans–isoeugenol	
1	DMSO	5	76	2	90	197
2	Benzene	74.2	71.6	7	85	87
3	Toluene	97.5	85	43	88	115
4	Cyclohexane	64.3	74	15	77	86
5	*n*–Hexane	54	78.6	11	75	72
6	Ethanol	99.8	95.6	14	82	85
7	Methanol	93.6	84.2	2	92	85
8	*iso*–Propanol	99.8	95.2	33	81	85
9	*n*–Propanol	99.7	94	11	85	85
10	*iso*–Butanol	99.7	94.6	21	82	112
11	*n*–Butanol	99.5	92.2	38	87	122
12	*n*–Hexanol	98.2	91	27	82	140
13	Acetonitrile	5.4	91	2.5	83	85
14	Tetrahydofuran	99.1	87	4	80	70
15	Dichloromethane	39	82	48	68	48
16	*n*–Decane	96.6	84	35	81	160

[a] **Reaction conditions:** eugenol = 6.75 mmol, solvent = 65.22 mmol, solvent* = 93.75 mmol, catalyst = 5.2 x 10^{-3} mmol, catalyst* = 5.88 x 10^{-3} mmol, reaction time = 3 h.

The non–polar, non–coordinating solvents showed better performance as compared to the

highly polar aprotic solvents for double bond isomerization of methyl chavicol and eugenol. The highest conversion (87.4%) of methyl chavicol was observed using cyclohexane as a solvent followed by toluene (82.8%) in $RuCl_2(PPh_3)_3$ catalyzed isomerization reaction. Whereas, $RuCl_3(AsPh_3)_2.CH_3OH$ catalyst showed 90.6% conversion of methyl chavicol with 93.0% selectivity of *trans*–anethole using toluene as a solvent. The non–polar solvents gave slightly lower conversion as compared to polar protic solvents, for the isomerization of eugenol using $RuCl_2(PPh_3)_3$ catalyst. The 99.1% conversion of eugenol was observed in tetrahydrofuran, 97.5% in toluene and 96.6% in *n*–decane as a solvent. However, lower selectivity of *trans*–isoeugenol was observed in case of non–polar solvents, as compared to polar protic solvents. For example, the selectivity of the *trans*–isoeugenol was found to be 87% in tetrahydrofuran, 74.2% in toluene and 84% in *n*–decane. The selectivity of *trans* isomer was significantly influenced by the nature of solvents used in the isomerization reactions. The maximum selectivity of *trans* isomers was observed in alcoholic solvents, while the solvent systems other than alcohols have given relatively lower selectivity for the *trans*–isomers and the magnitude of selectivity were almost similar with all the solvent systems other than alcohols.

The double bond isomerization reaction catalyzed by transition metal complex follows, generally two types of mechanistic pathways, one is π–allylic mechanism (1,3–hydrogen shift) and other is the alkyl mechanism (1,2–hydrogen shift). Generally, metal hydride complexes follow the alkyl mechanism. The key feature of the π–allylic mechanism is the β–C–H activation, a step that includes three–carbon arrangement in π–bonding to the metal. In this mechanism, the proposed active catalyst species $RuCl_2(PPh_3)_2$, is formed by the dissociation of on PPh_3 from the precursor $RuCl_2(PPh_3)_3$ complex (Scheme 7.1, step **I**) [28]. The next step, **II,** is the interaction of π–allylic electron from **1** to form a π–complex **1c** with the coordinatively unsaturated metal complex, $RuCl_2(PPh_3)_2$. The equilibrium step **III** gives π–allyl metal complex **1d** through allyl–H–migration (oxidative additions) from γ–carbon atom to metal. The hydride shift (reductive eliminations) from π–allyl metal–hydride complex **1d** to α–carbon atom gives complex **1e** via next equilibrium step **IV**. The dissociation of active catalyst species from the complex **1e** results in the formation of products **2** and **3**. For the alkyl mechanism, 1,2–insertion of coordinated alkene to Ru–H bond or β–elimination might be the rate–determining step. While for π–allylic mechanism, the slowest step is the oxidative addition step which leads to the formation of hydride–α–allyl complex. From the macroscopic point of view, factors such as rate of homogenization of catalyst precursor, and formation of active catalyst species involved in the catalytic cycle, may also strongly influence the overall rate of reaction [29]. These two factors are certainly connected with homogenization, which is in equilibrium with ligand dissociation and formation of the active catalyst species. There is an

additional set of equilibrium reactions, like coordination of catalyst by substrate, products or products of decomposition, which also influences the rate–determining step [29].

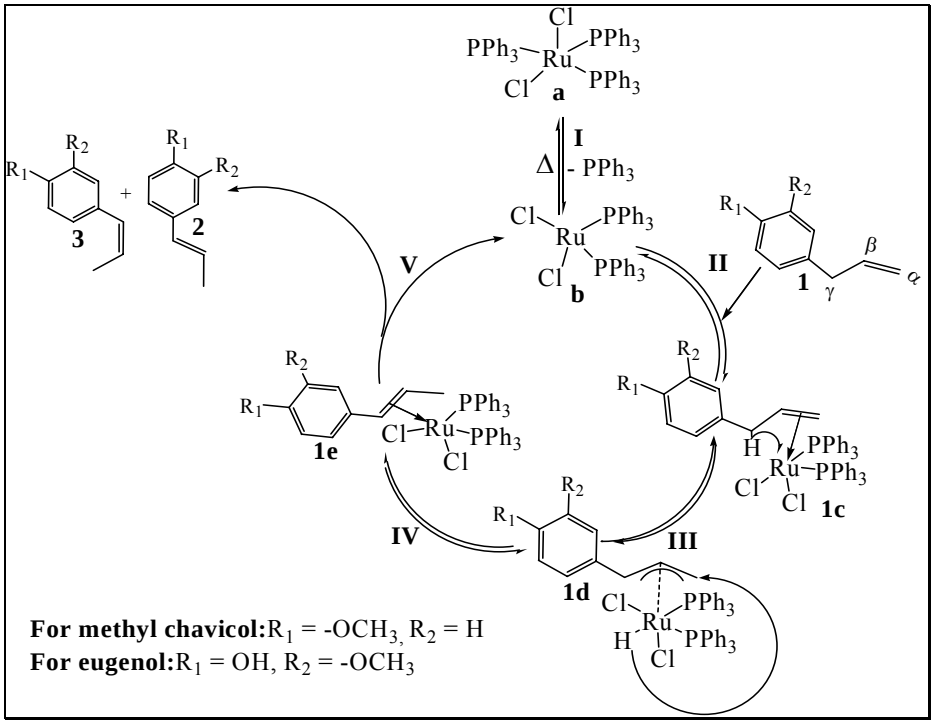

Scheme 7.1. Possible mechanistic pathway for the isomerization of methyl chavicol and eugenol using $RuCl_2(PPh_3)_3$ catalyst.

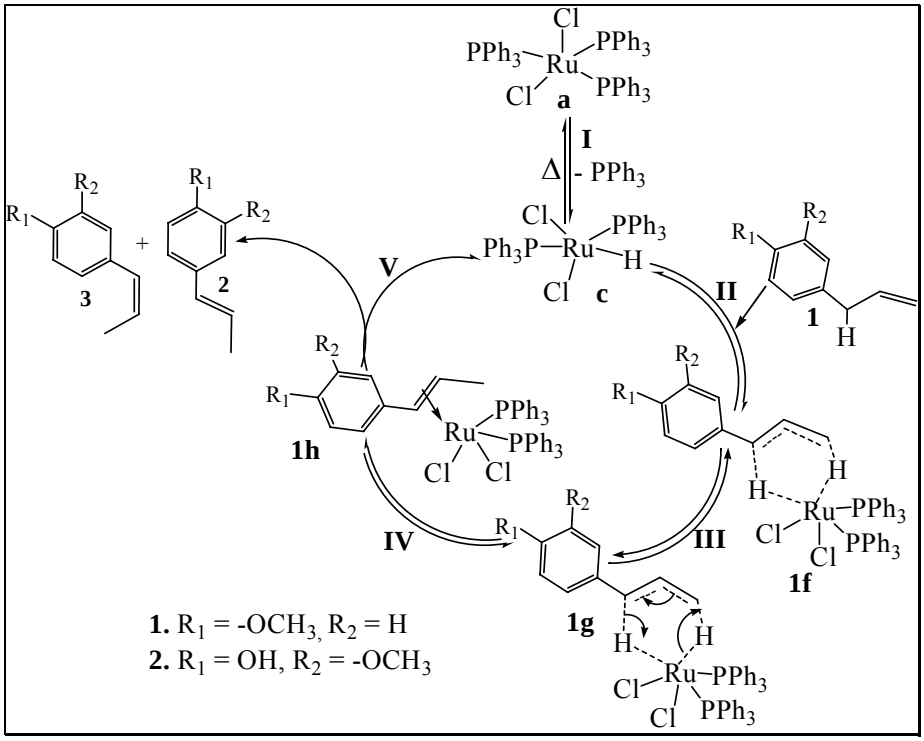

Scheme 7.2. Possible reaction mechanism for the isomerization of methyl chavicol and eugenol in protic polar solvents.

The higher conversion and selectivity obtained in alcohols may be attributed to facile transformation of the catalytic precursor **a** into the active catalyst species **c** in the reaction conditions (Scheme 7.2). In fact, the ruthenium hydride complex may be formed in a preliminary step through an oxidative addition of alcohol to the complex, and this new hydride complex could be catalytically active species having a very high activity towards double bond isomerization [30–31]. Higher catalytic activity of ruthenium hydride complex has also been reported from the comparative catalytic activities of $RuCl_2(PPh_3)_3$ and $HRuCl(PPh_3)_3$ complexes for double bond isomerization of 1,4–diarylbutenes [31]. The replacement of $RuCl_2(PPh_3)_3$ complex with $HRuCl(PPh_3)_3$ showed 80–fold increase in the maximum rate of reaction. Effect of addition of 3% methanol to the above reaction mixture containing $RuCl_2(PPh_3)_3$ complex and 1,4–diarylbutenes resulted into 10 fold increase in the maximum rate of reaction and this increase in reaction rate has been attributed to formation metal hydride complex [31]. The formation of metal hydride is associated with the oxidative protonation of $RuCl_2(PPh_3)_3$ in polar protic solvents, probably oxidative protonation of dissociated form $RuCl_2(PPh_3)_2$. Another important factor influencing the conversion of allyl phenyl ether is the rate of dissolution of the catalyst precursor. General observations for ruthenium complexes, reveals that they dissolve faster in polar aprotic solvents, while in benzene they may even stay partially solidified till the end of the reaction period if the concentration of the complex is more. However, it may be noted that the proposed mechanisms in Schemes 7.1 and 7.2 needs to be confirmed by spectroscopic evidence of the actual intermediate species.

The lower conversion of substrate found in highly polar solvents like DMSO and acetonitrile might be attributed to a competition between the solvent and the substrate for a coordinative place available on the catalyst. In this type of reactions, usually active solvents such as acetonitrile, DMSO did not performed well, due to reason that, these solvents may react with ruthenium complexes by oxidative addition to C–X bond, most likely deactivate the catalyst resulting in a decreased conversion [32]. Relatively strong coordination properties of DMSO, acetonitrile are the most important factors causing such a low conversion.

The conversion of methyl chavicol increased upto 80% using the non–polar solvents such as, toluene, cyclohexane, *n*–decane, benzene, chloroform, etc. This may be perhaps due to the coordination properties of these solvents. THF is usually the most effective solvent probably due to its coordinating properties.

In view of higher conversion and selectivity observed with ethanol as a solvent, further detailed kinetics has been studied using ethanol as a solvent for double bond isomerization of methyl chavicol and eugenol using Ru/PPh_3 complex catalyst. However, in case of isomerization of

methyl chavicol using Ru/$AsPh_3$ complex catalyst, methanol has been chosen as a solvent for further detailed kinetic study as higher selectivity of *trans*–isomer was observed with methanol solvent.

7.3.5. Effect of Solvent Concentration

Effect of solvent concentration on initial rate of reaction using $RuCl_2(PPh_3)_3$ and $RuCl_3(AsPh_3)_2.CH_3OH$ complex catalysts are shown in Figures 7.4a and 7.4b, respectively, for isomerization of methyl chavicol. From these figures, one can observe that the concentration of solvent plays an active role in inhibiting the rate of reaction.

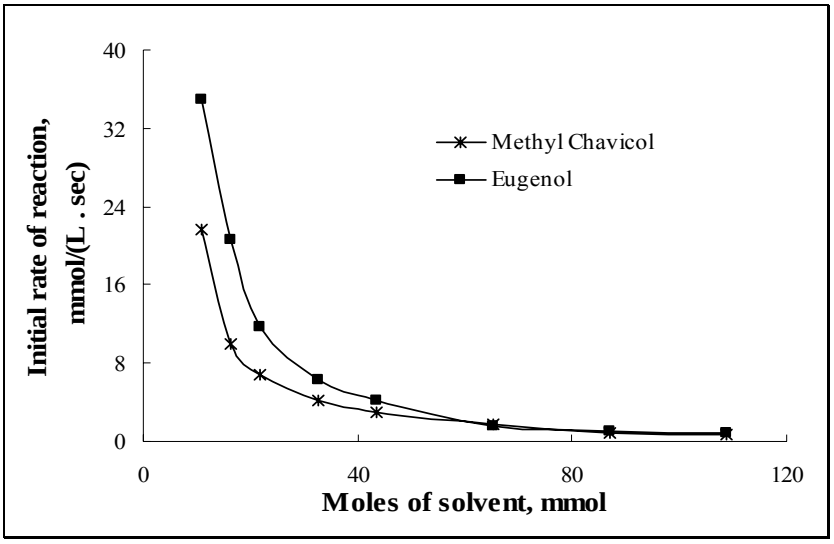

Figure 7.4a. Effect of solvent concentration on the isomerization of methyl chavicol and eugenol using $RuCl_2(PPh_3)_3$ complex catalyst.

Reaction conditions: reactant = 6.75 mmol, $RuCl_2(PPh_3)_3$ = 5.2 x 10^{-3} mmol, solvent (ethanol) = 11.0–109.0 mmol, at 85 °C.

At 10.87 mmol solvent concentration, the initial rate of reaction was found to be 21.67 mmol/(L sec). Further, by increasing the solvent concentration from 10.87 to 21.74 mmol, initial rate of reaction was observed to decrease from 21.67 to 6.8 mmol/(L sec). This trend was continued up to the solvent concentration of 65.22 mmol, which resulted least of value of the initial rate of reaction [1.67 mmol/(L sec)]. At the lower solvent concentration, the higher initial rate of reaction was found. As the concentration of solvent increased, the initial rate of reaction decreases sharply. Therefore, further kinetic experiments were performed at 65.22 mmol ethanol concentration because in this region rate of reaction was independent on solvent concentration.

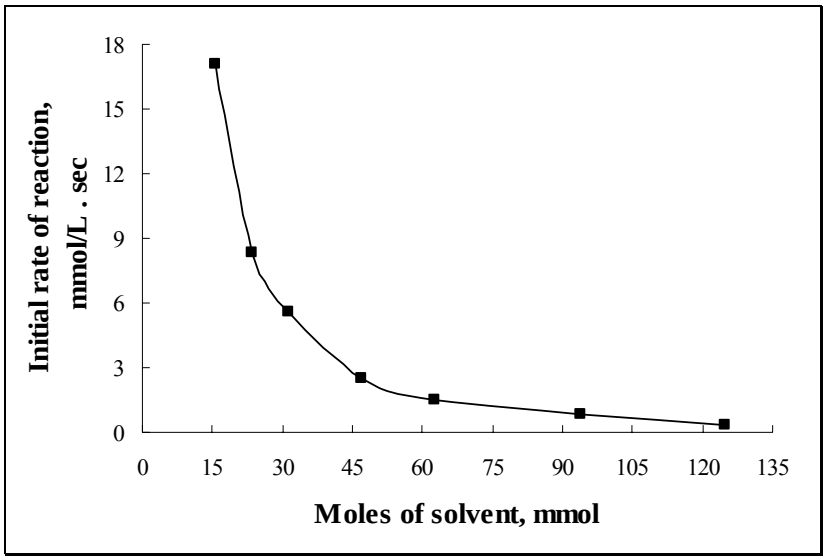

Figure 7.4b. Effect of solvent concentration on the isomerization of methyl chavicol using $RuCl_3(AsPh_3)_2.CH_3OH$ complex catalyst.

Reaction conditions: methyl chavicol]= 6.75 mmol, $RuCl_3(AsPh_3)_2.CH_3OH$ = 5.88 x 10^{-3} mmol, solvent (methanol) = 15.0–125.0 mmol, at 85 °C.

In case of $RuCl_3(AsPh_3)_2.CH_3OH$ complex, the initial rate of reaction decreased from 17.1 to 5.6 mmol/(L sec) on increasing the solvent concentration from 15.62 to 31.25 mmol. Therefore, for $RuCl_3(AsPh_3)_2.CH_3OH$ catalyzed isomerization reaction, the methanol concentration was taken 31.25 mmol for all kinetic experiments.

Similar behavior of the solvent concentration on initial rate of reaction was observed for eugenol isomerization using $RuCl_2(PPh_3)_3$ complex catalyst under studied experimental reaction conditions (Figure 7.4a). The concentration of solvent (ethanol) for isomerization of eugenol to isoeugenol was taken 65.22 mmol for the kinetic experiments.

7.3.6. Effect of Reactants Concentration

Effect of Methyl Chavicol Concentration

The effect of initial concentration of methyl chavicol on initial rate of reaction using $RuCl_2(PPh_3)_3$ complex catalyst is shown in Figure 7.5a. The initial rate of reaction showed positive order dependence on the concentration of methyl chavicol and found to increase linearly with increase in concentration of methyl chavicol. In the present study, maximum rate of reaction was found to be 3.5 mmol/(L sec) at 12.1 mmol methyl chavicol concentration using $RuCl_2(PPh_3)_3$ as a catalyst.

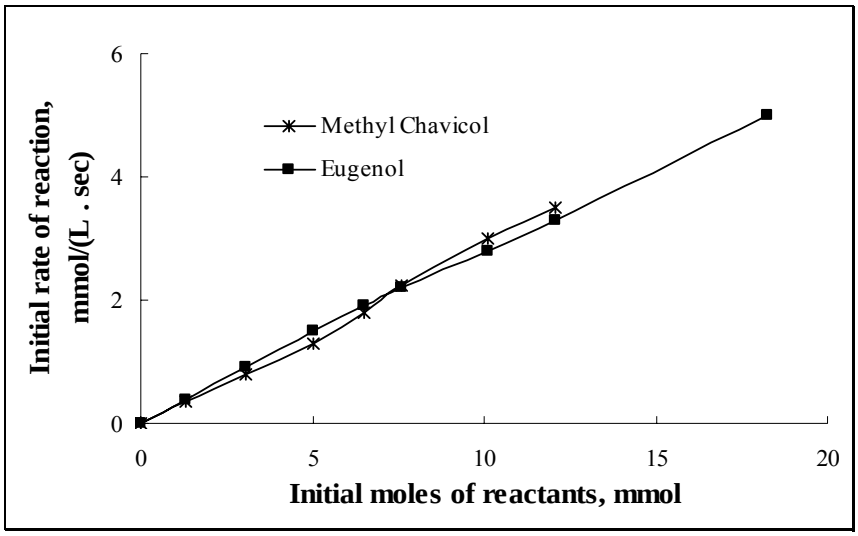

Figure 7.5a. Effect of Reactants concentration on the isomerization of methyl chavicol and eugenol using $RuCl_2(PPh_3)_3$ complex catalyst.

Reaction conditions: reactant = 1.35–18.27 mmol, $RuCl_2(PPh_3)_3$ = 5.2 x 10^{-3} mmol, solvent (ethanol) = 65.22 mmol, at 85 °C.

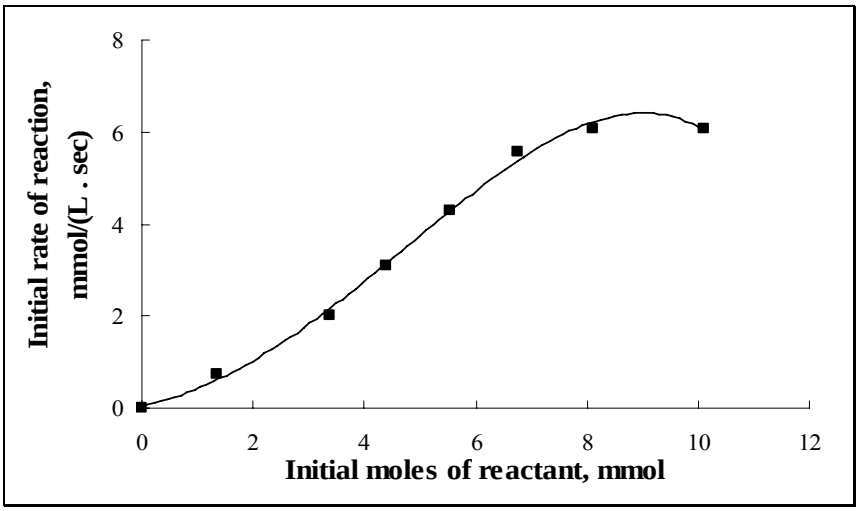

Figure 7.5b. Effect of methyl chavicol concentration on the isomerization of methyl chavicol using $RuCl_3(AsPh_3)_2.CH_3OH$ complex catalyst.

Reaction conditions: methyl chavicol = 1.35–10.15 mmol, $RuCl_3(AsPh_3)_2.CH_3OH$ = 5.88 x 10^{-3} mmol, solvent (methanol) = 31.25 mmol, at 85 °C.

The effect of initial concentration of methyl chavicol on initial rate of reaction using $RuCl_3(AsPh_3)_2.CH_3OH$ catalyst was also studied (Figure 7.5b). Trend of the dependence of initial rate of reaction upon the concentration of methyl chavicol was observed to be some what different than $RuCl_2(PPh_3)_3$ catalyst system. Firstly, the initial rate of reaction was found to increase linearly in methyl chavicol concentration range of 0.75 to 8.1 mmol and after that it remained constant with

further increase in the concentration of methyl chavicol.

Effect of Eugenol Concentration

The effect of initial concentration of eugenol on rate of reaction using $RuCl_2(PPh_3)_3$ complex catalyst is shown in Figure 7.5a. The trend observed was almost similar like the isomerization of methyl chavicol using $RuCl_2(PPh_3)_3$ catalyst. The initial rate of reaction increased from 1.5 to 5.0 mol/(L . sec), on increasing the concentration of eugenol from 5 to 18.3 mmol. The initial rate of reaction was found to be linearly dependent on the concentration of eugenol in entire range of experiments.

Effect of Reactants Concentration and Reaction Time on Selectivity of trans–Isomers

The trend of formation of *trans*–isomers was also studied and the obtained results are shown in Table 7.5. The selectivity of *trans*–anethole was observed to increase from 70.4 to 95.4% on increasing the reaction time upto 60 min. After that, the selectivity of *trans*–anethole was observed to be independent on reaction time even if it was double. Initially, lower selectivity of *trans*–isomer was observed due to simultaneous formation of the *cis* isomer (Scheme 7.1). The concentration of reactant was decreased significantly on increasing the reaction time. At lower concentration of methyl chavicol (<10%), the conversion of *cis* isomer to the trans–isomer was observed in the studied reaction conditions, due to thermodynamically instability of *cis* isomer. It was interesting to observe that the selectivity of *trans*–anethole is independent on the concentration of methyl chavicol. No significant change in the selectivity of *trans*–anethole was observed even when the concentration of methyl chavicol increased from 3.4 to 10.2 mmol.

Some relatively interesting results were found for the double bond isomerization of eugenol to isoeugenol using $RuCl_2(PPh_3)_3$ catalyst. At the lower reaction time (5 min), higher selectivity of *trans* isomer was observed. As the reaction time increased from 5 to 15 min, the selectivity of *trans*–isomer decreased from 89.7 to 80% at the 3.1 mmol of eugenol concentration, due to enhanced formation of *cis*–isomer. Initially, slow formation of the *cis*–isoeugenol was observed which favors to higher selectivity of *trans*–isomer. As reaction time increased, formation of *cis* isomer was observed to increase significantly, however, in this case also, when the concentration of reactant decreased, the *cis*–isomer was converted to the *trans*–isomer. No significant change in the selectivity of *trans*–isoeugenol was observed even on increasing the concentration of eugenol from 3.1 to 12.4 mmol.

Table 7.5. Effect of reaction time and concentration of reactant on the selectivity of *trans*–isomers

Time,	Moles of methyl chavicol			Moles of eugenol		
min	3.4 mmol	6.8 mmol	10.2 mmol	3.1 mmol	6.2 mmol	12.4 mmol
	% Selectivity of *trans*–isomer [a]					
5	70.4	70.7	70.5	89.7	90.1	89.8
10	83.3	82.5	83.5	88	88	87.9
15	84.5	84.1	84.4	85	85.6	85.1
30	91.2	91.4	90.8	93.3	92.5	92.2
60	95.4	95.4	95.3	95.5	95.6	95.5
120	95.4	95.4	95.4	95.5	95.6	95.6

[a] **Reaction conditions:** solvent (ethanol) = 65.22 mmol, $RuCl_2(PPh_3)_3$ = 5.2 x 10^{-3} mmol, reaction time = 2 h at 85 °C.

7.3.7. Effect of Catalyst Concentration

The effect of catalyst concentration on initial rate of reaction for isomerization of methyl chavicol using $RuCl_2(PPh_3)_3$ and $RuCl_3(AsPh_3)_2.CH_3OH$ catalyst is shown in Figures 7.6a and 7.6b, respectively.

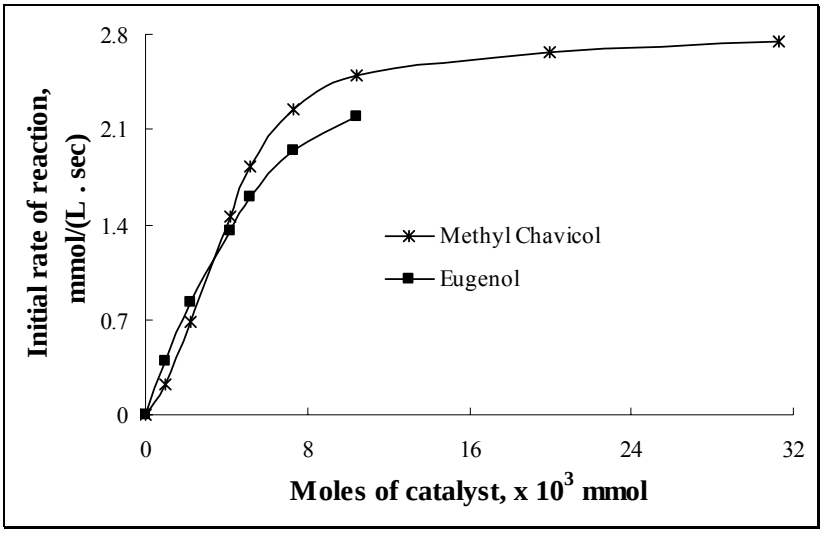

Figure 7.6a. Effect of catalyst concentration on the isomerization of methyl chavicol and eugenol using $RuCl_2(PPh_3)_3$ complex catalyst.

Reaction conditions: reactant = 6.75 mmol, $RuCl_2(PPh_3)_3$ = 1 x 10^{-3} – 31.3 x 10^{-3} mmol, solvent (ethanol) = 65.22 mmol, 85 °C.

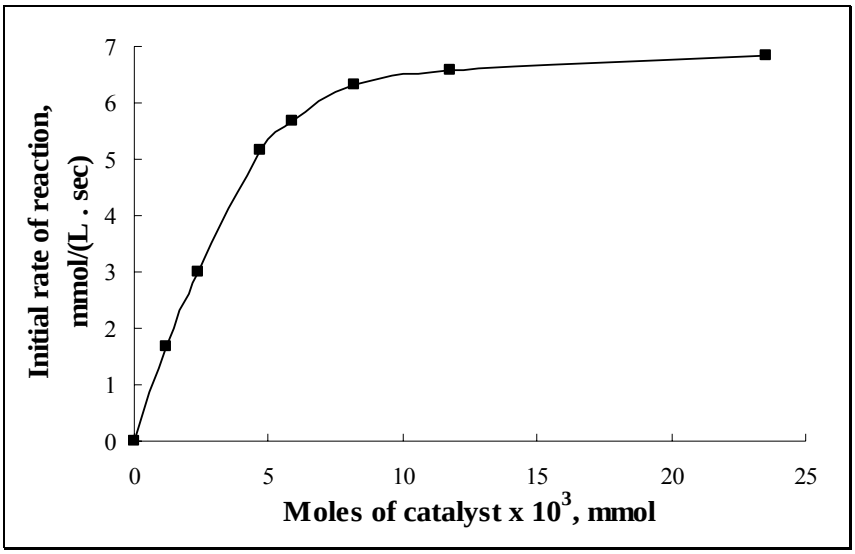

Figure 7.6b. Effect of catalyst concentration on the isomerization of methyl chavicol using $RuCl_3(AsPh_3)_2.CH_3OH$ complex catalyst.

Reaction conditions: methyl chavicol = 6.75 mmol, $RuCl_3(AsPh_3)_2.CH_3OH$ = 1.2 x 10^{-3} – 23.5 x 10^{-3} mmol, solvent (methanol) = 31.25 mmol, at 85 °C.

The initial rate of reaction linearly increased upto 2.4 mmol/(L sec) with increase in catalyst concentration upto 8.0 x 10^{-3} mmol. However, after 8.0 x 10^{-3} mmol catalyst concentration, lower extent of increment in the initial rate of reaction was observed. The initial rate of reaction increased from 2.4 to 2.75 mmol/(L sec) by increasing the concentration of catalyst from 8.0 x 10^{-3} to 31.3 x 10^{-3} mmol. The effect of catalyst concentration on initial rate of reaction for isomerization of eugenol using $RuCl_2(PPh_3)_3$ complex catalyst is shown in Figure 7.6a. The trend observed on varying the catalyst concentration on initial rate of reaction showed that the rate of reaction increases linearly on increasing the catalyst concentration upto 6 x 10^{-3} mmol, after that the slow increase in initial rate of reaction was observed. Similar type of the trend was observed when methyl chavicol was used as a reactant.

7.3.8. Rate Constant and Activation Energy

The effect of temperature on rates of reaction for isomerization of methyl chavicol and eugenol using $RuCl_2(PPh_3)_3$ and $RuCl_3(AsPh_3)_2.CH_3OH$ complex catalysts are shown in Figures 7.7a and 7.7b, respectively. It was observed that the initial rate of reaction increased by increasing the reaction temperature in case of isomerization of methyl chavicol using $RuCl_2(PPh_3)_3$ complex catalyst.

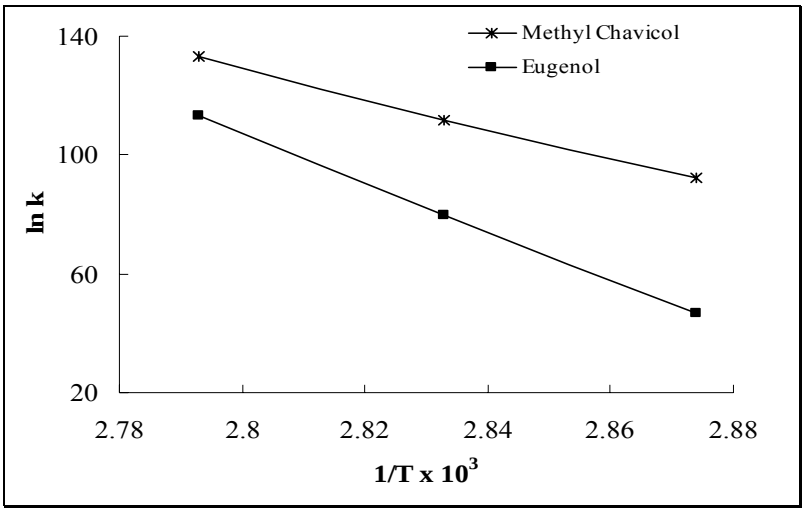

Figure 7.7a. Arrhenius plot for isomerization of methyl chavicol and eugenol using $RuCl_2(PPh_3)_3$ complex as a catalyst.

Reaction conditions: reactant = 6.75 mmol, $RuCl_2(PPh_3)_3$ = 5.2 x 10^{-3} mmol, solvent (ethanol) = 65.22 mmol, temperature = 75 –85 °C.

The lower conversion of methyl chavicol and lower selectivity of *trans*–anethole was found at lower reaction temperature. Similar types of trends in conversion and selectivity were observed in the case of isomerization of methyl chavicol using $RuCl_3(AsPh_3)_2.CH_3OH$ complex and isomerization of eugenol using $RuCl_2(PPh_3)_3$ as a catalyst.

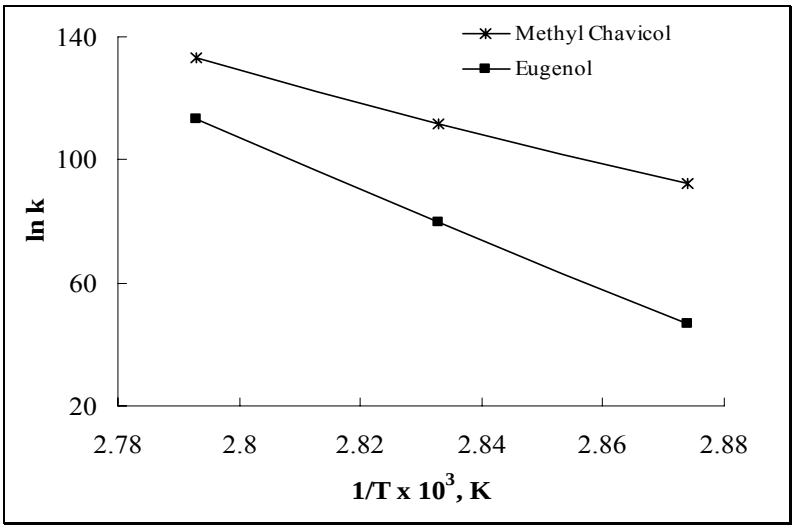

Figure 7.7b. Arrhenius plot for isomerization of methyl chavicol using $RuCl_3(AsPh_3)_2.CH_3OH$ complex as a catalyst.

Reaction conditions: methyl chavicol = 6.75 mmol, $RuCl_3(AsPh_3)_2.CH_3OH$ = 5.88x10^{-3} mmol, solvent (methanol) = 31.25 mmol, temperature = 75–85 °C.

Activation energies for isomerization of methyl chavicol under experimental reaction conditions were found to be 4.3 ± 0.08 kJ/mol (Figure 7.7a) with $RuCl_2(PPh_3)_3$ catalyst and 6.0 ± 0.12 kJ/mol (Figure 7.7b) with $RuCl_3(AsPh_3)_2.CH_3OH$ catalyst. For the isomerization of eugenol, the activation energy was found to be 6.9 ± 0.13 kJ/mol (Figure 7.7a) using $RuCl_2(PPh_3)_3$ complex as a catalyst, which is less than the reported value for rhodium (III) chloride system (42.6 kJ/mol) [33] and for KOH system (148 kJ/mol) [34].

From above detailed kinetic studies, it can be concluded that the $RuCl_2(PPh_3)_3$ complex showed higher conversion and reasonably excellent selectivity for isomerization of methyl chavicol and eugenol. Therefore, one reaction was performed in larger scale of methyl chavicol (methyl chavicol = 3.48 mol, $RuCl_2(PPh_3)_3$ = 2.2 mmol, ethanol = 32.61 mol, time = 2 h at 85 °C). The result was found identical to the previously observed results for isomerization of methyl chavicol at lower scale (6.75 mmol). The catalyst was recycled upto five times for the isomerization of methyl chavicol (Figure 7.8a) and eugenol (Figure 7.8b). No considerable changes were observed in the conversion and selectivity of respective isomers upto fifth cycles in both of the cases.

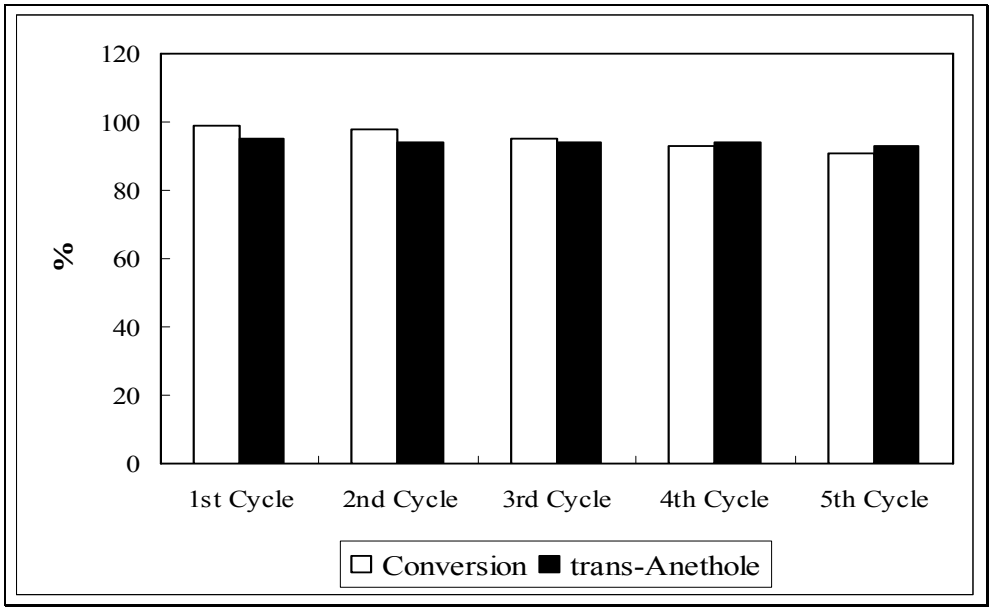

Figure 7.8a. Reusability of $RuCl_2(PPh_3)_3$ complex catalyst for the isomerization of methyl chavicol.

Reaction conditions: methyl chavicol = 6.75 mmol, $RuCl_2(PPh_3)_3$ = 5.2 x 10^{-3} mmol, solvent (ethanol) = 65.22 mmol, reaction time = 2 h, at 85 °C.

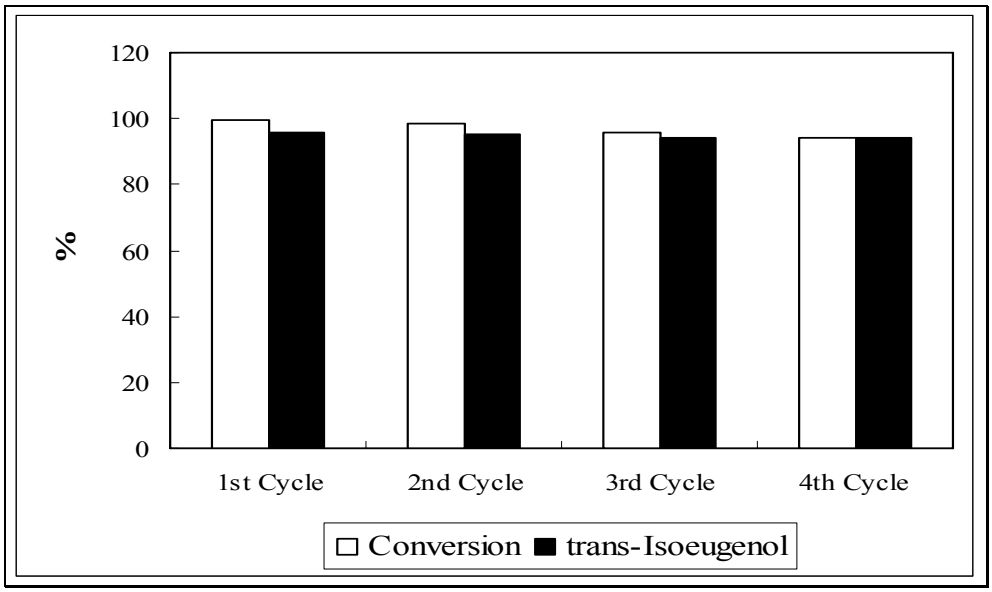

Figure 7.8b. Reusability of $RuCl_2(PPh_3)_3$ complex catalyst for the isomerization of eugenol.

Reaction conditions: eugenol = 6.75 mmol, $RuCl_2(PPh_3)_3$ = 5.2 x 10^{-3} mmol, solvent (ethanol) = 65.22 mmol, reaction time = 2 h, at 85 °C.

7.4. Heterogenization of Ruthenium Metal on the Solid Base Supports

The results discussed above for isomerization of methyl chavicol and eugenol showed very high selectivity of *trans*–anethole and *trans*–isoeugenol using $RuCl_2(PPh_3)_3$ and $RuCl_3(AsPh_3)_2.CH_3OH$ complexes as catalysts in homogeneous conditions using alcohols (ethanol and methanol) as polar protic solvents. Although excellent activity and maximum selectivity for the desired *trans* isomer was observed with the use of $RuCl_3(AsPh_3)_2.CH_3OH$ complex as a catalyst in catalytic amount and catalyst was also recycled several times without significantly loss in the activity, the role of arsine in environmental pollution (water) cannot be ignored. The major drawback of this process is the use of arsine in homogeneous system alongwith various organic solvents for the isomerization reaction. Therefore, the ruthenium, active component for double bond isomerization reaction, was heterogenized on different basic solid supports namely, hydrotalcite, magnesium oxide, calcium oxide, silica and alumina. The hydrotalcite or layered double hydroxides (*HT; $[M(II)_{1-x}M(III)_x(OH_2)]^{x+}(CO_3^{2-})_{x/n}{\cdot}mH_2O$; where M(II) = Mg or divalent cations and M(III) = Al or trivalent cations*) attracted main attention as a catalyst due to availability of wide range of basicity which can be achieved by tuning the proper molar ratio of M(II) and M(III) cations, intercalation of suitable anion in the interlayer space or activation of hydrotalcite at 450 °C. Various metal elements can be introduced into the brucite layer via isomorphic substitution of M(II) or M(III) cations at the octahedral sites, which are expected to be the active sites for organic transformation reactions [24, 35, 36]. The use of ruthenium grafted

hydrotalcite as a highly active catalyst is reported in the literature for oxidation of alcohols and aromatic compounds [37], direct alkylation of nitriles with primary alcohols and aldehydes [38–39] and for one pot synthesis of quinolines [40]. Apart from these applications, the literature is silent for further exploration of ruthenium containing hydrotalcite as the potential and versatile catalyst for various organic transformations.

The work presented in this part of the chapter describes the possibilities to overcome these limitations of the present existing processes for double bond isomerization of perfumery related compounds such as methyl chavicol, eugenol, safrole, allylbenzene, dimethoxy allylbenzene and 3–carene (Scheme 7.3). The use of non–hazardous reusable heterogeneous catalyst in place of hazardous liquid base like NaOH or KOH is an eco–friendly catalytic route for the production of *trans*–isomers. Present study explores the use of ruthenium grafted hydrotalcite (Ru–Mg–Al) as a reusable catalyst for double bond isomerization of methyl chavicol to *trans*–anethole and other perfumery related compounds in solvent free conditions in a very short reaction time.

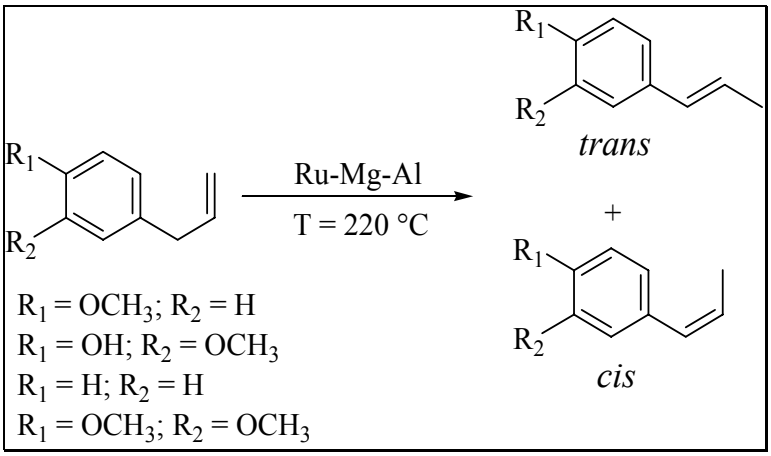

Scheme 7.3. Double bond isomerization of perfumery chemicals.

Synthesis of Ruthenium Grafted Hydrotalcite [Ru–Mg–Al]

Ruthenium grafted hydrotalcite was prepared by the co–precipitation method at pH = 9±0.5 [24]. In a typical synthesis procedure, an aqueous solution (A) containing $MgCl_2 \cdot 6H_2O$ (0.0522 mol), $AlCl_3 \cdot H_2O$ (0.0144 mol) and $RuCl_3.3H_2O$ (0.0005 mol) in 50 mL double distilled deionized water was prepared. The solution A was added drop wise into a second solution (B) containing Na_2CO_3 (0.079 mol) in 50 mL double distilled de–ionized water, in around 45 min under vigorous stirring at 30 °C. The constant pH of the mixture was maintained by adding 1 M NaOH solution. The content was then transferred into the teflon coated stainless steel autoclave and aged at 80 °C for 16 h under autogenous water vapor pressure. After 16 h, the precipitate formed was filtered and washed thoroughly with hot distilled water until the filtrate was free from Cl^- ions (silver nitrate

test). The obtained filter cake was dried in an oven at 80 °C for 14 h. The solid material (yield = 6.1 g) named as Ru–Mg–Al, was ground and stored under vacuum. The activation of Ru–Mg–Al was carried out in a muffle furnace at 450 °C for 4 h.

7.4.1. Characterization of Catalyst

The P–XRD patterns of HT(3.5) and Ru–Mg–Al samples were observed to be well crystalline materials similar to that of the pure hydrotalcite (Figure 7.9). Presence of CO_3^{2-} anions in the interlayer space of HT(3.5) and Ru–Mg–Al samples was confirmed by the characteristic basal spacing of (003) plane; d_{003} = 7.65Å. The sharp and symmetric reflections of (003) and (006) planes at low values of 2θ angles (11–23°) and broad, asymmetric reflections at higher values of 2θ (34–66°) were observed in the P–XRD patterns, which are typical characteristics of the pure hydrotalcite and revealed a good dispersion of aluminum and ruthenium in the brucite layers [25]. The P–XRD pattern of Ru–Mg–Al sample clearly shows that the characteristic original planes of HT(3.5) are retained after incorporation of ruthenium in the brucite like sheet. The peaks and their positions in the P–XRD of Ru–Mg–Al sample is identical with the HT(3.5). Any additional peaks other crystalline phases were not observed in the P–XRD pattern of HT(3.5) and Ru–Mg–Al samples under synthesis conditions. The intensities of (003) and (006) planes, which are directly related to the crystallinity were observed to decrease to 88% for Ru–Mg–Al sample (Table 7.6). The decrease in the crystallinity on introducing the ruthenium cations in hydrotalcite structure (Ru–Mg–Al) is due to increase in amount of cations of higher ionic radii in the brucite sheet.

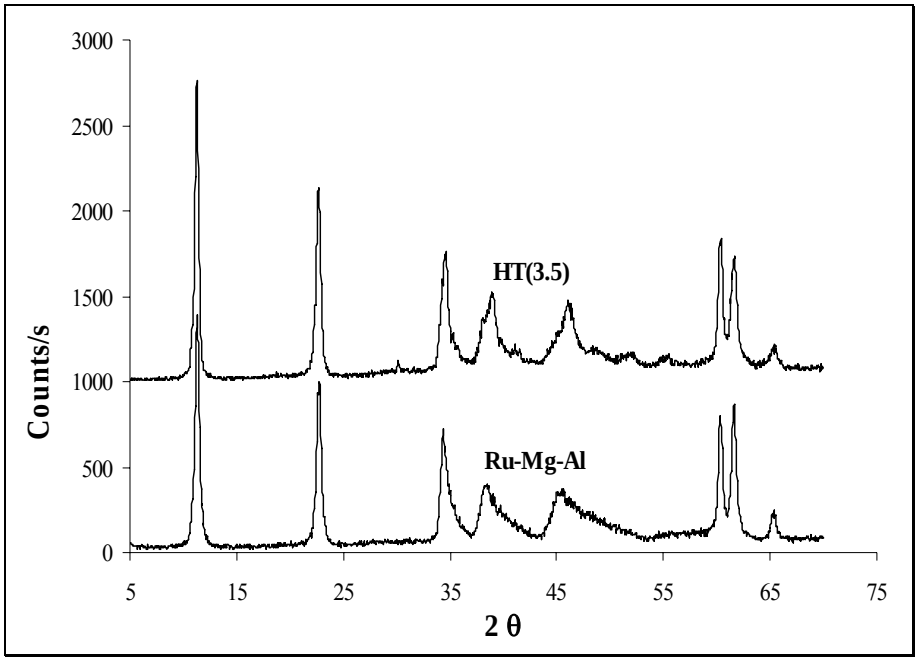

Figure 7.9. P–XRD patterns of HT(3.5) and Ru–Mg–Al samples.

Table 7.6. Physical characterization of the catalysts

	HT(3.5)	Ru–Mg–Al
Crystallinity, %	100	88
Unit cell parameter (a), Å	3.064	3.069
Unit cell parameter (c), Å	23.41	23.38
T_1, °C	80–160	180–220
W_1, %	8	13
T_2, °C	300–550	320–450
W_2, %	36	26
Surface area, m^2/g	76	80

W_1 =First weight loss at temperature T_1

W_2 =Second weight loss at temperature T_2

The values of unit cell parameters *a* and *c* were calculated for HT(3.5) and Ru–Mg–Al samples. Increase in the value of *a* was observed for Ru–Mg–Al sample (3.069 Å) as compared to the value (3.064 Å) for HT(3.5) due to larger ionic radii of ruthenium (0.68 Å) as compared to aluminum (0.53 Å). The decrease in the value of unit cell parameter *c* was observed for Ru–Mg–Al sample (23.38 Å) as compared to the value for HT(3.5) (23.41 Å). This results into decrease in charge density on layers due to weaker interaction (or decrease in Coulombic attractive force) between the negatively charged interlayer anions and positively charged brucite like layers [24, 25, 41].

FT–IR spectra of HT(3.5) and Ru–Mg–Al samples showed all characteristic peaks of the original hydrotalcite structure (Figure 7.10), and confirmed the formation of pure HT(3.5) sample. Generally, three types of IR–active vibrations; molecular vibration of the hydroxyl group, lattice vibrations of the octahedral layers and vibrations of the interlayer anions, are reported for hydrotalcite like materials [25].

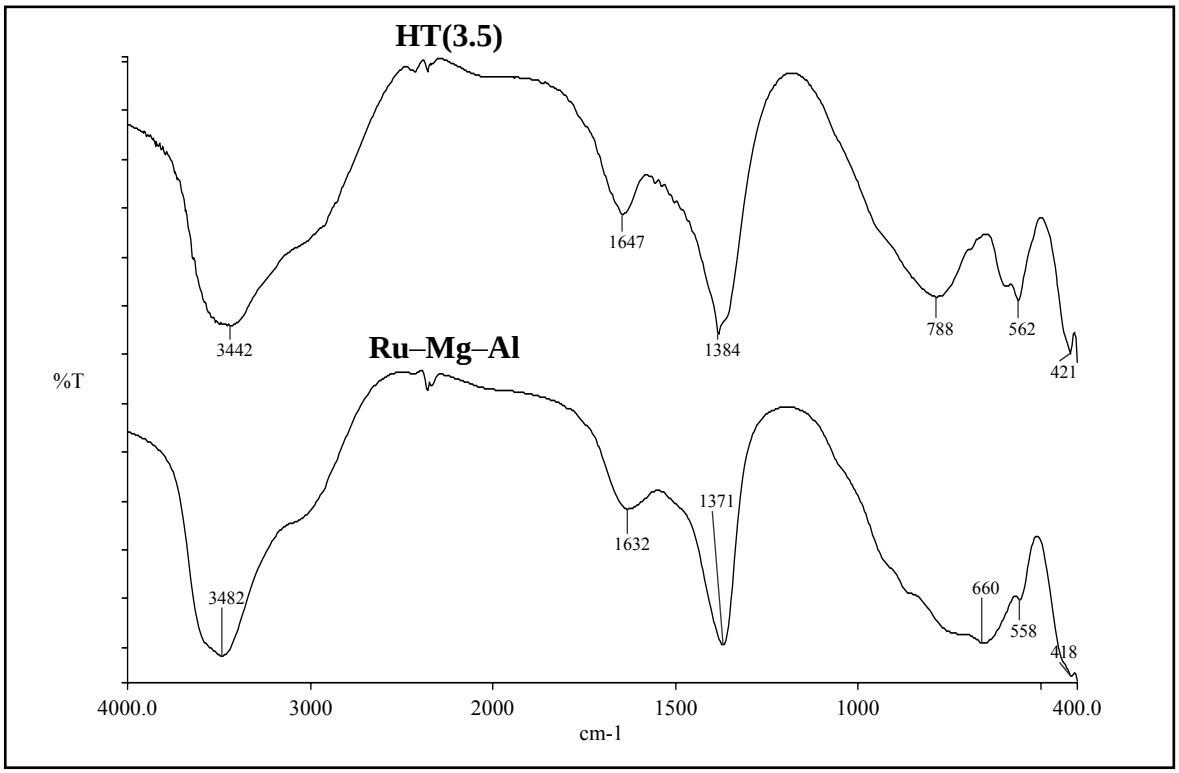

Figure 7.10. FT–IR spectra of HT(3.5) and Ru–Mg–Al samples.

The peak at around 3450–3480 cm^{-1} is due to the ν_{OH} mode of H–bonded hydroxyl groups in the layers and broadening of this peak is dependent on the strength of hydroxyl bonds. The shoulder present at 3000 cm^{-1} is attributed to the hydrogen bonding of hydroxyl groups of layered lattice and/or water molecules with interlayer carbonate anions [25]. Band that appeared at around 1640 cm^{-1} is due to the deformation mode of interlayer water molecules; intensity of this band suggests the content of water molecules in the material. The sharp, intense vibrational band at 1370 cm^{-1} is assigned to asymmetric ν_3 mode of interlayer carbonate anions. Absence of band at around 1050 cm^{-1}, suggests the retention of D_{3h} symmetry of carbonate anions in the interlayers. The bands in low frequency region (below 1000 cm^{-1}) are related with Mg–OH and Al–OH vibrational modes in brucite–type layers. The bands at 950 cm^{-1} for the deformation of Al–OH and at 760 cm^{-1} for Al–OH translation were also observed. The peak at around 660 cm^{-1} (ν_4) is assigned to the in–plane carbonate bending. The band at 554 cm^{-1} appeared in the lower wave number region, is assigned to the translation modes of hydroxyl groups, influenced by Al^{3+} cations (Mg/Al–OH translation) [42]. The band appeared at 418 cm^{-1} is attributed to the Mg–OH vibrational mode.

Thermogravimetric analysis (TGA) curves of HT(3.5) and Ru–Mg–Al are shown in Figure 7.11. The well defined weight loss patterns in two stages were observed, which clearly matched with TGA curve of pure hydrotalcite [25]. TGA curves of both samples [HT and Ru–Mg–Al] show similar weight loss patterns. 13% weight loss was observed in the Ru–Mg–Al sample at first stage in the temperature range of 180–220 °C, which is attributed to the loss of physically adsorbed

water molecules with relatively smaller amounts of condensed water molecules and CO_2. The weight loss in first steps is reversible without collapse of hydrotalcite structure.

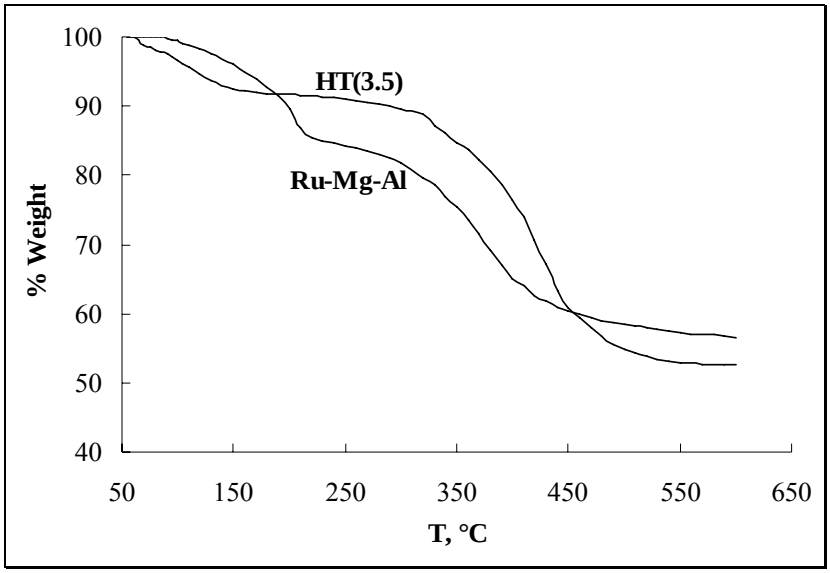

Figure 7.11. TGA of HT(3.5) and Ru–Mg–Al samples.

The weight loss in second stage (26%) was observed due to removal of condensed water molecules (dehydroxylation of hydroxyl groups) and carbon dioxide from the carbonate anion present in interlayer space of Ru–Mg–Al in the temperature range of 320–450 °C. In this weight loss, interlayer carbonate anions were thermally oxidized by a nearby interlayer water molecule to produce volatile CO_2 and interlayer hydroxyl anions. The observed lower weight loss in the TGA of Ru–Mg–Al sample as compared to HT(3.5) is due to the presence of ruthenium cations in the matrix which led to higher thermal stability of the catalyst. Due to higher thermal stability of Ru–Mg–Al sample, this material has potential applications as a catalyst.

The SEM images of HT(3.5) and Ru–Mg–Al hydrotalcite samples were recorded to observe the effect of ruthenium cations grafting in the brucite sheet on the morphology of hydrotalcite (Figure 7.12). The Ru–Mg–Al micrograph shows a well developed layered and platelet structure. However, spongy type structure is exhibited due to overlapping of such platelets. No significant difference were observed in the results obtained from EDX analysis related the Mg/Al molar ratio and ruthenium content in the hydrotalcite and were found to be in accordance with the calculated compositions. The ruthenium content in the Ru–Mg–Al hydrotalcite sample was analyzed by ICP and EDX and found to be 0.32 mg Ru per gram of Ru–Mg–Al catalyst.

The calculated BET surface area of HT(3.5) and Ru–Mg–Al samples were 76 and 80 m^2/g, respectively (Table 7.6). The increase in the surface area for ruthenium containing hydrotalcite sample is attributed to the observed decrease in the crystallinity as compared to [HT(3.5)] sample

(also seen from P–XRD patterns). The catalytic activity of Ru–Mg–Al was investigated for double bond isomerization of methyl chavicol to anethole, which is a base catalyzed reaction by varying the amount of catalyst and reaction temperature.

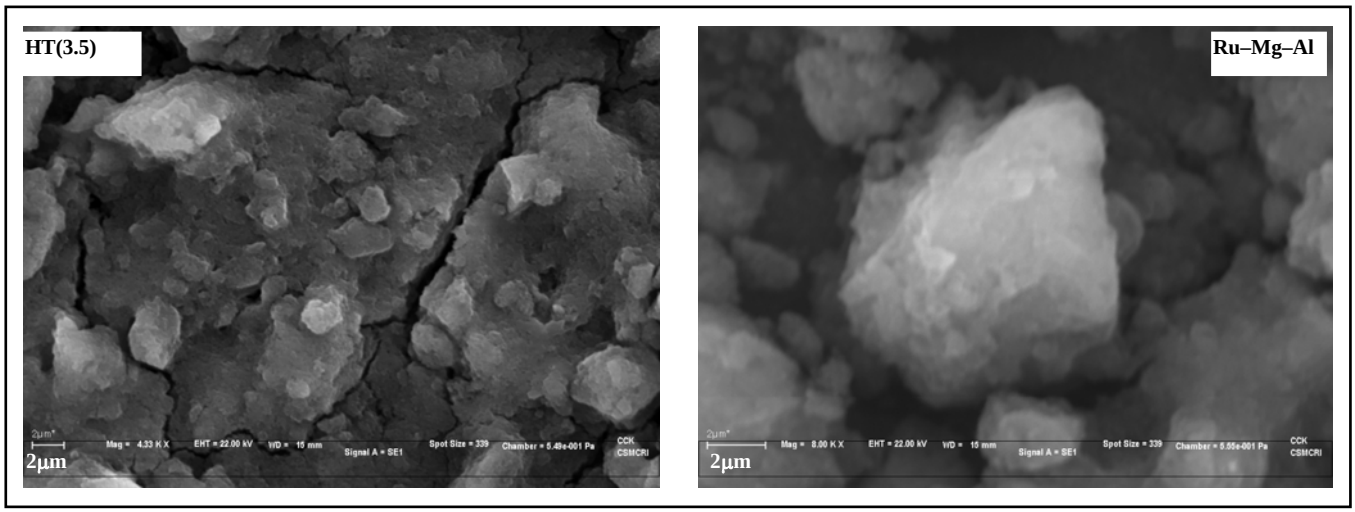

Figure 7.12. SEM images of HT(3.5) and Ru–Mg–Al samples.

7.4.2. Effect of Catalyst Amount on Catalytic Activity for Double Bond Isomerization of Methyl Chavicol

The effect of catalyst amount (Ru–Mg–Al) on the conversion and selectivity for isomerization of methyl chavicol is shown in Figure 7.13.

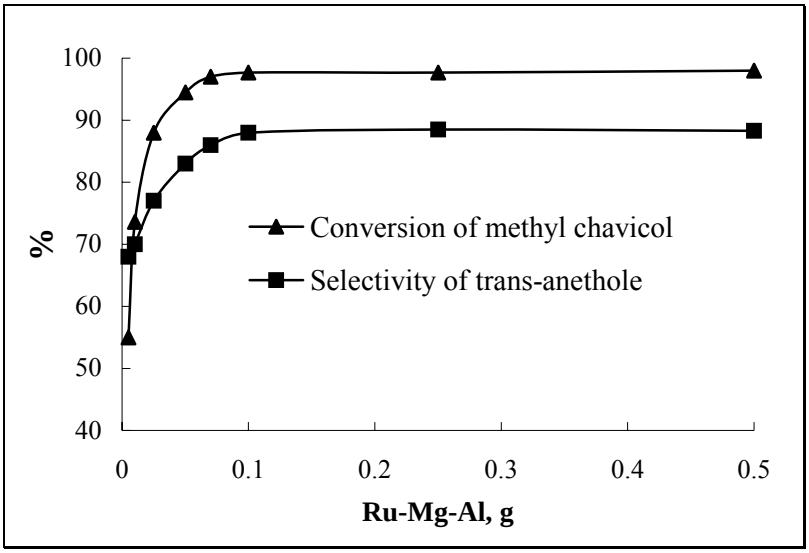

Figure 7.13. Effect of catalyst amount on conversion of methyl chavicol and selectivity of *trans*–anethole using Ru–Mg–Al as a catalyst.

Conversion of methyl chavicol and selectivity of *trans*–anethole was observed to increase linearly on increasing amount of catalyst from 0.01 g to 0.07g. After that slight increase in the

conversion and selectivity data was observed upto 0.1 g catalyst amount. On further increase in the amount of catalyst, no significant effect on conversion and selectivity of *trans*–anethole was observed. Therefore, 0.1 g catalyst amount was chosen for the further study. The lower catalytic activity at less catalyst amount is due to the unavailability of sufficient active basic sites for isomerization reaction. As the amount of catalyst increased, the availability of the active basic sites coordinated with the ruthenium for the double bond isomerization increases significantly. Therefore, higher conversion of methyl chavicol was observed on increasing the amount of the catalyst. At higher amount of the catalyst, similar conversion of methyl chavicol could be obtained within few minutes reaction time, but then the reaction will turn into stoichiometric reaction rather than catalytic reaction. No conversion of methyl chavicol was observed in the absence of the catalyst.

7.4.3. Effect of Reaction Temperature on Double Bond Isomerization of Methyl Chavicol

Figure 7.14 shows the effect of reaction temperature on conversion of methyl chavicol and selectivity of *trans*–anethole using Ru–Mg–Al as a catalyst. The conversion of methyl chavicol was found to increase on increasing the reaction temperature. At 100 °C, only 41% conversion of methyl chavicol was observed which increased to 74% on increasing the reaction temperature to 180 °C. Finally conversion of methyl chavicol reached to 98% at 210 °C. The selectivity of *trans*–anethole also changed significantly with respect to reaction temperature. At lower temperature (100 °C), 74% selectivity of *trans* isomer was observed, which increased to 88% at 210 °C.

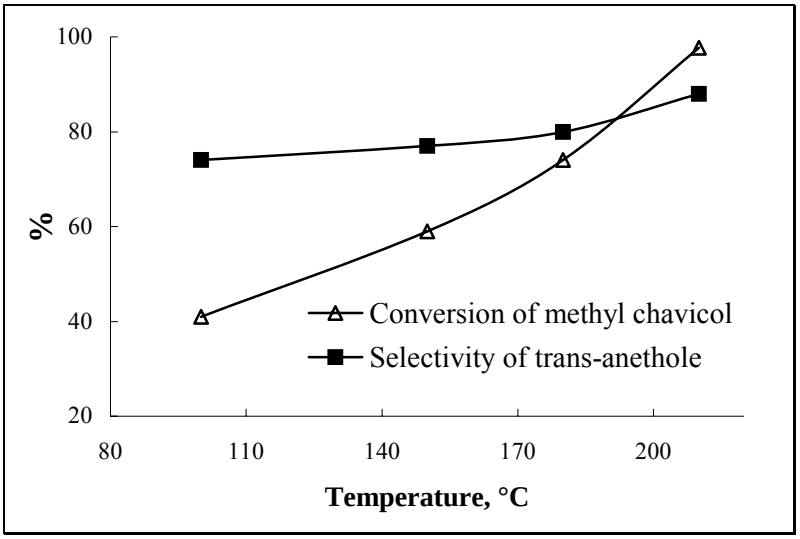

Figure 7.14. Effect of reaction temperature on conversion of methyl chavicol and selectivity of *trans*–anethole using Ru–Mg–Al as a catalyst.

7.4.4. Catalytic Activity and Reusability of Various Impregnated Catalysts

The catalytic activity and reusability of Ru–Mg–Al sample was compared with various ruthenium impregnated (similar amount) catalysts such as ruthenium impregnated on, hydrotalcite of Mg/Al molar ratio of 3.5 [Ru–HT(3.5)], magnesium oxide (Ru–MgO), calcium oxide (Ru–CaO), silica (Ru–SiO_2), alumina (Ru–Al_2O_3) (Table 7.7). Pristine hydrotalcite of Mg/Al molar ratio 3.5, magnesium oxide, calcium oxide, silica and alumina were also used as catalysts to observe the effect of impregnated ruthenium on the catalytic activity of respective sample for isomerization of methyl chavicol. The Ru–Mg–Al catalyst gave 98% conversion of methyl chavicol with 88% selectivity of *trans*–anethole within 2 h reaction time. The conversion and selectivity were observed to remain unchanged even at fourth run, shows that the catalyst is reusable several times for the isomerization reaction without loss in its activity. The higher activity of Ru–Mg–Al catalyst as compared to HT(3.5) is due to presence of, ruthenium cations in the hydrotalcite structure which is known as active metal for double bond isomerization reaction and hydroxyl groups which act as Brønsted basic sites for the reaction. The most of the active sites which are derived form the hydroxyl groups attached to the ruthenium cations are located at the outer surface of Ru–Mg–Al catalyst that makes Ru–Mg–Al as an active and reusable catalyst for isomerization reactions. Another reason for higher activity of Ru–Mg–Al catalyst is the higher surface area of Ru–Mg–Al sample which favors the enhanced catalytic activity of the material as compared to the pristine hydrotalcite. The leaching of the ruthenium metal from the hydrotalcite was not found due to the strong coordination of ruthenium cations in the hydrotalcite matrix as well as to the hydroxyl groups (anions). Similar to Ru–Mg–Al, [Ru–HT(3.5)] catalyst also showed comparable results, i.e. 97% conversion of methyl chavicol and 87% selectivity of *trans*–anethole. The conversion and selectivity was observed to decrease at the end of each cycle. The conversion of methyl chavicol decreased from 97 to 88% with 79% selectivity for *trans*–anethole at the end of fourth cycle. Decrease in the conversion and selectivity could be attributed to the leaching of ruthenium cations from the surface of impregnated catalyst during experiments, because in case of impregnation, the ruthenium is laying on the surface of the support without any bonding between ruthenium and the support. The above observed results were compared with the isomerization of methyl chavicol catalyzed by pristine hydrotalcite of similar Mg/Al molar ratio (3.5) and 20% conversion of methyl chavicol was achieved with 80% selectivity of *trans*–anethole in 2 h. In the second reusability experiment, only 4% conversion of methyl chavicol was found which showed that the [HT(3.5)] is not a reusable catalyst in the present study on double bond isomerization reaction. MgO, which is known as a strong solid base catalyst showed 24% conversion and 72% selectivity of *trans*–anethole.

Table 7.7. Comparison and reusability of various ruthenium containing catalysts for isomerization of methyl chavicol to anethole

Catalyst	Cycle	% Conversion	% Selectivity [a]	
			trans–Anethole	*cis*–Anethole
Ru–Mg–Al	first	98	88	12
	second	98	88	12
	third	98	88	12
	fourth	97	87	13
Ru–HT(3.5)	first	97	87	13
	second	95	85	15
	third	92	81	19
	fourth	88	79	21
HT(3.5)	first	20	80	20
	second	4	81	19
Ru–MgO	first	97	85	15
	second	97	82	18
	third	89	78	22
	fourth	84	75	25
MgO	first	24	72	28
	second	6	70	30
Ru–CaO	first	62	90	10
	second	15	87	13
	third	7	85	15
	fourth	3	84	16
CaO	first	15	75	25
	second	2	65	35
Ru–SiO_2	first	98	79	21
	second	85	73	27
	third	77	62	28
	fourth	70	59	41
SiO_2	first	5	45	55
	second	–	–	–
Ru–Alumina	first	98	84	16
	second	94	81	19
	third	90	79	21
	fourth	87	76	24
Alumina	first	10	72	28
	second	2	–	–

[a] **Reaction conditions:** methyl chavicol = 5.0 g, catalyst = 0.5 g, temperature = 210 °C, reaction time = 2 h

The higher conversion of methyl chavicol with lower selectivity of *trans*–anethole was observed using strong base catalyst (MgO) as compared to the mild base catalyst [HT(3.5)]. On impregnation of ruthenium on MgO, the conversion of methyl chavicol increased to 97% with 80% selectivity of *trans* isomer. The activity of Ru–MgO was also observed to decrease on reusability experiment. At the end of fourth cycle, conversion of methyl chavicol decreased to 84%. Among all ruthenium impregnated catalysts, lower conversion of methyl chavicol (62%) with higher selectivity of *trans*–anethole (90%) was observed in case of Ru–CaO as a catalyst. The conversion was found to decrease very rapidly on the consecutive reusability experiments. Only 3% conversion of methyl chavicol was achieved at the end of fourth cycle, which is lower than the conversion observed by the use of pristine CaO as a catalyst (15%). Rapid decrease in the conversion and selectivity data is due to the faster leaching of ruthenium metal which is known as active species for isomerization of methyl chavicol. Ruthenium impregnated silica and alumina also gave similar conversion of methyl chavicol (98%). However, higher selectivity of *trans*–anethole was observed for Ru–alumina (84%) as compared to Ru–SiO_2 (79%). On reusability of catalyst, rapid decrease in the conversion and selectivity was observed for Ru–SiO_2 as compared to Ru–alumina. The lower conversions of methyl chavicol, i.e. 5 and 10% were found when pristine SiO_2 and alumina respectively were used as catalysts.

7.4.5. Solvent free Isomerization of Other Perfumery Related Compounds using Ru–Mg–Al as a Catalyst

In view of observed higher catalytic activity and reusability of Ru–Mg–Al sample for isomerization of methyl chavicol in solvent free conditions, double bond isomerization of various other perfumery related compounds such as, eugenol, allylbenzene, dimethoxy allylbenzene, safrole, 3–carene were carried out using Ru–Mg–Al as a catalyst at substrate to catalyst ratio (by wt) 10 to ensure the catalytic reaction and optimum result was also observed at this ratio. The Ru–Mg–Al catalyst showed excellent conversion and selectivity of respective isomer in shorter reaction time (Table 7.8). For example, 98% conversion of methyl chavicol with 88% selectivity of *trans*–anethole was observed within 2 h reaction time.

Double bond isomerization of eugenol showed 94% conversion of eugenol with 89% selectivity of *trans*–isoeugenol. Lower conversion of eugenol as compared to methyl chavicol could be attributed to the higher boiling point and viscosity of the reactant. The allylbenzene isomerization showed 96% conversion with 88% selectivity for *trans* isomer. In case of isomerization of dimethoxy allylbenzene, 92% conversion was observed. For isomerization of safrole, 97% conversion with 89% selectivity of *trans*–isosafrole was achieved within 2 h using

Ru–Mg–Al as a catalyst (substrate to catalyst ratio 10:1). The solvent free catalytic isomerization of safrole and eugenol data presented in this study is comparable with the results reported by Kannan et al. using hydrotalcite as a catalyst (substrate to catalyst ratio 2:1) in DMSO as a solvent [43]. The catalytic activity of Ru–Mg–Al was also evaluated for the isomerization of other perfumery chemicals such as 3–carene in order to explore the versatility of the Ru–Mg–Al catalyst. Higher conversion (88%) for isomerization of 3–carene with 72% selectivity of 2–carene indicates that the Ru–Mg–Al as a catalyst is highly active for double bond isomerization of variety of substrates related to the fine and perfumery chemicals.

Table 7.8. Double bond isomerization of various perfumery related compounds

Run	Reactant	% Conversion	% Selectivity [a]	
			trans–Isomer	*cis*–Isomer
1	Methyl chavicol	98	88	12
2	Eugenol	94	89	11
3	Allylbenzene	96	88	12
4	Dimethoxy allylbenzene	92	88	12
5	Safrole	97	89	11
6	3–Carene	88	72	–

[a] **Reaction conditions:** reactant = 5.0 g, catalyst (Ru–Mg–Al) = 0.5 g, temperature = 210 °C, reaction time = 2 h.

Catalytic activity of as–synthesized Ru–Mg–Al and pristine hydrotalcite of varied Mg/Al molar ratio were compared to the respective activated samples for isomerization of methyl chavicol. The catalytic activities of Ru–Mg–Al and pristine hydrotalcite of varied Mg/Al molar ratio were observed to decrease on activation at 450 °C for 4 h (Table 7.9). For example, conversion of methyl chavicol and selectivity of *trans*–anethole were observed to decrease from 98 to 48% and 88 to 80%, respectively on activation of Ru–Mg–Al catalyst. The pristine activated hydrotalcite samples of varied Mg/Al molar ratio were also used as catalysts for double bond isomerization of methyl chavicol to anethole. The conversion of methyl chavicol was observed to increase on increasing on the Mg/Al molar ratio of hydrotalcite from 2.0 to 3.5. For activated hydrotalcite of Mg/Al molar ratio 2.0, 8% conversion of methyl chavicol was observed with 70% selectivity of *trans*–anethole in 10 h reaction time. The conversion increased to 20 with 80% selectivity of *trans*–anethole using activated hydrotalcite of Mg/Al molar ratio 3.5 as a catalyst. The longer reaction time (10 h) is required when pristine hydrotalcite samples were used as catalyst as compared to the Ru–Mg–Al samples as catalyst (only 2 h) for isomerization of methyl chavicol.

The as–synthesized hydrotalcite of varied Mg/Al molar ratio showed higher conversion and selectivity of *trans* isomer as compared to activated hydrotalcite as a catalyst. These results confirmed that the hydroxyl groups present in the hydrotalcite are playing an important role for double bond migration.

Table 7.9. Isomerization of methyl chavicol to anethole using activated catalysts

Run	Reactant	Catalyst*	% Conversion	% Selectivity [a]	
				trans–Iisomer	*cis*–Isomer
1	Methyl chavicol	Ru–Mg–Al	48	80	20
2	Eugenol	Ru–Mg–Al	41	81	19
3	Safrole	Ru–Mg–Al	43	77	23
4	Allylbenzene	Ru–Mg–Al	40	79	21
5	3–Carene	Ru–Mg–Al	38	70	30
6	Methyl chavicol	HT (3.5)	20	80	20
7	Methyl chavicol	HT (3.0)	16	78	22
8	Methyl chavicol	HT (2.5)	14	74	26
9	Methyl chavicol	HT (2.0)	8	70	30

[a] **Reaction conditions:** reactant = 5.0 g, catalyst = 0.5 g, temperature = 210 °C, reaction time = 2 h.
*Activated at 450 °C for 4 h.
Reaction time = 10 h for Runs 6 to 9.

When the catalyst was calcined at 450 °C, the material converted into respective mixed oxides phase of higher surface area and strong basic in nature (rich in Lewis basic sites) as compared to the as–synthesized hydrotalcite (Brønsted basic sites) as catalyst, which was not observed as active as the hydrotalcite without activation for isomerization of methyl chavicol. The above results again show that the as–synthesized Ru–Mg–Al as a versatile catalyst for double bond isomerization reactions.

7.4.6. Kinetic Study for Isomerization of Methyl Chavicol at Optimum Reaction Conditions

For kinetic experiment, the reaction was carried out by taking 10 g methyl chavicol with 1 g Ru–Mg–Al as a catalyst at 210 °C reaction temperature. The kinetic profile for consumption of methyl chavicol and formation of *cis*– and *trans*–anethole with respect to time is shown in Figure 7.15.

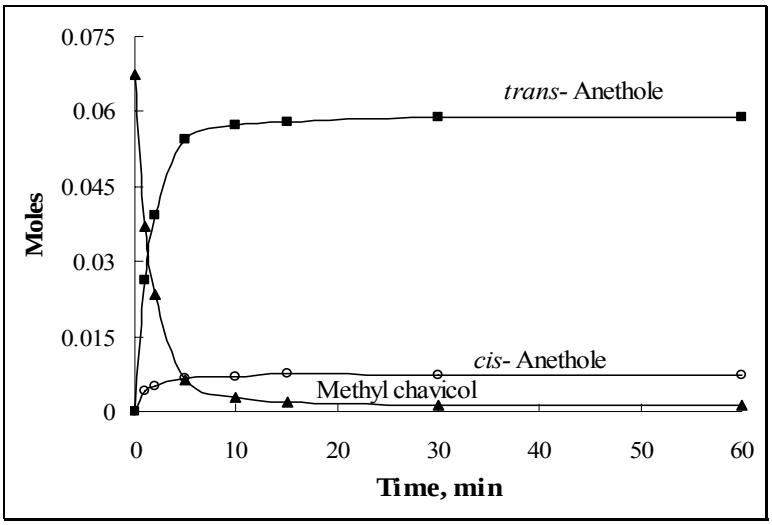

Figure 7.15. Progress of double bond isomerization of methyl chavicol to anethole with respect to time using Ru–Mg–Al as a catalyst.

Rapid consumption of methyl chavicol was observed in lower reaction time. 60% conversion of methyl chavicol was achieved within 2 min reaction time and increased to 95% in 10 min. Most of the methyl chavicol was consumed for the formation of *trans*–anethole, however, small amount of *cis*–anethole was also observed at the beginning of reaction. The higher selectivity of *trans* isomer is due to higher thermodynamic stability as compared to *cis* isomer. The *cis* isomer may also convert into *trans* isomer during the course of reaction. As the progress of reaction increased, the formation of *cis*–anethole was observed to increase. The initial rate of reaction for consumption of methyl chavicol, which was calculated in the conversion range of 25% was found to be 0.0026 mol/(g_{cat} min). The initial rate of reaction for the formation of *cis*– and *trans*–anethole was also calculated and found to be 0.0003 and 0.0023 mol/(g_{cat} min), respectively. The higher initial rate of reaction shows that the formation of *trans*–isomer is more favorable in the present reaction conditions as compared to *cis*–isomer.

7.5. Conclusions

The regioselective synthesis of *trans*–anethole from methyl chavicol via double bond isomerization of methyl chavicol using $RuCl_2(PPh_3)_3$ and $RuCl_3(AsPh_3)_2.CH_3OH$ complexes with detailed kinetic studies has been reported for the first time. The effects of different solvents on the isomerization of methyl chavicol to *trans*–anethole and eugenol to isoeugenol were studied in detail. The highest conversion (99.7%) with selectivity (95.4%) for *trans*–anethole was observed in ethanol followed by *iso*–propanol and methanol in relatively lesser reaction time using $RuCl_2(PPh_3)_3$ catalyst. Similar results were observed for eugenol isomerization in alcoholic solvents using $RuCl_2(PPh_3)_3$ catalyst. However, in case of $RuCl_3(AsPh_3)_2.CH_3OH$ catalyzed

isomerization of methyl chavicol, the highest conversion (94.2%) with selectivity (98.6%) for *trans*–anethole was observed in methanol followed by *iso*–propanol and ethanol. From the kinetic study, it was observed that the rate of reaction increased on increasing methyl chavicol, eugenol and catalyst concentrations. The rate of reaction was found strongly dependent on the solvent concentration and decreased on increasing the concentration of solvent. Activation energies for isomerization of methyl chavicol under experimental conditions were found to be 4.3 kJ/mol with $RuCl_2(PPh_3)_3$ catalyst and 6.0 kJ/mol using $RuCl_3(AsPh_3)_2.CH_3OH$ as a catalyst. For the isomerization of eugenol, the activation energy was found to be 6.9 kJ/mol using $RuCl_2(PPh_3)_3$ complex as a catalyst. The catalyst was recycled five times without significant loss in conversion and selectivity for isomerization of methyl chavicol and eugenol. The ruthenium metal was heterogenized by incorporation into the hydrotalcite matrix (Ru–Mg–Al) and characterized by the various physico–chemical characteristic techniques. The Ru–Mg–Al was used as a catalyst for isomerization of perfumery chemicals such as, methyl chavicol, eugenol, safrole, allylbenzene, dimethoxy allylbenzene, 3–carene. The Ru–Mg–Al catalyst shows excellent activity for the isomerization reaction in shorter reaction time. For example, 98% conversion of methyl chavicol with 88% selectivity of *trans*–anethole was observed in 1 h reaction time. The effect of reaction temperature showed 41% conversion of methyl chavicol and 74% selectivity of *trans*–anethole at 100 °C which increased to 98% with 88% selectivity of *trans*–anethole on increasing temperature to 210 °C using Ru–Mg–Al as a catalyst. The activity of Ru–Mg–Al was compared with the various ruthenium impregnated catalysts such as, Ru–HT(3.5), Ru–MgO, Ru–CaO, Ru–SiO_2, Ru–alumina. The Ru–Mg–Al catalyst was recycled upto fourth cycle without loss of its activity. Other ruthenium impregnated catalyst also showed comparable activity but significant loss in the catalytic activity was observed on reusability experiments for the isomerization of methyl chavicol. Kinetic study at optimum reaction conditions shows that 95% conversion of methyl chavicol was achieved within 10 min reaction time. The initial rate of reaction was calculated from the kinetic profile and found to be 0.0026 mol/(g_{cat} min).

7.6. References

[1] International Flavors & Fragrances Inc., New Release, New York, January 28, (2004).

[2] K. Bauer, D. Garbe, H. Surberg, Ullmann Encyclopedia of Industrial Chemistry, Electronic Release, 6th ed., (2002).

[3] P. Gandilhon, US Patent, 4138411 (1979).

[4] G.E. Svadkovskaya, L.A. Kheifits, A.I. Platova, V. Y. Denisenkova, Chem. Abst. 73 (1970) 14450r.

[5] A.P. Wagner, Manuf. Chemist 23 (1952) 56–60.

[6] M.R. Reddy, M. Periasamy, J. Organomet. Chem. 491 (1995) 263–266.

[7] M. Martan, P.H. Reichenbacher, US Patent, 4038325 to UOP.

[8] H.S. Lee, G.Y. Lee, Bull. Korean Chem. Soc. 26 (2005) 461–462.

[9] W. Wu, J.G. Verkade, ARKIVOC, ix (2004) 88–95.

[10] V.K. Srivastava, H.C. Bajaj, R.V. Jasra, Catal. Commun. 4 (2003) 543–548.

[11] C.H. Bibb, P. Fla, US Patent, 2052744 (1936).

[12] L. Cerveny, A. Krejeikova, A. Marhoul, V. Ruzicka. React. Kinet. Catal. Lett. 33 (1987) 471–476.

[13] A. Loupy, L. Thach, Syn. Commun. 23 (1993) 2571–2577.

[14] L.N. Thach, C.R. Strauss, J. Chem. Edu. 38 (2000) 76–79.

[15] J. Hartig, H.M. Weitz, R. Schnabel, DE Patent, 274 634 (1979) to BASF AG.

[16] J.D. Atwood, Mechanism of Inorganic and Organometallic Reactions, Brooks/Cole, California, (1985).

[17] P.N Rylander, Organic Synthesis with Nobel Metal Catalysts; Academic Press: New York, (1973) p. 145.

[18] P.A. Chaloner, Handbook of Coordination Catalysis in Organic Chemistry; Butterworths: London, (1986) p. 415.

[19] R.H. Crabtree, The Organometallic Chemistry of the Transition Metals; Wiley–InterSciences, New York, (1994).

[20] G. Yagupsky, C.K. Brown, G. Wilkinson, J. Chem. Soc. (A) (1970) 1392–1401.

[21] J.T. Mague, G. Wilkinson, J. Chem. Soc. (A) (1966) 1736–1740.

[22] T.A. Stephenson, G. Wilkinson, J. Inorg. Nucl. Chem. 28 (1966) 945–956.

[23] J.L. Burmeister, and F. Basolo, Inorg. Chem. 3 (1964) 1587–1593.

[24] F. Basile, L. Basini, G. Fornasari, M. Gazzano, F. Trifiro, A. Vaccari, Chem. Commun. (1996) 2435–2436.

[25] F. Cavani, F. Trifiro, A. Vaccari, Catal. Today 11 (1991) 173–301.

[26] N. Kuznik, O.F. Wendt, J. Chem Soc. Dalton Trans. (2002) 3074–3078.

[27] G.M. Bodner, M.P. May, L.E. McKinney, Inorg. Chem. 19 (1980) 1951–1958.

[28] S. Kaur, J.V. Crivello, N. Pascuzzi, J. Polym. Sci. Part A: Poly. Chem. 37 (1999) 199–209.

[29] S. Krompiec, N. Kuzynik, R. Penczek, J. Rzepa, J.M. Biaton, J. Mol. Catal. A: Chem. 219 (2004) 29–40.

[30] M.A. Bennett, T.W. Matheson, G. Wilkinson, F.G.A. Stone, F.W. Abel, Comprehensive Organometallic Chemistry, Vol. 4, Pergamon, New York, (1982) p. 942.

[31] J. Blum, Y. Becker, J.C.S. Perkin Trans. II (1972) 982–989.

[32] A. Salvini, F. Piacenti, P. Frediani, A. Devescovi, M. Caporali, J. Organomet. Chem. 625 (2001) 255–267.

[33] L. Cerveny, A. Krejeikova, A. Marhoul, V. Ruzicka, React. Kinet. Catal. Lett. 33 (1987) 471–476.

[34] L.N. Thach, C.R. Strauss, J. Chem. Edu. 38 (2000) 76–79.

[35] K. Kaneda, T. Yamashita, T. Matsushita, K. Ebitani, J. Org. Chem. 63 (1998) 1750–1751.

[36] F. Basile, G. Fornasari, M. Gazzano, A. Vaccari, Appl. Clay Sci. 16 (2000) 185–200.

[37] T. Matsushita, K. Ebitani and K. Kaneda, Chem. Commun. (1999) 265–266.

[38] K. Motokura, D. Nishimura, K. Mori, T. Mizugaki, K. Ebitani and K. Kaneda, J. Am. Chem. Soc. 126 (2004) 5662–5663.

[39] K. Motokura, N. Fujita, T. Mizugaki, K. Ebitani, K. Jitsukawa, K. Kaneda, Chem. Eur. J. 12 (2006) 8228–8239.

[40] K. Motokura, T. Mizugaki, K. Ebitani, K. Kaneda, Tetrahedran Lett. 45 (2004) 6029–6033.

[41] F. Basile, G. Fornasari, M. Gazzano, A. Vaccari, J. Mater. Chem. 12 (2002) 3296–3303.

[42] S. Abello, F. Medina, D. Tichit, J.P. Ramirez, J.C. Groen, J.E. Sueiras, P. Salagre, Y. Cesteros, Chem. Eur. J. 11 (2005) 728–739.

[43] D. Kishore, S. Kannan, J. Mol. Catal. A: Chem. 223 (2004) 225–230.

Chapter 8

Summary and Conclusions

8.1. Summary and Conclusions

Present thesis describes the development of green catalytic routes for the synthesis of fine and commercially important bulk chemicals using eco–friendly heterogeneous catalysts via hydroformylation, condensation and isomerization reactions. First part of the present study described the efforts to reduce a multi–step synthesis into a single pot for the synthesis of higher carbon number aldehydes/alcohol starting from lower carbon number alkenes. For example, C_8 aldol derivatives (2–ethylhexanal and 2–ethylhexanol), used as intermediates for the synthesis of dioctyl phthalate (DOP; used in PVC), were synthesized commercially from propylene in a three steps process. Hydroformylation of propylene in the presence of carbon monoxide is carried out in first step to produce *n*–butanal using rhodium based catalysts. In the second step, *n*–butanal undergoes aldol condensation in the presence of strong liquid base, like KOH or NaOH in stoichiometric amount for the production of 2–ethylhexenal and third step is the hydrogenation of 2–ethylhexenal using nickel or copper based catalysts to produce 2-ethylhexanol. The existing commercial processes for the production of C_8 aldol derivatives have drawbacks namely, i) being a multi–steps process, ii) use of hazardous liquid base KOH/NaOH in stoichiometric amount for aldol condensation reaction, iii) involving post synthesis work–up in the separation of spent KOH/NaOH from product mixture, iv) lower selectivity of product, corrosion of reactors and storage vessels, v) environmental and effluent treatment problems. It is estimated that approximately, 1.0–1.5 tons of spent liquid base is being generated for every 10 tones of the product formed in homogeneous aldol condensation. High capital expenses are also connected with the handling of strong liquid bases like KOH/NaOH. Therefore, our main concern was on the replacement of liquid bases, which are being used in stoichiometric amount, by the eco–friendly heterogeneous catalyst to carry out all three steps into a single pot by altering the reaction conditions. Similarly, synthesis of perfumery chemicals such as, *trans*–anethole and *trans*–isoeugenol by double bond isomerization of methyl chavicol and eugenol, respectively is done using liquid KOH and/or NaOH in stoichiometric amounts. Jasminaldehyde which has the fragrance of jasmine is also synthesized by the condensation of 1-heptanal with benzaldehyde in the presence of liquid KOH and/or NaOH in stoichiometric amounts. The existing commercial processes for these isomerization and condensation reactions also possess all the demerits stated above. With increased environmental awareness, replacement of stoichiometric technologies by atom efficient greener catalytic routes with low E factor (kg of byproducts generated per kg of desired product) and substitution of toxic and/or hazardous solvents/reagents with cleaner alternatives is today's need. Therefore, it is desirable to find eco-friendly solid base catalysts which could substitute these liquid bases.

The work presented in the thesis describes the synthesis of different heterogeneous catalysts, such as multi–functional catalyst synthesized by impregnation and intercalation of rhodium complex onto/into the hydrotalcite for hydroformylation, condensation, hydrogenation reactions in a single pot and hydrotalcite of varied M(II) and M(II)/Al molar ratio [M(II) = Mg, Ni, Zn] for aldol condensation and isomerization reactions. The intercalation of ruthenium metal in the hydrotalcite matrix (aluminum cations replaced by ruthenium) was also carried out and used as a catalyst for isomerization of perfumery chemicals. The structural and textural properties of the synthesized catalysts were studied by various instrumental techniques such as, ^{31}P–nuclear magnetic resonance (NMR), powder–X–ray diffraction (P–XRD), Fourier transform–infrared (FT–IR) spectrometer, thermogravimetric analysis (TGA), CHN analysis, scanning electron microscope (SEM) and surface area analyzer. Catalytic activity of these catalysts was studied for the hydroformylation, condensation and isomerization reactions.

The first chapter deals with a detailed literature survey on the use of heterogeneous catalysts for the hydroformylation of alkenes and applicability of the various solid base catalysts for aldol condensation (self and cross) and isomerization reactions. The development and applications of multi–functional catalyst is also discussed in the introduction part of the present thesis.

Second chapter is presented in two parts. The first part describes the synthesis of C_8 aldol derivatives (aldehydes/alcohol) from propylene in a single pot using a novel approach, in which multi–functional heterogeneous catalyst system [HF/HT] was prepared by impregnation of rhodium complex; $HRh(CO)(PPh_3)_3$ [HF] on the surface of a solid base hydrotalcite; $(Mg_{1-x}Al_x(OH_2))^{x+}(CO_3^{2-})_{x/n}\cdot mH_2O)$ [HT]. The [HF/HT] catalyst was characterized by powder X–ray diffraction (P–XRD), FT–IR spectroscopy, N_2 adsorption–desorption isotherm, scanning electron microscopy (SEM) and ^{31}P solid state NMR. The [HF/HT] catalyst has shown efficient catalytic activity for hydroformylation, aldol condensation and hydrogenation reactions in a single pot. The Mg/Al ratio of [HT], amount of [HF] complex and [HT], and reaction temperature showed pronounced effect on the selectivity and rate of formation of C_8 aldol derivatives. Aldol condensation temperature T_2 played a significant role in the formation of 2–ethylhexanol in a single pot. The selectivity for 2–ethylhexanol was observed 11% using Mg/Al molar ratio of [HT] 1.5 that increased to 21% on increasing the Mg/Al molar ratio of [HT] to 3.5 at 250 °C. As the Mg/Al molar ratio and amount of [HT] increased, the selectivity for 2–ethylhexanal was observed to increase due to enhancement in the basicity of the catalyst. The amount of [HF] complex in the [HF/HT] catalyst significantly influenced the selectivity of 2–ethylhexanal. From the kinetic experiments, it was observed that the rate of formation of 2–ethylhexanal depends on the rate of

aldol condensation which is catalyzed by [HT] component of the multi–functional catalyst. The reaction pathway and role of each component of multi–functional catalyst [HF/HT] for the synthesis of 2–ethylhexanol in a single pot was discussed with the help of the kinetic profile of the reaction with respect to time.

Second part of this chapter deals with the synthesis of 2–methylpentanol from ethylene in a single pot using the multi–functional catalyst [HF/HT–Act] synthesized by impregnation of $HRhCO(PPh_3)_3$ [HF] complex on the surface of activated hydrotalcite [HT–Act] of varied Mg/Al molar ratio. ^{31}P–NMR spectrum of [HF/HT–Act] catalyst showed that the [HF] complex impregnated on [HT–Act] without decomposition. The Mg/Al ratio of [HT], aldol condensation temperature T_2, CO to H_2 ratio of syn–gas and partial pressure of ethylene showed pronounced effect on the selectivity of 2–methylpentanol. As the Mg/Al molar ratio of [HT–Act] increased from 1.5 to 3.5, the selectivity for 2–methylpentanol also increased from 56 to 79% due to the enhancement in the basicity of catalyst. The selectivity of 2–methylpentanol was observed to increase from 0 to 79% on increasing the aldol temperature (T_2) from 60 to 130 °C. On further increase in the T_2 upto 180 °C, the selectivity of 2–methylpentanol decreased to 55% due to hydrogenation of propanal to propanol. The selectivity of 2–methylpentanol was observed to increase on increasing the partial pressure of ethylene. The polar solvents showed higher selectivity of 2–methylpentanol as compared to non polar solvents under identical reaction conditions. The [HF/HT–Act] catalyst was observed to be re-usable for hydroformylation and hydrogenation reactions even at the end of fourth cycle. However, it was not found to be active for aldol condensation of propanal. The reaction pathway and role of each component of multi–functional catalyst [HF/HT–Act] for the synthesis of 2–methylpentanol was discussed with the help of kinetic profile of the product formation with respect to time.

Third chapter comprises the development of a novel reusable heterogeneous catalyst by intercalation of $HRhCO(TPPTS)_3$ complex in the interlayer space of hydrotalcite for hydroformylation of alkenes. Intercalation of $HRh(CO)(TPPTS)_3$ complex into interlayer space of hydrotalcite was confirmed by ^{31}P–NMR, P–XRD and FT–IR spectra of intercalated [HT(3.5)–INT] catalyst. The catalytic activity of intercalated catalyst was evaluated for hydroformylation of linear alkenes of varied carbon chain length (C_5 to C_{13}) and cyclic alkenes. As carbon chain length of linear alkenes increases, the selectivity of aldehydes was observed to decrease. Activity of the catalyst for hydroformylation of linear alkenes under identical reaction conditions was found to be in the order of; 1–pentene > 1–hexene > 1–heptene > 1–octene> 1–nonene > 1–decene > 1–undecene > 1–dodecene > 1–tridecene. Order of the catalytic activity for hydroformylation of cyclic alkenes was observed as; cyclohexene > cycloheptene > cyclooctene under similar reaction

conditions. Effect of the reaction parameters such as, amount of catalyst, concentration of reactant, reaction temperature, partial pressure of carbon monoxide and hydrogen on conversion of alkenes and selectivity of aldehydes was studied by taking 1–hexene as a model reactant. The selectivity of aldehyde was observed to decrease on increasing the temperature and amount of catalyst due to the increased isomerization of 1–hexene to 2/3–hexene at higher reaction temperature and catalyst amount. The catalyst was recycled upto seven times for hydroformylation of 1–hexene. Complete conversion of 1–hexene (100%) was obtained in seventh cycle, however, the selectivity of aldehydes (n and iso) was observed to decrease after fifth cycle. The decrease in selectivity of aldehydes could be due to physical and handling loss of catalyst during reusability experiments. The P–XRD pattern and FT–IR spectrum of used [HT(3.5)–INT] catalyst showed that the structure of [HT(3.5)–INT] catalyst was retained after repeated experiments for the hydroformylation of 1–hexene. The rate of reaction was calculated from kinetic plot for hydroformylation of 1–hexene at optimum reaction conditions. Higher rate of reaction was obtained for isomerization of 1–hexene to 2/3–hexene as compared to the formation of aldehydes.

Fourth chapter describes the use of intercalated $HRhCO(TPPTS)_3$ complex into the interlayer space of hydrotalcite as a multi–functional catalyst [HF/HT–INT] for the synthesis of C_8 aldol derivatives (2–ethylhexanal and 2–ethylhexanol) from propylene via hydroformylation, aldol condensation and hydrogenation reactions in a single pot. The catalyst showed excellent activity for hydroformylation, aldol condensation and hydrogenation reaction in one pot by changing the reaction conditions. The effect of various reaction parameters on the selectivity of 2–ethylhexanal and 2–ethylhexanol was studied in order to optimize the reaction conditions. Formation of 2–ethylhexanol (12%) was observed at higher aldol condensation temperature (T_2 = 250 °C). The selectivity of C_8 aldehydes were observed to increase on increasing the T_2 and maximum selectivity (42%) obtained in the range of 150 to 200 °C aldol temperature at 10 atm partial pressure of propylene in 24 h reaction time. The amount of [HF/HT–INT] catalyst was varied form 100 to 1200 mg in order to optimize the amount of catalyst for the maximum selectivity of C_8 aldehydes. The selectivity of C_8 aldehydes increased from 21% at 100 mg to 51% at 1200 mg. The catalyst was reused upto second cycle without significant losses in the conversion and selectivity of C_8 aldehydes. The reusability experiments suggested that the [HF/HT–INT] catalyst is active even at fourth cycle for carrying out the hydroformylation reaction but hydrotalcite in [HF/HT–INT] catalyst gets deactivated. The rate of formation of various products was calculated from the kinetic profile and compared with the rate obtained from experiments performed separately for individual steps involved in the reaction.

The solvent free aldol condensation of propanal using various solid base catalysts such as

ion exchanged zeolites, alumina, KOH impregnated alumina, as–synthesized, activated and reconstructed hydrotalcite samples of varied Mg/Al molar ratio was reported in the fifth chapter. The alkali ion–exchanged zeolites, alumina, alkali impregnated alumina and hydrotalcite samples were synthesized, characterized by the various spectroscopic analysis. The higher conversion of propanal was observed using hydrotalcite as catalyst among the various studied solid base catalysts namely, alkali ion–exchanged zeolites, alumina, alkali treated alumina and hydrotalcite of varied Mg/Al molar ratio. The conversion and selectivity of 2–methylpentenal increased with increasing Mg/Al molar ratio of hydrotalcite. The maximum conversion (97%) of propanal with 99% selectivity of 2–methylpentenal was obtained at 100 °C and 10 h using activated hydrotalcite of Mg/Al molar ratio of 3.5 as a catalyst. To correlate the observed higher conversion and selectivity for propanal condensation with the basicity of activated hydrotalcite, the basicity of activated hydrotalcite of Mg/Al ratio 2.0, 2.5, 3.0 and 3.5 was evaluated by isomerization of β–isophorone to α– isophorone as a model test reaction reported for basicity measurement. Increase in the basicity of hydrotalcite with increasing Mg/Al molar ratio was confirmed from the test reaction. The effect of reconstruction of hydrotalcite on the selectivity of 2–methylpentenal was also studied. From the kinetic data for aldol condensation of propanal, the initial rate of reaction was observed to increase on increasing the amount of catalyst upto 0.1 g, on further increase in the amount of catalyst, initial rate of reaction did not change significantly. The reaction kinetics was also observed to be significantly influenced by the reaction temperature. The activation energy for the propanal condensation was calculated by Arrhenius plot and found to be 58 kJ/mol. The catalyst was recycled upto six cycles without any significant loss in its activity for aldol condensation of propanal.

Sixth chapter contains the synthesis of jasminaldehyde, which is an important perfumery chemical, by condensation of 1–heptanal with benzaldehyde using as–synthesized, activated and reconstructed hydrotalcite samples as catalysts. The catalytic activity of hydrotalcite ($[M(II)_{1-x}M(III)_x(OH_2)]^{x+}(CO_3^{2-})_{x/n}\cdot mH_2O$; where M(II) = Mg, Ni, Zn and M(III) = Al) was evaluated for the synthesis of jasminaldehyde by solvent free condensation of 1–heptanal with benzaldehyde. The effect of activation of as–synthesized Mg–Al hydrotalcite samples of varied Mg/Al molar ratio on catalytic activity was studied and correlated with their basicity as determined from the model test reaction. The effect of reaction parameters such as, amount of catalyst, benzaldehyde to 1–heptanal molar ratio and reaction temperature on conversion of 1–heptanal and selectivity of jasminaldehyde was studied in detail. The selectivity of jasminaldehyde was observed to increase on increasing the M(II)/Al molar ratio of as–synthesized as well as activated hydrotalcite. The maximum selectivity of jasminaldehyde (86%) with 98% conversion of 1–heptanal was observed using as–synthesized Mg–Al hydrotalcite of Mg/Al molar ratio of 3.5 as a catalyst. The activated

hydrotalcite was found to be more active for self condensation of 1–heptanal as compared to the condensation of 1–heptanal with benzaldehyde. The conversion of 1–heptanal was observed to increase from 70 to 100% with decrease in selectivity of jasminaldehyde from 86 to 70% on increasing the amount of Mg–Al(3.5) as a catalyst from 20 to 500 mg. Benzaldehyde to 1–heptanal molar ratio was observed to influence the selectivity of jasminaldehyde. The kinetics of the reaction was carried out to calculate the rate and order of reaction under optimum reaction conditions. The rate of reaction was calculated as 11.6×10^{-4} mol/(g_{cat} min) at optimum reaction conditions. The significant loss in the conversion of 1–heptanal and selectivity of jasminaldehyde was not observed upto three cycles, which shows the reusability of the catalyst. The base catalyzed reaction mechanism for condensation of 1–heptanal with benzaldehyde is proposed.

The effect of reconstruction of hydrotalcite on the selectivity of jasminaldehyde was also studied and found that the reconstructed hydrotalcite of Mg/Al molar ratio of 3.5 gave 98% conversion with 84% selectivity of jasminaldehyde within 2 h reaction time. The higher activity of the reconstructed hydrotalcite as compared to as–synthesized and activated hydrotalcite samples is due to the presence of higher numbers of Brønsted basic sites (OH^- groups), which are more active for the condensation of 1–heptanal with jasminaldehyde. The detail kinetics study was also carried out in order to obtain optimum reaction conditions for condensation of 1–heptanal with benzaldehyde using reconstructed hydrotalcite of Mg/Al molar ratio of 3.5 as a catalyst.

Seventh chapter of the thesis describes the isomerization of allyl phenyl ethers. The allyl phenyl ethers have unique importance in the perfumery, fragrance and food industries. Among the allyl phenyl ethers, *trans*–anethole and *trans*–isoeugenol have high industrial demand as intermediates for synthesis of various other perfumery chemicals. Double bond isomerization of methyl chavicol and eugenol to *trans*–anethole and *trans*–isoeugenol was studied using Pd, Rh, Ru metal precursors and their complexes of phosphine, arsine and antimony as catalysts in solvent free conditions. The ruthenium complexes showed better activity than palladium and rhodium metals complexes. Among the phosphine, arsine and antimony complexes of Pd, Rh and Ru, the $M/SbPh_3$ (M = Pd, Rh) system gave higher conversion and selectivity for isomerization of methyl chavicol and eugenol except for ruthenium complexes. In view of the higher conversion and selectivity for isomerization reaction using ruthenium complexes, the $RuCl_2(PPh_3)_3$ and $RuCl_3(AsPh_3)_2.CH_3OH$ complex as catalysts were studied for the double bond isomerization of methyl chavicol and eugenol in the polar aprotic (DMSO, acetonitrile), polar protic (ethanol, methanol, *n*–propanol, *iso*–propanol, *n*–butanol, *iso*–butanol, *n*–hexanol) and non–polar (benzene, toluene, *n*–hexane, cyclohexane, tetrahydrofuran,) solvents with detail kinetic studies. The highest conversion (99.7%) with selectivity (95.4%) for *trans*–anethole was observed in ethanol as a solvent followed by *iso*–

propanol and methanol in relatively lesser reaction time using $RuCl_2(PPh_3)_3$ catalyst. Similar results were observed for eugenol isomerization in alcoholic solvents using $RuCl_2(PPh_3)_3$ catalyst. However, in case of $RuCl_3(AsPh_3)_2.CH_3OH$ catalyzed isomerization of methyl chavicol, the highest conversion (94.2%) with selectivity (98.6%) for *trans*–anethole was observed in the methanol followed by *iso*–propanol and ethanol. The kinetics of isomerization of methyl chavicol and eugenol using $RuCl_2(PPh_3)_3$ and $RuCl_3(AsPh_3)_2.CH_3OH$ catalysts in ethanol or methanol involving the effect of substrate concentrations, catalyst amount, nature of solvents used and temperature on the initial rate of reaction was studied in detail. The initial rates of reaction were observed to increase on increasing the initial concentrations of methyl chavicol, eugenol, and catalysts. The rate of reaction was found strongly dependent on the solvent concentration and decreased with increasing the solvent concentration. Activation energies for the isomerization of methyl chavicol under experimental conditions were found to be 4.3 kJ/mol with $RuCl_2(PPh_3)_3$ catalyst and 6.0 kJ/mol with $RuCl_3(AsPh_3)_2.CH_3OH$ catalyst. For the isomerization of eugenol, the activation energy was found to be 6.9 kJ/mol using $RuCl_2(PPh_3)_3$ complex as a catalyst. The catalyst was recycled five times without significant loss in conversion and selectivity for isomerization of methyl chavicol and eugenol.

Ruthenium complexes were observed to give excellent results for double bond isomerization among all studied catalysts. Therefore, the ruthenium metal was heterogenized on various supports to take advantages of heterogeneous catalyst system over homogeneous catalyst. The ruthenium incorporated hydrotalcite (Ru–Mg–Al) was synthesized by the intercalation technique and characterized by the various spectroscopic methods. The Ru–Mg–Al was used as a catalyst for isomerization of perfumery chemicals such as, methyl chavicol, eugenol, safrole, allylbenzene, dimethoxy allylbenzene, 3–carene. The Ru–Mg–Al catalyst showed excellent activity for the isomerization reaction in shorter reaction time. For example, 98% conversion of methyl chavicol with 88% selectivity of *trans*–anethole was observed in 1 h reaction time. The activity of Ru–Mg–Al was compared with the various ruthenium impregnated catalysts such as, Ru–HT, Ru–MgO, Ru–CaO, Ru–SiO_2, Ru–alumina. The Ru–Mg–Al catalyst was recycled upto fourth cycle without loss of its activity. Other ruthenium impregnated catalysts also showed comparable activity but significant loss in the catalytic activity was observed on reusability experiments for isomerization of methyl chavicol. In order to optimize the reaction parameters for isomerization of methyl chavicol, the effect of reaction temperature and amount of catalyst was studied on the conversion and selectivity of *trans*–anethole. The conversion of methyl chavicol and selectivity of *trans*–anethole was found to increase on increasing the reaction temperature as well as amount of catalyst. At 0.005 g catalyst amount, 55% conversion of methyl chavicol with 68% selectivity of *trans*–anethole was observed which increased to 93% with 82% selectivity of *trans*–anethole at

0.05 g catalyst amount. On further increase in the amount of catalyst to 1 g, the conversion reached to 98% with 88% selectivity of *trans*–anethole. The effect of reaction temperature showed 41% conversion of methyl chavicol and 74% selectivity of *trans*–anethole at 100 °C that increased to 98% with 88% selectivity of *trans*–anethole at 210 °C using Ru–Mg–Al as a catalyst. Kinetic study at optimum reaction conditions showed that 95% conversion of methyl chavicol was achieved within 10 min reaction time. The initial rate of reaction was calculated from the kinetic profile and found to be 0.0026 mol/(g_{cat} min).

List of Publications

List of Publications in SCI Journals –

(1) **Sumeet K Sharma**, Parimal A Parikh, Raksh V Jasra, Ruthenium containing hydrotalcite as a solid base catalyst for >C=C< double bond isomerization of perfumery chemicals, *J. Mol. Catal. A Chem.* (Under Review).

(2) **Sumeet K Sharma**, Parimal A Parikh, Raksh V Jasra, Hydroformylation of alkenes using heterogeneous catalyst prepared by intercalation of $HRh(CO)(TPPTS)_3$ complex in hydrotalcite, *J. Mol. Catal. A: Chem.* (Revised).

(3) **Sumeet K Sharma,** Ram S Shukla, Parimal A Parikh, Raksh V Jasra, The multi–step reactions for the synthesis of C8 aldehydes and alcohol from propene in a single pot using an eco–friendly multi–functional catalyst system: Kinetic performance for parametric optimization, *J. Mol. Catal. A Chem.* (In Press).

(4) **Sumeet K Sharma**, Parimal A Parikh, Raksh V Jasra, Synthesis of 2–methylpentanol from ethylene in one pot using eco–friendly $HRhCO(PPh_3)_3$ supported on activated hydrotalcite as a multi–functional catalyst, *J. Mol. Catal. A: Chem.* (In Press).

(5) **Sumeet K Sharma,** Parimal A Parikh, Raksh V Jasra, Eco–friendly synthesis of jasminaldehyde by condensation of 1–heptanal with benzaldehyde using hydrotalcite as a solid base catalyst, *J. Mol. Catal. A Chem.* 286 (2008) 55–62.

(6) **Sumeet K Sharma**, Hasmukh A Patel, Raksh V Jasra, Synthesis of jasminaldehyde using magnesium organo silicates as a solid base catalyst, *J. Mol. Catal. A: Chem.* 280 (2008) 61–67.

(7) **Sumeet K Sharma**, Pushpendra K Kushwaha, Vivek K Srivastava, Sharad D. Bhatt, Raksh V Jasra, Effect of hydrothermal conditions on structural and textural properties of synthetic hydrotalcites of varied Mg/Al ratio, *Ind. Eng. Chem, Res*. 46 (2007) 4856–4865.

(8) **Sumeet K Sharma**, Parimal A Parikh, Raksh V Jasra, Solvent free aldol condensation of propanal to 2–methylpentenal using solid base catalysts, *J. Mol. Catal. A: Chem.* 278 (2007) 135–144.

(9) **Sumeet K Sharma**, Vivek K Srivastava, Ram S Shukla, Parimal A Parikh, Raksh V Jasra, One–pot synthesis of C_8 aldehydes/alcohols from propylene using eco–friendly hydrotalcite supported $HRh(CO)(PPh_3)_3$ catalyst, *New J. Chem.* 31 (2007) 277–286.

(10) **Sumeet K Sharma**, Vivek K Srivastava, Raksh V Jasra, Selective double bond isomerization of allyl phenyl ethers catalyzed by ruthenium metal complexes, *J. Mol. Catal. A: Chem.* 245 (2006) 200–209.

(11) **Sumeet K Sharma**, Vivek K Srivastava, Priti H Pandya, Raksh V Jasra, Isomerization of

methyl chavicol to *trans*–anethole using transition metal complexes as catalysts, *Catal. Commun*. 6 (2005) 205–209.

(12) Vivek K Srivastava, **Sumeet K Sharma**, Ram S Shukla, Raksh V Jasra, Rhodium metal complex and hydrotalcite based environment–friendly catalyst system for the selective synthesis of C_8 aldehydes from propylene ratio, *Ind. Eng. Chem, Res*. 47 (2008) 3795–3803.

(13) N Sudheesh, **Sumeet K Sharma**, Ram S Shukla, Raksh V Jasra, $HRh(CO)(PPh_3)_3$ encapsulated mesopores of hexagonal mesoporous silica (HMS) acting as nanophase reactor for effective catalytic hydroformylation of olefins, *J. Mol. Catal. A Chem.* 296 (2008) 61–70.

(14) Hasmukh A Patel, **Sumeet K Sharma**, Raksh V Jasra, Synthetic talc as a solid base catalyst for condensation of aldehydes and ketones, *J. Mol. Catal. A: Chem.* 286 (2008) 31–40.

(15) Vivek K Srivastava, **Sumeet K Sharma**, Ram S Shukla, Raksh V Jasra, The 'single–pot' synthesis of C_{2n+2}–aldol derivatives from C_n–alkenes using multi–functional catalyst, *Catal. Commun*. 7 (2006) 881–886.

(16) Vivek K Srivastava, **Sumeet K Sharma**, Ram S.Shukla, N Subrahmanyam, Raksh V Jasra, Kinetic studies on the hydroformylation of 1–hexene using $RhCl(AsPh_3)_3$ as a catalyst, *Ind. Eng. Chem. Res*. 44 (2005) 1764 –1771.

Chapter in a Book -

(17) **Sumeet K Sharma**, Vivek K Srivastava, Raksh V Jasra, Catalytic processes for the hydroformylation of alkenes for producing oxo–products, book entitled "*Catalysis in hydrocarbon processing and fertilizer industry*" edited by MA Siddiqui, RP Verma, Lovraj Kumar Memorial Trust, New Delhi.

List of Seminars/Conferences –

(1) **Sumeet K. Sharma**, Parimal A. Parikh, Raksh V. Jasra, *Intercalation of $HRh(CO)(TPPTS)_3$ complex in the interlayer space of hydrotalcite to prepare a heterogeneous catalyst for hydroformylation of alkenes***,** 19th National Symposium on Catalysis (CATSYMP-19), 18–21st January 2009, organized by NCL-Pune and Catalysis Society of India.

(2) **Sumeet K. Sharma**, Ram S. Shukla, Parimal A. Parikh, Raksh V. Jasra, *A rhodium-hydrotalcite based eco–friendly multi–functional catalyst system in the effective synthesis of C_8 aldehydes and alcohol from propylene: Kinetic investigations***,** 19th National Symposium on Catalysis (CATSYMP-19), 18–21st January 2009, organized by NCL-Pune and Catalysis

Society of India.

(3) **Sumeet K Sharma**, Parimal A Parikh, Raksh V Jasra, *Selective synthesis of 2–methylpentanol from ethylene in a single pot using eco–friendly multi–functional [HF/HT–Act] catalyst system,* Petrotech–2009, 8th International Oil and gas Conference & Exhibition, January 11–15th , 2009 at New Delhi, India.

(4) **Sumeet K Sharma**, Parimal A Parikh, Raksh V Jasra, *Eco-friendly multi-functional catalyst system for selective synthesis of 2-methylpentanol from ethylene in single pot*, 14th International Conference on Catalysis, Seoul, Korea 2008 from 19-21st July 2008.

(5) **Sumeet K Sharma**, Parimal A Parikh, Raksh V Jasra, *Hydrotalcite (rehydrated) as highly active solid base catalyst for synthesis of jasminaldehyde by condensation of 1-heptanal with benzaldehyde,* 14th International Conference on Catalysis, Seoul, Korea 2008 from 19-21st July 2008.

(6) **Sumeet K. Sharma,** Vivek K. Srivastava, Ram S. Shukla, Parimal A. Parikh, Raksh V. Jasra, *Synthesis of 2-ethylhexanol and 2-ethylhexanal from propylene in one pot using heterogeneous eco-friendly multi-functional catalyst,* 22nd Gujarat Science Congress at Bhavnagar University, Bhavnagar, on 9th March 2008.

(7) **Sumeet K. Sharma**, Vivek K. Srivastava, Ram S. Shukla, Parimal A. Parikh, Raksh V. Jasra, *A novel eco-friendly multi-functional catalyst system for the synthesis of C_8 aldehydes and alcohols from propylene in a single pot,* 5th All Gujarat Research Scholars Meet at Department of Applied Chemistry, The M.S. University of Baroda, Vadodara on 17th February 2008 (***Won First Prize in Oral Presentation***).

(8) **Sumeet K Sharma**, Parimal A Parikh and Raksh V Jasra, *Solvent free aldol condensation of propanal using solid base catalysts,* 18th National Symposium on Catalysis at IIP Dehradun from 16–18th April 2007.

(9) **Sumeet K Sharma**, Parimal A Parikh and Raksh V Jasra, *Recent developments in the hydroformylation processes in manufacturing of fine chemicals,* CHEMCON-2006 at GNFC Bharuch from 27–30th December 2006.

(10) **Sumeet K. Sharma**, V.K. Srivastava, R.V. Jasra, *Selective isomerization of methyl chavicol to trans-anethole using ruthenium complexes as catalysts,* 17th National Symposium on Catalysis at CSMCRI Bhavnagar from 18-20th January 2005 ***(Won Hindustan Platinum Award for Best Poster Presentation)***.